

**A Comparative Risk Analysis of
Composite and Steel Production Risers**

By

**E.G. Ward, O.A. Ochoa, and Won Kim (OTRC at TAMU)
R.M. Gilbert and Anubhav Jain (OTRC at UT)
Charles Miller (Stress Engineering Services)
Early Denison (Consultant)**

**Phase I & II Final Project Report
Prepared for the Minerals Management Service
Under the MMS/OTRC Cooperative Research Agreement
1435-01-99-CA-31003
Task Order 73632
1435-01-04-CA-35515
Task Order 35985
MMS Project Number 490**

and

OTRC Industry Consortium

April, 2007

OTRC Library Number: 3/07A180

"The views and conclusions contained in this document are those of the authors and should not be interpreted as representing the opinions or policies of the U.S. Government. Mention of trade names or commercial products does not constitute their endorsement by the U. S. Government".



For more information contact:

Offshore Technology Research Center
Texas A&M University
1200 Mariner Drive
College Station, Texas 77845-3400
(979) 845-6000

or

Offshore Technology Research Center
The University of Texas at Austin
1 University Station C3700
Austin, Texas 78712-0318
(512) 471-6989

A National Science Foundation Graduated Engineering Research Center

Table of Contents

Table of Contents	i
List of Tables and Figures	ii
Introduction	1
General Description of Riser System & Functional Requirements	3
Risers	4
Steel Riser	4
Configuration	4
Cross Section	5
Composite Riser	5
Configuration	5
Cross Section	7
Failure Modes	9
Expected Riser Performance	10
Global Riser Analyses	10
Metocean Environments	10
TLP	11
Riser Properties	11
Load Cases	12
Fatigue	12
Steel Riser	14
Riser Sizing (Burst & Collapse)	14
Load Cases	14
Fatigue Life	16
Composite Riser	17
Riser Sizing (Burst)	17
Collapse	17
Load Cases	18
Fatigue Life	21
Thermal Response of the Liner & Tubing	23
Impact Loads	24
Comparisons of the Steel and Composite Risers	25
Comparative Risk Results	27
Acknowledgements	30
References	30
Appendices	30

List of Tables and Figures

Tables

Table 1. Composite Tube Layup Matrix.....	8
Table 2. Wave & Current Conditions	10
Table 3. 100-Year Hurricane & 1-Year Winter Storm Current Profile	11
Table 4. 100-Year Loop Current Profile.....	11
Table 5. Comparison of Steel & Composite Riser Properties used for Global Analyses	12
Table 6. Riser Design Load Cases.....	12
Table 7. Maximum Mid-Wall von-Mises Stress Measurements along Steel Riser.....	14
Table 8. Fatigue Life for Steel Riser	16
Table 9. Nodal Forces & Moments	20
Table 10. Maximum Stresses in Upper 10 Feet of Riser for Load Cases.....	21
Table 11. Fatigue Life for Steel Liner	22
Table 12. Fatigue Life for Steel Components in the Composite Riser System	22
Table 13. Top Tension for the Steel & Composite Risers for the Three Load Cases ...	25
Table 14. Global Analysis of Load Cases for the TSJ and TJ for the Steel and Composite Risers: Maximum Stresses vs. Allowables	25
Table 15. Results for Predicted Failures for the Steel Riser	28
Table 16. Results for Predicted Failures for the Composite Riser	29

Figures

Figure 1. Steel Riser Configuration	4
Figure 2. Steel Riser Cross Section	5
Figure 3. Composite Riser Configuration	6
Figure 4. Composite Riser Cross Section	7
Figure 5. Fault Tree & Failure Modes.....	9
Figure 6. Bending Moments for Steel Riser for Load Cases PHN-1 (100-Year Hurricane) & PCN-1 (100-Year Loop Current)	15
Figure 7. Bending Moments for Composite Riser for Load Case PHN-1 (100-Year Hurricane) &	19
Load Case PCN-1 (100-Year Loop Current)	19
Figure 8. Relationship between Global Beam & Detailed FE Analyses.....	20
Figure 9. Finite Element Shell Analysis of the Top 10 feet of the Composite Riser.....	21

A Comparative Risk Analysis of Composite and Steel Production Risers

E.G. Ward, O.A. Ochoa, and Won Kim (OTRC at TAMU)
R.M. Gilbert and Anubhav Jain (OTRC at UT)
Charles Miller (Stress Engineering Services)
Early Denison (Consultant)

Introduction

As offshore activities move into deep water, there is a growing interest in the use of composite production risers to replace steel risers. There are a number of potential benefits using composite risers on floating production systems in deep water. The most significant advantage is in the reduction in weight and thus payload for floating production systems. Other potential advantages include excellent fatigue, thermal and damping properties and high corrosion resistance.

Composite risers have not been used in the Gulf of Mexico to date. The Minerals Management Service's Deepwater Operating Plan (DWOP) requires that new technology introduced in a deepwater development project must be shown to be as safe as existing technology. This project was undertaken to examine the relative risks of composite and steel production risers. A Comparative Risk Analysis was completed for a steel and a composite production riser system for a deepwater floating production system operating in the Gulf of Mexico. The risks for a composite production riser and a steel riser that both had the same functional requirements and service life were compared to demonstrate the relative safety of the composite and steel riser.

The steel riser analyzed in this study was an example riser configuration developed for this study. It was based on conventional and proven technology and design practices that have provided numerous deepwater risers that have been successfully used in many Gulf of Mexico projects, and had no special attributes specifically that were included for the purposes of this study.

A similar background of experience and well-established design practices are not available for composite production risers. Therefore a composite riser had to be "configured" for the purposes of this project. The configuration sought to include all the design consideration needed to meet the functional requirements and service life, but only in sufficient detail for the comparative risk study. The resulting composite riser configuration should not be taken as a final design. Rather we believe that it represents a realistic configuration that could be taken to a successful final design and application, and is detailed enough to evaluate the major risks for a composite production system. Details of the description and analyses of the CPR will be highlighted in this document.

The results of this study indicate that a composite production riser can be designed to be as safe as a steel production riser for deepwater applications in the Gulf of Mexico.

This report presents a summary of the results of this study. More detailed information and results are available in Appendices A, B, and C to this report.

Appendix A is the report Global Riser Analysis for the Composite and Steel Production Riser CRA by Charles Miller of Stress Engineering Services. The report provides a description of the steel and composite risers and summarizes their global analyses of both risers in design and fatigue seastates, their detailed design and fatigue studies of the steel riser.

Appendix B is the report Comparative Risk Analysis of Composite and Steel Production Risers: Composite Riser Response Assessment by Won Kim and Dr. Ozden Ochoa, his PhD advisor, of Texas A&M University, which focuses on the composite riser. It includes a more detailed description of that riser and summarizes the various analyses completed assess the performance and failure modes of the composite riser.

Appendix C is the MS thesis Risk Analysis of Steel Production Risers for Deepwater Offshore Facilities by Anubhav Jain (his MS advisor Dr. Robert Gilbert) of The University of Texas at Austin. That report includes the risk framework developed for this study and an example application to the steel riser.

General Description of Riser System & Functional Requirements

This section describes provides a description of the riser system and the functional requirements for the steel riser and the composite production riser (CPR) analyzed in this study. Each riser was a “conventional” single-casing (single-barrier) top-tensioned production riser operating on a multi-well Tension Leg Platform in located in 6000 feet of water in the Gulf of Mexico (GOM). The CPR riser joints were expected to meet the same requirements as the steel production riser joints, i.e. all functional and operational requirements such as operating loads, chemical resistance, internal and external damage tolerances, and geometric, operational and interface compatibility etc.

Production risers are an extension of the well casing from the subsea wellhead to the surface wellhead.

The production riser system:

- Connects the subsea wellhead to the surface wellhead and production tree
- Contains the production tubing and conduits for methanol injection, chemical injection, fluid displacement, control of SCSSV, and measurement of temperature and pressure
- Limits the bending moments (curvatures) of the tubing
- Supports the surface tree during production and the BOP for completions and workovers.

A through wall leak leading to loss of pressure and fluid containment of the riser is considered to be a riser failure for the purposes of this study.

For production and workover operations, the production riser:

- Is removable/replaceable from the surface to the mud-line
- Contains well-bore pressure if the tubing leaks during normal production operations
- Provides a conduit for monitoring and bleeding annulus pressures
- Provides at least two pressure barriers for well control during production (i.e., tubing string, and production riser string)
- Provides necessary integrity and pressure test capabilities throughout its life.

The combined well and riser system provide insulation to mitigate hydrate formation during production and shut-in conditions.

The riser diameter is designed to accommodate the production tubing, methanol injection, chemical injection, displacement and control lines, and should be full bore to the production casing string below the mudline.

Major components of the production risers include:

- Tieback connector
- Stress joint (SJ)
- Riser joints and pup joints for space-out
- Tensioner joint (TJ)

For the CPR analyzed in this study, only the riser joints and pup joints will be Composite. The tieback connector, SJ, and TJ were selected to be made from conventional steel. The primary goal of the CPR system evaluated in this study was to save weight through the use of composite pipe for the majority of the riser. The steel components were used at the top and bottom of the riser because of the complexity and service requirements of these components. The high strength to weight ratio and/or other properties of composites might be shown to be an attractive alternative for some of these components, but studying these alternatives was beyond the scope of this project.

The maximum bottom-hole pressure for this riser system will be assumed to be 8500 psi. The riser system will be tested after installation to a pressure of 10,000 psi.

Risers

Steel Riser

Configuration The steel riser configuration is shown in Figure 1. The riser system model includes the surface tree, a tensioner joint (TJ), 6005 feet of riser joints (each 62 feet long), a tapered stress joint (TSJ), and the wellhead and top portion of the surface casing. The riser is assumed to be vertical with no offset between the well and the TLP.

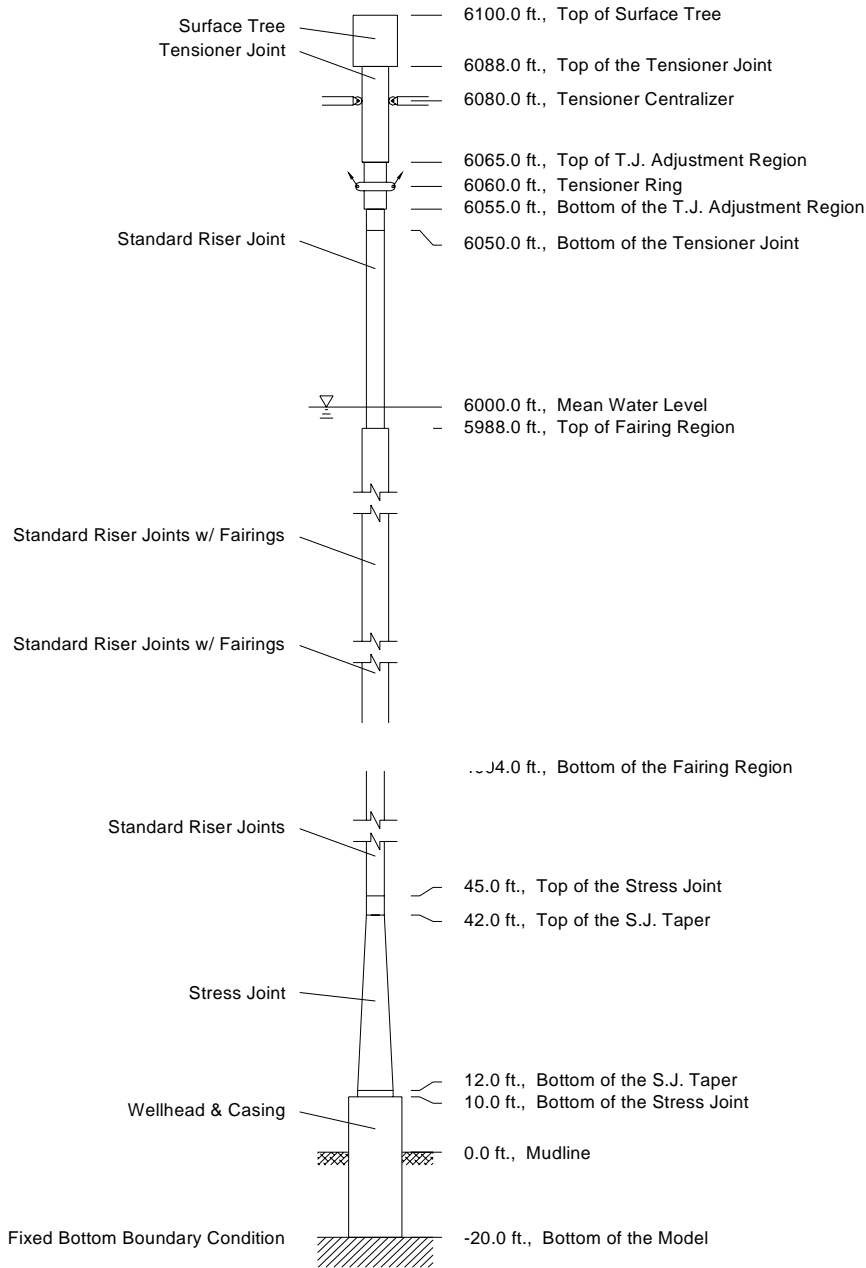


Figure 1. Steel Riser Configuration

Cross Section The cross section is shown in Figure 2 below. The outer riser casing has an 11.750 inch OD and a 1.014 inch thick wall, and is made from X80 pipe. The casing was sized for a burst pressure of 8,500 psi. The production tubing has a 5.500 inch OD, a 0.415 inch wall thickness, and is made of C95 pipe.

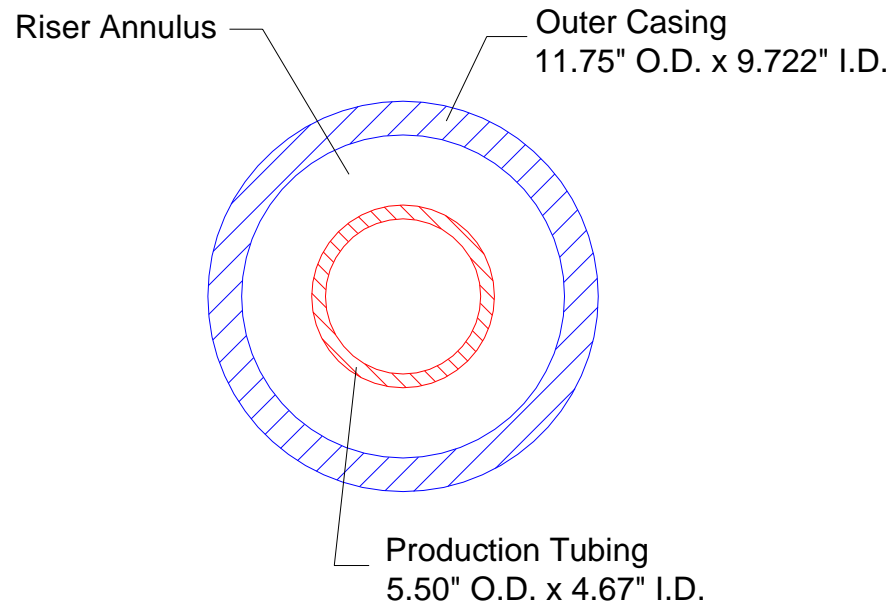


Figure 2. Steel Riser Cross Section

More details of the steel riser system are given in Appendix A.

Composite Riser

Configuration The composite riser configuration is shown in Figure 3 below. The riser system model includes the steel surface tree, a steel tensioner joint (TJ), 2 steel riser joints just above and below the mean water line, 5824 feet of composite riser joints (each 62 feet long), one steel riser joint, a tapered stress joint (TSJ), and the wellhead and top portion of the surface casing. The CPR riser is assumed to be vertical with no offset between the well and the TLP.

The primary goal of the CPR system evaluated in this study was to save weight through the use of composite pipe for the majority of the riser. The steel components were used at the top and bottom of the riser because of the complexity and service requirements of these components. The high strength to weight ratio and/or other properties of composites might be shown to be an attractive alternative for some of these components, but studying these alternatives was beyond the scope of this project.

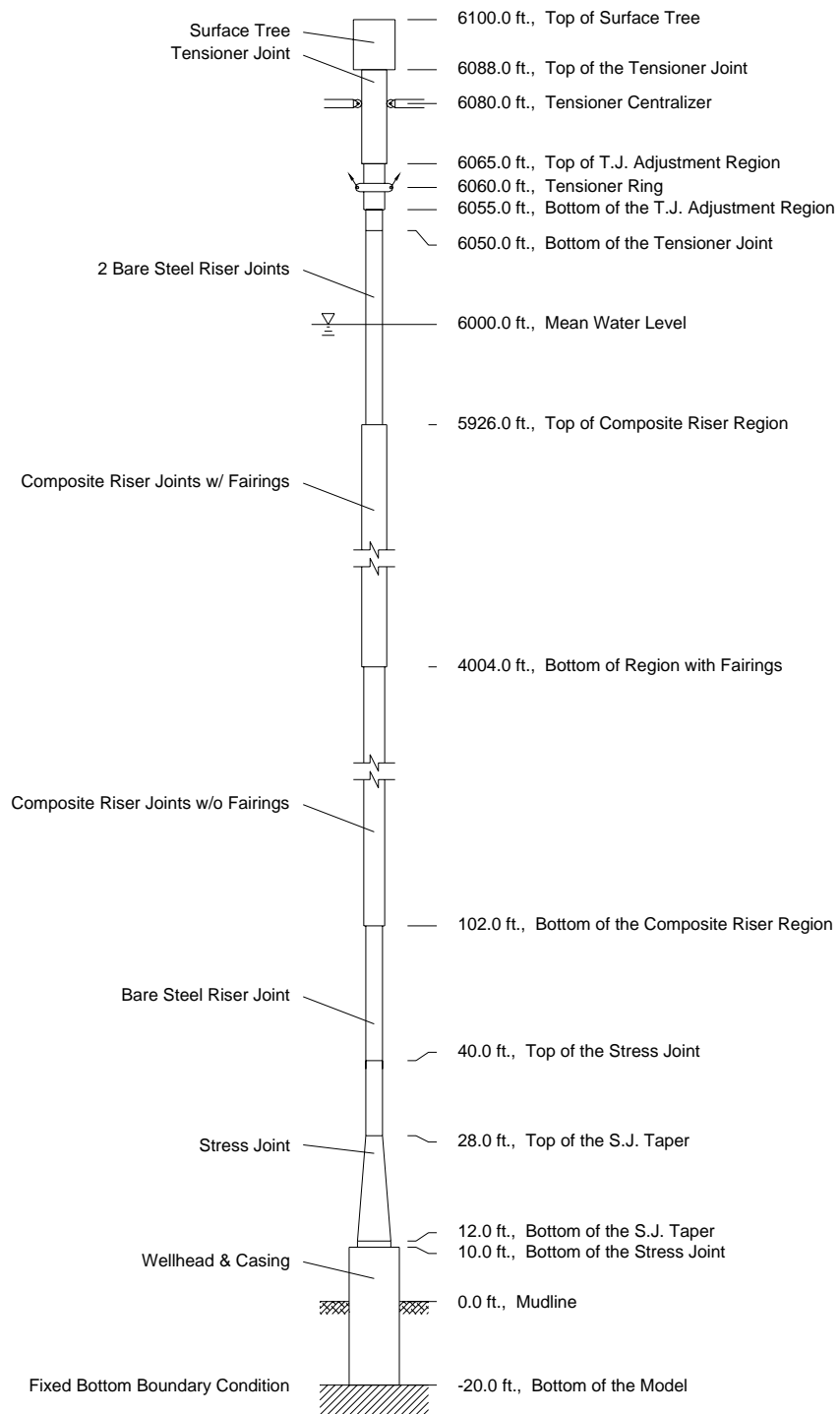


Figure 3. Composite Riser Configuration

Cross Section The cross section of the composite riser is shown in Figure 4 below. The composite riser consists of a 12.164 inch OD composite tube with a 0.974 inch thick wall and a 10.220 OD steel liner with a 0.250 thick wall. A 0.125 inch thick coating of E-Glass is applied to the exterior of the composite tube, and a flexible coating would be applied over the E-Glass layer as a protective coating. The production tubing is the same as used for the steel riser - a 5.500 inch OD, a 0.415 inch wall thickness, and made of C95 pipe.

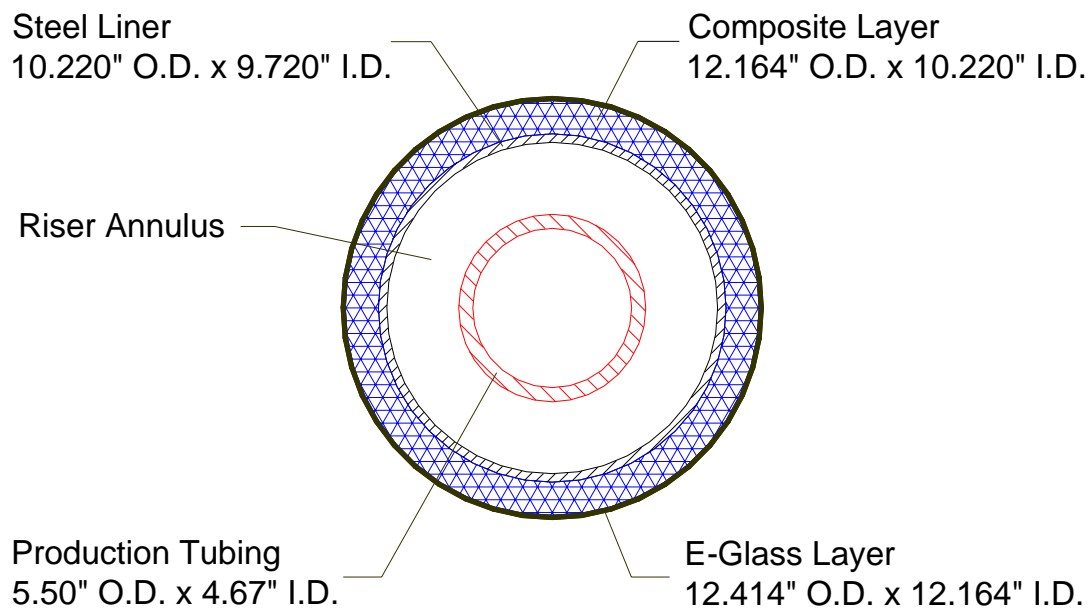


Figure 4. Composite Riser Cross Section

A steel mechanical-composite interface (MCI) is on each end of the riser joint. The functions of the MCI are to provide threaded connectors for joining composite riser joints, and to act as a load path to transfer all loads (axial, bending, and torsion) from the MCI to the composite tube and to contain pressure. In fabrication, the liner is welded to the MCI's to provide pressure containment in the riser.

The composite tube is permeable enough to allow liquids or gas to “weep” at high pressure differentials. The E-Glass layer provides a barrier to prevent seawater from entering the composite wall of the riser. If that fails, the internal steel liner can experience pressure build up on its exterior, but the liner wall thickness was sized to prevent collapse when supported by the surrounding composite tube. The steel liner also acts as a barrier to internal pressures or fluid build up in the annulus from tubing leaks. And lastly, the steel liner provides a wear surface to protect the composite tubing from gouges or wear when tools are run through the riser during drilling or workover operations.

The composite tube for the riser is made up of carbon fibers and an epoxy matrix. The layup is shown in the following Table 1.

Table 1. Composite Tube Layup Matrix

Layer	Orientation (deg)	Thickness (in)	Layer	Orientation (deg)	Thickness (in)
Liner		0.2500	10	0	0.0450
1	88	0.0810	11	88	0.0405
2	0	0.0450	12	0	0.0450
3	88	0.0810	13	88	0.0405
4	0	0.0450	14	0	0.0450
5	88	0.0810	15	88	0.0405
6	0	0.0450	16	0	0.0450
7	88	0.0810	17	88	0.0405
8	0	0.0450	18	0	0.0450
9	88	0.0405	19	88	0.0405

The 0 degree orientation is parallel to the longitudinal axis of the riser and fibers in this orientation provide the axial strength. The 88 degree orientation refers to the circumferential wraps that provide hoop strength.

Failure Modes

Analyses were performed to examine the resistance of each riser to the same failure modes. The failures modes studied and the conditions that could cause them are shown in the fault tree in Figure 5 below. Riser failure was defined as the development of a through wall crack (steel) or damage (composite that would lead to the loss of pressure and/or fluid containment).

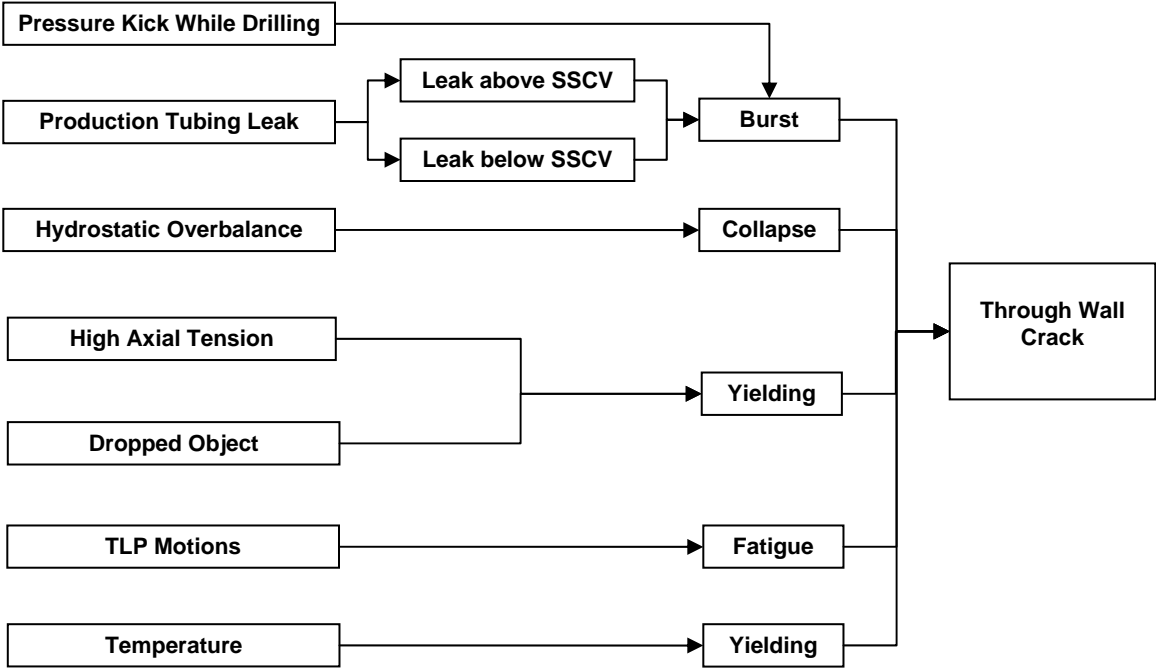


Figure 5. Fault Tree & Failure Modes

Fatigue damage due to VIV caused by waves and loop currents was not included in this study. It was assumed that riser VIV could be suppressed by fairings, and thereby mitigated such that it would not significantly impact riser fatigue.

Expected Riser Performance

Expected riser performance was assessed for each of the riser failure modes shown in Figure 5 above by several processes. For other areas, expected performance was estimated by analyses, including:

- Riser Sizing - In certain well-established areas, expected performance was simply based upon sizing the riser in accordance with established design practices and experience.
- Load Cases - Expected performance for some failure modes was estimated by analyzing selected Load Cases that considered both conditions within the riser and the external forces on the riser caused by the TLP motion in various metocean environments.
- Fatigue Analysis - Expected fatigue life was estimated by computing the motions of the TLP and the resulting fatigue damage to the risers by appropriate damage laws.
- Special Finite Element Analyses - required to predict the responses and failures of the composite riser.

The global riser analyses required for both the Load Cases and the Fatigue Analyses are described in the next section.

Global Riser Analyses

The global analyses to predict the motions of the TLP and the attached risers in various metocean environments were performed by Stress Engineering Services of both steel and composite production risers. Their global analysis program is a fully coupled program that models the TLP, its tendons, and attached risers and can provide both time and frequency domain solutions for the motions of the TLP and its tendons and risers, and loads and stresses in the tendons and risers.

The frequency domain analysis approach was used for this study. The TLP motion characteristics were described by Response Amplitude Operators (RAOs) that relate the TLP motions to various wave heights and periods or sea states. The riser is represented by a 3-dimensional rod finite element which models both the axial and bending responses of the riser due to the TLP motions.

Metocean Environments The metocean conditions used in this study are summarized below.

Table 2. Wave & Current Conditions

Condition	Height (ft.)	Period (sec.)	Surface Velocity "V" (ft/sec)
1 Year Winter Storm	16.0	9.0	1.2
100 Year Hurricane	41.0	14.0	4.0
100 Year Loop Current	9.0	8.0	7.0

Table 3. 100-Year Hurricane & 1-Year Winter Storm Current Profile

Depth (ft.)	Velocity (ft/sec)
0	V
300	V
400	0.2
6000	0.2

Table 4. 100-Year Loop Current Profile

Depth (ft.)	Velocity (ft/sec)
0	7.00
82	7.00
164	6.94
656	2.86
1230	1.62
2214	0.87
2870	0.50
3280	0.31
6000	0.00

These values used here were representative of values commonly used in studies of deepwater floating production systems and design at the time this study was initiated (in 2004 before hurricane Ivan). The severe hurricanes that occurred in 2004 and 2005 led to studies to reassess wind, wave, and current conditions in severe hurricanes, and are expected to result in higher values for 100-year conditions in certain Gulf of Mexico locations. These increased conditions are not expected to change the relative performance of the steel and composite risers nor the assessed relative risk of failure.

The long-term Gulf of Mexico wave height and period conditions used to study the fatigue of the risers was taken from a wave scatter diagram or chart also developed by DeepStar for such studies. That chart describes the long term wave environment as a number of individual sea states, i.e., wave height and period combinations, and the percentage of time that each sea state would be expected to occur over the long term.

More details on the metocean environments and global analysis techniques are provided in Appendix A.

TLP The TLP used in this study was a representative and realistic design developed by DeepStar for general research studies on TLP¹. The configuration and response functions are shown in Appendix A.

Riser Properties The following riser properties were used for the global analyses of the steel and composite risers. The composite riser properties are equivalent properties based on the combined properties of the composite tube and the steel liner. Note that the composite riser is both lighter (~ 3 x) and more flexible (~ 2 X) than the steel riser.

Table 5. Comparison of Steel & Composite Riser Properties used for Global Analyses

Riser	Air Weight (lbs/joint)	Submerged Weight (lbs/joint)	Bending Stiffness (EI) (lbs-ft ² x 10 ⁻⁷)	Axial Stiffness (EA) (lbs x 10 ⁻⁸)
Steel	8214	6838	10.01	9.92
Composite	4220	2404	5.73	5.44

Load Cases

Some of these failure modes were studied by determining the extreme responses due to Load Cases that considered both conditions within the riser and the external forces on the riser with the TLP in various positions. These Design Load Cases were chosen to be consistent with API RP2RD (ref). The most important load combinations used for the design of the steel and composite risers are shown in the table below. These load cases tend to govern the design of deepwater risers in the Gulf of Mexico, and were used for this study.

The API load categories and associated allowable stress factors are detailed, but all of these are not directly applicable for the CPR. However, the stress format should be applied for the metal part of the Metal Composite Interface (MCI), spool piece and the steel connector (steel connectors in a CPR joint are expected to be less loaded compared to connectors in a steel riser joint). The CPR design did not take advantage of the load bearing contribution from the steel liner, and the requirement for the in-place riser is that the liner shall not yield when subjected to extreme loads.

Table 6. Riser Design Load Cases

Case	Riser Condition	Contents (ppg)		Int. Press. (psi) at surface		Design Environment	Damage Condition	Cf	Tension Factor
		Annulus	Tubing	Annulus	Tubing				
PNS-1	Normal shut-in	0.04	5.50	0	8,500	1 Yr. Winter Storm	Intact	1.00	1.30
PHN-1	Shut-in w/ Hurricane	0.04	5.50	100	8,500	100 Yr. Hurricane	Intact	1.20	1.30
PCN-1	Maximum Producing	0.04	5.50	100	8,500	100 Yr. Loop Current	Intact	1.20	1.60

The rationale for each load case was:

- PNS-1: Normal shut-in pressure in a normal operating environment
- PHN-1: Normal shut-in in a 100-year hurricane condition
- PNC-1: Maximum production in a 100-year loop current – maximum offset

The mean and extreme responses for the TLP and attached risers were estimated by the Global Riser Analysis Techniques described above.

Fatigue The steel and composite riser joints were analyzed for wave-generated fatigue damage to ensure the fatigue life was at least 10 times the riser service life. The riser service life was taken to be 20 years, so that the required fatigue life was 200 years.

Standard practices were used to estimate the long term motions of the TLP and attached risers. The TLP motion characteristics were described by Response Amplitude Operators (RAOs) for use in the frequency

domain analysis. The wave scatter diagram was simplified, and applied to predict the TLP motions and wave loads for various sea states, i.e., wave height and wave period combinations.

The predicted riser response for each sea state in the scatter diagrams was used to compute the stresses at points along the riser due to that sea state. The percentage of time that each sea state was expected to occur during the 20-year riser design lifetime was used with the computed the number of stress cycles to estimate the fatigue damage caused by that sea state using an appropriate damage law. Summing up all the damages at all points along the riser from all sea states provided an estimate of the total damage and the expected fatigue life for each point along the riser.

Fatigue damage due to VIV caused by waves and loop currents was not included in this study. It was presumed that riser VIV could be suppressed by fairings, and thereby mitigated such that it would not significantly impact riser fatigue.

Steel Riser

Riser Sizing (Burst & Collapse)

The steel riser was sized to meet the stated functional requirements and to meet the Burst and Collapse criteria per API RP-1111 and API 5C3.

Load Cases

Results for the bending stresses [including the tensioner joint (TJ) and the tapered stress joint (TSJ)] are presented in Figure 6 for the 100-year hurricane and loop current cases. The first panel plots the mean, minimum, and maximum bending moments along the riser length, and the second and third panels plot the bending moments in the lower 200 feet and upper 300 feet of the riser. Note that the bending moments throughout the riser section are small and only increases near and in the TJ at the top at the TSJ and the bottom.

Table 7 below presents the maximum mid-wall von-Mises stresses at points along the riser.

Table 7. Maximum Mid-Wall von-Mises Stress Measurements along Steel Riser

Location along Steel Riser	Elevation (ft.)	Max von-Mises Stresses		
		1 Year Winter Storm PNS-1 (ksi)	100-Year Hurricane PHN-1 (ksi)	100-Year Loop Current PCH-1 (ksi)
Base of the Stress Joint	10.0	19.52	48.94	60.79
Base of the Stress Joint Taper	12.0	18.63	45.83	56.49
Top of the Stress Joint Taper	42.0	31.96	58.04	59.83
Stress Joint Top Connector	45.0	29.52	52.19	52.27
Mean Water Level	6000.0	23.27	29.33	31.77
Tensioner Joint's Bottom Connector	6050.0	22.87	29.53	31.63
Bottom of the Tensioner Joint Threads	6055.0	23.06	30.86	32.41
Tensioner Joint at the Tensioner Ring	6060.0	7.78	10.76	11.08
Tensioner Joint at the Tensioner Guide	6080.0	0.32	0.93	0.34
Top of the Tensioner Joint	6088.0	0.69	0.31	0.78

The maximum stresses occur at the top of the stress joint taper, and are below the allowable stresses for PNS-1 (67% yield = 53.3 ksi) and PHN-1 and PCN-1 (80% of yield = 64.0 ksi). The stresses in the riser sections (45 ft < elevation < 6000 ft) are even lower and range from about 30 to 50 ksi.

Steel Riser

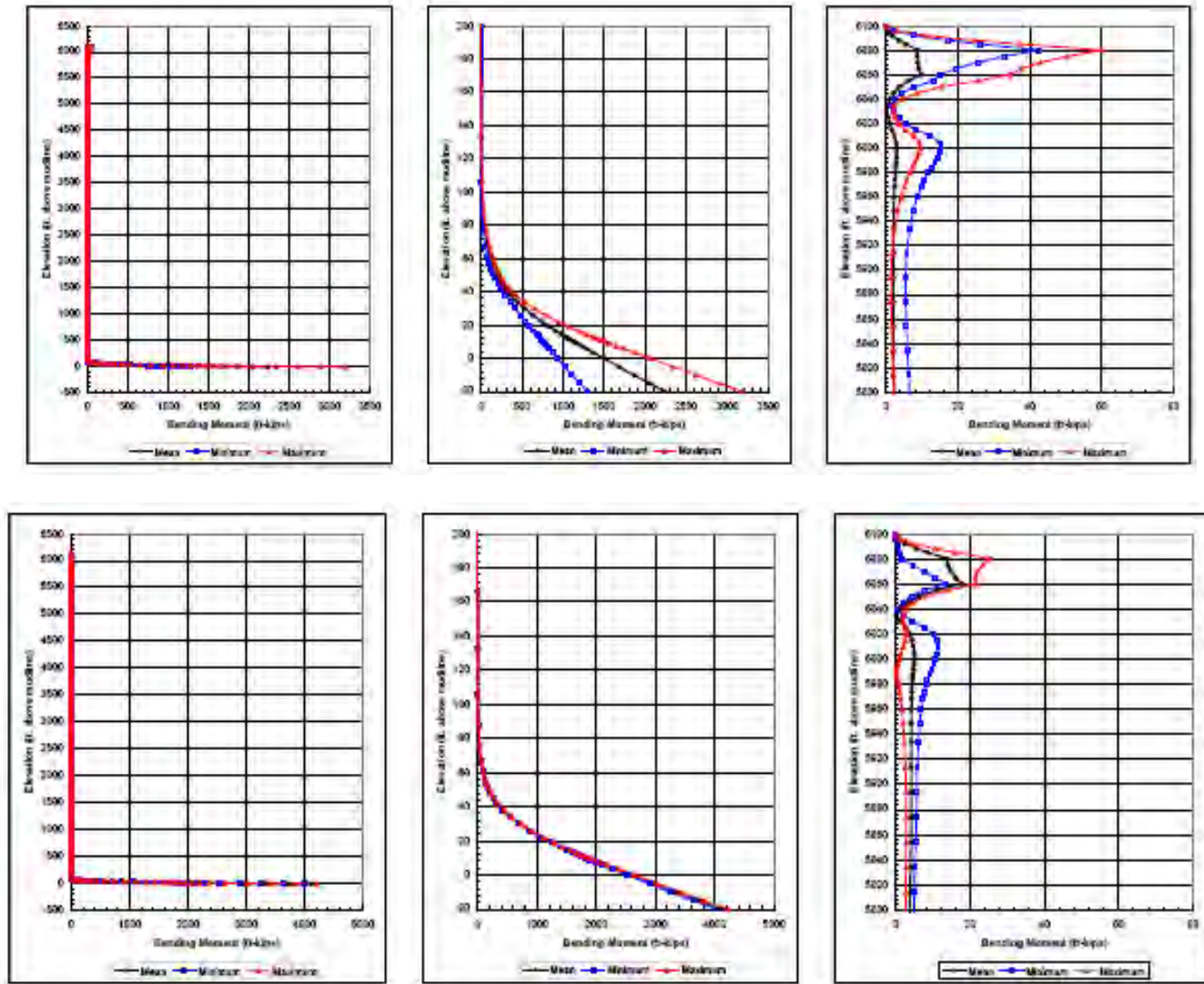


Figure 6. Bending Moments for Steel Riser for Load Cases PHN-1 (100-Year Hurricane) & PCN-1 (100-Year Loop Current)

Fatigue Life

A conventional S-N approach was used to estimate the fatigue damage and life. The number of cycles for each stress range S was determined from the global analysis results for each sea state. The fatigue life was estimated using S-N curves that included the DnV-B curve for machined parent metal, and the DnV-C and DnV-F2 for welded sections. Results are shown in Table 8. Note that the estimated fatigue life for the welds in the lower portion of the steel riser have fatigue lives of < 200 years using the F2 quality underground welds, and will require C quality ground welds to achieve satisfactory fatigue lives.

Table 8. Fatigue Life for Steel Riser

Steel Riser Component	Location	Elevation (ft.)	Estimated Life (years)		
			Machined Parent Mat'l DnV-B	Welded Sections DnV-F2	Welded Sections DnV-C
Stress Joint	Base of Stress Joint	10.0	395	35	584
	Base of Stress Joint Taper	12.0	3593	41	717
	Top of Stress Joint Taper	42.0	1990	26	416
	Top of Stress Joint	45.0	489	39	683
Weld-on Connectors for Stnd. Riser Joints	Region 1 (48 ft. to 202 ft.)	48.0	866	61	1127
	Region 2 (240 ft. to 5934 ft.)	281.0	426133	4068	196474
	Region 3 (5949 ft. to 6045 ft.)	5992.0	1508610	13368	705394
Tensioner Joint	Bottom of Tensioner Joint	6050.0	14601802	331240	12095507
	Bottom of T.J. Adjust. Region	6055.0	5728327	-	-
	Tensioner Ring Top of T.J.	6060.0	155181620	-	-
	Adjust. Region	6065.0	98471151	-	-
	Tensioner Centralizer	6080.0	25401570	-	-
	Top of Tensioner Joint	6088.0	84790540	292276	24024095

Composite Riser

Riser Sizing (Burst)

The composite riser was sized to meet the functional requirements and meet the Burst criteria. The sizing was determined based on the 10,000 psi pressure test that follows riser installation. A finite element analysis (FEA) approach was used to model the layered structure of the steel liner and the carbon/epoxy layers or lamina that made up the composite tube. The composite tube and liner were sized to prevent (1) the maximum hoop stresses in the steel liner from exceeding its 80 ksi yield stress, and (2) to prevent the lamina from exceeding their long term strength criteria. Rather than simply increasing the liner thickness, the liner thickness and composite tube thickness were both increased to the values shown in Figure 7 in a tradeoff study of riser weight and cost to optimize the design. Increasing the liner thickness also benefited welding inspection issues.

Collapse

The sized riser was then analyzed to ensure that it could meet the collapse requirements. A FEA model was used to study the hydrostatic buckling or collapse of the composite riser. The riser was first assumed to have a perfect bond between the steel liner and the composite tube. Analyses showed that a riser section six feet long was sufficient to determine the critical pressure. The predicted critical pressure was taken to be 30,200 psi, but varied between 25,000 and 35,000 psi depending upon details of the assumptions and the analyses. An analytical solution used to benchmark the FE analyses predicted a critical pressure of ~35,000 psi. Since the maximum hydrostatic pressure near the seafloor in 6000 feet of water is less than 2,660 psi, the composite riser with a perfectly bonded liner and composite tubular will not buckle.

The effect of an unbonded area between the steel liner and composite tube on hydrostatic collapse was also analyzed. The hydrostatic pressure was assumed to be directly applied to the liner under the unbonded area, and various geometries of unbonded area were studied. Patch-shaped debonded areas with dimensions ranging from 1 x 1 to 4 x 4 inches resulted in critical pressures of 30,200 psi, no change from the perfectly bonded case. An 8 x 8 inch debond resulted in a slight decrease in critical pressure to 29,500 psi. Debonded areas that extended circumferentially all the way around the liner were also considered.

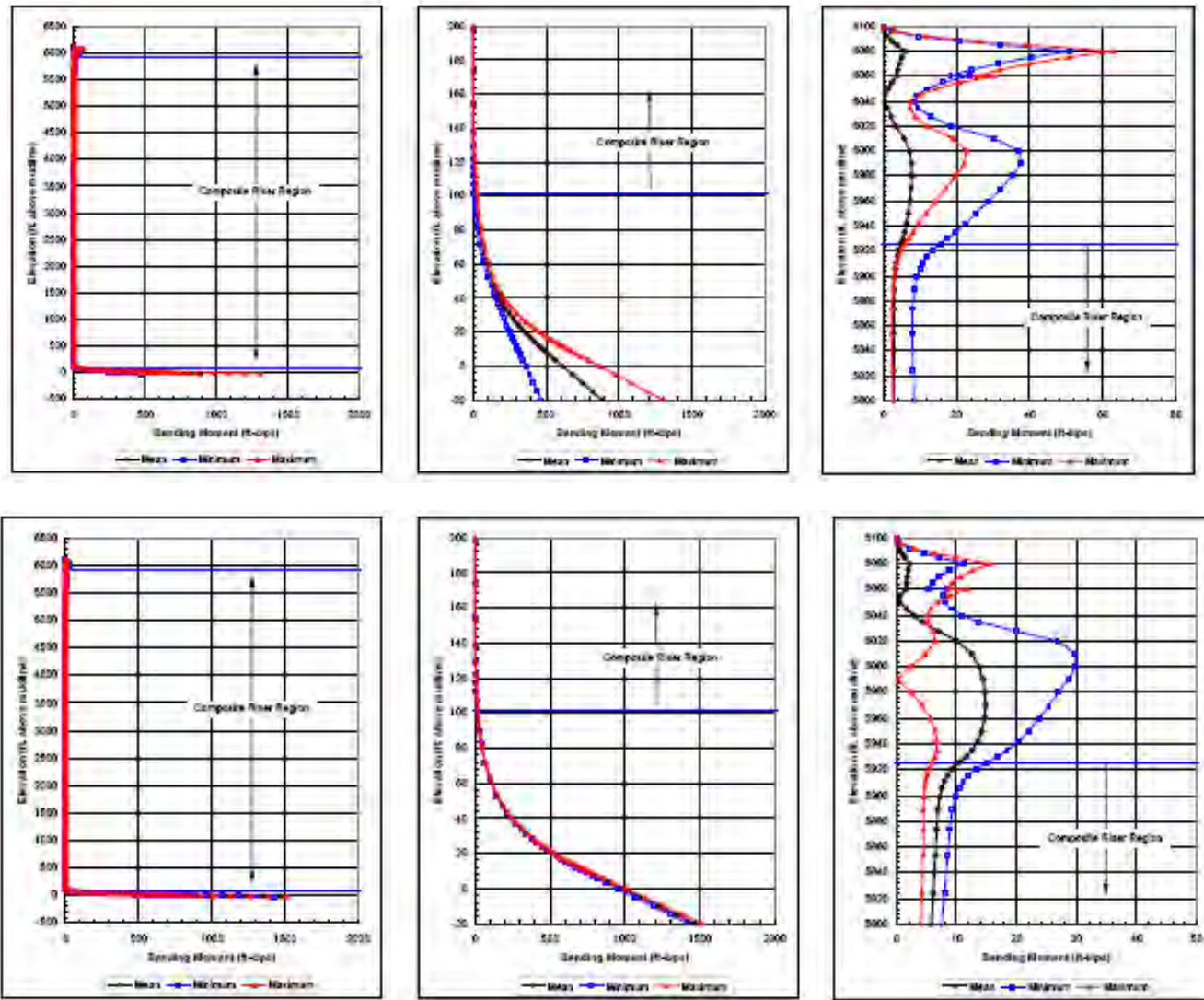
As the length of the circumferentially debonded area increased, the critical pressure decreased and asymptotically approached ~11,500 psi, the critical pressure of the completely debond liner, when 50% and more of the area was debonded. Lastly, debonded areas that extended along the riser longitudinally and were debonded over an arc of the circumference were also analyzed. The critical pressures decreased with increasing size of the arc, and approached the critical pressure of ~ 11,500 psi as the percent of unbonded area became 100%.

With even the extreme assumptions of unbonded areas studied, the critical pressures for hydrostatic buckling remained well above the maximum hydrostatic pressure of 2,660 psi in 6,000 feet. However, severe separation of the steel liner from the composite tube can limit the serviceability of the riser even though the riser as a whole does not lose its structural integrity. Under the condition of no bonding between the steel liner and composite tube along with an ovality of one percent, the steel liner collapses plastically at 3,700 psi. Note that the state of the structure and loading assumed in the analysis is extremely severe; it is highly unlikely that there is no bonding whatsoever between the steel liner and composite tube. Also, the pressure built up at the OD of the liner is assumed conservatively to be equal to the external pressure. In spite of the conservative assumptions, the riser is safe from buckling and collapse.

Load Cases

A global analyses that used a riser with equivalent properties to represent the composite riser (composite tube and steel liner) (see Table 5 above) provided global riser responses such as bending moments illustrated in Figure 7 below. Results for the bending moments [including the tensioner joint (TJ) and the tapered stress joint (TSJ)] are presented in Figure 7 for the 100-year hurricane and loop current cases. The first panel plots the mean, minimum, and maximum along the riser length, and the second and third panels plot the bending moments in the lower 200 feet and upper 300 feet of the riser. Note that the bending moments throughout the riser section are small and only increases near and in the TJ at the top and the TSJ and the bottom.

Composite Riser



C

Figure 7. Bending Moments for Composite Riser for Load Case PHN-1 (100-Year Hurricane) & Load Case PCN-1 (100-Year Loop Current)

These global results for the basis for the detailed local analysis of the composite riser that was needed to investigate potential failures due to the three Load Cases. Nodal displacements and forces from the global results were transferred to an FEA model of the composite riser. This schematically displayed in Figure 8 below.

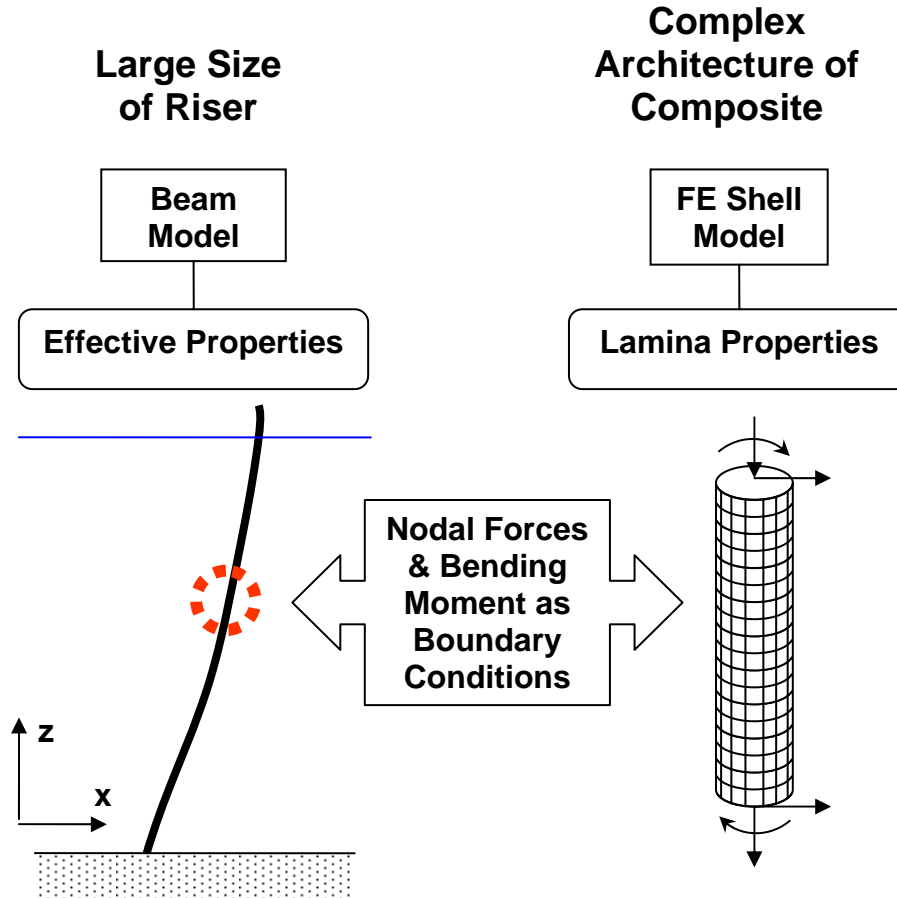


Figure 8. Relationship between Global Beam & Detailed FE Analyses

A detailed analysis following this scheme of the top 10 feet of the composite riser, which experienced the highest total stress, is illustrated below. The maximum nodal output from the global analysis for 100-year loop current Load Case PCN-1 is shown in the Table 9 below.

Table 9. Nodal Forces & Moments

Elevation (ft)	X-Force (lb)	Z-Force (lb)	Y-Moment (ft-lb)	X Position (ft)	Z-Position (ft)	Slope
5926	9995	346495	-15144	545.0	-100.7	0.0284
5916	10314	346154	-11988	544.7	-110.7	0.0298

The nodal forces and locations are used as the boundary conditions in the FE shell analysis shown in Figure 9 below. The various colors illustrate the stress results from the FE shell analysis.

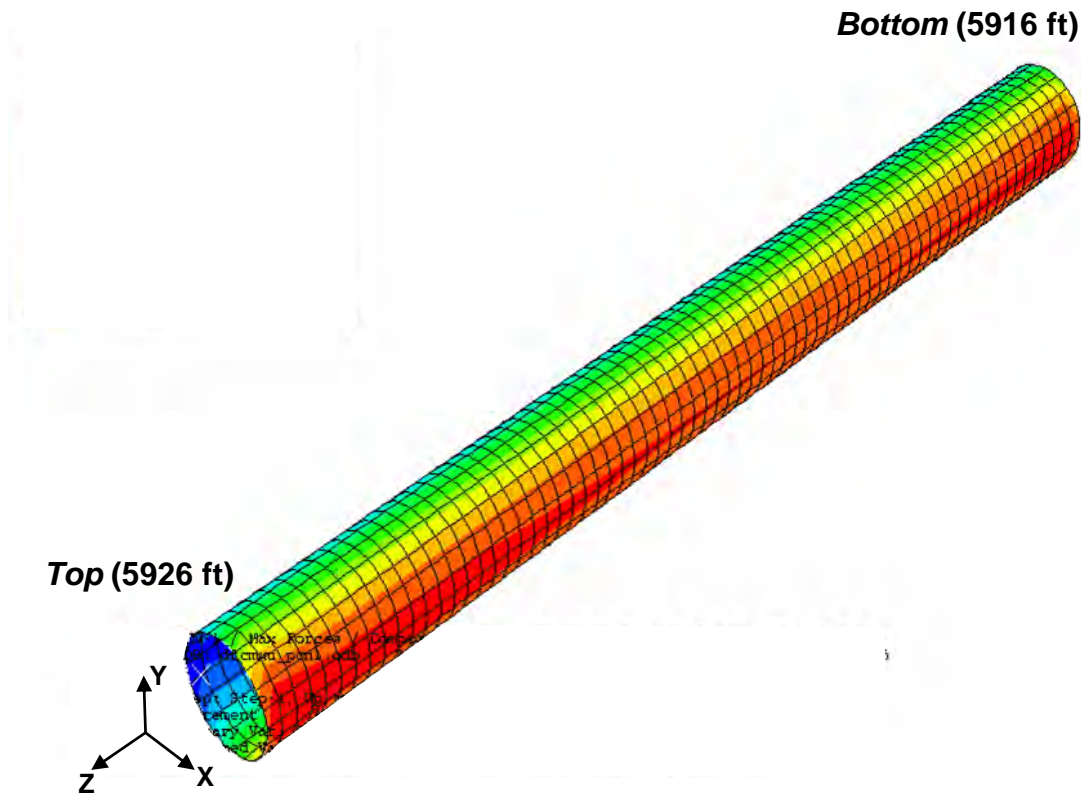


Figure 9. Finite Element Shell Analysis of the Top 10 feet of the Composite Riser

The resulting maximum stresses in select layers of the composite riser are shown in Table 10 below.

Table 10. Maximum Stresses in Upper 10 Feet of Riser for Load Cases

Load Case	Liner Axial Stress (ksi)	Layer 18 Axial Stress (ksi)	Layer 19 Hoop Stress (ksi)
1-Year Winter Storm	17.4	11.3	0.5
100-Year Hurricane	31.3	21.5	1.0
100-Year Loop Current	23.0	15.1	0.7

The stresses here are substantially below failure.

Fatigue Life

The results from the global analysis provided RMS values and the zero crossing periods T_z 's for the axial tensions and bending moments at specific locations along the riser for each sea state in the wave scatter diagram. The tensions and bending moments were converted to RMS stresses, which were used with the associated T_z 's to describe the number of stress cycles expected during the 20-year design life. Appropriate S-N laws were used with Miner's rule to sum the damage

and estimate the fatigue life. This procedure was used to estimate the fatigue lives of the axial fiber layers and the liner for locations 10 feet from the top and bottom ends of the riser section just above the TSJ and below the TJ.

The S-N law used for the axial carbon fibers was based on recently reported experimental data. Carbon fibers are known for their excellent fatigue properties, as evidenced by the flat slope of the S-N curve, which is much flatter than is typical for steel.

The S-N relationship used for the steel liner was the DnV-C curve for machined surfaces.

The resulting fatigue lives are shown in Table 11 below.

Table 11. Fatigue Life for Steel Liner

Elevation (ft)	Location	Fatigue Life (years)	
		Composite Axial Layers	Steel Liner
102	10 ft above TSJ	$1.61(10)^{30}$	$1.42 (10)^6$
5926	10 ft below TJ	$2.72 (10)^{30}$	$1.50 (10)^6$

These fatigue lives reflect the excellent fatigue resistance of the composite material and the low stress levels in the riser.

Fatigue properties of carbon-epoxy composites may vary depending on the choice of constituent materials and manufacturing process. Fatigue lives were also estimated using more conservative hypothetical S-N curves with a range of steeper slopes. Fatigue lives ranged from 7 million years to 2 to 3 thousand years, which may be considered as the lower limit.²

The fatigue lives of the Tapered Stress Joint and the Tensioner Joint were estimated for the composite riser system using the same analysis methods as describe previously for the steel riser system. Results are shown in Table 12 below.

Table 12. Fatigue Life for Steel Components in the Composite Riser System

Composite Riser Component	Location	Elevation (ft.)	Estimated Fatigue Life (years)		
			Machined Surfaces DnV-B	Welded Sections DnV-C	Welded Sections DnV-F2
Stress Joint	Base of TSJ	10.0	622	802	43
	Base of TSJ Taper	12.0	772	968	50
	Top of TSJ	28.0	666	850	45
	Top of TSJ	40.0	3223	3443	453
Tensioner Joint	Bottom of TJ	6050.0	9742305	3678457	50623
	Bottom of T.J. Adjust.	6055.0	4564317	1929221	29862
	Region Tensioner Ring	6060.0	126571946	38205406	416925
	Top of T.J. Adjust. Region	6065.0	58108771	16025924	185380
	Tensioner Centralizer	6080.0	1820869	852567	16789
	Top of TJ	6088.0	63105984	18890663	237596

The fatigue life was estimated using S-N curves that included the DnV-B curve for machined parent metal, and the DnV-C and DnV-F2 for welded sections. Note that the estimated fatigue life for welds in the TSJ have fatigue lives of < 200 years using the F2 quality unground welds, and will require C quality ground welds to achieve satisfactory fatigue lives.

Thermal Response of the Liner & Tubing

The thermal response on the composite riser system during the start of production in a well is examined though considering the impacts of a well start up on the steel liner and tubing performance.

The thermal conductivity for transverse heat flow in carbon fiber structures is roughly an order of magnitude less that of the steel liner. Brine is sometimes used in the riser annulus to conduct heat from the tubing string to the riser wall. So we will assume that the composite tube is a perfect insulator and that the inner temperature of the liner will be the same as that of the produced fluids. When production in a well is initiated, there could be a rapid heating up of the tubing string, annulus fluid, and the steel riser liner. We will assume a fairly conservative case in which the tubing string is initially at 40 degrees F due to the cold ambient seafloor temperatures, and the produced fluid is at 180 degrees F. During startup, the tubing string, annular fluid, and the steel liner would experience a rapid heating while the composite tubular remained at near ambient temperatures, and the steel liner would try to expand both axially and circumferentially.

The strain in the tubing is estimated as

$$\text{Strain (both directions)} = \text{coefficient of thermal expansion} \times \Delta T$$

With a coefficient of thermal expansion of 6.5×10^{-6} in/ (in-deg F for steel and a delta T of 140 degrees F, the strain would be 9×10^{-4} in/in. Assuming that the liner is rigidly constrained, this strain would correspond to a compressive stress of 26.4 ksi, which is well below its yield strength. Thus the liner would not yield and buckle under this conservative description of a well startup scenario.

The behavior of the tubing in the composite riser is also examined under the assumption that the riser will not experience any thermal growth during startup. The tubing will likely be axially constrained at the surface and below the mudline (via a hanger). An average starting temperature of the tubing string can be approximated as the average of the temperature throughout the water column, or roughly 60 degrees F in the Gulf of Mexico. Assuming the final temperature of the tubing is 180 degrees F when the well is producing at a maximum rate, then the average change in temperature will be 120 degrees F. The axial stress reduction in the tubing string due to this temperature change would be 22.6 ksi, assuming the riser length does not grow. For the assumed 5-1/2", 23 lb/ft tubing, the tension in the tubing would be reduced by 50 kips. Depending on how much residual bottom tension is left in the tubing string when it is run and hung off, the tubing could be in compression at the mudline. It could also buckle helically but should not yield, due to the modest compressive stress. This tubing performance prediction is no different than would be experienced with an insulated steel riser.

These conservative examples illustrate that no special thermal issues should be expected for the composite riser.

Impact Loads

Impact due to a dropped object or mishandling were not evaluated as part of this study. However, an experiment has been conducted in a composite riser test sample was subjected to a 10 KJ Joule impact. No gross failures were observable. Detailed test results were not available to this study. (M. Salama, personal communication).

Comparisons of the Steel and Composite Risers

Some useful comparisons of the steel and composite risers are summarized here.

The top tensions applied to the steel and composite risers for the three load cases are shown in Table 13.

Table 13. Top Tension for the Steel & Composite Risers for the Three Load Cases

Riser	Load Case	Nominal Applied Tension (kips)
Steel	PNS-1: Normal Shut-in with a 1-Year Winter Storm	864
	PHN-1: Shut-in with a 100-Year Hurricane	864
	PCN-1: Maximum Producing with a 100-Year Loop Current	1054
Composite	PNS-1: Normal Shut-in with a 1-Year Winter Storm	319
	PHN-1: Shut-in with a 100-Year Hurricane	319
	PCN-1: Maximum Producing with a 100-Year Loop Current	319

Note that significantly less tension is required for the composite riser due to its lighter weight. The maximum bending moments at the TP were about the same, but were significantly smaller at the TSJ for the composite riser.

Results for the maximum stresses and percentage of the allowable stresses for critical locations in the TSJ and the TJ for steel and composite riser are compared in Table 14 for the three Load Cases.

Table 14. Global Analysis of Load Cases for the TSJ and TJ for the Steel and Composite Risers: Maximum Stresses vs. Allowables

Riser	Load Case	Allowable Stress (ksi)	Tapered Joint Stress		Tensioner Joint	
			Max Stress (ksi)	% of Allowable	Max Stress (ksi)	% of Allowable
Steel	PNS-1: Normal Shut-in in a 1-Year Winter Storm	53.3	32.0	60%	23.3	44%
	PHN-1: Shut-in in a 100-Year Hurricane	64.0	58.0	91%	30.9	48%
	PCN-1: Max Production in a 100-Year Loop Current	64.0	60.8	95%	32.4	51%
Composite	PNS-1: Normal Shut-in in a 1-Year Winter Storm	53.3	25.3	47%	6.5	12%
	PHN-1: Shut-in in a 100-Year Hurricane	64.0	50.7	79%	10.4	16%
	PCN-1: Max Production in a 100-Year Loop Current	64.0	58.0	91%	8.4	13%

All maximum stress levels are smaller than the allowables and satisfy existing codes. Note that the percentages of the allowables are smaller for the composite riser than the steel riser.

Other key comparisons include:

- A stress joint needed for the composite riser was considerably smaller and lighter than that required for the steel riser. Critical wall thicknesses in the TSJ for the composite were about one half that needed for the steel riser, and the taper length was 16 feet for the composite and 30 feet for the steel riser. The smaller TSJ and smaller tension requirements results in lower loads on the wellheads for the composite riser.
- The smaller tension requirements for the composite riser also allow a significantly smaller TJ to be used for the composite riser.

Comparative Risk Results

The results of this study are compiled and summarized in Tables 15 and 16 in terms of the hazards and failure modes introduced in Figure 5, and provide a basis for comparing the risks of the steel and composite risers.

Table 15 provides the values of the (1) allowable or design target, (2) predicted performance, and (3) minimum failure for each failure mode for the steel riser. Similarly, Table 16 provides values for the composite riser.

Comparisons of the results for each failure mode indicate that composite production riser can be designed to be at least as safe as a steel production riser for deepwater applications in the Gulf of Mexico.

Table 15. Results for Predicted Failures for the Steel Riser

Steel Riser						
Hazard	Failure Mode	Limiting Design Criteria	Predicted Performance	Expected Minimum Failure Value	Risk	Remarks
Kick control while drilling	Burst	8500 psi	8500 psi (60% of calculated minimum burst)	14,170 psi (minimum burst)	Loss of pressure containment	API RP-1111 Calculation, 12.5% mill tolerance, 0.050" corrosion and wear allowance.
Tubing leak						
Riser evacuation (hydrostatic overbalance)	Collapse	6,000 ft WD (2,660 psi)	2,660 psi (6,000 ft WD)	12,680 psi		API 5C3 Calculation, elastic collapse, using nominal wall.
Excessive riser tension (axial stress)	Axial yielding of liner	64 ksi (80% yield)	Max above SJ is 52 ksi, max below TJ is 30 ksi (see Note 1)	80 ksi (yield)	Loss of pressure containment, parted riser	100-year Hurricane, API RP 2RD
			Max above SJ is 60 ksi, max below TJ is 32 ksi (see Note 1)			100-year Loop current, API RP 2RD
Wave-induced fatigue	Crack through liner wall, parting of liner	Minimum life = 200 years	Minimum fatigue life along riser > 800 years	Cumulative Damage > 1.0		Damage calculations for 20 year life with factor of 10 for non-inspectable components. VIV fatigue mitigated by suppression equipment.
Dropped objects	Denting, leakage in connector				Loss of pressure containment	This is typically not evaluated for steel riser systems. Tests have shown the joints and connectors to be robust. No information exists on riser joints that have been damaged in service by external collisions or dropped objects.
Riser-to-riser collisions						

Note 1: Study focused on riser joints. Forged TSJ above the seabed and TJ just above the sea surface were not carefully designed and analyzed for this study. Stresses in the long middle portion of the riser are lower than at the two extremes.

Note 2: Forged steel tapered stress joints (TSJ) and tensioner joints (TJ) can achieve the required fatigue performance. Welds in the riser joints near the bottom (first 200 ft above the TSJ) must be ground to achieve DNV C-curve performance. Unground welds meet the DNV F2 curve and provide the needed fatigue life above this elevation.

Table 16. Results for Predicted Failures for the Composite Riser

Composite Riser						
Hazard	Failure Mode	Limiting Design Criteria	Predicted Performance	Expected Minimum Failure Value	Risk	Remarks
Kick control while drilling	Burst	8500 psi	11,000 liner yield, body is significantly stronger	18,000 psi matrix yield, 30,000 psi fiber limit	Loss of pressure containment, parted riser	
Tubing leak						
Riser evacuation (hydrostatic overbalance)	Collapse	6,000 ft WD (2,660 psi)	11,500 psi (leak in outer liner, complete debonding of steel liner)	Riser collapse at 11,500 psi w/ fully debonded liner Liner collapse at 3,700 psi w/ fully debonded liner		With no breach of outer structure, riser is stronger than the 29,400 psi figure. Liner collapse limits serviceability, but riser will not lose structural integrity.
Excessive riser tension (axial stress)	Axial yielding of liner	64 ksi (80% yield)	Max at Top of Composite Riser (74 ft WD) is 31 ksi (Note 3)	80 ksi (yield)		100-year Hurricane, API RP 2RD, riser will remain intact even with yielded liner.
			Max at Top of Composite Riser (74 ft WD) is 23 ksi (Note 3)			100-year Loop current, API RP 2RD, riser will remain intact even with yielded liner.
Wave-induced fatigue	Crack through liner wall, parting of liner	Minimum life = 200 years	Minimum life of steel liner >100,000 years	Cumulative Damage > 1.0		Liner: damage calculations for 20 year life of liner welds with factor of 10 for non-inspectable components. Life based on DNV E curve for unground welds - no need to grind welds. Composite tube: predicted life >> steel liner. Steel sections (TJ & TSJ) would be designed using normal practices.
	Crack through composite wall, parting of tube		Minimum life of composite tube is >> 100,000 years			
Dropped objects	Denting, leakage in connector					A prototype riser joint has been tested to a 10 MJ impact load as part of another project. BNo gross failures were observable. Detailed tests results are not available to this study, and it is noted that the design details regarding the steel liner were significantly different.
Riser-to-riser collisions						

Note 3: Composite riser joints run between 102 ft, which is 54 ft above the SJ, to 5926 ft, which is 124 ft below the bottom of the tensioner joint and 74 ft below the mean water level. Maximum composite joint liner stress is near the surface rather than near the stress joint above the seabed. Composite structure is much stronger than the liner.

Acknowledgements

We acknowledge with appreciation the discussions with Mamdouh Salama and Robert Sokoll of Conoco during this project. Their advice and experiences based on their work on composite risers was very useful and added value to this study.

References

1. Zou, J; Omberg, H; Stansberg, T; (2004) "Prediction of TLP Responses: Model Test vs. Analysis", OTC Paper 16584, Houston, Texas, May.
2. Kim, Won Ki, (2007) "Composite Production Riser Assessment", PhD Dissertation, Texas A&M University, May.

Appendices

Appendix A: Global Riser Analysis for the Composite and Steel Production Riser CRA, Prepared For Offshore Technology Research Center, March, 2006 by Charles Miller, Stress Engineering Services, Inc. Houston, Texas

Appendix B: Comparative Risk Analysis of Composite and Steel Production Risers: Composite Riser Response Assessment, Project Report, by Won K. Kim & Advisor: Ozden Ochoa, Texas A&M University, December 2005

Appendix C: Risk Analysis Of Steel Production Risers For Deepwater Offshore Facilities by Anubhav Jain, MS Thesis ,The University of Texas at Austin, December 2004

Appendix A:

Global Riser Analysis for the Composite and Steel Production Riser

CRA

Prepared For

Offshore Technology Research Center, March, 2006

by

Charles Miller, Stress Engineering Services, Inc.

Houston, Texas

**GLOBAL RISER ANALYSIS FOR
THE COMPOSITE AND STEEL
PRODUCTION RISER CRA**

**Prepared For
Offshore Technology Research Center
College Station Texas**

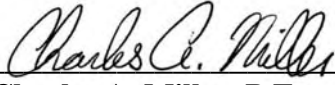
APRIL, 2007

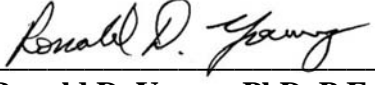


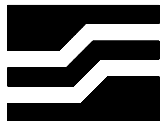
**Stress Engineering Services, Inc.
Houston, Texas**

**GLOBAL RISER ANALYSIS FOR
THE COMPOSITE AND STEEL
PRODUCTION RISER CRA**

**Prepared for:
Offshore Technology Research Center
College Station, TX**

Prepared By: 
Charles A. Miller, P.E.
Principal

Reviewed By: 
Ronald D. Young, PhD, P.E.
Principal



**Stress Engineering Services, Inc.
13800 Westfair East Drive
Houston, Texas 77041-1101**

April, 2007

EXECUTIVE SUMMARY

This document provides a summary of the global riser analyses performed on a composite top tensioned riser and a traditional steel top tensioned production riser. The results of these analyses were used in the Comparative Risk Analysis (CRA) performed on these two riser systems. The analyses performed included design storm analyses and wave-generated fatigue analyses. The design storm analyses included the extreme response analyses for the operating, extreme, and survival storm conditions. The fatigue analyses included fatigue generated by the day-to-day wave environment.

Two riser configurations were used in the analyses. One of the riser configurations was an “All-Steel” configuration similar to those that have been used in the Gulf of Mexico. The other riser configuration was a “Composite-Steel” configuration. Sketches of the “All-Steel” and “Composite-Steel” production risers used for this study are provided in Fig. 1 and 2. Both riser configurations were assumed to be single-casing risers.

The riser’s were assumed to be deployed from a TLP in 6,000 ft. of water in the Gulf of Mexico. Typical TLP motions and Gulf of Mexico environmental conditions were used in the analyses.

KEY FINDINGS

The following key findings were obtained from the global riser analyses performed in this study.

- The tension requirements for the “Composite-Steel” riser configuration used in the study are ~40% of the “All-Steel” riser configuration tension requirements.
- The stress joint needed for the “Composite-Steel” riser configuration was considerably smaller than the “All-Steel” riser configuration’s stress joint. The “Composite-Steel” riser’s stress joint base thickness was 1.6 inches compared to a thickness of 3.0 inches required for the “All-Steel” riser’s stress joint. The “Composite-Steel” riser’s stress joint

taper length is also ~50% of the “All-Steel” riser’s stress joint taper length (16 ft. compared to 30 ft.).

- The wellhead loads generated by the “All-Composite” riser are considerably smaller than those generated by the “All-Steel” riser configuration.
- The bending moments generated in the tensioner joint are about the same for both riser configurations.
- The maximum stresses generated in the “All-Steel” riser components and the “Composite-Steel” riser’s stress joint and tensioner joint satisfy the specified stress criteria.
- The fatigue life estimates obtained for the “All-Steel” riser components and the “Composite-Steel” riser’s stress joint and tensioner joint satisfy the specified 200-year target life required for a 20-year service life.

ADDITIONAL COMMENTS

The analyses performed in this global riser analysis did not include a detailed evaluation of the composite riser joints. The results generated from these analyses were used by others for additional detailed analyses of the composite riser joints. The results of the global riser analyses performed in this study offer insights into the benefits that may be realized provided the composite joints used in this study, could be dependably designed, manufactured, and successfully operated.

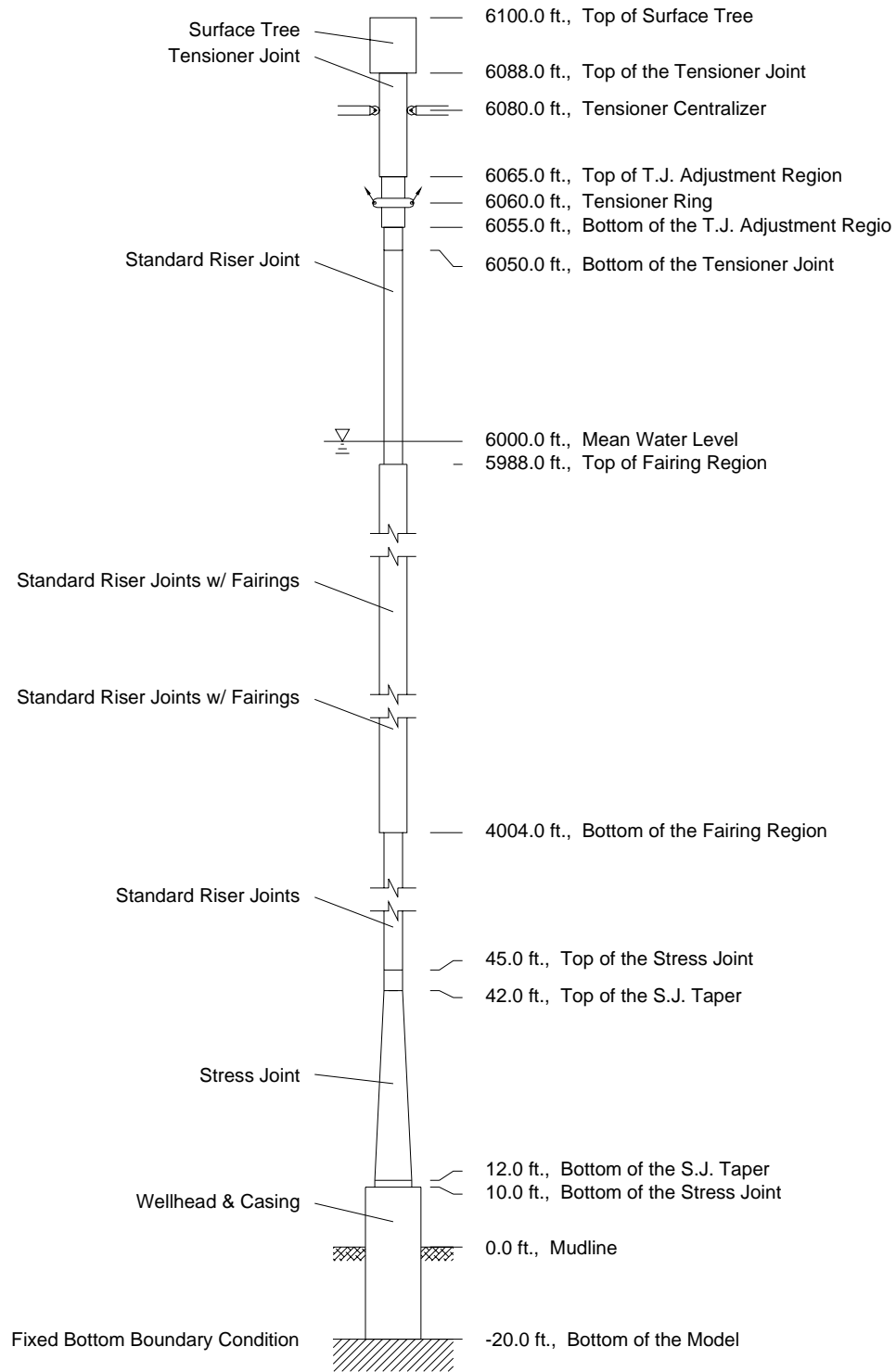


Fig. 1 “All-Steel” Riser Configuration

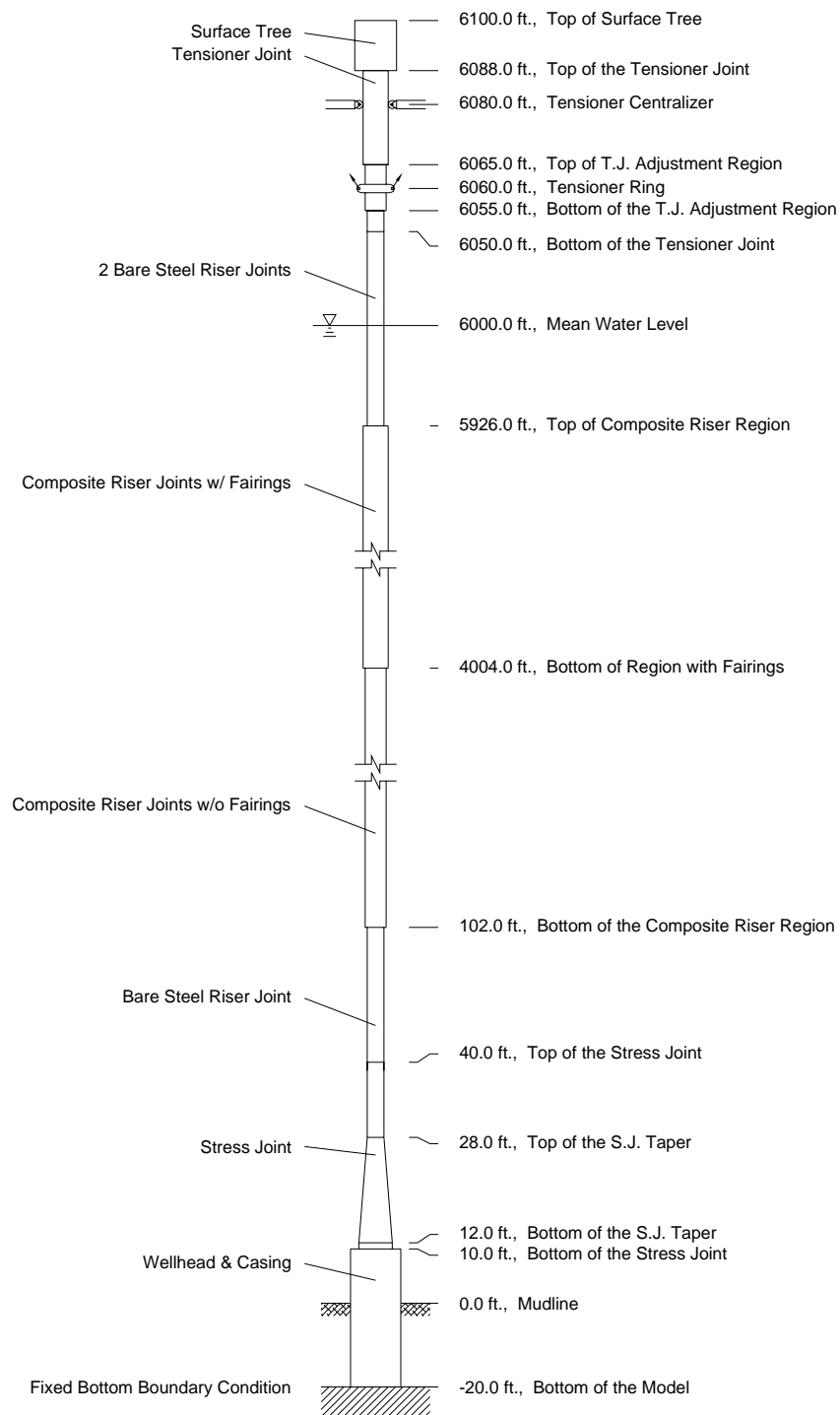


Fig. 2 “Composite-Steel” Riser Configuration

TABLE OF CONTENTS

	<u>Page No.</u>
1 GENERAL.....	1
2 RISER DESCRIPTION, MODELING, AND ASSUMPTIONS	2
2.1 “All-Steel” Riser Configuration.....	2
2.2 “Composite-Steel” Riser Configuration	3
3 ENVIRONMENT, HOST MOTIONS, AND LOAD CASES	22
3.1 Oceanographic Data.....	22
3.1.1 Design Storm and Current Definitions	22
3.1.2 Fatigue Seastate Definitions	23
3.2 Required Analyses	23
3.2.1 Global Analysis of Design Load Cases	23
3.2.2 Global Analysis Required for Estimating Fatigue Life	24
3.3 Host Motion Description.....	24
3.3.1 TLP Motions for the Design Storm Analysis	24
3.3.2 TLP Motions for the Cumulative Wave-Generated Fatigue Analysis.....	26
4 ANALYSIS DETAILS.....	40
4.1 Dynamic Analysis Program	40
4.2 Extreme Response Calculations.....	40
4.3 Application of Environmental Loads.....	41
4.4 Fatigue Curves	41
5 RESULTS OF THE DESIGN STORM ANALYSIS	45
5.1 General.....	45
5.2 “All-Steel” Riser Configuration Design Storm Analysis.....	45
5.2.1 Load Case PNS-1: Normal Shut-in with a 1-Year Winter Storm.....	45
5.2.2 Load Case PHN-1: Shut-in with a 100-Year Hurricane	46
5.2.3 Load Case PCN-1: Maximum Producing with a 100-Year Loop Current.....	46
5.3 “Composite-Steel” Riser Configuration Design Storm Analysis	47
5.3.1 Load Case PNS-1: Normal Shut-in with a 1-Year Winter Storm.....	47
5.3.2 Load Case PHN-1: Shut-in with a 100-Year Hurricane	47
5.3.3 Load Case PCN-1: Maximum Producing with a 100-Year Loop Current.....	48
5.4 Riser Configuration Result Comparison.....	48
6 RESULTS OF THE FATIGUE ANALYSIS.....	70
6.1 General.....	70
6.2 “All-Steel” Riser Configuration Fatigue.....	70
6.3 “Composite-Steel” Riser Configuration Fatigue	72
7 REFERENCES.....	96

1 GENERAL

This document provides a summary of the global riser analyses performed on a composite top tensioned riser and a traditional steel top tensioned production riser. The results of these analyses were used in the Comparative Risk Analysis (CRA) performed on these two riser systems. The analyses performed included design storm analyses and wave-generated fatigue analyses. The design storm analyses included the extreme response analyses for the operating, extreme, and survival storm conditions. The fatigue analyses included fatigue generated by the day-to-day wave environment. Discussions of modeling procedures and analysis methodology are also presented.

2 RISER DESCRIPTION, MODELING, AND ASSUMPTIONS

Single-casing riser configurations in 6,000 ft. of water were used for this study. One “all-steel” riser configuration and one “composite-steel” riser configuration were evaluated. These riser configurations are described below.

2.1 “ALL-STEEL” RISER CONFIGURATION

Fig. 2.1 contains a sketch of the “all-steel” riser configuration used for this study. The riser was assumed to be a truly vertical riser with no well offset. Table 2.1 contains a summary of the parameters used to model this riser configuration. The riser’s cross-section is shown in Fig. 2.2. The outer casing has an 11.750-inch O.D., a 1.014-inch thick wall, and is made from x-80 pipe. This casing was sized for a maximum shut-in pressure of 8,500 psi.

The production tubing has a 5.500-inch O.D., a 0.415-inch wall thickness, and is made from C-95 pipe. The production tubing was also sized for a maximum shut-in pressure of 8,500 psi.

A simplified model of the foundation casing and wellhead was used. The model used approximates the lateral and rotational restraint provided by a conventional wellhead system used in the Gulf of Mexico. The bottom of the 36-inch casing was “fixed” 20 ft. below the mudline. No soil springs were used in the model. The top of the wellhead was assumed to be located 10 ft. above the mudline. The dimensions used for the wellhead/foundation casing are given in Table 2.1.

A tapered stress joint (TSJ) was modeled at the bottom of the riser string and attached to the top of the wellhead. The dimensions used to model the TSJ are given in Table 2.1. A straight section was used at the bottom of the TSJ to model the TSJ’s lower connector. The TSJ was assumed to have a 30 ft. taper and a constant O.D. section extending 12 ft. above the top of the tapered portion of the TSJ. The TSJ dimensions given in Table 2.1

are the final values and were optimized using the design storm and wave-fatigue solutions.

Standard riser joints were modeled from the top of the TSJ to the bottom of the tensioner joint located 50 ft. above the mean water level (6,050 ft. above the mudline). The assumed joint lengths and weights are given in Table 2.1. It was assumed that fairings would be needed over the top ~2,000 ft. of the riser for VIV suppression purposes. The assumed fairing weights are included in the riser joint weights used from 4,004 ft. to 5,988 ft. above the mudline.

The tensioner joint extended from 6,050 ft. to 6,088 ft. above the mudline. The tensioner joint modeled had three (3) sections with different outside diameters and wall thicknesses. These sections are described in Table 2.1. The tensioner ring was assumed to be attached to the tensioner joint at an elevation of 6,060 ft. The tensioner also passes through the production deck which is assumed to be located 6,080 ft. above the mudline. The riser is centralized by rollers at the production deck.

A 12-ft. tall surface tree was assumed to be attached to the top of the riser's tensioner joint. Therefore, the top of the riser model was assumed to be located 6,100 ft. above the mudline.

The assumed riser tensioner stiffness used in the study is given in Table 2.1.

Table 2.2 contains a summary of the dimensions, effective weights, and nominal tensioner setting used for the normal operating conditions.

2.2 “COMPOSITE-STEEL” RISER CONFIGURATION

Fig. 2.3 contains a sketch of the “composite-steel” riser configuration used for this study. The riser was assumed to be a truly vertical riser with no well offset. Table 2.3 contains a summary of the parameters used to model this riser configuration. The riser's cross-section is shown in Fig. 2.4. The composite riser joints have a steel inner liner, a 0.972-inch thick layer of carbon fiber composite material, and an outer layer of an E-glass

composite material. These composite joints were sized for a maximum shut-in pressure of 8,500 psi.

The production tubing has a 5.500-inch O.D., a 0.415-inch wall thickness, and is made from C-95 pipe. The production tubing was also sized for a maximum shut-in pressure of 8,500 psi. This is the same production tubing modeled in the “all-steel” riser configuration.

The foundation casing, tensioner joint, and surface tree models used for the “all-steel” configuration were also used for the “composite-steel” configuration.

A tapered stress joint (TSJ) was modeled at the bottom of the riser string and attached to the top of the wellhead. The dimensions used to model the TSJ are given in Table 2.3. A straight section was used at the bottom of the TSJ to model the TSJ’s lower connector. The TSJ was assumed to have a 16 ft. taper and a constant O.D. section extending 12 ft. above the top of the tapered portion of the TSJ. The TSJ dimensions given in Table 2.3 are the final values and were optimized using the design storm and wave-fatigue solutions.

One steel riser joint was modeled above the TSJ and two steel joints were modeled below the tensioner joint. These riser joints were 62 ft. long and were identical to the standard riser joints used in the “all-steel” riser configuration.

The composite riser joints were modeled from the top of the lower steel riser joint (located 102 ft. above the mudline) to the bottom of the upper two steel riser joints (located 5926 ft. above the mudline or 74 ft. below the mean water level). The assumed joint lengths, weights, and stiffness properties used for the composite riser joints are given in Table 2.3. It was assumed that fairings would be needed over the top ~2,000 ft. of the riser for VIV suppression purposes. The assumed fairing weights are included in the riser joint weights used from 4,004 ft. to 5,926 ft. above the mudline.

The assumed riser tensioner stiffness used in the study is given in Table 2.3. Table 2.4 contains a summary of the dimensions, effective weights, and nominal tensioner setting

used for the normal operating conditions. The composite riser joints are considerably lighter than the steel riser joints. Therefore, the composite riser system is considerably lighter than the “all-steel” riser configuration. The same tension factors were used for the “all-steel” and “composite-steel” riser configurations. Since the “composite-steel” configuration is considerably lighter than the “all-steel” configuration, use of the same tension factor for both configurations resulted in a lower tensioner setting for the “composite-steel” configuration. This also produced lower tensions at the lower stress joint. The lower TSJ tensions in the “composite-steel” configuration produced a smaller stress joint for the “composite-steel” configuration over the “all-steel” configuration.

Table 2.1
“All-Steel” Riser Configuration Definition

1.	Water Depth, ft.	6,000
2.	Wellhead/Foundation Region	
	a. Region Extremities, ft. above the mudline	-20 to 10
	b. Outside Diameter, in.	36.0
	c. Inside Diameter, in.	32.0
	d. Wall Thickness, in.	2.0
3.	Tapered Joint Region	
	a. Extremities, ft. above the mudline	10 to 45
	b. Yield Stress, ksi	80
	c. Modulus of Elasticity, ksi	29×10^3
	d. Air Weight, lbs/joint	10,698
	e. Submerged Weight, lbs/joint	9,300
	f. Drag Coefficient	1.00
	g. Bottom Section	
	i. Extremities, ft. above the mudline	10 to 12
	ii. Outside Diameter, in.	15.722
	iii. Inside Diameter, in.	9.722
	iv. Wall Thickness, in.	3.000
	v. Drag Diameter, in.	15.722
	h. Tapered Section	
	i. Extremities, ft. above the mudline	12 to 42
	ii. Base Outside Diameter, in.	15.722
	iii. Base Inside Diameter, in.	9.722
	iv. Base Wall Thickness, in.	3.000
	v. Base Drag Diameter, in.	15.722

Table 2.1 Continued
“All-Steel” Riser Configuration Definition

vi.	Tip Outside Diameter, in.	11.750
vii.	Tip Inside Diameter, in.	9.722
viii.	Tip Wall Thickness, in.	1.014
ix.	Tip Drag Diameter, in.	11.750
i.	Upper Section	
i.	Extremities, ft. above the mudline	42 to 45
ii.	Outside Diameter, in.	11.750
iii.	Inside Diameter, in.	9.722
iv.	Wall Thickness, in.	1.014
v.	Drag Diameter, in.	11.750
4.	Lower Standard Riser Joints without VIV Suppression	
a.	Extremities, ft. above the mudline	45 to 4,004
b.	Outside Diameter, in.	11.750
c.	Inside Diameter, in.	9.722
d.	Wall Thickness, in.	1.014
e.	Joint Length, ft.	62
f.	Air Weight, lbs/joint	7,692
g.	Submerged Weight, lbs/joint	6,687
h.	Drag Diameter, in.	11.750
i.	Drag Coefficient	1.00
j.	Yield Stress, ksi	80
k.	Modulus of Elasticity, ksi	29 x 10 ³
5.	Standard Riser Joints with VIV Suppression	
a.	Extremities, ft. above the mudline	4,004 to 5,988
b.	Outside Diameter, in.	11.750

Table 2.1 Continued
“All-Steel” Riser Configuration Definition

c.	Inside Diameter, in.	9.722
d.	Wall Thickness, in.	1.014
e.	Joint Length, ft.	62
f.	Air Weight, lbs/joint	8,214
g.	Submerged Weight, lbs/joint	6,838
h.	Drag Diameter, in.	11.750
i.	Drag Coefficient	0.70
j.	Yield Stress, ksi	80
k.	Modulus of Elasticity, ksi	29×10^3
6.	Upper Standard Riser Joints without VIV Suppression	
a.	Extremities, ft. above the mudline	5,988 to 6,050
b.	Outside Diameter, in.	11.750
c.	Inside Diameter, in.	9.722
d.	Wall Thickness, in.	1.014
e.	Joint Length, ft.	62
f.	Air Weight, lbs/joint	7,692
g.	Submerged Weight, lbs/joint	6,687
h.	Drag Diameter, in.	11.750
i.	Drag Coefficient	1.00
j.	Yield Stress, ksi	80
k.	Modulus of Elasticity, ksi	29×10^3
7.	Tensioner Joint Region	
a.	Extremities, ft. above the mudline	6,050 to 6,088
b.	Yield Stress, ksi	80
c.	Modulus of Elasticity, ksi	29×10^3

Table 2.1 Continued
“All-Steel” Riser Configuration Definition

d. Air Weight, lbs/joint	12,821
e. Bottom Section	
i. Extremities, ft. above the mudline	6,050 to 6,055
ii. Outside Diameter, in.	11.750
iii. Inside Diameter, in.	9.722
iv. Wall Thickness, in.	1.014
f. Middle Section	
i. Extremities, ft. above the mudline	6,055 to 6,065
ii. Outside Diameter, in.	15.000
iii. Inside Diameter, in.	9.722
iv. Wall Thickness, in.	2.639
g. Upper Section	
i. Extremities, ft. above the mudline	6,065 to 6,088
ii. Outside Diameter, in.	15.250
iii. Inside Diameter, in.	9.722
iv. Wall Thickness, in.	2.764
8. Surface Tree	
a. Extremities, ft. above the mudline	6,088 to 6,100
b. Air Weight, lbs	20,000
c. Weight of Flex Hose, ..., lbs	3,000
9. Production Tubing	
a. Extremities, ft. above the mudline	10 to 6,088
b. Outside Diameter, in.	5.500
c. Inside Diameter, in.	4.670
d. Wall Thickness, in.	0.415

Table 2.1 Continued
“All-Steel” Riser Configuration Definition

e. Joint Length, ft.	40
f. Air Weight, lbs/joint	902
g. Yield Stress, ksi	95
h. Modulus of Elasticity, ksi	29×10^3

Table 2.2
“All-Steel” Riser Configuration – Normal Operating Condition

Single Casing Riser; Production Tubing Shut-in Pressure = 8,500 psi
Riser Weight Estimate; Nominal Position (Vertical); Water Depth = 6,000 ft.
TLP Centered Over the Well Pattern; No Environment
Outer Casing Contents = 0.04 ppg; Production Tubing Contents = 5.50 ppg
Recommended Riser Tensioner Setting = 865 kips

Region	O.D. (in.)	I.D. (in.)	Region Extremities		Joint Length (ft.)	Air Wts.		Submerged Wts.		Ext. Fluid Density (ppg)	Int. Fluid Density (ppg)	Effective Wts.			Tension Factor	Tension Rqmts. (lbs)
			Bottom (ft.)	Top (ft.)		Joint (lbs)	Unit (lbs/ft)	Joint (lbs)	Unit (lbs/ft)			Unit (lbs/ft)	Joint (lbs)	Total Reg. (lbs)		
Foundation Casing	36.000	32.000	-20.0	10.0	30	21808	726.93	18960	631.98	8.56	0.04	276.2	8286	8286	-	-
Stress Jt. Btm. Straight Reg.	15.722	9.722	10.0	12.0	2.0	1310	655.16	1139	569.59	8.56	0.04	536.8	1074	1074	1.30	1396
Stress Jt. Taper Reg.	15.722	9.722	12.0	42.0	30.0	8655	288.49	7524	250.81	8.56	0.04	218.0	6539	6539	1.30	8501
Stress Jt. Straight Reg.	11.750	9.722	42.0	45.0	3.0	733	244.25	637	212.33	8.56	0.04	179.5	538	538	1.30	700
Bare Std. Jt.	11.750	9.722	45.0	4004.0	62.0	7692	124.07	6687	107.86	8.56	0.04	75.0	4651	297013	1.30	386117
Std. Jt. with Fairings	11.750	9.722	4004.0	5988.0	62.0	8214	132.48	6838	110.28	8.56	0.04	77.4	4802	153654	1.30	199750
Std. Jt. Below MWL	11.750	9.722	5988.0	6000.0	62.0	7692	124.07	6687	107.86	8.56	0.04	75.0	4651	900	1.30	1170
Bare Std. Jt.	11.750	9.722	6000.0	6050.0	62.0	7692	124.07	7692	124.07	0.00	0.04	124.2	7702	6211	1.30	8074
Tensioner Joint - Reg. 1	11.750	9.722	6050.0	6055.0	5.0	849	169.83	849	169.83	0.00	0.04	170.0	850	850	1.30	1105
Tensioner Joint - Reg. 2	15.000	9.722	6055.0	6065.0	10.0	3487	348.72	3487	348.72	0.00	0.04	348.9	3489	3489	1.30	4535
Tensioner Joint - Reg. 3	15.250	9.722	6065.0	6088.0	23.0	8485	368.93	8485	368.93	0.00	0.04	369.1	8489	8489	1.30	11036
Production Tubing	5.500	4.670	10.0	6088.0	40.0	902	22.56	902	22.55	0.04	5.50	27.40	1096	166558	1.30	216525
													644241	837513		
Flex. Flowline Hose	-	-	-	-	-	3000	-	3000	-	0.00	0.00	-	3000	3000	1.00	3000
Surface Tree	-	-	-	-	-	24000	-	24000	-	0.00	0.00	-	24000	24000	1.00	24000
													27000	27000		
TOTALS (REQUIRED TOP TENSION)													671241		864513	

Table 2.3
“Composite-Steel” Riser Configuration Definition

1.	Water Depth, ft.	6,000
2.	Wellhead/Foundation Region	
	a. Region Extremities, ft. above the mudline	-20 to 10
	b. Outside Diameter, in.	36.0
	c. Inside Diameter, in.	32.0
	d. Wall Thickness, in.	2.0
3.	Tapered Joint Region	
	a. Extremities, ft. above the mudline	10 to 40
	b. Yield Stress, ksi	80
	c. Modulus of Elasticity, ksi	29×10^3
	d. Air Weight, lbs/joint	6,359
	e. Submerged Weight, lbs/joint	5,528
	f. Drag Coefficient	1.00
	g. Bottom Section	
	i. Extremities, ft. above the mudline	10 to 12
	ii. Outside Diameter, in.	12.920
	iii. Inside Diameter, in.	9.722
	iv. Wall Thickness, in.	1.600
	v. Drag Diameter, in.	12.920
	h. Tapered Section	
	i. Extremities, ft. above the mudline	12 to 28
	ii. Base Outside Diameter, in.	12.920
	iii. Base Inside Diameter, in.	9.720
	iv. Base Wall Thickness, in.	1.600
	v. Base Drag Diameter, in.	12.920

Table 2.3 Continued
“Composite-Steel” Riser Configuration Definition

vi.	Tip Outside Diameter, in.	11.750
vii.	Tip Inside Diameter, in.	9.720
viii.	Tip Wall Thickness, in.	1.015
ix.	Tip Drag Diameter, in.	11.750
i.	Upper Section	
i.	Extremities, ft. above the mudline	28 to 40
ii.	Outside Diameter, in.	11.750
iii.	Inside Diameter, in.	9.720
iv.	Wall Thickness, in.	1.015
v.	Drag Diameter, in.	11.750
4.	Lower Steel Riser Joint	
a.	Extremities, ft. above the mudline	40 to 102
b.	Outside Diameter, in.	11.750
c.	Inside Diameter, in.	9.722
d.	Wall Thickness, in.	1.014
e.	Joint Length, ft.	62
f.	Air Weight, lbs/joint	7,692
g.	Submerged Weight, lbs/joint	6,687
h.	Drag Diameter, in.	11.750
i.	Drag Coefficient	1.00
j.	Yield Stress, ksi	80
k.	Modulus of Elasticity, ksi	29 x 10 ³
5.	Composite Riser Joints without VIV Suppression	
a.	Extremities, ft. above the mudline	102 to 4,004
b.	Outside Diameter, in.	12.414
c.	Inside Diameter, in.	9.720

Table 2.3 Continued
“Composite-Steel” Riser Configuration Definition

d.	Wall Thickness, in.	1.347
e.	Joint Length, ft.	62
f.	Air Weight, lbs/joint	3,698
g.	Submerged Weight, lbs/joint	2,254
h.	Drag Diameter, in.	12.414
i.	Drag Coefficient	1.00
j.	EA, kips	5.444×10^5
k.	EI, kips-ft ²	5.729×10^4
6.	Composite Riser Joints with VIV Suppression	
a.	Extremities, ft. above the mudline	4,004 to 5,926
b.	Outside Diameter, in.	12.414
c.	Inside Diameter, in.	9.720
d.	Wall Thickness, in.	1.347
e.	Joint Length, ft.	62
f.	Air Weight, lbs/joint	4,220
g.	Submerged Weight, lbs/joint	2,404
h.	Drag Diameter, in.	12.414
i.	Drag Coefficient	0.70
j.	EA, kips	5.444×10^5
k.	EI, kips-ft ²	5.729×10^4
7.	Upper Steel Riser Joints	
a.	Extremities, ft. above the mudline	5,926 to 6,050
b.	Outside Diameter, in.	11.750
c.	Inside Diameter, in.	9.722
d.	Wall Thickness, in.	1.014
e.	Joint Length, ft.	62

Table 2.3 Continued
“Composite-Steel” Riser Configuration Definition

f.	Air Weight, lbs/joint	7,692
g.	Submerged Weight, lbs/joint	6,687
h.	Drag Diameter, in.	11.750
i.	Drag Coefficient	1.00
j.	Yield Stress, ksi	80
k.	Modulus of Elasticity, ksi	29 x 10 ³
8.	Tensioner Joint Region	
a.	Extremities, ft. above the mudline	6,050 to 6,088
b.	Yield Stress, ksi	80
c.	Modulus of Elasticity, ksi	29 x 10 ³
d.	Air Weight, lbs/joint	12,821
e.	Bottom Section	
i.	Extremities, ft. above the mudline	6,050 to 6,055
ii.	Outside Diameter, in.	11.750
iii.	Inside Diameter, in.	9.722
iv.	Wall Thickness, in.	1.014
f.	Middle Section	
i.	Extremities, ft. above the mudline	6,055 to 6,065
ii.	Outside Diameter, in.	15.000
iii.	Inside Diameter, in.	9.722
iv.	Wall Thickness, in.	2.639
g.	Upper Section	
i.	Extremities, ft. above the mudline	6,065 to 6,088
ii.	Outside Diameter, in.	15.250
iii.	Inside Diameter, in.	9.722
iv.	Wall Thickness, in.	2.764

Table 2.3 Continued
“Composite-Steel” Riser Configuration Definition

9.	Surface Tree	
	a. Extremities, ft. above the mudline	6,088 to 6,100
	b. Air Weight, lbs	20,000
	c. Weight of Flex Hose, ..., lbs	3,000
10.	Production Tubing	
	a. Extremities, ft. above the mudline	10 to 6,088
	b. Outside Diameter, in.	5.500
	c. Inside Diameter, in.	4.670
	d. Wall Thickness, in.	0.415
	e. Joint Length, ft.	40
	f. Air Weight, lbs/joint	902
	g. Yield Stress, ksi	95
	h. Modulus of Elasticity, ksi	29×10^3

Table 2.4
“Composite-Steel” Riser Configuration – Normal Operating Condition

Single Casing Riser; Production Tubing Shut-in Pressure = 8,500 psi
Riser Weight Estimate; Nominal Position (Vertical); Water Depth = 6,000 ft.
TLP Centered Over the Well Pattern; No Environment
Outer Casing Contents = 0.04 ppg; Production Tubing Contents = 5.50 ppg
Recommended Riser Tensioner Setting = 319 kips

Region	O.D. (in.)	I.D. (in.)	Region Extremities		Joint Length (ft.)	Air Wts.		Submerged Wts.		Ext. Fluid Density (ppg)	Int. Fluid Density (ppg)	Effective Wts.			Tension Factor	Tension Rqmts. (lbs)
			Bottom (ft.)	Top (ft.)		Joint (lbs)	Unit (lbs/ft)	Joint (lbs)	Unit (lbs/ft)			Unit (lbs/ft)	Joint (lbs)	Total Reg. (lbs)		
Foundation Casing	36.000	32.000	-20.0	10.0	30	21808	726.93	18960	631.98	8.56	0.04	276.2	8286	8286	-	-
Stress Jt. Btm. Straight Reg.	12.920	9.720	10.0	12.0	2.0	1109	554.38	964	481.97	8.56	0.04	449.1	898	898	1.30	1168
Stress Jt. Taper Reg.	12.920	9.720	12.0	28.0	16.0	3470	216.88	3017	188.55	8.56	0.04	155.7	2492	2492	1.30	3239
Stress Jt. Straight Reg.	11.748	9.720	28.0	40.0	12.0	1780	148.32	1547	128.94	8.56	0.04	96.1	1153	1153	1.30	1499
Bare Steel Jt.	11.750	9.722	40.0	102.0	62.0	7692	124.07	6687	107.86	8.56	0.04	75.0	4651	4651	1.30	6047
Bare Composite Jt.	12.414	9.720	102.0	4004.0	62.0	3698	59.65	2254	36.36	8.56	0.04	3.53	219	13784	1.30	17919
Composite Jt. with Fairings	12.414	9.720	4004.0	5926.0	62.0	4220	68.07	2404	38.78	8.56	0.04	5.96	369	11449	1.30	14883
Bare Steel Jt. Below MWL	11.750	9.722	5926.0	6000.0	62.0	7692	124.07	6687	107.86	8.56	0.04	75.0	4651	5552	1.30	7217
Bare Steel Jt. Above MWL	11.750	9.722	6000.0	6050.0	62.0	7692	124.07	7692	124.07	0.00	0.04	124.2	7702	6211	1.30	8074
Tensioner Joint - Reg. 1	11.750	9.722	6050.0	6055.0	5.0	849	169.83	849	169.83	0.00	0.04	170.0	850	850	1.30	1105
Tensioner Joint - Reg. 2	15.000	9.722	6055.0	6065.0	10.0	3487	348.72	3487	348.72	0.00	0.04	348.9	3489	3489	1.30	4535
Tensioner Joint - Reg. 3	15.250	9.722	6065.0	6088.0	23.0	8485	368.93	8485	368.93	0.00	0.04	369.1	8489	8489	1.30	11036
Production Tubing	5.500	4.670	10.0	6088.0	40.0	902	22.56	901	22.52	0.04	5.50	27.38	1095	166391	1.30	216308
													224510		291863	
Flex. Flowline Hose	-	-	-	-	-	3000	-	3000	-	0.00	0.00	-	3000	3000	1.00	3000
Surface Tree	-	-	-	-	-	24000	-	24000	-	0.00	0.00	-	24000	24000	1.00	24000
													27000		27000	
TOTALS (REQUIRED BUOYANCY)													251510		318863	

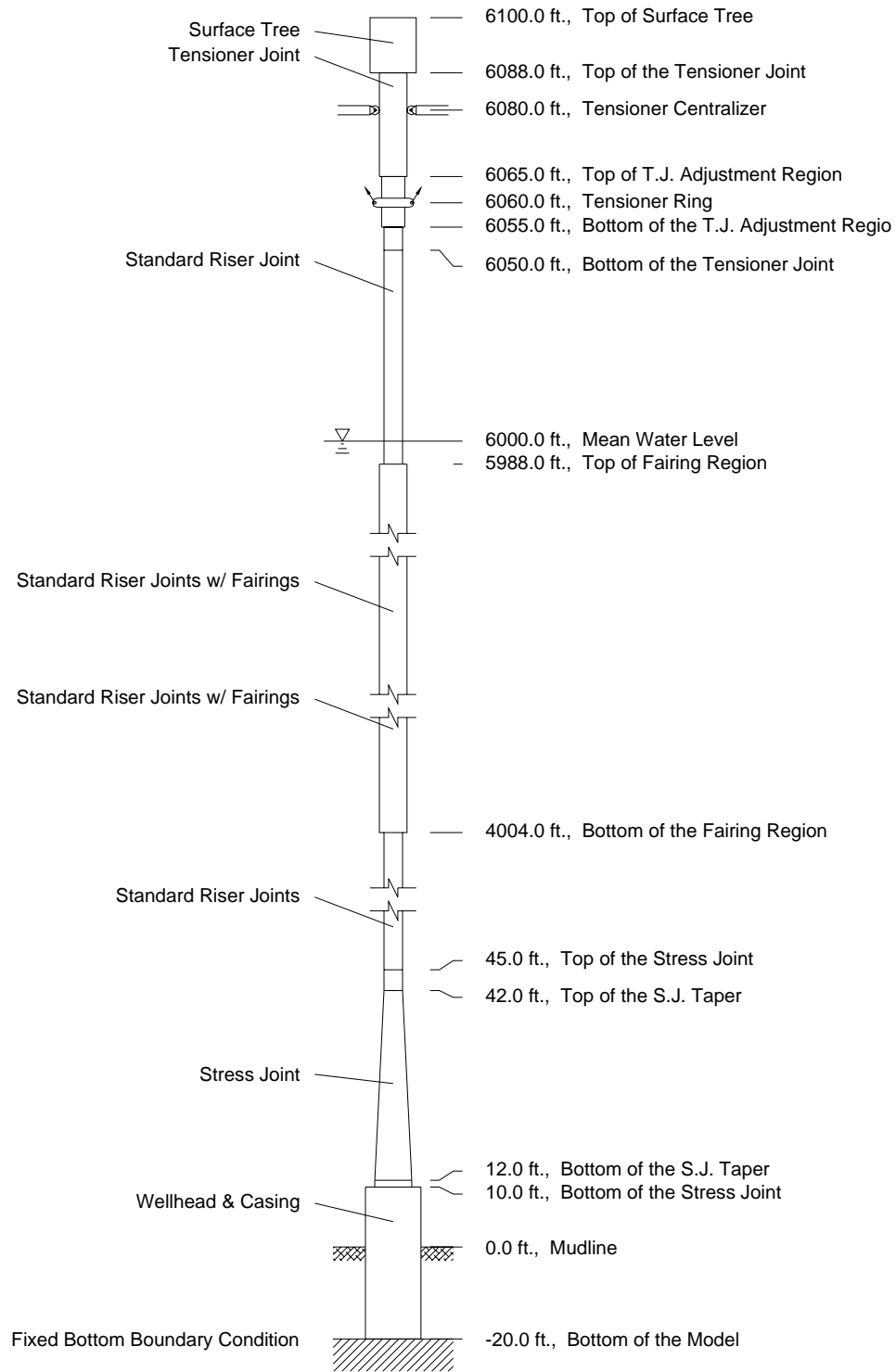


Fig. 2.1 “All-Steel” Riser Configuration

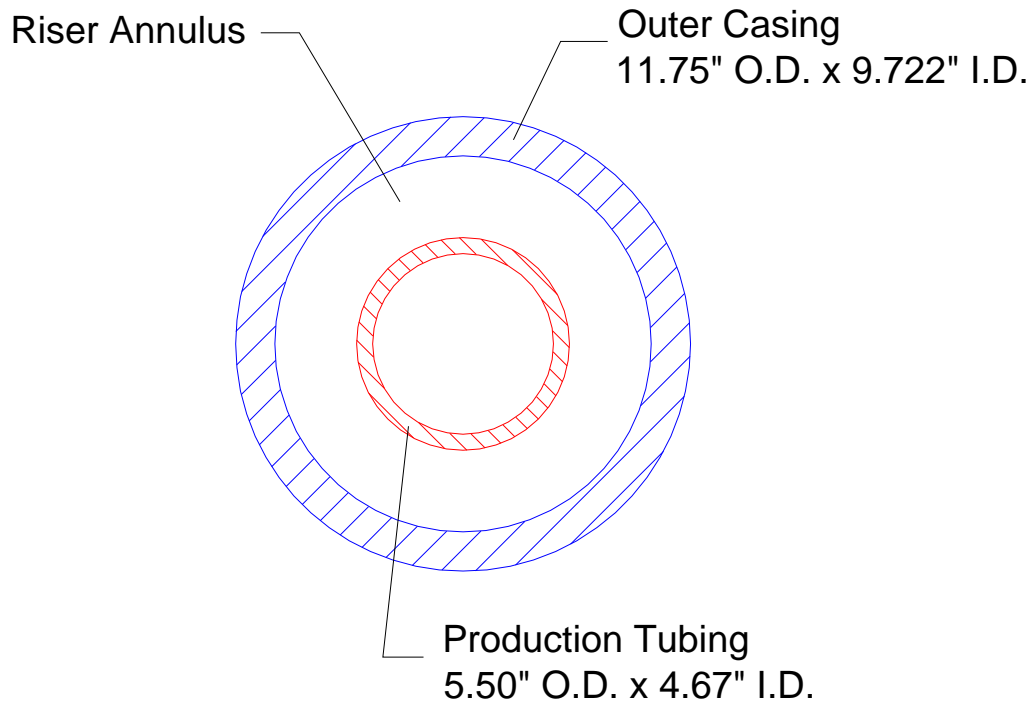


Fig. 2.2 "All-Steel" Riser Cross-Section

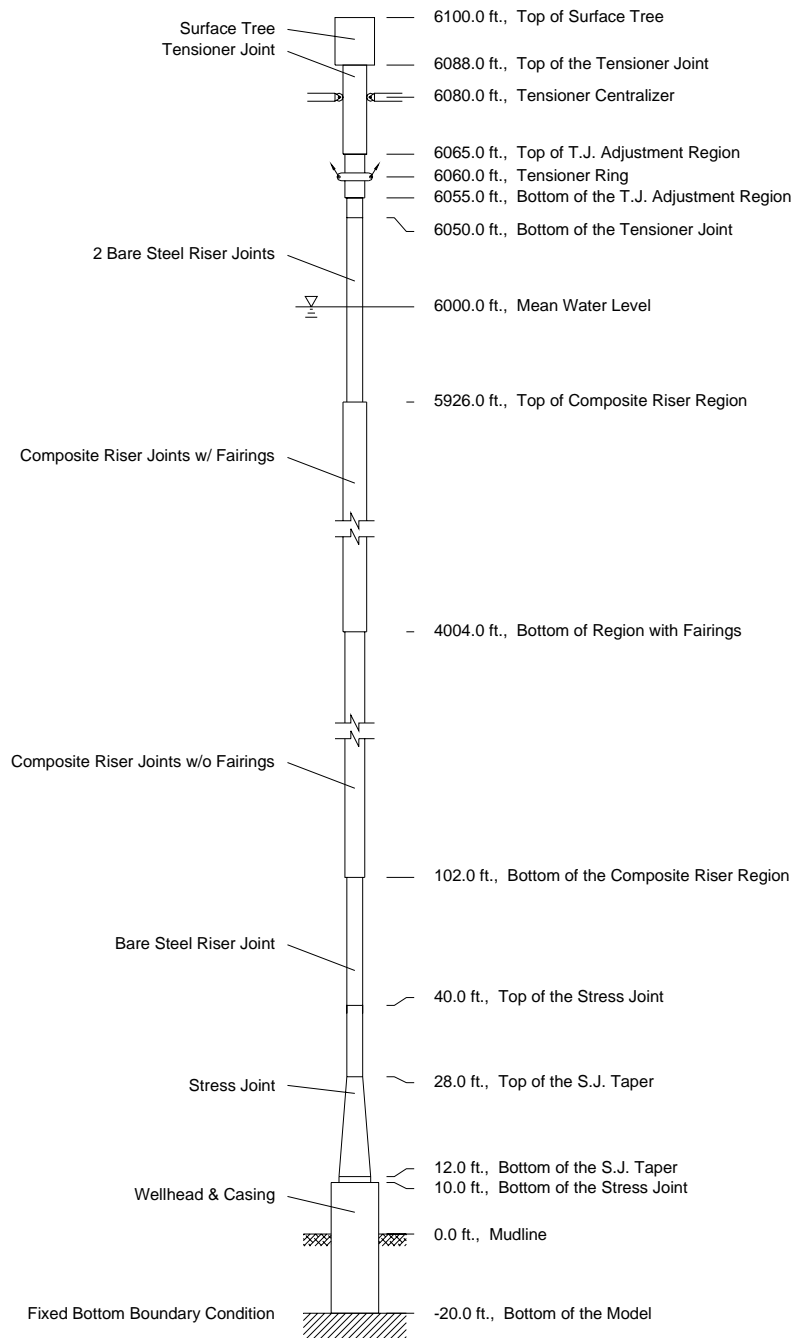


Fig. 2.3 “Composite-Steel” Riser Configuration

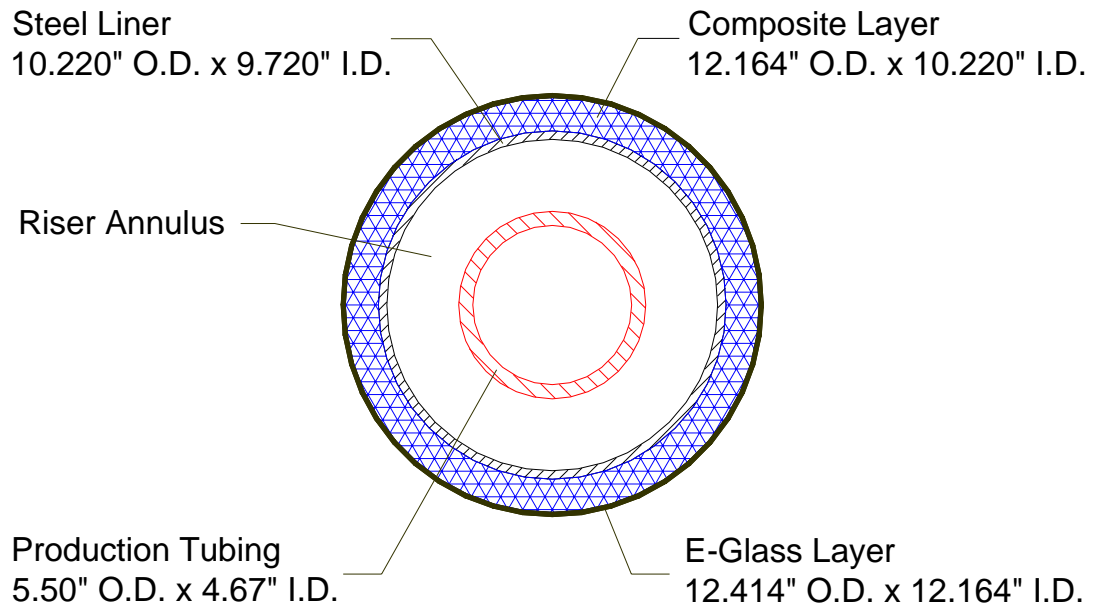


Fig. 2.4 "Composite-Steel" Riser Cross-Section

3 ENVIRONMENT, HOST MOTIONS, AND LOAD CASES

3.1 OCEANOGRAPHIC DATA

This section provides environmental parameters for the three (3) “design storm events” used in this study:

- 1-year Winter Storm
- 100-year Hurricane
- 100-year Loop Current Event

Also provided are 27 bins of wave parameters and corresponding probabilities of occurrence. These will be used for fatigue analysis.

Table 3.1.1 contains the Goda 3-parameter form [1] used to describe the wave spectrum in terms of significant wave height H_S , peak period T_P , and peakedness γ . This form is a specialization of the 5-parameter JONSWAP spectrum, and its use is implied by the specification of the 3 spectral parameters H_S , T_P , and γ . Wind, waves, and current shall be assumed collinear.

Data in this section were obtained from information provided by OTRC and are typical of Gulf of Mexico (GOM) conditions.

3.1.1 Design Storm and Current Definitions

The design storm and current environments represent particular design conditions for which extreme riser response quantities are determined. The definitions of the spectral waves used for the design events appear in Table 3.1.1.1. Table 3.1.1.2 contains the current profile information for the 1-year winter storm and 100-year hurricane events.

The 100-year loop current profile is provided in Table 3.1.1.3. Although the loop currents may have a predominant direction, for evaluation of extreme riser responses, the loop current is assumed to be able to come from any direction.

3.1.2 Fatigue Seastate Definitions

Table 3.1.2.1 contains a copy of the wave fatigue scatter diagram used for the riser fatigue analysis. The scatter diagram contains descriptions of each of the 27 seastates used to define the day-to-day wave environment for the purpose of performing the cumulative wave-generated fatigue analysis. The wave scatter diagram provided is an omni-directional scatter diagram. Wave directionality was not considered in this analysis.

The current velocity is set to zero throughout the water column for the fatigue analyses performed using the seastates defined in Table 3.1.2.1. This is a conservative assumption that removes any damping that may be generated by current loads. This assumption is made because the waves and currents are not necessarily correlated, therefore, there is no guarantee that the current loading used in the analysis will be present to provide any damping of the riser response.

3.2 REQUIRED ANALYSES

Two primary types of criteria must be met in order to qualify a riser design for dynamic service: (1) the riser system response must remain within allowable bounds when subjected to prescribed design load cases, and (2) the fatigue life of the riser system must be demonstrated to equal or exceed its specified design life. In both cases, several individual analyses must be performed to qualify the riser system.

3.2.1 Global Analysis of Design Load Cases

Design load cases are analyzed for the purpose of verifying that response quantities (primary pipe wall stress and support loads) do not exceed allowable values. Three (3) levels of service are considered: (1) (Normal) Operating, (2) Extreme, and (3) Survival, each with its own allowable stress increase factor. The design load cases for this study are presented in Table 3.2.1.1. The C_f values in Table 3.2.1.1 are consistent with those found in Table 2 of API RP 2RD [2].

3.2.2 Global Analysis Required for Estimating Fatigue Life

Fatigue analyses were performed to determine fatigue damage rates for wave-generated loads and TLP motions. All of the analyses were performed assuming the risers to be filled with their normal-operating contents.

For cumulative wave-generated fatigue, global dynamic analysis was performed for each of the 27 fatigue bin seastates contained in Table 3.1.2.1.

3.3 HOST MOTION DESCRIPTION

Dynamic analysis of risers attached to a floating host is typically a two-step process. First, the response of the host itself is determined using a detailed model of the host and a simplified model of any risers that are being modeled. This is done for each set of environmental conditions of interest. The detailed analysis of the riser system is then performed separately by imposing this host displacement response at the riser/host attachment point as displacement boundary conditions on the interface elements (i.e., springs, flexjoints, etc.) that connect the riser to the host.

Since this is a comparative study the main concern regarding these motions is to apply the same realistic motions to both riser systems. The floating production system used in this study was a TLP. The motions used were provided by OTRC.

The coordinate system used for the TLP motions is shown in Fig. 3.3.1. The wave heading (direction) assumes a “toward which” interpretation of wave velocity. Positive wave headings are measured counter-clockwise from the positive X-axis. Therefore, a wave heading of 0° corresponds to a wave traveling along the positive X-axis as shown in Fig. 3.3.1. A wave heading of 90° corresponds to a wave traveling along the positive Y-axis.

3.3.1 TLP Motions for the Design Storm Analysis

TLP Mean Offsets and Low-Frequency Design Storm Motions

The TLP mean offset and low-frequency motion data used for the design storm load cases are summarized in Table 3.1.1.1. The mean offsets and low frequency motions/periods are typical values for a TLP in the Gulf of Mexico.

Because the TLP is tied to the seafloor by its vertical tendons, the TLP will also move down into the water as the environment moves the TLP laterally. This vertical downward motion is referred to as “setdown”. Table 3.3.1.1 contains a summary of the relationship between TLP offset and setdown used in this study. The TLP setdown factor was calculated for the water depth used in the study assuming no tendon stretch. The equation used is provided below:

$$SD_{mean} = (-8.333 \times 10^{-5}) (H_{mean})^2 \quad (3.3.1.1)$$

where,

SD_{mean} = TLP mean setdown measured in feet (positive value corresponds to upward TLP motion)

H_{mean} = TLP mean offset measured in feet

TLP Wave-Frequency Design Storm Motions

The TLP wave-frequency motions used for the design storm analysis were generated from TLP RAOs provided by OTRC. Appendix A-3.3.1.1 contains definitions of the provided RAOs in tabular form. RAOs were provided for wave headings of 0°, 22.5°, 45°, 67.5°, and 90°. Only the 0° heading RAOs were used in this study. Fig. 3.3.1.1 contains plots of the RAOs used for the analyses.

A positive phase angle indicates that a parameter reaches its peak value after the wave crest has passed the CoG of the structure. Therefore, the following relationship was used to calculate the wave-frequency motions using the TLP RAOs:

$$a = A \cos(\omega t - \phi) \quad (3.3.1.2)$$

where,

a = Value of the TLP response at time “ t ”

$A =$ Amplitude of the TLP response at frequency “ ω ”

$\omega =$ Angular frequency (rad/sec)

$t =$ Time (sec)

$\phi =$ Phase angle at frequency “ ω ”

3.3.2 TLP Motions for the Cumulative Wave-Generated Fatigue Analysis

TLP Mean Offsets for the Wave-Generated Fatigue Seastates

TLP mean offsets were provided by OTRC for six (6) seastates. The seastates were selected to provide a coarse representation of the fatigue wave scatter diagram. The six (6) seastates used are defined in Table 3.3.2.1. A relationship between the TLP mean offset and significant wave height was developed using this seastates. The equation derived from the provided data is defined in Table 3.3.2.1. The “Raw” values are the values provided by OTRC and the “Estimated” values are the values obtained from the equation provided in Table 3.3.2.1.

The “TLP Offset – Significant Wave Height” relationship was used to calculate the TLP offsets used for each seastate defined in the wave scatter diagram. Fig. 3.3.2.1 contains a plot of the estimated mean offsets calculated for each fatigue seastate. Table 3.1.2.1 contains a tabular summary of the estimated mean offsets obtained for each fatigue seastate. The corresponding mean TLP setdown estimates are also included in Table 3.1.2.1.

TLP Low-Frequency Motions for the Wave-Generated Fatigue Seastates

Estimated low frequency motions were also provided by OTRC for the same six (6) seastates used for the mean offset estimates. A relationship between the TLP low-frequency motion and significant wave height was developed using this seastates. The equation derived from the provided data is defined in Table 3.3.2.2. Again, the “Raw” values are the values provided by OTRC and the “Estimated” values are the values obtained from the equation provided in Table 3.3.2.2.

The “TLP Low-Frequency Motion – Significant Wave Height” relationship was used to calculate the TLP low-frequency motions used for each seastate defined in the wave scatter diagram. Fig. 3.3.2.2 contains a plot of the estimated mean offsets calculated for each fatigue seastate. Table 3.1.2.1 includes a tabular summary of the estimated low-frequency motions obtained for each fatigue seastate. The corresponding heave motions generated by the TLP setdown are also included in Table 3.1.2.1.

TLP Wave-Frequency Motions for the Fatigue Seastates

The TLP wave-frequency motions used for the wave-generated fatigue analysis were generated from the TLP surge, sway, pitch, roll, and yaw RAOs shown in Fig. 3.3.1.1. Since the magnitude of the dynamic TLP setdown is affected by the TLP’s mean offset different heave RAOs were generated for the different fatigue seastates. The heave RAOs used for the fatigue analysis are shown in Fig. 3.3.2.3.

Table 3.1.1
Goda Three-parameter Wave Spectral Form

$$S(\omega) = \alpha H_s^2 \frac{\omega^{-5}}{\omega_p^{-4}} \exp\left[-1.25(\omega/\omega_p)^{-4}\right] \gamma^\beta$$

$$\alpha = \frac{0.0624}{0.230 + 0.0336\gamma - 0.185(1.9 + \gamma)^{-1}}$$

$$\beta = \exp\left[\frac{-(\omega - \omega_p)^2}{2\tau^2 \omega_p^2}\right]$$

$$\tau = 0.07 \quad \text{for } \omega \leq \omega_p$$

$$\tau = 0.09 \quad \text{for } \omega > \omega_p$$

$$\omega = \frac{2\pi}{T}; \quad \omega_p = \frac{2\pi}{T_p}$$

H_s = Significant Wave Height

T = period in seconds

T_p = peak period

γ = peakedness; ($\gamma = 1$ results in Pierson-Moskowitz)

**Table 3.1.1.1
Design Storm Definitions**

Storm Condition	Sig. Wave Height (ft.)	Peak Period (sec.)	JONSWAP Peakedness Factor	Surf. Cur. "V" (ft/sec)	Mean TLP Offset		Low Freq. Motion	
					Offset (% W.D.)	Offset (ft.)	RMS (ft.)	Tz (sec.)
1 Year Winter Storm	16.0	9.0	1.0	1.2	2%	120	6.0	200
100 Year Hurricane	41.0	14.0	2.0	4.0	6%	360	22.2	200
100 Year Loop Current	9.0	8.0	1.0	7.0	9%	540	2.0	200

**Table 3.1.1.2
Hurricane and Winter Storm Current Profiles**

Depth (ft.)	Velocity (ft/sec)
0	V
300	V
400	0.2
6000	0.2

**Table 3.1.1.3
100-year Loop Current Current Profile**

Depth (ft.)	Elevation (ft. from Mud)	Velocity (ft/sec)
0	6000	7.00
82	5918	7.00
164	5836	6.94
656	5344	2.86
1230	4770	1.62
2214	3786	0.87
2870	3130	0.50
3280	2720	0.31
6000	0	0.00

Table 3.1.2.1
Wave Fatigue Scatter Diagram

TLP Offsets and Low Frequency Motions are Derived Using Data from OTRC

Fatigue Bin	Wave Definition		Mean Offset (ft.)	Mean Setdown (ft.)	Estimated Low Freq. Motions			Probability
	Hs (ft.)	Tz (sec.)			Surge RMS (ft.)	Heave RMS (ft.)	Tz (sec.)	
1	2.0	2.0	6.0	0.00	0.1	0.00	200	4.1895E-02
2	2.0	3.0	6.0	0.00	0.1	0.00	200	2.2055E-01
3	2.0	4.0	6.0	0.00	0.1	0.00	200	1.0194E-01
4	4.0	3.0	16.0	0.02	4.0	0.01	200	8.1279E-02
5	4.0	4.0	16.0	0.02	4.0	0.01	200	1.9041E-01
6	4.0	5.0	16.0	0.02	4.0	0.01	200	5.3197E-02
7	6.0	4.0	28.0	0.07	7.9	0.04	200	8.8356E-02
8	6.0	5.0	28.0	0.07	7.9	0.04	200	7.2831E-02
9	6.0	6.0	28.0	0.07	7.9	0.04	200	1.3813E-02
10	8.0	5.0	42.0	0.15	11.8	0.08	200	4.1781E-02
11	8.0	6.0	42.0	0.15	11.8	0.08	200	1.6324E-02
12	10.0	6.0	59.0	0.29	15.8	0.16	200	1.3242E-02
13	12.0	6.0	76.0	0.48	19.7	0.25	200	5.1368E-03
14	14.0	6.5	95.0	0.75	23.5	0.37	200	3.3107E-03
15	16.0	7.5	116.0	1.12	27.2	0.53	200	5.1368E-04
16	18.0	7.7	137.0	1.56	30.7	0.70	200	3.5386E-04
17	20.0	7.9	158.0	2.08	34.0	0.90	200	2.5117E-04
18	22.0	8.1	180.0	2.70	37.1	1.11	200	1.5982E-04
19	24.0	8.3	202.0	3.40	39.9	1.34	200	1.0270E-04
20	26.0	8.6	224.0	4.18	42.4	1.58	200	6.8494E-05
21	28.0	8.8	245.0	5.00	44.6	1.82	200	5.1368E-05
22	30.0	9.0	265.0	5.85	46.4	2.05	200	3.0319E-05
23	32.0	9.2	285.0	6.77	46.6	2.21	200	2.2828E-05
24	34.0	9.4	303.0	7.65	46.8	2.36	200	1.3703E-05
25	36.0	9.7	319.0	8.48	47.0	2.50	200	9.7024E-06
26	38.0	9.9	334.0	9.30	47.2	2.63	200	6.5070E-06
27	41.0	10.3	352.0	10.32	47.6	2.79	200	4.3377E-06
Total								0.946

**Table 3.2.1.1
Riser Design Load Cases**

Case	Riser Condition	Contents (ppg)		Int. Press. (psi) ¹		Design Environment	Damage Condition	Cf	Tension Factor
		Annulus	Tubing	Annulus	Tubing				
WPT-1	Riser Pressure Test	8.60	NA	10,000	NA	1 Yr. Winter Storm	Intact	1.20	1.30
PNS-1	Normal Shut-in	0.04	5.50	0	8,500	1 Yr. Winter Storm	Intact	1.00	1.30
PHN-1	Shut-in w/ Hurricane	0.04	5.50	100	8,500	100 Yr. Hurricane	Intact	1.20	1.30
PCN-1	Maximum Producing	0.04	5.50	100	8,500	100 Yr. Loop Current	Intact	1.20	1.60
PCL-1	Shut-in with Leak	5.50	5.50	8,500	8,500	100 Yr. Loop	Intact	1.50	1.60
PCK-T1	Well Killed - Tubing	15.50	15.50	0	0	100 Yr. Loop	Intact	1.50	1.60
PNK-T1D	Well Killed - Tubing	15.50	15.50	0	0	1 Yr. Winter Storm	Lost 1 Ten. Cyl.	1.20	1.08

Notes:

1. Internal Pressure at the Surface.
2. Load Case Rationale
 - WPT-1: Maximum internal pressure.
 - PNS-1: Maximum pressure with a normal operating stress criterion
 - PHN-1: Maximum storm condition with extreme stress criterion
 - PCL-1: Maximum pressure condition with survival stress criterion
 - PCK-T1: Heaviest riser with an extreme storm condition.
 - PNK-T1D: Heaviest riser with lowest tension. This may be most severe for joints above the lower stress joint.

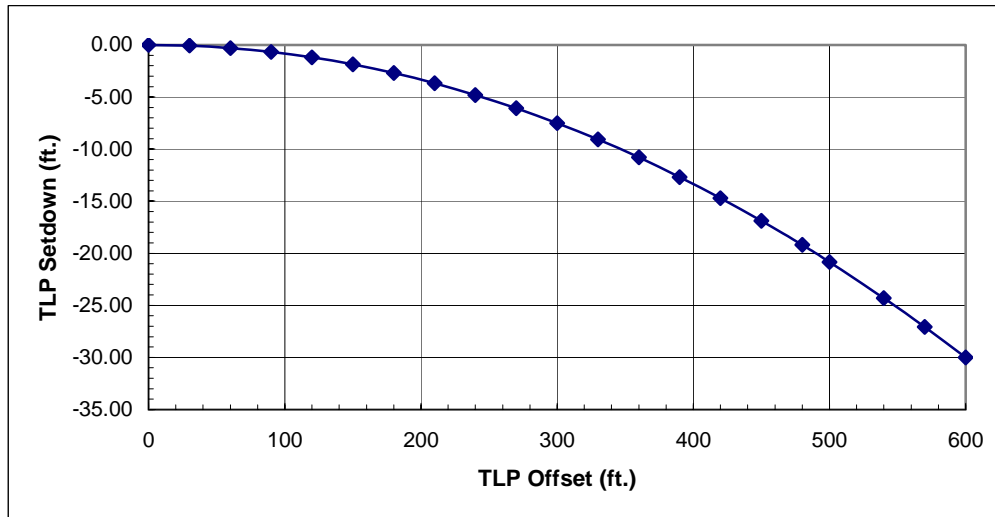
Table 3.3.1.1
TLP Setdown Estimate

TLP Setdown Factor = -8.333E-05

Estimated TLP Setdown = (TLP Setdown Factor) * (TLP Offset)²

TLP Offset (ft.)	TLP "Setdown" (ft.)
0	0.00
30	-0.08
60	-0.30
90	-0.68
120	-1.20
150	-1.88
180	-2.70
210	-3.68
240	-4.80
270	-6.08
300	-7.50

TLP Offset (ft.)	TLP "Setdown" (ft.)
300	-7.50
330	-9.08
360	-10.80
390	-12.68
420	-14.70
450	-16.88
480	-19.20
500	-20.83
540	-24.30
570	-27.08
600	-30.00



Note: This Estimate of TLP Setdown Does Not Include Tendon Stretch.

Table 3.3.2.1
TLP Offset Estimates for
Six Fatigue Seastates

Raw Data Provided by OTRC
Offset Estimate = $Ax^3 + Bx^2 + Cx + D$
A = -0.0055; B = 0.3660
C = 2.8434; D = -1.4867

Wave Description		TLP Offset	
Hsig (ft.)	Tz (sec.)	Raw (ft.)	Estimated (ft.)
3.0	3.2	10.3	10.2
6.0	5.0	27.9	27.6
11.0	6.1	65.5	66.8
18.0	7.7	137.5	136.2
30.0	9.0	264.7	264.7
41.0	13.6	352.6	351.3

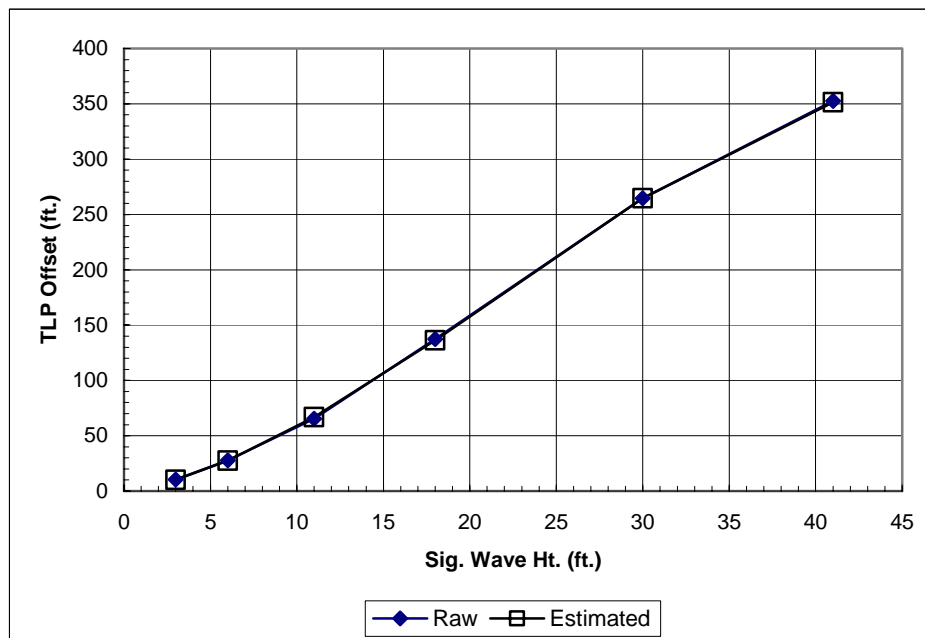


Table 3.3.2.2
TLP Offset Estimates for
Six Fatigue Seastates

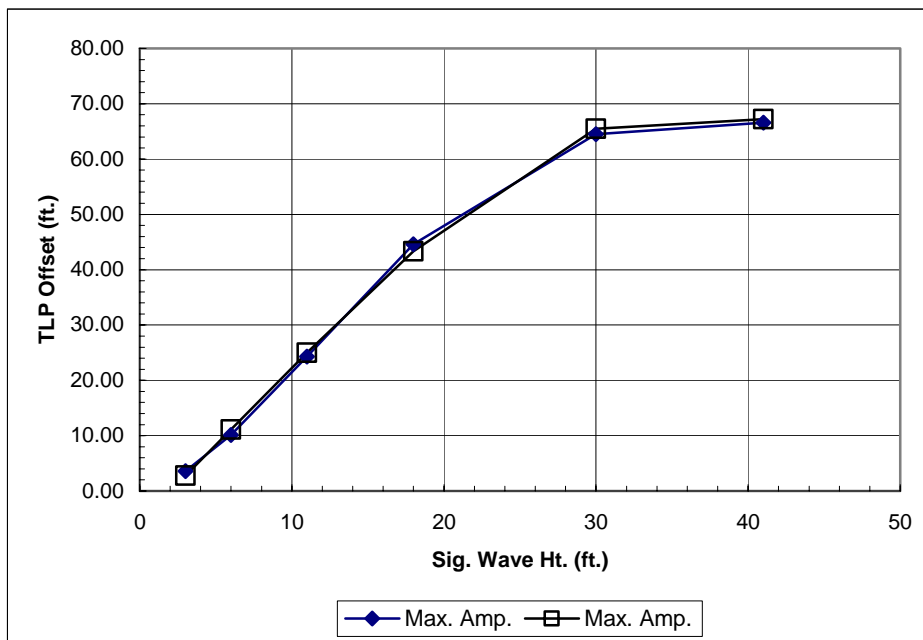
Raw Data Provided by OTRC

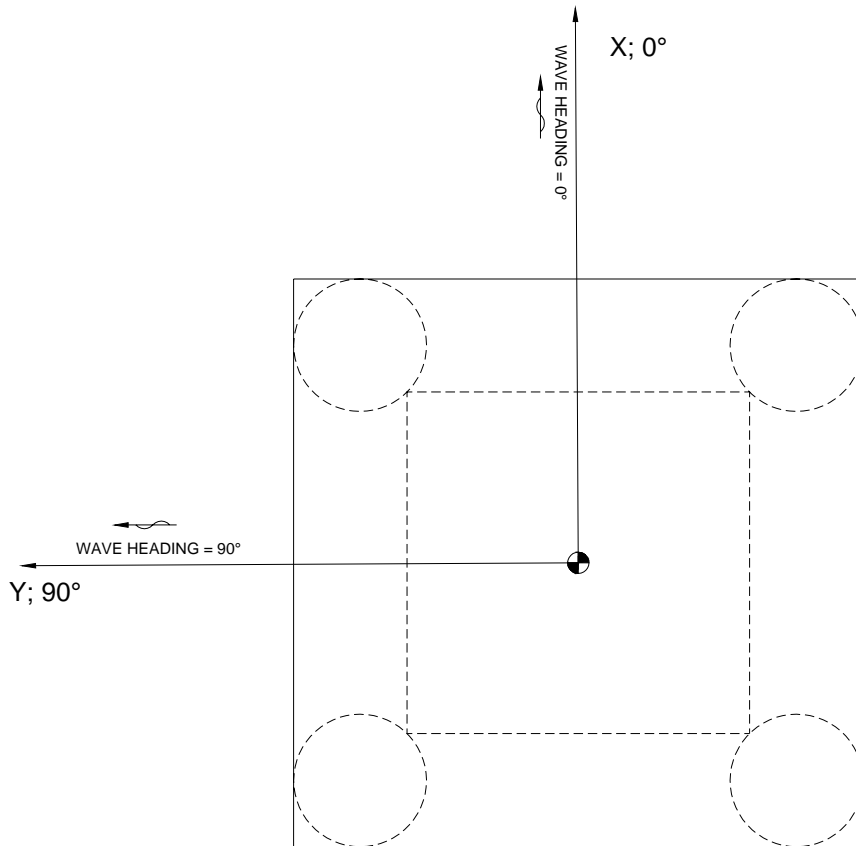
Surge Low Freq. Motion Estimate = $Ax^3 + Bx^2 + Cx + D$

A = -0.0011; B = 0.0244

C = 2.6158; D = -5.2550

Wave Description		Surge Low Freq. Motion			
Hsig (ft.)	Tz (sec.)	Raw Values		Estimated Values	
		Max. Amp. (ft.)	Tz (sec.)	Max. Amp. (ft.)	Tz (sec.)
3.0	3.2	3.60	200	2.8	200
6.0	5.0	10.10	200	11.1	200
11.0	6.1	24.30	200	25.0	200
18.0	7.7	44.60	200	43.3	200
30.0	9.0	64.50	200	65.5	200
41.0	10.3	66.60	200	67.2	200





Z-COORDINATE IS POSITIVE UPWARD
ORIGIN OF (X, Y, Z) SYSTEM IS AT MEAN WATER SURFACE
NOMINAL TLP DRAFT = 102 FEET

Fig. 3.3.1 TLP Motion Coordinate System

Storm Heading = 0 deg.; 100-Year Hurricane

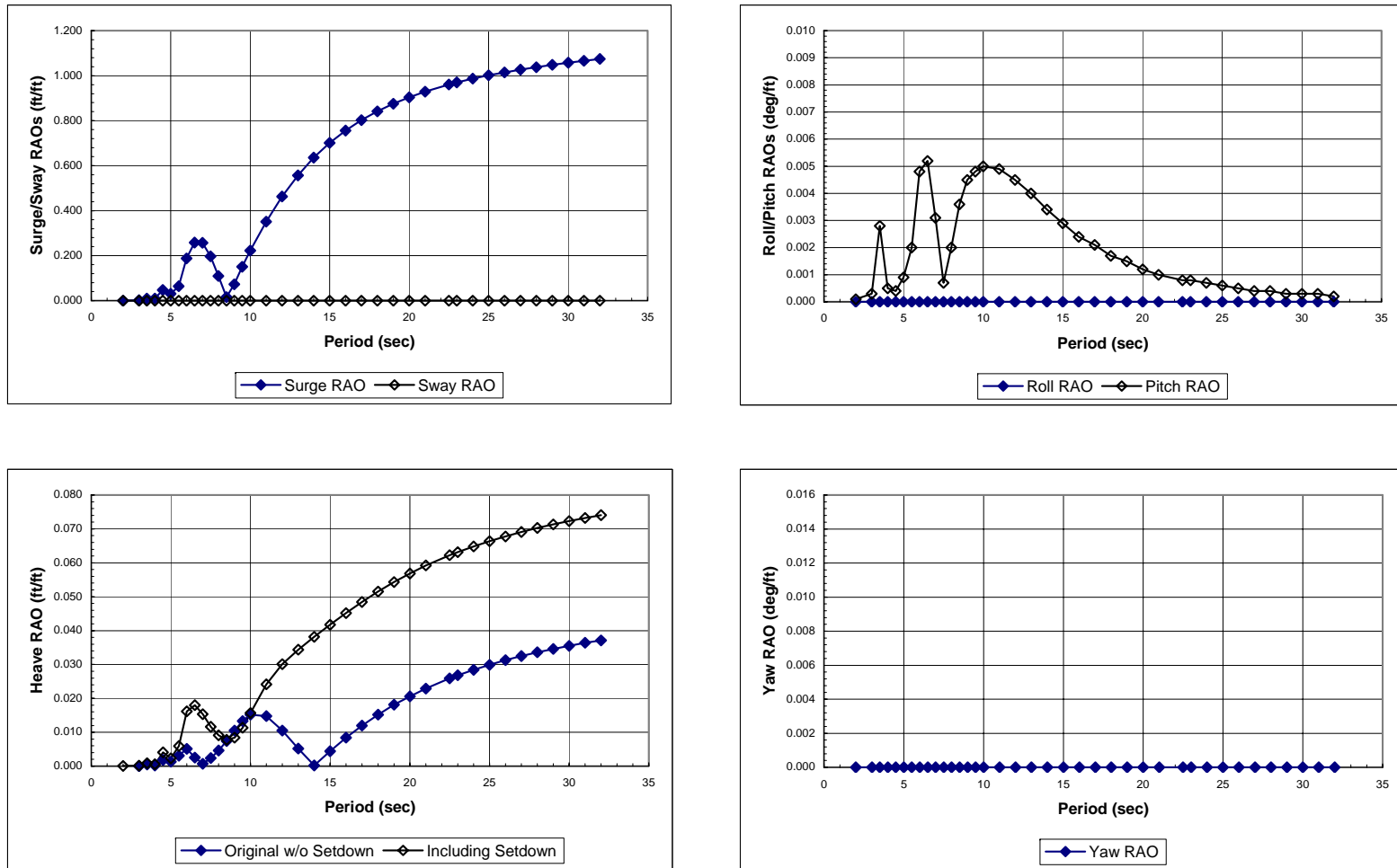


Fig. 3.3.1.1 TLP RAOs

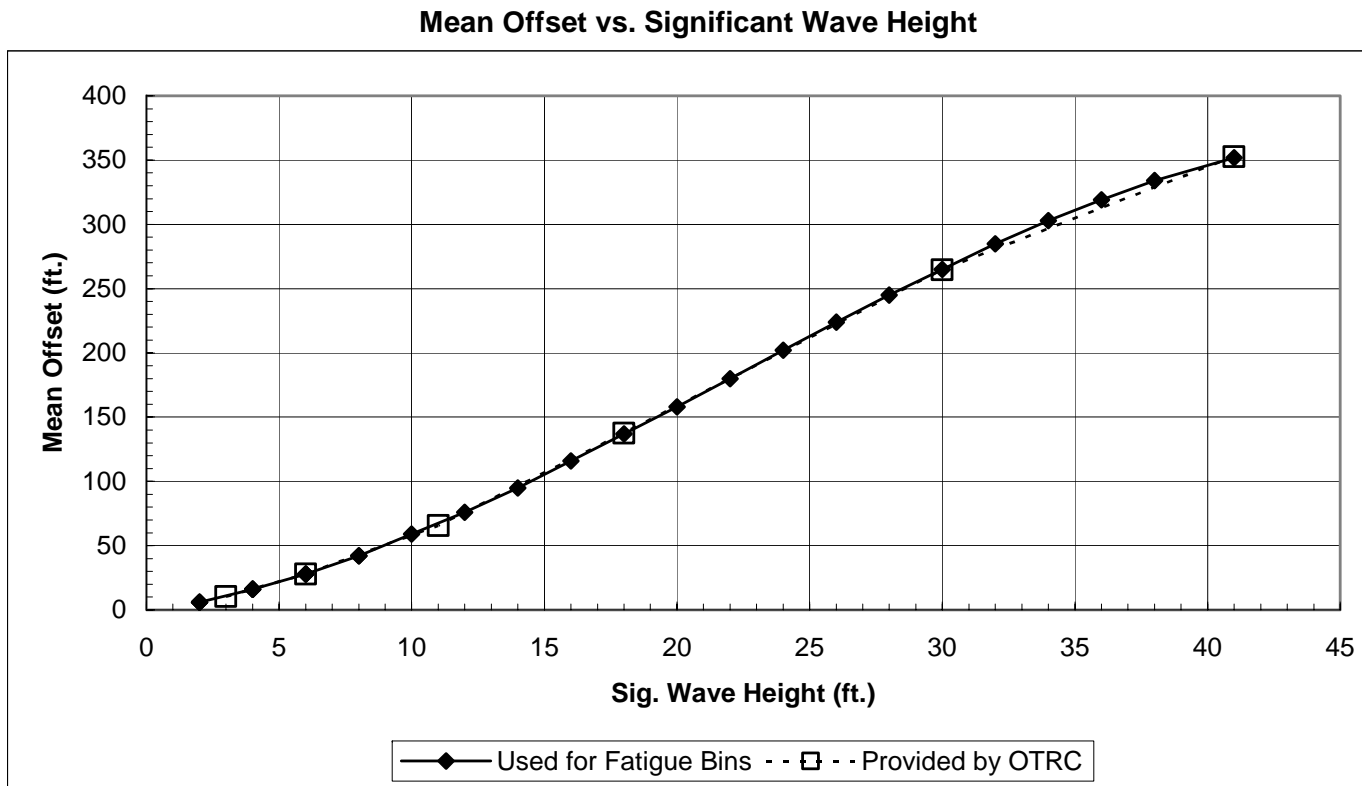


Fig. 3.3.2.1 TLP Mean Offsets Used for the Fatigue Seastates

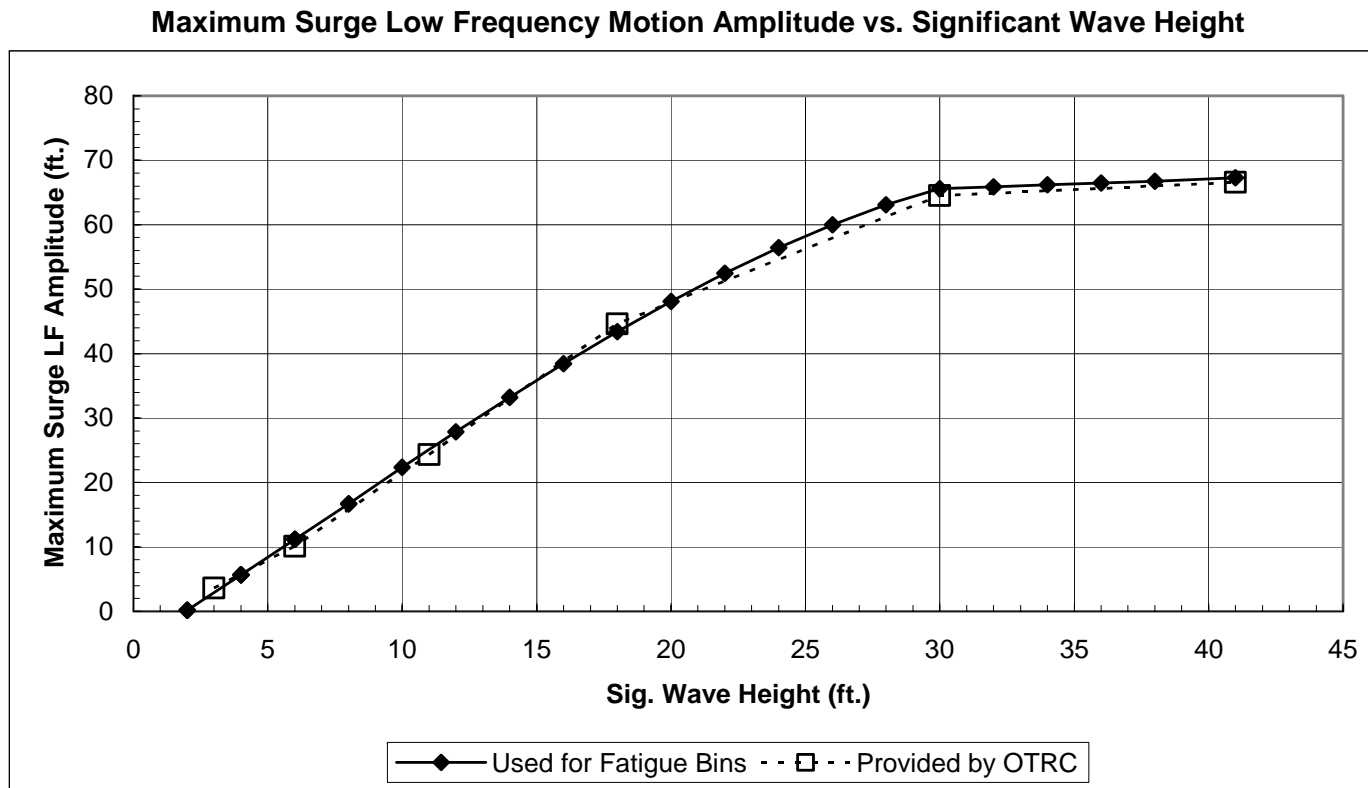


Fig. 3.3.2.2 TLP Surge Low Frequency Motion Amplitudes Used for the Fatigue Seastates

Storm Heading = 0 deg.

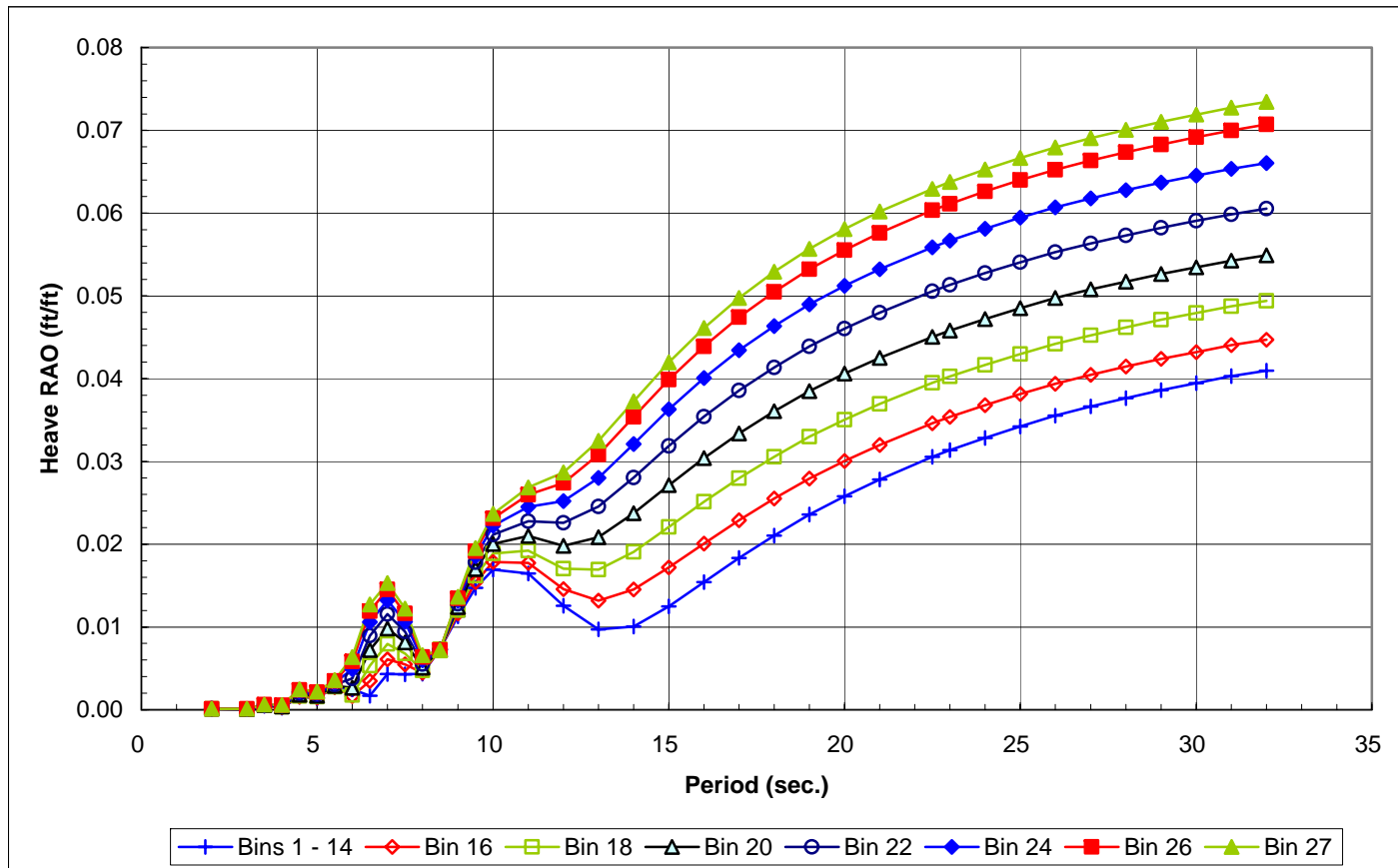


Fig. 3.3.2.3 TLP Heave RAOs Used for the Fatigue Seastates

4 ANALYSIS DETAILS

4.1 DYNAMIC ANALYSIS PROGRAM

Dynamic analyses of the “all-steel” and “composite-steel” risers were performed using SES’s proprietary coupled analysis program, RAMS. RAMS has the ability to perform fully coupled frequency-domain and/or time-domain solutions. These fully coupled solutions include models of host, moorings/tendons, and risers. The coupled analysis capabilities of RAMS were not used for these riser analyses. Instead, the motions of the TLP were provided to SES.

RAMS uses a three-dimensional rod finite element formulation to represent the riser. Both axial and bending deformations are modeled, but torsion is ignored. Large deflections and rotations are accommodated, though strains are assumed to remain small. Material behavior is assumed to be linearly elastic.

The dynamic analyses of the risers were performed using the frequency-domain capabilities of RAMS.

Frequency-domain Analysis

The frequency-domain approach linearizes the equations of motion about a mean or static configuration that is calculated using the full nonlinearity of the rod element formulation. This static solution includes the effects of gravity, buoyancy, drag from steady ocean currents, and host offset, subject to imposed boundary conditions. Results of the dynamic analysis are available as statistics (i.e., means and variances) for each of the response quantities of interest.

4.2 EXTREME RESPONSE CALCULATIONS

For stochastic processes such as dynamic riser response, response extremes may be expressed as a value with a certain probability of being exceeded during an event of a given duration. Extreme values reported in this study are “Most Probable Maximum” (MPM) values unless otherwise noted. The MPM values provided correspond to a 63%

exceedance probability and are based on 3-hour event durations. The extreme values are calculated from the predicted mean and RMS (square-root of variance) values according to:

$$Extreme = mean + factor \times RMS$$

where *factor* is a dynamic peak factor calculated by RAMS, which depends on the specified exceedance probability, event duration, and zero up-crossing period.

4.3 APPLICATION OF ENVIRONMENTAL LOADS

A conservative approach is adopted which assumes that wind, waves, and current all act in the same direction (the “environmental heading”) for any given event being analyzed.

No current was applied to the riser in the cumulative wave-generated fatigue analyses. This is a conservative assumption that removes any damping that may be generated by current loads. This assumption is made because the waves and currents are not necessarily correlated, therefore, there is no guarantee that the current loading will be present to provide any damping of the response.

4.4 FATIGUE CURVES

The fatigue analysis was performed using the S-N Curve Approach. The S-N curves used for the fatigue analyses are defined in Table 4.4.1 and Fig. 4.4.1. The S-N curves are defined in terms of two empirical constants and take the following form:

$$N = C(\Delta\sigma)^{-m} \quad (4.7.1)$$

where,

N = Number of cycles to failure

$\Delta\sigma$ = Stress range (twice the stress amplitude)

C, m = Empirical constants developed from testing

The S-N curves used include the DnV-B, DnV-C, and DnV-F2. The DnV-B S-N curve was used for machined parent material locations. The DnV-C and DnV-F2 curves were

used for welded sections. The DnV-C curve produces longer fatigue lives than does the DnV-F2 curve. It is also more difficult to produce a weld that satisfies the DnV-C curve requirements compared to the DnV-F2 curve.

Table 4.4.1
S-N Curve Definitions

Fatigue Curve	Inverse Slope of the S-N Curve	Fatigue Curve Constant "K"	
		for Stress Range in ksi	for Stress Range in psi
DnV-D	3.00	4.62E+09	4.62E+18
DnV-E	3.00	3.19E+09	3.19E+18
DnV-F2	3.00	1.30E+09	1.30E+18
API-X'	3.74	1.79E+10	2.98E+21

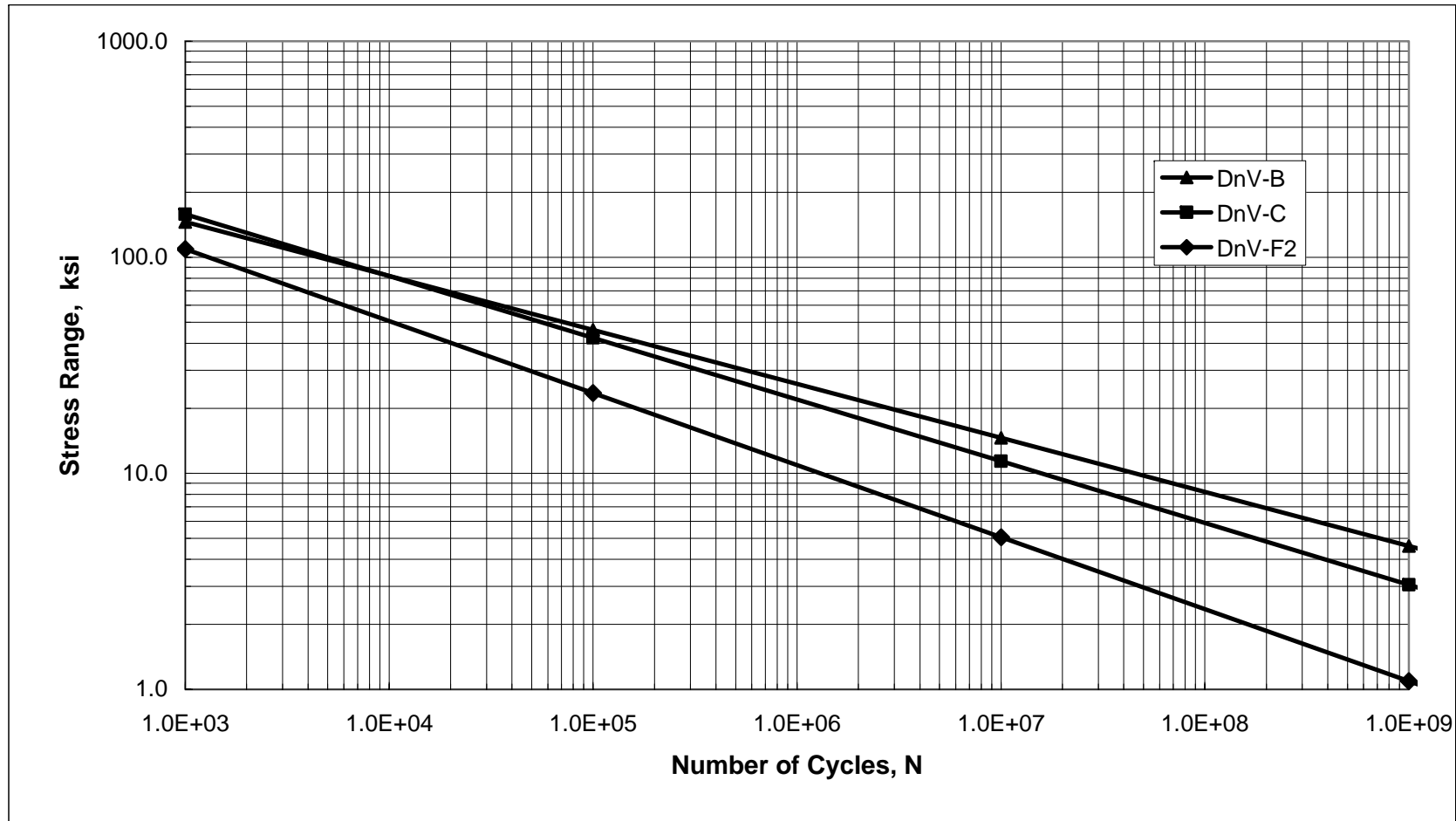


Fig. 4.4.1 Plots of the Fatigue S-N Curves

5 RESULTS OF THE DESIGN STORM ANALYSIS

5.1 GENERAL

Design storm analyses were performed for the “all-steel” and “composite-steel” riser configurations. These analyses were performed to verify that the maximum stresses generated by the imposed loads and displacements do not exceed allowable values. Maximum loads for the critical riser components were also generated and tabulated for the design load cases evaluated.

Table 3.2.1.1 contains a description of the design storm load cases considered for these analyses. The designs of typical top tensioned risers in the Gulf of Mexico are generally governed by the equivalent of Load Cases PNS-1, PHN-1, and PCN-1. Therefore, only these load cases were evaluated in this study.

Maximum stresses were generated for the components along the entire length of the “all-steel” riser configuration. Mean, dynamic, and maximum loads were also tabulated for critical locations along the length of the riser.

Maximum stresses were generated for the stress joint and tensioner joint in the “composite-steel” riser configuration. Mean, dynamic, and maximum loads were also tabulated for critical locations along the entire length of the riser. The stress evaluation of the composite riser joints were performed by others using the load information generated in these analyses.

5.2 “ALL-STEEL” RISER CONFIGURATION DESIGN STORM ANALYSIS

5.2.1 Load Case PNS-1: Normal Shut-in with a 1-Year Winter Storm

Table 5.2.1.1 contains a summary of the mean, RMS, and maximum loads (effective tensions, shear forces, and bending moments) obtained at critical locations along the length of the riser. The tabulated loads are the loads obtained for the combined riser cross-section (combined section properties of the outer casing and production tubing). Fig. 5.2.1.1 contains plots of the mean, minimum, and maximum bending moment distributions along the length of the riser. Fig. 5.2.1.1 contains a plot of the bending

moment distribution along the entire length of the riser. Fig. 5.2.1.1 also contains plots of the bending moment distributions in the lower 200 ft. of the riser and the upper 300 ft. of the riser. Note that “peaks” in the bending moment distributions occur at the bottom boundary condition and at the tensioner centralizer location.

Table 5.2.1.2 contains a summary of the maximum stresses obtained for critical outer casing components. A maximum stress of ~32 ksi occurs at the top of the stress joint taper. This maximum stress is equal to 40% of the yield stress (S_{yield}) of 80 ksi. This is well below the maximum allowable stress of 53.3 ksi (67% of S_{yield}) specified for this load case.

5.2.2 Load Case PHN-1: Shut-in with a 100-Year Hurricane

Table 5.2.2.1 contains a summary of the mean, RMS, and maximum loads (effective tensions, shear forces, and bending moments) obtained at critical locations along the length of the riser. The tabulated loads are the loads obtained for the combined riser cross-section (combined section properties of the outer casing and production tubing). Fig. 5.2.2.1 contains plots of the mean, minimum, and maximum bending moment distributions along the length of the riser.

Table 5.2.2.2 contains a summary of the maximum stresses obtained for critical outer casing components. A maximum stress of ~58 ksi occurs at the top of the stress joint taper. This maximum stress is equal to ~73% of the yield stress (S_{yield}) of 80 ksi. This is below the maximum allowable stress of 64.0 ksi (80% of S_{yield}) specified for this load case.

5.2.3 Load Case PCN-1: Maximum Producing with a 100-Year Loop Current

Table 5.2.3.1 contains a summary of the mean, RMS, and maximum loads (effective tensions, shear forces, and bending moments) obtained at critical locations along the length of the riser. The tabulated loads are the loads obtained for the combined riser cross-section (combined section properties of the outer casing and production tubing). Fig. 5.2.3.1 contains plots of the mean, minimum, and maximum bending moment distributions along the length of the riser.

Table 5.2.3.2 contains a summary of the maximum stresses obtained for critical outer casing components. A maximum stress of ~60 ksi occurs at the top of the stress joint taper. This maximum stress is equal to ~75% of the yield stress (S_{yield}) of 80 ksi. This is below the maximum allowable stress of 64.0 ksi (80% of S_{yield}) specified for this load case.

5.3 “COMPOSITE-STEEL” RISER CONFIGURATION DESIGN STORM ANALYSIS

5.3.1 Load Case PNS-1: Normal Shut-in with a 1-Year Winter Storm

Table 5.3.1.1 contains a summary of the mean, RMS, and maximum loads (effective tensions, shear forces, and bending moments) obtained at critical locations along the length of the “composite-steel” riser. The tabulated loads are the loads obtained for the combined riser cross-section (combined section properties of the outer casing and production tubing). Fig. 5.3.1.1 contains plots of the mean, minimum, and maximum bending moment distributions along the length of the riser. Note that “peaks” in the bending moment distributions occur at the bottom boundary condition and at the tensioner centralizer location.

Table 5.3.1.2 contains a summary of the maximum stresses obtained for critical locations in the stress joint and tensioner joint. A maximum stress of ~26 ksi occurs at the top of the stress joint taper. This maximum stress is equal to ~33% of the yield stress (S_{yield}) of 80 ksi. This is well below the maximum allowable stress of 53.3 ksi (67% of S_{yield}) specified for this load case.

5.3.2 Load Case PHN-1: Shut-in with a 100-Year Hurricane

Table 5.3.2.1 contains a summary of the mean, RMS, and maximum loads (effective tensions, shear forces, and bending moments) obtained at critical locations along the length of the “composite-steel” riser. The tabulated loads are the loads obtained for the combined riser cross-section (combined section properties of the outer casing and production tubing). Fig. 5.3.2.1 contains plots of the mean, minimum, and maximum bending moment distributions along the length of the riser.

Table 5.3.2.2 contains a summary of the maximum stresses obtained for critical outer casing components. A maximum stress of ~50 ksi occurs at the top of the stress joint taper. This maximum stress is equal to ~63% of the yield stress (S_{yield}) of 80 ksi. This is below the maximum allowable stress of 64.0 ksi (80% of S_{yield}) specified for this load case.

5.3.3 Load Case PCN-1: Maximum Producing with a 100-Year Loop Current

Table 5.3.3.1 contains a summary of the mean, RMS, and maximum loads (effective tensions, shear forces, and bending moments) obtained at critical locations along the length of the “composite-steel” riser. The tabulated loads are the loads obtained for the combined riser cross-section (combined section properties of the outer casing and production tubing). Fig. 5.3.3.1 contains plots of the mean, minimum, and maximum bending moment distributions along the length of the riser.

Table 5.3.3.2 contains a summary of the maximum stresses obtained for critical outer casing components. A maximum stress of ~58 ksi occurs at the bottom of the stress joint. This maximum stress is equal to ~73% of the yield stress (S_{yield}) of 80 ksi. This is below the maximum allowable stress of 64.0 ksi (80% of S_{yield}) specified for this load case.

5.4 RISER CONFIGURATION RESULT COMPARISON

Table 5.4.1 contains a summary and comparison of the mean and maximum bending moments obtained at the bottom of the stress joint and at the tensioner centralizer for the “all-steel” and “composite-steel” riser configurations. The maximum bending moments obtained at the bottom of the “composite-steel” riser’s stress joint are significantly less than those obtained at the base of the “all-steel” riser stress joint. These lower values are a product of the smaller stress joint and lower tension required by the “composite-steel” riser configuration.

The bending moments generated in the tensioner joint at the location of the tensioner centralizer are about the same for both riser configurations.

Table 5.4.2 contains a summary of the mean and maximum stresses obtained at the bottom of the stress joint and at the tensioner centralizer for the “all-steel” and “composite-steel” riser configurations. All of the stresses satisfy the allowable stress criteria. The maximum stresses generated for the “composite-steel” riser’s stress joint are a little smaller than those obtained for the “all-steel” riser.

The “composite-steel” riser’s stresses at the tensioner centralizer are significantly smaller than those generated in the “all-steel” riser configuration. This is due to the lower tension required for the “composite-steel” riser over the “all-steel” riser.

Table 5.2.1.1
“All-Steel” Riser Configuration
Design Storm Load Summary for the Combined Cross-Section
Load Case PNS-1: Normal Shut-in with a 1-Year Winter Storm

Wellhead Tilt = 1 deg.
Cd = 0.7 in the Region with Fairings; Cd = 1.0 in the Regions without Fairings
Nominal Applied Tension = 864 kips; Well Offset = 0 ft.
Riser Contents: Annulus = 0.04 ppg; Production Tube = 5.50 ppg
Riser Surface Pressures: Annulus = 100 psi; Production Tube = 8,500 psi

Location	Elevation (ft.)	Effective Tension			Shear			Bending Moment		
		Mean (kips)	RMS (kips)	Maximum (kips)	Mean (kips)	RMS (kips)	Maximum (kips)	Mean (ft-kips)	RMS (ft-kips)	Maximum (ft-kips)
Base of the Stress Joint	10.0	213.6	4.6	231.5	9.6	0.8	12.9	446.1	27.3	551.9
Base of the Stress Joint Taper	12.0	214.7	4.6	232.7	9.6	0.8	12.9	420.9	25.7	520.4
Top of the Stress Joint Taper	42.0	222.3	4.6	240.4	9.6	0.8	12.9	134.5	7.6	164.0
Stress Joint Top Connector	45.0	222.7	4.6	240.7	9.6	0.8	12.9	117.1	6.5	142.5
Mean Water Level	6000.0	837.6	4.5	854.9	8.3	1.7	15.1	0.5	1.4	6.0
Tensioner Joint's Bottom Connector	6050.0	845.2	4.4	862.5	8.3	1.7	15.1	0.3	0.2	1.3
Bottom of the Tensioner Joint Threads	6055.0	846.2	4.4	863.5	8.3	1.7	15.1	0.6	0.5	2.6
Tensioner Joint at the Tensioner Ring	6060.0	848.0	4.4	865.4	8.3	1.7	15.1	1.0	1.0	4.9
Tensioner Joint at the Tensioner Guide	6080.0	-23.2	0.0	-23.2	0.0	0.4	1.4	2.9	4.8	22.0
Top of the Tensioner Joint	6088.0	-20.0	0.0	-20.0	0.0	0.3	1.3	1.2	2.0	9.1

Table 5.2.1.2
“All-Steel” Riser Configuration
Outer Casing Mid-Wall von-Mises Stresses
Load Case PNS-1: Normal Shut-in with a 1-Year Winter Storm

Wellhead Tilt = 1 deg.
Cd = 0.7 in the Region with Fairings; Cd = 1.0 in the Regions without Fairings
Nominal Applied Tension = 864 kips; Well Offset = 0 ft.
Riser Contents: Annulus = 0.04 ppg; Production Tube = 5.50 ppg
Riser Surface Pressures: Annulus = 100 psi; Production Tube = 8,500 psi

Location	Elevation (ft.)	Pressure		Effective Tension		Bending Moment		von-Mises Stresses	
		Internal (psi)	External (psi)	Mean (kips)	Maximum (kips)	Mean (ft-kips)	Maximum (ft-kips)	Mean (ksi)	Maximum (ksi)
Base of the Stress Joint	10.0	113	2662	301	316	442	547	16.38	19.52
Base of the Stress Joint Taper	12.0	113	2661	302	317	417	516	15.68	18.63
Top of the Stress Joint Taper	42.0	113	2648	307	322	129	157	28.18	31.96
Stress Joint Top Connector	45.0	113	2647	308	323	112	137	26.25	29.52
Mean Water Level	6000.0	100	0	756	770	1	6	22.17	23.27
Tensioner Joint's Bottom Connector	6050.0	100	0	762	777	0	1	22.32	22.87
Bottom of the Tensioner Joint Threads	6055.0	100	0	763	777	1	3	22.38	23.06
Tensioner Joint at the Tensioner Ring	6060.0	100	0	765	779	1	5	7.50	7.78
Tensioner Joint at the Tensioner Guide	6080.0	100	0	-107	-107	3	22	0.91	0.32
Top of the Tensioner Joint	6088.0	100	0	-104	-104	1	9	0.94	0.69

Table 5.2.2.1
“All-Steel” Riser Configuration
Design Storm Load Summary for the Combined Cross-Section
Load Case PHN-1: Shut-in with a 100-Year Hurricane

Wellhead Tilt = 1 deg.
Cd = 0.7 in the Region with Fairings; Cd = 1.0 in the Regions without Fairings
Nominal Applied Tension = 864 kips; Well Offset = 0 ft.
Riser Contents: Annulus = 0.04 ppg; Production Tube = 5.50 ppg
Riser Surface Pressures: Annulus = 100 psi; Production Tube = 8,500 psi

Location	Elevation (ft.)	Effective Tension			Shear			Bending Moment		
		Mean (kips)	RMS (kips)	Maximum (kips)	Mean (kips)	RMS (kips)	Maximum (kips)	Mean (ft-kips)	RMS (ft-kips)	Maximum (ft-kips)
Base of the Stress Joint	10.0	284.1	39.2	431.4	33.3	4.8	51.3	1131.1	103.2	1511.3
Base of the Stress Joint Taper	12.0	285.4	39.2	432.8	33.3	4.8	51.3	1060.2	93.8	1405.4
Top of the Stress Joint Taper	42.0	294.4	39.4	442.6	33.3	4.8	51.3	290.6	14.3	342.4
Stress Joint Top Connector	45.0	294.9	39.4	443.2	33.3	4.8	51.2	247.9	12.5	294.0
Mean Water Level	6000.0	908.9	39.0	1055.3	26.9	8.7	59.5	2.9	3.1	15.3
Tensioner Joint's Bottom Connector	6050.0	916.4	39.0	1062.8	26.6	8.6	58.8	3.7	3.1	15.4
Bottom of the Tensioner Joint Threads	6055.0	917.4	39.0	1063.8	26.6	8.5	58.8	6.3	5.2	25.9
Tensioner Joint at the Tensioner Ring	6060.0	919.3	39.0	1065.7	26.6	8.5	58.6	9.8	8.6	42.4
Tensioner Joint at the Tensioner Guide	6080.0	-23.2	0.0	-23.3	0.0	0.9	3.5	8.8	13.3	59.9
Top of the Tensioner Joint	6088.0	-20.0	0.0	-20.1	0.0	0.8	3.0	3.6	5.5	24.6

Table 5.2.2.2
“All-Steel” Riser Configuration
Outer Casing Mid-Wall von-Mises Stresses
Load Case PHN-1: Shut-in with a 100-Year Hurricane

Wellhead Tilt = 1 deg.
Cd = 0.7 in the Region with Fairings; Cd = 1.0 in the Regions without Fairings
Nominal Applied Tension = 864 kips; Well Offset = 0 ft.
Riser Contents: Annulus = 0.04 ppg; Production Tube = 5.50 ppg
Riser Surface Pressures: Annulus = 100 psi; Production Tube = 8,500 psi

Location	Elevation (ft.)	Pressure		Effective Tension		Bending Moment		von-Mises Stresses	
		Internal (psi)	External (psi)	Mean (kips)	Maximum (kips)	Mean (ft-kips)	Maximum (ft-kips)	Mean (ksi)	Maximum (ksi)
Base of the Stress Joint	10.0	113	2662	361	484	1122	1499	36.74	48.94
Base of the Stress Joint Taper	12.0	113	2661	362	485	1051	1394	34.68	45.83
Top of the Stress Joint Taper	42.0	113	2648	367	491	279	328	48.23	58.04
Stress Joint Top Connector	45.0	113	2647	367	492	238	282	43.12	52.19
Mean Water Level	6000.0	100	0	815	938	3	15	24.21	29.33
Tensioner Joint's Bottom Connector	6050.0	100	0	822	944	4	15	24.49	29.53
Bottom of the Tensioner Joint Threads	6055.0	100	0	823	945	6	25	24.84	30.86
Tensioner Joint at the Tensioner Ring	6060.0	100	0	824	947	10	42	8.40	10.76
Tensioner Joint at the Tensioner Guide	6080.0	100	0	-119	-119	9	59	0.82	0.93
Top of the Tensioner Joint	6088.0	100	0	-116	-116	4	24	0.97	0.31

Table 5.2.3.1
“All-Steel” Riser Configuration
Design Storm Load Summary for the Combined Cross-Section
Load Case PCN-1: Maximum Producing with a 100-Year Loop Current

Wellhead Tilt = 1 deg.
Cd = 0.7 in the Region with Fairings; Cd = 1.0 in the Regions without Fairings
Nominal Applied Tension = 1,054 kips; Well Offset = 0 ft.
Riser Contents: Annulus = 0.04 ppg; Production Tube = 5.50 ppg
Riser Surface Pressures: Annulus = 100 psi; Production Tube = 8,500 psi

Location	Elevation (ft.)	Effective Tension			Shear			Bending Moment		
		Mean (kips)	RMS (kips)	Maximum (kips)	Mean (kips)	RMS (kips)	Maximum (kips)	Mean (ft-kips)	RMS (ft-kips)	Maximum (ft-kips)
Base of the Stress Joint	10.0	500.5	3.7	515.2	71.2	0.6	73.4	1847.7	9.6	1884.8
Base of the Stress Joint Taper	12.0	502.1	3.7	516.8	71.2	0.6	73.4	1705.4	8.6	1738.8
Top of the Stress Joint Taper	42.0	513.7	3.8	528.5	71.2	0.6	73.4	327.0	1.6	333.0
Stress Joint Top Connector	45.0	514.2	3.8	529.0	71.2	0.6	73.4	265.3	1.4	270.7
Mean Water Level	6000.0	1126.9	3.5	1140.8	52.0	1.5	57.8	4.9	1.5	10.7
Tensioner Joint's Bottom Connector	6050.0	1134.4	3.5	1148.4	50.7	1.7	57.4	6.1	0.5	8.1
Bottom of the Tensioner Joint Threads	6055.0	1135.4	3.5	1149.4	50.7	1.7	57.4	10.9	0.8	14.1
Tensioner Joint at the Tensioner Ring	6060.0	1137.3	3.5	1151.2	50.7	1.7	57.4	17.6	1.4	23.2
Tensioner Joint at the Tensioner Guide	6080.0	-23.1	0.0	-23.2	0.0	0.2	0.9	13.7	3.0	25.6
Top of the Tensioner Joint	6088.0	-20.0	0.0	-20.0	0.0	0.2	0.8	5.6	1.2	10.5

Table 5.2.3.2
“All-Steel” Riser Configuration
Outer Casing Mid-Wall von-Mises Stresses
Load Case PCN-1: Maximum Producing with a 100-Year Loop Current

Wellhead Tilt = 1 deg.
Cd = 0.7 in the Region with Fairings; Cd = 1.0 in the Regions without Fairings
Nominal Applied Tension = 1,054 kips; Well Offset = 0 ft.
Riser Contents: Annulus = 0.04 ppg; Production Tube = 5.50 ppg
Riser Surface Pressures: Annulus = 100 psi; Production Tube = 8,500 psi

Location	Elevation (ft.)	Pressure		Effective Tension		Bending Moment		von-Mises Stresses	
		Internal (psi)	External (psi)	Mean (kips)	Maximum (kips)	Mean (ft-kips)	Maximum (ft-kips)	Mean (ksi)	Maximum (ksi)
Base of the Stress Joint	10.0	113	2662	574	586	1832	1869	59.59	60.79
Base of the Stress Joint Taper	12.0	113	2661	575	587	1691	1724	55.41	56.49
Top of the Stress Joint Taper	42.0	113	2648	580	593	313	319	58.73	59.83
Stress Joint Top Connector	45.0	113	2647	581	594	254	259	51.27	52.27
Mean Water Level	6000.0	100	0	1029	1041	5	10	30.71	31.77
Tensioner Joint's Bottom Connector	6050.0	100	0	1036	1047	6	8	31.04	31.63
Bottom of the Tensioner Joint Threads	6055.0	100	0	1036	1048	10	14	31.66	32.41
Tensioner Joint at the Tensioner Ring	6060.0	100	0	1038	1050	17	23	10.76	11.08
Tensioner Joint at the Tensioner Guide	6080.0	100	0	-123	-123	14	25	0.70	0.34
Top of the Tensioner Joint	6088.0	100	0	-120	-120	6	10	0.94	0.78

Table 5.3.1.1
“Composite-Steel” Riser Configuration
Design Storm Load Summary for the Combined Cross-Section
Load Case PNS-1: Normal Shut-in with a 1-Year Winter Storm

Wellhead Tilt = 1 deg.
Cd = 0.7 in the Region with Fairings; Cd = 1.0 in the Regions without Fairings
Nominal Applied Tension = 319 kips; Well Offset = 0 ft.
Riser Contents: Annulus = 0.04 ppg; Production Tube = 5.50 ppg
Riser Surface Pressures: Annulus = 100 psi; Production Tube = 8,500 psi

Location	Elevation (ft.)	Effective Tension			Shear			Bending Moment		
		Mean (kips)	RMS (kips)	Maximum (kips)	Mean (kips)	RMS (kips)	Maximum (kips)	Mean (ft-kips)	RMS (ft-kips)	Maximum (ft-kips)
Base of the Stress Joint	10.0	78.8	2.1	86.8	3.5	0.3	4.6	193.6	9.9	231.5
Base of the Stress Joint Taper	12.0	79.8	2.1	87.8	3.5	0.3	4.6	184.1	9.3	220.0
Top of the Stress Joint Taper	28.0	82.8	2.1	90.8	3.5	0.3	4.6	118.9	5.7	140.9
Stress Joint Top Connector	40.0	84.3	2.1	92.3	3.5	0.3	4.6	83.9	3.9	98.8
Bottom of Composite Riser Section	102.0	90.7	2.1	98.7	3.5	0.3	4.5	10.7	0.4	12.2
Bottom of VIV Suppression Region	4004.0	211.2	2.0	219.1	3.2	0.4	4.9	0.2	0.6	2.5
Top of Composite Riser Section	5926.0	275.3	2.0	283.0	2.7	0.9	6.1	0.8	1.4	6.5
Mean Water Level	6000.0	282.9	2.0	290.6	2.4	1.0	6.3	1.3	3.2	14.0
Tensioner Joint's Bottom Connector	6050.0	290.5	2.0	298.2	2.4	1.0	6.4	0.2	0.6	2.7
Bottom of the Tensioner Joint Threads	6055.0	291.4	2.0	299.2	2.4	1.0	6.4	0.4	0.9	3.9
Tensioner Joint at the Tensioner Ring	6060.0	293.3	2.0	301.0	2.4	1.0	6.4	0.7	1.4	6.1
Tensioner Joint at the Tensioner Guide	6080.0	-23.2	0.0	-23.2	0.0	0.4	1.5	2.5	5.1	22.6
Top of the Tensioner Joint	6088.0	-20.0	0.0	-20.0	0.0	0.3	1.3	1.0	2.1	9.3

Table 5.3.1.2
“Composite-Steel” Riser Configuration
Outer Casing Mid-Wall von-Mises Stresses
Load Case PNS-1: Normal Shut-in with a 1-Year Winter Storm

Wellhead Tilt = 1 deg.
Cd = 0.7 in the Region with Fairings; Cd = 1.0 in the Regions without Fairings
Nominal Applied Tension = 319 kips; Well Offset = 0 ft.
Riser Contents: Annulus = 0.04 ppg; Production Tube = 5.50 ppg
Riser Surface Pressures: Annulus = 100 psi; Production Tube = 8,500 psi

Location	Elevation (ft.)	Pressure		Material Tension		Effective Tension		Bending Moment		von-Mises Stresses	
		Internal (psi)	External (psi)	Mean (kips)	Maximum (kips)	Mean (kips)	Maximum (kips)	Mean (ft-kips)	Maximum (ft-kips)	Mean (ksi)	Maximum (ksi)
Base of the Stress Joint	10.0	13	2662	-196	-190	152	158	189	226	18.39	20.95
Base of the Stress Joint Taper	12.0	13	2661	-195	-189	153	159	180	215	17.79	20.20
Top of the Stress Joint Taper	28.0	13	2654	-131	-125	156	162	114	135	22.77	25.28
Stress Joint Top Connector	40.0	13	2649	-130	-124	157	163	80	95	19.25	20.86
Bottom of Composite Riser Section	102.0	12	2621	-142	-136	161	167	10.0	11.4	-	-
Bottom of VIV Suppression Region	4004.0	4	887	72	78	175	181	0.2	2.3	-	-
Top of Composite Riser Section	5926.0	0	33	183	189	186	192	0.8	6.2	-	-
Mean Water Level	6000.0	0	0	192	198	192	198	1.3	13.4	5.78	7.51
Tensioner Joint's Bottom Connector	6050.0	0	0	198	204	198	204	0.1	2.6	5.82	6.30
Bottom of the Tensioner Joint Threads	6055.0	0	0	199	205	199	205	0.4	3.9	5.87	6.49
Tensioner Joint at the Tensioner Ring	6060.0	0	0	201	207	201	207	0.7	6.0	1.98	2.23
Tensioner Joint at the Tensioner Guide	6080.0	0	0	-116	-116	-116	-116	2.5	22.3	0.99	0.32
Top of the Tensioner Joint	6088.0	0	0	-113	-113	-113	-113	0.5	4.6	1.03	0.89

Table 5.3.2.1
“Composite-Steel” Riser Configuration
Design Storm Load Summary for the Combined Cross-Section
Load Case PHN-1: Shut-in with a 100-Year Hurricane

Wellhead Tilt = 1 deg.
Cd = 0.7 in the Region with Fairings; Cd = 1.0 in the Regions without Fairings
Nominal Applied Tension = 319 kips; Well Offset = 0 ft.
Riser Contents: Annulus = 0.04 ppg; Production Tube = 5.50 ppg
Riser Surface Pressures: Annulus = 100 psi; Production Tube = 8,500 psi

Location	Elevation (ft.)	Effective Tension			Shear			Bending Moment		
		Mean (kips)	RMS (kips)	Maximum (kips)	Mean (kips)	RMS (kips)	Maximum (kips)	Mean (ft-kips)	RMS (ft-kips)	Maximum (ft-kips)
Base of the Stress Joint	10.0	104.5	17.1	168.5	12.1	2.0	19.5	477.6	46.1	648.0
Base of the Stress Joint Taper	12.0	105.5	17.1	169.5	12.1	2.0	19.5	451.0	41.9	605.7
Top of the Stress Joint Taper	28.0	108.9	17.2	173.1	12.1	2.0	19.5	273.7	17.3	336.5
Stress Joint Top Connector	40.0	110.5	17.2	174.9	12.1	2.0	19.5	183.8	8.5	214.0
Bottom of Composite Riser Section	102.0	117.0	17.2	181.5	12.1	2.0	19.5	17.3	2.7	27.6
Bottom of VIV Suppression Region	4004.0	237.3	17.2	301.5	11.5	1.0	15.0	0.5	0.6	2.6
Top of Composite Riser Section	5926.0	301.3	17.1	365.1	7.9	4.2	23.8	4.8	2.8	15.6
Mean Water Level	6000.0	308.9	17.0	372.6	6.4	4.5	23.2	7.2	7.6	37.1
Tensioner Joint's Bottom Connector	6050.0	316.5	17.0	380.2	6.0	4.5	22.9	1.3	3.5	14.6
Bottom of the Tensioner Joint Threads	6055.0	317.5	17.0	381.1	6.0	4.4	22.8	2.3	4.9	20.9
Tensioner Joint at the Tensioner Ring	6060.0	319.3	17.0	383.0	6.0	4.4	22.6	3.6	7.1	30.6
Tensioner Joint at the Tensioner Guide	6080.0	-23.2	0.0	-23.2	0.0	0.9	3.5	5.9	14.8	62.7
Top of the Tensioner Joint	6088.0	-20.0	0.0	-20.0	0.0	0.8	3.0	2.4	6.1	25.8

Table 5.3.2.2
“Composite-Steel” Riser Configuration
Outer Casing Mid-Wall von-Mises Stresses
Load Case PHN-1: Shut-in with a 100-Year Hurricane

Wellhead Tilt = 1 deg.
Cd = 0.7 in the Region with Fairings; Cd = 1.0 in the Regions without Fairings
Nominal Applied Tension = 319 kips; Well Offset = 0 ft.
Riser Contents: Annulus = 0.04 ppg; Production Tube = 5.50 ppg
Riser Surface Pressures: Annulus = 100 psi; Production Tube = 8,500 psi

Location	Elevation (ft.)	Pressure		Material Tension		Effective Tension		Bending Moment		von-Mises Stresses	
		Internal (psi)	External (psi)	Mean (kips)	Maximum (kips)	Mean (kips)	Maximum (kips)	Mean (ft-kips)	Maximum (ft-kips)	Mean (ksi)	Maximum (ksi)
Base of the Stress Joint	10.0	113	2662	-173	-125	168	215	467	633	37.87	50.66
Base of the Stress Joint Taper	12.0	113	2661	-172	-124	169	216	441	592	36.03	47.70
Top of the Stress Joint Taper	28.0	113	2654	-108	-60	171	219	262	322	40.66	49.53
Stress Joint Top Connector	40.0	113	2649	-106	-59	172	220	176	205	30.17	34.97
Bottom of Composite Riser Section	102.0	112	2621	-119	-71	177	225	16.1	25.7	-	-
Bottom of VIV Suppression Region	4004.0	104	887	95	143	191	238	0.4	2.4	-	-
Top of Composite Riser Section	5926.0	100	33	206	253	202	250	4.6	14.9	-	-
Mean Water Level	6000.0	100	0	215	262	208	255	6.9	35.5	6.98	12.07
Tensioner Joint's Bottom Connector	6050.0	100	0	221	269	214	261	1.2	13.9	6.43	9.46
Bottom of the Tensioner Joint Threads	6055.0	100	0	222	270	215	262	2.3	20.7	6.60	10.36
Tensioner Joint at the Tensioner Ring	6060.0	100	0	224	271	217	264	3.6	30.3	2.25	3.68
Tensioner Joint at the Tensioner Guide	6080.0	100	0	-119	-119	-126	-126	5.8	62.1	0.99	0.95
Top of the Tensioner Joint	6088.0	100	0	-116	-116	-123	-123	1.2	12.9	1.12	0.73

Table 5.3.3.1
“Composite-Steel” Riser Configuration
Design Storm Load Summary for the Combined Cross-Section
Load Case PCN-1: Maximum Producing with a 100-Year Loop Current

Wellhead Tilt = 1 deg.
Cd = 0.7 in the Region with Fairings; Cd = 1.0 in the Regions without Fairings
Nominal Applied Tension = 319 kips; Well Offset = 0 ft.
Riser Contents: Annulus = 0.04 ppg; Production Tube = 5.50 ppg
Riser Surface Pressures: Annulus = 100 psi; Production Tube = 8,500 psi

Location	Elevation (ft.)	Effective Tension			Shear			Bending Moment		
		Mean (kips)	RMS (kips)	Maximum (kips)	Mean (kips)	RMS (kips)	Maximum (kips)	Mean (ft-kips)	RMS (ft-kips)	Maximum (ft-kips)
Base of the Stress Joint	10.0	143.1	1.6	149.2	22.3	0.2	23.2	738.8	4.4	755.4
Base of the Stress Joint Taper	12.0	144.2	1.6	150.3	22.3	0.2	23.2	691.7	3.9	706.5
Top of the Stress Joint Taper	28.0	148.2	1.6	154.4	22.3	0.2	23.2	388.5	1.3	393.5
Stress Joint Top Connector	40.0	150.1	1.6	156.3	22.3	0.2	23.2	245.3	0.7	247.8
Bottom of Composite Riser Section	102.0	156.7	1.6	162.9	22.3	0.2	23.2	16.1	0.2	17.0
Bottom of VIV Suppression Region	4004.0	276.6	1.6	282.7	21.7	0.1	22.2	0.8	0.0	1.0
Top of Composite Riser Section	5926.0	340.6	1.6	346.6	7.3	0.7	10.0	10.6	1.2	15.1
Mean Water Level	6000.0	348.1	1.6	354.1	3.8	0.8	7.1	13.7	4.0	29.8
Tensioner Joint's Bottom Connector	6050.0	355.7	1.6	361.7	2.4	1.1	6.9	0.6	1.9	8.1
Bottom of the Tensioner Joint Threads	6055.0	356.7	1.6	362.7	2.4	1.1	6.9	0.5	2.1	8.7
Tensioner Joint at the Tensioner Ring	6060.0	358.6	1.6	364.6	2.4	1.1	6.9	1.6	2.6	11.8
Tensioner Joint at the Tensioner Guide	6080.0	-23.2	0.0	-23.2	0.0	0.2	0.9	2.2	3.4	15.6
Top of the Tensioner Joint	6088.0	-20.0	0.0	-20.0	0.0	0.2	0.8	0.9	1.4	6.4

Table 5.3.3.2
“Composite-Steel” Riser Configuration
Outer Casing Mid-Wall von-Mises Stresses
Load Case PCN-1: Maximum Producing with a 100-Year Loop Current

Wellhead Tilt = 1 deg.
Cd = 0.7 in the Region with Fairings; Cd = 1.0 in the Regions without Fairings
Nominal Applied Tension = 319 kips; Well Offset = 0 ft.
Riser Contents: Annulus = 0.04 ppg; Production Tube = 5.50 ppg
Riser Surface Pressures: Annulus = 100 psi; Production Tube = 8,500 psi

Location	Elevation (ft.)	Pressure		Material Tension		Effective Tension		Bending Moment		von-Mises Stresses	
		Internal (psi)	External (psi)	Mean (kips)	Maximum (kips)	Mean (kips)	Maximum (kips)	Mean (ft-kips)	Maximum (ft-kips)	Mean (ksi)	Maximum (ksi)
Base of the Stress Joint	10.0	113	2662	-144	-139	197	202	722	738	56.76	58.01
Base of the Stress Joint Taper	12.0	113	2661	-143	-138	198	202	676	691	53.44	54.57
Top of the Stress Joint Taper	28.0	113	2654	-79	-74	200	205	372	377	55.30	56.04
Stress Joint Top Connector	40.0	113	2649	-77	-73	202	206	235	238	38.14	38.56
Bottom of Composite Riser Section	102.0	112	2621	-90	-85	206	211	15.0	15.8	-	-
Bottom of VIV Suppression Region	4004.0	104	887	125	129	220	224	0.7	0.9	-	-
Top of Composite Riser Section	5926.0	100	33	235	240	231	236	10.1	14.5	-	-
Mean Water Level	6000.0	100	0	244	249	237	241	13.2	28.5	8.65	10.76
Tensioner Joint's Bottom Connector	6050.0	100	0	251	255	243	248	0.6	7.7	7.20	8.25
Bottom of the Tensioner Joint Threads	6055.0	100	0	251	256	244	248	0.5	8.6	7.21	8.39
Tensioner Joint at the Tensioner Ring	6060.0	100	0	253	258	246	250	1.6	11.7	2.46	2.87
Tensioner Joint at the Tensioner Guide	6080.0	100	0	-129	-129	-137	-136	2.2	15.4	1.20	0.76
Top of the Tensioner Joint	6088.0	100	0	-126	-126	-134	-134	0.5	3.2	1.23	1.14

Table 5.4.1
Comparison of Bending Moments Obtained for the
“All-Steel” and “Composite-Steel” Riser Configurations

Bending Moments at the Base of the Stress Joint
and in the Tensioner Joint at the Tensioner Centralizer

Riser Configuration	Load Case	Base of the Stress Joint		Tensioner Joint at the Tensioner Centralizers	
		Mean (ft-kips)	Maximum (ft-kips)	Mean (ft-kips)	Maximum (ft-kips)
"All-Steel" Riser Configuration	PNS-1: Normal Shut-in with a 1-Year Winter Storm	446	552	3	22
	PHN-1: Shut-in with a 100-Year Hurricane	1131	1511	13	60
	PCN-1: Maximum Producing with a 100-Year Loop Current	1848	1885	14	26
"Composite-Steel" Riser Configuration	PNS-1: Normal Shut-in with a 1-Year Winter Storm	194	232	3	23
	PHN-1: Shut-in with a 100-Year Hurricane	478	648	6	63
	PCN-1: Maximum Producing with a 100-Year Loop Current	739	755	2	16

Table 5.4.2
Comparison of Maximum Stresses Obtained for the
“All-Steel” and “Composite-Steel” Riser Configurations

Mid-Wall von-Mises Stresses in the Stress Joint
in the Tensioner Joint

Riser Configuration	Load Case	Allowable Stress (ksi)	Stress Joint		Tensioner Joint	
			Max. Stress (ksi)	% of Allowable	Max. Stress (ksi)	% of Allowable
"All-Steel" Riser Configuration	PNS-1: Normal Shut-in with a 1-Year Winter Storm	53.3	32.0	60%	23.3	44%
	PHN-1: Shut-in with a 100-Year Hurricane	64.0	58.0	91%	30.9	48%
	PCN-1: Maximum Producing with a 100-Year Loop Current	64.0	60.8	95%	32.4	51%
"Composite-Steel" Riser Configuration	PNS-1: Normal Shut-in with a 1-Year Winter Storm	53.3	25.3	47%	6.5	12%
	PHN-1: Shut-in with a 100-Year Hurricane	64.0	50.7	79%	10.4	16%
	PCN-1: Maximum Producing with a 100-Year Loop Current	64.0	58	91%	8.4	13%

Fig. 5.2.1.1
“All-Steel” Riser Configuration
Bending Moment Distributions for the Combined Cross-Section
Load Case PNS-1: Normal Shut-in with a 1-Year Winter Storm

Wellhead Tilt = 1 deg.
Cd = 0.7 in the Region with Fairings; Cd = 1.0 in the Regions without Fairings
Nominal Applied Tension = 864 kips; Well Offset = 0 ft.
Riser Contents: Annulus = 0.04 ppg; Production Tube = 5.50 ppg
Riser Surface Pressures: Annulus = 100 psi; Production Tube = 8,500 psi

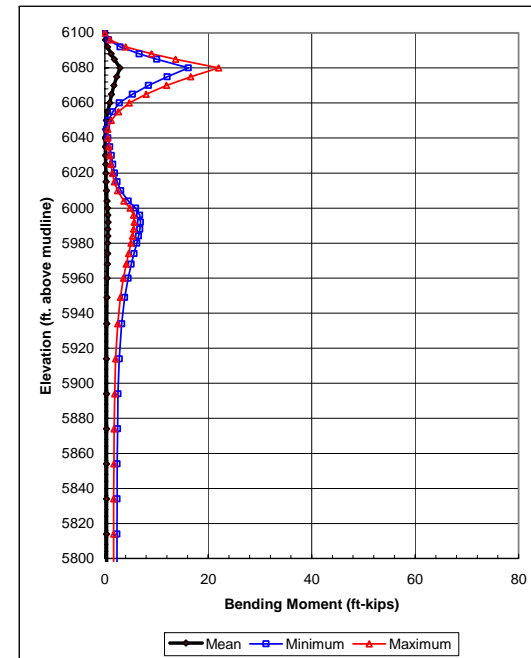
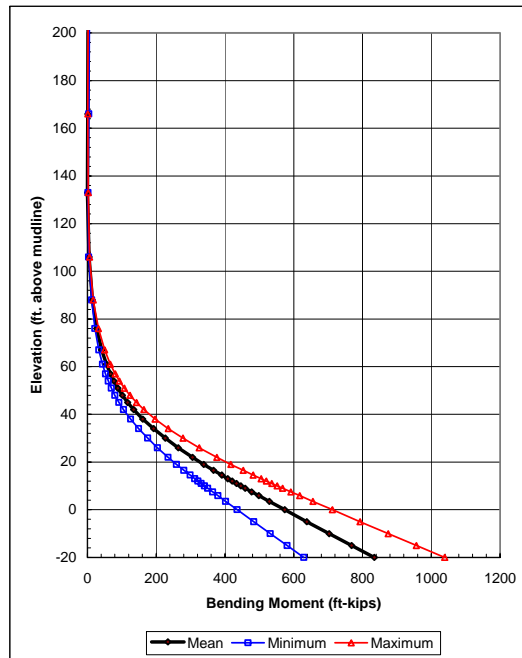
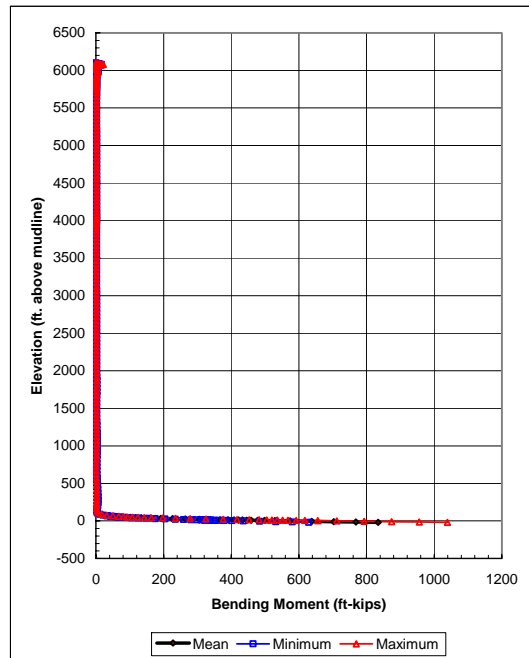


Fig. 5.2.2.1
“All-Steel” Riser Configuration
Bending Moment Distributions for the Combined Cross-Section
Load Case PHN-1: Shut-in with a 100-Year Hurricane

Wellhead Tilt = 1 deg.
Cd = 0.7 in the Region with Fairings; Cd = 1.0 in the Regions without Fairings
Nominal Applied Tension = 864 kips; Well Offset = 0 ft.
Riser Contents: Annulus = 0.04 ppg; Production Tube = 5.50 ppg
Riser Surface Pressures: Annulus = 100 psi; Production Tube = 8,500 psi

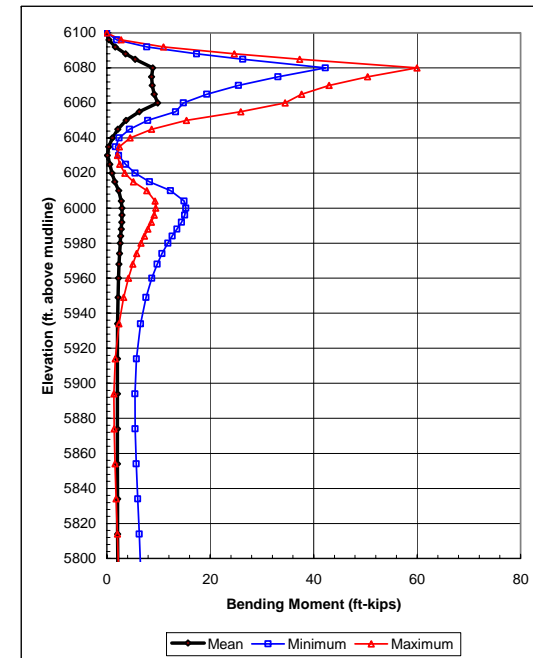
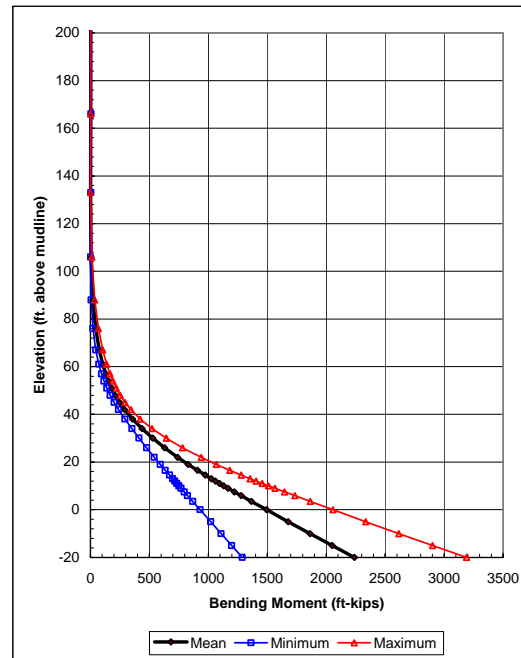
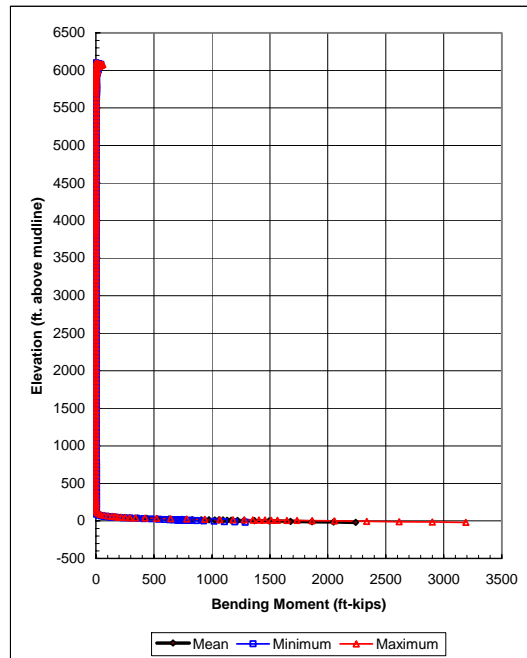


Fig. 5.2.3.1
“All-Steel” Riser Configuration
Bending Moment Distributions for the Combined Cross-Section
Load Case PCN-1: Maximum Producing with a 100-Year Loop Current

Wellhead Tilt = 1 deg.
Cd = 0.7 in the Region with Fairings; Cd = 1.0 in the Regions without Fairings
Nominal Applied Tension = 1,054 kips; Well Offset = 0 ft.
Riser Contents: Annulus = 0.04 ppg; Production Tube = 5.50 ppg
Riser Surface Pressures: Annulus = 100 psi; Production Tube = 8,500 psi

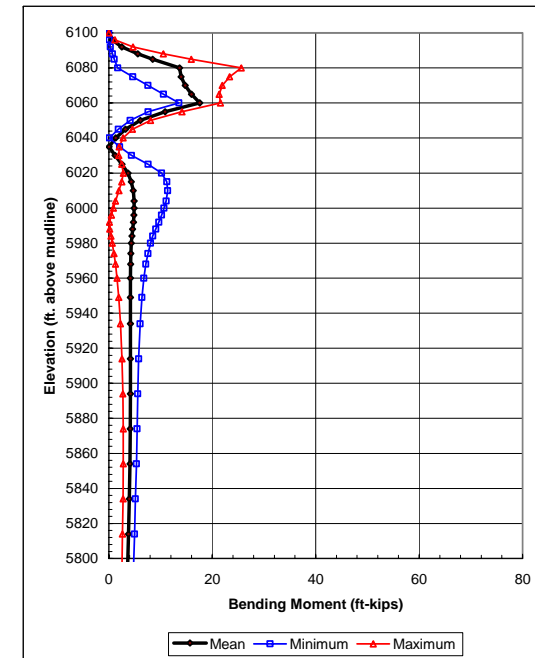
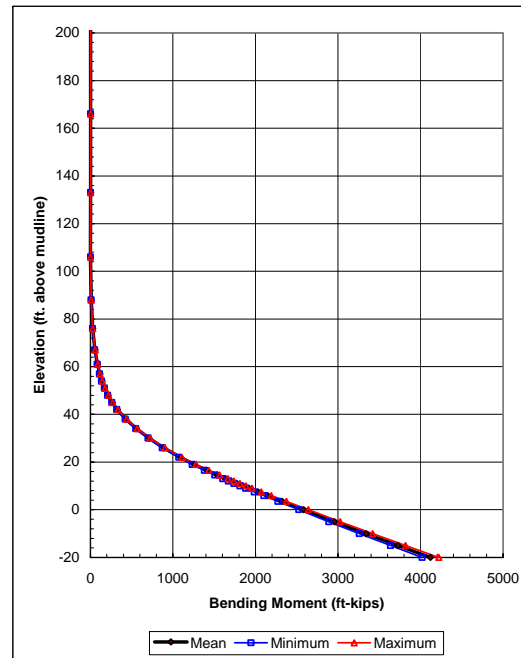
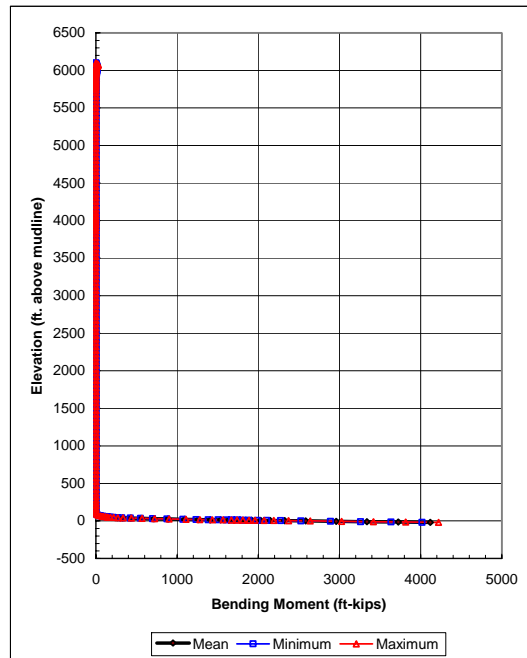


Fig. 5.3.1.1
“Composite-Steel” Riser Configuration
Bending Moment Distributions for the Combined Cross-Section
Load Case PNS-1: Normal Shut-in with a 1-Year Winter Storm

Wellhead Tilt = 1 deg.
Cd = 0.7 in the Region with Fairings; Cd = 1.0 in the Regions without Fairings
Nominal Applied Tension = 319 kips; Well Offset = 0 ft.
Riser Contents: Annulus = 0.04 ppg; Production Tube = 5.50 ppg
Riser Surface Pressures: Annulus = 100 psi; Production Tube = 8,500 psi

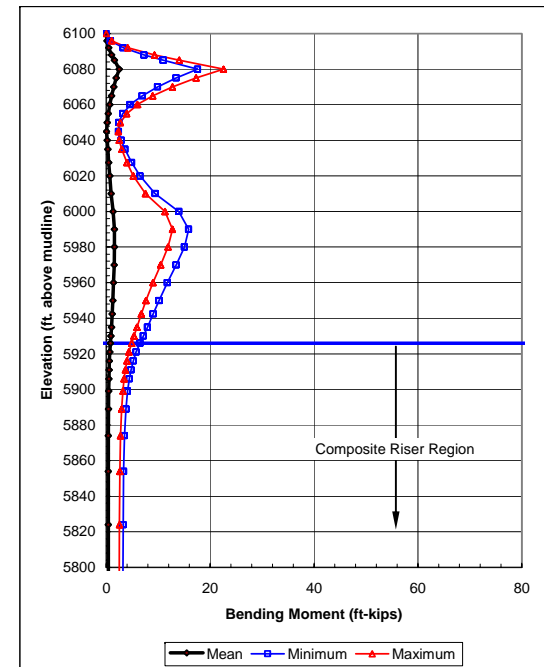
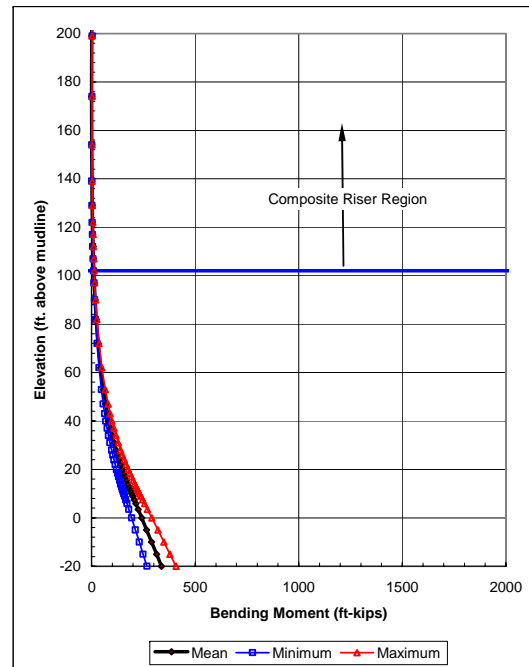
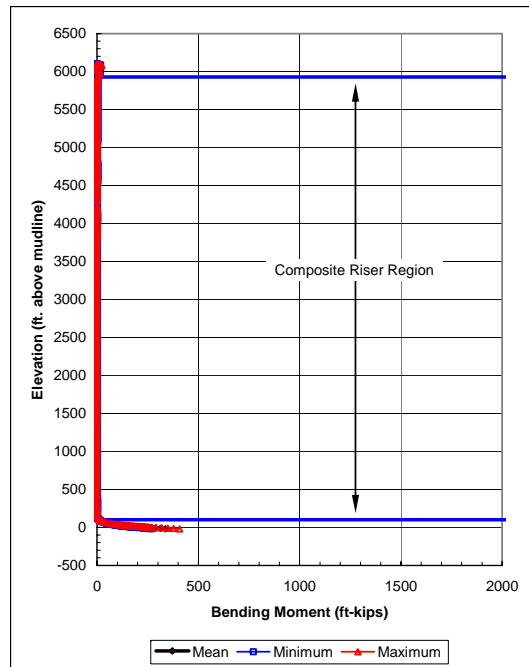


Fig. 5.3.2.1
“Composite-Steel” Riser Configuration
Bending Moment Distributions for the Combined Cross-Section
Load Case PHN-1: Shut-in with a 100-Year Hurricane

Wellhead Tilt = 1 deg.
 Cd = 0.7 in the Region with Fairings; Cd = 1.0 in the Regions without Fairings
 Nominal Applied Tension = 319 kips; Well Offset = 0 ft.
 Riser Contents: Annulus = 0.04 ppg; Production Tube = 5.50 ppg
 Riser Surface Pressures: Annulus = 100 psi; Production Tube = 8,500 psi

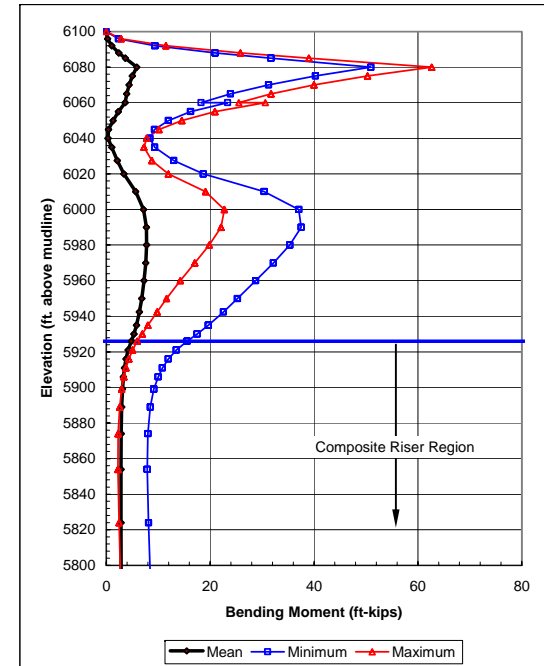
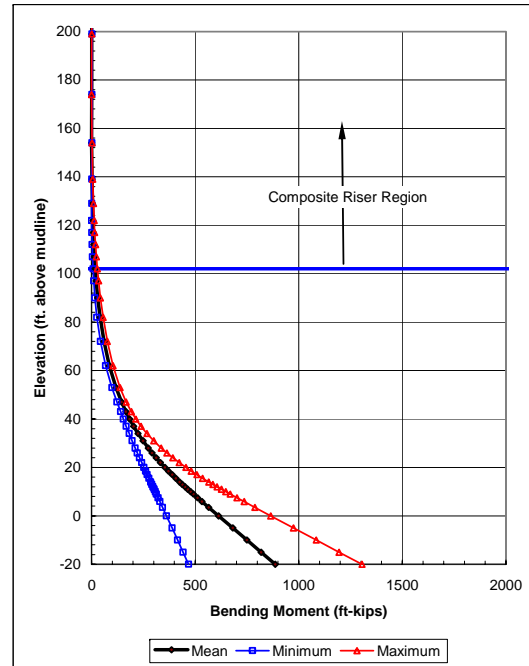
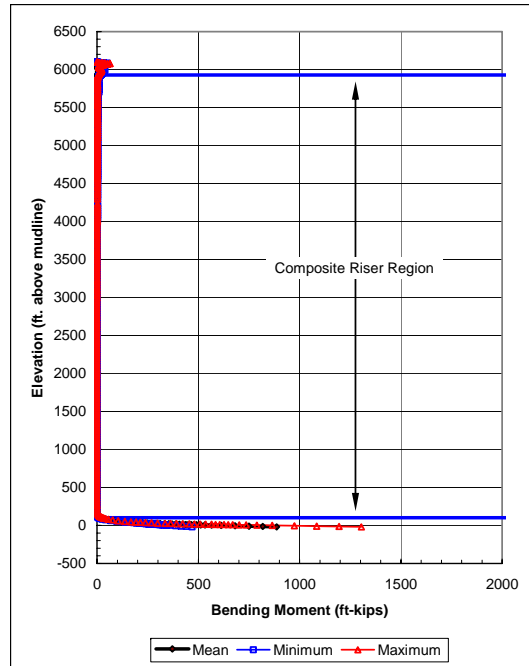
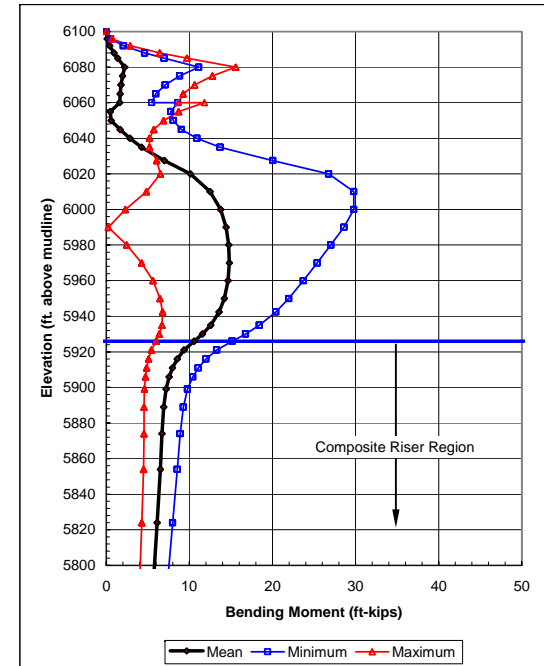
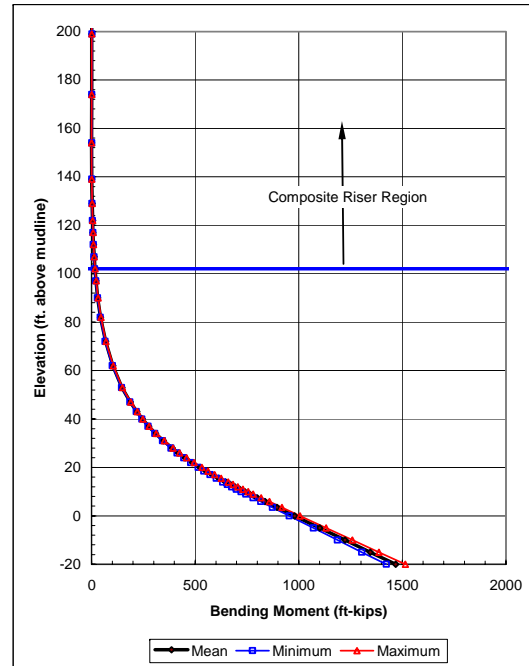
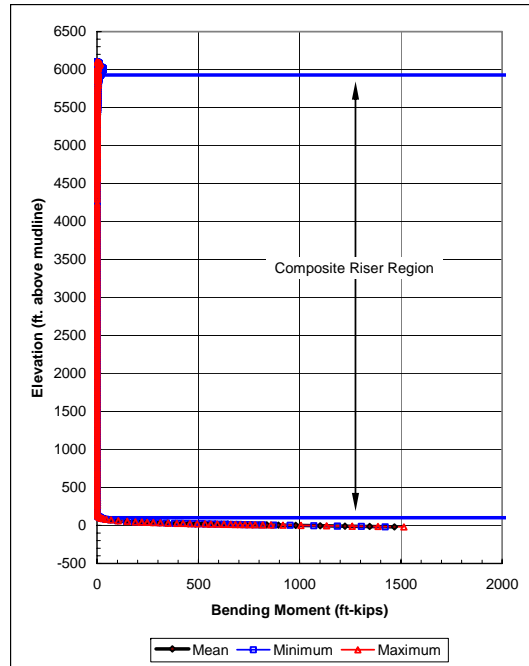


Fig. 5.3.3.1
“Composite-Steel” Riser Configuration
Bending Moment Distributions for the Combined Cross-Section
Load Case PCN-1: Maximum Producing with a 100-Year Loop Current

Wellhead Tilt = 1 deg.
 Cd = 0.7 in the Region with Fairings; Cd = 1.0 in the Regions without Fairings
 Nominal Applied Tension = 319 kips; Well Offset = 0 ft.
 Riser Contents: Annulus = 0.04 ppg; Production Tube = 5.50 ppg
 Riser Surface Pressures: Annulus = 100 psi; Production Tube = 8,500 psi



6 RESULTS OF THE FATIGUE ANALYSIS

6.1 GENERAL

The “all-steel” and “composite-steel” risers are required to have a service life (SL) of 20 years. A factor of safety of 10 is used in conjunction with the service life so that the target design fatigue life for the risers is 10×20 years, or 200 years.

The fatigue life estimates were made for the parent material sections and the welds in the “all-steel” riser configuration. The stress amplification factors used for the machined parent material sections of the critical riser components are summarized in Table 6.1.1. An SAF of 1.2 was used for all of the welded sections. The SAF’s used are representative of values typically obtained for these riser components.

Fatigue life estimates were also made for the stress joint components and tensioner joint components in the “composite-steel” riser configuration. The same SAF’s used for the “all-steel” riser stress joint and tensioner joint components were used for these “composite-steel” components. Fatigue life estimates were not made for the composite riser joints. Instead, fatigue loads were generated for the composite joints and fatigue life estimates were generated by others.

6.2 “ALL-STEEL” RISER CONFIGURATION FATIGUE

Table 6.2.1 contains a summary of the minimum wave-generated fatigue life estimates obtained for the parent material sections of the critical riser components. These fatigue life estimates were generated using the DnV-B fatigue curve. All of the lives given in the table exceed the target design fatigue life of 200 years. The lowest life estimate of 395 years occurs at the bottom of the stress joint.

Fig. 6.2.1 contains a plot of the fatigue life along the entire length of the riser. These life estimates were obtained using the DnV-B curve with an SAF of 1.0. This plot shows that the lowest estimated fatigue lives occur in the stress joint region. Fig. 6.2.2 contains a “zoomed-in” plot of the fatigue life estimates in the stress joint region. This plot shows

that the fatigue life estimates in the stress joint are pretty uniform when using the same SAF along the entire length of the stress joint.

Fig. 6.2.3 contains a plot of the fatigue life results obtained for the upper riser. The lowest estimated fatigue lives were obtained near the mean water level (6,000 ft. elevation) and at the tensioner centralizer.

Table 6.2.2 contains a summary of the fatigue damage obtained at the base of the stress joint for each fatigue seastate. The results show that most of the fatigue damage is generated by fatigue bins 5 through 14 with the most damaging fatigue bin being bin 10 ($H_s = 8.0$ ft., $T_z = 5.0$ sec.). This is typical of results obtained for most top tensioned production risers in the Gulf of Mexico.

Table 6.2.3 contains a summary of the minimum wave-generated fatigue life estimates obtained for the welded sections of the critical riser components. These fatigue life estimates were generated using the DnV-C fatigue curve. Again, all of the lives given in the table exceed the target design fatigue life of 200 years. The lowest life estimate of 416 years occurs at the top of the stress joint taper.

Fig. 6.2.4 contains a plot of the fatigue life along the entire length of the riser. These life estimates were obtained using the DnV-C curve with an SAF of 1.0. The lowest estimated fatigue lives occur in the stress joint region. Fig. 6.2.5 contains a “zoomed-in” plot of the fatigue life estimates in the stress joint region.

Fig. 6.2.6 contains a plot of the fatigue life results obtained for the upper riser. The lowest estimated fatigue lives were obtained at the mean water level and at the tensioner centralizer.

Table 6.2.4 contains a summary of the fatigue damage obtained at the base of the stress joint for each fatigue seastate. The results show that most of the fatigue damage is generated by fatigue bins 5 through 14 with the most damaging fatigue bin being bin 10 ($H_s = 8.0$ ft., $T_z = 5.0$ sec.).

Table 6.2.5 contains a summary of the minimum wave-generated fatigue life estimates obtained for the welded sections of the critical riser components using the DnV-F2 S-N curve. The estimated fatigue lives obtained in the stress joint region do not meet the 200-year design life requirement. Therefore, DnV-C quality welds will be required in the lower portion of the riser. This is also typical of the results obtained for top-tensioned production risers in the Gulf of Mexico.

Tables containing the dynamic stresses obtained for each riser node and each fatigue seastate are provided in Appendix A-6.2.1. The stresses provided are the stress standard deviation (or RMS stress). The zero-crossing periods for each stress value are also provided in the tables. This information can be used to produce stress histograms for each location along the length of the riser.

6.3 “COMPOSITE-STEEL” RISER CONFIGURATION FATIGUE

Fatigue life estimates were generated for the steel components of the “composite-steel” riser configuration. While the composite riser joints were included in the riser models, due to the complex nature of the composite riser construction and stress fields within these joints, the fatigue life estimates for the composite joints were generated by others. The loads used for those composite riser fatigue life estimates were generated by this global riser analysis.

Table 6.3.1 contains a summary of the minimum wave-generated fatigue life estimates obtained for the parent material sections of the critical “all-steel” components. These fatigue life estimates were generated using the DnV-B fatigue curve. All of the lives given in the table exceed the target design fatigue life of 200 years. The lowest life estimate of 622 years occurs at the bottom of the stress joint. This life is ~50% greater than the minimum life obtained for the “all-steel” riser configuration.

Fig. 6.3.1 contains a plot of the fatigue life along the lower portion of the riser. These life estimates were obtained using the DnV-B curve with an SAF of 1.0. As with the “all-

steel” riser configuration, the fatigue life estimates in the stress joint are pretty uniform when using the same SAF along the entire length of the stress joint.

Fig. 6.3.2 contains a plot of the fatigue life results obtained for the upper riser. The lowest estimated fatigue lives were obtained near the mean water level (6,000 ft. elevation) and at the tensioner centralizer.

Table 6.3.2 contains a summary of the fatigue damage obtained at the base of the stress joint for each fatigue seastate. As with the “all-steel” configuration, most of the fatigue damage is generated by fatigue bins 5 through 14. The most damaging fatigue bin is bin 7 ($H_s = 6.0$ ft., $T_z = 4.0$ sec.).

Table 6.3.3 contains a summary of the minimum wave-generated fatigue life estimates obtained for the welded sections of the critical “all-steel” components. These fatigue life estimates were generated using the DnV-C fatigue curve. Again, all of the lives given in the table exceed the target design fatigue life of 200 years. The lowest life estimate of 802 years occurs at the bottom of the stress joint taper.

Fig. 6.3.3 contains a plot of the fatigue life along the lower portion of the riser using the DnV-C curve with an SAF of 1.0. Fig. 6.3.4 contains a plot of the fatigue life results obtained for the upper riser. The lowest estimated fatigue lives were obtained near the mean water level and at the tensioner centralizer.

Table 6.3.4 contains a summary of the fatigue damage obtained at the base of the stress joint for each fatigue seastate. The results show that most of the fatigue damage is generated by fatigue bins 5 through 14 with the most damaging fatigue bin being bin 7 ($H_s = 6.0$ ft., $T_z = 4.0$ sec.).

Table 6.3.5 contains a summary of the minimum wave-generated fatigue life estimates obtained for the welded sections of the critical “all-steel” components using the DnV-F2 S-N curve. The estimated fatigue lives obtained in the stress joint region do not meet the 200-year design life requirement. Therefore, DnV-C quality welds will be required in the lower portion of the riser.

Tables summarizing the tension loads and bending moments generated at the top of the composite riser joint section (elevation 5,926 ft. above the mudline) and at the bottom of the composite riser joint section (elevation 102 ft. above the mudline) were produced. These tables are provided in Appendix A-6.3.1. Tension and bending moment histograms were generated from the load given in the table are provided in Appendices A-6.3.2 and A-6.3.3.

Table 6.1.1
Stress Amplification Factors (SAFs) Used
For the “All-Steel” Riser Configuration
Fatigue Analysis

Material	Fatigue Curve	Component	Location	Elevation (ft.)	SAF	Component Feature
Machined Surfaces	DnV-B	Stress Joint	Base of Stress Joint	10.0	1.8	Tieback Connector
			Base of Stress Joint Taper	12.0	1.1	Tieback Connector / Stress Joint Transition
			Top of Stress Joint Taper	42.0	1.1	Transition at the Top of the Stress Joint Taper
			Top of Stress Joint	45.0	1.8	Connector at the Top of the Stress Joint
		Weld-on Connectors for the Standard Joints	Region 1 (from 48 ft. to 202 ft.)	48.0	1.8	Connector
			Region 2 (from 240 ft. to 5934 ft.)	281.0	1.8	Connector
			Region 3 (from 5949 ft. to 6045 ft.)	5992.0	1.8	Connector
		Tensioner Joint	Bottom of Tensioner Joint	6050.0	1.8	Connector at the Bottom of the Tensioner Joint
			Bottom of T.J. Adjust. Region	6055.0	2.0	Tensioner Ring Adjustment Grooves
			Tensioner Ring	6060.0	2.0	Tensioner Ring Adjustment Grooves
Top of T.J. Adjust. Region	6065.0		2.0	Tensioner Ring Adjustment Grooves		
Tensioner Centralizer	6080.0		1.0	Straight Barrel of the Tensioner Joint		
Top of Tensioner Joint	6088.0	1.8	Connector at the Top of the Tensioner Joint			
Welded Sections	DnV-C and DnV-F2	Stress Joint	Base of Stress Joint	10.0	1.2	Tieback Connector Weld
			Base of Stress Joint Taper	12.0	1.2	Tieback Connector / Stress Joint Weld
			Top of Stress Joint Taper	42.0	1.2	Weld at the Top of the Stress Joint Taper
			Top of Stress Joint	45.0	1.2	Stress Joint/Connector Weld
		Weld-on Connectors for the Standard Joints	Region 1 (from 48 ft. to 202 ft.)	48.0	1.2	Connector Weld
			Region 2 (from 240 ft. to 5934 ft.)	281.0	1.2	Connector Weld
			Region 3 (from 5949 ft. to 6045 ft.)	5992.0	1.2	Connector Weld
		Tensioner Joint	Bottom of Tensioner Joint	6050.0	1.2	Tensioner Joint / Connector Weld
			Top of Tensioner Joint	6088.0	1.2	Connector at the Top of the Tensioner Joint

Table 6.2.1
Estimated Fatigue Life Summary for the
“All-Steel” Riser Configuration Machined Surfaces

Fatigue Curve: DnV-B

Component	Location	Elevation (ft.)	SAF	Wave Gen. Ftg. Damage	Estimated Life (years)
Stress Joint	Base of Stress Joint	10.0	1.8	2.529E-03	395
	Base of Stress Joint Taper	12.0	1.1	2.783E-04	3593
	Top of Stress Joint Taper	42.0	1.1	5.025E-04	1990
	Top of Stress Joint	45.0	1.8	2.044E-03	489
Weld-on Connectors for the Standard Joints	Region 1 (from 48 ft. to 202 ft.)	48.0	1.8	1.155E-03	866
	Region 2 (from 240 ft. to 5934 ft.)	281.0	1.8	2.347E-06	426133
	Region 3 (from 5949 ft. to 6045 ft.)	5992.0	1.8	6.629E-07	1508610
Tensioner Joint	Bottom of Tensioner Joint	6050.0	1.8	6.848E-08	14601802
	Bottom of T.J. Adjust. Region	6055.0	2.0	1.746E-07	5728327
	Tensioner Ring	6060.0	2.0	6.444E-09	155181620
	Top of T.J. Adjust. Region	6065.0	2.0	1.016E-08	98471151
	Tensioner Centralizer	6080.0	1.0	3.937E-08	25401570
	Top of Tensioner Joint	6088.0	1.8	1.179E-08	84790540

Table 6.2.2
Fatigue Damage Histogram for the Base of the Stress Joint
“All-Steel” Riser Configuration Machined Surfaces
Fatigue Curve: DnV-B

Bin	Significant Wave Ht. (ft.)	Zero-Cross. Period (sec.)	Bin Occurrence Probability	Damage	Percent of Total Damage	Bin	Significant Wave Ht. (ft.)	Zero-Cross. Period (sec.)	Bin Occurrence Probability	Damage	Percent of Total Damage
1	2.0	2.0	4.190E-02	3.330E-07	0.01%	15	16.0	7.5	5.137E-04	6.857E-05	2.71%
2	2.0	3.0	2.206E-01	1.438E-06	0.06%	16	18.0	7.7	3.539E-04	7.028E-05	2.78%
3	2.0	4.0	1.019E-01	7.434E-06	0.29%	17	20.0	7.9	2.512E-04	7.137E-05	2.82%
4	4.0	3.0	8.128E-02	2.592E-05	1.02%	18	22.0	8.1	1.598E-04	6.149E-05	2.43%
5	4.0	4.0	1.904E-01	1.349E-04	5.33%	19	24.0	8.3	1.027E-04	5.224E-05	2.07%
6	4.0	5.0	5.320E-02	5.158E-05	2.04%	20	26.0	8.6	6.849E-05	4.345E-05	1.72%
7	6.0	4.0	8.836E-02	2.649E-04	10.47%	21	28.0	8.8	5.137E-05	4.032E-05	1.59%
8	6.0	5.0	7.283E-02	2.507E-04	9.91%	22	30.0	9.0	3.032E-05	2.782E-05	1.10%
9	6.0	6.0	1.381E-02	5.242E-05	2.07%	23	32.0	9.2	2.283E-05	2.355E-05	0.93%
10	8.0	5.0	4.178E-02	3.655E-04	14.45%	24	34.0	9.4	1.370E-05	1.524E-05	0.60%
11	8.0	6.0	1.632E-02	1.604E-04	6.34%	25	36.0	9.7	9.702E-06	1.168E-05	0.46%
12	10.0	6.0	1.324E-02	2.766E-04	10.94%	26	38.0	9.9	6.507E-06	8.611E-06	0.34%
13	12.0	6.0	5.137E-03	1.972E-04	7.80%	27	41.0	10.3	4.338E-06	6.859E-06	0.27%
14	14.0	6.5	3.311E-03	2.386E-04	9.43%		Totals		0.9457	2.529E-03	100.00%

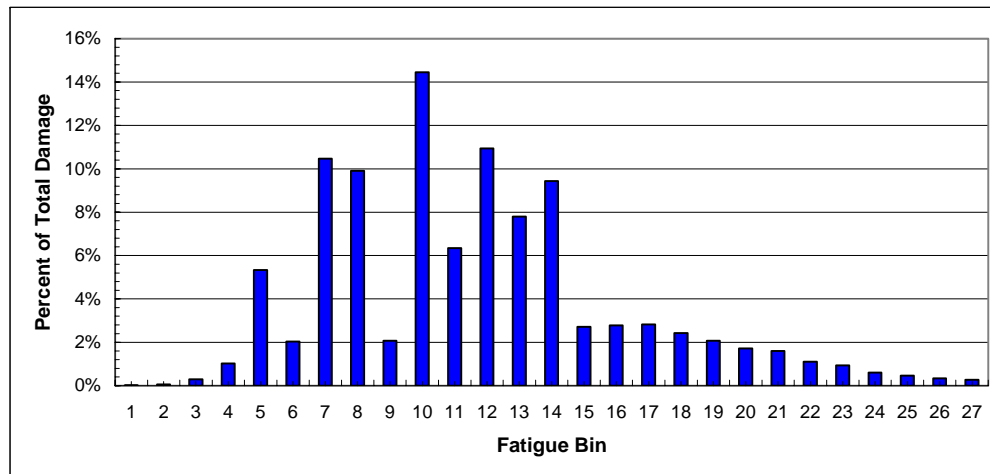


Table 6.2.3
Estimated Fatigue Life Summary for the
“All-Steel” Riser Configuration Welded Sections

Fatigue Curve: DnV-C

Component	Location	Elevation (ft.)	SAF	Wave Gen. Ftg. Damage	Estimated Life (years)
Stress Joint	Base of Stress Joint	10.0	1.2	1.713E-03	584
	Base of Stress Joint Taper	12.0	1.2	1.395E-03	717
	Top of Stress Joint Taper	42.0	1.2	2.406E-03	416
	Top of Stress Joint	45.0	1.2	1.465E-03	683
Weld-on Connectors for the Standard Joints	Region 1 (from 48 ft. to 202 ft.)	48.0	1.2	8.876E-04	1127
	Region 2 (from 240 ft. to 5934 ft.)	281.0	1.2	5.090E-06	196474
	Region 3 (from 5949 ft. to 6045 ft.)	5992.0	1.2	1.418E-06	705394
Tensioner Joint	Bottom of Tensioner Joint	6050.0	1.2	8.268E-08	12095507
	Top of Tensioner Joint	6088.0	1.2	4.162E-08	24024095

Table 6.2.4
Fatigue Damage Histogram for the Base of the Stress Joint
“All-Steel” Riser Configuration Welded Sections
Fatigue Curve: DnV-C

Bin	Significant Wave Ht. (ft.)	Zero-Cross. Period (sec.)	Bin Occurrence Probability	Damage	Percent of Total Damage
1	2.0	2.0	4.190E-02	7.817E-07	0.05%
2	2.0	3.0	2.206E-01	3.184E-06	0.19%
3	2.0	4.0	1.019E-01	1.144E-05	0.67%
4	4.0	3.0	8.128E-02	3.049E-05	1.78%
5	4.0	4.0	1.904E-01	1.512E-04	8.83%
6	4.0	5.0	5.320E-02	5.601E-05	3.27%
7	6.0	4.0	8.836E-02	2.291E-04	13.37%
8	6.0	5.0	7.283E-02	2.186E-04	12.76%
9	6.0	6.0	1.381E-02	4.474E-05	2.61%
10	8.0	5.0	4.178E-02	2.668E-04	15.57%
11	8.0	6.0	1.632E-02	1.143E-04	6.67%
12	10.0	6.0	1.324E-02	1.704E-04	9.95%
13	12.0	6.0	5.137E-03	1.081E-04	6.31%
14	14.0	6.5	3.311E-03	1.176E-04	6.86%

Bin	Significant Wave Ht. (ft.)	Zero-Cross. Period (sec.)	Bin Occurrence Probability	Damage	Percent of Total Damage
15	16.0	7.5	5.137E-04	3.089E-05	1.80%
16	18.0	7.7	3.539E-04	2.962E-05	1.73%
17	20.0	7.9	2.512E-04	2.841E-05	1.66%
18	22.0	8.1	1.598E-04	2.330E-05	1.36%
19	24.0	8.3	1.027E-04	1.897E-05	1.11%
20	26.0	8.6	6.849E-05	1.521E-05	0.89%
21	28.0	8.8	5.137E-05	1.369E-05	0.80%
22	30.0	9.0	3.032E-05	9.215E-06	0.54%
23	32.0	9.2	2.283E-05	7.739E-06	0.45%
24	34.0	9.4	1.370E-05	4.975E-06	0.29%
25	36.0	9.7	9.702E-06	3.791E-06	0.22%
26	38.0	9.9	6.507E-06	2.779E-06	0.16%
27	41.0	10.3	4.338E-06	2.111E-06	0.12%
Totals			0.9457	1.713E-03	100.00%

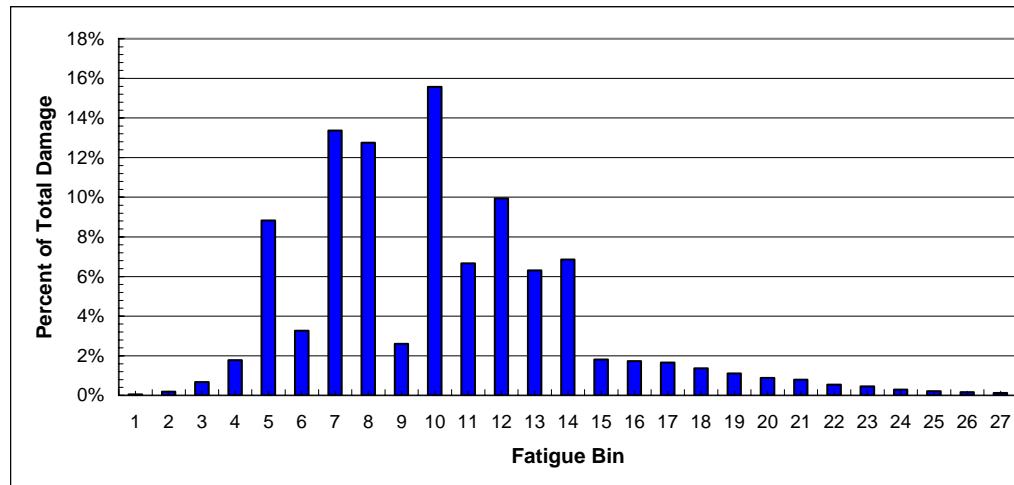


Table 6.2.5
Estimated Fatigue Life Summary for the
“All-Steel” Riser Configuration Welded Sections

Fatigue Curve: DnV-F2

Component	Location	Elevation (ft.)	SAF	Wave Gen. Ftg. Damage	Estimated Life (years)
Stress Joint	Base of Stress Joint	10.0	1.2	2.879E-02	35
	Base of Stress Joint Taper	12.0	1.2	2.418E-02	41
	Top of Stress Joint Taper	42.0	1.2	3.896E-02	26
	Top of Stress Joint	45.0	1.2	2.543E-02	39
Weld-on Connectors for the Standard Joints	Region 1 (from 48 ft. to 202 ft.)	48.0	1.2	1.651E-02	61
	Region 2 (from 240 ft. to 5934 ft.)	281.0	1.2	2.458E-04	4068
	Region 3 (from 5949 ft. to 6045 ft.)	5992.0	1.2	7.481E-05	13368
Tensioner Joint	Bottom of Tensioner Joint	6050.0	1.2	3.019E-06	331240
	Top of Tensioner Joint	6088.0	1.2	3.421E-06	292276

Table 6.3.1
Estimated Fatigue Life Summary for the
“Composite-Steel” Riser Configuration Steel Machined Surfaces

Fatigue Curve: DnV-B

Component	Location	Elevation (ft.)	SAF	Wave Gen. Ftg. Damage	Estimated Life (years)
Stress Joint	Base of Stress Joint	10.0	1.8	1.608E-03	622
	Base of Stress Joint Taper	12.0	1.8	1.295E-03	772
	Top of Stress Joint Taper	28.0	1.8	1.501E-03	666
	Top of Stress Joint	40.0	1.8	3.103E-04	3223
Tensioner Joint	Bottom of Tensioner Joint	6050.0	1.8	1.026E-07	9742305
	Bottom of T.J. Adjust. Region	6055.0	1.8	2.191E-07	4564317
	Tensioner Ring	6060.0	1.8	7.901E-09	126571946
	Top of T.J. Adjust. Region	6065.0	1.8	1.721E-08	58108771
	Tensioner Centralizer	6080.0	1.8	5.492E-07	1820869
	Top of Tensioner Joint	6088.0	1.8	1.585E-08	63105984

Table 6.3.2
Fatigue Damage Histogram for the Base of the Stress Joint
“Composite-Steel” Riser Configuration Steel Machined Surfaces
Fatigue Curve: DnV-B

Bin	Significant Wave Ht. (ft.)	Zero-Cross. Period (sec.)	Bin Occurrence Probability	Damage	Percent of Total Damage
1	2.0	2.0	4.190E-02	2.587E-06	0.16%
2	2.0	3.0	2.206E-01	6.359E-06	0.40%
3	2.0	4.0	1.019E-01	9.193E-06	0.57%
4	4.0	3.0	8.128E-02	4.960E-05	3.08%
5	4.0	4.0	1.904E-01	1.663E-04	10.34%
6	4.0	5.0	5.320E-02	4.483E-05	2.79%
7	6.0	4.0	8.836E-02	2.911E-04	18.10%
8	6.0	5.0	7.283E-02	1.918E-04	11.93%
9	6.0	6.0	1.381E-02	3.097E-05	1.93%
10	8.0	5.0	4.178E-02	2.453E-04	15.26%
11	8.0	6.0	1.632E-02	8.225E-05	5.12%
12	10.0	6.0	1.324E-02	1.296E-04	8.06%
13	12.0	6.0	5.137E-03	8.513E-05	5.29%
14	14.0	6.5	3.311E-03	8.825E-05	5.49%

Bin	Significant Wave Ht. (ft.)	Zero-Cross. Period (sec.)	Bin Occurrence Probability	Damage	Percent of Total Damage
15	16.0	7.5	5.137E-04	2.244E-05	1.40%
16	18.0	7.7	3.539E-04	2.250E-05	1.40%
17	20.0	7.9	2.512E-04	2.286E-05	1.42%
18	22.0	8.1	1.598E-04	2.035E-05	1.27%
19	24.0	8.3	1.027E-04	1.819E-05	1.13%
20	26.0	8.6	6.849E-05	1.615E-05	1.00%
21	28.0	8.8	5.137E-05	1.630E-05	1.01%
22	30.0	9.0	3.032E-05	1.217E-05	0.76%
23	32.0	9.2	2.283E-05	1.108E-05	0.69%
24	34.0	9.4	1.370E-05	7.645E-06	0.48%
25	36.0	9.7	9.702E-06	6.432E-06	0.40%
26	38.0	9.9	6.507E-06	5.024E-06	0.31%
27	41.0	10.3	4.338E-06	3.536E-06	0.22%
Totals			0.9457	1.608E-03	100.00%

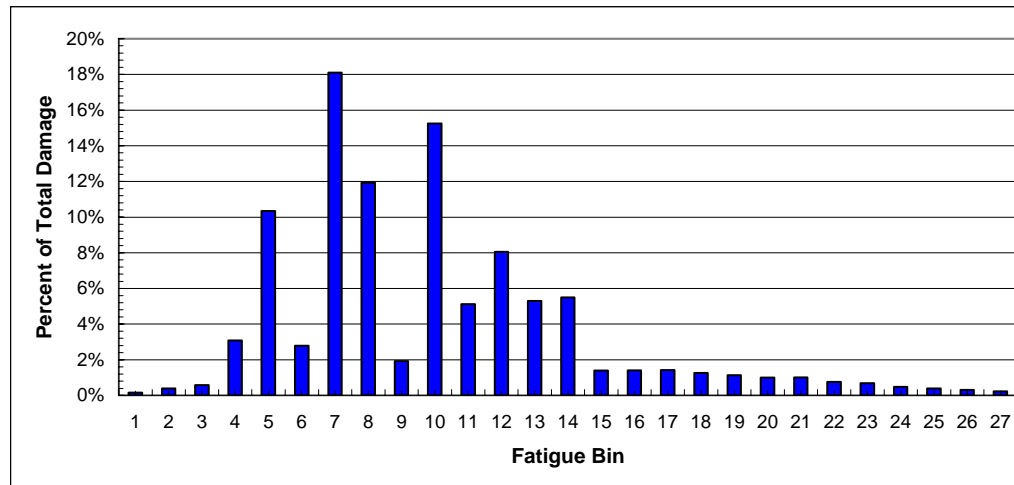


Table 6.3.3
Estimated Fatigue Life Summary for the
“Composite-Steel” Riser Configuration Steel Component Welded Sections

Fatigue Curve: DnV-C

Component	Location	Elevation (ft.)	SAF	Wave Gen. Ftg. Damage	Estimated Life (years)
Stress Joint	Base of Stress Joint	10.0	1.2	1.247E-03	802
	Base of Stress Joint Taper	12.0	1.2	1.033E-03	968
	Top of Stress Joint Taper	28.0	1.2	1.176E-03	850
	Top of Stress Joint	40.0	1.2	2.904E-04	3443
Tensioner Joint	Bottom of Tensioner Joint	6050.0	1.2	2.719E-07	3678457
	Bottom of T.J. Adjust. Region	6055.0	1.2	5.183E-07	1929221
	Tensioner Ring	6060.0	1.2	2.617E-08	38205406
	Top of T.J. Adjust. Region	6065.0	1.2	6.240E-08	16025924
	Tensioner Centralizer	6080.0	1.2	1.173E-06	852567
	Top of Tensioner Joint	6088.0	1.2	5.294E-08	18890663

Table 6.3.4
Fatigue Damage Histogram for the Base of the Stress Joint
“Composite-Steel” Riser Configuration Steel Component Welded Sections
Fatigue Curve: DnV-C

Bin	Significant Wave Ht. (ft.)	Zero-Cross. Period (sec.)	Bin Occurrence Probability	Damage	Percent of Total Damage	Bin	Significant Wave Ht. (ft.)	Zero-Cross. Period (sec.)	Bin Occurrence Probability	Damage	Percent of Total Damage
1	2.0	2.0	4.190E-02	4.658E-06	0.37%	15	16.0	7.5	5.137E-04	1.072E-05	0.86%
2	2.0	3.0	2.206E-01	1.202E-05	0.96%	16	18.0	7.7	3.539E-04	1.011E-05	0.81%
3	2.0	4.0	1.019E-01	1.392E-05	1.12%	17	20.0	7.9	2.512E-04	9.735E-06	0.78%
4	4.0	3.0	8.128E-02	5.745E-05	4.61%	18	22.0	8.1	1.598E-04	8.251E-06	0.66%
5	4.0	4.0	1.904E-01	1.827E-04	14.65%	19	24.0	8.3	1.027E-04	7.052E-06	0.57%
6	4.0	5.0	5.320E-02	4.923E-05	3.95%	20	26.0	8.6	6.849E-05	6.012E-06	0.48%
7	6.0	4.0	8.836E-02	2.470E-04	19.81%	21	28.0	8.8	5.137E-05	5.848E-06	0.47%
8	6.0	5.0	7.283E-02	1.670E-04	13.39%	22	30.0	9.0	3.032E-05	4.234E-06	0.34%
9	6.0	6.0	1.381E-02	2.713E-05	2.18%	23	32.0	9.2	2.283E-05	3.794E-06	0.30%
10	8.0	5.0	4.178E-02	1.780E-04	14.28%	24	34.0	9.4	1.370E-05	2.582E-06	0.21%
11	8.0	6.0	1.632E-02	5.984E-05	4.80%	25	36.0	9.7	9.702E-06	2.143E-06	0.17%
12	10.0	6.0	1.324E-02	8.138E-05	6.53%	26	38.0	9.9	6.507E-06	1.655E-06	0.13%
13	12.0	6.0	5.137E-03	4.791E-05	3.84%	27	41.0	10.3	4.338E-06	1.145E-06	0.09%
14	14.0	6.5	3.311E-03	4.541E-05	3.64%	Totals			0.9457	1.247E-03	100.00%

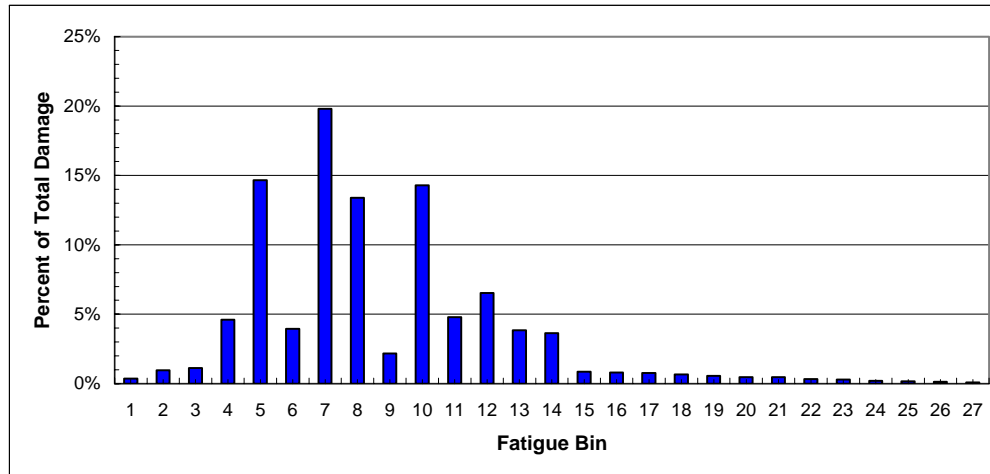


Table 6.3.5
Estimated Fatigue Life Summary for the
“Composite-Steel” Riser Configuration Steel Component Welded Sections

Fatigue Curve: DnV-F2

Component	Location	Elevation (ft.)	SAF	Wave Gen. Ftg. Damage	Estimated Life (years)
Stress Joint	Base of Stress Joint	10.0	1.2	2.346E-02	43
	Base of Stress Joint Taper	12.0	1.2	1.997E-02	50
	Top of Stress Joint Taper	28.0	1.2	2.213E-02	45
	Top of Stress Joint	40.0	1.2	6.526E-03	153
Tensioner Joint	Bottom of Tensioner Joint	6050.0	1.2	1.975E-05	50623
	Bottom of T.J. Adjust. Region	6055.0	1.2	3.349E-05	29862
	Tensioner Ring	6060.0	1.2	2.399E-06	416925
	Top of T.J. Adjust. Region	6065.0	1.2	5.394E-06	185380
	Tensioner Centralizer	6080.0	1.2	5.956E-05	16789
	Top of Tensioner Joint	6088.0	1.2	4.209E-06	237596

Fig. 6.2.1
Fatigue Life Estimates Along the Length of the Riser
“All-Steel” Riser Configuration Machined Sections
Fatigue Curve: DnV-B

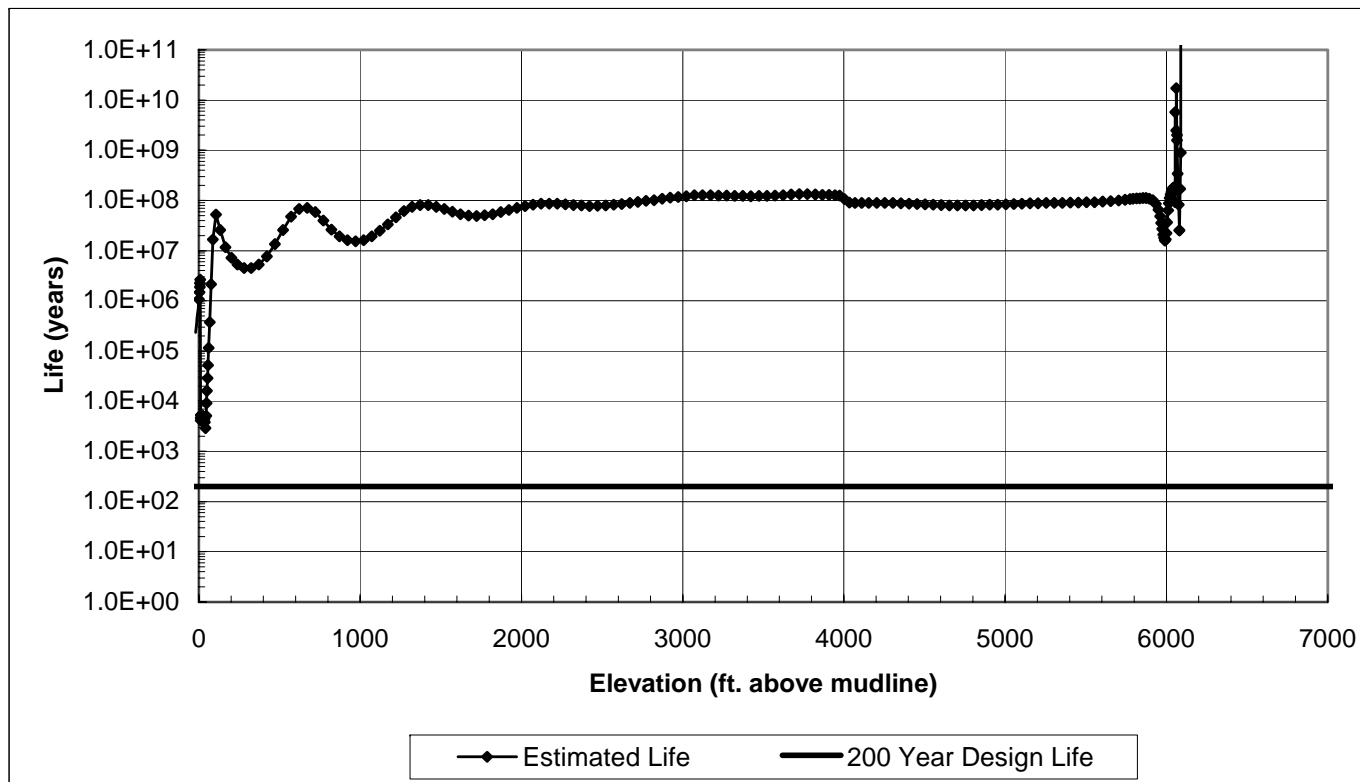


Fig. 6.2.2
Fatigue Life Estimates in the Lower Portion of the Riser
“All-Steel” Riser Configuration Machined Sections
Fatigue Curve: DnV-B

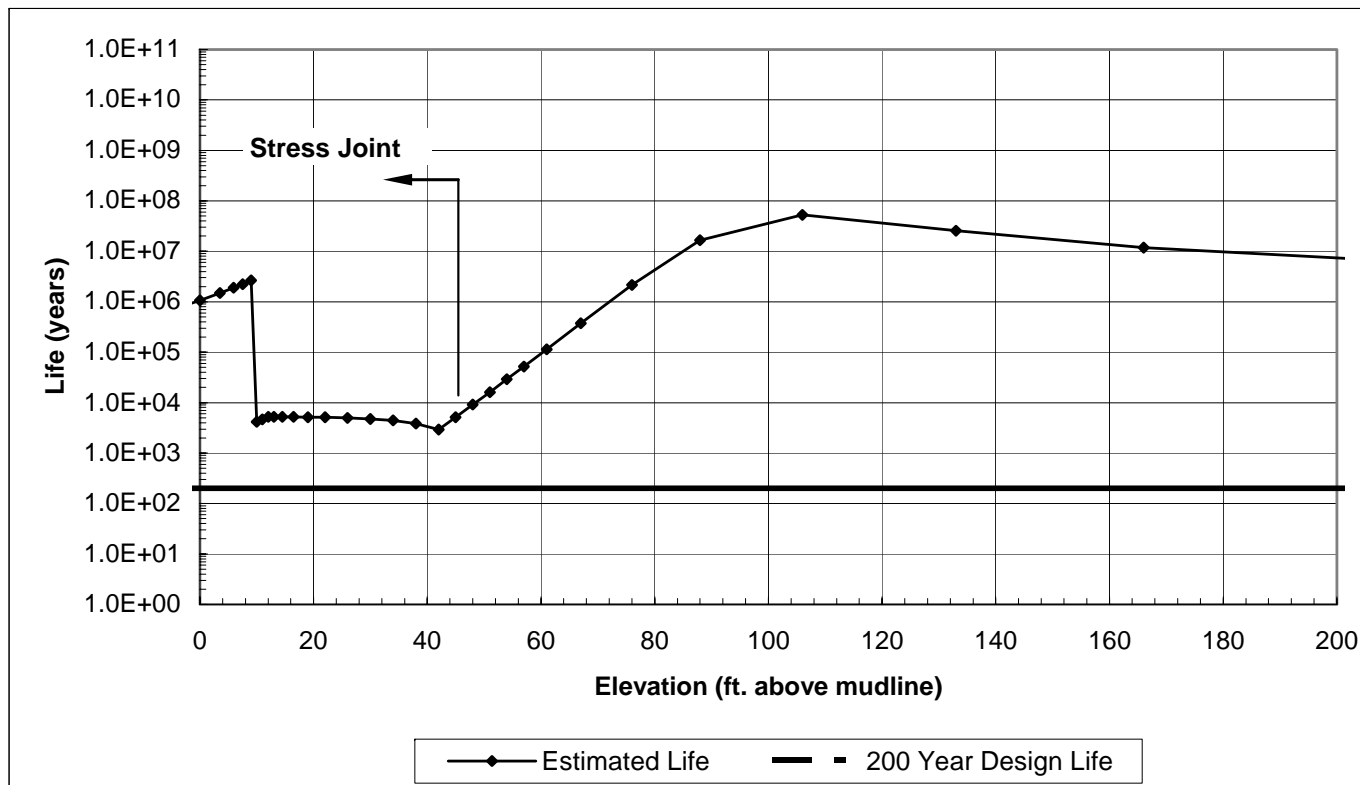


Fig. 6.2.3
Fatigue Life Estimates in the Upper Portion of the Riser
“All-Steel” Riser Configuration Machined Sections
Fatigue Curve: DnV-B

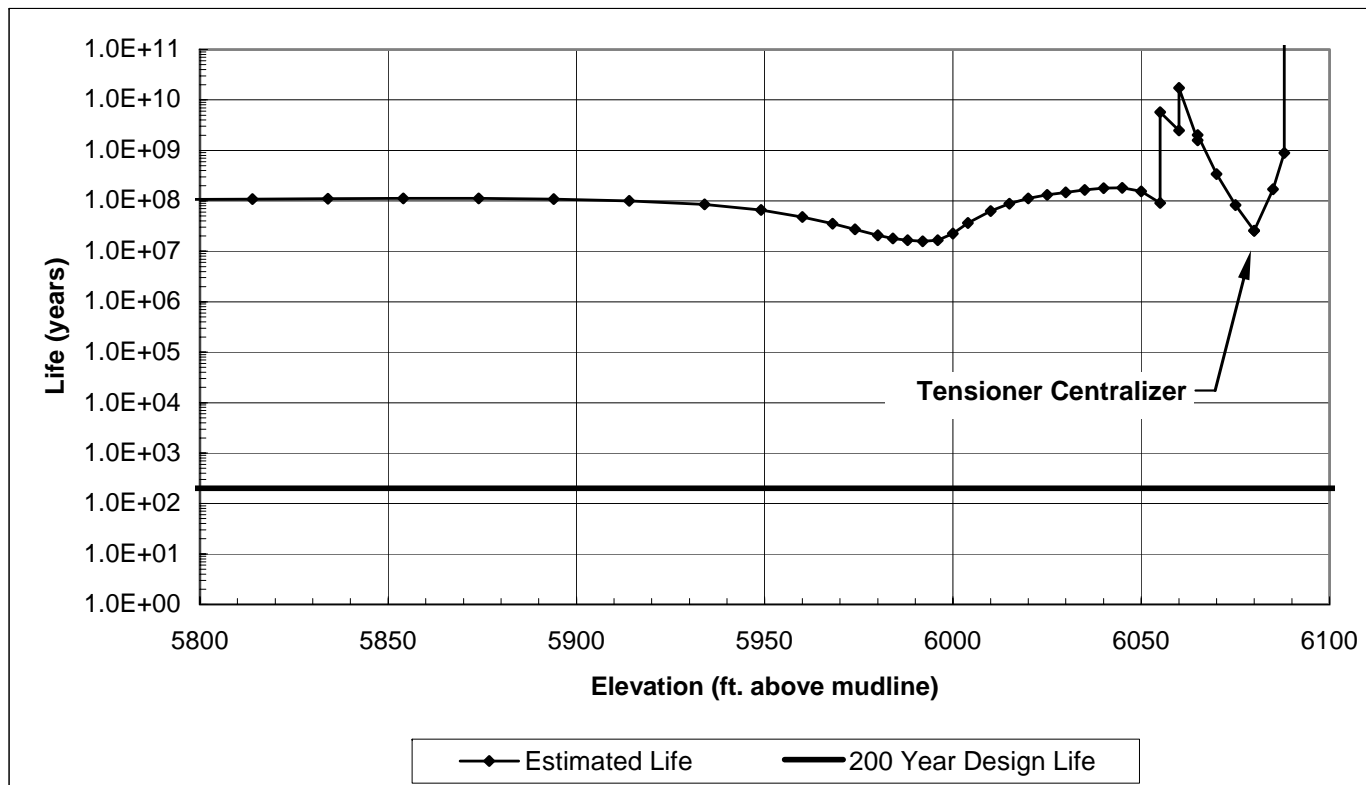


Fig. 6.2.4
Fatigue Life Estimates Along the Length of the Riser
“All-Steel” Riser Configuration Welded Sections
Fatigue Curve: DnV-C

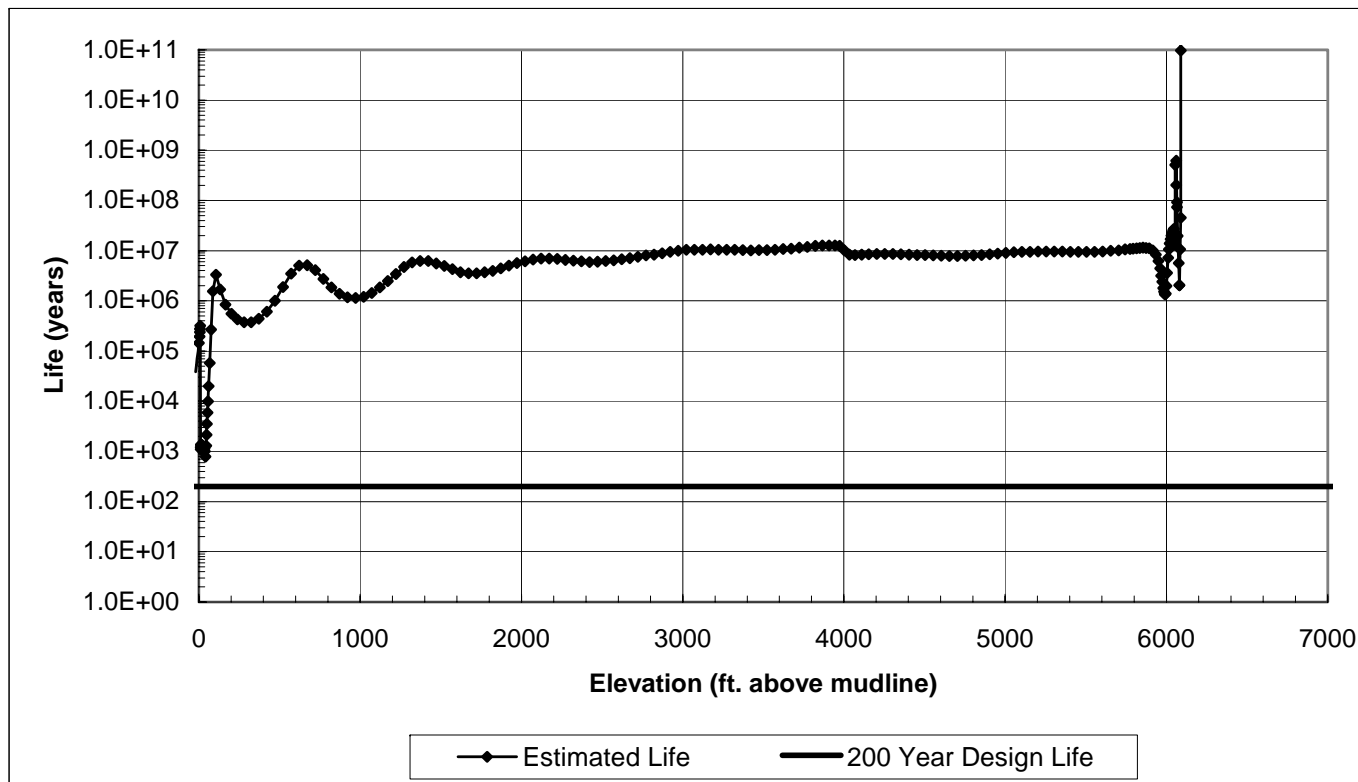


Table 6.2.5
Fatigue Life Estimates in the Lower Portion of the Riser
“All-Steel” Riser Configuration Welded Sections
Fatigue Curve: DnV-C

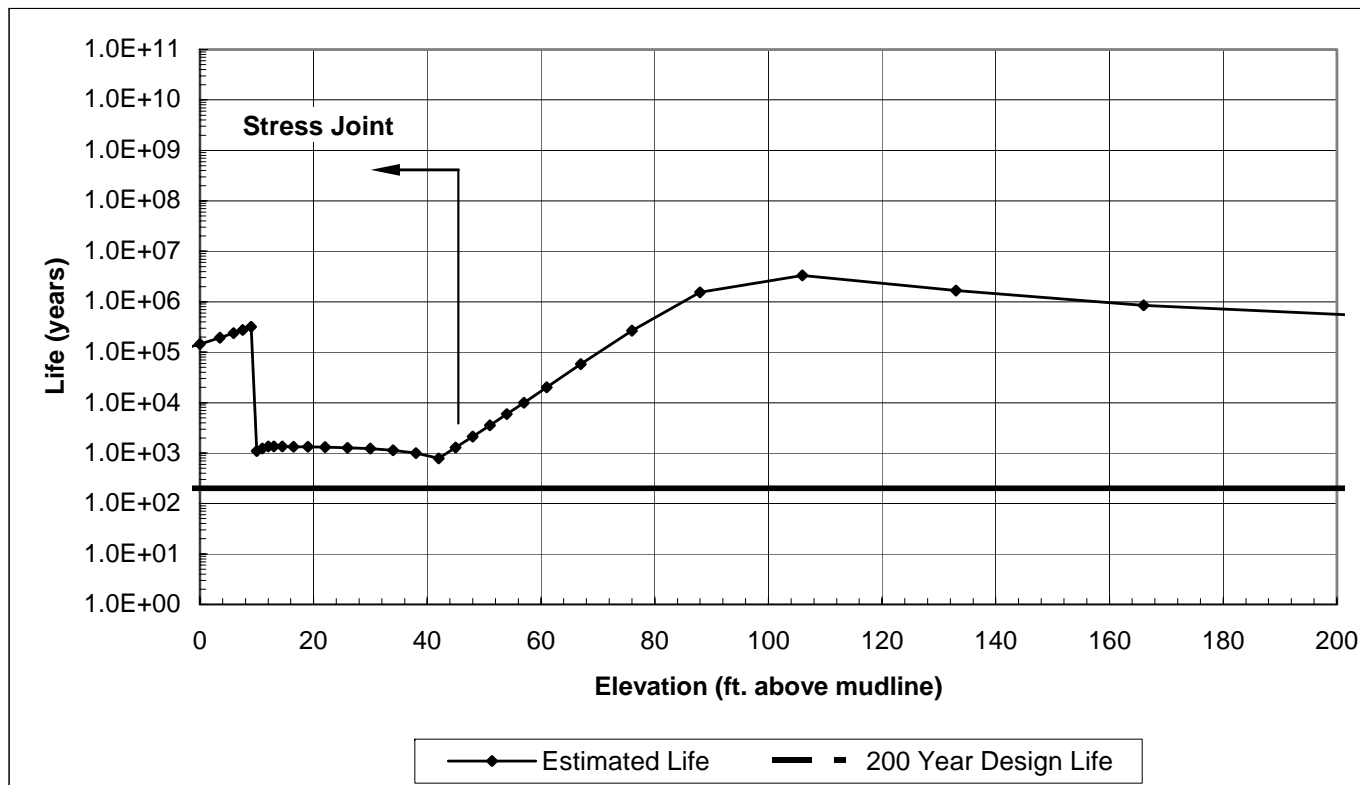


Table 6.2.6
Fatigue Life Estimates in the Upper Portion of the Riser
“All-Steel” Riser Configuration Welded Sections
Fatigue Curve: DnV-C

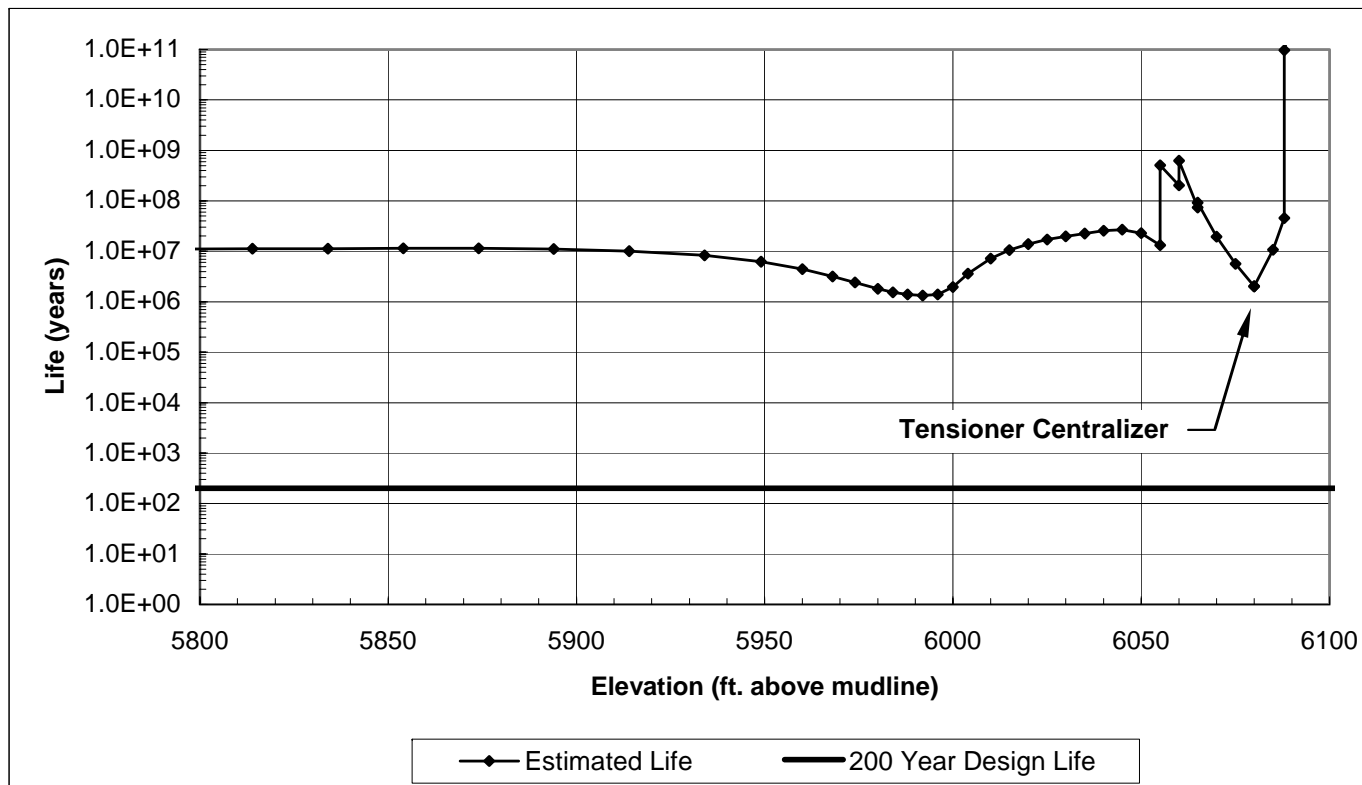


Fig. 6.3.1
Fatigue Life Estimates in the Lower Portion of the Riser
“Composite-Steel” Riser Configuration Steel Component Machined Sections
Fatigue Curve: DnV-B

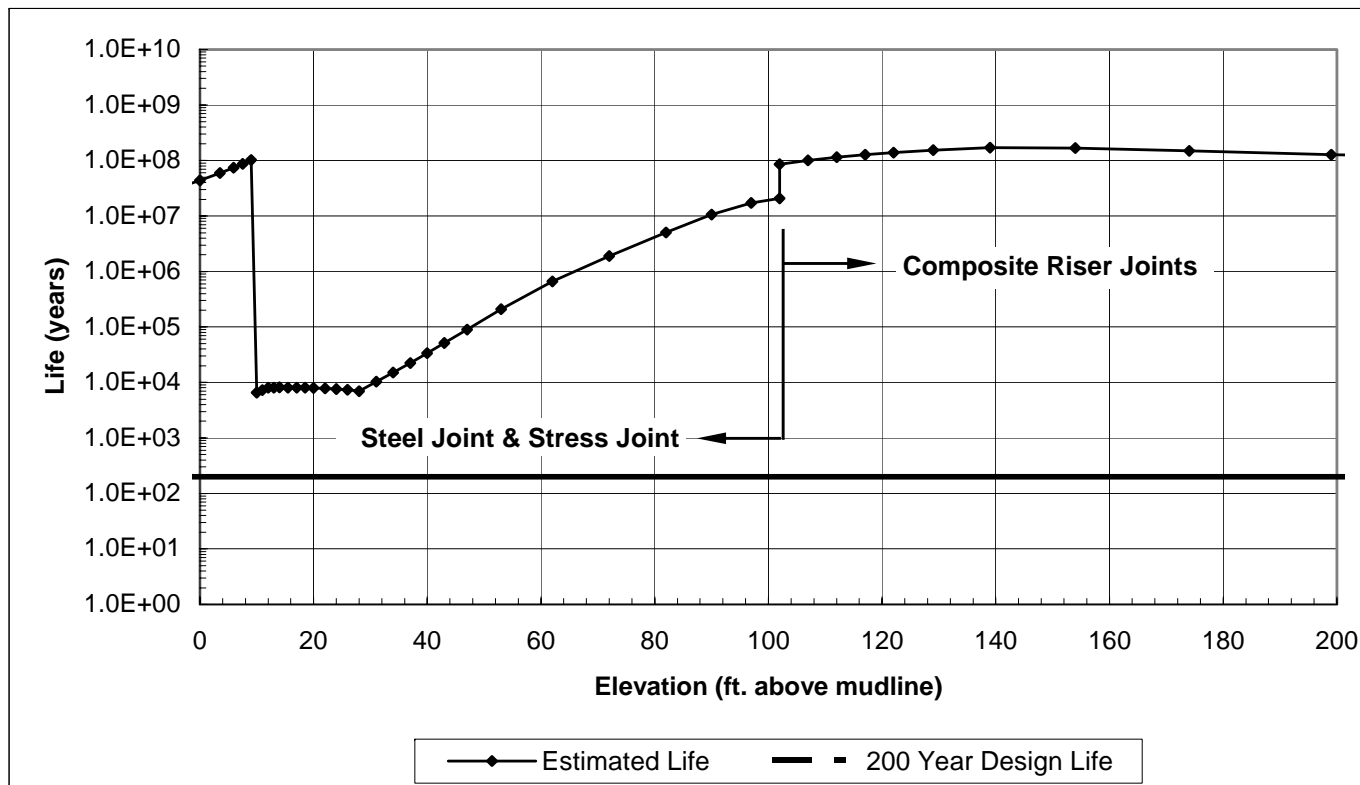


Fig. 6.3.2
Fatigue Life Estimates in the Upper Portion of the Riser
“Composite-Steel” Riser Configuration Steel Component Machined Sections
Fatigue Curve: DnV-B

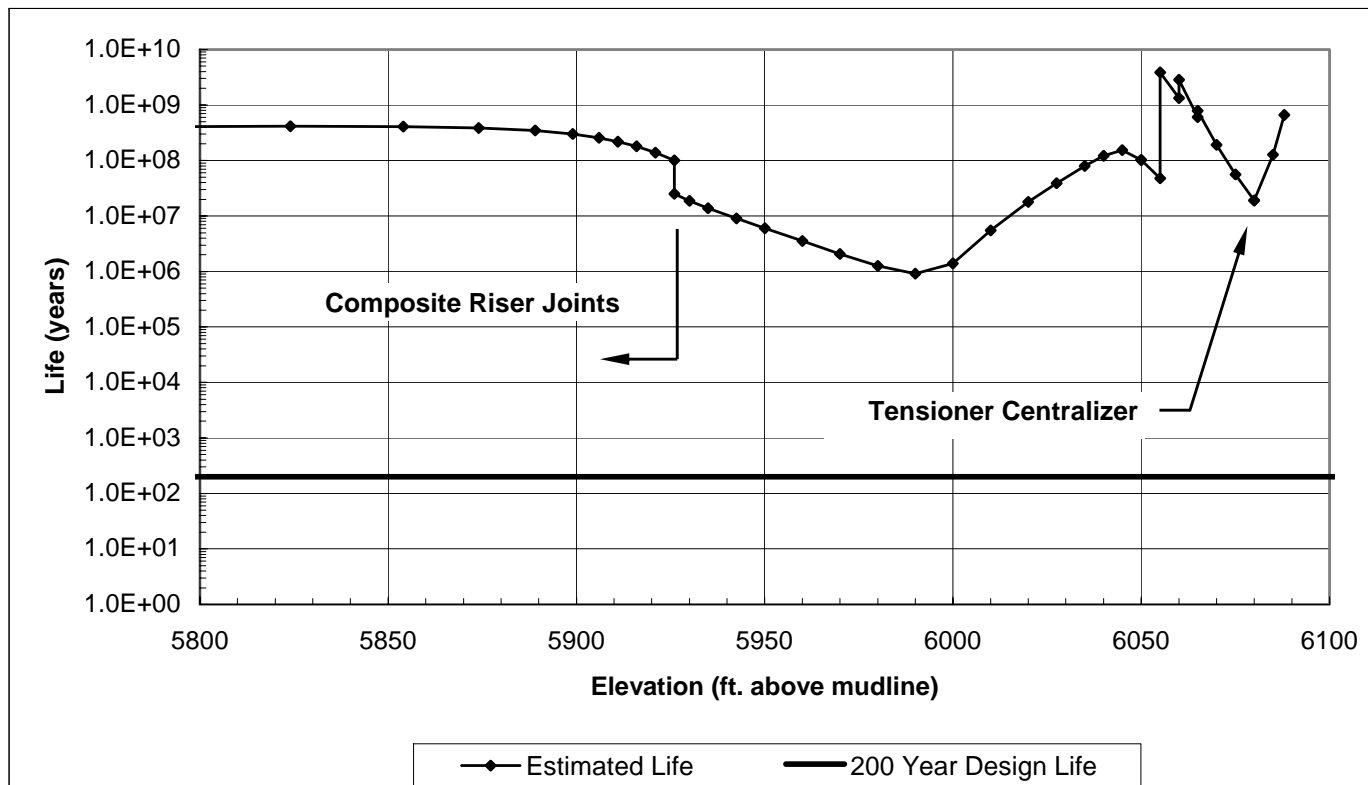


Fig. 6.3.3
Fatigue Life Estimates in the Lower Portion of the Riser
“Composite-Steel” Riser Configuration Steel Component Welded Sections
Fatigue Curve: DnV-C

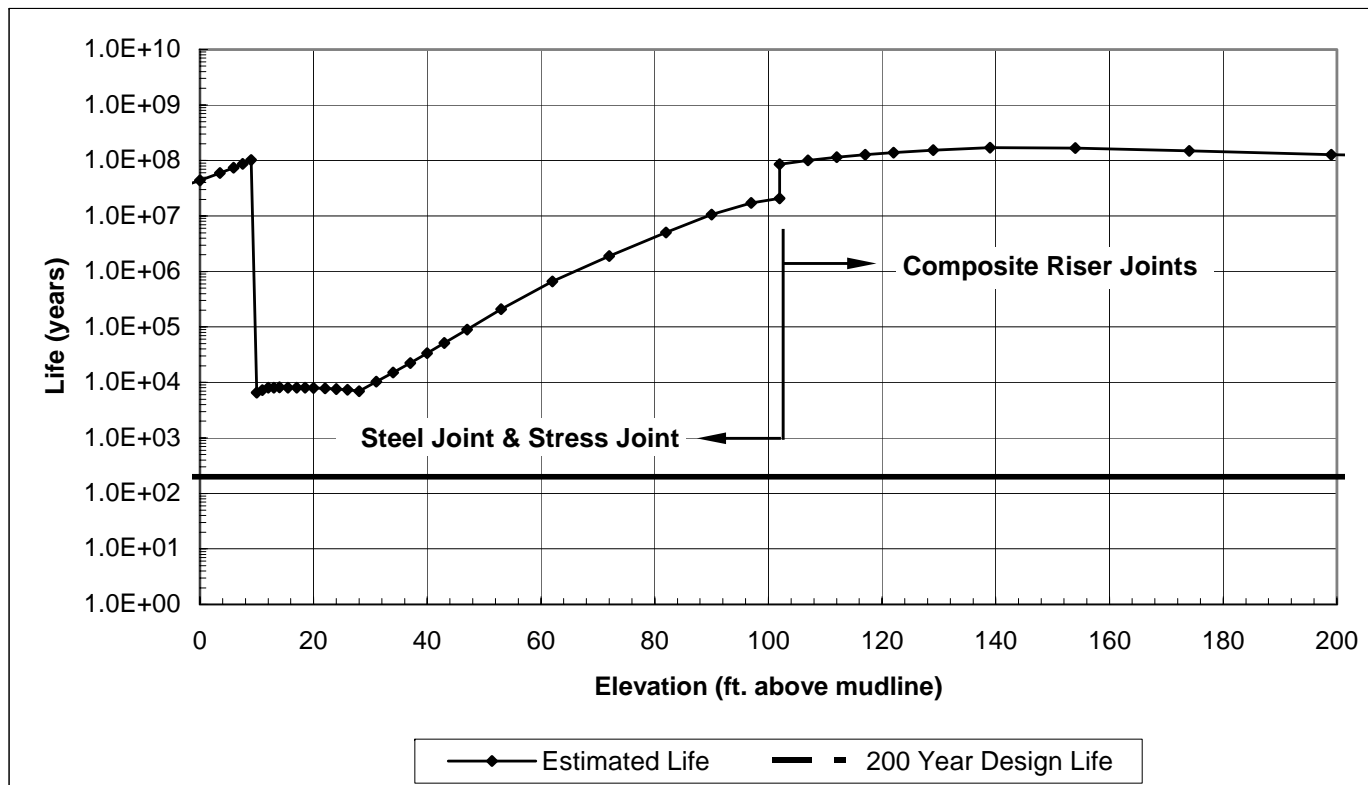
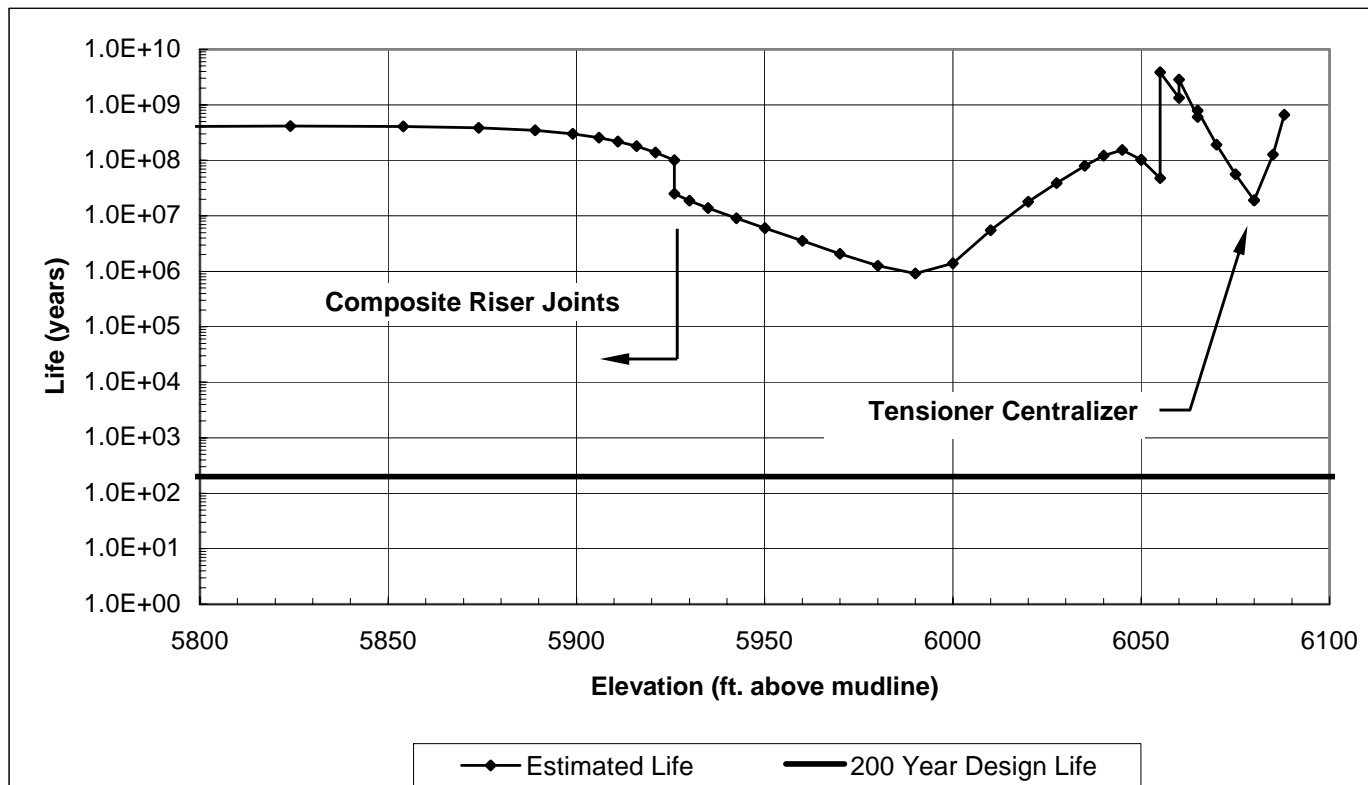


Fig. 6.3.4
Fatigue Life Estimates in the Upper Portion of the Riser
“Composite-Steel” Riser Configuration Steel Component Welded Sections
Fatigue Curve: DnV-C



7 REFERENCES

1. “A Review on Statistical Interpretation of Wave Data,” Goda, Y., in Report of the Port and Harbour Research Institute, March, 1979, vol. 18 (1), pp. 5-32.
2. Recommended Practice for Floating Production Systems (FPSs) and Tension-Leg Platforms (TLPs), API RP 2RD, First Edition, June, 1998.

Appendix A-3.3.1.1
TLP RAOs Provided by OTRC

**** HEADING: 0 DEG ****												
**** REGULAR WAVE RESPONSES ABOUT VESSEL CG ****												
WAVE PERIOD (SEC)	SURGE AMP (FT/FT)	SURGE (PHASE) (DEG)	SWAY AMP (FT/FT)	SWAY (PHASE) (DEG)	HEAVE AMP (FT/FT)	HEAVE (PHASE) (DEG)	ROLL AMP (DEG/FT)	ROLL (PHASE) (DEG)	PITCH AMP (DEG/FT)	PITCH (PHASE) (DEG)	YAW AMP (DEG/FT)	YAW (PHASE) (DEG)
32.0	1.0741	-90.1	0.0	0.0	0.0371	0.5	0.0	0.0	0.0002	-104.6	0.0	0.0
31.0	1.0661	-90.2	0.0	0.0	0.0364	0.5	0.0	0.0	0.0003	-102.8	0.0	0.0
30.0	1.0575	-90.2	0.0	0.0	0.0355	0.6	0.0	0.0	0.0003	-101.1	0.0	0.0
29.0	1.0482	-90.3	0.0	0.0	0.0346	0.6	0.0	0.0	0.0003	-99.6	0.0	0.0
28.0	1.0381	-90.3	0.0	0.0	0.0336	0.7	0.0	0.0	0.0004	-98.3	0.0	0.0
27.0	1.0271	-90.4	0.0	0.0	0.0325	0.8	0.0	0.0	0.0004	-97.1	0.0	0.0
26.0	1.0149	-90.5	0.0	0.0	0.0313	0.9	0.0	0.0	0.0005	-96.1	0.0	0.0
25.0	1.0015	-90.6	0.0	0.0	0.0299	1.0	0.0	0.0	0.0006	-95.2	0.0	0.0
24.0	0.9865	-90.7	0.0	0.0	0.0284	1.1	0.0	0.0	0.0007	-94.5	0.0	0.0
23.0	0.9696	-90.9	0.0	0.0	0.0268	1.2	0.0	0.0	0.0008	-94.0	0.0	0.0
22.5	0.9604	-91.0	0.0	0.0	0.0259	1.3	0.0	0.0	0.0008	-93.7	0.0	0.0
21.0	0.9290	-91.4	0.0	0.0	0.0229	1.5	0.0	0.0	0.0010	-93.3	0.0	0.0
20.0	0.9041	-91.8	0.0	0.0	0.0206	1.7	0.0	0.0	0.0012	-93.3	0.0	0.0
19.0	0.8754	-92.3	0.0	0.0	0.0181	1.9	0.0	0.0	0.0015	-93.4	0.0	0.0
18.0	0.8419	-92.9	0.0	0.0	0.0152	2.0	0.0	0.0	0.0017	-93.7	0.0	0.0
17.0	0.8027	-93.7	0.0	0.0	0.0120	2.1	0.0	0.0	0.0021	-94.3	0.0	0.0
16.0	0.7564	-94.7	0.0	0.0	0.0084	2.1	0.0	0.0	0.0024	-95.2	0.0	0.0
15.0	0.7013	-95.9	0.0	0.0	0.0044	2.0	0.0	0.0	0.0029	-96.3	0.0	0.0
14.0	0.6354	-97.1	0.0	0.0	0.0002	171.4	0.0	0.0	0.0034	-97.6	0.0	0.0
13.0	0.5566	-98.1	0.0	0.0	0.0052	178.4	0.0	0.0	0.0040	-98.8	0.0	0.0
12.0	0.4624	-98.2	0.0	0.0	0.0105	174.2	0.0	0.0	0.0045	-99.1	0.0	0.0
11.0	0.3510	-96.3	0.0	0.0	0.0148	166.3	0.0	0.0	0.0049	-97.1	0.0	0.0
10.0	0.2220	-90.4	0.0	0.0	0.0152	155.8	0.0	0.0	0.0050	-90.5	0.0	0.0
9.5	0.1504	-85.5	0.0	0.0	0.0133	151.8	0.0	0.0	0.0048	-84.8	0.0	0.0
9.0	0.0723	-79.0	0.0	0.0	0.0105	150.6	0.0	0.0	0.0045	-78.8	0.0	0.0
8.5	0.0161	80.6	0.0	0.0	0.0074	153.6	0.0	0.0	0.0036	-77.1	0.0	0.0
8.0	0.1093	90.7	0.0	0.0	0.0046	162.2	0.0	0.0	0.0020	-90.6	0.0	0.0
7.5	0.1969	75.6	0.0	0.0	0.0024	176.1	0.0	0.0	0.0007	136.6	0.0	0.0
7.0	0.2577	51.3	0.0	0.0	0.0007	155.7	0.0	0.0	0.0031	61.4	0.0	0.0
6.5	0.2583	37.6	0.0	0.0	0.0025	47.7	0.0	0.0	0.0052	38.0	0.0	0.0
6.0	0.1878	43.4	0.0	0.0	0.0051	25.4	0.0	0.0	0.0048	43.8	0.0	0.0
5.5	0.0643	56.0	0.0	0.0	0.0031	-5.8	0.0	0.0	0.0020	82.3	0.0	0.0
5.0	0.0311	-131.9	0.0	0.0	0.0013	140.0	0.0	0.0	0.0009	113.2	0.0	0.0
4.5	0.0479	-96.8	0.0	0.0	0.0018	-157.4	0.0	0.0	0.0004	-98.9	0.0	0.0
4.0	0.0093	129.0	0.0	0.0	0.0002	-140.0	0.0	0.0	0.0005	-61.5	0.0	0.0
3.5	0.0097	149.7	0.0	0.0	0.0005	-137.9	0.0	0.0	0.0028	-19.6	0.0	0.0
3.0	0.0018	84.3	0.0	0	0.0000	124.9	0.0	0.0	0.0003	82.7	0.0	0.0

**** HEADING: 22.5 DEG ****												
**** REGULAR WAVE RESPONSES ABOUT VESSEL CG ****												
WAVE PERIOD (SEC)	SURGE AMP (FT/FT)	SURGE (PHASE) (DEG)	SWAY AMP (FT/FT)	SWAY (PHASE) (DEG)	HEAVE AMP (FT/FT)	HEAVE (PHASE) (DEG)	ROLL AMP (DEG/FT)	ROLL (PHASE) (DEG)	PITCH AMP (DEG/FT)	PITCH (PHASE) (DEG)	YAW AMP (DEG/FT)	YAW (PHASE) (DEG)
32.0	0.9925	-90.1	0.4113	-90.1	0.0371	0.5	0.0001	89.9	0.0002	-105.6	0.0000	-180.0
31.0	0.9851	-90.2	0.4083	-90.2	0.0364	0.5	0.0001	89.9	0.0002	-103.7	0.0001	-180.0
30.0	0.9772	-90.2	0.4051	-90.2	0.0355	0.6	0.0001	89.9	0.0003	-101.9	0.0001	-180.0
29.0	0.9686	-90.3	0.4016	-90.3	0.0346	0.6	0.0001	89.8	0.0003	-100.3	0.0001	-180.0
28.0	0.9593	-90.3	0.3978	-90.3	0.0336	0.7	0.0002	89.8	0.0003	-98.8	0.0001	-180.0
27.0	0.9491	-90.4	0.3936	-90.4	0.0325	0.8	0.0002	89.7	0.0004	-97.6	0.0001	-180.0
26.0	0.9380	-90.5	0.3891	-90.5	0.0313	0.9	0.0002	89.6	0.0005	-96.5	0.0002	-180.0
25.0	0.9256	-90.6	0.3841	-90.6	0.0299	1.0	0.0002	89.5	0.0005	-95.5	0.0002	-180.0
24.0	0.9118	-90.7	0.3785	-90.7	0.0284	1.1	0.0003	89.4	0.0006	-94.7	0.0003	-180.0
23.0	0.8963	-90.9	0.3722	-90.9	0.0268	1.2	0.0003	89.3	0.0007	-94.1	0.0003	-180.0
22.5	0.8879	-91.0	0.3688	-91.0	0.0259	1.3	0.0004	89.2	0.0008	-93.9	0.0004	-180.0
21.0	0.8590	-91.4	0.3571	-91.4	0.0229	1.5	0.0005	88.8	0.0010	-93.4	0.0006	-180.0
20.0	0.8362	-91.8	0.3480	-91.8	0.0206	1.7	0.0005	88.5	0.0012	-93.3	0.0007	-180.0
19.0	0.8099	-92.3	0.3375	-92.3	0.0181	1.9	0.0007	88.1	0.0014	-93.4	0.0010	-180.0
18.0	0.7794	-92.9	0.3253	-92.9	0.0153	2.0	0.0008	87.5	0.0017	-93.7	0.0013	-180.0
17.0	0.7436	-93.7	0.3111	-93.7	0.0121	2.1	0.0010	86.8	0.0020	-94.2	0.0018	-180.0
16.0	0.7014	-94.7	0.2944	-94.8	0.0085	2.1	0.0012	86.0	0.0024	-95.0	0.0025	-180.0
15.0	0.6514	-95.9	0.2748	-96.0	0.0045	2.0	0.0014	85.0	0.0028	-96.1	0.0036	-180.0
14.0	0.5920	-97.2	0.2516	-97.4	0.0000	121.9	0.0018	84.0	0.0034	-97.3	0.0051	180.0
13.0	0.5214	-98.3	0.2242	-98.9	0.0050	178.5	0.0022	82.9	0.0040	-98.4	0.0075	180.0
12.0	0.4376	-98.6	0.1916	-100.2	0.0101	174.5	0.0027	82.1	0.0046	-98.8	0.0112	180.0
11.0	0.3393	-97.3	0.1518	-101.3	0.0141	167.0	0.0034	81.5	0.0052	-97.6	0.0170	179.9
10.0	0.2256	-93.4	0.1003	-104.3	0.0143	157.3	0.0041	79.5	0.0056	-94.0	0.0261	179.5
9.5	0.1621	-90.6	0.0672	-109.6	0.0124	153.9	0.0044	76.4	0.0057	-91.5	0.0323	179.0
9.0	0.0934	-88.4	0.0285	-128.9	0.0097	153.3	0.0044	69.9	0.0054	-89.9	0.0399	177.7
8.5	0.0216	-89.0	0.0203	100.4	0.0067	156.2	0.0038	58.2	0.0046	-91.8	0.0489	175.0
8.0	0.0436	85.8	0.0496	60.6	0.0038	162.7	0.0026	41.6	0.0032	-100.5	0.0592	168.9
7.5	0.0908	71.5	0.0591	31.5	0.0011	173.0	0.0011	32.3	0.0014	-117.0	0.0697	156.1
7.0	0.1133	50.2	0.0486	-0.5	0.0017	-2.6	0.0006	112.0	0.0005	34.4	0.0778	135.6
6.5	0.0991	39.3	0.0246	-23.2	0.0043	0.5	0.0010	124.2	0.0018	38.1	0.0789	118.7
6.0	0.0499	49.1	0.0075	-110.8	0.0054	-5.4	0.0008	94.2	0.0020	61.9	0.0685	120.4
5.5	0.0099	102.4	0.0192	-168.2	0.0030	-17.9	0.0008	16.0	0.0017	82.1	0.0424	137.9
5.0	0.0043	-14.2	0.0043	172.6	0.0001	-115.6	0.0000	-79.8	0.0008	75.2	0.0041	-151.3
4.5	0.0201	73.0	0.0068	110.6	0.0011	154.8	0.0002	54.5	0.0001	86.8	0.0073	-21.1
4.0	0.0179	102.7	0.0117	88.7	0.0004	155.2	0.0004	91.9	0.0007	-81.1	0.0072	4.4
3.5	0.0088	-21.6	0.0050	-17.6	0.0006	149.4	0.0014	-12.8	0.0026	165.9	0.0035	65.2
3.0	0.0034	50.0	0.0011	85.3	0.0000	-2.0	0.0002	-96.1	0.0006	47.3	0.0022	-41.7

**** HEADING: 45 DEG ****												
**** REGULAR WAVE RESPONSES ABOUT VESSEL CG ****												
WAVE PERIOD (SEC)	SURGE AMP (FT/FT)	SURGE (PHASE) (DEG)	SWAY AMP (FT/FT)	SWAY (PHASE) (DEG)	HEAVE AMP (FT/FT)	HEAVE (PHASE) (DEG)	ROLL AMP (DEG/FT)	ROLL (PHASE) (DEG)	PITCH AMP (DEG/FT)	PITCH (PHASE) (DEG)	YAW AMP (DEG/FT)	YAW (PHASE) (DEG)
32.0	0.7599	-90.1	0.7598	-90.1	0.0371	0.5	0.0002	89.9	0.0002	-109.6	0.0000	0.0
31.0	0.7543	-90.2	0.7542	-90.2	0.0364	0.5	0.0002	89.9	0.0002	-107.1	0.0000	0.0
30.0	0.7482	-90.2	0.7482	-90.2	0.0355	0.6	0.0002	89.9	0.0002	-104.9	0.0000	0.0
29.0	0.7417	-90.3	0.7417	-90.3	0.0346	0.6	0.0002	89.8	0.0002	-102.9	0.0000	0.0
28.0	0.7346	-90.3	0.7346	-90.3	0.0336	0.7	0.0003	89.8	0.0003	-101.0	0.0000	0.0
27.0	0.7269	-90.4	0.7269	-90.4	0.0325	0.8	0.0003	89.7	0.0003	-99.4	0.0000	0.0
26.0	0.7185	-90.5	0.7184	-90.5	0.0313	0.9	0.0004	89.6	0.0004	-98.0	0.0000	0.0
25.0	0.7091	-90.6	0.7090	-90.6	0.0299	1.0	0.0004	89.5	0.0004	-96.8	0.0000	0.0
24.0	0.6986	-90.7	0.6986	-90.7	0.0284	1.1	0.0005	89.4	0.0005	-95.7	0.0000	0.0
23.0	0.6870	-90.9	0.6869	-90.9	0.0268	1.2	0.0006	89.2	0.0006	-94.9	0.0000	0.0
22.5	0.6806	-91.0	0.6805	-91.0	0.0259	1.3	0.0006	89.1	0.0006	-94.6	0.0000	0.0
21.0	0.6588	-91.4	0.6587	-91.4	0.0229	1.5	0.0008	88.7	0.0008	-93.8	0.0000	0.0
20.0	0.6416	-91.8	0.6416	-91.8	0.0206	1.7	0.0009	88.4	0.0010	-93.5	0.0000	0.0
19.0	0.6219	-92.3	0.6218	-92.3	0.0181	1.9	0.0011	87.9	0.0011	-93.5	0.0000	-0.1
18.0	0.5990	-92.9	0.5989	-92.9	0.0153	2.0	0.0014	87.4	0.0014	-93.7	0.0000	-0.1
17.0	0.5723	-93.7	0.5722	-93.7	0.0121	2.1	0.0016	86.6	0.0016	-94.1	0.0000	-0.1
16.0	0.5409	-94.7	0.5409	-94.7	0.0085	2.1	0.0020	85.7	0.0020	-94.7	0.0000	-0.2
15.0	0.5040	-96.0	0.5040	-96.0	0.0046	1.9	0.0024	84.6	0.0024	-95.6	0.0000	-0.4
14.0	0.4604	-97.3	0.4604	-97.3	0.0001	9.4	0.0029	83.4	0.0029	-96.6	0.0000	-0.7
13.0	0.4090	-98.6	0.4090	-98.6	0.0047	178.7	0.0036	82.3	0.0036	-97.6	0.0000	-1.1
12.0	0.3485	-99.4	0.3484	-99.4	0.0097	174.8	0.0043	81.6	0.0043	-98.2	0.0000	-1.7
11.0	0.2773	-99.4	0.2773	-99.4	0.0134	167.7	0.0052	81.6	0.0052	-98.2	0.0000	-2.4
10.0	0.1922	-98.9	0.1922	-98.9	0.0134	158.9	0.0061	81.5	0.0061	-98.3	0.0000	-2.2
9.5	0.1419	-99.3	0.1419	-99.4	0.0115	156.3	0.0064	80.3	0.0064	-99.6	0.0000	-1.3
9.0	0.0853	-101.0	0.0853	-101.0	0.0089	156.4	0.0064	76.9	0.0064	-102.9	0.0000	0.4
8.5	0.0287	-96.9	0.0287	-96.9	0.0060	159.4	0.0056	70.4	0.0056	-109.5	0.0000	2.7
8.0	0.0190	8.6	0.0190	8.6	0.0030	163.6	0.0041	63.0	0.0041	-116.9	0.0000	4.3
7.5	0.0319	-13.3	0.0319	-13.3	0.0003	14.3	0.0026	65.9	0.0026	-114.1	0.0000	4.3
7.0	0.0329	-82.5	0.0329	-82.5	0.0042	-7.0	0.0020	76.3	0.0020	-103.9	0.0000	4.3
6.5	0.0547	-137.3	0.0547	-137.3	0.0075	-17.0	0.0016	56.0	0.0016	-124.5	0.0000	4.3
6.0	0.0798	-139.4	0.0798	-139.4	0.0072	-37.1	0.0015	30.4	0.0015	-150.1	0.0000	-41.7
5.5	0.0851	-121.1	0.0851	-121.1	0.0020	-65.7	0.0011	44.6	0.0011	-135.6	0.0000	-41.7
5.0	0.0549	-103.0	0.0549	-103.0	0.0021	53.2	0.0004	109.8	0.0004	-70.8	0.0000	-41.7
4.5	0.0084	-78.0	0.0084	-78.0	0.0005	-161.0	0.0000	11.4	0.0000	-169.0	0.0000	-41.7
4.0	0.0185	-75.9	0.0185	-75.9	0.0005	-13.5	0.0004	-61.8	0.0004	118.4	0.0000	-41.7
3.5	0.0038	-9.6	0.0038	-9.5	0.0004	135.8	0.0011	-3.9	0.0011	176.4	0.0000	-41.7
3.0	0.0042	44.0	0.0042	44.0	0.0000	84.3	0.0007	-138.6	0.0007	41.4	0.0000	-41.7

**** HEADING: 67.5 DEG ****												
**** REGULAR WAVE RESPONSES ABOUT VESSEL CG ****												
WAVE PERIOD (SEC)	SURGE AMP (FT/FT)	SURGE (PHASE) (DEG)	SWAY AMP (FT/FT)	SWAY (PHASE) (DEG)	HEAVE AMP (FT/FT)	HEAVE (PHASE) (DEG)	ROLL AMP (DEG/FT)	ROLL (PHASE) (DEG)	PITCH AMP (DEG/FT)	PITCH (PHASE) (DEG)	YAW AMP (DEG/FT)	YAW (PHASE) (DEG)
32.0	0.4114	-90.2	0.9924	-90.1	0.0371	0.5	0.0002	89.9	0.0001	-122.6	0.0001	0.0
31.0	0.4084	-90.2	0.9850	-90.2	0.0364	0.5	0.0002	89.9	0.0001	-118.9	0.0001	0.0
30.0	0.4051	-90.2	0.9771	-90.2	0.0355	0.6	0.0003	89.9	0.0001	-115.4	0.0001	0.0
29.0	0.4016	-90.3	0.9685	-90.3	0.0346	0.6	0.0003	89.8	0.0001	-112.1	0.0001	0.0
28.0	0.3978	-90.3	0.9592	-90.3	0.0336	0.7	0.0003	89.8	0.0002	-109.0	0.0001	0.0
27.0	0.3937	-90.4	0.9491	-90.4	0.0325	0.8	0.0004	89.7	0.0002	-106.2	0.0001	0.0
26.0	0.3891	-90.5	0.9379	-90.5	0.0313	0.9	0.0005	89.6	0.0002	-103.7	0.0002	0.0
25.0	0.3841	-90.6	0.9255	-90.6	0.0299	1.0	0.0005	89.5	0.0002	-101.5	0.0002	0.0
24.0	0.3785	-90.7	0.9117	-90.7	0.0284	1.1	0.0006	89.4	0.0003	-99.6	0.0003	0.0
23.0	0.3722	-90.9	0.8963	-90.9	0.0268	1.2	0.0007	89.2	0.0003	-98.0	0.0003	0.0
22.5	0.3688	-91.0	0.8878	-91.0	0.0259	1.3	0.0008	89.1	0.0004	-97.3	0.0004	0.0
21.0	0.3572	-91.4	0.8589	-91.4	0.0229	1.5	0.0010	88.7	0.0005	-95.6	0.0006	0.0
20.0	0.3480	-91.8	0.8362	-91.8	0.0206	1.7	0.0012	88.3	0.0005	-94.9	0.0007	0.0
19.0	0.3375	-92.3	0.8099	-92.3	0.0181	1.9	0.0014	87.8	0.0007	-94.4	0.0010	0.0
18.0	0.3253	-92.9	0.7793	-92.9	0.0153	2.0	0.0016	87.2	0.0008	-94.2	0.0013	0.0
17.0	0.3111	-93.7	0.7435	-93.7	0.0121	2.1	0.0020	86.3	0.0010	-94.3	0.0018	0.0
16.0	0.2944	-94.8	0.7013	-94.7	0.0085	2.1	0.0024	85.3	0.0012	-94.6	0.0025	0.0
15.0	0.2748	-96.0	0.6514	-95.9	0.0045	1.9	0.0028	84.1	0.0014	-95.2	0.0036	0.0
14.0	0.2517	-97.4	0.5920	-97.2	0.0000	142.1	0.0034	82.7	0.0018	-96.0	0.0052	0.0
13.0	0.2242	-98.9	0.5213	-98.3	0.0050	178.7	0.0040	81.5	0.0022	-96.8	0.0075	0.0
12.0	0.1916	-100.2	0.4376	-98.6	0.0101	174.6	0.0046	81.0	0.0027	-97.5	0.0113	0.0
11.0	0.1518	-101.3	0.3393	-97.3	0.0141	167.0	0.0052	82.1	0.0034	-98.1	0.0170	-0.1
10.0	0.1003	-104.3	0.2256	-93.4	0.0143	157.3	0.0056	85.8	0.0041	-100.2	0.0261	-0.5
9.5	0.0672	-109.6	0.1621	-90.6	0.0124	153.9	0.0057	88.3	0.0044	-103.4	0.0323	-1.0
9.0	0.0285	-128.9	0.0934	-88.4	0.0097	153.3	0.0054	89.9	0.0044	-109.8	0.0399	-2.3
8.5	0.0203	100.4	0.0216	-89.1	0.0067	156.2	0.0046	88.1	0.0038	-121.6	0.0489	-5.0
8.0	0.0496	60.6	0.0436	85.8	0.0038	162.9	0.0032	79.4	0.0026	-138.3	0.0592	-11.1
7.5	0.0591	31.5	0.0908	71.5	0.0011	173.3	0.0014	63.0	0.0011	-147.6	0.0697	-23.9
7.0	0.0486	-0.5	0.1133	50.2	0.0017	-2.4	0.0005	-145.9	0.0006	-68.2	0.0778	-44.4
6.5	0.0246	-23.2	0.0991	39.3	0.0043	0.8	0.0018	-142.0	0.0010	-56.2	0.0789	-61.3
6.0	0.0075	-110.9	0.0499	49.1	0.0054	-5.1	0.0020	-118.5	0.0008	-86.6	0.0685	-59.6
5.5	0.0192	-168.2	0.0099	102.4	0.0030	-17.4	0.0017	-98.1	0.0008	-164.3	0.0424	-42.1
5.0	0.0043	172.6	0.0043	-14.2	0.0001	-116.5	0.0008	-104.8	0.0000	99.8	0.0041	28.7
4.5	0.0068	110.6	0.0201	73.0	0.0011	154.5	0.0001	-91.7	0.0002	-124.5	0.0073	158.9
4.0	0.0117	88.7	0.0179	102.7	0.0004	156.0	0.0007	98.8	0.0004	-87.8	0.0072	-175.6
3.5	0.0050	-17.7	0.0088	-21.5	0.0004	149.9	0.0026	-14.3	0.0015	167.4	0.0035	-114.8
3.0	0.0011	85.3	0.0034	50.0	0.0000	-75.7	0.0006	-132.8	0.0002	83.9	0.0022	138.3

**** HEADING: 90 DEG ****												
**** REGULAR WAVE RESPONSES ABOUT VESSEL CG ****												
WAVE PERIOD (SEC)	SURGE AMP (FT/FT)	SURGE (PHASE) (DEG)	SWAY AMP (FT/FT)	SWAY (PHASE) (DEG)	HEAVE AMP (FT/FT)	HEAVE (PHASE) (DEG)	ROLL AMP (DEG/FT)	ROLL (PHASE) (DEG)	PITCH AMP (DEG/FT)	PITCH (PHASE) (DEG)	YAW AMP (DEG/FT)	YAW (PHASE) (DEG)
32.0	0.0000	-179.5	1.0740	-90.1	0.0371	0.5	0.0002	89.9	0.0001	-179.5	0.0000	-61.3
31.0	0.0000	-179.5	1.0660	-90.2	0.0364	0.5	0.0002	89.9	0.0001	-179.4	0.0000	-61.3
30.0	0.0000	-179.4	1.0574	-90.2	0.0355	0.6	0.0003	89.9	0.0001	-179.4	0.0000	-61.3
29.0	0.0000	-179.3	1.0481	-90.3	0.0346	0.6	0.0003	89.8	0.0001	-179.3	0.0000	-61.3
28.0	0.0000	-179.3	1.0380	-90.3	0.0336	0.7	0.0004	89.8	0.0001	-179.2	0.0000	-61.3
27.0	0.0000	-179.2	1.0270	-90.4	0.0325	0.8	0.0004	89.7	0.0001	-179.1	0.0000	-61.3
26.0	0.0000	-179.1	1.0148	-90.5	0.0313	0.9	0.0005	89.6	0.0000	-179.1	0.0000	-61.3
25.0	0.0000	-179.0	1.0014	-90.6	0.0299	1.0	0.0006	89.5	0.0000	-178.9	0.0000	-61.3
24.0	0.0000	-178.8	0.9864	-90.7	0.0284	1.1	0.0006	89.4	0.0000	-178.8	0.0000	-61.3
23.0	0.0000	-178.7	0.9696	-90.9	0.0268	1.2	0.0008	89.2	0.0000	-178.7	0.0000	-61.3
22.5	0.0000	-178.6	0.9603	-91.0	0.0259	1.3	0.0008	89.1	0.0000	-178.6	0.0000	-61.3
21.0	0.0000	-178.3	0.9289	-91.4	0.0229	1.5	0.0010	88.6	0.0000	-178.4	0.0000	-61.3
20.0	0.0000	-178.0	0.9040	-91.8	0.0206	1.7	0.0012	88.2	0.0000	-178.2	0.0000	-61.3
19.0	0.0000	-177.8	0.8753	-92.3	0.0181	1.8	0.0015	87.7	0.0000	-178.1	0.0000	-61.3
18.0	0.0000	-177.5	0.8419	-92.9	0.0152	2.0	0.0017	87.1	0.0000	-177.9	0.0000	-61.3
17.0	0.0000	-177.2	0.8027	-93.7	0.0120	2.1	0.0021	86.2	0.0000	-177.8	0.0000	-61.3
16.0	0.0000	-176.9	0.7563	-94.7	0.0084	2.0	0.0024	85.1	0.0000	-177.8	0.0000	-61.3
15.0	0.0000	-176.9	0.7012	-95.9	0.0044	1.7	0.0029	83.8	0.0000	-178.1	0.0000	-61.3
14.0	0.0000	0.0	0.6354	-97.1	0.0002	-179.8	0.0034	82.4	0.0000	-178.1	0.0000	-61.3
13.0	0.0000	2.4	0.5565	-98.1	0.0052	178.7	0.0040	81.1	0.0000	-1.1	0.0000	-61.3
12.0	0.0000	-0.9	0.4623	-98.2	0.0105	174.4	0.0045	80.7	0.0000	-5.4	0.0000	-61.3
11.0	0.0000	-7.6	0.3510	-96.3	0.0148	166.4	0.0049	82.6	0.0000	-13.3	0.0000	-61.3
10.0	0.0000	-17.5	0.2220	-90.4	0.0152	155.9	0.0050	89.2	0.0000	-23.8	0.0000	-61.3
9.5	0.0000	-22.0	0.1504	-85.5	0.0133	152.0	0.0048	94.9	0.0000	-27.7	0.0000	-61.3
9.0	0.0000	-25.0	0.0723	-79.0	0.0105	150.8	0.0045	101.0	0.0000	-28.8	0.0000	-61.3
8.5	0.0000	-25.3	0.0161	80.6	0.0074	153.8	0.0036	102.7	0.0000	-25.8	0.0000	-61.3
8.0	0.0000	-19.1	0.1093	90.7	0.0046	162.4	0.0020	89.2	0.0000	-17.2	0.0000	-61.3
7.5	0.0000	-4.6	0.1969	75.6	0.0024	176.0	0.0007	-43.1	0.0000	-3.6	0.0000	-61.3
7.0	0.0000	0.0	0.2577	51.3	0.0007	153.4	0.0031	-118.6	0.0000	-3.6	0.0000	-61.3
6.5	0.0000	-124.1	0.2583	37.6	0.0026	47.4	0.0052	-142.0	0.0000	-132.0	0.0000	-61.3
6.0	0.0000	-145.7	0.1878	43.4	0.0051	25.5	0.0049	-136.2	0.0000	-153.9	0.0000	138.3
5.5	0.0000	178.1	0.0643	56.0	0.0032	-5.3	0.0020	-97.9	0.0000	175.3	0.0000	138.3
5.0	0.0000	-39.3	0.0311	-131.9	0.0013	139.8	0.0009	-66.7	0.0000	-39.5	0.0000	138.3
4.5	0.0000	24.0	0.0479	-96.8	0.0018	-157.2	0.0004	80.4	0.0000	23.8	0.0000	138.3
4.0	0.0000	0.0	0.0093	129.0	0.0002	-136.3	0.0005	118.3	0.0000	23.8	0.0000	138.3
3.5	0.0000	10.9	0.0097	149.7	0.0008	-175.1	0.0028	160.1	0.0000	11.3	0.0000	138.3
3.0	0.0000	0.0	0.0018	84.3	0.0000	140.0	0.0003	-97.3	0.0000	11.3	0.0000	138.3

Appendix A-6.2.1

Dynamic Stresses Obtained from the “All-Steel” Riser Configuration Fatigue Solutions

**Dynamic Stresses Along the Length of the Riser
for the Wave Fatigue Bins**

Riser Configuration_07-20-04
Nominal Tensioner Setting = 865 kips; Wave Heading = 0 deg.

Elevation (ft. above Mudline)	Fatigue Bin = 1		Fatigue Bin = 2		Fatigue Bin = 3		Fatigue Bin = 4		Fatigue Bin = 5		Fatigue Bin = 6		Fatigue Bin = 7		Fatigue Bin = 8	
	Stress Std. Dev. (psi)	Zero Cross. Period (sec.)														
10.00	112.806	1.911	126.751	3.714	262.199	6.059	440.869	9.253	564.369	8.693	613.419	8.634	936.867	11.776	981.779	11.273
11.00	109.383	1.914	123.130	3.718	254.832	6.059	428.512	9.270	548.547	8.695	596.221	8.635	910.591	11.779	954.241	11.274
12.00	106.007	1.918	119.556	3.723	247.562	6.060	416.318	9.287	532.933	8.697	579.250	8.637	884.665	11.782	927.070	11.276
13.00	105.896	1.922	119.672	3.728	247.931	6.061	416.971	9.305	533.767	8.700	580.157	8.638	886.035	11.785	928.505	11.277
14.50	105.711	1.928	119.848	3.735	248.505	6.062	417.991	9.334	535.067	8.703	581.571	8.639	888.177	11.790	930.748	11.279
16.50	105.416	1.937	120.074	3.746	249.280	6.064	419.382	9.376	536.838	8.708	583.495	8.642	891.104	11.797	933.811	11.283
19.00	104.976	1.951	120.366	3.762	250.315	6.066	421.262	9.436	539.223	8.716	586.086	8.646	895.067	11.808	937.955	11.289
22.00	104.360	1.969	120.766	3.783	251.743	6.069	423.882	9.519	542.534	8.727	589.681	8.652	900.607	11.824	943.743	11.297
26.00	103.432	2.000	121.488	3.818	254.216	6.074	428.444	9.656	548.281	8.744	595.919	8.662	910.288	11.850	953.852	11.312
30.00	102.521	2.040	122.687	3.860	257.944	6.081	435.298	9.828	556.902	8.767	605.273	8.674	924.872	11.886	969.079	11.332
34.00	101.912	2.091	124.863	3.913	264.072	6.088	446.460	10.046	570.943	8.796	620.507	8.691	948.651	11.932	993.909	11.360
38.00	102.201	2.158	128.999	3.977	274.835	6.098	465.851	10.324	595.367	8.834	647.008	8.713	989.969	11.993	1037.069	11.398
42.00	104.699	2.242	137.199	4.054	294.989	6.109	501.805	10.673	640.730	8.882	696.237	8.741	1066.553	12.073	1117.102	11.448
45.00	87.173	2.316	118.232	4.121	256.353	6.119	437.725	10.997	558.289	8.929	606.577	8.770	930.584	12.155	974.486	11.502
48.00	71.817	2.391	101.516	4.195	222.338	6.131	381.528	11.385	485.884	8.987	527.819	8.807	811.364	12.258	849.409	11.571
51.00	58.523	2.435	86.799	4.270	192.389	6.144	332.265	11.833	422.300	9.059	458.640	8.853	706.847	12.387	739.731	11.659
54.00	47.281	2.373	73.861	4.333	166.016	6.158	289.109	12.314	366.474	9.147	397.886	8.911	615.245	12.546	643.578	11.770
57.00	38.194	2.124	62.508	4.355	142.772	6.173	251.320	12.761	317.444	9.254	344.511	8.983	534.952	12.742	559.267	11.911
61.00	30.428	1.609	49.567	4.239	115.977	6.191	208.175	13.035	261.202	9.432	283.249	9.110	443.070	13.076	462.740	12.158
67.00	28.877	1.205	34.408	3.516	83.271	6.196	156.485	11.710	193.137	9.785	209.017	9.394	332.270	13.763	346.233	12.717
76.00	38.641	1.202	21.086	2.006	47.209	5.949	102.059	6.999	119.398	10.381	128.284	10.199	212.755	15.135	220.295	14.329
88.00	52.938	1.338	20.707	1.559	17.179	3.581	61.874	3.313	59.568	8.436	61.644	12.380	114.770	13.288	116.412	19.229
106.00	65.563	1.532	30.925	1.943	19.746	3.171	48.163	2.138	36.649	3.822	34.255	5.685	58.592	4.988	56.554	7.684
133.00	68.748	1.823	40.661	2.502	39.796	4.482	57.082	2.455	60.174	4.462	62.015	5.615	74.404	4.504	76.803	5.679
166.00	62.405	1.839	45.390	2.884	52.750	5.144	63.794	2.860	79.687	5.150	84.455	5.948	97.773	5.151	103.731	5.959
202.00	54.740	1.656	46.239	2.899	61.113	5.492	64.568	2.892	92.315	5.494	99.311	6.145	113.290	5.487	121.948	6.149
240.00	52.066	1.607	44.062	3.133	66.476	5.587	61.318	3.089	100.413	5.581	109.352	6.230	123.259	5.576	134.280	6.234
281.00	52.957	1.480	41.093	2.907	69.021	5.684	56.980	2.869	104.286	5.688	115.092	6.258	128.073	5.691	141.361	6.263
325.00	48.862	1.530	37.508	2.702	68.408	5.791	52.354	2.681	103.453	5.788	115.816	6.302	127.154	5.789	142.322	6.304
372.00	48.444	1.526	33.837	2.779	64.494	5.755	48.295	2.737	97.662	5.734	110.962	6.357	120.170	5.731	136.459	6.356
422.00	52.806	1.628	32.344	2.413	57.233	5.676	46.665	2.427	86.788	5.674	100.426	6.368	106.928	5.676	123.623	6.369
472.00	54.570	1.659	30.620	2.493	47.630	5.550	44.535	2.495	72.370	5.535	85.612	6.360	89.314	5.530	105.528	6.364
522.00	50.002	1.585	30.434	2.425	36.916	5.150	43.191	2.410	56.217	5.130	68.103	6.359	70.785	5.413	84.519	6.732
572.00	43.786	1.534	30.494	2.355	26.740	4.474	42.097	2.480	40.745	4.518	50.098	6.189	54.356	5.083	64.732	6.808
622.00	46.365	1.547	29.129	2.452	20.074	3.790	41.716	2.458	31.852	4.014	35.798	5.842	45.400	4.643	50.193	6.644
672.00	48.706	1.551	28.369	2.483	21.462	3.979	41.892	2.540	34.365	4.125	32.968	5.486	47.983	4.646	47.077	6.342
722.00	44.492	1.572	28.876	2.430	28.137	4.524	42.869	2.541	43.934	4.646	40.948	5.594	58.445	5.022	55.605	6.152
772.00	42.682	1.529	29.512	2.634	35.542	4.949	43.656	2.659	54.775	5.017	52.808	5.774	70.841	5.278	68.952	6.116
822.00	45.021	1.596	30.608	2.652	41.748	5.283	44.175	2.698	63.970	5.316	63.996	5.945	81.623	5.509	81.947	6.181
872.00	46.380	1.560	31.244	2.862	46.081	5.473	43.890	2.775	70.414	5.515	72.733	6.080	89.284	5.682	92.272	6.262
922.00	40.756	1.515	31.469	2.685	48.278	5.574	42.921	2.741	73.725	5.618	78.352	6.171	93.279	5.763	98.985	6.324
972.00	38.496	1.626	29.599	2.666	48.326	5.658	41.075	2.667	73.871	5.694	80.672	6.250	93.512	5.829	101.787	6.391
1022.00	45.393	1.486	26.696	2.684	46.448	5.663	38.714	2.596	71.157	5.693	79.834	6.331	90.308	5.841	100.809	6.471
1072.00	39.749	1.536	24.756	2.275	42.970	5.624	36.442	2.386	66.042	5.649	76.229	6.396	84.230	5.815	96.504	6.546
1122.00	34.579	1.545	22.693	2.495	38.338	5.586	33.936	2.494	59.161	5.617	70.409	6.446	76.042	5.817	89.540	6.618
1172.00	41.446	1.520	22.984	2.206	33.158	5.412	33.470	2.329	51.407	5.479	63.069	6.499	66.815	5.748	80.765	6.708

**Dynamic Stresses Along the Length of the Riser
for the Wave Fatigue Bins**

Riser Configuration_07-20-04
Nominal Tensioner Setting = 865 kips; Wave Heading = 0 deg.

Elevation (ft. above Mudline)	Fatigue Bin = 1		Fatigue Bin = 2		Fatigue Bin = 3		Fatigue Bin = 4		Fatigue Bin = 5		Fatigue Bin = 6		Fatigue Bin = 7		Fatigue Bin = 8	
	Stress Std. Dev. (psi)	Zero Cross. Period (sec.)														
1222.00	42.473	1.571	22.980	2.215	28.081	5.121	32.981	2.346	43.781	5.240	55.077	6.529	57.789	5.590	71.236	6.799
1272.00	36.483	1.556	22.070	2.393	23.895	4.876	32.173	2.450	37.487	5.002	47.479	6.473	50.381	5.411	62.207	6.830
1322.00	35.310	1.527	22.335	2.332	21.596	4.642	32.493	2.379	33.929	4.714	41.450	6.320	46.088	5.151	55.038	6.775
1372.00	37.846	1.429	23.193	2.667	22.266	4.590	33.113	2.502	34.029	4.555	38.091	6.131	45.569	5.009	50.941	6.644
1422.00	35.161	1.614	24.905	2.501	24.612	4.735	34.118	2.478	37.518	4.761	39.121	5.836	48.124	5.102	50.404	6.457
1472.00	37.236	1.492	24.958	2.541	27.548	4.928	34.188	2.533	42.000	4.936	42.358	5.804	52.422	4.959	53.529	5.870
1522.00	36.136	1.518	23.511	2.767	30.313	5.141	33.275	2.649	46.280	5.091	46.472	5.844	57.717	5.100	58.507	5.902
1572.00	33.686	1.545	22.961	2.608	32.517	5.304	32.627	2.650	49.658	5.254	50.434	5.924	61.900	5.262	63.320	5.973
1622.00	34.952	1.514	22.931	2.511	33.952	5.375	32.330	2.573	51.820	5.365	53.614	6.007	64.581	5.389	67.208	6.047
1672.00	35.949	1.564	22.398	2.539	34.480	5.458	31.690	2.534	52.626	5.459	55.684	6.083	65.617	5.488	69.760	6.118
1722.00	33.979	1.430	21.492	2.544	34.108	5.568	30.736	2.509	52.103	5.550	56.515	6.153	65.041	5.566	70.812	6.188
1772.00	28.506	1.545	20.521	2.366	32.974	5.577	29.761	2.419	50.425	5.554	56.126	6.218	63.047	5.563	70.381	6.254
1822.00	32.291	1.448	19.373	2.395	31.217	5.506	28.521	2.428	47.798	5.490	54.640	6.277	59.875	5.507	68.615	6.315
1872.00	34.523	1.511	18.474	2.203	29.000	5.481	27.343	2.342	44.477	5.443	52.266	6.333	55.848	5.466	65.765	6.374
1922.00	32.229	1.578	17.456	2.236	26.607	5.433	26.037	2.355	40.859	5.370	49.282	6.380	51.599	5.734	62.164	6.427
1972.00	30.671	1.492	17.349	2.362	24.360	5.267	25.474	2.381	37.394	5.238	46.015	6.400	48.340	5.618	58.205	6.457
2022.00	31.023	1.559	18.264	2.114	22.500	5.110	25.939	2.217	34.480	5.131	42.808	6.383	45.908	5.513	55.032	6.800
2072.00	31.988	1.470	17.910	2.380	21.217	5.061	25.827	2.362	32.959	5.031	39.988	6.329	44.619	5.438	52.840	6.776
2122.00	29.211	1.490	18.014	2.520	20.843	4.919	26.181	2.460	32.833	4.979	38.195	6.307	44.545	5.384	51.488	6.716
2172.00	27.003	1.462	18.958	2.347	21.318	4.902	27.164	2.447	33.598	4.997	37.744	6.210	45.453	5.398	51.046	6.623
2222.00	28.971	1.474	19.202	2.708	22.164	4.933	27.748	2.677	34.895	5.058	38.021	6.126	46.960	5.447	51.400	6.525
2272.00	30.352	1.502	19.740	2.627	23.096	5.032	28.387	2.632	36.343	5.129	38.805	6.083	48.663	5.476	52.305	6.457
2322.00	28.968	1.508	19.976	2.617	23.926	5.141	28.378	2.677	37.638	5.208	39.841	6.077	50.201	5.511	53.477	6.428
2372.00	27.599	1.610	19.650	2.824	24.542	5.184	27.861	2.753	38.591	5.265	40.896	6.094	51.332	5.553	54.660	6.424
2422.00	29.765	1.464	19.269	2.411	24.859	5.208	27.234	2.477	39.098	5.295	41.789	6.129	51.934	5.586	55.652	6.440
2472.00	27.709	1.460	17.412	2.404	24.842	5.309	25.335	2.476	39.114	5.361	42.399	6.181	51.958	5.646	56.315	6.477
2522.00	24.121	1.505	15.057	2.536	24.560	5.444	23.114	2.466	38.694	5.466	42.669	6.242	51.451	5.744	56.581	6.528
2572.00	25.775	1.399	14.308	2.079	24.116	5.482	21.826	2.221	37.964	5.525	42.592	6.295	50.537	5.819	56.440	6.581
2622.00	27.304	1.535	13.916	2.052	23.561	5.469	20.761	2.223	37.023	5.540	42.186	6.335	49.346	5.852	55.917	6.627
2672.00	27.970	1.508	13.725	2.104	22.921	5.519	20.192	2.204	35.948	5.575	41.492	6.367	47.990	5.881	55.063	6.668
2722.00	25.989	1.489	13.910	2.075	22.267	5.541	20.210	2.211	34.851	5.569	40.563	6.387	46.596	5.871	53.945	6.703
2772.00	24.099	1.595	14.160	2.219	21.659	5.418	20.720	2.324	33.816	5.456	39.461	6.387	45.264	5.788	52.638	6.726
2822.00	26.228	1.397	14.705	2.317	21.078	5.276	21.790	2.306	32.843	5.337	38.248	6.367	44.018	5.705	51.219	6.730
2872.00	24.196	1.419	15.414	2.490	20.493	5.220	22.614	2.442	31.910	5.284	36.982	6.339	42.862	5.671	49.756	6.726
2922.00	21.653	1.590	16.260	2.620	19.908	5.156	23.309	2.593	31.030	5.227	35.720	6.311	41.813	5.635	48.312	6.721
2972.00	25.409	1.432	17.013	2.569	19.369	5.011	23.950	2.548	30.200	5.147	34.519	6.282	40.867	5.587	46.945	6.714
3022.00	26.217	1.524	17.110	2.601	19.006	4.930	23.821	2.641	29.581	4.967	33.434	6.252	39.996	5.576	45.708	6.705
3072.00	24.367	1.573	16.514	2.529	18.601	4.962	23.135	2.642	29.268	4.996	32.505	6.235	39.206	5.586	44.637	6.699
3122.00	23.353	1.414	15.306	2.565	18.220	5.020	22.154	2.550	28.987	5.034	32.197	6.089	38.529	5.571	43.757	6.706
3172.00	21.874	1.498	14.251	2.689	17.933	5.036	21.063	2.570	28.776	5.070	32.274	6.126	38.335	5.253	43.340	6.286
3222.00	22.830	1.437	14.037	2.284	17.763	5.072	20.408	2.352	28.649	5.138	32.501	6.163	38.318	5.323	43.633	6.314
3272.00	23.045	1.377	13.478	2.216	17.719	5.170	19.551	2.247	28.627	5.220	32.839	6.196	38.354	5.380	43.995	6.339
3322.00	20.845	1.543	12.578	2.484	17.817	5.274	18.416	2.407	28.728	5.271	33.237	6.230	38.449	5.406	44.376	6.363
3372.00	22.350	1.489	12.604	2.173	18.054	5.312	18.207	2.275	28.932	5.291	33.640	6.263	38.576	5.425	44.727	6.388
3422.00	24.104	1.455	12.606	2.094	18.377	5.304	18.280	2.201	29.190	5.303	33.994	6.283	38.701	5.448	45.002	6.407
3472.00	22.451	1.542	12.169	2.331	18.707	5.326	18.007	2.395	29.433	5.320	34.246	6.287	38.781	5.464	45.158	6.418

**Dynamic Stresses Along the Length of the Riser
for the Wave Fatigue Bins**

Riser Configuration_07-20-04
Nominal Tensioner Setting = 865 kips; Wave Heading = 0 deg.

Elevation (ft. above Mudline)	Fatigue Bin = 1		Fatigue Bin = 2		Fatigue Bin = 3		Fatigue Bin = 4		Fatigue Bin = 5		Fatigue Bin = 6		Fatigue Bin = 7		Fatigue Bin = 8	
	Stress Std. Dev. (psi)	Zero Cross. Period (sec.)														
3522.00	20.955	1.486	12.198	2.153	18.979	5.403	18.199	2.328	29.600	5.356	34.351	6.282	38.769	5.485	45.158	6.422
3572.00	20.977	1.465	12.111	2.188	19.162	5.475	18.474	2.293	29.644	5.400	34.271	6.278	38.621	5.520	44.974	6.426
3622.00	21.532	1.458	12.087	2.544	19.232	5.471	18.546	2.490	29.536	5.414	33.987	6.272	38.474	5.780	44.593	6.431
3672.00	20.999	1.427	12.913	2.316	19.148	5.412	19.030	2.416	29.245	5.388	33.497	6.262	38.492	5.756	44.018	6.434
3722.00	19.523	1.448	13.420	2.273	18.869	5.374	19.309	2.381	28.743	5.357	32.810	6.247	38.359	5.754	43.264	6.435
3772.00	19.215	1.436	13.128	2.661	18.389	5.357	18.996	2.618	28.034	5.328	31.952	6.233	38.077	5.778	42.358	6.438
3822.00	20.522	1.497	13.096	2.568	17.738	5.293	18.924	2.597	27.398	5.335	30.964	6.224	37.680	5.786	41.343	6.447
3867.00	21.704	1.548	13.160	2.351	17.031	5.191	18.982	2.456	26.818	5.292	30.006	6.220	37.254	5.763	40.377	6.458
3908.00	22.156	1.462	12.818	2.440	16.387	5.123	18.697	2.510	26.228	5.252	29.119	6.217	36.827	5.742	39.721	6.630
3944.00	20.806	1.418	12.416	2.570	15.856	5.093	18.347	2.594	25.715	5.233	28.391	6.216	36.477	5.732	39.477	6.636
3974.00	18.687	1.471	12.368	2.542	15.585	5.081	18.360	2.576	25.569	5.219	28.120	6.213	36.530	5.717	39.690	6.630
4004.00	19.286	1.555	13.804	2.464	16.945	5.060	20.293	2.498	27.980	5.180	30.661	6.186	39.703	5.611	43.402	6.530
4034.00	21.766	1.492	15.195	2.486	18.204	5.029	22.105	2.499	30.265	5.152	33.143	6.174	42.777	5.543	47.079	6.465
4069.00	23.265	1.408	15.125	2.593	17.698	4.980	21.851	2.588	29.804	5.151	32.818	6.121	42.484	5.571	47.115	6.493
4109.00	23.053	1.467	14.942	2.512	16.955	4.920	21.413	2.550	28.950	5.157	32.356	6.171	41.685	5.612	46.673	6.539
4154.00	21.903	1.533	14.561	2.327	16.247	4.889	20.951	2.419	28.087	5.153	31.954	6.215	40.811	5.627	46.187	6.579
4204.00	21.953	1.415	13.421	2.307	15.740	4.943	20.032	2.431	27.391	5.155	31.744	6.244	40.006	5.623	45.775	6.604
4254.00	21.055	1.501	12.107	2.354	15.625	5.063	19.116	2.448	27.041	5.200	31.794	6.276	39.436	5.649	45.535	6.629
4304.00	21.497	1.455	11.775	2.306	15.928	5.144	18.780	2.405	27.068	5.257	32.073	6.319	39.140	5.685	45.475	6.661
4354.00	21.584	1.470	12.346	2.128	16.560	5.156	18.888	2.334	27.438	5.274	32.526	6.355	39.128	5.688	45.581	6.688
4404.00	21.460	1.618	12.512	2.149	17.347	5.202	18.857	2.316	28.030	5.292	33.076	6.367	39.335	5.689	45.818	6.700
4454.00	22.832	1.452	12.189	2.308	18.136	5.338	18.566	2.368	28.698	5.365	33.626	6.362	39.665	5.734	46.121	6.700
4504.00	20.646	1.447	12.146	2.212	18.837	5.467	18.382	2.342	29.334	5.450	34.081	6.357	40.031	5.790	46.416	6.700
4554.00	17.746	1.512	12.301	2.402	19.386	5.485	18.299	2.431	29.850	5.477	34.362	6.351	40.352	5.812	46.631	6.701
4604.00	19.900	1.426	12.912	2.593	19.698	5.444	18.600	2.526	30.144	5.468	34.411	6.340	40.531	5.817	46.706	6.698
4654.00	21.763	1.488	13.879	2.368	19.699	5.439	19.196	2.361	30.125	5.477	34.196	6.321	40.483	5.833	46.596	6.692
4704.00	20.804	1.461	14.066	2.577	19.433	5.361	19.321	2.498	29.768	5.319	33.704	6.304	40.169	5.838	46.272	6.691
4754.00	18.039	1.475	13.945	2.829	18.887	5.309	19.203	2.671	29.303	5.287	32.949	6.295	39.581	5.817	45.731	6.700
4804.00	18.327	1.546	13.994	2.437	18.046	5.217	19.372	2.482	28.501	5.233	31.973	6.296	38.730	5.796	44.996	6.719
4854.00	21.360	1.447	13.234	2.512	16.954	5.146	19.014	2.504	27.408	5.190	30.846	6.301	37.659	5.795	44.112	6.742
4904.00	20.673	1.499	12.190	2.749	15.698	5.081	18.287	2.608	26.119	5.146	29.659	6.309	36.570	5.386	43.144	6.771
4954.00	17.935	1.546	11.889	2.307	14.410	4.954	17.865	2.427	24.763	5.075	28.515	6.329	35.426	5.355	42.168	6.806
5004.00	17.839	1.409	11.538	2.263	13.228	4.789	17.355	2.382	23.477	5.002	27.524	6.363	34.276	5.338	41.265	6.846
5054.00	18.474	1.449	11.068	2.376	12.293	4.691	16.733	2.390	22.398	4.963	26.791	6.399	33.238	5.338	40.515	6.882
5104.00	18.888	1.506	10.968	2.202	11.754	4.701	16.280	2.291	21.661	4.958	26.391	6.421	32.612	5.794	39.982	6.902
5154.00	19.047	1.458	10.829	2.256	11.716	4.770	15.843	2.295	21.360	4.979	26.348	6.425	32.420	5.786	39.697	6.903
5204.00	17.793	1.438	10.791	2.330	12.166	4.860	15.815	2.335	21.508	5.036	26.632	6.426	32.616	5.801	39.662	6.891
5254.00	16.528	1.461	10.976	2.199	12.966	4.980	15.994	2.320	22.126	5.221	27.169	6.425	33.160	5.817	39.843	6.867
5304.00	17.493	1.480	10.932	2.243	13.941	5.134	16.160	2.379	23.174	5.276	27.863	6.407	33.961	5.808	40.185	6.830
5354.00	19.169	1.523	10.687	2.331	14.962	5.272	16.331	2.385	24.310	5.335	28.602	6.369	34.894	5.803	40.613	6.779
5404.00	19.461	1.523	10.614	2.373	15.959	5.379	16.422	2.441	25.392	5.398	29.278	6.325	35.833	5.817	41.043	6.725
5454.00	17.934	1.524	10.855	2.369	16.775	5.417	16.554	2.521	26.313	5.433	29.796	6.294	36.678	5.822	41.398	6.680
5504.00	16.559	1.479	11.152	2.311	17.344	5.426	16.825	2.460	26.988	5.437	30.088	6.275	37.341	5.806	41.611	6.646
5554.00	16.409	1.359	11.189	2.504	17.619	5.454	16.904	2.560	27.350	5.448	30.256	6.329	37.752	5.803	41.638	6.616
5604.00	15.867	1.421	11.381	2.701	17.592	5.476	17.031	2.723	27.373	5.471	30.166	6.317	37.872	5.822	41.453	6.587
5654.00	16.332	1.455	11.894	2.488	17.271	5.430	17.464	2.591	27.064	5.454	29.793	6.303	37.700	5.820	41.046	6.565

**Dynamic Stresses Along the Length of the Riser
for the Wave Fatigue Bins**

Riser Configuration_07-20-04
Nominal Tensioner Setting = 865 kips; Wave Heading = 0 deg.

Elevation (ft. above Mudline)	Fatigue Bin = 1		Fatigue Bin = 2		Fatigue Bin = 3		Fatigue Bin = 4		Fatigue Bin = 5		Fatigue Bin = 6		Fatigue Bin = 7		Fatigue Bin = 8	
	Stress Std. Dev. (psi)	Zero Cross. Period (sec.)														
5704.00	17.447	1.399	12.064	2.601	16.666	5.333	17.641	2.647	26.443	5.389	29.161	6.302	37.255	5.783	40.438	6.560
5744.00	17.009	1.454	12.011	2.866	15.986	5.276	17.590	2.818	25.732	5.348	28.503	6.311	36.712	5.763	39.838	6.566
5744.00	16.424	1.521	12.066	2.780	15.370	5.251	17.622	2.778	25.086	5.335	27.950	6.315	36.204	5.767	39.344	6.574
5794.00	16.344	1.530	12.128	2.620	14.919	5.230	17.666	2.678	24.613	5.328	27.569	6.314	35.827	5.774	39.008	6.579
5814.00	16.582	1.510	12.142	2.494	14.446	5.192	17.669	2.591	24.121	5.312	27.204	6.308	35.439	5.777	38.700	6.585
5834.00	17.005	1.496	12.054	2.444	13.954	5.125	17.584	2.554	23.617	5.279	26.862	6.299	35.046	5.771	38.490	6.586
5854.00	17.442	1.518	11.848	2.467	13.464	5.028	17.396	2.567	23.139	5.228	26.599	6.291	34.699	5.753	38.440	6.588
5874.00	17.875	1.576	11.550	2.526	12.999	4.912	17.129	2.601	22.738	5.166	26.516	6.290	34.471	5.728	38.661	6.594
5894.00	18.364	1.657	11.210	2.541	12.608	4.801	16.835	2.598	22.517	5.113	26.783	6.304	34.514	5.707	39.407	6.605
5914.00	18.912	1.687	10.877	2.438	12.419	4.736	16.581	2.520	22.745	5.102	27.759	6.340	35.213	5.707	41.211	6.622
5934.00	19.453	1.622	10.657	2.263	12.856	4.897	16.658	2.419	24.147	5.167	30.199	6.379	37.617	5.727	45.216	6.613
5949.00	19.732	1.540	10.968	2.206	14.157	4.995	17.987	2.465	27.133	5.226	33.856	6.344	42.243	5.676	50.987	6.521
5960.00	19.902	1.491	12.193	2.320	16.145	5.010	21.332	2.681	31.418	5.176	38.068	6.213	48.735	5.502	57.572	6.344
5968.00	20.258	1.485	14.270	2.530	18.382	4.919	26.311	2.928	36.135	5.030	42.028	6.027	55.870	5.266	63.769	6.129
5974.00	21.025	1.519	16.769	2.729	20.491	4.774	31.935	3.092	40.572	4.855	45.278	5.826	62.591	5.029	68.899	5.911
5980.00	22.754	1.608	20.052	2.893	22.734	4.559	39.079	3.171	45.334	4.611	48.208	5.568	69.844	4.750	73.621	5.643
5984.00	24.700	1.697	22.465	2.950	24.000	4.377	44.205	3.155	48.064	4.417	49.412	5.364	74.111	4.542	75.701	5.437
5988.00	27.260	1.792	24.559	2.932	24.624	4.159	48.708	3.067	49.533	4.194	49.247	5.132	76.596	4.312	75.781	5.209
5992.00	30.469	1.857	26.206	2.845	24.618	3.907	52.353	2.938	49.737	3.940	47.859	4.873	77.232	4.059	74.009	4.957
5996.00	33.535	1.857	26.848	2.698	23.750	3.639	53.911	2.764	48.146	3.673	45.069	4.613	75.083	3.798	69.970	4.708
6000.00	31.572	1.767	23.495	2.531	20.220	3.468	47.222	2.591	41.036	3.506	38.523	4.523	64.445	3.656	59.983	4.635
6004.00	23.876	1.692	17.126	2.469	15.223	3.552	34.267	2.559	30.919	3.618	30.510	4.758	49.297	3.821	47.695	4.904
6010.00	16.720	1.544	10.996	2.322	10.486	3.745	21.946	2.518	21.443	3.864	23.025	5.216	35.315	4.228	36.311	5.451
6015.00	13.355	1.416	7.957	2.144	8.159	3.965	15.881	2.457	16.855	4.157	19.359	5.643	28.750	4.731	30.822	5.989
6020.00	11.426	1.309	6.131	1.964	6.696	4.201	12.223	2.387	14.022	4.489	16.985	6.036	24.818	5.331	27.343	6.523
6025.00	10.403	1.228	5.064	1.803	5.710	4.384	10.085	2.312	12.143	4.782	15.260	6.352	22.277	5.925	24.901	7.006
6030.00	10.006	1.169	4.482	1.674	4.932	4.440	8.860	2.223	10.680	4.958	13.754	6.594	20.329	6.429	22.871	7.462
6035.00	10.159	1.125	4.239	1.571	4.191	4.287	8.183	2.099	9.292	4.951	12.176	6.797	18.495	6.800	20.870	7.991
6040.00	10.945	1.090	4.311	1.493	3.484	3.682	7.916	1.937	7.870	4.673	10.400	6.994	16.589	6.954	18.806	8.781
6045.00	12.608	1.064	4.804	1.451	3.254	3.332	8.194	1.773	6.942	4.166	8.875	7.048	15.052	6.579	17.351	9.720
6050.00	15.588	1.045	5.961	1.460	4.517	3.695	9.774	1.745	8.583	4.134	10.828	6.443	17.337	6.237	19.123	8.746
6055.00	20.457	1.033	8.127	1.515	8.071	4.422	13.375	1.811	15.185	4.817	18.537	6.255	26.167	5.816	28.623	7.127
6055.00	6.562	1.034	2.611	1.517	2.613	4.438	4.380	1.852	4.963	4.894	6.166	6.362	8.846	6.099	9.691	7.444
6060.00	8.377	1.027	3.584	1.623	4.600	5.024	6.140	2.006	8.856	5.331	10.739	6.307	14.321	5.918	16.084	6.451
6060.00	8.315	1.024	3.548	1.616	4.484	4.999	5.685	1.856	8.572	5.199	9.960	6.140	12.715	5.340	14.834	6.203
6065.00	10.873	1.021	5.231	1.800	8.251	5.419	8.864	2.158	16.065	5.572	18.987	6.262	23.976	5.671	28.394	6.305
6065.00	10.216	1.021	4.915	1.800	7.752	5.419	8.328	2.158	15.093	5.572	17.839	6.262	22.526	5.671	26.677	6.305
6070.00	12.229	1.020	6.663	2.006	11.991	5.623	11.781	2.466	23.540	5.741	28.018	6.310	35.228	5.816	41.974	6.345
6075.00	13.979	1.021	8.636	2.226	16.945	5.739	15.769	2.769	33.421	5.832	39.929	6.335	50.091	5.893	59.877	6.366
6080.00	15.613	1.024	10.879	2.446	22.616	5.808	20.334	3.048	44.733	5.886	53.564	6.349	67.105	5.938	80.370	6.377
6085.00	10.204	1.021	6.869	2.383	14.085	5.792	12.765	2.972	27.842	5.874	33.322	6.346	41.757	5.928	49.992	6.375
6088.00	7.045	1.019	4.602	2.329	9.317	5.778	8.507	2.905	18.406	5.863	22.019	6.343	27.598	5.918	33.029	6.372

**Dynamic Stresses Along the Length of the Riser
for the Wave Fatigue Bins**

Riser Configuration_07-20-04
Nominal Tensioner Setting = 865 kips; Wave Heading = 0 deg.

Elevation (ft. above Mudline)	Fatigue Bin = 9		Fatigue Bin = 10		Fatigue Bin = 11		Fatigue Bin = 12		Fatigue Bin = 13		Fatigue Bin = 14		Fatigue Bin = 15		Fatigue Bin = 16	
	Stress Std. Dev. (psi)	Zero Cross. Period (sec.)														
10.00	980.537	12.076	1365.292	13.842	1363.542	14.840	1766.168	17.778	2165.829	20.691	2570.213	25.047	2984.420	31.687	3382.696	35.921
11.00	953.048	12.078	1326.852	13.842	1325.164	14.840	1716.073	17.776	2103.801	20.684	2495.583	25.031	2896.289	31.653	3280.919	35.871
12.00	925.924	12.079	1288.931	13.843	1287.305	14.841	1666.669	17.773	2042.650	20.677	2422.045	25.014	2809.498	31.620	3180.751	35.820
13.00	927.372	12.080	1290.769	13.844	1289.154	14.841	1668.656	17.770	2044.466	20.669	2423.144	24.996	2809.261	31.583	3178.558	35.765
14.50	929.635	12.082	1293.635	13.845	1292.051	14.841	1671.784	17.766	2047.346	20.657	2424.935	24.969	2809.011	31.527	3175.309	35.680
16.50	932.728	12.086	1297.583	13.847	1296.016	14.843	1676.059	17.761	2051.266	20.642	2427.338	24.932	2808.580	31.451	3170.715	35.565
19.00	936.913	12.091	1302.937	13.850	1301.408	14.845	1681.924	17.755	2056.728	20.623	2430.869	24.886	2808.448	31.354	3165.177	35.416
22.00	942.759	12.098	1310.491	13.857	1309.015	14.851	1690.366	17.751	2064.871	20.603	2436.765	24.832	2809.887	31.234	3159.919	35.230
26.00	952.957	12.112	1323.884	13.871	1322.492	14.863	1705.806	17.751	2080.603	20.581	2449.960	24.762	2817.335	31.070	3158.327	34.972
30.00	968.293	12.132	1344.398	13.892	1343.105	14.881	1730.300	17.758	2107.064	20.567	2475.228	24.697	2837.834	30.905	3170.281	34.702
34.00	993.257	12.158	1378.277	13.924	1377.104	14.910	1771.872	17.777	2153.951	20.565	2523.818	24.642	2884.059	30.741	3209.655	34.425
38.00	1036.587	12.194	1437.664	13.969	1436.635	14.952	1846.112	17.812	2240.096	20.580	2617.579	24.603	2980.641	30.587	3303.414	34.149
42.00	1116.848	12.242	1548.323	14.031	1547.474	15.011	1986.062	17.868	2405.390	20.620	2802.742	24.591	3179.644	30.456	3508.488	33.891
45.00	974.458	12.294	1351.018	14.104	1350.465	15.081	1732.278	17.949	2095.704	20.700	2437.574	24.652	2758.559	30.453	3034.711	33.813
48.00	849.586	12.361	1178.275	14.201	1177.987	15.175	1510.606	18.062	1825.884	20.822	2120.507	24.764	2394.417	30.516	2626.823	33.813
51.00	740.095	12.447	1027.059	14.325	1027.006	15.296	1317.005	18.212	1590.809	20.991	1845.196	24.940	2079.473	30.658	2275.569	33.908
54.00	644.113	12.556	894.723	14.484	894.883	15.451	1147.970	18.410	1386.069	21.221	1606.219	25.191	1807.173	30.897	1973.196	34.116
57.00	559.961	12.694	778.897	14.686	779.249	15.650	1000.376	18.668	1207.742	21.526	1398.784	25.538	1571.757	31.254	1712.934	34.465
61.00	463.630	12.937	646.582	15.046	647.164	16.004	832.248	19.132	1005.201	22.085	1164.127	26.193	1306.701	31.966	1421.427	35.205
67.00	347.384	13.491	487.393	15.863	488.271	16.812	630.790	20.204	763.523	23.393	885.748	27.761	994.405	33.732	1080.558	37.130
76.00	221.743	15.122	316.107	18.225	317.310	19.192	415.271	23.376	506.568	27.299	592.373	32.493	668.778	39.045	729.352	43.071
88.00	117.865	21.516	175.023	25.326	176.292	28.243	238.488	35.224	297.342	41.611	356.408	49.335	411.110	55.233	456.705	60.484
106.00	55.289	9.960	84.204	9.938	83.473	12.987	117.643	16.648	152.610	20.158	193.904	26.479	237.332	33.569	278.679	38.058
133.00	71.375	6.286	89.359	5.808	83.961	6.495	103.769	7.968	129.753	9.489	166.784	12.854	214.017	18.635	267.630	23.078
166.00	96.348	6.384	122.488	6.542	114.854	7.105	138.646	7.993	165.888	9.160	199.295	11.743	239.311	16.785	288.081	20.670
202.00	113.266	6.484	142.338	6.668	133.011	7.080	156.906	7.790	183.324	8.729	213.196	10.827	248.048	15.155	294.218	18.565
240.00	124.910	6.556	155.241	6.684	144.976	7.054	168.627	7.652	194.243	8.454	221.591	10.273	252.918	14.133	297.669	17.228
281.00	132.021	6.598	162.611	6.667	152.198	7.037	175.701	7.571	200.845	8.294	226.783	9.968	256.076	13.563	300.050	16.463
325.00	133.904	6.632	163.553	6.695	153.949	7.044	177.388	7.555	202.405	8.249	228.196	9.871	257.192	13.368	300.976	16.176
372.00	129.898	6.689	157.300	6.768	149.472	7.112	172.888	7.643	198.111	8.362	225.126	10.014	255.785	13.552	300.010	16.366
422.00	119.819	6.782	143.795	6.840	138.593	7.265	162.061	7.872	187.857	8.685	217.457	10.488	251.732	14.205	297.018	17.124
472.00	105.197	6.898	125.111	6.972	123.100	7.501	146.824	8.262	173.575	9.256	206.710	11.371	245.847	15.420	292.590	18.530
522.00	87.855	7.051	103.814	7.269	105.203	7.881	129.568	8.914	157.668	10.211	194.804	12.799	239.196	17.307	287.518	20.671
572.00	70.101	7.295	83.561	7.678	87.741	8.540	113.224	10.033	142.912	11.801	183.788	14.945	232.882	19.845	282.623	23.467
622.00	55.276	8.064	69.353	7.957	74.403	9.375	101.118	11.484	132.123	13.838	175.480	17.564	227.818	22.489	278.583	26.315
672.00	49.774	7.792	66.148	7.737	68.939	9.308	95.997	11.712	127.311	14.383	171.046	18.817	224.552	23.869	275.814	27.916
722.00	53.637	7.085	73.810	7.142	72.235	8.303	98.263	10.335	128.652	12.716	170.643	17.242	223.197	23.028	274.422	27.349
772.00	63.052	6.717	86.806	6.760	81.135	7.572	105.613	9.086	134.451	10.966	173.420	14.835	223.468	20.874	274.238	25.289
822.00	73.584	6.589	100.090	6.639	91.618	7.208	114.863	8.353	142.232	9.838	177.950	13.052	224.811	18.725	274.897	22.988
872.00	82.665	6.557	110.949	6.624	100.956	7.041	123.470	7.962	149.780	9.189	182.770	11.952	226.575	17.120	275.950	21.121
922.00	89.077	6.578	118.138	6.635	107.684	6.989	129.854	7.785	155.551	8.861	186.720	11.330	228.165	16.098	276.964	19.847
972.00	92.356	6.636	121.192	6.680	111.173	7.014	133.241	7.752	158.696	8.755	189.055	11.048	229.150	15.561	277.605	19.124
1022.00	92.503	6.717	120.181	6.763	111.351	7.090	133.452	7.820	158.952	8.811	189.449	11.041	229.302	15.413	277.682	18.868
1072.00	89.821	6.812	115.574	6.860	108.513	7.205	130.734	7.969	156.497	8.999	187.944	11.279	228.595	15.591	277.148	19.007
1122.00	84.826	6.931	108.106	6.975	103.219	7.367	125.632	8.210	151.831	9.330	184.875	11.753	227.161	16.061	276.083	19.485
1172.00	78.215	7.086	98.722	7.141	96.234	7.597	118.922	8.570	145.686	9.838	180.776	12.469	225.247	16.800	274.658	20.262

**Dynamic Stresses Along the Length of the Riser
for the Wave Fatigue Bins**

Riser Configuration_07-20-04
Nominal Tensioner Setting = 865 kips; Wave Heading = 0 deg.

Elevation (ft. above Mudline)	Fatigue Bin = 9		Fatigue Bin = 10		Fatigue Bin = 11		Fatigue Bin = 12		Fatigue Bin = 13		Fatigue Bin = 14		Fatigue Bin = 15		Fatigue Bin = 16	
	Stress Std. Dev. (psi)	Zero Cross. Period (sec.)														
1222.00	70.851	7.274	88.600	7.352	88.506	7.898	111.550	9.062	138.951	10.546	176.279	13.438	223.158	17.768	273.088	21.277
1272.00	63.726	7.465	79.092	7.546	81.094	8.240	104.538	9.654	132.556	11.417	172.019	14.638	221.201	18.858	271.599	22.418
1322.00	57.874	7.610	71.573	7.670	75.044	8.553	98.831	10.244	127.324	12.318	168.540	15.902	219.635	19.877	270.383	23.491
1372.00	54.180	7.648	67.161	7.665	71.186	8.726	95.117	10.643	123.825	12.989	166.209	16.865	218.626	20.584	269.575	24.256
1422.00	53.064	7.542	66.262	7.472	69.877	8.661	93.667	10.662	122.276	13.140	165.162	17.160	218.235	20.813	269.230	24.535
1472.00	54.246	7.344	68.276	7.203	70.851	8.402	94.260	10.321	122.510	12.744	165.298	16.778	218.419	20.575	269.328	24.319
1522.00	56.908	7.165	71.953	7.017	73.360	8.111	96.298	9.855	124.064	12.098	166.345	16.034	219.052	20.026	269.787	23.755
1572.00	60.113	7.063	76.045	6.934	76.516	7.900	99.035	9.463	126.332	11.499	167.938	15.238	219.963	19.357	270.484	23.033
1622.00	63.118	7.030	79.640	6.908	79.565	7.784	101.798	9.201	128.734	11.060	169.705	14.558	220.964	18.718	271.278	22.312
1672.00	65.440	7.038	82.183	6.921	81.994	7.735	104.090	9.049	130.815	10.776	171.320	14.058	221.878	18.197	272.034	21.689
1722.00	66.825	7.071	83.412	6.969	83.510	7.734	105.603	8.984	132.274	10.623	172.543	13.747	222.565	17.831	272.636	21.214
1772.00	67.185	7.129	83.296	7.042	84.000	7.779	106.202	8.999	132.960	10.588	173.236	13.607	222.930	17.625	272.999	20.905
1822.00	66.571	7.215	81.979	7.131	83.502	7.870	105.897	9.090	132.856	10.662	173.355	13.607	222.928	17.564	273.076	20.759
1872.00	65.143	7.320	79.729	7.241	82.173	7.995	104.820	9.241	132.060	10.825	172.939	13.716	222.563	17.624	272.855	20.755
1922.00	63.135	7.427	76.909	7.369	80.253	8.134	103.188	9.426	130.752	11.041	172.088	13.904	221.872	17.778	272.356	20.864
1972.00	60.823	7.521	73.942	7.486	78.022	8.267	101.253	9.615	129.150	11.274	170.934	14.141	220.919	17.997	271.619	21.054
2022.00	58.490	7.591	71.239	7.559	75.765	8.378	99.274	9.785	127.474	11.490	169.626	14.385	219.782	18.250	270.701	21.291
2072.00	56.397	7.620	69.137	7.579	73.736	8.446	97.475	9.907	125.921	11.655	168.301	14.588	218.540	18.499	269.659	21.543
2122.00	54.749	7.592	67.848	7.544	72.130	8.449	96.026	9.951	124.636	11.732	167.071	14.710	217.265	18.710	268.551	21.780
2172.00	53.660	7.507	67.430	7.451	71.052	8.379	95.019	9.902	123.703	11.701	166.008	14.736	216.013	18.859	267.423	21.977
2222.00	53.134	7.388	67.772	7.327	70.502	8.262	94.457	9.783	123.131	11.580	165.139	14.677	214.821	18.936	266.312	22.120
2272.00	53.082	7.271	68.646	7.219	70.397	8.132	94.271	9.634	122.870	11.414	164.457	14.558	213.708	18.951	265.237	22.210
2322.00	53.356	7.176	69.779	7.150	70.598	8.016	94.348	9.489	122.830	11.244	163.925	14.410	212.674	18.926	264.209	22.259
2372.00	53.790	7.106	70.923	7.112	70.948	7.923	94.556	9.365	122.901	11.093	163.487	14.263	211.708	18.887	263.224	22.291
2422.00	54.228	7.062	71.878	7.099	71.299	7.858	94.765	9.272	122.978	10.977	163.081	14.145	210.791	18.854	262.275	22.330
2472.00	54.542	7.045	72.502	7.115	71.527	7.824	94.867	9.218	122.964	10.907	162.647	14.077	209.902	18.849	261.350	22.399
2522.00	54.644	7.052	72.721	7.157	71.542	7.822	94.779	9.208	122.789	10.892	162.137	14.071	209.021	18.886	260.436	22.513
2572.00	54.489	7.076	72.520	7.212	71.300	7.846	94.459	9.237	122.411	10.930	161.519	14.130	208.132	18.978	259.524	22.682
2622.00	54.064	7.107	71.926	7.268	70.787	7.886	93.894	9.295	121.817	11.013	160.778	14.248	207.225	19.131	258.609	22.915
2672.00	53.383	7.141	70.994	7.328	70.018	7.936	93.096	9.376	121.017	11.131	159.915	14.422	206.298	19.346	257.687	23.215
2722.00	52.478	7.174	69.792	7.392	69.026	7.993	92.095	9.476	120.037	11.281	158.942	14.648	205.353	19.619	256.763	23.583
2772.00	51.394	7.208	68.403	7.451	67.855	8.058	90.934	9.595	118.915	11.461	157.882	14.924	204.399	19.943	255.841	24.017
2822.00	50.183	7.239	66.911	7.496	66.560	8.126	89.662	9.726	117.695	11.665	156.762	15.239	203.447	20.309	254.932	24.507
2872.00	48.904	7.264	65.386	7.533	65.198	8.191	88.333	9.861	116.426	11.882	155.616	15.583	202.511	20.712	254.046	25.043
2922.00	47.611	7.284	63.892	7.570	63.826	8.252	86.997	9.996	115.153	12.103	154.475	15.944	201.604	21.142	253.195	25.610
2972.00	46.357	7.302	62.484	7.606	62.490	8.310	85.698	10.128	113.917	12.323	153.367	16.311	200.741	21.591	252.390	26.197
3022.00	45.990	7.175	61.209	7.635	61.234	8.368	84.474	10.259	112.751	12.539	152.317	16.676	199.935	22.044	251.642	26.788
3072.00	46.087	7.199	60.100	7.659	60.092	8.423	83.354	10.383	111.681	12.745	151.347	17.029	199.196	22.489	250.961	27.368
3122.00	46.266	7.218	59.172	7.689	59.877	7.699	82.361	10.492	110.728	12.930	150.472	17.352	198.534	22.908	250.353	27.919
3172.00	46.511	7.231	58.434	7.725	60.232	7.704	81.507	10.579	109.904	13.081	149.704	17.629	197.956	23.288	249.827	28.418
3222.00	46.798	7.239	57.885	7.755	60.590	7.707	80.795	10.644	109.212	13.196	149.050	17.848	197.466	23.620	249.386	28.845
3272.00	47.095	7.245	57.509	7.771	60.923	7.708	80.220	10.688	108.651	13.277	148.510	18.005	197.068	23.895	249.033	29.184
3322.00	47.368	7.247	57.278	7.776	61.203	7.710	80.036	8.713	108.214	13.324	148.083	18.099	196.762	24.104	248.770	29.423
3372.00	47.582	7.242	57.438	6.807	61.402	7.709	80.230	8.715	107.891	13.337	147.765	18.130	196.550	24.240	248.598	29.558
3422.00	47.703	7.232	57.636	6.826	61.493	7.706	80.311	8.719	107.670	13.314	147.550	18.100	196.430	24.301	248.516	29.589
3472.00	47.699	7.219	57.705	6.841	61.453	7.704	80.263	8.728	107.538	13.262	147.433	18.014	196.401	24.287	248.522	29.517

**Dynamic Stresses Along the Length of the Riser
for the Wave Fatigue Bins**

Riser Configuration_07-20-04
Nominal Tensioner Setting = 865 kips; Wave Heading = 0 deg.

Elevation (ft. above Mudline)	Fatigue Bin = 9		Fatigue Bin = 10		Fatigue Bin = 11		Fatigue Bin = 12		Fatigue Bin = 13		Fatigue Bin = 14		Fatigue Bin = 15		Fatigue Bin = 16	
	Stress Std. Dev. (psi)	Zero Cross. Period (sec.)														
3522.00	47.546	7.209	57.618	6.854	61.266	7.707	80.076	8.748	107.482	13.194	147.405	17.884	196.461	24.206	248.615	29.348
3572.00	47.231	7.204	57.358	6.870	60.924	7.717	79.746	8.779	107.491	13.119	147.459	17.724	196.606	24.065	248.792	29.092
3622.00	46.749	7.201	56.971	7.674	60.427	7.733	79.280	8.822	107.557	13.040	147.590	17.545	196.836	23.873	249.050	28.761
3672.00	46.109	7.202	56.837	7.660	59.785	7.754	78.860	10.538	107.677	12.956	147.791	17.353	197.145	23.636	249.387	28.371
3722.00	45.326	7.206	56.656	7.647	59.016	7.780	78.918	10.509	107.846	12.867	148.059	17.150	197.533	23.361	249.798	27.936
3772.00	44.426	7.218	56.440	7.639	58.145	7.814	79.017	10.485	108.064	12.779	148.389	16.941	197.994	23.054	250.278	27.471
3822.00	43.446	7.237	56.212	7.639	57.203	7.857	79.167	10.465	108.331	12.693	148.778	16.728	198.525	22.721	250.824	26.984
3867.00	42.529	7.260	56.016	7.644	56.324	7.900	79.348	10.450	108.613	12.618	149.175	16.538	199.059	22.407	251.367	26.536
3908.00	41.694	7.282	55.863	7.650	55.522	7.940	79.557	10.435	108.905	12.549	149.573	16.369	199.590	22.112	251.903	26.124
3944.00	41.018	7.299	55.804	7.652	55.453	8.507	79.813	10.411	109.221	12.478	149.973	16.210	200.107	21.837	252.419	25.748
3974.00	40.805	7.298	56.190	7.623	55.954	8.479	80.373	10.327	109.809	12.331	150.566	15.968	200.745	21.485	253.040	25.301
4004.00	43.646	7.177	60.393	7.359	59.611	8.159	84.021	9.748	113.367	11.500	153.549	14.811	203.242	20.091	255.374	23.669
4034.00	46.499	7.085	64.634	7.170	63.388	7.920	87.857	9.301	117.152	10.845	156.780	13.864	205.993	18.870	257.952	22.218
4069.00	46.171	7.150	64.828	7.189	63.861	7.935	88.407	9.285	117.748	10.794	157.467	13.745	206.851	18.624	258.798	21.886
4109.00	46.153	7.211	64.444	7.237	63.914	7.988	88.514	9.329	117.898	10.826	157.821	13.735	207.522	18.493	259.483	21.685
4154.00	46.144	7.276	63.939	7.282	63.917	8.050	88.533	9.389	117.939	10.881	158.109	13.758	208.215	18.384	260.195	21.509
4204.00	46.222	7.334	63.408	7.314	63.936	8.108	88.517	9.449	117.913	10.944	158.357	13.802	208.947	18.282	260.947	21.345
4254.00	46.409	7.375	62.962	7.344	64.006	8.152	88.504	9.501	117.857	11.005	158.563	13.855	209.653	18.189	261.673	21.199
4304.00	46.694	7.409	62.632	7.382	64.139	8.191	88.521	9.551	117.804	11.068	158.754	13.911	210.344	18.098	262.380	21.059
4354.00	47.056	7.436	62.439	7.416	64.338	8.227	88.585	9.599	117.782	11.133	158.954	13.968	211.029	18.003	263.077	20.922
4404.00	47.460	7.454	62.381	7.434	64.595	8.254	88.706	9.639	117.810	11.192	159.178	14.021	211.714	17.901	263.769	20.782
4454.00	47.864	7.458	62.430	7.441	64.888	8.267	88.882	9.664	117.896	11.234	159.435	14.061	212.398	17.791	264.457	20.639
4504.00	48.219	7.454	62.535	7.448	65.186	8.269	89.093	9.674	118.034	11.259	159.724	14.087	213.077	17.671	265.138	20.491
4554.00	48.479	7.450	62.642	7.455	65.449	8.271	89.314	9.679	118.205	11.273	160.034	14.098	213.739	17.546	265.804	20.338
4604.00	48.605	7.453	62.698	7.458	65.642	8.277	89.512	9.686	118.383	11.285	160.349	14.099	214.372	17.420	266.445	20.185
4654.00	48.574	7.463	62.652	7.459	65.733	8.290	89.656	9.698	118.539	11.299	160.647	14.099	214.957	17.301	267.045	20.038
4704.00	48.376	7.480	62.467	7.468	65.704	8.308	89.722	9.715	118.646	11.316	160.905	14.104	215.478	17.194	267.590	19.904
4754.00	48.017	7.505	62.121	7.490	65.543	8.334	89.690	9.740	118.682	11.339	161.105	14.119	215.916	17.105	268.065	19.790
4804.00	47.518	7.543	61.617	7.521	65.254	8.371	89.550	9.776	118.630	11.373	161.230	14.145	216.258	17.039	268.456	19.702
4854.00	46.912	7.594	60.977	7.559	64.851	8.422	89.302	9.828	118.482	11.424	161.271	14.185	216.492	16.996	268.753	19.639
4904.00	46.246	7.655	60.239	7.603	64.359	8.482	88.959	9.891	118.241	11.489	161.224	14.238	216.611	16.978	268.948	19.603
4954.00	45.572	7.718	59.454	7.655	63.813	8.544	88.540	9.961	117.918	11.563	161.092	14.304	216.613	16.984	269.039	19.593
5004.00	44.941	7.773	58.681	7.710	63.250	8.602	88.071	10.029	117.533	11.638	160.885	14.379	216.499	17.011	269.024	19.606
5054.00	44.396	7.819	57.982	7.756	62.705	8.651	87.581	10.091	117.110	11.711	160.617	14.457	216.275	17.057	268.908	19.640
5104.00	43.968	7.850	57.409	7.786	62.205	8.690	87.095	10.145	116.670	11.775	160.304	14.529	215.950	17.118	268.697	19.693
5154.00	43.672	7.861	57.001	7.795	61.773	8.712	86.636	10.184	116.239	11.827	159.964	14.588	215.533	17.191	268.399	19.759
5204.00	43.504	7.843	56.771	7.786	61.418	8.710	86.222	10.201	115.837	11.856	159.612	14.628	215.038	17.269	268.024	19.834
5254.00	43.442	7.799	56.716	7.758	61.136	8.682	85.860	10.192	115.477	11.859	159.263	14.646	214.474	17.351	267.582	19.913
5304.00	43.446	7.738	56.808	7.712	60.912	8.636	85.549	10.161	115.165	11.834	158.924	14.641	213.851	17.432	267.079	19.992
5354.00	43.467	7.670	57.006	7.651	60.719	8.579	85.277	10.114	114.900	11.788	158.600	14.612	213.177	17.512	266.521	20.069
5404.00	43.455	7.602	57.254	7.586	60.527	8.520	85.029	10.059	114.675	11.729	158.290	14.564	212.454	17.589	265.909	20.145
5454.00	43.363	7.537	57.493	7.527	60.303	8.460	84.786	10.000	114.475	11.660	157.987	14.499	211.684	17.667	265.243	20.222
5504.00	43.152	7.474	57.671	7.479	60.020	8.402	84.526	9.942	114.285	11.587	157.684	14.426	210.867	17.746	264.518	20.302
5554.00	42.795	7.420	57.746	7.439	59.655	8.352	84.231	9.888	114.089	11.517	157.367	14.354	209.995	17.830	263.723	20.388
5604.00	42.272	7.380	57.688	7.408	59.188	8.317	83.883	9.848	113.865	11.456	157.017	14.289	209.052	17.924	262.835	20.486
5654.00	41.584	7.358	57.480	7.390	58.614	8.300	83.468	9.826	113.597	11.412	156.615	14.237	208.019	18.032	261.823	20.602

**Dynamic Stresses Along the Length of the Riser
for the Wave Fatigue Bins**

Riser Configuration_07-20-04
Nominal Tensioner Setting = 865 kips; Wave Heading = 0 deg.

Elevation (ft. above Mudline)	Fatigue Bin = 9		Fatigue Bin = 10		Fatigue Bin = 11		Fatigue Bin = 12		Fatigue Bin = 13		Fatigue Bin = 14		Fatigue Bin = 15		Fatigue Bin = 16	
	Stress Std. Dev. (psi)	Zero Cross. Period (sec.)														
5704.00	40.763	7.351	57.132	7.391	57.955	8.299	82.999	9.821	113.288	11.383	156.154	14.197	206.885	18.156	260.667	20.741
5744.00	40.329	7.215	56.777	7.404	57.398	8.306	82.606	9.824	113.026	11.369	155.749	14.173	205.898	18.266	259.616	20.870
5774.00	40.040	7.229	56.483	7.419	56.988	8.315	82.324	9.830	112.840	11.361	155.438	14.156	205.118	18.351	258.755	20.976
5794.00	39.830	7.235	56.287	7.429	56.735	8.322	82.158	9.834	112.738	11.356	155.241	14.144	204.590	18.407	258.152	21.046
5814.00	39.631	7.238	56.128	7.440	56.540	8.329	82.049	9.836	112.693	11.346	155.090	14.124	204.095	18.452	257.569	21.109
5834.00	39.453	7.240	56.029	7.451	56.435	8.336	82.037	9.833	112.748	11.327	155.033	14.089	203.679	18.475	257.052	21.148
5854.00	39.368	7.239	56.078	7.461	56.518	8.339	82.223	9.816	113.015	11.286	155.177	14.019	203.439	18.448	256.703	21.132
5874.00	39.515	7.234	56.435	7.465	56.955	8.331	82.794	9.769	113.696	11.200	155.722	13.880	203.553	18.319	256.707	21.002
5894.00	40.141	7.221	57.398	7.458	58.043	8.297	84.084	9.664	115.166	11.028	157.040	13.611	204.336	18.002	257.394	20.656
5914.00	41.760	7.195	59.622	7.416	60.384	8.206	86.784	9.450	118.206	10.701	159.880	13.111	206.390	17.348	259.384	19.913
5934.00	45.397	7.128	64.539	7.285	65.166	7.999	92.302	9.042	124.434	10.107	165.776	12.231	210.875	16.130	263.847	18.498
5949.00	50.509	7.005	71.764	7.046	71.641	7.705	99.906	8.546	133.146	9.416	174.082	11.237	217.249	14.716	270.272	16.827
5960.00	56.100	6.832	80.212	6.743	78.680	7.382	108.357	8.059	143.015	8.769	183.531	10.334	224.452	13.418	277.588	15.280
5968.00	61.106	6.640	88.349	6.439	85.012	7.077	116.137	7.642	152.294	8.238	192.442	9.619	231.158	12.394	284.460	14.057
5974.00	65.017	6.449	95.238	6.163	90.116	6.638	122.410	7.301	159.960	7.821	199.806	9.077	236.587	11.633	290.091	13.150
5980.00	68.291	6.216	101.790	5.849	94.895	6.384	127.913	6.942	166.959	7.402	206.493	8.558	241.287	10.936	295.090	12.324
5984.00	69.405	6.037	104.904	5.621	96.764	6.198	130.044	6.701	170.000	7.133	209.349	8.246	243.014	10.547	297.094	11.870
5988.00	68.750	5.847	105.557	5.319	96.385	6.007	129.488	6.472	170.056	6.890	209.284	7.991	242.310	10.278	296.740	11.560
5992.00	66.526	5.644	103.894	5.069	93.930	5.808	126.425	6.248	167.170	6.662	206.286	7.777	239.199	10.106	293.964	11.364
5996.00	62.566	5.462	99.096	4.823	89.023	5.634	120.639	5.920	160.502	6.489	199.532	7.654	233.168	10.096	288.135	11.347
6000.00	54.493	5.507	86.108	4.759	78.404	5.696	107.858	6.035	145.351	6.659	184.845	7.975	221.436	10.726	276.416	12.000
6004.00	45.400	5.920	69.434	5.208	65.809	6.204	92.092	6.718	125.949	7.613	165.577	9.343	205.959	12.874	259.516	14.412
6010.00	37.374	6.672	54.492	6.066	54.865	7.168	78.819	8.063	109.735	9.542	149.772	12.002	194.919	14.049	244.962	18.993
6015.00	33.683	7.300	47.628	6.976	49.965	8.017	73.152	9.296	102.852	11.349	143.224	14.327	192.226	16.210	241.925	18.438
6020.00	31.378	7.837	43.462	7.940	47.013	8.784	69.909	10.453	98.845	13.058	139.420	16.384	191.073	17.932	241.289	20.543
6025.00	29.716	8.277	40.627	8.867	44.996	9.451	67.843	11.496	96.145	14.568	137.378	16.793	190.528	19.316	241.228	22.226
6030.00	28.246	8.676	38.296	9.785	43.333	10.093	66.290	12.524	94.328	15.024	136.577	18.392	190.225	20.596	241.445	23.766
6035.00	26.690	9.127	35.989	10.855	41.708	10.852	64.935	13.745	93.289	16.694	136.161	20.170	190.101	22.056	241.987	25.492
6040.00	24.947	9.742	33.679	12.027	40.057	11.913	63.784	15.417	92.664	18.896	136.299	22.378	190.390	23.994	243.260	27.739
6045.00	23.355	10.461	32.866	13.995	38.852	13.177	63.415	17.287	93.150	21.128	137.764	24.520	191.886	26.468	246.339	30.499
6050.00	25.098	9.424	35.487	12.078	39.898	12.721	65.705	16.442	96.777	19.659	142.601	23.435	196.630	27.807	253.754	31.764
6055.00	33.368	7.919	46.617	8.620	47.863	8.715	75.283	12.016	108.456	14.020	155.617	17.548	209.396	23.714	271.055	27.000
6055.00	11.638	8.203	16.222	9.236	16.977	9.194	27.025	12.922	39.152	15.154	56.540	18.840	76.476	24.989	98.874	28.442
6060.00	17.229	7.308	24.018	7.469	23.640	7.636	34.400	9.532	47.700	10.780	65.582	13.340	85.277	18.283	109.792	20.836
6060.00	13.916	6.631	19.830	6.243	18.593	6.673	23.468	6.741	28.578	6.825	32.962	7.291	37.245	8.457	43.787	9.060
6065.00	26.727	6.684	37.947	6.333	35.714	6.715	44.899	6.753	54.276	6.794	61.793	7.150	69.104	8.104	78.797	8.428
6065.00	25.111	6.684	35.653	6.334	33.554	6.715	42.183	6.753	50.993	6.794	58.056	7.150	64.925	8.104	74.032	8.428
6070.00	39.557	6.705	56.102	6.369	52.873	6.731	66.407	6.762	80.137	6.793	91.007	7.124	101.861	8.041	115.493	8.313
6075.00	56.461	6.715	80.039	6.388	75.483	6.740	94.771	6.768	114.292	6.795	129.696	7.117	145.355	8.024	164.578	8.283
6080.00	75.807	6.721	107.438	6.399	101.358	6.745	127.234	6.772	153.389	6.797	174.002	7.114	195.179	8.018	220.892	8.273
6085.00	47.152	6.720	66.825	6.396	63.042	6.744	79.134	6.770	95.401	6.796	108.223	7.113	121.396	8.017	137.389	8.272
6088.00	31.152	6.718	44.149	6.394	41.648	6.743	52.279	6.769	63.025	6.794	71.495	7.112	80.200	8.016	90.765	8.271

**Dynamic Stresses Along the Length of the Riser
for the Wave Fatigue Bins**

Riser Configuration_07-20-04
Nominal Tensioner Setting = 865 kips; Wave Heading = 0 deg.

Elevation (ft. above Mudline)	Fatigue Bin = 17		Fatigue Bin = 18		Fatigue Bin = 19		Fatigue Bin = 20		Fatigue Bin = 21		Fatigue Bin = 22		Fatigue Bin = 23		Fatigue Bin = 24	
	Stress Std. Dev. (psi)	Zero Cross. Period (sec.)														
10.00	3773.495	39.941	4150.792	43.892	4511.180	46.890	4850.548	49.941	5164.284	51.205	5423.218	52.911	5529.271	50.351	5614.053	49.910
11.00	3657.654	39.875	4020.688	43.808	4366.696	46.805	4691.775	49.844	4991.710	51.128	5238.763	52.831	5337.674	50.303	5416.539	49.860
12.00	3543.724	39.809	3892.820	43.723	4224.801	46.718	4535.964	49.744	4822.481	51.048	4942.567	52.747	5150.041	50.252	5223.223	49.807
13.00	3538.934	39.738	3884.842	43.632	4213.023	46.625	4519.867	49.636	4801.812	50.962	5033.087	52.657	5121.134	50.196	5190.932	49.748
14.50	3531.703	39.628	3872.722	43.492	4195.081	46.480	4495.309	49.469	4770.261	50.826	4995.052	52.514	5077.002	50.105	5141.640	49.653
16.50	3521.595	39.477	3855.853	43.298	4170.178	46.278	4461.290	49.235	4726.628	50.632	4942.522	52.309	5016.131	49.969	5073.726	49.511
19.00	3508.883	39.281	3834.344	43.043	4138.227	46.010	4417.503	48.922	4670.389	50.366	4874.782	52.025	4937.633	49.775	4986.164	49.306
22.00	3494.684	39.033	3809.144	42.720	4099.965	45.663	4364.433	48.513	4601.779	50.010	4791.849	51.642	4841.298	49.499	4878.575	49.014
26.00	3480.804	38.682	3779.999	42.256	4052.621	45.155	4296.403	47.908	4512.088	49.463	4682.231	51.045	4712.932	49.045	4734.532	48.529
30.00	3480.581	38.307	3764.259	41.753	4018.132	44.590	4240.412	47.225	4433.582	48.819	4583.016	50.334	4593.863	48.469	4598.952	47.912
34.00	3508.908	37.912	3777.657	41.213	4012.902	43.966	4213.375	46.459	4383.602	48.068	4511.856	49.491	4501.542	47.747	4489.138	47.134
38.00	3594.742	37.504	3850.781	40.644	4068.812	43.290	4248.132	45.616	4395.750	47.205	4502.886	48.512	4469.606	46.863	4438.336	46.174
42.00	3799.124	37.105	4047.999	40.070	4252.781	42.586	4413.406	44.723	4540.085	46.255	4626.984	47.420	4567.558	45.828	4514.910	45.047
45.00	3274.879	36.936	3476.213	39.788	3637.220	42.206	3758.288	44.210	3849.932	45.678	3909.007	46.737	3843.484	45.150	3786.545	44.296
48.00	2825.711	36.857	2988.768	39.605	3115.231	41.929	3205.816	43.807	3270.995	45.203	3309.472	46.157	3241.846	44.554	3183.821	43.627
51.00	2440.718	36.885	2573.002	39.544	2672.278	41.780	2739.505	43.544	2784.837	44.863	2808.197	45.719	2741.175	44.083	2684.171	43.084
54.00	2110.862	37.043	2218.524	39.630	2296.563	41.789	2366.107	43.452	2376.781	44.697	2389.251	45.463	2324.662	43.783	2270.059	42.717
57.00	1828.302	37.360	1916.384	39.897	1977.989	41.992	2014.362	43.574	2034.438	44.749	2039.269	45.440	1978.303	43.706	1926.951	42.578
61.00	1513.606	38.095	1581.858	40.605	1627.441	42.643	1651.679	44.152	1662.424	45.253	1660.838	45.872	1605.761	44.057	1559.437	42.856
67.00	1148.664	40.111	1197.270	42.696	1228.100	44.714	1242.473	46.221	1246.451	47.249	1240.789	47.848	1195.474	45.888	1157.142	44.617
76.00	777.656	46.415	811.802	49.480	833.975	51.497	845.219	53.323	849.093	54.112	844.926	54.986	814.603	52.517	801.463	52.604
88.00	496.184	62.468	526.761	66.170	551.264	64.890	569.763	66.999	583.799	63.777	644.792	62.588	712.309	25.776	759.858	26.746
106.00	320.702	39.625	358.951	43.018	426.616	28.235	501.924	31.579	580.297	31.362	640.040	33.402	688.341	31.147	720.327	31.817
133.00	328.081	26.626	387.093	30.759	450.574	32.256	510.361	35.713	570.636	35.158	614.964	37.071	647.624	34.196	668.063	34.675
166.00	342.277	24.349	394.612	28.425	450.456	30.747	502.984	34.411	555.793	34.616	594.206	36.658	621.524	34.120	638.249	34.633
202.00	345.790	22.059	395.715	25.905	449.221	28.581	499.659	32.286	550.616	33.084	587.653	35.241	614.033	33.144	630.111	33.741
240.00	348.089	20.531	397.139	24.167	450.018	26.954	499.946	30.615	550.633	31.754	587.467	33.966	613.922	32.197	629.981	32.857
281.00	349.938	19.622	398.653	23.099	451.428	25.898	501.281	29.483	552.092	30.795	588.983	33.016	615.711	31.457	631.856	32.149
325.00	350.819	19.257	399.560	22.637	452.527	25.403	502.530	28.912	553.635	30.267	590.690	32.465	617.759	30.996	634.035	31.692
372.00	350.320	19.432	399.448	22.778	452.896	25.478	503.261	28.919	554.813	30.201	592.130	32.352	619.596	30.855	636.053	31.527
422.00	348.301	20.228	398.172	23.591	452.384	26.168	503.323	29.537	555.471	30.616	593.150	32.695	621.064	31.046	637.754	31.670
472.00	345.168	21.688	395.997	25.091	451.142	27.442	502.781	30.713	555.607	31.446	593.703	33.427	622.076	31.517	639.029	32.072
522.00	341.496	23.829	393.342	27.256	449.472	29.209	501.848	32.332	555.373	32.568	593.907	34.428	622.728	32.169	639.953	32.644
572.00	337.888	26.474	390.657	29.874	447.705	31.230	500.765	34.165	554.953	33.791	593.907	35.525	623.142	32.878	640.631	33.274
622.00	334.849	29.005	388.328	32.362	446.131	33.040	499.757	35.816	554.518	34.850	593.842	36.491	623.444	33.492	641.170	33.832
672.00	332.694	30.398	386.609	33.826	444.955	34.071	498.983	36.822	554.199	35.477	593.825	37.096	623.734	33.872	641.662	34.195
722.00	331.522	30.027	385.597	33.694	444.265	34.006	498.527	36.902	554.069	35.522	593.922	37.201	624.077	33.934	642.167	34.287
772.00	331.233	28.346	385.243	32.266	444.039	33.019	498.391	36.147	554.141	35.030	594.154	36.824	624.496	33.683	642.712	34.100
822.00	331.586	26.279	385.387	30.318	444.174	31.575	498.511	34.910	554.376	34.196	594.498	36.111	624.978	33.201	643.291	33.696
872.00	332.267	24.451	385.811	28.467	444.517	30.103	498.784	33.565	554.700	33.244	594.900	35.254	625.481	32.607	643.872	33.173
922.00	332.966	23.100	386.288	27.010	444.902	28.857	499.093	32.365	555.028	32.352	595.296	34.420	625.948	32.010	644.410	32.629
972.00	333.427	22.256	386.622	26.033	445.180	27.952	499.330	31.443	555.275	31.629	595.619	33.717	626.323	31.490	644.857	32.142
1022.00	333.490	21.874	386.684	25.527	445.247	27.414	499.414	30.847	555.378	31.127	595.817	33.204	626.557	31.096	645.172	31.759
1072.00	333.102	21.892	386.416	25.445	445.050	27.228	499.299	30.579	555.299	30.860	595.857	32.903	626.620	30.850	645.327	31.507
1122.00	332.302	22.246	385.838	25.724	444.592	27.349	498.982	30.609	555.031	30.817	595.730	32.808	626.504	30.755	645.314	31.389
1172.00	331.205	22.874	385.024	26.294	443.921	27.719	498.494	30.887	554.595	30.968	595.453	32.895	626.220	30.797	645.140	31.398

**Dynamic Stresses Along the Length of the Riser
for the Wave Fatigue Bins**

Riser Configuration_07-20-04
Nominal Tensioner Setting = 865 kips; Wave Heading = 0 deg.

Elevation (ft. above Mudline)	Fatigue Bin = 17		Fatigue Bin = 18		Fatigue Bin = 19		Fatigue Bin = 20		Fatigue Bin = 21		Fatigue Bin = 22		Fatigue Bin = 23		Fatigue Bin = 24	
	Stress Std. Dev. (psi)	Zero Cross. Period (sec.)														
1222.00	329.963	23.704	384.085	27.067	443.119	28.263	497.892	31.343	554.036	31.266	595.058	33.126	625.799	30.953	644.833	31.513
1272.00	328.742	24.631	383.144	27.935	442.279	28.892	497.248	31.890	553.412	31.651	594.594	33.448	625.283	31.189	644.428	31.705
1322.00	327.686	25.509	382.316	28.763	441.494	29.508	496.633	32.435	552.782	32.057	594.111	33.802	624.723	31.464	643.971	31.940
1372.00	326.906	26.169	381.689	29.403	440.837	30.014	496.108	32.890	552.203	32.423	593.660	34.129	624.167	31.738	643.506	32.181
1422.00	326.457	26.478	381.314	29.731	440.358	30.332	495.718	33.186	551.717	32.699	593.278	34.383	623.658	31.976	643.073	32.396
1472.00	326.337	26.407	381.200	29.705	440.076	30.422	495.482	33.285	551.348	32.857	592.992	34.534	623.225	32.154	642.704	32.560
1522.00	326.499	26.035	381.317	29.372	439.977	30.296	495.397	33.191	551.101	32.892	592.812	34.575	622.886	32.262	642.416	32.662
1572.00	326.856	25.498	381.608	28.848	440.026	30.009	495.439	32.943	550.965	32.820	592.730	34.517	622.641	32.302	642.215	32.703
1622.00	327.308	24.922	381.993	28.256	440.166	29.641	495.568	32.601	550.914	32.673	592.729	34.387	622.479	32.288	642.095	32.693
1672.00	327.751	24.398	382.391	27.694	440.335	29.265	495.736	32.233	550.911	32.492	592.780	34.219	622.379	32.241	642.037	32.650
1722.00	328.094	23.981	382.725	27.225	440.472	28.941	495.894	31.896	550.918	32.316	592.849	34.047	622.312	32.184	642.019	32.595
1772.00	328.265	23.698	382.934	26.881	440.526	28.703	495.996	31.632	550.897	32.179	592.905	33.904	622.251	32.139	642.014	32.547
1822.00	328.220	23.558	382.973	26.674	440.456	28.569	496.006	31.464	550.817	32.104	592.918	33.813	622.166	32.124	641.996	32.524
1872.00	327.941	23.556	382.821	26.603	440.241	28.544	495.900	31.401	550.655	32.106	592.864	33.791	622.037	32.154	641.944	32.541
1922.00	327.436	23.672	382.475	26.657	439.873	28.623	495.668	31.441	550.399	32.187	592.729	33.844	621.847	32.236	641.840	32.604
1972.00	326.730	23.879	381.947	26.816	439.358	28.794	495.307	31.575	550.045	32.341	592.507	33.971	621.588	32.372	641.673	32.719
2022.00	325.866	24.143	381.265	27.052	438.715	29.040	494.829	31.788	549.599	32.560	592.198	34.165	621.260	32.557	641.442	32.884
2072.00	324.888	24.432	380.464	27.332	437.969	29.334	494.251	32.063	549.073	32.827	591.810	34.414	620.867	32.785	641.146	33.093
2122.00	323.842	24.716	379.578	27.626	437.148	29.651	493.592	32.377	548.483	33.129	591.356	34.704	620.421	33.044	640.795	33.338
2172.00	322.770	24.972	378.643	27.910	436.283	29.966	492.876	32.711	547.847	33.448	590.849	35.022	619.933	33.323	640.398	33.608
2222.00	321.702	25.183	377.686	28.169	435.398	30.260	492.126	33.046	547.185	33.769	590.307	35.352	619.418	33.611	639.968	33.893
2272.00	320.663	25.344	376.731	28.397	434.514	30.524	491.359	33.367	546.513	34.080	589.742	35.685	618.890	33.896	639.517	34.184
2322.00	319.664	25.460	375.791	28.595	433.648	30.756	490.591	33.670	545.845	34.371	589.171	36.012	618.363	34.173	639.059	34.474
2372.00	318.710	25.544	374.877	28.770	432.809	30.961	489.835	33.955	545.193	34.642	588.602	36.328	617.847	34.437	638.603	34.756
2422.00	317.798	25.619	373.990	28.939	432.003	31.149	489.096	34.230	544.564	34.894	588.046	36.632	617.351	34.685	638.159	35.029
2472.00	316.921	25.706	373.129	29.116	431.230	31.333	488.380	34.504	543.963	35.133	587.509	36.928	616.883	34.918	637.735	35.292
2522.00	316.073	25.825	372.293	29.322	430.492	31.526	487.689	34.790	543.394	35.368	586.994	37.221	616.446	35.140	637.335	35.546
2572.00	315.245	25.990	371.476	29.571	429.784	31.741	487.024	35.097	542.858	35.608	586.506	37.518	616.044	35.355	636.965	35.795
2622.00	314.432	26.208	370.677	29.876	429.107	31.987	486.385	35.433	542.355	35.859	586.045	37.825	615.678	35.567	636.627	36.039
2672.00	313.632	26.482	369.895	30.241	428.458	32.273	485.773	35.803	541.886	36.127	585.614	38.146	615.350	35.781	636.323	36.284
2722.00	312.846	26.811	369.131	30.666	427.837	32.601	485.190	36.210	541.452	36.412	585.215	38.484	615.063	35.999	636.057	36.530
2772.00	312.077	27.193	368.389	31.148	427.248	32.969	484.639	36.655	541.055	36.716	584.850	38.837	614.816	36.221	635.829	36.778
2822.00	311.329	27.624	367.674	31.679	426.692	33.372	484.121	37.134	540.698	37.035	584.521	39.203	614.613	36.448	635.644	37.027
2872.00	310.611	28.095	366.991	32.253	426.173	33.801	483.642	37.639	540.382	37.365	584.233	39.577	614.456	36.675	635.503	37.275
2922.00	309.930	28.595	366.348	32.857	425.698	34.247	483.207	38.159	540.112	37.701	583.989	39.952	614.348	36.899	635.411	37.516
2972.00	309.294	29.111	365.752	33.480	425.270	34.701	482.819	38.682	539.891	38.034	583.792	40.320	614.293	37.114	635.371	37.745
3022.00	308.712	29.627	365.209	34.104	424.896	35.151	482.485	39.192	539.724	38.356	583.648	40.671	614.294	37.314	635.387	37.957
3072.00	308.190	30.131	364.728	34.710	424.580	35.586	482.210	39.677	539.615	38.657	583.561	40.997	614.355	37.495	635.463	38.145
3122.00	307.735	30.609	364.313	35.278	424.328	35.994	481.997	40.121	539.567	38.926	583.533	41.285	614.479	37.651	635.602	38.302
3172.00	307.351	31.048	363.969	35.788	424.142	36.360	481.852	40.510	539.584	39.156	583.570	41.526	614.670	37.774	635.808	38.423
3222.00	307.044	31.435	363.700	36.225	424.028	36.673	481.776	40.831	539.668	39.337	583.674	41.712	614.930	37.860	636.085	38.504
3272.00	306.815	31.756	363.510	36.573	423.987	36.921	481.773	41.073	539.824	39.465	583.848	41.833	615.261	37.905	636.434	38.538
3322.00	306.668	32.000	363.400	36.821	424.022	37.096	481.845	41.226	540.051	39.532	584.094	41.885	615.667	37.904	636.858	38.524
3372.00	306.603	32.157	363.371	36.960	424.133	37.193	481.993	41.281	540.351	39.535	584.413	41.863	616.148	37.855	637.358	38.458
3422.00	306.620	32.224	363.423	36.984	424.322	37.207	482.217	41.235	540.725	39.472	584.807	41.767	616.704	37.756	637.936	38.339
3472.00	306.720	32.201	363.557	36.890	424.588	37.137	482.517	41.089	541.173	39.340	585.275	41.595	617.337	37.607	638.591	38.169

**Dynamic Stresses Along the Length of the Riser
for the Wave Fatigue Bins**

Riser Configuration_07-20-04
Nominal Tensioner Setting = 865 kips; Wave Heading = 0 deg.

Elevation (ft. above Mudline)	Fatigue Bin = 17		Fatigue Bin = 18		Fatigue Bin = 19		Fatigue Bin = 20		Fatigue Bin = 21		Fatigue Bin = 22		Fatigue Bin = 23		Fatigue Bin = 24	
	Stress Std. Dev. (psi)	Zero Cross. Period (sec.)														
3522.00	306.901	32.090	363.771	36.685	424.931	36.984	482.893	40.846	541.695	39.142	585.816	41.351	618.044	37.411	639.322	37.947
3572.00	307.161	31.897	364.063	36.377	425.348	36.749	483.343	40.514	542.288	38.878	586.430	41.039	618.825	37.167	640.130	37.679
3622.00	307.499	31.628	364.432	35.980	425.840	36.439	483.865	40.102	542.951	38.555	587.115	40.664	619.678	36.880	641.011	37.366
3672.00	307.913	31.291	364.874	35.508	426.402	36.061	484.457	39.620	543.682	38.177	587.868	40.232	620.601	36.553	641.963	37.015
3722.00	308.398	30.896	365.385	34.977	427.032	35.624	485.114	39.079	544.478	37.752	588.687	39.752	621.590	36.191	642.983	36.629
3772.00	308.953	30.453	365.963	34.399	427.727	35.139	485.835	38.492	545.335	37.288	589.568	39.233	622.642	35.797	644.068	36.215
3822.00	309.570	29.972	366.601	33.787	428.480	34.614	486.611	37.869	546.245	36.790	590.503	38.683	623.748	35.377	645.208	35.776
3867.00	310.179	29.517	367.227	33.218	429.209	34.118	487.359	37.288	547.114	36.320	591.396	38.169	624.794	34.981	646.288	35.366
3908.00	310.774	29.090	367.835	32.692	429.910	33.651	488.077	36.748	547.940	35.878	592.244	37.688	625.783	34.610	647.307	34.982
3944.00	311.343	28.695	368.413	32.214	430.570	33.221	488.750	36.257	548.709	35.472	593.033	37.251	626.697	34.269	648.249	34.633
3974.00	312.007	28.237	369.074	31.682	431.309	32.747	489.494	35.734	549.549	35.041	593.886	36.794	627.678	33.912	649.257	34.270
4004.00	314.374	26.633	371.355	29.924	433.757	31.227	491.907	34.121	552.212	33.734	596.537	35.437	630.718	32.854	652.359	33.205
4034.00	316.976	25.151	373.862	28.285	436.423	29.760	494.530	32.557	555.080	32.436	599.391	34.088	633.966	31.789	655.673	32.135
4069.00	317.892	24.759	374.776	27.819	437.434	29.293	495.543	32.034	556.202	31.968	600.529	33.591	635.256	31.383	656.997	31.723
4109.00	318.670	24.483	375.569	27.474	438.334	28.919	496.456	31.604	557.222	31.566	601.575	33.158	636.441	31.021	658.219	31.355
4154.00	319.496	24.216	376.414	27.141	439.299	28.540	497.439	31.170	558.322	31.148	602.707	32.710	637.721	30.640	659.540	30.970
4204.00	320.379	23.948	377.319	26.807	440.337	28.147	498.496	30.722	559.503	30.710	603.924	32.241	639.093	30.236	660.958	30.563
4254.00	321.237	23.695	378.199	26.496	441.346	27.774	499.525	30.301	560.649	30.292	605.109	31.797	640.422	29.849	662.333	30.175
4304.00	322.075	23.448	379.057	26.199	442.327	27.413	500.524	29.899	561.756	29.888	606.256	31.372	641.700	29.476	663.656	29.803
4354.00	322.898	23.203	379.898	25.911	443.282	27.059	501.496	29.511	562.824	29.496	607.365	30.963	642.925	29.114	664.927	29.445
4404.00	323.707	22.957	380.724	25.627	444.210	26.712	502.439	29.135	563.851	29.116	608.434	30.568	644.095	28.765	666.142	29.099
4454.00	324.502	22.711	381.533	25.347	445.108	26.372	503.352	28.770	564.833	28.748	609.461	30.188	645.204	28.428	667.297	28.767
4504.00	325.278	22.465	382.323	25.073	445.973	26.042	504.230	28.419	565.766	28.396	610.440	29.824	646.247	28.106	668.387	28.451
4554.00	326.025	22.222	383.086	24.804	446.795	25.725	505.068	28.083	566.642	28.061	611.366	29.480	647.218	27.802	669.405	28.152
4604.00	326.732	21.989	383.812	24.546	447.565	25.426	505.857	27.767	567.452	27.748	612.230	29.157	648.107	27.518	670.343	27.873
4654.00	327.386	21.769	384.491	24.303	448.270	25.149	506.586	27.474	568.186	27.461	613.024	28.861	648.904	27.258	671.191	27.618
4704.00	327.970	21.571	385.108	24.083	448.899	24.899	507.245	27.210	568.835	27.202	613.737	28.594	649.599	27.025	671.941	27.388
4754.00	328.470	21.400	385.652	23.891	449.437	24.681	507.823	26.978	569.385	26.977	614.360	28.360	650.182	26.822	672.581	27.187
4804.00	328.873	21.261	386.108	23.731	449.873	24.499	508.310	26.782	569.828	26.788	614.883	28.162	650.643	26.652	673.103	27.018
4854.00	329.166	21.155	386.468	23.606	450.196	24.356	508.696	26.626	570.155	26.638	615.298	28.001	650.971	26.517	673.499	26.881
4904.00	329.342	21.083	386.724	23.517	450.398	24.253	508.974	26.509	570.357	26.528	615.598	27.881	651.162	26.418	673.760	26.779
4954.00	329.395	21.047	386.871	23.463	450.475	24.191	509.139	26.433	570.430	26.461	615.777	27.801	651.209	26.358	673.883	26.713
5004.00	329.326	21.044	386.906	23.443	450.423	24.169	509.189	26.397	570.371	26.434	615.833	27.761	651.109	26.336	673.862	26.684
5054.00	329.136	21.072	386.832	23.456	450.244	24.186	509.123	26.400	570.180	26.449	615.765	27.762	650.862	26.352	673.698	26.691
5104.00	328.831	21.129	386.651	23.498	449.941	24.239	508.944	26.440	569.860	26.505	615.574	27.802	650.469	26.406	673.390	26.734
5154.00	328.418	21.212	386.371	23.566	449.519	24.327	508.656	26.514	569.414	26.599	615.262	27.880	649.933	26.499	672.941	26.813
5204.00	327.907	21.317	385.997	23.658	448.987	24.448	508.264	26.622	568.847	26.731	614.834	27.995	649.257	26.629	672.352	26.927
5254.00	327.307	21.441	385.538	23.770	448.351	24.600	507.773	26.760	568.165	26.901	614.291	28.146	648.446	26.797	671.625	27.077
5304.00	326.628	21.580	385.000	23.897	447.618	24.780	507.186	26.926	567.371	27.107	613.634	28.332	647.500	27.001	670.758	27.261
5354.00	325.875	21.733	384.386	24.038	446.793	24.987	506.504	27.121	566.465	27.349	612.861	28.552	646.418	27.244	669.747	27.482
5404.00	325.054	21.898	383.696	24.191	445.877	25.221	505.724	27.342	565.446	27.627	611.964	28.809	645.192	27.525	668.579	27.739
5454.00	324.164	22.075	382.929	24.359	444.867	25.480	504.839	27.590	564.305	27.942	610.930	29.103	643.811	27.848	667.238	28.036
5504.00	323.203	22.267	382.077	24.541	443.757	25.768	503.834	27.869	563.028	28.298	609.737	29.438	642.252	28.214	665.692	28.376
5554.00	322.161	22.475	381.120	24.743	442.532	26.087	502.685	28.183	561.588	28.697	608.350	29.819	640.478	28.630	663.894	28.767
5604.00	321.019	22.704	380.032	24.971	441.160	26.442	501.349	28.539	559.944	29.149	606.712	30.255	638.434	29.103	661.780	29.215
5654.00	319.745	22.960	378.768	25.232	439.598	26.842	499.767	28.949	558.034	29.662	604.748	30.760	636.045	29.645	659.256	29.735

**Dynamic Stresses Along the Length of the Riser
for the Wave Fatigue Bins**

Riser Configuration_07-20-04
Nominal Tensioner Setting = 865 kips; Wave Heading = 0 deg.

Elevation (ft. above Mudline)	Fatigue Bin = 17		Fatigue Bin = 18		Fatigue Bin = 19		Fatigue Bin = 20		Fatigue Bin = 21		Fatigue Bin = 22		Fatigue Bin = 23		Fatigue Bin = 24	
	Stress Std. Dev. (psi)	Zero Cross. Period (sec.)														
5704.00	318.321	23.247	377.296	25.534	437.818	27.294	497.901	29.425	555.826	30.247	602.411	31.348	633.274	30.265	656.279	30.341
5744.00	317.053	23.501	375.931	25.811	436.199	27.697	496.144	29.862	553.783	30.776	600.191	31.890	630.700	30.827	653.466	30.899
5774.00	316.028	23.703	374.791	26.039	434.867	28.022	494.660	30.225	552.082	31.207	598.304	32.342	628.551	31.286	651.087	31.363
5794.00	315.317	23.838	373.978	26.196	433.925	28.246	493.586	30.480	550.861	31.507	596.927	32.662	626.999	31.607	649.351	31.691
5814.00	314.632	23.965	373.177	26.349	433.006	28.465	492.520	30.736	549.662	31.806	595.556	32.987	625.471	31.930	647.626	32.023
5834.00	314.027	24.065	372.443	26.477	432.170	28.658	491.520	30.971	548.545	32.084	594.253	33.298	624.032	32.235	645.977	32.344
5854.00	313.609	24.103	371.888	26.544	431.541	28.786	490.715	31.146	547.652	32.302	593.164	33.554	622.842	32.488	644.568	32.617
5874.00	313.577	24.009	371.725	26.475	431.345	28.773	490.341	31.181	547.234	32.385	592.552	33.681	622.181	32.624	643.690	32.782
5894.00	314.278	23.665	372.320	26.141	431.974	28.485	490.798	30.935	547.716	32.200	592.864	33.547	622.519	32.532	643.825	32.730
5914.00	316.345	22.861	374.333	25.305	434.107	27.675	492.779	30.145	549.813	31.500	594.839	32.898	624.619	32.002	645.751	32.258
5934.00	320.935	21.259	378.939	23.582	438.917	25.924	497.441	28.352	554.679	29.838	599.651	31.268	629.659	30.630	650.647	30.972
5949.00	327.498	19.316	385.595	21.447	445.781	23.678	504.174	25.988	561.620	27.568	606.618	28.983	636.873	28.650	657.767	29.071
5960.00	334.944	17.485	393.176	19.406	453.533	21.476	511.795	23.627	569.405	25.228	614.474	26.589	644.962	26.506	665.801	26.980
5968.00	341.948	16.026	400.343	17.766	460.847	19.673	519.000	21.671	576.740	23.240	621.911	24.531	652.624	24.608	673.457	25.106
5974.00	347.731	14.940	406.317	16.541	466.968	18.309	525.066	20.179	582.933	21.692	628.243	22.915	659.190	23.082	680.071	23.585
5980.00	352.960	13.951	411.841	15.421	472.719	17.049	530.854	18.790	588.921	20.227	634.481	21.372	665.771	21.590	686.808	22.083
5984.00	355.197	13.407	414.377	14.801	475.499	16.342	533.786	18.004	592.080	19.382	637.921	20.468	669.545	20.695	690.801	21.172
5988.00	355.167	13.032	414.763	14.366	476.252	15.830	534.876	17.423	593.526	18.737	639.799	19.761	671.886	19.970	693.514	20.417
5992.00	352.725	12.787	412.799	14.065	474.743	15.453	533.893	16.974	593.035	18.209	639.913	19.157	672.653	19.318	694.868	19.718
5996.00	347.140	12.732	407.688	13.952	470.138	15.252	530.035	16.686	589.827	17.817	637.521	18.659	671.184	18.736	694.290	19.059
6000.00	335.531	13.370	396.520	14.504	459.535	15.681	520.539	16.984	581.211	17.948	630.025	18.622	664.942	18.527	689.385	18.715
6004.00	317.236	16.004	377.247	17.097	439.899	18.061	502.219	18.989	563.941	19.516	614.166	19.797	650.641	19.270	676.972	19.165
6010.00	301.407	16.779	357.154	23.141	415.889	24.722	474.669	26.203	532.263	26.714	579.401	26.765	613.415	25.217	639.516	24.316
6015.00	299.931	19.469	354.275	21.273	415.391	21.555	470.689	23.124	529.567	22.803	571.729	23.343	607.085	21.816	628.664	21.554
6020.00	299.817	21.568	354.772	23.752	416.514	23.923	472.578	25.845	532.145	25.353	574.862	26.225	610.268	24.450	631.838	24.409
6025.00	300.166	23.222	355.688	25.699	417.909	25.748	474.673	27.939	534.773	27.276	578.022	28.401	613.617	26.403	635.402	26.539
6030.00	300.739	24.730	356.860	27.452	419.474	27.379	476.977	29.797	537.504	28.960	581.280	30.284	617.073	28.060	639.163	28.328
6035.00	301.662	26.440	358.552	29.411	421.570	29.211	480.041	31.870	541.002	30.838	585.443	32.349	621.478	29.857	644.032	30.239
6040.00	303.458	28.739	361.520	31.998	425.115	31.688	485.109	34.653	546.724	33.394	592.266	35.120	628.767	32.271	652.218	32.774
6045.00	307.415	31.863	367.470	35.401	432.135	35.192	494.817	38.515	557.738	37.113	605.444	39.049	643.073	35.793	668.494	36.396
6050.00	316.480	34.484	380.143	37.922	447.056	38.823	514.764	42.212	580.584	41.461	632.828	43.244	673.232	40.083	703.054	40.481
6055.00	336.937	31.297	407.222	33.999	478.843	37.241	555.951	39.897	628.033	41.579	689.574	42.376	736.089	41.161	774.995	40.707
6055.00	122.906	32.669	148.234	35.560	174.178	38.509	201.678	41.392	227.577	42.626	249.289	43.718	265.635	41.997	278.903	41.788
6060.00	135.233	24.587	163.711	26.704	191.762	30.239	223.849	32.238	252.629	35.046	279.051	35.232	298.496	35.792	316.788	34.878
6060.00	50.302	9.777	58.936	10.636	67.106	11.659	78.523	12.925	88.346	14.248	100.160	15.270	108.763	16.335	119.268	17.032
6065.00	88.071	8.756	98.663	9.125	108.144	9.487	119.968	9.998	129.564	10.393	141.366	10.783	149.392	11.019	160.391	11.336
6065.00	82.746	8.756	92.697	9.125	101.605	9.487	112.714	9.998	121.731	10.393	132.819	10.783	140.360	11.019	150.694	11.336
6070.00	128.880	8.583	143.094	8.866	156.455	9.133	171.291	9.499	184.366	9.756	198.858	10.015	210.225	10.137	223.932	10.358
6075.00	183.882	8.542	203.773	8.806	223.282	9.060	243.758	9.395	263.112	9.634	283.102	9.868	300.568	9.980	319.551	10.181
6080.00	247.082	8.532	273.697	8.791	300.501	9.047	327.873	9.375	354.850	9.617	381.659	9.847	406.522	9.965	432.003	10.162
6085.00	153.681	8.531	170.234	8.790	186.909	9.046	203.932	9.374	220.713	9.616	237.388	9.846	252.855	9.963	268.702	10.161
6088.00	101.530	8.530	112.466	8.789	123.484	9.045	134.730	9.373	145.818	9.615	156.833	9.845	167.054	9.962	177.523	10.160

**Dynamic Stresses Along the Length of the Riser
for the Wave Fatigue Bins**

Riser Configuration_07-20-04
Nominal Tensioner Setting = 865 kips; Wave Heading = 0 deg.

Elevation (ft. above Mudline)	Fatigue Bin = 25		Fatigue Bin = 26		Fatigue Bin = 27	
	Stress Std. Dev. (psi)	Zero Cross. Period (sec.)	Stress Std. Dev. (psi)	Zero Cross. Period (sec.)	Stress Std. Dev. (psi)	Zero Cross. Period (sec.)
10.00	5705.671	48.049	5780.864	47.879	6347.503	49.701
11.00	5502.039	48.034	5571.994	47.864	6100.739	49.599
12.00	5302.848	48.016	5367.778	47.845	5859.967	49.491
13.00	5267.179	47.995	5329.131	47.823	5799.801	49.374
14.50	5212.750	47.957	5270.174	47.783	5707.903	49.184
16.50	5137.845	47.893	5189.111	47.716	5581.605	48.901
19.00	5041.333	47.789	5084.717	47.607	5418.528	48.495
22.00	4922.710	47.622	4956.379	47.430	5216.509	47.915
26.00	4763.465	47.308	4783.755	47.095	4939.661	46.948
30.00	4612.136	46.859	4618.553	46.613	4662.490	45.702
34.00	4486.004	46.236	4478.019	45.942	4400.484	44.108
38.00	4418.140	45.404	4395.030	45.044	4182.945	42.114
42.00	4476.164	44.362	4436.462	43.915	4068.778	39.742
45.00	3743.177	43.631	3700.185	43.115	3305.796	38.097
48.00	3138.919	42.957	3095.269	42.374	2697.780	36.584
51.00	2639.718	42.391	2597.069	41.744	2213.618	35.280
54.00	2227.304	41.988	2186.678	41.282	1829.347	34.269
57.00	1886.624	41.805	1848.592	41.048	1525.486	33.633
61.00	1522.889	42.021	1488.690	41.209	1218.666	33.534
67.00	1126.570	43.681	1098.191	42.835	1203.009	22.757
76.00	879.895	22.392	930.224	23.098	1256.002	28.279
88.00	824.023	25.748	864.926	26.400	1221.780	33.604
106.00	763.720	29.790	790.705	30.246	1105.161	38.120
133.00	697.472	32.243	715.159	32.582	977.890	40.451
166.00	663.242	32.423	678.149	32.783	918.844	40.610
202.00	654.351	31.844	668.808	32.261	932.062	36.696
240.00	654.251	31.211	670.577	28.024	934.300	36.153
281.00	656.307	30.678	670.766	31.175	933.353	35.698
325.00	658.733	30.308	673.249	30.818	931.684	35.374
372.00	661.061	30.139	675.671	30.642	929.735	35.222
422.00	663.138	30.184	677.883	30.662	927.549	35.267
472.00	664.818	30.408	679.726	30.848	925.265	35.497
522.00	666.154	30.746	681.243	31.142	922.918	35.873
572.00	667.227	31.120	682.500	31.472	920.555	36.346
622.00	668.122	31.447	683.570	31.767	922.068	39.109
672.00	668.914	31.654	684.519	31.961	923.521	39.259
722.00	669.655	31.697	685.397	32.012	924.847	39.293
772.00	670.372	31.569	686.228	31.912	926.068	39.202
822.00	671.063	31.302	687.016	31.685	927.193	39.002
872.00	671.708	30.954	687.746	31.377	928.219	38.729
922.00	672.274	30.585	688.390	31.042	929.136	38.427
972.00	672.722	30.247	688.918	30.728	929.930	38.140
1022.00	673.021	29.978	689.304	30.471	930.588	37.901
1072.00	673.151	29.797	689.528	30.291	931.105	37.735
1122.00	673.106	29.712	689.586	30.196	931.480	37.651
1172.00	672.896	29.717	689.486	30.185	931.720	37.648

**Dynamic Stresses Along the Length of the Riser
for the Wave Fatigue Bins**

Riser Configuration_07-20-04
Nominal Tensioner Setting = 865 kips; Wave Heading = 0 deg.

Elevation (ft. above Mudline)	Fatigue Bin = 25		Fatigue Bin = 26		Fatigue Bin = 27	
	Stress Std. Dev. (psi)	Zero Cross. Period (sec.)	Stress Std. Dev. (psi)	Zero Cross. Period (sec.)	Stress Std. Dev. (psi)	Zero Cross. Period (sec.)
1222.00	672.544	29.802	689.249	30.246	931.842	37.719
1272.00	672.085	29.947	688.906	30.365	931.867	37.849
1322.00	671.560	30.130	688.493	30.521	931.819	38.019
1372.00	671.013	30.328	688.050	30.693	931.724	38.209
1422.00	670.482	30.516	687.613	30.860	931.608	38.401
1472.00	670.000	30.678	687.214	31.006	931.492	38.577
1522.00	669.589	30.803	686.876	31.121	931.391	38.726
1572.00	669.259	30.887	686.611	31.200	931.317	38.843
1622.00	669.011	30.936	686.422	31.246	931.275	38.928
1672.00	668.832	30.961	686.300	31.269	931.262	38.987
1722.00	668.705	30.974	686.232	31.280	931.273	39.030
1772.00	668.609	30.988	686.199	31.291	931.299	39.068
1822.00	668.522	31.017	686.181	31.314	931.331	39.114
1872.00	668.424	31.070	686.159	31.358	931.357	39.176
1922.00	668.300	31.153	686.118	31.430	931.370	39.262
1972.00	668.138	31.269	686.045	31.533	931.363	39.376
2022.00	667.934	31.419	685.936	31.669	931.333	39.519
2072.00	667.688	31.599	685.787	31.834	931.279	39.690
2122.00	667.405	31.804	685.601	32.025	931.203	39.885
2172.00	667.093	32.026	685.385	32.236	931.110	40.099
2222.00	666.761	32.258	685.146	32.460	931.003	40.325
2272.00	666.420	32.491	684.894	32.689	930.889	40.557
2322.00	666.081	32.720	684.638	32.918	930.775	40.789
2372.00	665.753	32.939	684.386	33.142	930.666	41.016
2422.00	665.444	33.146	684.147	33.358	930.568	41.233
2472.00	665.160	33.341	683.927	33.564	930.486	41.439
2522.00	664.908	33.525	683.731	33.761	930.422	41.632
2572.00	664.689	33.698	683.564	33.949	930.382	41.813
2622.00	664.508	33.864	683.429	34.129	930.366	41.982
2672.00	664.366	34.023	683.329	34.303	930.378	42.140
2722.00	664.266	34.177	683.265	34.471	930.419	42.288
2772.00	664.209	34.328	683.241	34.634	930.491	42.426
2822.00	664.197	34.473	683.259	34.791	930.596	42.554
2872.00	664.233	34.614	683.322	34.940	930.736	42.671
2922.00	664.319	34.746	683.433	35.080	930.912	42.775
2972.00	664.459	34.868	683.594	35.207	931.127	42.862
3022.00	664.656	34.976	683.810	35.319	931.383	42.931
3072.00	664.913	35.066	684.084	35.411	931.682	42.979
3122.00	665.233	35.135	684.419	35.481	932.027	43.003
3172.00	665.619	35.178	684.819	35.524	932.419	43.000
3222.00	666.074	35.193	685.286	35.538	932.860	42.967
3272.00	666.601	35.178	685.823	35.519	933.352	42.904
3322.00	667.200	35.131	686.431	35.467	933.895	42.808
3372.00	667.873	35.051	687.113	35.381	934.491	42.679
3422.00	668.621	34.936	687.869	35.259	935.140	42.516
3472.00	669.443	34.788	688.699	35.103	935.843	42.320

**Dynamic Stresses Along the Length of the Riser
for the Wave Fatigue Bins**

Riser Configuration_07-20-04
Nominal Tensioner Setting = 865 kips; Wave Heading = 0 deg.

Elevation (ft. above Mudline)	Fatigue Bin = 25		Fatigue Bin = 26		Fatigue Bin = 27	
	Stress Std. Dev. (psi)	Zero Cross. Period (sec.)	Stress Std. Dev. (psi)	Zero Cross. Period (sec.)	Stress Std. Dev. (psi)	Zero Cross. Period (sec.)
3522.00	670.339	34.606	689.602	34.914	936.597	42.092
3572.00	671.308	34.392	690.579	34.693	937.404	41.834
3622.00	672.347	34.149	691.626	34.443	938.262	41.547
3672.00	673.455	33.878	692.741	34.165	939.168	41.234
3722.00	674.627	33.583	693.923	33.864	940.122	40.898
3772.00	675.860	33.267	695.166	33.542	941.120	40.542
3822.00	677.145	32.932	696.461	33.203	942.157	40.168
3867.00	678.352	32.618	697.678	32.886	943.126	39.820
3908.00	679.484	32.324	698.822	32.590	944.035	39.494
3944.00	680.527	32.056	699.874	32.320	944.873	39.197
3974.00	681.644	31.775	701.000	32.040	945.801	38.888
4004.00	685.137	30.949	704.523	31.217	949.004	37.975
4034.00	688.837	30.112	708.253	30.384	952.363	37.046
4069.00	690.269	29.783	709.695	30.056	953.525	36.680
4109.00	691.577	29.485	711.014	29.757	954.551	36.344
4154.00	692.983	29.168	712.433	29.440	955.651	35.986
4204.00	694.483	28.831	713.948	29.104	956.823	35.605
4254.00	695.926	28.507	715.408	28.782	957.949	35.240
4304.00	697.303	28.195	716.804	28.472	959.020	34.890
4354.00	698.610	27.894	718.131	28.174	960.033	34.553
4404.00	699.844	27.602	719.386	27.886	960.986	34.229
4454.00	701.001	27.323	720.565	27.611	961.872	33.920
4504.00	702.073	27.056	721.663	27.348	962.690	33.626
4554.00	703.054	26.804	722.671	27.100	963.433	33.350
4604.00	703.935	26.570	723.584	26.870	964.095	33.094
4654.00	704.708	26.357	724.391	26.659	964.671	32.862
4704.00	705.363	26.166	725.085	26.470	965.154	32.654
4754.00	705.890	26.000	725.656	26.305	965.537	32.476
4804.00	706.280	25.862	726.095	26.166	965.814	32.327
4854.00	706.525	25.753	726.395	26.056	965.979	32.212
4904.00	706.618	25.675	726.548	25.975	966.029	32.131
4954.00	706.553	25.630	726.549	25.925	965.959	32.087
5004.00	706.329	25.617	726.396	25.906	965.765	32.080
5054.00	705.943	25.639	726.085	25.920	965.447	32.112
5104.00	705.397	25.694	725.617	25.965	965.003	32.183
5154.00	704.690	25.784	724.990	26.044	964.435	32.294
5204.00	703.826	25.908	724.207	26.155	963.740	32.446
5254.00	702.806	26.066	723.265	26.299	962.917	32.639
5304.00	701.627	26.260	722.160	26.477	961.962	32.876
5354.00	700.284	26.490	720.882	26.689	960.865	33.157
5404.00	698.764	26.758	719.415	26.938	959.612	33.487
5454.00	697.047	27.067	717.732	27.227	958.178	33.871
5504.00	695.102	27.420	715.795	27.560	956.532	34.315
5554.00	692.882	27.823	713.545	27.943	954.627	34.829
5604.00	690.317	28.285	710.904	28.387	952.398	35.429
5654.00	687.318	28.818	707.766	28.904	949.764	36.131

**Dynamic Stresses Along the Length of the Riser
for the Wave Fatigue Bins**

Riser Configuration_07-20-04
Nominal Tensioner Setting = 865 kips; Wave Heading = 0 deg.

Elevation (ft. above Mudline)	Fatigue Bin = 25		Fatigue Bin = 26		Fatigue Bin = 27	
	Stress Std. Dev. (psi)	Zero Cross. Period (sec.)	Stress Std. Dev. (psi)	Zero Cross. Period (sec.)	Stress Std. Dev. (psi)	Zero Cross. Period (sec.)
5704.00	683.855	29.429	704.097	29.506	946.711	36.951
5744.00	680.645	29.984	700.652	30.060	943.864	37.710
5774.00	677.972	30.439	697.755	30.519	941.488	38.339
5794.00	676.038	30.756	695.643	30.843	939.761	38.784
5814.00	674.138	31.074	693.554	31.171	938.064	39.231
5834.00	672.336	31.376	691.550	31.486	936.443	39.661
5854.00	670.806	31.633	689.809	31.759	935.033	40.037
5874.00	669.851	31.791	688.644	31.940	934.075	40.293
5894.00	669.969	31.763	688.562	31.942	933.953	40.327
5914.00	671.943	31.387	690.361	31.609	935.265	39.959
5934.00	676.922	30.340	695.192	30.627	938.859	38.843
5949.00	684.069	28.761	702.238	29.115	944.092	37.110
5960.00	692.051	26.972	710.154	27.377	949.951	35.094
5968.00	699.608	25.319	717.687	25.754	955.509	33.176
5974.00	706.125	23.942	724.228	24.389	960.328	31.536
5980.00	712.786	22.551	731.004	22.997	965.313	29.839
5984.00	716.787	21.689	735.181	22.125	968.385	28.762
5988.00	719.620	20.961	738.325	21.375	970.698	27.830
5992.00	721.255	20.266	740.460	20.641	972.328	26.906
5996.00	721.216	19.582	741.195	19.894	973.061	25.946
6000.00	717.291	19.156	738.456	19.361	971.418	25.232
6004.00	706.526	19.389	729.442	19.389	965.281	25.159
6010.00	670.349	23.537	695.778	22.613	941.212	28.377
6015.00	661.361	20.685	680.600	20.358	928.589	25.686
6020.00	664.910	23.253	684.035	23.133	935.125	29.118
6025.00	668.729	25.119	688.027	25.164	944.551	31.666
6030.00	672.545	26.660	692.086	26.820	957.806	33.875
6035.00	677.293	28.294	697.187	28.543	978.069	36.368
6040.00	685.302	30.471	705.915	30.800	1011.450	39.817
6045.00	701.694	33.650	724.047	34.018	1069.119	44.859
6050.00	737.568	37.603	764.100	37.731	1170.798	50.933
6055.00	813.730	39.182	849.159	38.542	1344.939	53.614
6055.00	292.583	39.821	304.571	39.403	477.253	54.198
6060.00	332.733	34.990	349.840	33.908	566.022	48.915
6060.00	126.590	18.182	136.701	18.701	215.350	28.482
6065.00	167.471	11.690	178.288	11.982	230.595	15.054
6065.00	157.346	11.690	167.510	11.982	216.652	15.054
6070.00	234.962	10.620	248.546	10.835	283.485	11.946
6075.00	337.269	10.443	356.132	10.641	389.449	11.212
6080.00	457.695	10.432	483.041	10.627	521.851	11.042
6085.00	284.684	10.431	300.447	10.626	324.585	11.040
6088.00	188.083	10.430	198.496	10.625	214.441	11.039

Appendix A-6.3.1

Tension Loads and Bending Moments from the “Composite-Steel” Riser Configuration Fatigue Solutions

**Composite Riser Used for the CRA Study
Tension and Bending Moments for a Composite Riser Section
Located 102 ft. above the Mudline**

Riser Configuration 05-04-05
Omni-Directional Seas; Wave Heading = 0 deg.
Nominal Tensioner Setting = 319 kips

Fatigue Bin	Wave Definition		Probability	Effective Tension					Bending Moment				
	Hs (ft.)	Tz (sec.)		Mean (kips)	RMS (kips)	Tz (sec.)	Minimum (kips)	Maximum (kips)	Mean (ft-kips)	RMS (ft-kips)	Tz (sec.)	Minimum (ft-kips)	Maximum (ft-kips)
1	2.0	2.0	4.1895E-02	85.40	0.61	1.43	82.75	88.05	4.46	0.65	1.80	1.67	7.24
2	2.0	3.0	2.2055E-01	85.40	0.12	1.44	84.86	85.94	4.46	0.38	2.11	2.86	6.06
3	2.0	4.0	1.0194E-01	85.40	0.06	1.59	85.14	85.66	4.46	0.17	2.29	3.72	5.19
4	4.0	3.0	8.1279E-02	85.50	0.22	1.51	84.53	86.47	5.03	0.56	2.37	2.67	7.38
5	4.0	4.0	1.9041E-01	85.50	0.12	1.98	84.98	86.01	5.03	0.36	3.41	3.55	6.50
6	4.0	5.0	5.3197E-02	85.50	0.14	8.24	84.96	86.03	5.03	0.30	5.31	3.81	6.25
7	6.0	4.0	8.8356E-02	85.67	0.26	3.62	84.60	86.74	5.70	0.57	4.93	3.39	8.01
8	6.0	5.0	7.2831E-02	85.67	0.29	12.11	84.57	86.78	5.70	0.53	8.41	3.63	7.77
9	6.0	6.0	1.3813E-02	85.67	0.41	11.21	84.11	87.23	5.70	0.52	13.08	3.73	7.68
10	8.0	5.0	4.1781E-02	85.97	0.59	19.01	83.78	88.16	6.48	0.74	11.54	3.67	9.30
11	8.0	6.0	1.6324E-02	85.97	0.70	14.63	83.34	88.61	6.48	0.73	18.10	3.78	9.19
12	10.0	6.0	1.3242E-02	86.47	1.20	20.30	82.04	90.89	7.41	0.91	22.04	4.08	10.74
13	12.0	6.0	5.1368E-03	87.10	1.90	26.84	80.26	93.94	8.31	1.05	26.15	4.51	12.11
14	14.0	6.5	3.3107E-03	87.96	2.90	30.89	77.66	98.26	9.28	1.15	35.54	5.24	13.32
15	16.0	7.5	5.1368E-04	89.08	4.16	33.60	74.37	103.80	10.30	1.20	48.47	6.17	14.42
16	18.0	7.7	3.5386E-04	90.38	5.55	40.04	71.06	109.70	11.26	1.23	49.30	7.05	15.48
17	20.0	7.9	2.5117E-04	91.82	7.10	43.53	67.26	116.38	12.17	1.26	46.96	7.85	16.50
18	22.0	8.1	1.5982E-04	93.48	8.76	49.75	63.50	123.45	13.06	1.31	46.25	8.54	17.58
19	24.0	8.3	1.0270E-04	95.26	10.52	51.26	59.36	131.16	13.88	1.42	43.89	8.96	18.81
20	26.0	8.6	6.8494E-05	97.16	12.20	56.48	55.88	138.43	14.64	1.57	45.48	9.22	20.07
21	28.0	8.8	5.1368E-05	99.05	13.88	55.71	52.03	146.08	15.31	1.80	44.52	9.11	21.52
22	30.0	9.0	3.0319E-05	100.93	15.38	59.55	49.13	152.73	15.90	2.04	47.90	8.89	22.91
23	32.0	9.2	2.2828E-05	102.87	16.24	55.13	47.81	157.92	16.45	2.23	44.85	8.76	24.13
24	34.0	9.4	1.3703E-05	104.65	16.95	56.19	47.29	162.02	16.90	2.39	46.29	8.66	25.14
25	36.0	9.7	9.7024E-06	106.27	17.71	52.14	45.93	166.61	17.27	2.58	43.83	8.35	26.19
26	38.0	9.9	6.5070E-06	107.81	18.30	52.79	45.53	170.10	17.60	2.73	44.94	8.19	27.01
27	41.0	10.3	4.3377E-06	109.69	17.96	47.28	47.99	171.38	17.96	2.17	32.51	10.29	25.64

**Composite Riser Used for the CRA Study
Tension and Bending Moments for a Composite Riser Section
Located 5926 ft. above the Mudline**

Riser Configuration 05-04-05
Omni-Directional Seas; Wave Heading = 0 deg.
Nominal Tensioner Setting = 319 kips

Fatigue Bin	Wave Definition		Probability	Effective Tension					Bending Moment				
	Hs (ft.)	Tz (sec.)		Mean (kips)	RMS (kips)	Tz (sec.)	Minimum (kips)	Maximum (kips)	Mean (ft-kips)	RMS (ft-kips)	Tz (sec.)	Minimum (ft-kips)	Maximum (ft-kips)
1	2.0	2.0	4.1895E-02	270.07	0.02	1.47	269.98	270.16	-0.02	0.26	1.91	-1.12	1.08
2	2.0	3.0	2.2055E-01	270.07	0.01	3.29	270.01	270.13	-0.02	0.19	2.48	-0.80	0.77
3	2.0	4.0	1.0194E-01	270.07	0.03	5.59	269.97	270.17	-0.02	0.18	4.24	-0.73	0.70
4	4.0	3.0	8.1279E-02	270.16	0.07	9.07	269.89	270.43	-0.04	0.26	2.44	-1.14	1.07
5	4.0	4.0	1.9041E-01	270.16	0.08	9.27	269.85	270.48	-0.04	0.32	4.45	-1.34	1.26
6	4.0	5.0	5.3197E-02	270.16	0.13	9.20	269.65	270.68	-0.04	0.38	5.83	-1.54	1.47
7	6.0	4.0	8.8356E-02	270.34	0.24	18.19	269.46	271.22	-0.06	0.47	4.56	-1.97	1.84
8	6.0	5.0	7.2831E-02	270.34	0.29	13.42	269.26	271.42	-0.06	0.56	5.91	-2.31	2.19
9	6.0	6.0	1.3813E-02	270.34	0.40	11.37	268.82	271.87	-0.06	0.53	6.42	-2.16	2.03
10	8.0	5.0	4.1781E-02	270.64	0.59	20.94	268.48	272.79	-0.09	0.76	5.96	-3.12	2.93
11	8.0	6.0	1.6324E-02	270.64	0.69	14.97	268.04	273.23	-0.09	0.71	6.47	-2.92	2.73
12	10.0	6.0	1.3242E-02	271.13	1.20	20.90	266.74	275.51	-0.13	0.91	6.49	-3.73	3.47
13	12.0	6.0	5.1368E-03	271.75	1.89	27.72	264.96	278.55	-0.17	1.11	6.52	-4.57	4.24
14	14.0	6.5	3.3107E-03	272.60	2.89	31.81	262.36	282.85	-0.21	1.23	6.73	-5.07	4.66
15	16.0	7.5	5.1368E-04	273.72	4.15	34.46	259.07	288.37	-0.25	1.20	7.03	-4.98	4.47
16	18.0	7.7	3.5386E-04	274.99	5.54	41.08	255.74	294.24	-0.30	1.32	7.14	-5.50	4.91
17	20.0	7.9	2.5117E-04	276.42	7.09	44.63	251.95	300.90	-0.34	1.43	7.26	-6.00	5.31
18	22.0	8.1	1.5982E-04	278.06	8.76	51.00	248.17	307.95	-0.39	1.54	7.37	-6.45	5.68
19	24.0	8.3	1.0270E-04	279.82	10.51	52.49	244.02	315.62	-0.43	1.63	7.48	-6.87	6.00
20	26.0	8.6	6.8494E-05	281.69	12.19	57.81	240.51	322.86	-0.48	1.69	7.60	-7.14	6.18
21	28.0	8.8	5.1368E-05	283.56	13.88	56.96	236.65	330.47	-0.53	1.76	7.70	-7.45	6.40
22	30.0	9.0	3.0319E-05	285.41	15.38	60.86	233.72	337.10	-0.57	1.82	7.78	-7.72	6.58
23	32.0	9.2	2.2828E-05	287.31	16.23	56.29	232.38	342.25	-0.61	1.87	7.77	-7.95	6.73
24	34.0	9.4	1.3703E-05	289.07	16.94	57.34	231.83	346.32	-0.65	1.89	7.78	-8.06	6.77
25	36.0	9.7	9.7024E-06	290.66	17.70	53.14	230.45	350.88	-0.68	1.88	7.81	-8.06	6.70
26	38.0	9.9	6.5070E-06	292.18	18.30	53.78	230.02	354.34	-0.71	1.89	7.82	-8.14	6.72
27	41.0	10.3	4.3377E-06	294.02	17.92	48.02	232.53	355.51	-0.75	1.88	7.89	-8.10	6.61

Appendix A-6.3.2

Tension Histograms Generated from the “Composite-Steel” Riser Configuration Fatigue Solutions

**Composite Riser Used for the CRA Study
Tension Histogram for a Composite Riser Section
Located 102 ft. above the Mudline**

Riser Configuration 05-04-05
Omni-Directional Seas; Wave Heading = 0 deg.
Nominal Tensioner Setting = 319 kips

Tension Histogram Bin	Tension Range Interval Midpoint (lbs)	Number of Tension Cycles per Year	Tension Histogram Bin	Tension Range Interval Midpoint (lbs)	Number of Tension Cycles per Year
1	15	1.271E+05	51	8986	3.285E+02
2	46	3.963E+05	52	9556	2.882E+02
3	79	6.631E+05	53	10159	2.523E+02
4	113	8.920E+05	54	10798	2.200E+02
5	150	1.055E+06	55	11476	1.907E+02
6	189	1.144E+06	56	12195	1.643E+02
7	231	1.166E+06	57	12957	1.407E+02
8	274	1.142E+06	58	13764	1.198E+02
9	321	1.086E+06	59	14620	1.015E+02
10	370	1.003E+06	60	15527	8.568E+01
11	422	8.935E+05	61	16489	7.222E+01
12	478	7.632E+05	62	17508	6.101E+01
13	536	6.249E+05	63	18588	5.189E+01
14	598	4.949E+05	64	19734	4.463E+01
15	664	3.859E+05	65	20948	3.890E+01
16	734	3.031E+05	66	22235	3.436E+01
17	808	2.440E+05	67	23599	3.067E+01
18	887	2.022E+05	68	25045	2.756E+01
19	970	1.706E+05	69	26577	2.483E+01
20	1058	1.448E+05	70	28202	2.237E+01
21	1152	1.227E+05	71	29924	2.012E+01
22	1251	1.042E+05	72	31750	1.804E+01
23	1356	8.947E+04	73	33685	1.613E+01
24	1467	7.844E+04	74	35736	1.436E+01
25	1585	7.053E+04	75	37910	1.273E+01
26	1710	6.479E+04	76	40214	1.123E+01
27	1843	6.018E+04	77	42657	9.857E+00
28	1984	5.585E+04	78	45247	8.604E+00
29	2133	5.120E+04	79	47991	7.462E+00
30	2290	4.597E+04	80	50901	6.422E+00
31	2458	4.015E+04	81	53985	5.478E+00
32	2635	3.395E+04	82	57254	4.624E+00
33	2823	2.766E+04	83	60719	3.855E+00
34	3023	2.164E+04	84	64392	3.166E+00
35	3234	1.621E+04	85	68286	2.556E+00
36	3458	1.162E+04	86	72413	2.022E+00
37	3696	7.992E+03	87	76788	1.563E+00
38	3948	5.318E+03	88	81425	1.176E+00
39	4214	3.492E+03	89	86341	8.578E-01
40	4497	2.335E+03	90	91551	6.040E-01
41	4797	1.647E+03	91	97074	4.084E-01
42	5115	1.253E+03	92	102929	2.639E-01
43	5452	1.020E+03	93	109134	1.619E-01
44	5809	8.671E+02	94	115712	9.365E-02
45	6188	7.503E+02	95	122685	5.074E-02
46	6589	6.519E+02	96	130076	2.553E-02
47	7014	5.662E+02	97	137911	1.182E-02
48	7465	4.920E+02	98	146216	4.985E-03
49	7943	4.286E+02	99	155018	1.894E-03
50	8449	3.747E+02	100	164350	6.401E-04

**Composite Riser Used for the CRA Study
Tension Histogram for a Composite Riser Section
Located 5926 ft. above the Mudline**

Riser Configuration 05-04-05
Omni-Directional Seas; Wave Heading = 0 deg.
Nominal Tensioner Setting = 319 kips

Tension Histogram Bin	Tension Range Interval Midpoint (lbs)	Number of Tension Cycles per Year	Tension Histogram Bin	Tension Range Interval Midpoint (lbs)	Number of Tension Cycles per Year
1	15	1.218E+06	51	8986	3.155E+02
2	46	1.662E+06	52	9556	2.770E+02
3	79	7.031E+05	53	10159	2.427E+02
4	113	2.861E+05	54	10798	2.117E+02
5	150	1.830E+05	55	11476	1.836E+02
6	189	1.652E+05	56	12195	1.582E+02
7	231	1.534E+05	57	12957	1.355E+02
8	274	1.325E+05	58	13764	1.154E+02
9	321	1.064E+05	59	14620	9.784E+01
10	370	8.157E+04	60	15527	8.262E+01
11	422	6.202E+04	61	16489	6.968E+01
12	478	4.890E+04	62	17508	5.891E+01
13	536	4.103E+04	63	18588	5.016E+01
14	598	3.643E+04	64	19734	4.319E+01
15	664	3.342E+04	65	20948	3.770E+01
16	734	3.103E+04	66	22235	3.334E+01
17	808	2.881E+04	67	23599	2.979E+01
18	887	2.653E+04	68	25045	2.678E+01
19	970	2.410E+04	69	26577	2.414E+01
20	1058	2.152E+04	70	28202	2.176E+01
21	1152	1.887E+04	71	29924	1.958E+01
22	1251	1.629E+04	72	31750	1.756E+01
23	1356	1.392E+04	73	33685	1.570E+01
24	1467	1.188E+04	74	35736	1.398E+01
25	1585	1.021E+04	75	37910	1.240E+01
26	1710	8.884E+03	76	40214	1.094E+01
27	1843	7.848E+03	77	42657	9.611E+00
28	1984	7.014E+03	78	45247	8.392E+00
29	2133	6.304E+03	79	47991	7.280E+00
30	2290	5.657E+03	80	50901	6.268E+00
31	2458	5.039E+03	81	53985	5.348E+00
32	2635	4.438E+03	82	57254	4.516E+00
33	2823	3.859E+03	83	60719	3.765E+00
34	3023	3.314E+03	84	64392	3.093E+00
35	3234	2.819E+03	85	68286	2.498E+00
36	3458	2.387E+03	86	72413	1.976E+00
37	3696	2.025E+03	87	76788	1.528E+00
38	3948	1.732E+03	88	81425	1.149E+00
39	4214	1.499E+03	89	86341	8.383E-01
40	4497	1.314E+03	90	91551	5.902E-01
41	4797	1.163E+03	91	97074	3.990E-01
42	5115	1.035E+03	92	102929	2.577E-01
43	5452	9.190E+02	93	109134	1.580E-01
44	5809	8.121E+02	94	115712	9.139E-02
45	6188	7.129E+02	95	122685	4.948E-02
46	6589	6.222E+02	96	130076	2.487E-02
47	7014	5.412E+02	97	137911	1.151E-02
48	7465	4.708E+02	98	146216	4.847E-03
49	7943	4.106E+02	99	155018	1.839E-03
50	8449	3.594E+02	100	164350	6.206E-04

Appendix A-6.3.3

Bending Moment Histograms Generated from the “Composite-Steel” Riser Configuration Fatigue Solutions

**Composite Riser Used for the CRA Study
Bending Moment Histogram for a Composite Riser Section
Located 102 ft. above the Mudline**

Riser Configuration 05-04-05
Omni-Directional Seas; Wave Heading = 0 deg.
Nominal Tensioner Setting = 319 kips

Bend. Mom. Histogram Bin	Bnd. Mom. Range Interval Midpoint (ft-lbs)	Number of Tension Cycles per Year	Bend. Mom. Histogram Bin	Bnd. Mom. Range Interval Midpoint (ft-lbs)	Number of Tension Cycles per Year
1	15	1.548E+04	51	2578	5.728E+04
2	45	4.746E+04	52	2659	5.049E+04
3	76	8.070E+04	53	2742	4.435E+04
4	108	1.147E+05	54	2827	3.880E+04
5	140	1.491E+05	55	2914	3.379E+04
6	173	1.832E+05	56	3002	2.927E+04
7	206	2.166E+05	57	3092	2.522E+04
8	240	2.486E+05	58	3184	2.159E+04
9	275	2.788E+05	59	3278	1.836E+04
10	311	3.066E+05	60	3373	1.550E+04
11	347	3.318E+05	61	3471	1.299E+04
12	384	3.540E+05	62	3570	1.080E+04
13	421	3.731E+05	63	3672	8.910E+03
14	460	3.890E+05	64	3775	7.289E+03
15	499	4.018E+05	65	3881	5.915E+03
16	539	4.115E+05	66	3988	4.762E+03
17	580	4.185E+05	67	4098	3.804E+03
18	621	4.231E+05	68	4210	3.016E+03
19	664	4.255E+05	69	4324	2.375E+03
20	707	4.260E+05	70	4441	1.859E+03
21	751	4.250E+05	71	4559	1.447E+03
22	796	4.226E+05	72	4681	1.122E+03
23	842	4.189E+05	73	4804	8.672E+02
24	889	4.141E+05	74	4930	6.692E+02
25	937	4.082E+05	75	5059	5.164E+02
26	986	4.010E+05	76	5190	3.990E+02
27	1035	3.926E+05	77	5324	3.093E+02
28	1086	3.829E+05	78	5460	2.407E+02
29	1138	3.719E+05	79	5599	1.883E+02
30	1190	3.595E+05	80	5741	1.482E+02
31	1244	3.458E+05	81	5886	1.174E+02
32	1299	3.308E+05	82	6034	9.350E+01
33	1355	3.148E+05	83	6185	7.485E+01
34	1412	2.979E+05	84	6338	6.018E+01
35	1470	2.802E+05	85	6495	4.852E+01
36	1530	2.621E+05	86	6655	3.918E+01
37	1590	2.438E+05	87	6818	3.166E+01
38	1652	2.256E+05	88	6985	2.557E+01
39	1715	2.077E+05	89	7154	2.062E+01
40	1780	1.902E+05	90	7327	1.660E+01
41	1845	1.734E+05	91	7504	1.333E+01
42	1912	1.574E+05	92	7684	1.067E+01
43	1980	1.424E+05	93	7868	8.530E+00
44	2050	1.283E+05	94	8055	6.805E+00
45	2121	1.153E+05	95	8246	5.424E+00
46	2193	1.033E+05	96	8441	4.323E+00
47	2267	9.224E+04	97	8640	3.451E+00
48	2343	8.220E+04	98	8843	2.763E+00
49	2419	7.307E+04	99	9049	2.222E+00
50	2498	6.478E+04	100	9260	1.798E+00

**Composite Riser Used for the CRA Study
Bending Moment Histogram for a Composite Riser Section
Located 5926 ft. above the Mudline**

Riser Configuration 05-04-05
Omni-Directional Seas; Wave Heading = 0 deg.
Nominal Tensioner Setting = 319 kips

Bend. Mom. Histogram Bin	Bnd. Mom. Range Interval Midpoint (ft-lbs)	Number of Tension Cycles per Year	Bend. Mom. Histogram Bin	Bnd. Mom. Range Interval Midpoint (ft-lbs)	Number of Tension Cycles per Year
1	15	1.194E+04	51	2578	6.238E+03
2	45	3.656E+04	52	2659	5.631E+03
3	76	6.199E+04	53	2742	5.074E+03
4	108	8.776E+04	54	2827	4.563E+03
5	140	1.134E+05	55	2914	4.095E+03
6	173	1.382E+05	56	3002	3.667E+03
7	206	1.617E+05	57	3092	3.276E+03
8	240	1.834E+05	58	3184	2.920E+03
9	275	2.025E+05	59	3278	2.596E+03
10	311	2.188E+05	60	3373	2.303E+03
11	347	2.317E+05	61	3471	2.038E+03
12	384	2.409E+05	62	3570	1.800E+03
13	421	2.464E+05	63	3672	1.586E+03
14	460	2.480E+05	64	3775	1.394E+03
15	499	2.460E+05	65	3881	1.223E+03
16	539	2.405E+05	66	3988	1.071E+03
17	580	2.319E+05	67	4098	9.352E+02
18	621	2.208E+05	68	4210	8.150E+02
19	664	2.077E+05	69	4324	7.087E+02
20	707	1.932E+05	70	4441	6.149E+02
21	751	1.777E+05	71	4559	5.322E+02
22	796	1.620E+05	72	4681	4.596E+02
23	842	1.465E+05	73	4804	3.960E+02
24	889	1.315E+05	74	4930	3.405E+02
25	937	1.174E+05	75	5059	2.921E+02
26	986	1.043E+05	76	5190	2.500E+02
27	1035	9.243E+04	77	5324	2.136E+02
28	1086	8.173E+04	78	5460	1.821E+02
29	1138	7.221E+04	79	5599	1.550E+02
30	1190	6.379E+04	80	5741	1.317E+02
31	1244	5.636E+04	81	5886	1.117E+02
32	1299	4.984E+04	82	6034	9.458E+01
33	1355	4.410E+04	83	6185	7.993E+01
34	1412	3.906E+04	84	6338	6.742E+01
35	1470	3.463E+04	85	6495	5.674E+01
36	1530	3.074E+04	86	6655	4.764E+01
37	1590	2.731E+04	87	6818	3.990E+01
38	1652	2.431E+04	88	6985	3.331E+01
39	1715	2.167E+04	89	7154	2.773E+01
40	1780	1.936E+04	90	7327	2.300E+01
41	1845	1.734E+04	91	7504	1.900E+01
42	1912	1.556E+04	92	7684	1.563E+01
43	1980	1.399E+04	93	7868	1.281E+01
44	2050	1.261E+04	94	8055	1.045E+01
45	2121	1.138E+04	95	8246	8.488E+00
46	2193	1.029E+04	96	8441	6.863E+00
47	2267	9.311E+03	97	8640	5.526E+00
48	2343	8.428E+03	98	8843	4.430E+00
49	2419	7.629E+03	99	9049	3.538E+00
50	2498	6.902E+03	100	9260	2.815E+00

Appendix B:

Comparative Risk Analysis of Composite and Steel Production
Risers: Composite Riser Response Assessment

Project Report

By

Won K. Kim & Advisor: Ozden Ochoa,
Texas A&M University, December 2005

**Comparative Risk Analysis of
Composite and Steel Production Risers:
Composite Riser Response Assessment**

by

Won K. Kim, Dept. of Mechanical Engineering, Texas A&M University
Advisor: Ozden Ochoa, Texas A&M University

**Project Report
Prepared for Minerals Management Service
Under the MMS/OTRC Cooperative Research Agreements
1435-01-99-CA-31003
Task Order 73632
1435-01-04-CA-35515
Task Order 35985
MMS Project Number 490**

December 2005

OTRC Library Number: 12/05A158

“The views and conclusions contained in this document are those of the authors and should not be interpreted as representing the opinions or policies of the U.S. Government. Mention of trade names or commercial products does not constitute their endorsement by the U. S. Government”.



For more information contact:

Offshore Technology Research Center

Texas A&M University
1200 Mariner Drive
College Station, Texas 77845-3400
(979) 845-6000

or

Offshore Technology Research Center

The University of Texas at Austin
1 University Station C3700
Austin, Texas 78712-0318
(512) 471-6989

A National Science Foundation Graduated Engineering Research Center

Table of Contents

1. Introduction	4
1.1. Background	4
1.2. TLP Production Riser System	4
1.3. Material Properties	5
2. Burst Analysis	7
2.1. Initial Composite Riser Configuration	7
2.2. Preliminary Burst Simulation	7
2.3. Modified Configuration	8
2.4. Burst Pressure Estimation	10
3. Hydrostatic Buckling Analysis	12
3.1. Effect of Geometry and Finite Element Selection	12
3.2. Effect of Debond between Liner and Composite	13
3.2.1. Patch-Shaped Debond	13
3.2.2. Through-Circumference Debond	15
3.2.3. Through-Length Debond	16
4. Global Static Analysis	18
4.1. Static Loads	18
4.2. Composite Riser Effective Properties	19
4.3. Benchmark Study	19
4.4. 100 Year Hurricane Condition	21
5. Local Analysis for Static Solution	24
5.1. Global-Local Link	24
5.2. Damage Analysis	25
5.3. Damage Initiation and Progression	25
6. Local Analyses for Dynamic Solutions	29
6.1. PNS-1: 1 Year Winter Storm	29

6.1.1.	Dynamic Mean Solution	30
6.1.2.	Dynamic Maximum Solution	32
6.2.	PHN-1: 100 Year Hurricane	34
6.2.1.	Dynamic Mean Solution	34
6.2.2.	Dynamic Maximum Solution	36
6.3.	PCN-1: 100 Year Loop Current	38
6.3.1.	Dynamic Mean Solution	38
6.3.2.	Dynamic Maximum Solution	40
7.	Fatigue Analysis	42
7.1.	Procedure	42
7.2.	S-N Curves	43
7.3.	Input Data	44
7.4.	Damage Due to Individual Loading	47
7.5.	Combined Loading	50
8.	Summary	53
	REFERENCES	54

Introduction

1.1. Background

As offshore activities move into deep water, there is a growing interest in the use of composite production risers instead of metallic risers. Among numerous benefits that composite materials offer, the most significant impact is in weight reduction and subsequent increase in specific strength. In addition to weight reduction, composite materials are known to have excellent fatigue, thermal, and damping properties and high corrosion resistance. Top tensioned production systems, such as Tension Leg Platform (TLP) and spar, feature vertical access to wells and are relatively insensitive to increase in water depth in terms of cost [1, 2].

The MMS Deepwater Operating Plan (DWOP) requires that the new technology introduced in a deepwater development project must be shown to be as safe as existing technology. Therefore, the risks of a composite production riser need to be addressed with those of a steel riser that has the same functional requirements and service life. The main purpose of this report is to compile various finite element structural analyses results, which are expected to serve as inputs for risk assessments.

1.2. TLP Production Riser System

The composite riser analysis performed in this report is based on the Gulf of Mexico environment. The water depth for the TLP system to be installed in is 6000 ft. Figure 1 shows the configuration of the composite riser system for this study. The composite riser joints extend from 102 ft elevation to 5926 ft. To the joints above 4004 ft, fairings will be attached to mitigate vortex-induced vibration (VIV). Between the top of the stress joint and the bottom of the composite riser is a conventional steel riser joint, and there are two steel joints between the top of the composite riser and the bottom of the tensioner joint.

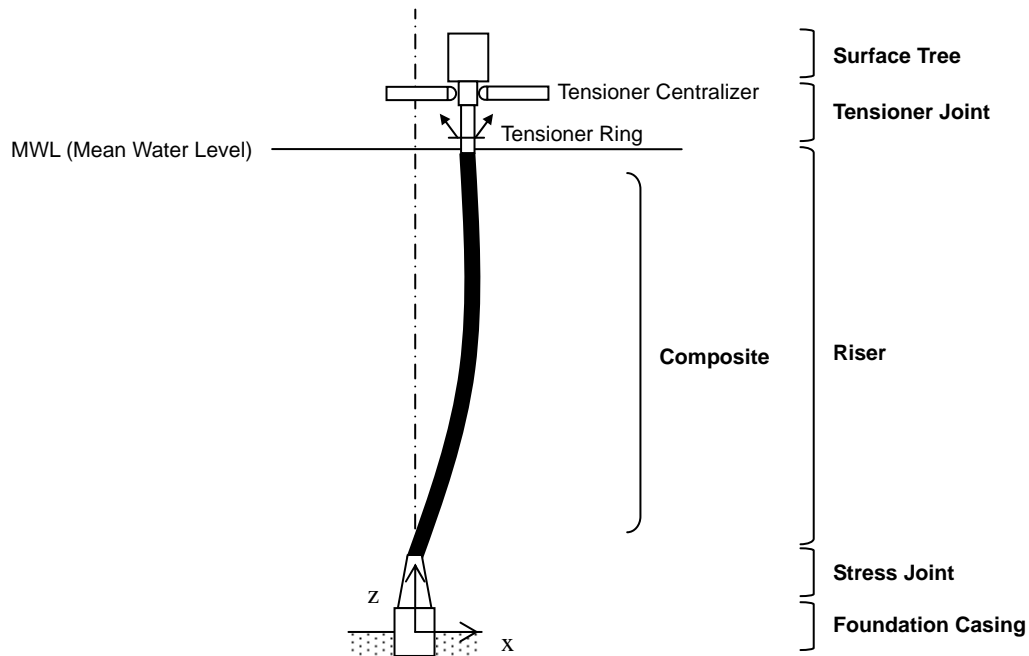


Figure 1. Composite Riser System Configuration

1.3. Material Properties

The structural part of the composite riser consists of a metal liner and carbon/epoxy composite. The thicknesses of the layers vary from one layer to another, and the orientations alternate between 0° and 88° . The configuration of the composite will be presented in the next chapter. Table 1 shows the material properties of the carbon/epoxy lamina and steel liner. Other steel parts, such as standard steel joints, stress joint, tensioner joint, etc., shares the properties of steel presented in the table.

Table 1. Material Properties of Steel and Composite Lamina

Material	E_1 (msi)	E_2 (msi)	G_{12} (msi)	ν_{12}
Steel	30.00	30.00	1.54	0.300
Composite	20.14	0.96	0.43	0.373

The subscripts 1 and 2 denote the fiber and transverse directions in material coordinates, respectively. For damage analysis, the following long term strength properties were used [3].

Table 2. Long-Term Strength Properties of Lamina (in ksi)

s_1^+	s_1^-	s_2^+	s_2^-	s_{12}
220	150	5	22	10

2. Burst Analysis

2.1. Initial Composite Riser Configuration

The initial configuration of the composite riser consists of a 0.17 in thick steel liner and 19 carbon/epoxy composite layers which alternate between 0° and 88°. The inner diameter and the total wall thickness of the liner and structural composite are 9.720 in and 0.985 in, respectively. Table 3 shows the initial configuration of the composite riser.

Table 3. Composite Riser Layup – Initial Configuration

Layer	Orientation	Thickness (in)	Layer	Orientation	Thickness (in)
Liner		0.170	10	0	0.045
1	88	0.060	11	88	0.030
2	0	0.045	12	0	0.045
3	88	0.060	13	88	0.030
4	0	0.045	14	0	0.045
5	88	0.060	15	88	0.030
6	0	0.045	16	0	0.045
7	88	0.060	17	88	0.030
8	0	0.045	18	0	0.045
9	88	0.030	19	88	0.030

2.2. Preliminary Burst Simulation

The simulation was performed using ABAQUS finite element analysis software [4]. Based on the riser pressure test condition, a uniform internal pressure of 10,000 psi has been applied. The following five finite element models were used to examine the effects of model length and element selection.

- FE 1: Shell (S8R) / 1 element through thickness / 10 ft long
- FE 2: Shell (S8R) / 1 element through thickness / 1ft long
- FE 3: Shell (S8R & S8R5) / 2 elements through thickness (liner separated) / 1ft long
- FE 4: Solid (C3D20) / 1 element through thickness / 1ft long
- FE 5: Solid (C3D20) / 2 elements through thickness (liner separated) / 1ft long

The stress data for each model were obtained from an element in the middle of the length. The results from the above five models generally agree well with each other. Due to the nature of the applied load, the most critical stress components are 1) hoop stress in the liner, 2) σ_{11} in 88° layers, and 3) σ_{22} in 0° layers. The hoop stress in the liner which results from the internal pressure is about 120 ksi, which exceed 80 ksi, the yield strength of steel. σ_{22} in 0° layers reached 70% of the long term allowable for the matrix direction, and σ_{11} in 88° layers are about 35% of the long term allowable. The liner yielding requires changes in the initial geometry, and a few options will be considered in the next section.

2.3. Modified Configuration

First, only liner thickness was increased to reduce the hoop stress in the liner. To bring the stress below 80 ksi, liner thickness needed to be at least 0.35 in. In this case, the effective weight of the structural part of the riser, excluding outer protective layer, becomes almost twice that of the original configuration. To seek for other ways to keep the liner stress below the yield strength without introducing a drastic increase in weight, the thicknesses of the hoop layers were also increased while gradually increasing liner thickness. Table 4 summarizes possible design options and weight penalties.

The last option, 0.25 in liner with the hoop layers increased by 35%, was decided as the most reasonable compromise between cost and weight. The combined wall thickness for the structural parts is increased to 1.222 in. The subsequent analyses presented in this study will be performed on the modified configuration. Table 5 and 6 present the modified configuration and geometry. Over the structural carbon/epoxy composite, 0.125 in of glass/epoxy protective layer will be wrapped. However, its contribution as a structural part will be neglected in subsequent analyses.

Table 4. Alternative Configurations

Liner t (in)	Hoop t inc. (%)	Liner σ (ksi)	$\sigma_2, 0^\circ$ (ksi)	$\sigma_1, 88^\circ$ (ksi)	Air Wt. (lbs/ft)	Submerged Wt. (lbs/ft)	Effective Wt. (lbs/ft)	Wt. Penalty (%)
0.17	0	110	3.4	71.4	40.5	23.6	18.2	
0.35	0	78.2	2.4	51.7	61.0	41.0	35.5	50 / 74 / 96
0.17	60	79.9	2.5	52.6	47.0	25.7	20.3	16 / 9 / 12
0.20	50	79.5	2.5	52.4	49.3	28.2	22.8	21 / 20 / 25
0.25	35	78.4	2.5	51.8	53.3	32.5	27.0	31 / 38 / 49

Table 5. Composite Riser Layup – Modified Configuration

Layer	Orientation	Thickness (in)	Layer	Orientation	Thickness (in)
Liner		0.2500	10	0	0.0450
1	88	0.0810	11	88	0.0405
2	0	0.0450	12	0	0.0450
3	88	0.0810	13	88	0.0405
4	0	0.0450	14	0	0.0450
5	88	0.0810	15	88	0.0405
6	0	0.0450	16	0	0.0450
7	88	0.0810	17	88	0.0405
8	0	0.0450	18	0	0.0450
9	88	0.0405	19	88	0.0405

Table 6. Composite Riser Geometry

ID (in)	OD (in)	Thickness (in)			
		Liner	Structural Composite	Protective Layer	Total
9.720	12.414	0.25	0.972	0.125	1.347

Based on the new geometry, the weights of the composite riser have been re-calculated. Table 7 shows the calculated values and also compares them with the weights of the 1 in wall thickness steel riser.

Table 7. Riser Weights [5]

	Air Wt. (lb/ft)	Submerged Wt. (lb/ft)	Effective Wt. (lb/ft)	Effective Wt. w/ Tubing (lb/ft)
Bare Composite	59.65	36.36	3.53	30.93
Composite w/ Fairings	68.07	38.78	5.96	33.36
Bare Steel	124.07	107.86	75.0	102.40

2.4. Burst Pressure Estimation

To estimate the burst capacity of the riser, the internal pressure is increased incrementally from 10,000 psi. To detect damage in the individual layers and take appropriate reductions in stiffness after damage occurs, a user material (UMAT) subroutine, which enables a user to define the constitutive behavior of a material, is incorporated with the ABAQUS input. In the UMAT subroutine, the maximum stress theory is implemented, and every local stress component is compared with the corresponding allowable. Table 8 shows the pressures at which different types of layers fail. As was shown in Table 4, the liner nearly yielded under the test pressure, and as expected, the yielding of the steel liner occurs immediately after the pressure increase. However, the last ply failure does not take place until the pressure is increased to 30 ksi.

Table 8. Failure Pressure

Liner Yield	0° Layers, Matrix Cracking	88° Layers, Fiber Fracture
11 ksi	18 ksi	30 ksi

3. Hydrostatic Buckling Analysis

3.1. Effect of Geometry and Finite Element Selection

Although the length of a composite riser joint is as long as 62 ft, hydrostatic buckling pressure can be estimated with a relatively short finite element model. To ensure accuracy of solution and to minimize computation cost in subsequent analyses, hydrostatic buckling analyses for various model lengths have been carried out using ABAQUS, and their solutions were compared. Also, solutions from shell element model and solid element model have been compared.

As the length of composite riser is increased, critical buckling pressure decreases significantly. When the length is 6 ft or greater, the effect of length on the first buckling mode becomes negligible, and therefore, a 6 ft model is sufficient for this particular riser. The ratios of this length to the wall thickness and mid-wall radius are 59.0 and 13.2, respectively. The numbers of circumferential and longitudinal waves for the first mode are 2 and 0.5, respectively. It should be mentioned that cases where higher buckling modes need to be sought may require longer models since higher modes converge later as the length increases. For the particular riser configuration under consideration, good convergence on the second and third modes can be observed when the length is 12 ft. Also, caution should be used when deciding the number of elements along the circumference. In general, minimum number of elements for circular cross-section is 18, but it may not be sufficient for some mode shapes and may result in inaccurate mode shapes and pressures. For the composite riser, 40 elements turned out to be sufficient for calculating the first three modes; doubling the number does not change the solution at all.

Although the critical pressure converges at 6 ft regardless of finite element selection, the estimations from shell and solid elements do show a significant difference. The critical pressure from the shell model is 26.7 ksi, whereas the solution from the solid model is 38.6 ksi. Another solid model has been created where the liner is modeled as separate elements, i.e., 2 layers of elements in the radial direction. This new solid model estimates a critical pressure of 30.2 ksi. Various test analyses have been performed to study the disagreement between the shell and 1-layered solid models. When the outer 10 composite layers are removed, the difference between two models decreases, but the disagreement is still notable. For a thin composite pipe where there are only four alternating layers, shell

and solid elements show no difference in critical pressure. A thick steel pipe, whose wall thickness is about 1 in, showed very little effect of element selection. Therefore, the significant disagreement between the shell and solid riser models is due to the combined effect of the wall thickness and material.

In addition to the finite element solutions, an analytical solution has been used as a benchmark [6]. The calculation resulted in a critical buckling pressure of 34.6 ksi. Since the hydrostatic pressure near the sea floor is less than 3 ksi, it can be concluded that the ideal composite riser is highly unlikely to buckle under hydrostatic pressure only.

3.2. Effect of Debond between Liner and Composite

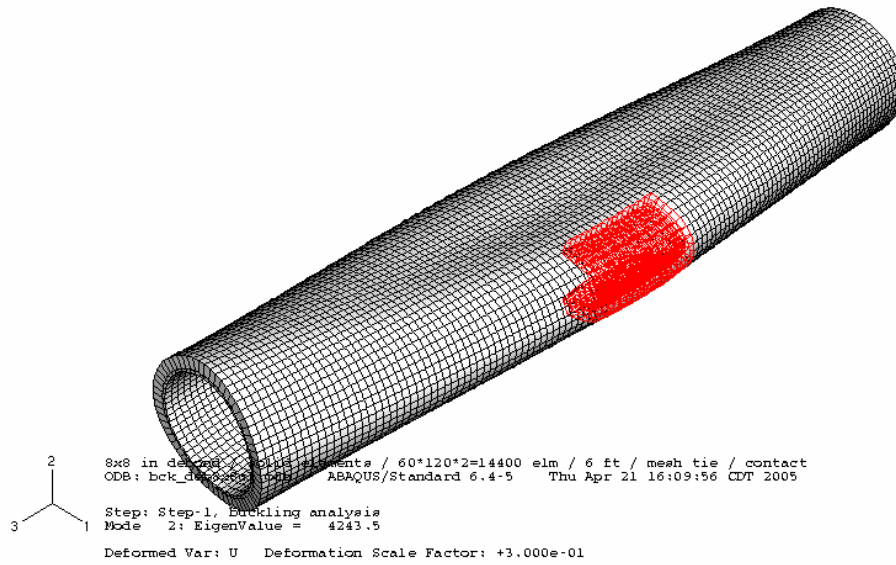
3.2.1. Patch-Shaped Debond

To investigate the effect of debond, 2 layer solid models with four different sizes of debond in the middle of the riser have been created. On both debond faces, same amount of pressures as the external pressure were applied, pushing the liner and composite away from each other. The four models have debond areas of 1 in \times 1 in, 2 in \times 2 in, 4 in \times 4 in, and 8 in \times 8 in and the critical pressures of the four cases have been compared to study the effect of increasing debond area.

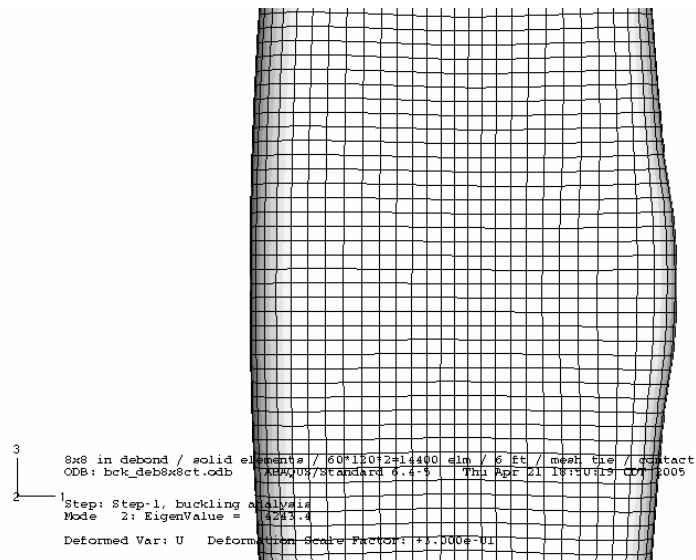
Three different methods were tried to model debond. First, the elements in the liner side and the composite side of the bonded region share the nodes at the interface, and the ones in the debond area have separate nodes with gap elements placed between each set of nodes. The second method is same as the previous method, except the gap elements are replaced by contact pair interaction for the debond interface. In the last method, instead of node sharing, tie constraints are used for the nodes on the interface of the bonded region, and contact pair is defined for the debond region. These three methods produced the same results.

1 \times 1, 2 \times 2, and 4 \times 4 debond models give a critical pressure of 30.2 ksi, which is exactly the same as the result from the completely bonded model. A small decrease in the critical pressure can be observed when the debond area is 8 \times 8 where the buckling pressure is 29.5 ksi. The mode shape is essentially identical with the completely bonded model, except that there is a slight bulge where the composite is debonded from the liner. Figure 2 (a) and (b) show the first mode shape of the whole model and a close-up view of

the bulge, respectively. The highlighted area in Figure 2 (a) shows the debond region.



(a)



(b)

Figure 2. 8 in × 8 in Debond Model

3.2.2. Through-Circumference Debond

Since small, patch-shaped debond areas hardly affect the critical buckling pressure, severer debond conditions are taken into consideration. First severe debond type is through-circumference debond, which is a fully debonded ring with varying length. Although 40 elements in the circumferential direction are sufficient, a highly refined mesh is used hereafter in case geometric imperfections are required to be introduced in the future. Geometric imperfection may be given as ovality, or multiple superimposed buckling modes. Note again that the mesh refinement has no effect on the critical buckling pressure for the perfect geometry considered at this time.

Debond is located in the middle of the model, and the initial length of debond area is 10 in. Then debond is expanded along axial coordinate with an increment of 10 in. Again, pressure is also applied on the debond surfaces. The first mode shape is similar to that of the perfectly bonded case, having 2 circumferential waves and 0.5 longitudinal wave. However, the waves are confined within the debond region, as shown in Figure 3. Through-circumference debond shows a sharp initial decrease in critical buckling pressure. However, expansion of debond hardly affects critical pressure after 40-50% of liner-composite interface is debonded. Figure 5 shows changes in critical pressure for increasing debond size.

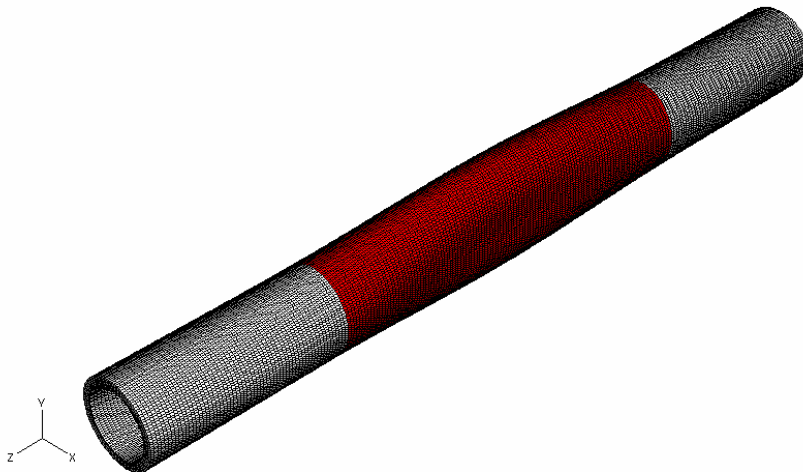


Figure 3. First Mode of Through-Circumference Debond Model (50% debond shown)

3.2.3. Through-Length Debond

Through-length debond extends throughout the longitudinal direction and is initially set at a 30° arc. Its growth is studied in 30° increments. This type of debond also shows relatively sharp decrease in critical buckling pressure at the early stage of debond growth, but when compared with through-circumference type debond, the decrease is not as severe, as shown in Figure 5. While through-circumference approaches the critical pressure of the complete debond case at less than 50% debond, through-length shows relatively continuous decrease in critical pressure.

The mode shape of through-length debond is also same as the completely bonded case, with one exception. At intermediate debond size, the cross-section is not symmetric with respect to y-z plane, as shown in Figure 4 where circumferential wave is confined within the debond region.

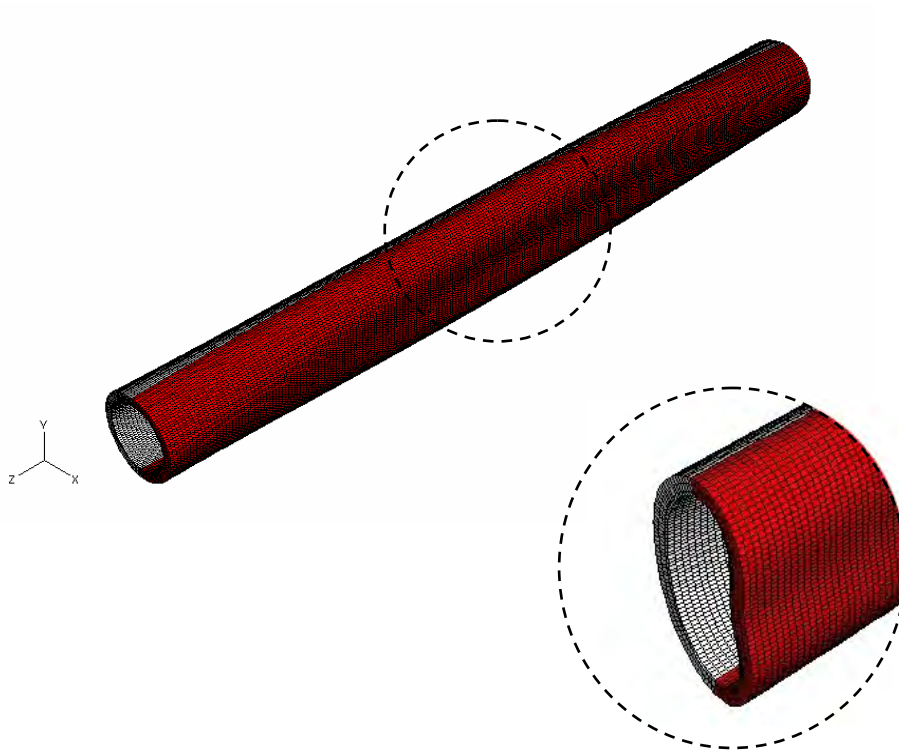


Figure 4. First Mode of Through-Length Debond Model (50% debond shown)

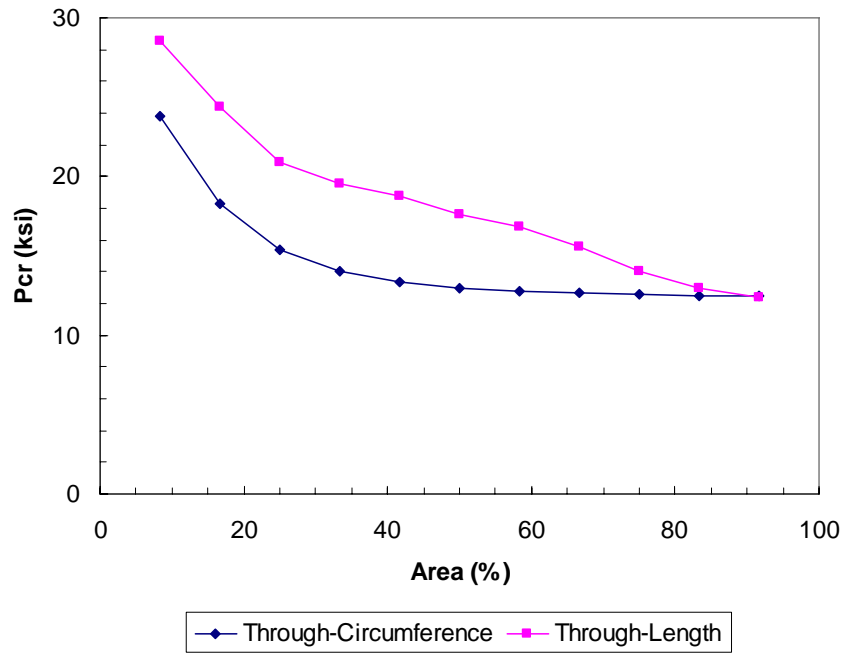


Figure 5. Critical Buckling Pressure for Various Debond Size

4. Global Static Analysis

4.1. Static Loads

Based on the riser system configuration in Section 1.2 and the new composite riser configuration presented in Section 2.3, the sum of the effective weights of all the regions, from the stress joint to the tensioner joint, has been calculated. For a tension factor of 1.3, the tensioner requirement is 319 kips. Although the composite riser gained a significant weight in comparison to the initial configuration, the tensioner requirement is still considerably lower than the steel riser system, where 1 in wall thickness standard steel joints are used. The tensioner requirement for the steel riser system is 864 kips.

The effective weights are applied to the global beam model as distributed loads. The top tension is applied as a concentrated load through a linear spring at 6060 ft elevation, where the tensioner ring is located. The stiffness of the spring is generally set to be 12% of top tension, and in this case the stiffness is 38.28 kips/ft. Static offset of the platform is conveyed to the riser tensioner through the tensioner centralizer which is initially located at 6080 ft elevation. As a result of the horizontal displacement of the TLP, downward movement of the platform called setdown also occurs. When tendon stretch is negligible, TLP setdown and offset have the following relationship.

$$Setdown = (SetdownFactor) \times (Offset)^2 \quad (1)$$

where the setdown factor used in this study is -8.333×10^{-5} . Finally, current drag is applied to the in-water regions of the system. Table 8 shows the current profile used in the analysis.

Table 8. Current Profile

Depth (ft)	0	300	400	6000
Velocity (ft/sec)	4.0	4.0	0.2	0.2

4.2. Composite Riser Effective Properties

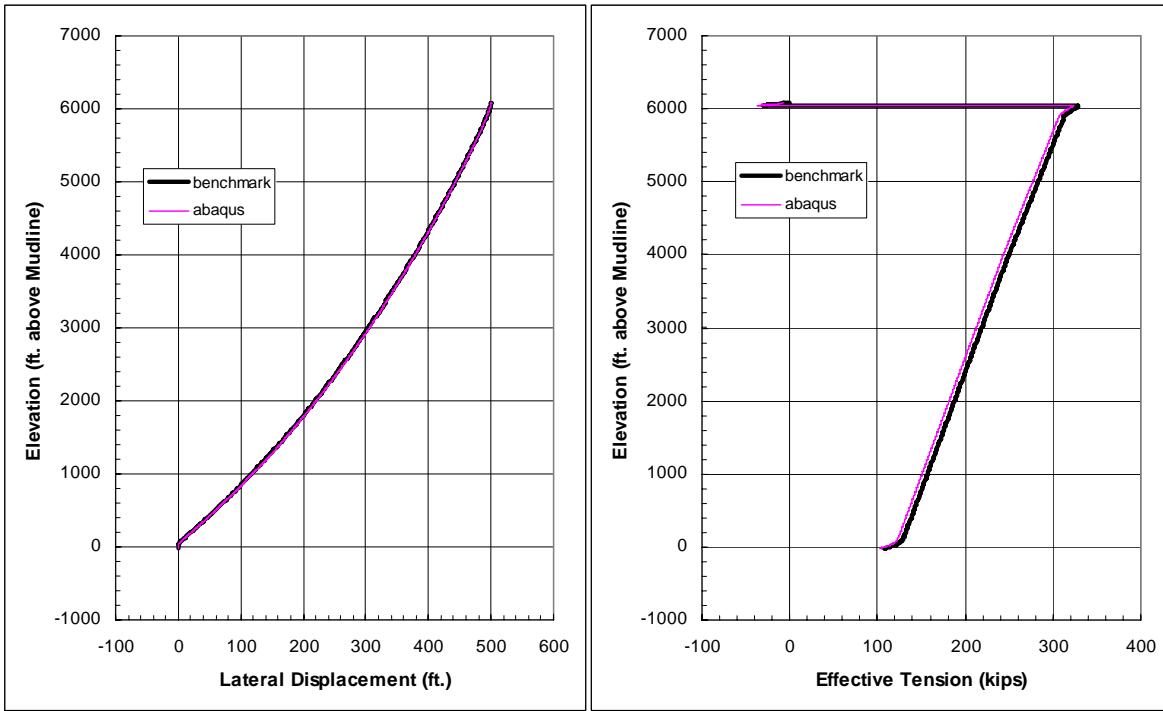
Using the lamina mechanical properties presented in Table 1, the effective properties of the laminate in global coordinates can be calculated. Instead of specifying the lamina properties on a layer-by-layer basis, the effective properties of the whole laminate are defined for global beam analysis. In the calculation, the steel liner is considered as one of the composite layers to include its contribution to the effective properties. The effective properties of the composite riser are presented in Table 9. The subscripts x and y denote the axial and tangential directions in global coordinates, respectively. In terms of stiffnesses, E_x results in bending stiffness (EI) and axial stiffness (EA) of 5.729×10^7 lbs-ft² and 5.444×10^8 lbs, respectively. The stiffnesses of the standard steel riser joints are 1.081×10^8 lbs-ft² and 1.225×10^9 lbs.

Table 9. Effective Properties

E_x (msi)	E_y (msi)	G_{xy} (msi)	ν_{xy}
12.96	11.85	0.5278	0.078

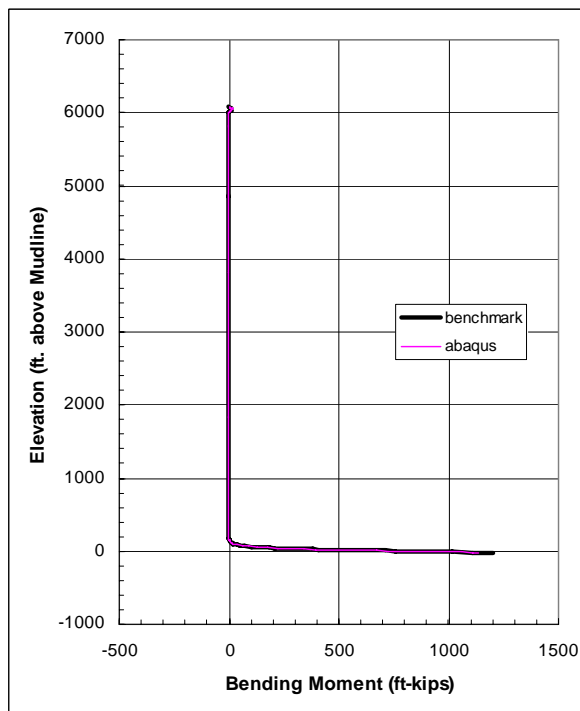
4.3. Benchmark Study

The aforementioned loads are applied to a 637 beam element model, created using ABAQUS, and the axial tension and bending moment profiles are compared with existing finite element analysis data provided by Stress Engineering Services, Inc. [5]. The magnitudes of the loads applied are as specified in the previous section, except the static TLP offset is arbitrarily chosen as 500 ft. This value does not necessarily correspond to any real environmental condition. The setdown for this offset value, according to Eqn. 1, is -20.83 ft. Figure 6 and 7 present the plots for the lateral displacement, axial tension and bending moment along the elevation from the sea floor. The analysis results agree well with the existing data.



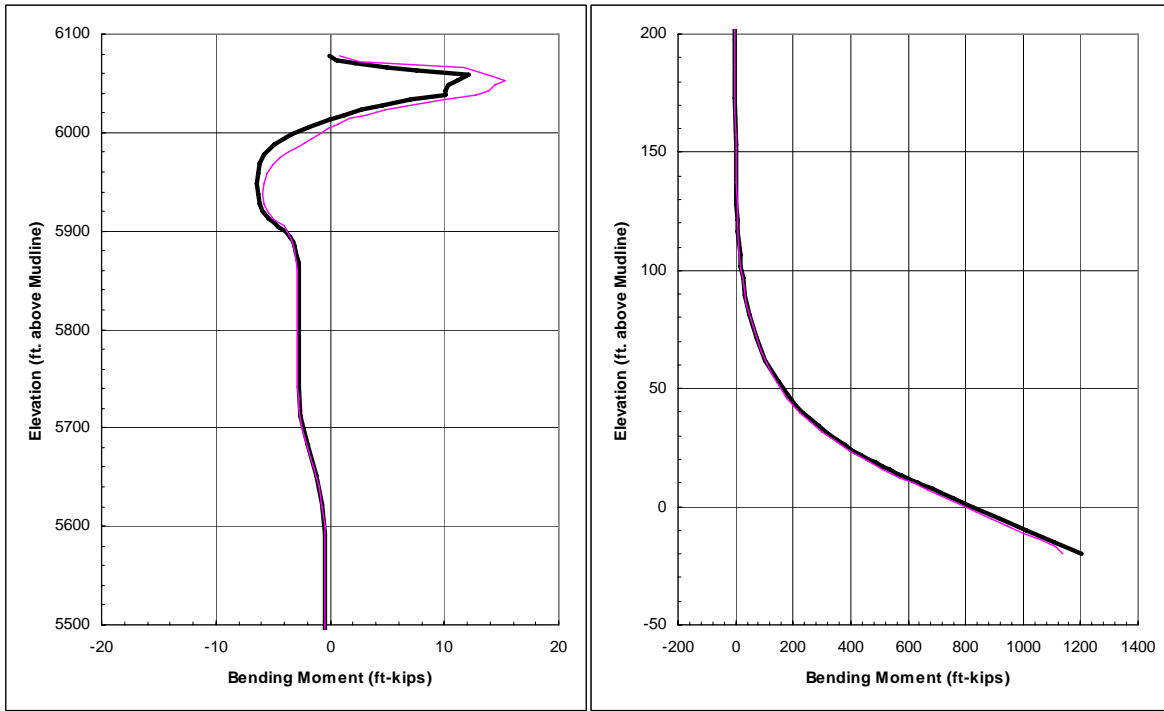
(a)

(b)



(c)

Figure 6. Benchmark Study: (a) Lateral Displacement (b) Tension (c) Bending Moment



(a) (b)
 Figure 7. Benchmark Study: Local View of Bending Moment (a) Top (b) Bottom

4.4. 100 Year Hurricane Condition

TLP offset can be estimated through the significant wave height for a particular environmental load condition. For the 100 year hurricane condition, whose significant wave height is 41 ft., the TLP offset is estimated to be 360 ft. The setdown for this offset value is -10.80 ft. The top tension, tensioner stiffness, effective weights, and current profile remain unchanged from the previous analysis. It should be noted that the wave particle velocity is not included in the analysis. Figure 8 shows the axial tension and bending moment profiles for this case.

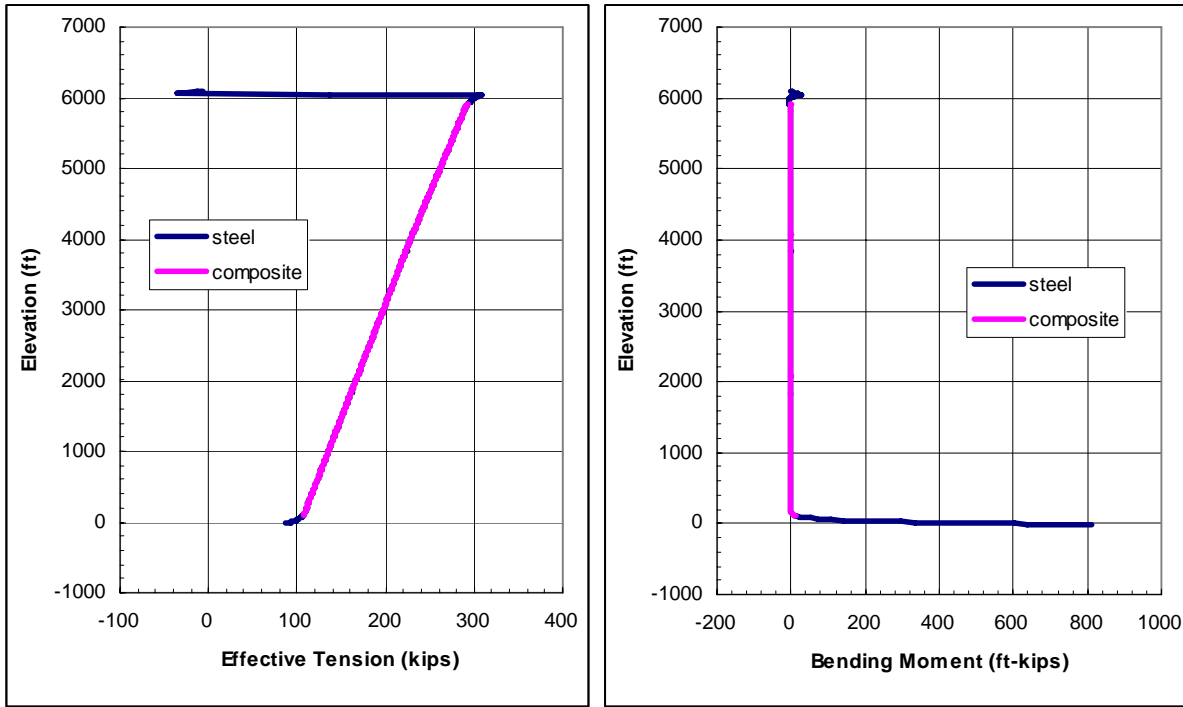


Figure 8. Axial Tension and Bending Moment Profiles of Static Analysis

Effective tension varies linearly within the composite riser region due to the uniform weight. No significant bending moment is observed throughout the composite riser region. Within this region, the bottom part shows relatively large bending moment, and the very top also shows non-zero bending moment. Figure 9 shows the bending moment distribution at the top of the composite riser region. Mainly due to the effective tension, and with a small degree of bending moment, the very top of the composite riser is most likely to experience the highest level of stress. Therefore, a short section from the top will be analyzed in the subsequent local analysis.

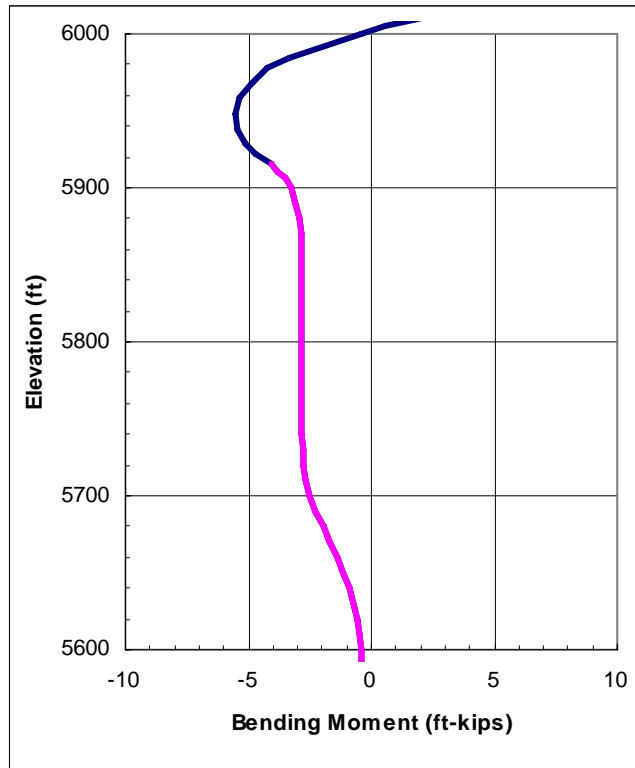


Figure 9. Bending Moment at Top of Composite Riser

5. Local Analysis for Static Solution

5.1. Global-Local Link

The link between the global and local analysis is achieved through transferring the nodal displacements and/or nodal forces from the global analysis to the local analysis. For the local model, the nodal displacements and/or forces serve as boundary conditions. When the nodal displacements from the global analysis are used, relative values of translations are applied at the top of the local section model while the translations of the bottom are constrained. The rotations applied are the actual values at the respective locations.

To decide a reasonable length for the section to be analyzed in the local analysis, three different lengths, 6 ft., 10 ft., and 16 ft., were analyzed and their results were compared. For all the cases, the elevation of the top of the section is 5926 ft., which is the top end of the composite riser region. In other words, only the elevation and displacements of the bottom are different from one case to another. The analysis results show that the 10 ft. and 16 ft. models produce similar results in terms of damage initiation, while the 6 ft. model predicts earlier damage initiation. Therefore, 10 ft. is concluded to be sufficient for the length of the local section model. Table 10 shows the nodal displacements obtained from the global static analysis. The values to be applied as boundary conditions for the local model are italicized.

Table 10. Boundary Conditions for 10 ft. Section

	Elevation (ft)	x-displacement (ft)	z-displacement (ft)	y- rotation (rad)
Top	5926	356.3	-9.879000	<i>0.027307</i>
Bottom	5916	356	-9.88	<i>0.027904</i>
Relative		<i>0.3</i>	<i>0.001</i>	

5.2. Damage Analysis

When the boundary conditions presented earlier are applied to the local model, no damage is predicted. No stress component in any layer was near the applicable allowable. For study purpose, the boundary conditions are now multiplied equally by a factor m . Note that multiplying the boundary conditions is not equivalent to multiplying the loads on the global level, such as static offset and top tension.

For damage analysis, three sets of damage criteria were used: maximum stress, Hashin, and Hashin-Rotem. For all three cases, only maximum stress criteria were used for the steel liner. Maximum stress theory simply compares each stress component with its corresponding strength. For example, fiber fracture occurs when σ_{11} exceeds s_1^+ , tensile strength in the fiber direction, if the stress is tensile. Hashin-Rotem criteria [7] share the same fiber failure criteria with maximum stress criteria, but take the interaction between the transverse normal and shear stresses into account for matrix mode failure estimation, as shown in Eqn. 2. For a compressive stress, the superscript in the first term is replaced by a negative sign.

$$\left(\frac{\sigma_{22}}{s_2^+}\right)^2 + \left(\frac{\tau}{s_{12}}\right)^2 = 1 \quad (2)$$

Hashin criteria [8] extend the idea of normal-shear interaction to fiber modes. Also, this theory replaces the compressive matrix mode with the following equation. The criterion for the tensile matrix mode is identical to Hashin-Rotem.

$$\left(\frac{\sigma_{22}}{2s_{23}}\right)^2 + \left[\left(\frac{s_2^-}{2s_{23}}\right)^2 - 1\right] \left[\left(\frac{\sigma_{22}}{s_2^-}\right) + \left(\frac{\sigma_{12}}{s_{12}}\right)\right]^2 = 1 \quad (3)$$

The aforementioned failure criteria are implemented in UMAT subroutines. UMAT checks for failure using the failure criteria and reduces relevant stiffness(es) of the current layer of the current element if any failure is detected.

5.3. Damage Initiation and Progression

The load amplification factor m , is increased from 1 to 4.5 with an increment of 0.5. When $m=2$, localized liner failure occurs in 5.8% of the entire liner. At the next increment, $m=2.5$, the damage area expands to 77%. At $m=3$, matrix failure in the hoop layers occurs. The percentage of damaged elements is 6 to 7%, depending on layers. Generally, outer layers show more damage than inner layers do due to the bending moment. However, layer 1 shows larger damage area than layer 3 since the liner carries no loads any more with the failure area approaching 99.9%. The damage area of the hoop layers expands up to 74% at $m=3.5$. Figure 10 shows the layer-by-layer damage in the hoop layers at $m=3$ and 3.5.

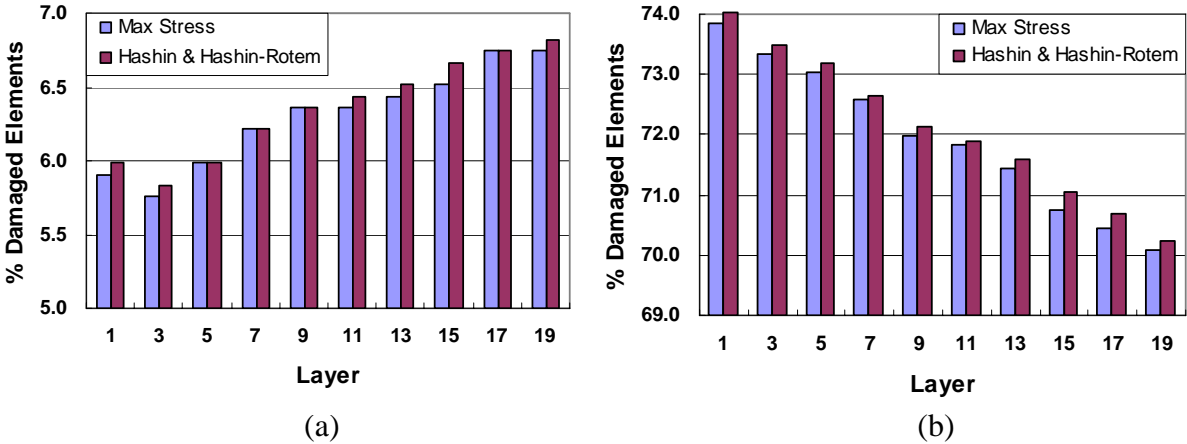


Figure 10. Matrix Damage in Hoop Layers (a) $m=3$ (b) $m=3.5$

When $m=4$, fiber fracture in the axial layers occurs in layers 2, 4, and 6. The percentage of damaged elements is less than 1%. At $m=4.5$, every the axial layer shows a localized damage area up to 4.8%. Some of the elements show simultaneous occurrences of fiber fracture and matrix cracking. Figure 11 shows the damage status in the axial layers at $m=4.5$. Figure 12 and 13 visualize the expansion of damage areas for the liner and a hoop layer, respectively, as predicted by maximum stress criteria. As was already shown in Figure 10 and 11, the predictions by different damage theories show no significant difference, which is explained by the fact the effect of shear stress is not consequential.

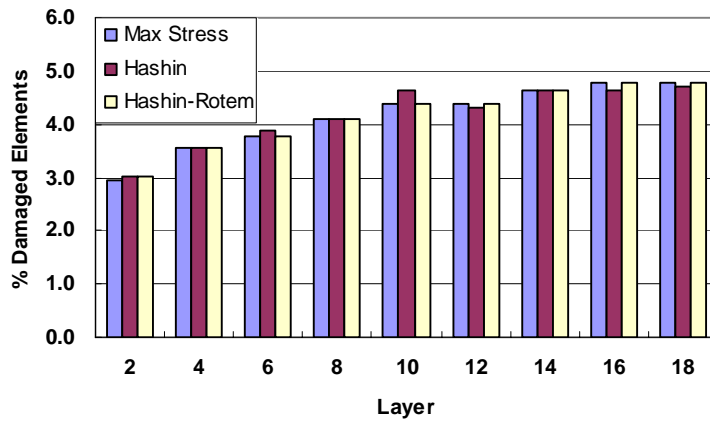


Figure 11. Fiber Damage in Axial Layers at m=4.5

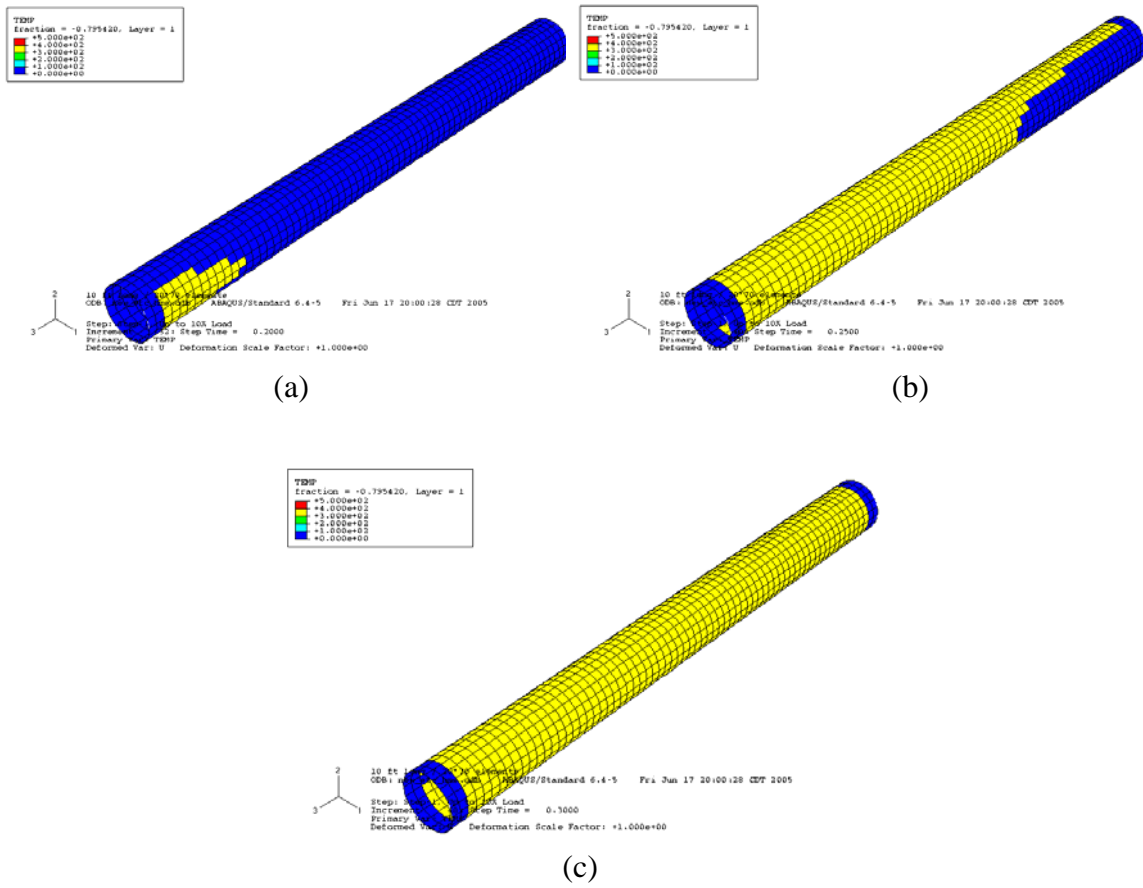


Figure 12. Damage Expansion in Liner (a) m=2 (b) m=2.5 (c) m=3

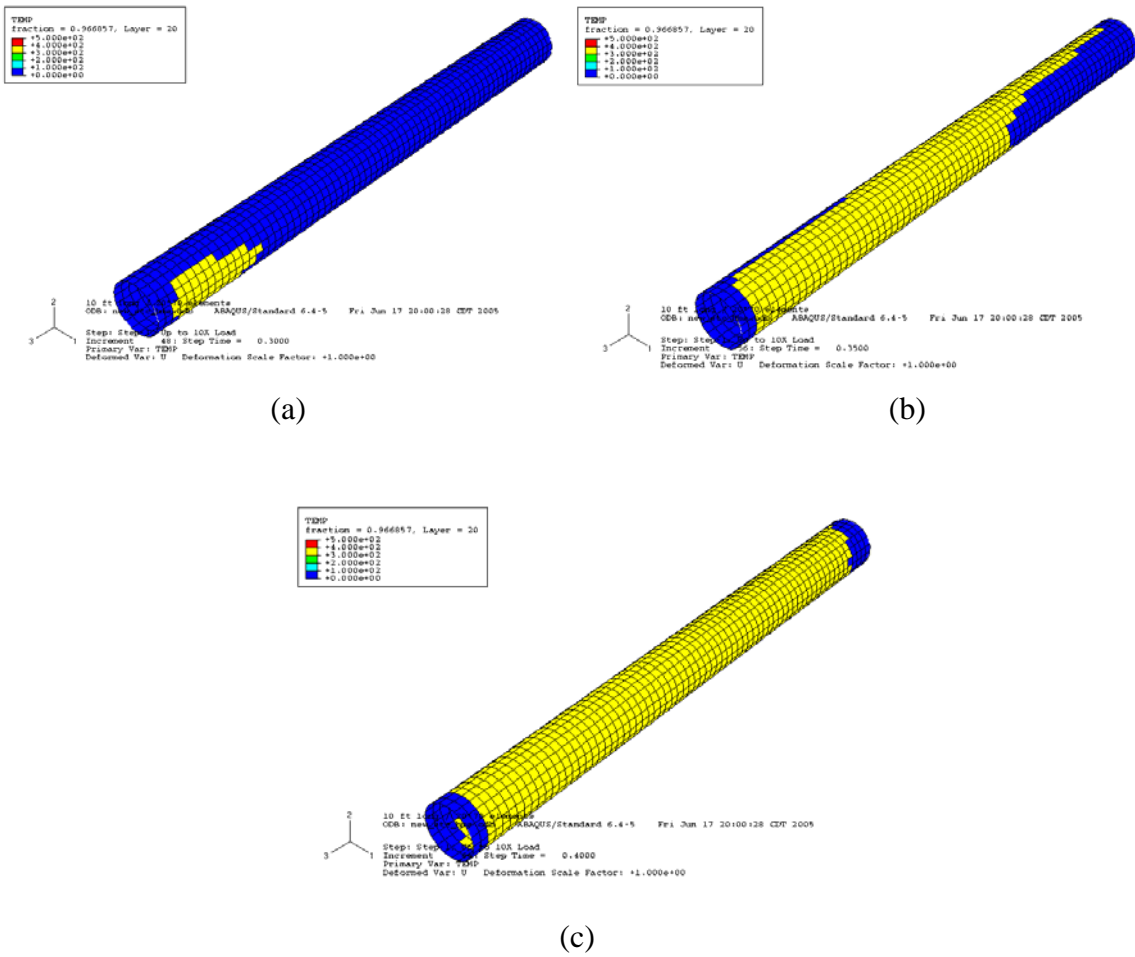


Figure 13. Damage Expansion in Layer 19 (0°) (a) $m=3$ (b) $m=3.5$ (c) $m=4$

6. Local Analyses for Dynamic Solutions

Local analyses are performed using the global frequency domain analyses data provided by Stress Engineering Services, Inc. [9]. The load cases considered in the global analyses include PNS-1, PHN-1, and PCN-1, for which corresponding environmental conditions are 1 year winter storm, 100 year hurricane, and 100 year loop current, respectively. Table 11 presents the details of the load cases.

Table 11. Definitions of Load Cases

Case	Significant Wave Ht. (ft)	Peak Period (sec)	JONSWAP Peakedness Factor	Surface Cur. Vel. (ft/s)	Mean TLP Offset (ft)	Low Freq. Motion	
						RMS (ft)	T _z (sec)
PNS-1	16.0	9.0	1.0	1.2	120	6.0	200
PHN-1	41.0	14.0	2.0	4.0	360	22.2	200
PCn-1	9.0	8.0	1.0	7.0	540	2.0	200

The same model geometry as the local analysis for the static solution is used. First the mean values of the nodal forces are applied to the local model, and then the maximum values are applied. The translations of the bottom of the local section are constrained, but the rotation as obtained from the global analysis is applied. At the top of the section, forces in horizontal and vertical directions are applied along with bending moment acting counterclockwise. The weight of the section is applied as a force equally distributed over the entire model. The environmental force acting on the local section is neglected. When the reaction forces and moment at the bottom of the local model are compared with the corresponding nodal forces and moment from the global solution, the differences are negligible for the mean solutions, about 0.1% at most. On the other hand, the maximum solutions show greater difference, up to 20%.

6.1. PNS-1: 1 Year Winter Storm

6.1.1. Dynamic Mean Solution

Table 12 shows the mean values of the nodal forces and displacements from the global dynamic analysis. The values which are applied to the local model as the boundary conditions are italicized. Figure 14 through 16 show stress contours of selected layers. Since the major load coincides with the global axial direction, σ_{11} of the axial layers and σ_{22} of the hoop layers are most critical.

Table 12. Mean Nodal Output from Global Dynamic Analysis: PNS-1

Elevations	X-Force	Z-Force	Y-Moment	X-Position	Z-Position	Slope
5926	<i>2657.50</i>	<i>275291.03</i>	<i>-806.96</i>	118.6485	-75.3376	0.0095559
5916	<i>2672.25</i>	<i>274957.56</i>	<i>-607.94</i>	118.5523	-85.3372	<i>0.0096661</i>

(units in lb and ft)

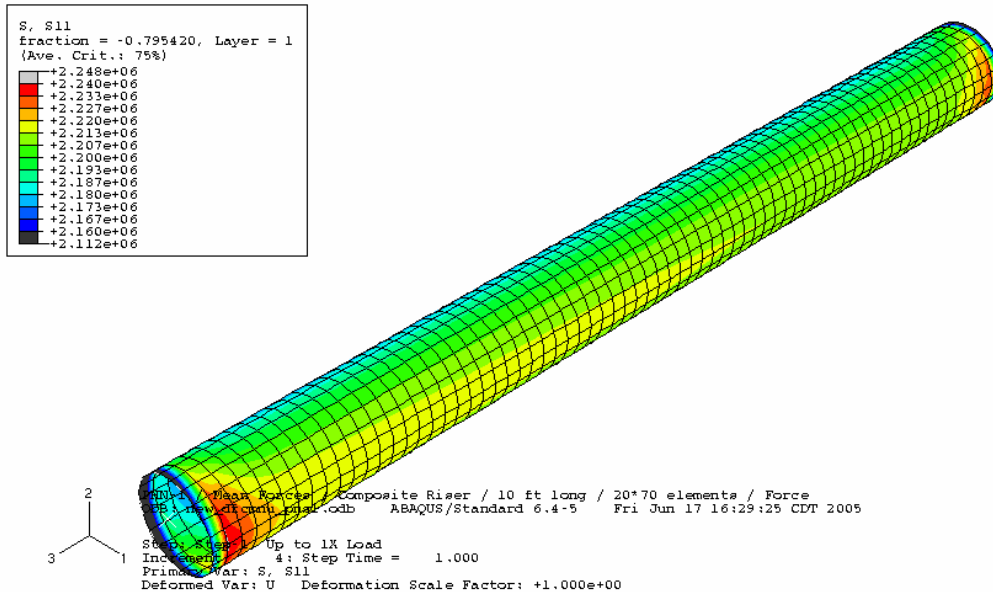


Figure 14. Axial Stress (σ_{11}) Contour of Liner (min: 15 ksi / max: 15.6 ksi): PNS-1 / Mean

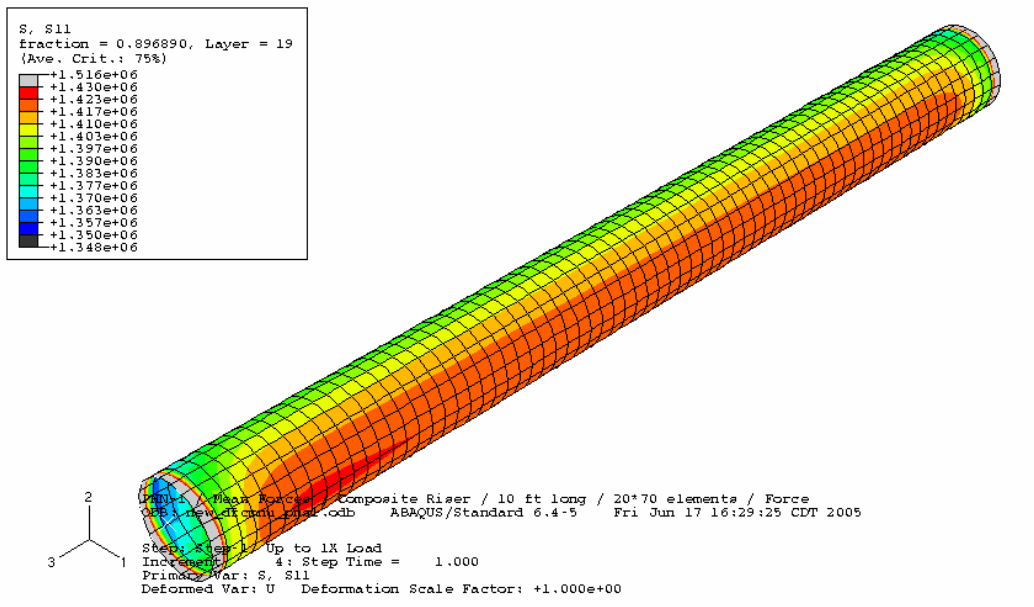


Figure 15. σ_{11} Contour of Layer 18 (0°) (min: 9.4 ksi / max: 9.9 ksi): PNS-1 / Mean

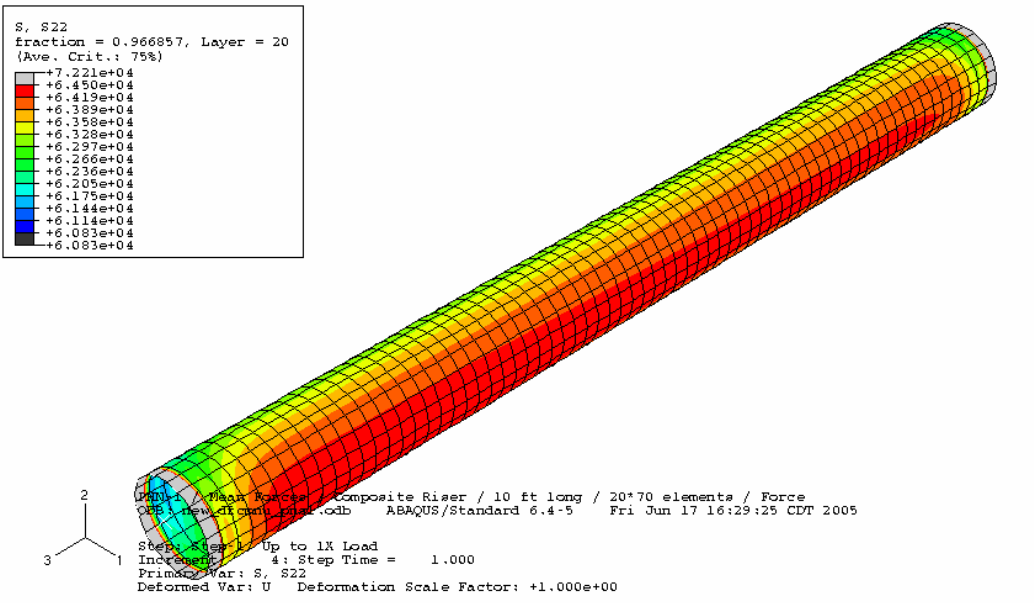


Figure 16. σ_{22} Contour of Layer 19 (88°) (min: 0.42 ksi / max: 0.45 ksi): PNS-1 / Mean

6.1.2. Dynamic Maximum Solution

Table 13 presents the maximum values of the nodal forces and displacement from the global dynamic analysis, and Figure 17 through 19 shows the stress contours when the maximum solution is applied as the boundary conditions.

Table 13. Maximum Nodal Output from Global Dynamic Analysis: PNS-1

Elevations	X-Force	Z-Force	Y-Moment	X-Position	Z-Position	Slope
5926	6103.77	283007.32	-6485.48	138.6544	-75.7584	0.0218761
5916	6132.10	282674.23	-5190.56	138.5268	-85.7586	0.0220408

(units in lb and ft)

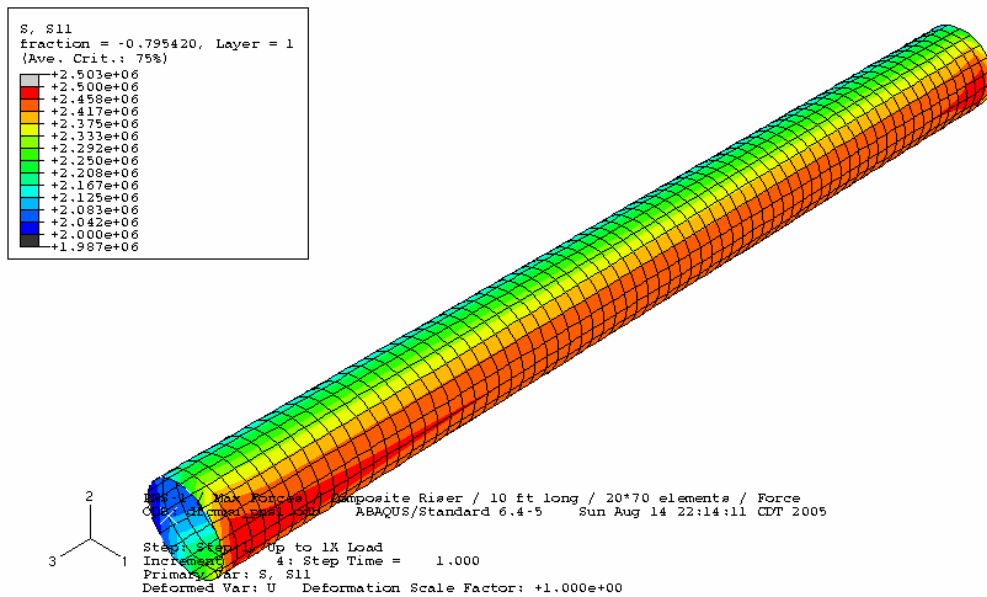


Figure 17. Axial Stress (σ_{11}) Contour of Liner (min: 13.9 ksi / max: 17.4 ksi): PNS-1 / Max

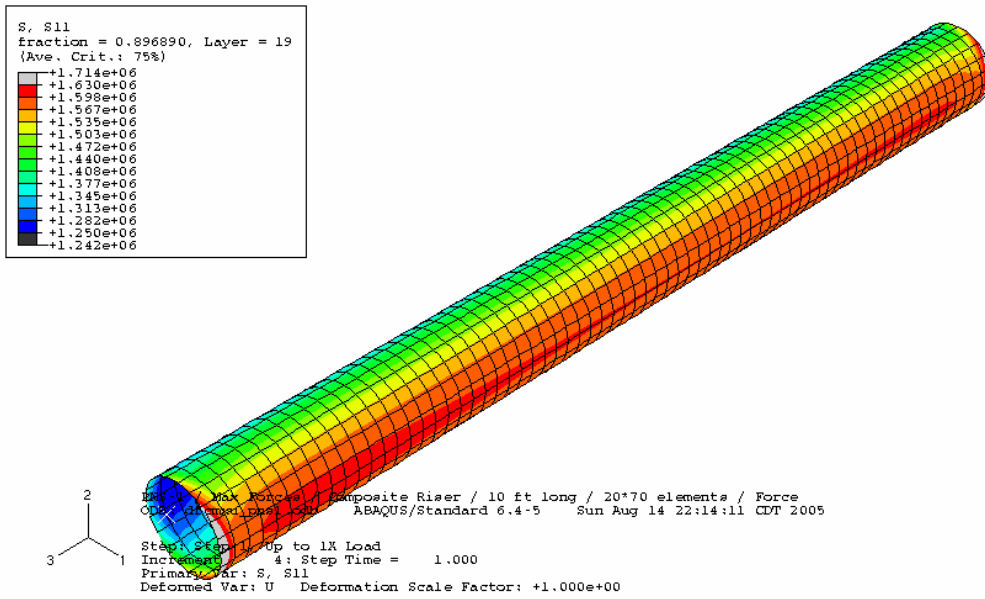


Figure 18. σ_{11} Contour of Layer 18 (0°) (min: 8.7 ksi / max: 11.3 ksi): PNS-1 / Max

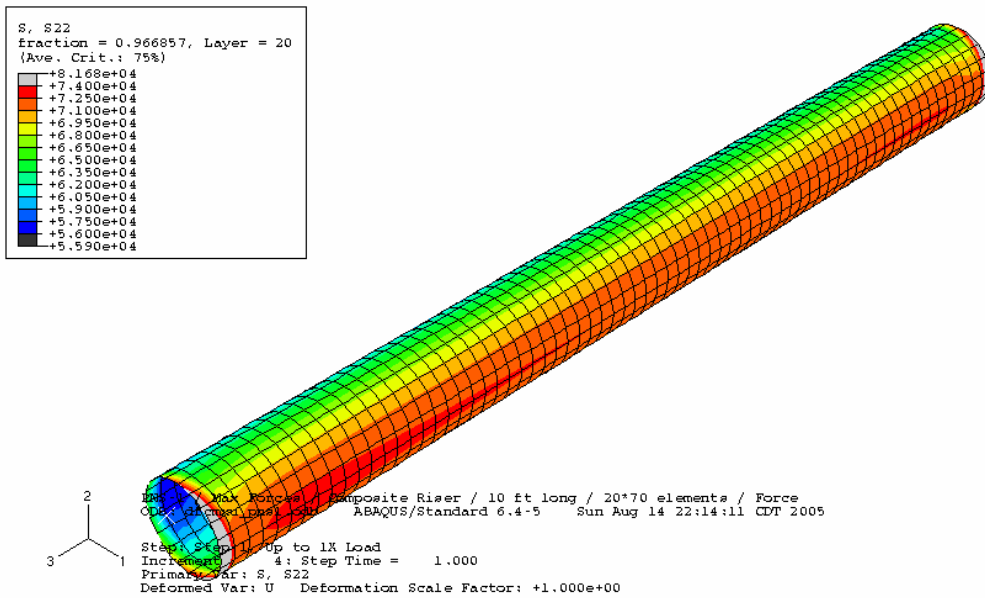


Figure 19. σ_{22} Contour of Layer 19 (88°) (min: 0.39 ksi / max: 0.51 ksi): PNS-1 / Max

6.2. PHN-1: 100 Year Hurricane

6.2.1. Dynamic Mean Solution

Table 14 shows the nodal output from the global analysis, and Figure 20 through 22 present stress contours.

Table 14. Mean Nodal Output from Global Dynamic Analysis: PHN-1

Elevations	X-Force	Z-Force	Y-Moment	X-Position	Z-Position	Slope
5926	7904.68	301213.96	-4800.83	356.6630	-85.5899	0.0257821
5916	8031.08	300877.32	-3809.85	356.4017	-95.5869	0.0264541

(units in lb and ft)

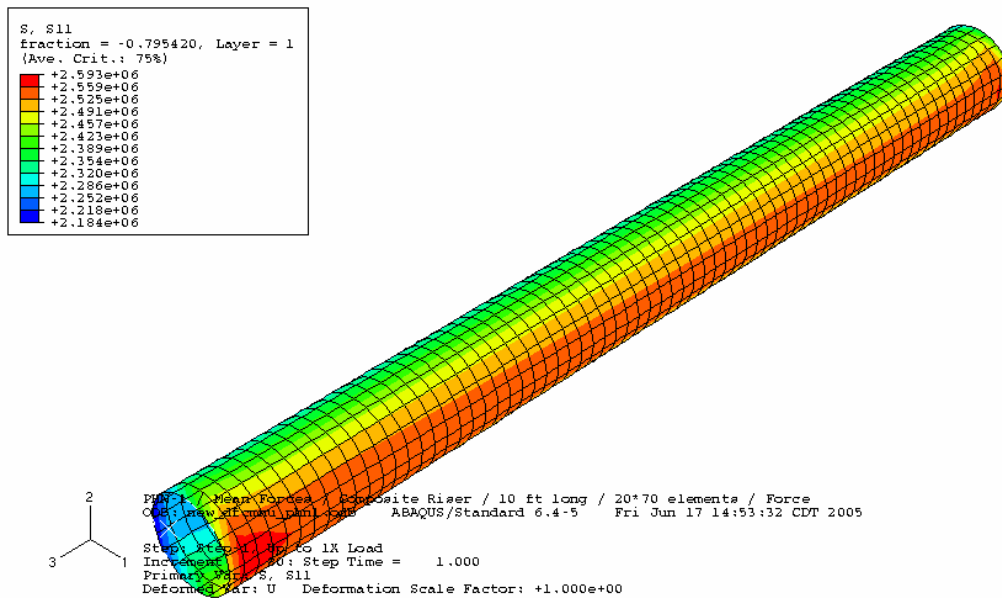


Figure 20. Axial Stress (σ_{11}) Contour of Liner (min: 15.2 ksi / max: 18.0 ksi): PHN-1 / Mean

6.2.2. Dynamic Maximum Solution

Table 15 shows the nodal output from the global analysis, and Figure 23 through 25 present stress contours of selected layers.

Table 15. Maximum Nodal Output from Global Dynamic Analysis: PHN-1

Elevations	X-Force	Z-Force	Y-Moment	X-Position	Z-Position	Slope
5926	23769.88	364819.75	-15568.12	430.0070	-89.6571	0.0764229
5916	23772.60	364485.84	-11952.46	429.4957	-99.6525	0.0767332

(units in lb and ft)

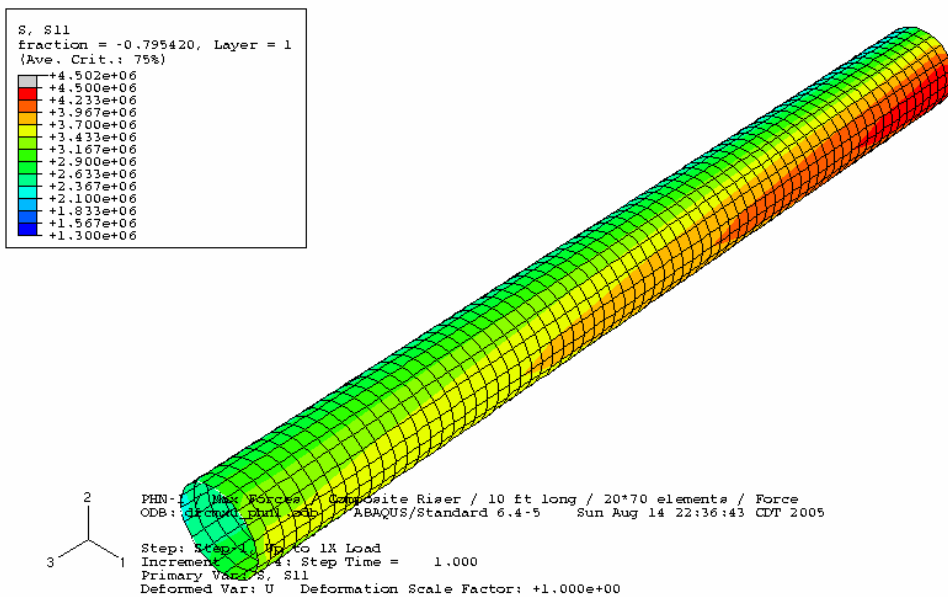


Figure 23. Axial Stress (σ_{11}) Contour of Liner (min: 9.0 ksi / max: 31.3 ksi): PHN-1 / Max

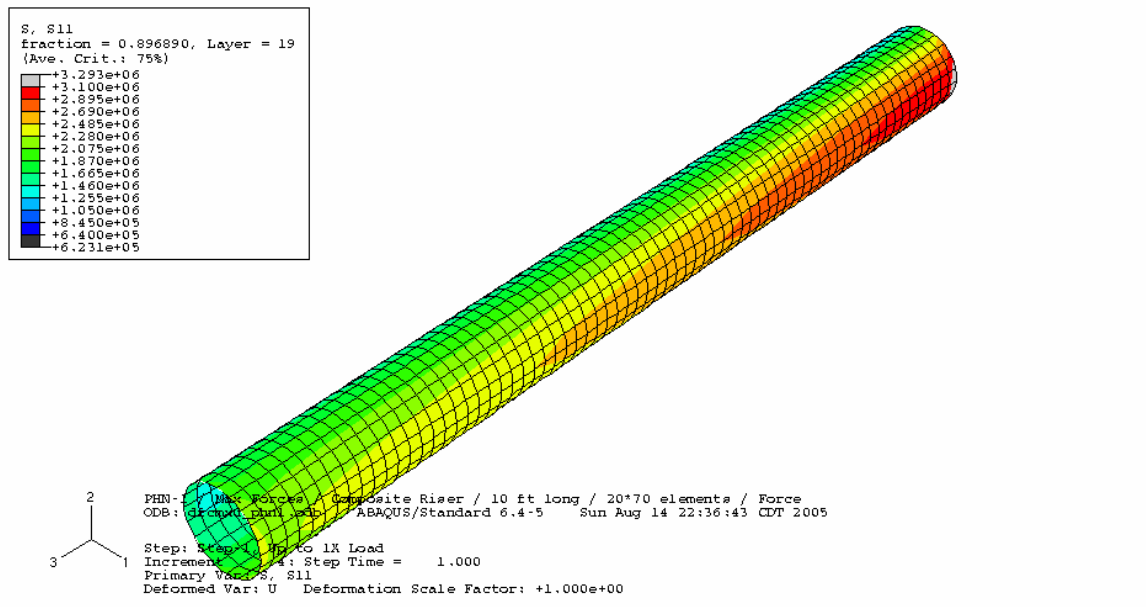


Figure 24. σ_{11} Contour of Layer 18 (0°) (min: 4.4 ksi / max: 21.5 ksi): PHN-1 / Max

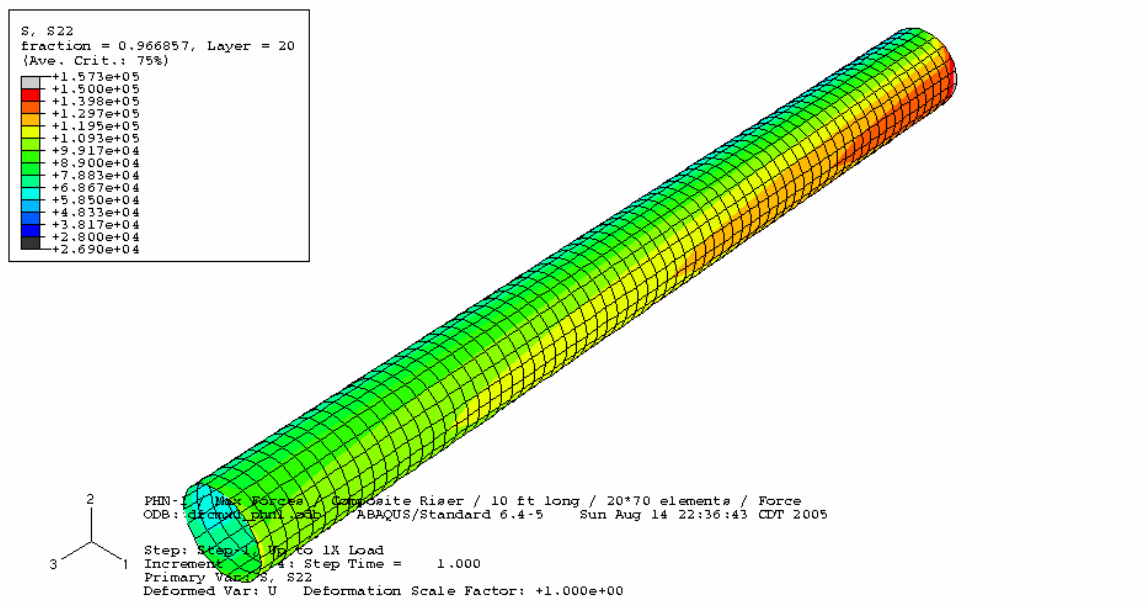


Figure 25. σ_{22} Contour of Layer 19 (88°) (min: 0.19 ksi / max: 1.04 ksi): PHN-1 / Max

6.3. PCN-1: 100 Year Loop Current

6.3.1. Dynamic Mean Solution

Table 16 shows the nodal output from the global analysis, and Figure 26 through 28 present stress contours.

Table 16. Mean Nodal Output from Global Dynamic Analysis: PCN-1

Elevations	X-Force	Z-Force	Y-Moment	X-Position	Z-Position	Slope
5926	7311.45	340489.85	-10558.37	538.1579	-100.1437	0.0206310
5916	7662.99	340148.99	-8532.66	537.9439	-110.1423	0.0221212

(units in lb and ft)

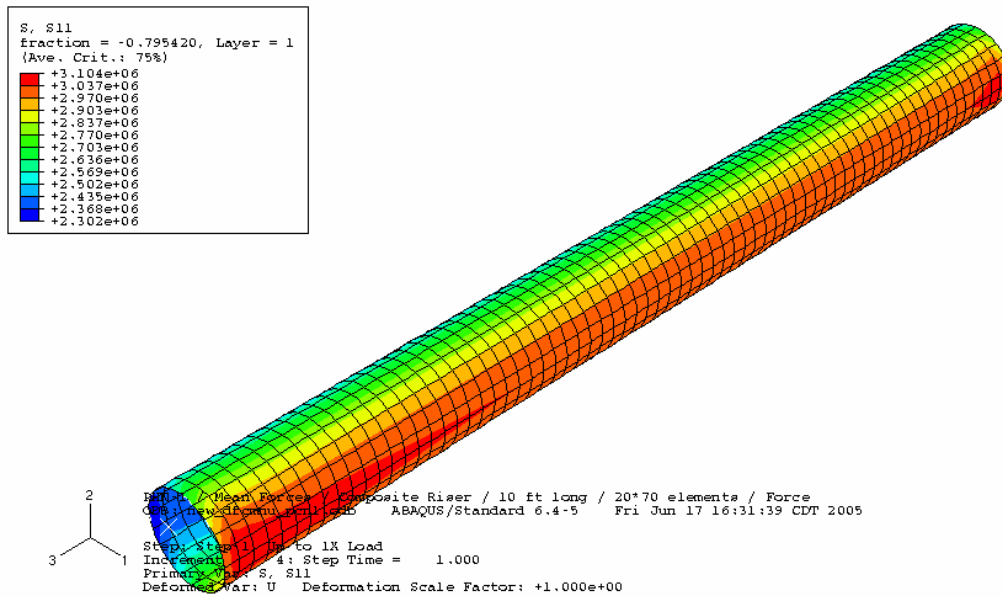


Figure 26. Axial Stress (σ_{11}) Contour of Liner (min: 16.0 ksi / max: 21.6 ksi): PCN-1 / Mean

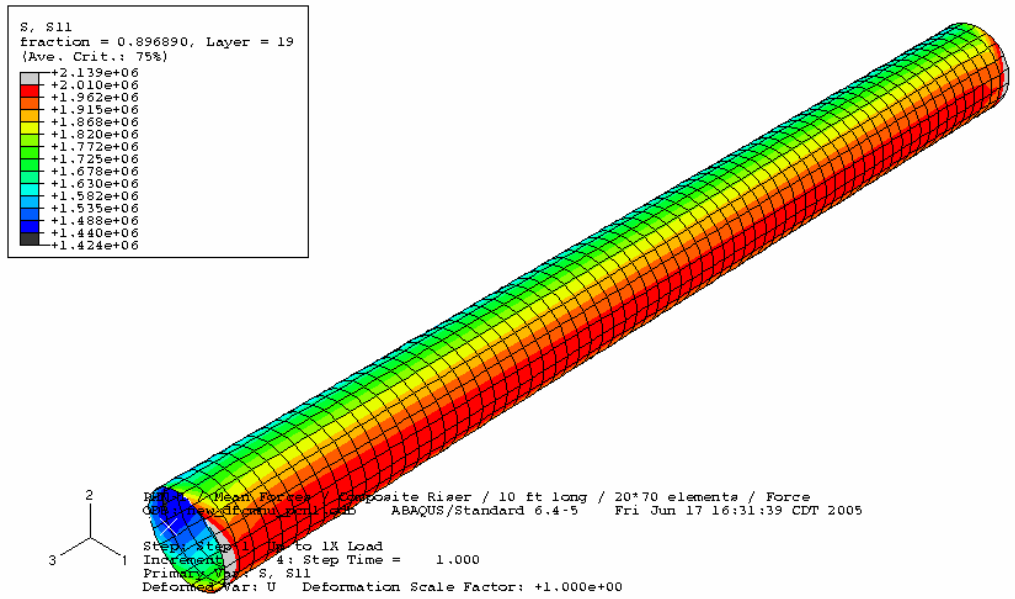


Figure 27. σ_{11} Contour of Layer 18 (0°) (min: 10.0 ksi / max: 14.0 ksi): PCN-1 / Mean

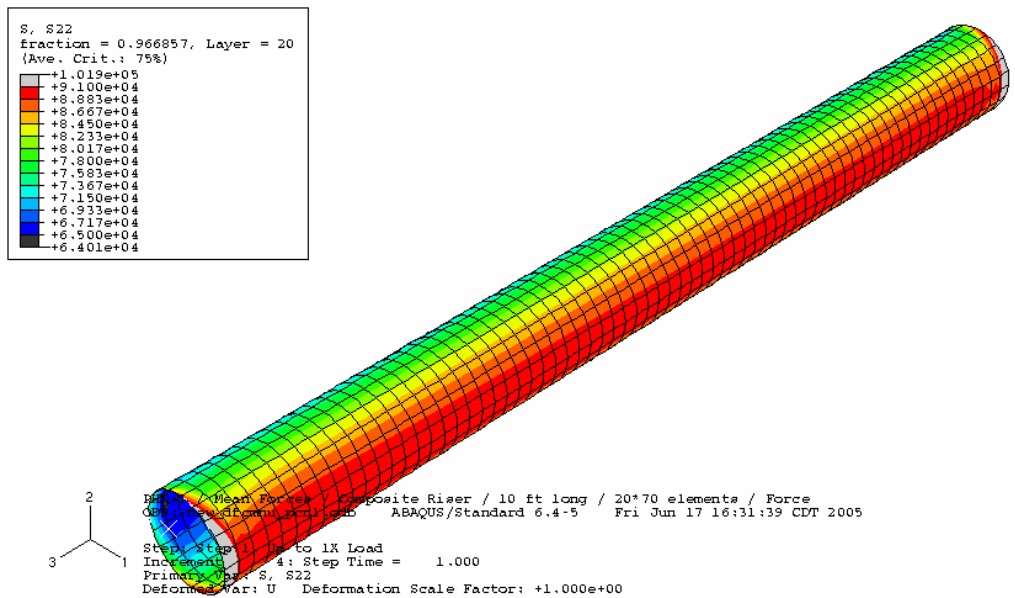


Figure 28. σ_{22} Contour of Layer 19 (88°) (min: 0.45 ksi / max: 0.63 ksi): PCN-1 / Mean

6.3.2. Dynamic Maximum Solution

Table 17 shows the nodal output from the global analysis, and Figure 29 through 31 present stress contours.

Table 17. Maximum Nodal Output from Global Dynamic Analysis: PCN-1

Elevations	X-Force	Z-Force	Y-Moment	X-Position	Z-Position	Slope
5926	9994.78	346495.03	-15144.42	544.9844	-100.7176	0.0284770
5916	10313.61	346154.38	-11987.75	544.7413	-110.7168	0.0298441

(units in lb and ft)

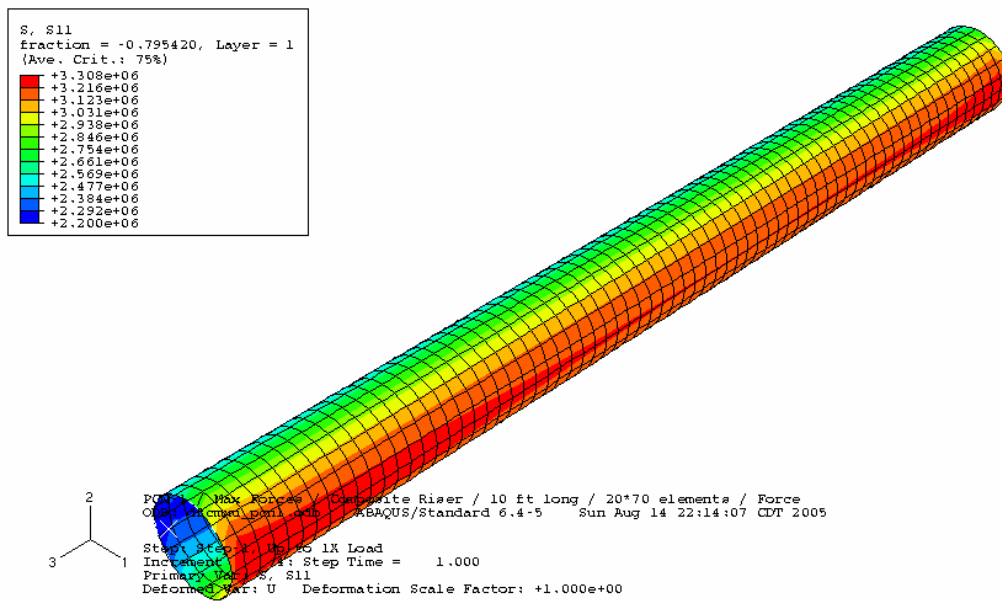


Figure 29. Axial Stress (σ_{11}) Contour of Liner (min: 15.3 ksi / max: 23.0 ksi): PCN-1 / Max

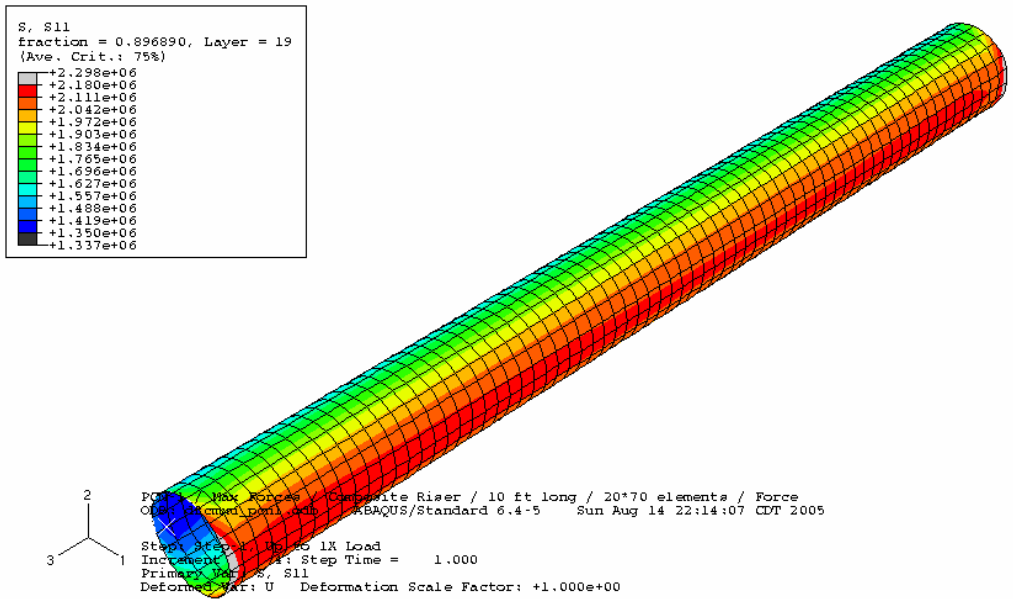


Figure 30. σ_{11} Contour of Layer 18 (0°) (min: 9.4 ksi / max: 15.1 ksi): PCN-1 / Max

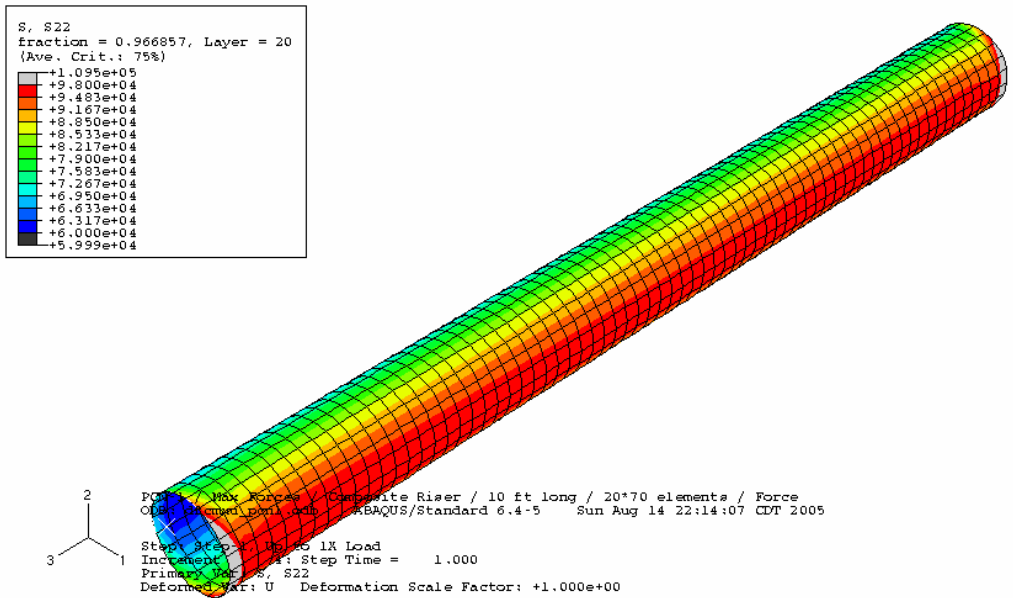


Figure 31. σ_{22} Contour of Layer 19 (88°) (min: 0.42 ksi / max: 0.68 ksi): PCN-1 / Max

7. Fatigue Analysis

7.1. Procedure

Spectral fatigue analysis of a steel riser generally utilizes a transfer function, which, in this case, is the ratio of the stress to the wave height as a function of frequency [10, 11]. The transfer function, H_σ , is then used to generate a stress energy spectrum, S_σ , from the wave energy spectrum, S_η , as shown in the following equation.

$$S_\sigma(\omega|H_s, T_z) = |H_\sigma(\omega)|^2 S_\eta(\omega|H_s, T_z) \quad (4)$$

The Rayleigh probability density function for stress range distribution can be obtained through the spectral moments of the stress energy spectrum.

Since the transfer function for the composite riser is not readily available, this study uses an alternative method for generating the Rayleigh probability density function. First, global analysis is performed for each fatigue bin (sea state). From the output, the root mean square (RMS) value and T_z of axial tension and bending moment at a particular location are obtained. Second, the RMS tension and bending moment are converted to RMS stresses, σ_{RMS} , and the Rayleigh probability density function for each RMS stress is obtained using the following equation.

$$p(S) = \frac{2S}{S_{RMS}^2} \exp\left[\frac{-S^2}{S_{RMS}^2}\right] = \frac{S}{4\sigma_{RMS}^2} \exp\left[\frac{-S^2}{8\sigma_{RMS}^2}\right] \quad (5)$$

where S : stress range

Then the Rayleigh probability density function is converted to a stress histogram, where the probability is replaced by the number of cycles per year, using the probability of occurrence of the fatigue bin and T_z . Finally, using an S-N relationship, each data point in the histogram is converted into damage using Miner's rule [12], and the sum of the individual damage values represents the damage caused by the particular fatigue bin. When this procedure is applied to every fatigue bin and the total damage is calculated, the life at the location under consideration is obtained simply by inverting the total damage. In this study, the fatigue lives of the axial layers and steel liner at the top and bottom ends of the composite riser region, which are 102 ft and 5926 ft in elevation, will be estimated.

When calculating the RMS stresses, it is assumed that the transverse normal direction of the hoop layers have no load-carrying capability, and thus rendering the analysis conservative.

7.2. S-N Curves

In the literature, only a few S-N curves for unidirectional composites are available [13-17], whereas extensive experimental studies on fatigue of cross-ply and quasi-isotropic composites have been carried out. In this study, the most recent data in Ref. 15 is used for the calculation of life, where G40-700/5245C material with 0° orientation was tested. Generally, S-N relationship of composite materials is best represented by a semi-log equation of the following form.

$$S = a - b \log N \quad (6)$$

Where

a, b : constants

N : life

The constants a and b for the selected S-N curve normalized by the static strength are 0.861 and 0.01, respectively. Carbon fiber composites are well-known for their excellent fatigue properties, which is evidenced by the small value of constant b in the S-N equation.

S-N relationship of steel, on the other hand, is usually represented by the following power law equation.

$$S^m N = C \quad (7)$$

Where

m, C : constants

Choices of the values for the constants should be made according to the structural details. In this study, DNV-C curve for machined section is used where m and C are 4.51×10^{11} and 4.0, respectively.

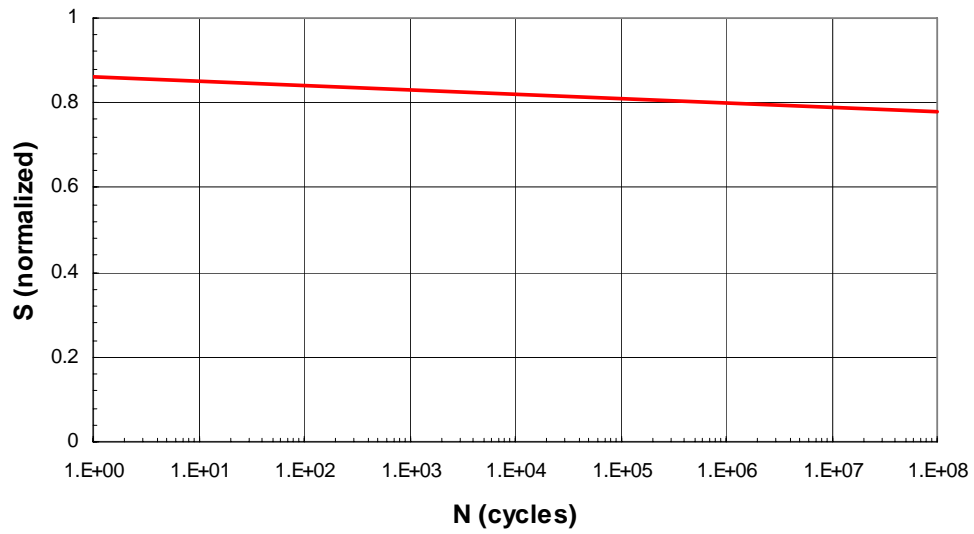


Figure 32. S-N Curve for Unidirectional Composite (0°)

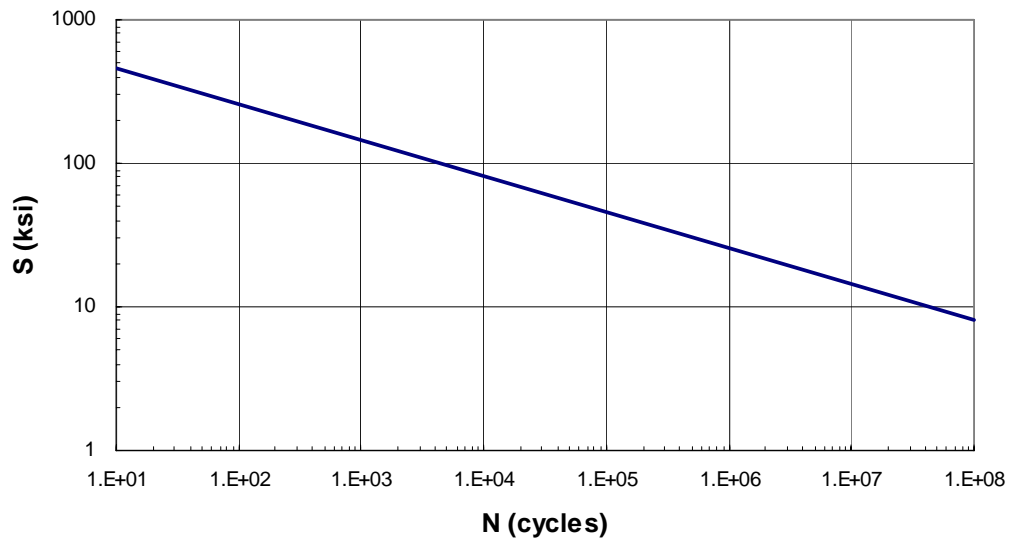


Figure 33. S-N Curve for Steel

7.3. Input Data

Table 18 and 19 present the wave definition, RMS tension and bending moment, and

T_z for each of 27 fatigue bins, which were provided by Stress Engineering Services, Inc.

Table 18. Input Data for Fatigue Analysis (102 ft elevation)

Fatigue Bin	Wave Definition		Probability	Effective Tension			Bending Moment		
	Hs (ft.)	Tz (sec.)		Mean (kips)	RMS (kips)	Tz (sec.)	Mean (ft-kips)	RMS (ft-kips)	Tz (sec.)
1	2.0	2.0	4.1895E-02	85.40	0.61	1.43	4.46	0.65	1.80
2	2.0	3.0	2.2055E-01	85.40	0.12	1.44	4.46	0.38	2.11
3	2.0	4.0	1.0194E-01	85.40	0.06	1.59	4.46	0.17	2.29
4	4.0	3.0	8.1279E-02	85.50	0.22	1.51	5.03	0.56	2.37
5	4.0	4.0	1.9041E-01	85.50	0.12	1.98	5.03	0.36	3.41
6	4.0	5.0	5.3197E-02	85.50	0.14	8.24	5.03	0.30	5.31
7	6.0	4.0	8.8356E-02	85.67	0.26	3.62	5.70	0.57	4.93
8	6.0	5.0	7.2831E-02	85.67	0.29	12.11	5.70	0.53	8.41
9	6.0	6.0	1.3813E-02	85.67	0.41	11.21	5.70	0.52	13.08
10	8.0	5.0	4.1781E-02	85.97	0.59	19.01	6.48	0.74	11.54
11	8.0	6.0	1.6324E-02	85.97	0.70	14.63	6.48	0.73	18.10
12	10.0	6.0	1.3242E-02	86.47	1.20	20.30	7.41	0.91	22.04
13	12.0	6.0	5.1368E-03	87.10	1.90	26.84	8.31	1.05	26.15
14	14.0	6.5	3.3107E-03	87.96	2.90	30.89	9.28	1.15	35.54
15	16.0	7.5	5.1368E-04	89.08	4.16	33.60	10.30	1.20	48.47
16	18.0	7.7	3.5386E-04	90.38	5.55	40.04	11.26	1.23	49.30
17	20.0	7.9	2.5117E-04	91.82	7.10	43.53	12.17	1.26	46.96
18	22.0	8.1	1.5982E-04	93.48	8.76	49.75	13.06	1.31	46.25
19	24.0	8.3	1.0270E-04	95.26	10.52	51.26	13.88	1.42	43.89
20	26.0	8.6	6.8494E-05	97.16	12.20	56.48	14.64	1.57	45.48
21	28.0	8.8	5.1368E-05	99.05	13.88	55.71	15.31	1.80	44.52
22	30.0	9.0	3.0319E-05	100.93	15.38	59.55	15.90	2.04	47.90
23	32.0	9.2	2.2828E-05	102.87	16.24	55.13	16.45	2.23	44.85
24	34.0	9.4	1.3703E-05	104.65	16.95	56.19	16.90	2.39	46.29
25	36.0	9.7	9.7024E-06	106.27	17.71	52.14	17.27	2.58	43.83
26	38.0	9.9	6.5070E-06	107.81	18.30	52.79	17.60	2.73	44.94
27	41.0	10.3	4.3377E-06	109.69	17.96	47.28	17.96	2.17	32.51

Table 19. Input Data for Fatigue Analysis (5926 ft elevation)

Fatigue Bin	Wave Definition		Probability	Effective Tension			Bending Moment		
	Hs (ft.)	Tz (sec.)		Mean (kips)	RMS (kips)	Tz (sec.)	Mean (ft-kips)	RMS (ft-kips)	Tz (sec.)
1	2.0	2.0	4.1895E-02	270.07	0.02	1.47	-0.02	0.26	1.91
2	2.0	3.0	2.2055E-01	270.07	0.01	3.29	-0.02	0.19	2.48
3	2.0	4.0	1.0194E-01	270.07	0.03	5.59	-0.02	0.18	4.24
4	4.0	3.0	8.1279E-02	270.16	0.07	9.07	-0.04	0.26	2.44
5	4.0	4.0	1.9041E-01	270.16	0.08	9.27	-0.04	0.32	4.45
6	4.0	5.0	5.3197E-02	270.16	0.13	9.20	-0.04	0.38	5.83
7	6.0	4.0	8.8356E-02	270.34	0.24	18.19	-0.06	0.47	4.56
8	6.0	5.0	7.2831E-02	270.34	0.29	13.42	-0.06	0.56	5.91
9	6.0	6.0	1.3813E-02	270.34	0.40	11.37	-0.06	0.53	6.42
10	8.0	5.0	4.1781E-02	270.64	0.59	20.94	-0.09	0.76	5.96
11	8.0	6.0	1.6324E-02	270.64	0.69	14.97	-0.09	0.71	6.47
12	10.0	6.0	1.3242E-02	271.13	1.20	20.90	-0.13	0.91	6.49
13	12.0	6.0	5.1368E-03	271.75	1.89	27.72	-0.17	1.11	6.52
14	14.0	6.5	3.3107E-03	272.60	2.89	31.81	-0.21	1.23	6.73
15	16.0	7.5	5.1368E-04	273.72	4.15	34.46	-0.25	1.20	7.03
16	18.0	7.7	3.5386E-04	274.99	5.54	41.08	-0.30	1.32	7.14
17	20.0	7.9	2.5117E-04	276.42	7.09	44.63	-0.34	1.43	7.26
18	22.0	8.1	1.5982E-04	278.06	8.76	51.00	-0.39	1.54	7.37
19	24.0	8.3	1.0270E-04	279.82	10.51	52.49	-0.43	1.63	7.48
20	26.0	8.6	6.8494E-05	281.69	12.19	57.81	-0.48	1.69	7.60
21	28.0	8.8	5.1368E-05	283.56	13.88	56.96	-0.53	1.76	7.70
22	30.0	9.0	3.0319E-05	285.41	15.38	60.86	-0.57	1.82	7.78
23	32.0	9.2	2.2828E-05	287.31	16.23	56.29	-0.61	1.87	7.77
24	34.0	9.4	1.3703E-05	289.07	16.94	57.34	-0.65	1.89	7.78
25	36.0	9.7	9.7024E-06	290.66	17.70	53.14	-0.68	1.88	7.81
26	38.0	9.9	6.5070E-06	292.18	18.30	53.78	-0.71	1.89	7.82
27	41.0	10.3	4.3377E-06	294.02	17.92	48.02	-0.75	1.88	7.89

7.4. Damage Due to Individual Loading

When RMS tension and RMS bending moment are converted to corresponding RMS stresses, it can be seen that the RMS stresses due to bending moment are greater than those due to axial tension, in the low-numbered fatigue bins. The procedure presented in Section 7.1 is separately applied to axial tension and bending moment at the bottom of the composite riser, and the damage values of the tension only case and bending moment only cases are compared. As can be seen in Table 20, fatigue damage in the composite is mainly influenced by T_z , while damage in the steel liner is governed by RMS stress. In the table, the smaller T_z and the larger value from each set of RMS stresses and damage are highlighted in boldface. For the composite, the larger RMS stress does not necessarily lead to larger damage, but it is number of cycles per year that primarily decides the amount of damage. The fatigue life estimates of the composite are infinite, regardless of the loading; the fatigue life from the tension only case is slightly smaller. On the other hand, the fatigue life of the steel liner from the tension only case is larger than the life from the bending moment only case. The fatigue responses of the composite and steel are quite different from each other, even to the same set of axial tension and bending moment.

The top of the composite riser shows the same trend, which is shown in Table 21; fatigue damage in the composite is decided by T_z , whereas the steel liner is mainly influenced by RMS stress. Since it cannot be said that one type of loading is dominant over the other, the stresses by the two different types of loading need to be combined. In the next section, the Rayleigh probability distribution function for combined stress will be derived.

Table 20. Effects of Stress and T_z on Damage (102 ft)

Fatigue Bin	Tz		Composite				Steel Liner			
			RMS Stress (ksi)		Damage		RMS Stress (ksi)		Damage	
	Tension	B. M.	Tension	B. M.	Tension	B. M.	Tension	B. M.	Tension	B. M.
1	1.43	1.80	0.0223	0.1203	3.84E-32	3.42E-32	0.0350	0.1556	3.88E-10	1.22E-07
2	1.44	2.11	0.0046	0.0697	1.97E-31	1.45E-31	0.0071	0.0902	3.04E-12	6.18E-08
3	1.59	2.29	0.0022	0.0322	8.21E-32	5.90E-32	0.0034	0.0417	7.96E-14	1.20E-09
4	1.51	2.37	0.0082	0.1032	6.93E-32	4.93E-32	0.0128	0.1335	1.21E-11	9.76E-08
5	1.98	3.41	0.0044	0.0661	1.23E-31	7.69E-32	0.0069	0.0855	1.91E-12	2.67E-08
6	8.24	5.31	0.0050	0.0561	7.42E-33	1.36E-32	0.0078	0.0726	1.93E-13	2.49E-09
7	3.62	4.93	0.0095	0.1059	3.15E-32	2.59E-32	0.0149	0.1369	1.06E-11	5.64E-08
8	12.11	8.41	0.0106	0.0981	7.77E-33	1.24E-32	0.0166	0.1269	4.08E-12	2.01E-08
9	11.21	13.08	0.0149	0.0964	1.60E-33	1.51E-33	0.0233	0.1247	3.24E-12	2.29E-09
10	19.01	11.54	0.0216	0.1363	2.88E-33	5.42E-33	0.0339	0.1763	2.60E-11	3.13E-08
11	14.63	18.10	0.0256	0.1352	1.47E-33	1.35E-33	0.0401	0.1749	2.58E-11	7.56E-09
12	20.30	22.04	0.0440	0.1687	8.76E-34	9.34E-34	0.0689	0.2183	1.32E-10	1.22E-08
13	26.84	26.15	0.0695	0.1953	2.65E-34	3.15E-34	0.1087	0.2526	2.40E-10	7.16E-09
14	30.89	35.54	0.1058	0.2125	1.55E-34	1.53E-34	0.1656	0.2750	7.21E-10	4.77E-09
15	33.60	48.47	0.1521	0.2228	2.33E-35	1.76E-35	0.2382	0.2882	4.41E-10	6.54E-10
16	40.04	49.30	0.2026	0.2278	1.43E-35	1.20E-35	0.3172	0.2946	8.01E-10	4.84E-10
17	43.53	46.96	0.2593	0.2328	1.00E-35	8.99E-36	0.4060	0.3012	1.40E-09	3.94E-10
18	49.75	46.25	0.3201	0.2428	6.02E-36	5.88E-36	0.5012	0.3142	1.81E-09	3.01E-10
19	51.26	43.89	0.3844	0.2636	4.07E-36	4.09E-36	0.6018	0.3410	2.35E-09	2.83E-10
20	56.48	45.48	0.4457	0.2914	2.67E-36	2.72E-36	0.6978	0.3770	2.57E-09	2.72E-10
21	55.71	44.52	0.5071	0.3324	2.20E-36	2.20E-36	0.7939	0.4300	3.28E-09	3.53E-10
22	59.55	47.90	0.5619	0.3781	1.28E-36	1.28E-36	0.8797	0.4891	2.73E-09	3.24E-10
23	55.13	44.85	0.5932	0.4121	1.07E-36	1.07E-36	0.9288	0.5331	2.76E-09	3.68E-10
24	56.19	46.29	0.6191	0.4432	6.50E-37	6.49E-37	0.9693	0.5733	1.83E-09	2.86E-10
25	52.14	43.83	0.6470	0.4774	5.08E-37	5.08E-37	1.0130	0.6175	1.75E-09	2.88E-10
26	52.79	44.94	0.6686	0.5049	3.45E-37	3.45E-37	1.0468	0.6532	1.32E-09	2.36E-10
27	47.28	32.51	0.6560	0.4010	2.77E-37	2.77E-37	1.0271	0.5187	9.14E-10	8.65E-11

Table 21. Effects of Stress and T_z on Damage (5926 ft)

Fatigue Bin	T _z		Composite				Steel Liner			
			RMS Stress (ksi)		Damage		RMS Stress (ksi)		Damage	
	Tension	B. M.	Tension	B. M.	Tension	B. M.	Tension	B. M.	Tension	B. M.
1	1.47	1.91	0.0008	0.0477	3.64E-32	2.96E-32	0.0012	0.0617	5.64E-16	2.85E-09
2	3.29	2.48	0.0005	0.0345	8.56E-32	1.18E-31	0.0008	0.0446	2.55E-16	3.15E-09
3	5.59	4.24	0.0009	0.0326	2.33E-32	3.19E-32	0.0015	0.0422	7.63E-16	6.84E-10
4	9.07	2.44	0.0025	0.0485	1.15E-32	4.50E-32	0.0040	0.0628	1.98E-14	4.64E-09
5	9.27	4.45	0.0030	0.0592	2.63E-32	5.85E-32	0.0047	0.0766	8.86E-14	1.32E-08
6	9.20	5.83	0.0048	0.0697	7.42E-33	1.65E-32	0.0076	0.0902	1.68E-13	1.67E-08
7	18.19	4.56	0.0087	0.0869	6.26E-33	2.73E-32	0.0136	0.1124	1.47E-12	2.77E-08
8	13.42	5.91	0.0104	0.1042	7.01E-33	1.78E-32	0.0163	0.1348	3.43E-12	3.65E-08
9	11.37	6.42	0.0146	0.0975	1.58E-33	3.07E-33	0.0228	0.1262	2.93E-12	4.88E-09
10	20.94	5.96	0.0215	0.1402	2.61E-33	1.05E-32	0.0336	0.1814	2.28E-11	6.79E-08
11	14.97	6.47	0.0253	0.1316	1.43E-33	3.75E-33	0.0396	0.1702	2.39E-11	1.89E-08
12	20.90	6.49	0.0437	0.1676	8.50E-34	3.17E-33	0.0684	0.2168	1.24E-10	4.03E-08
13	27.72	6.52	0.0692	0.2052	2.56E-34	1.28E-33	0.1083	0.2655	2.28E-10	3.50E-08
14	31.81	6.73	0.1054	0.2272	1.50E-34	8.21E-34	0.1651	0.2940	6.92E-10	3.29E-08
15	34.46	7.03	0.1518	0.2214	2.27E-35	1.21E-34	0.2376	0.2864	4.25E-10	4.40E-09
16	41.08	7.14	0.2023	0.2441	1.40E-35	8.45E-35	0.3167	0.3158	7.76E-10	4.41E-09
17	44.63	7.26	0.2590	0.2655	9.77E-36	6.05E-35	0.4055	0.3434	1.36E-09	4.31E-09
18	51.00	7.37	0.3199	0.2850	5.87E-36	3.89E-35	0.5008	0.3686	1.76E-09	3.58E-09
19	52.49	7.48	0.3841	0.3024	3.98E-36	2.52E-35	0.6014	0.3913	2.29E-09	2.88E-09
20	57.81	7.60	0.4455	0.3134	2.61E-36	1.67E-35	0.6975	0.4054	2.51E-09	2.18E-09
21	56.96	7.70	0.5069	0.3264	2.15E-36	1.26E-35	0.7936	0.4222	3.20E-09	1.90E-09
22	60.86	7.78	0.5618	0.3370	1.28E-36	7.46E-36	0.8795	0.4360	2.67E-09	1.26E-09
23	56.29	7.77	0.5930	0.3460	1.09E-36	5.69E-36	0.9285	0.4476	2.70E-09	1.06E-09
24	57.34	7.78	0.6189	0.3496	6.65E-37	3.43E-36	0.9690	0.4523	1.89E-09	6.60E-10
25	53.14	7.81	0.6468	0.3480	5.28E-37	2.41E-36	1.0126	0.4502	1.72E-09	4.57E-10
26	53.78	7.82	0.6683	0.3505	3.61E-37	1.62E-36	1.0464	0.4534	1.30E-09	3.15E-10
27	48.02	7.89	0.6547	0.3472	2.64E-37	1.07E-36	1.0250	0.4492	8.92E-10	2.00E-10

7.5. Combined Loading

The variance, V , of total stress range can be expressed in terms of individual stress ranges.

$$V(S^{Total}) = V(S^T + S^{BM}) = V(S^T) + V(S^{BM}) \quad (8)$$

Also, variance can be expressed in terms of RMS and mean, μ .

$$V(S) = S_{RMS}^2 - \mu_S^2 \quad (9)$$

In addition, the relationship between RMS and mean is

$$\mu_S^2 = \frac{\pi}{4} S_{RMS}^2 \quad (10)$$

Combining Eqn. (8) through (10) yields

$$S^{Total}_{RMS}{}^2 = S^T_{RMS}{}^2 + S^{BM}_{RMS}{}^2 = 8[(\sigma^T_{RMS})^2 + (\sigma^{BM}_{RMS})^2] \quad (11)$$

Therefore, from Eqn. (5) and (11), Rayleigh probability density function for combined stress is given by the following equation.

$$\begin{aligned} p(S^{Total}) &= \frac{2S^{Total}}{(S^{Total})_{RMS}^2} \exp\left[\frac{-(S^{Total})^2}{(S^{Total}_{RMS})^2}\right] \\ &= \frac{S^{Total}}{4[(\sigma^T_{RMS})^2 + (\sigma^{BM}_{RMS})^2]} \exp\left[\frac{-(S^{Total})^2}{8[(\sigma^T_{RMS})^2 + (\sigma^{BM}_{RMS})^2]}\right] \end{aligned} \quad (12)$$

Using Eqn. (12), fatigue damage and life for combined stress cases can be estimated. For conservative results, the T_z of the combined stress is assumed to be equal to the smaller one between those of axial tension and bending moment of each fatigue bin. Table 22 and 23 summarize the results from all three cases: tension only, bending moment only, and combined. The fatigue lives at the top and the bottom are not significantly different from each other. However, it should be noted that the contribution of each fatigue bin to the total damage is dependent on the location, especially for the steel liner.

Table 22. Damage at 102 ft Elevation

Bin	Composite						Steel Liner					
	Tension Only		B. M. Only		Combined		Tension Only		B. M. Only		Combined	
	Damage	%	Damage	%	Damage	%	Damage	%	Damage	%	Damage	%
1	3.84E-32	6.8	3.42E-32	8.0	4.31E-32	6.9	3.88E-10	1.5	1.22E-07	26.7	1.70E-07	24.1
2	1.97E-31	34.9	1.45E-31	34.0	2.12E-31	34.1	3.04E-12	0.0	6.18E-08	13.5	9.17E-08	13.0
3	8.21E-32	14.6	5.90E-32	13.9	8.49E-32	13.7	7.96E-14	0.0	1.20E-09	0.3	1.75E-09	0.2
4	6.93E-32	12.3	4.93E-32	11.6	7.75E-32	12.5	1.21E-11	0.0	9.76E-08	21.3	1.56E-07	22.1
5	1.23E-31	21.9	7.69E-32	18.1	1.32E-31	21.3	1.91E-12	0.0	2.67E-08	5.8	4.66E-08	6.6
6	7.42E-33	1.3	1.36E-32	3.2	1.36E-32	2.2	1.93E-13	0.0	2.49E-09	0.5	2.54E-09	0.4
7	3.15E-32	5.6	2.59E-32	6.1	3.52E-32	5.7	1.06E-11	0.0	5.64E-08	12.3	7.86E-08	11.1
8	7.77E-33	1.4	1.24E-32	2.9	1.24E-32	2.0	4.08E-12	0.0	2.01E-08	4.4	2.08E-08	2.9
9	1.60E-33	0.3	1.51E-33	0.4	1.76E-33	0.3	3.24E-12	0.0	2.29E-09	0.5	2.86E-09	0.4
10	2.88E-33	0.5	5.42E-33	1.3	5.43E-33	0.9	2.60E-11	0.1	3.13E-08	6.8	3.37E-08	4.8
11	1.47E-33	0.3	1.35E-33	0.3	1.67E-33	0.3	2.58E-11	0.1	7.56E-09	1.7	1.04E-08	1.5
12	8.76E-34	0.2	9.34E-34	0.2	1.02E-33	0.2	1.32E-10	0.5	1.22E-08	2.7	1.60E-08	2.3
13	2.65E-34	0.0	3.15E-34	0.1	3.20E-34	0.1	2.40E-10	0.9	7.16E-09	1.6	1.01E-08	1.4
14	1.55E-34	0.0	1.53E-34	0.0	1.81E-34	0.0	7.21E-10	2.8	4.77E-09	1.0	1.02E-08	1.4
15	2.33E-35	0.0	1.76E-35	0.0	2.69E-35	0.0	4.41E-10	1.7	6.54E-10	0.1	2.67E-09	0.4
16	1.43E-35	0.0	1.20E-35	0.0	1.62E-35	0.0	8.01E-10	3.1	4.84E-10	0.1	2.78E-09	0.4
17	1.00E-35	0.0	8.99E-36	0.0	1.12E-35	0.0	1.40E-09	5.5	3.94E-10	0.1	3.37E-09	0.5
18	6.02E-36	0.0	5.88E-36	0.0	7.19E-36	0.0	1.81E-09	7.1	3.01E-10	0.1	3.79E-09	0.5
19	4.07E-36	0.0	4.09E-36	0.0	5.29E-36	0.0	2.35E-09	9.2	2.83E-10	0.1	4.79E-09	0.7
20	2.67E-36	0.0	2.72E-36	0.0	3.72E-36	0.0	2.57E-09	10.1	2.72E-10	0.1	5.33E-09	0.8
21	2.20E-36	0.0	2.20E-36	0.0	3.15E-36	0.0	3.28E-09	12.8	3.53E-10	0.1	6.86E-09	1.0
22	1.28E-36	0.0	1.28E-36	0.0	1.91E-36	0.0	2.73E-09	10.7	3.24E-10	0.1	5.81E-09	0.8
23	1.07E-36	0.0	1.07E-36	0.0	1.64E-36	0.0	2.76E-09	10.8	3.68E-10	0.1	5.99E-09	0.8
24	6.50E-37	0.0	6.49E-37	0.0	1.01E-36	0.0	1.83E-09	7.2	2.86E-10	0.1	4.26E-09	0.6
25	5.08E-37	0.0	5.08E-37	0.0	8.02E-37	0.0	1.75E-09	6.9	2.88E-10	0.1	3.93E-09	0.6
26	3.45E-37	0.0	3.45E-37	0.0	5.51E-37	0.0	1.32E-09	5.2	2.36E-10	0.1	3.00E-09	0.4
27	2.77E-37	0.0	2.77E-37	0.0	4.59E-37	0.0	9.14E-10	3.6	8.65E-11	0.0	2.09E-09	0.3
Total	5.64E-31	100	4.26E-31	100	6.22E-31	100	2.55E-08	100	4.58E-07	100	7.06E-07	100
Life*	1.77E+24		2.35E+24		1.61E+24		3.92E+01		2.18E+00		1.42E+00	

*: million years

Table 23. Damage at 5926 ft Elevation

Bin	Composite						Steel Liner					
	Tension Only		B. M. Only		Combined		Tension Only		B. M. Only		Combined	
	Damage	%	Damage	%	Damage	%	Damage	%	Damage	%	Damage	%
1	3.64E-32	17.3	2.96E-32	8.0	2.96E-32	8.0	5.64E-16	0.0	2.85E-09	0.9	2.85E-09	0.4
2	8.56E-32	40.6	1.18E-31	32.1	1.18E-31	32.1	2.55E-16	0.0	3.15E-09	0.9	3.15E-09	0.5
3	2.33E-32	11.1	3.19E-32	8.7	3.19E-32	8.7	7.63E-16	0.0	6.84E-10	0.2	6.86E-10	0.1
4	1.15E-32	5.4	4.50E-32	12.2	4.50E-32	12.2	1.98E-14	0.0	4.64E-09	1.4	4.68E-09	0.7
5	2.63E-32	12.5	5.85E-32	15.9	5.85E-32	15.9	8.86E-14	0.0	1.32E-08	4.0	1.33E-08	2.0
6	7.42E-33	3.5	1.65E-32	4.5	1.65E-32	4.5	1.68E-13	0.0	1.67E-08	5.0	1.68E-08	2.5
7	6.26E-33	3.0	2.73E-32	7.4	2.74E-32	7.4	1.47E-12	0.0	2.77E-08	8.3	2.85E-08	4.3
8	7.01E-33	3.3	1.78E-32	4.8	1.78E-32	4.8	3.43E-12	0.0	3.65E-08	11.0	3.75E-08	5.6
9	1.58E-33	0.7	3.07E-33	0.8	3.08E-33	0.8	2.93E-12	0.0	4.88E-09	1.5	5.21E-09	0.8
10	2.61E-33	1.2	1.05E-32	2.9	1.06E-32	2.9	2.28E-11	0.1	6.79E-08	20.4	7.27E-08	10.9
11	1.43E-33	0.7	3.75E-33	1.0	3.76E-33	1.0	2.39E-11	0.1	1.89E-08	5.7	2.11E-08	3.2
12	8.50E-34	0.4	3.17E-33	0.9	3.19E-33	0.9	1.24E-10	0.5	4.03E-08	12.1	4.88E-08	7.3
13	2.56E-34	0.1	1.28E-33	0.3	1.30E-33	0.4	2.28E-10	0.9	3.50E-08	10.5	4.76E-08	7.1
14	1.50E-34	0.1	8.21E-34	0.2	8.45E-34	0.2	6.92E-10	2.8	3.29E-08	9.9	5.69E-08	8.5
15	2.27E-35	0.0	1.21E-34	0.0	1.28E-34	0.0	4.25E-10	1.7	4.40E-09	1.3	1.25E-08	1.9
16	1.40E-35	0.0	8.45E-35	0.0	9.25E-35	0.0	7.76E-10	3.2	4.41E-09	1.3	1.78E-08	2.7
17	9.77E-36	0.0	6.05E-35	0.0	6.91E-35	0.0	1.36E-09	5.5	4.31E-09	1.3	2.47E-08	3.7
18	5.87E-36	0.0	3.89E-35	0.0	4.67E-35	0.0	1.76E-09	7.2	3.58E-09	1.1	2.86E-08	4.3
19	3.98E-36	0.0	2.52E-35	0.0	3.20E-35	0.0	2.29E-09	9.3	2.88E-09	0.9	3.23E-08	4.8
20	2.61E-36	0.0	1.67E-35	0.0	2.26E-35	0.0	2.51E-09	10.2	2.18E-09	0.7	3.31E-08	5.0
21	2.15E-36	0.0	1.26E-35	0.0	1.81E-35	0.0	3.20E-09	13.0	1.90E-09	0.6	3.90E-08	5.8
22	1.28E-36	0.0	7.46E-36	0.0	1.14E-35	0.0	2.67E-09	10.9	1.26E-09	0.4	3.24E-08	4.9
23	1.09E-36	0.0	5.69E-36	0.0	8.98E-36	0.0	2.70E-09	11.0	1.06E-09	0.3	2.97E-08	4.4
24	6.65E-37	0.0	3.43E-36	0.0	5.57E-36	0.0	1.89E-09	7.7	6.60E-10	0.2	2.06E-08	3.1
25	5.28E-37	0.0	2.41E-36	0.0	4.07E-36	0.0	1.72E-09	7.0	4.57E-10	0.1	1.68E-08	2.5
26	3.61E-37	0.0	1.62E-36	0.0	2.80E-36	0.0	1.30E-09	5.3	3.15E-10	0.1	1.26E-08	1.9
27	2.64E-37	0.0	1.07E-36	0.0	1.82E-36	0.0	8.92E-10	3.6	2.00E-10	0.1	7.72E-09	1.2
Total	2.11E-31	100	3.68E-31	100	3.68E-31	100	2.46E-08	100	3.33E-07	100	6.67E-07	100
Life*	4.74E+24		2.72E+24		2.72E+24		4.07E+01		3.00E+00		1.50E+00	

*: million years

8. Summary

A series of computational simulations has been carried out to identify possible failure modes and mechanisms of a composite riser. Burst analysis shows that the steel liner is the weakest element, and chances that the composite layers will experience any type of failure are remote. Although the steel liner is in relative vulnerability, it should be noted that the limit state set for the liner is not the ultimate strength, but the yield strength. Therefore, it is unlikely that the test pressure will lead to structural failure of the liner, considering that it will not be exposed to the maximum internal pressure throughout the service life. The internal pressure under the normal producing condition is merely 1/100 of the test pressure.

Buckling analysis shows that hydrostatic buckling will not be a possibility, either. Although the presence of the most extreme debond can significantly lower the critical buckling pressure, it is still over four times greater than the maximum hydrostatic pressure for 6000 ft water depth. For greater water depths, however, more detailed analysis should be performed, introducing geometric imperfections.

Under combined axial tension and bending moment, the stresses in the structural composite are further away from its long term allowables. The maximum observed stresses in the transverse normal and fiber directions are about 20% and 10% of the respective allowables. Again, the steel liner shows the highest stress to strength ratio of 40%. Although the combined thickness of the axial layers are smaller than that of the hoop layers, the stresses caused by the axial loadings are substantially smaller than those in the hoop direction.

Due to the combined effect of small axial stresses and excellent fatigue property of carbon fiber, the estimated fatigue life of the composite is practically infinite. The fatigue life of the steel liner is also shown to be sufficient. However, it should be mentioned that the fatigue life of the liner welds can be significantly lower and will need separate calculations.

REFERENCES

1. Demirbilek, Z., Tension Leg Platform: An Overview of the Concept, Analysis, and Design, Tension Leg Platform, Z. Demirbilek, ed. ASCE, New York, pp. 1-14, 1989.
2. Saad, P., Salama, M. M., and Jahnsen, O., Application of Composites to Deepwater Top Tensioned Riser Systems, Proceedings of 21st International Conference on Offshore Mechanics and Arctic Engineering, Oslo, Norway, OMAE 2002-28325, 2002.
3. Salama, M. M., Some Challenges and Innovations for Deepwater Developments, Offshore Technology Conference, Houston, TX, OTC 8455, 1997.
4. ABAQUS User's Manual,
5. Miller, C., Project Report, May 2005 Project Meeting at Stress Engineering Services, Inc., Houston, TX.
6. Zou, R. D. & Foster, C. G., Simple Solution for Buckling of Orthotropic Circular Cylindrical Shells, Thin-Walled Structures, Vol. 22, pp 143-158, 1995.
7. Hashin, Z. and Rotem, A., A Fatigue Failure Criterion for Fiber Reinforced Materials, Journal of Composite Materials, Vol. 7, pp. 448-464, 1973.
8. MIL-HDBK-17, The Composite Materials Handbook, ASTM International, 2002.
9. Miller, C., Private Communication, June 2005.
10. Guidance Notes on Spectral-Based Fatigue Analysis for Vessels, American Bureau of Shipping, 2004.
11. Recommended Practice for Planning, Designing, and Constructing Fixed Offshore Platforms – Load and Resistance Factor Design, API RP 2A-LRFD, American Petroleum Institute, 1993.

12. Miner, M. A., Cumulative Damage in Fatigue, *Journal of Applied Mechanics*, Vol. 12, pp. 159-164, 1945.
13. Green, A. K. and Pratt, P. L., The Axial Fatigue Behavior of Unidirectional Type IIS Carbon Fibre-Epoxy Resin Composites, *Composites*, Vol. 5, pp. 63-66, 1974.
14. Sims, D. F. and Brogdon, V. H., Fatigue Behavior of Composites Under Different Loading Modes, *Fatigue of Filamentary Composite Materials*, ASTM STP 636, American Society for Testing and Materials, pp. 185-205, 1977.
15. Lorenzo, L. and Hahn, H. T., Fatigue Failure Mechanisms in Unidirectional Composites, *Composite Materials: Fatigue and Fracture*, ASTM STP 907, American Society for Testing and Materials, pp. 210-232, 1986.
16. Lee, J. W., Daniel, I. M., and Yaniv, G., Fatigue Life Prediction of Cross-Ply Composite Laminates, *Composite Materials: Fatigue and Fracture*, 2nd Volume, ASTM STP 1012, American Society for Testing and Materials, pp. 19-28, 1989.
17. Halverson, H. G., Curtin, W. A., and Reifsnider, K. L., Fatigue Life of Individual Composite Specimens Based on Intrinsic Fatigue Behavior, *International Journal of Fatigue*, Vol. 19, No. 5, pp. 369-377, 1996.

Conversion Factors for Different Units of Measurements			
Quantity	SI Unit	Other Unit	Inverse Factor
Length	1 m	3.281 feet (ft)	0.3048 m
	1 km	0.540 nautical miles	1.852 km
	1 km	0.6213712 mile	1.609344 km
Area	1 m ²	10.764 ft ²	0.0929m ²
Volume	1 m ³	35.315 ft ³	0.0283 m ³
	1 m ³	264.2 gallon (US)	0.00379 m ³
	1 m ³	220.0 gallon (UK)	0.00455 m ³
	1 m ³	6.29 barrel (US Petroleum)	0.1589 m ³
Velocity	1 m/s	3.281 ft/s	0.305 m/s
	1 m/s	1.943 knot	0.515 m/s
	1 m/s	2.2369 mph	0.44704 m/s
	1 km/hr	0.62137 mph	1.6093 km/hr
Mass	1 kg	2.205 pound	0.454 kg
	1 Mg	0.984 ton (long)	1.016 Mg
	1 Mg	1 tonne (metric)	1 Mg
Force	1 N	0.225 pound force	4.448 N
	1 MN	100.4 ton force	9964 N
	1 MN	224.81 kip	4448 N
	1 kg-force	0.0022046 kip	453.592 kg-force
Pressure	1 N/m ²	0.000145 psi	6895 N/m ²
	1 kg-force/cm ²	0.01422 ksi	70.307 kg-force/cm ²
	1 MN/m ²	20.885 kip/ft ²	47880 N/m ²
Energy	1 J	0.738 foot pounds	1.356 J
Power	1 W	0.00134 horsepower	745.7 W
Temperature	0 ⁰ Celsius	32 ⁰ Fahrenheit	-17.78 ⁰ Celsius
Frequency	1 cycle/s	1 hertz	1 cycle/second
Flow Rates	1 m ³ /day	6.289 barrel/day	0.1589 m ³ /day
	1 m ³ /day	35.3146 ft ³ /day	0.0283 m ³ /day
Density	1 g/cm ³	0.578 oz./inch ³	1.73 g/cm ³

Appendix C:

Risk Analysis Of Steel Production Risers For Deepwater Offshore Facilities

by

Anubhav Jain,
MS Thesis The University of Texas at Austin, December 2004

**RISK ANALYSIS OF STEEL PRODUCTION
RISERS FOR DEEPWATER OFFSHORE
FACILITIES**

by
Anubhav Jain, B. Tech.

**Masters Thesis
Presented to the Faculty of the Graduate School of the University of Texas at Austin**

**Supported by Funding From:
Minerals Management Service
Under the MMS/OTRC Cooperative Research Agreement
1435-01-99-CA-31003
Task Order 73632
MMS Project Number 490**

December 2004

OTRC Library Number: 12/04B146

“The views and conclusions contained in this document are those of the authors and should not be interpreted as representing the opinions or policies of the U.S. Government. Mention of trade names or commercial products does not constitute their endorsement by the U. S. Government”.



For more information contact:

Offshore Technology Research Center

Texas A&M University
1200 Mariner Drive
College Station, Texas 77845-3400
(979) 845-6000

or

Offshore Technology Research Center

The University of Texas at Austin
1 University Station C3700
Austin, Texas 78712-0318
(512) 471-6989

A National Science Foundation Graduated Engineering Research Center

Copyright
by
Anubhav Jain
2004

**RISK ANALYSIS OF STEEL PRODUCTION RISERS FOR DEEPWATER
OFFSHORE FACILITIES**

by

ANUBHAV JAIN, B. TECH.

THESIS

Presented to the Faculty of the Graduate School of
The University of Texas at Austin
in Partial Fulfillment
of the Requirements
for the Degree of

MASTER OF SCIENCE IN ENGINEERING

The University of Texas at Austin

December 2004

**RISK ANALYSIS OF STEEL PRODUCTION RISERS FOR DEEPWATER
OFFSHORE FACILITIES**

**APPROVED BY
SUPERVISING COMMITTEE:**

Robert B. Gilbert

Elmira Popova

Dedicated to my parents

Acknowledgements

I wish to express my deep sense of gratitude to my co-supervisors Dr. Robert Gilbert and Dr. Elmira Popova, for their valuable guidance, consent for me to work with them and generous help at every stage of the report in all possible manners. Nothing helped me more than their encouragement and the insights that they had provided into the technical details of the project. I also take this opportunity to thank other team members of the project, who provided all the valuable information when needed and constant support throughout the life of the project. I would specially like to thank Dr. Robert Gilbert for his constructive comments, valuable insights and assistance provided during the development of the problem solution and during the organization and structure of the report.

I am also thankful to my friends and colleagues for their help and support. In the end I would like to thank my family for their unconditional support, constant encouragement and inspiration without which this work would not have been accomplished.

RISK ANALYSIS OF STEEL PRODUCTION RISERS FOR DEEPWATER
OFFSHORE FACILITIES

by

ANUBHAV JAIN, M.S.E

The University of Texas at Austin, 2004

CO-SUPERVISORS: Robert Gilbert, Elmira Popova

A probabilistic methodology is developed to quantify the risks associated with structural failure of a steel production riser and in deepwater oil and gas production. First, background on the steel production riser is presented, detailing its functions, main components, operational phases and design considerations. Next, the study riser, developed by Stress Engineering, is described and its design basis is presented. A fault tree of failure scenarios is then developed and analyzed. Fatigue is identified as the primary failure mechanism affecting the risk for a production riser between its base at the mud-line and its top at the sea level. Bursting, collapsing and yielding are not likely for the riser. Probabilistic fatigue analysis is carried out to better understand and quantify the probability of a fatigue failure. This analysis includes development of probabilistic model and quantifying the uncertainties in the input to the model.

It was concluded that the probability of fatigue failure in a 20 yr design life is on the order of 1 in 1000 or smaller. This probability is consistent with the levels that are accepted in the offshore industry. The risk is very sensitive to the parameters of the weld, including the size and frequency of cracks in the weld and the properties of the intact weld material. The size and frequency of the crack in the weld depend on the quality of initial weld and the level of quality control in inspecting the weld for defects to the repaired. The critical location in the production riser with respect to the fatigue is at its base.

Table of Contents

ACKNOWLEDGEMENTS	V
ABSTRACT	VI
TABLE OF CONTENTS	VII
LIST OF FIGURES	X
LIST OF TABLES.....	XII
LIST OF TABLES.....	XII
CHAPTER 1: INTRODUCTION	1
1.1 Objectives of the Study	1
1.2 Motivation.....	1
1.3 Composite Risers.....	2
1.4 Steel Risers: Conventional Technology	2
1.5 Scope.....	3
1.6 Methodology	3
1.7 Thesis Structure	4
CHAPTER 2: BACKGROUND ON PRODUCTION RISERS.....	5
2.1 Production Riser.....	5
2.2 Components of Production Riser	5
2.3 Operation Phases of Production Riser	7
2.4 Design Considerations for a Production Riser	7
2.4.1 Yielding	8
2.4.2 Burst Pressure	10
2.4.3 Collapse Pressure.....	11
2.4.4 Propagating Collapse Pressure.....	12
2.4.5 Fatigue	12
2.5 Summary.....	13
CHAPTER 3: DESIGN OF THE STUDY RISER	14
3.1 Design Approach	14

3.2	Design Load Cases.....	15
3.3	Study Riser Design	16
CHAPTER 4: FAILURE ANALYSIS OF THE STUDY RISER		18
4.1	Methodology	18
4.2	Fault Tree.....	19
4.3	Analysis of Fault Trees	22
4.3.1	Collapse	22
4.3.2	Bursting	23
4.3.3	Yielding	26
4.3.4	Propagating Collapse.....	27
4.3.5	Fatigue Failure.....	28
4.4	Summary.....	28
CHAPTER 5: PROBABILISTIC FATIGUE ANALYSIS OF STUDY RISER		29
5.1	Literature Review on Fatigue Crack Growth Models	29
5.2	Integration of Random Load Cycles Fatigue Model	33
5.3	Verification of Model	34
5.4	Evaluation of Final Crack Length with Stress Path.....	35
5.5	Flowchart for Probabilistic Fatigue Analysis	37
5.6	Summary.....	38
CHAPTER 6: STRESS AMPLITUDE DISTRIBUTION FOR STUDY RISER...39		
6.1	Introduction.....	39
6.2	Wave Scatter Diagram.....	40
6.3	Wave Spectrum	40
6.4	Stress Response.....	44
6.5	Stress Amplitude versus Number of Cycles.....	46
6.6	Summary.....	49
CHAPTER 7: FATIGUE FAILURE ANALYSIS WITH RANDOM LOAD FOR STUDY RISER		50
7.1	Moments of Z.....	50
7.2	Coefficient of Variation of Z	52
7.3	Final Crack length: Uncertainty Analysis.....	53
7.4	Sensitivity of Crack Growth to Weld Joints	56
7.5	Sensitivity of Crack Growth with Material Properties	58

7.6	Failure Envelope.....	60
7.7	Sensitivity of Crack Growth with Life of Study Riser	60
7.8	Summary.....	61
CHAPTER 8: FATIGUE FAILURE PROBABILITY FOR STUDY RISER.....		63
8.1	Uncertainty in Initial Crack Length, a_i	63
8.2	Uncertainty in Initial Crack Density, v_i	67
8.3	Uncertainty in m and C	69
8.4	Critical Failure Point	70
8.5	Fatigue Failure Probability	72
8.5.1	Fatigue Failure probability with constant m and C	72
8.5.2	Final Fatigue Failure Probability	73
8.6	Sensitivity of Final Fatigue Failure Probability with $E[C]$ and $E[m]$	73
8.7	Summary.....	75
CHAPTER 9: CONCLUSIONS		76
9.1	Conclusions	76
9.2	Future Work.....	77
APPENDIX A: EXPECTATION AND VARIANCE OF 'Z'		79
APPENDIX B: MOMENTS OF A RAYLEIGH DISTRIBUTION		80
APPENDIX C: DYNAMIC STRESSES ALONG THE LENGTH OF THE RISER FOR 27 SEA STATES.....		81
APPENDIX D: RESULTS		89
REFERENCES		96
VITA		99

List of Figures

Figure 2-1: Schematic Illustration of Top-Tensioned Production Riser, API 2RD (1998)	6
Figure 3-1: Riser Design.....	17
Figure 4-1: Schematic Representation of a Riser with SCSSV	20
Figure 4-2: Fault Tree Leading to a Through Wall Crack.....	21
Figure 4-3: Net Inter Pressure and Burst Strengths	26
Figure 5-1: Schematic S-N curve.....	29
Figure 5-2: Crack length vs Number of Cycles for Different Stress Amplitudes.....	31
Figure 5-3: Crack growth at Stress Amplitude of 100 MPa and 150 MPa, as in Figure 4 of Ref [15](reproduced and scaled).....	35
Figure 5-4: Crack Growth at Stress Amplitude of 100 MPa and 150 MPa	35
Figure 5-5: Stress Histogram	36
Figure 5-6: Fatigue Crack Growth for Different Stress Paths	36
Figure 5-7: Flowchart of the Data Flow among the Key Components of Fatigue	38
Figure 6-1: Frequency Distribution of the 27 Sea States.....	40
Figure 6-2: Wave Pattern from Combining Four Regular Waves, Michel (1967)	41
Figure 6-3: Energy Spectrum for the Resultant Wave Depicted in Figure 6-2, Michel (1967).....	43
Figure 6-4: Figure Illustrating the Connection between a Frequency Domain and Time Domain Representation of Waves in a Short Term Sea-State, Stress Engineering ..	43
Figure 6-5: An Example of Stand Deviations of Stress Ranges for Sea-states at 54feet Elevation above Mud-line, Stress Engineering.....	47
Figure 6-6: An Example of Zero-Crossing Time Period of Stress Load Cycles for Different Sea-States at 54feet Elevation above Mud-line.....	47
Figure 6-7: Example, Rayleigh Distribution Function for the Stress Amplitude at 54feet Elevation above Mud line under 2 nd Sea State.....	48
Figure 6-8: Expected Number of Stress Range Load Cycles vs its Standard Deviation ..	49
Figure 7-1: C.o.v. of Z at Different Points of Riser for Different m Values	53
Figure 7-2: Variation of a_N with Z for $a_i=.5$, $m=3$ and $C=1e-13$ at 54feet of Elevation above Mud-line.	54
Figure 7-3: Change in $E[s^m]$ with the Location of Weld in Riser.....	57
Figure 7-4: Change in $E[s^m]$ with the Elevation Point of Riser, Magnified for Range between 0 feet and 180 feet	57
Figure 7-5: Sensitivity of the Final Crack Length with m for Different C at 54 feet of Elevation above Mud-line for $a_i=4mm$	58
Figure 7-6: Sensitivity of the Final Crack Length with m for Different a_i at 54 feet of Elevation above Mud-line for $C=7E-13$	59
Figure 7-7: Sensitivity of the Final Crack Length with C for Different a_i at 54 feet of Elevation above Mud-line for $m=3$	59
Figure 7-8: Failure Envelope with Respect to m, C, a_i at 54 feet of Elevation above Mud- line.....	61

Figure 7-9: Sensitivity of Crack Growth with Life of Study Riser at $m=3$ and $a_i=.5$ mm	61
Figure 8-1: Probability of Detection Curve Based on ref [14]	65
Figure 8-2: Probability Density Function of the Crack Length	67
Figure 8-3: Failure Envelope w.r to m, C, a_i at 106 feet Elevation above Mud-line	71
Figure 8-4: Failure Envelope w.r to m, C, a_i at 54 feet Elevation above Mud-line	72
Figure 8-5: Sensitivity of Probability of Failure with $E[C]$ and $E[m]$ at 54 feet Elevation above Mud-line	74
Figure 8-6: Sensitivity of Probability of Failure with $E[C]$ and $E[m]$ at 116 feet Elevation above Mud-line	74

List of Tables

Table 3-1: Design Properties for Riser Pipe Steel	14
Table 3-2: Design Load Cases	15
Table 3-3: Design Load Cases Rationale.....	16
Table 3-4: Design of Steel Production Riser	16
Table 4-1: List of Meetings.....	18
Table 4-2: Calculation of Collapse Strength of the riser	23
Table 4-3: Internal Pressure Calculations for Case WPT-1	24
Table 4-4: Burst Strength Calculations for (4004feet<X<5988feet).....	25
Table 4-5: Burst Strength Calculation Changes for (54feet<X<4004feet).....	25
Table 4-6: Summary of Maximum Stress during extreme Sea- States.....	27
Table 4-7: Calculations for Propagating Collapse	27
Table 6-1: Deep Water Characteristics of Regular Waves, [18]	42
Table 8-1: Numerically Solved to Find the Chances of g Cracks in a Weld.....	68
Table 8-2: Probabilistic Models of C and m.....	70
Table 8-3: Failure or Safe Regions for Welded Joints at 54feet and 106feet Elevation...	71

Chapter 1: Introduction

1.1 Objectives of the Study

The primary objective of the study is to assess the risk analysis of steel production risers for deepwater offshore production facilities. It also creates the foundation for comparative risk analysis of the composite and steel production risers in Gulf of Mexico.

1.2 Motivation

Deepwater (more than 3000 feet deep) production risers face lot of problems due to its high weight, large size, high hydrostatic pressure, low stability, and have not been very common in Gulf of Mexico. Failure of these risers results in high cost, more pollution to the environment, and may also lead to high fatality rates. It is good to understand the risks associated with these deepwater risers before they get more common in Gulf of Mexico.

A lot of emphasis has been made on the use of composite production riser in the last few years owing to its low weight, excellent fatigue and corrosion performance and high strength. Thus major industries have shown major interest in the development, qualification and commercialization of composite risers for deepwater offshore applications. Kvaerner Oilfield Products, [1], installed several joints of composite riser on ConocoPhillips' Heidrum tension leg platform in the North Sea. With the emergence of this new technology, there is a need to identify the risks associated with it in comparison to the existing technology and understand that the proposed system with the new technologies is at least as reliable as existing systems, particularly in the deep water domain. This study will also form the basis for the comparative study of the risks between the steel and composite production risers in deep water offshore production facilities.

1.3 Composite Risers

The composite is not a new technology and has been around for more than 40 years with the aerospace industry. This industry, being very particular about its weight and quality sensitive, has recognized its unique properties. It is because of the success in this industry, Deepwater Offshore industry too is venturing in it to take advantage of it. Deepwater operations (more than 3000 feet water depth) require high tension carrying capacities due to increased length of the production risers. Lester Bruno, [1], in ABB Vetco Gray's Capital Drilling Equipment's sales department said "If you took an existing string of steel riser on a rig that is rated for 5000 feet of water and only put composite choke and kill lines or a composite auxiliary line on it, then you could probably take that rig to 6000 or 6500 feet without additional tensioning capacities, deck load considerations or buoyancy considerations". This implies that the cost of tensioning capacity is greatly reduced with the use of composites, which would also favor small size of the tension leg platforms and less buoyancy materials. The composites are also seen to be more corrosion resistant and can be designed to offer more strength and stiffness.

1.4 Steel Risers: Conventional Technology

Steel Production risers have been used in deepwater oil and gas applications for many years.. Steel risers have been proved to be successful through out the life cycle of the risers and have been seen to withstand all the extreme conditions imposed on it by the environment. It is very unlikely that a steel riser will fail due to high ductility of steel. A steel riser first yields and then fails after it has exceeded its ultimate tensile strength. Due to high steel toughness, steel risers are also very robust against the impacts due to dropped objects or collisions with another riser.

1.5 Scope

The scope of this thesis is to assess the risks for the deepwater (approximately 6000 feet deep) production risers. A generic riser design that is representative of existing technology in the Gulf of Mexico is described in Chapter 3. The study riser serves the purpose to develop the probability methodology and understand the sensitivity of the various factors leading to failure scenarios for a riser. The results are limited to the design of the riser considered, but could easily be extended to other risers using the same methodology.

1.6 Methodology

The methodology for the project is defined in the following steps:

- i) Study the production riser
- ii) Be a part of a cross functional team comprising of the following team members.
 - a. E.G.Ward, Associate Director, Offshore Technology Research Center, College Station
 - b. Chuck Miller, Principal, Stress Engineering Services, Inc, Houston
 - c. Early Denison, Consultant
 - d. Robert Gilbert, Associate Professor, University of Texas at Austin, Austin
 - e. Ozden Ochoa, Expert in Composites, Texas A&M University, College Station
 - f. Representative of Material Management Services
- iii) Development of fault tree
- iv) Identification of critical failure modes of the study riser
- v) Probabilistic fatigue failure analysis
- vi) Uncertainty analyses of the critical factors
- vii) Failure probability analyses
- viii) Sensitivity analyses of failure probability with factors affecting it

1.7 Thesis Structure

This report is divided into nine chapters. After presenting the objectives, motivation, study barriers and methodology in this chapter, background on steel production risers is described in Chapter 2. The study riser, developed by Stress Engineering, is explained in Chapter 3, with the design basis. Chapter 4 presents the fault tree explaining the multiple scenarios of failure followed with a preliminary analysis to identify critical failure mechanisms for the study riser.

After identification of the fatigue as the critical failure mechanism, Chapter 5 develops a foundation of the fatigue model with the necessary literature review. Chapter 6 presents the detailed spectral analysis conducted by Stress Engineering to quantify the uncertainties in the stress range cycles, required for fatigue analyses. Chapter 7 customizes the fatigue model (adopted in Chapter 5) for the current needs and uses it to make inference about the final crack length subjected to random load history. All other factors were kept constant at this stage. Chapter 8 discusses the uncertainties associated with the other factors (initial crack length, total number of cracks, material parameters m and C) to find the final fatigue failure probability. Chapter 9 discusses the conclusions of the thesis and the future work.

In addition there are four appendices supporting the information required during the development of the thesis. Finally the References section is included containing the list of references cited in the report.

Chapter 2: Background on Production Risers

The objective of the chapter is to provide an overview on production risers in the context of the offshore oil and gas production, which is very important before any risk analysis is carried out. This chapter describes the functions, the components, the phases of operation and the design considerations for a production riser.

2.1 Production Riser

In offshore oil and gas industry, various fluids (including oil, gas and water) are produced from a reservoir and carried from a sub-sea well to a surface platform for processing and transport. A production riser is a protective casing for the fluid conduit between the sub-sea equipment and the surface platform. It comprises metal pipe cross-sections that may be thought of as a continuation of the well bore to the ocean's surface (Figure 2-1). The main functions of the riser, described in APIRP-2RD (1998), can be summarized as follows:

- i. Provide structural support to limit bending stresses during production in the production tubing that carries the production fluids from the well head to the surface through the water column.
- ii. Provide a secondary containment during production in the event of a leak in the production tubing.
- iii. Provide primary containment of drilling fluids during well drilling and maintenance activities.

2.2 Components of Production Riser

The riser is made by connecting small pipe segments, called joints, together with welded connections. There are three main types of joints.

- a. *Standard joint*: These joints comprise most of the riser length and are steel pipes that are normally 10 inch in diameter, 1 inch thick and 60 feet long. They start after one joint above the mud-line (stress joint) and end just before the tensioner joint.
- b. *Stress Joint*: The lowermost pipe segment is the tapered stress joint. The joint's function is to withstand the bending moments in the riser and at the sea-floor.

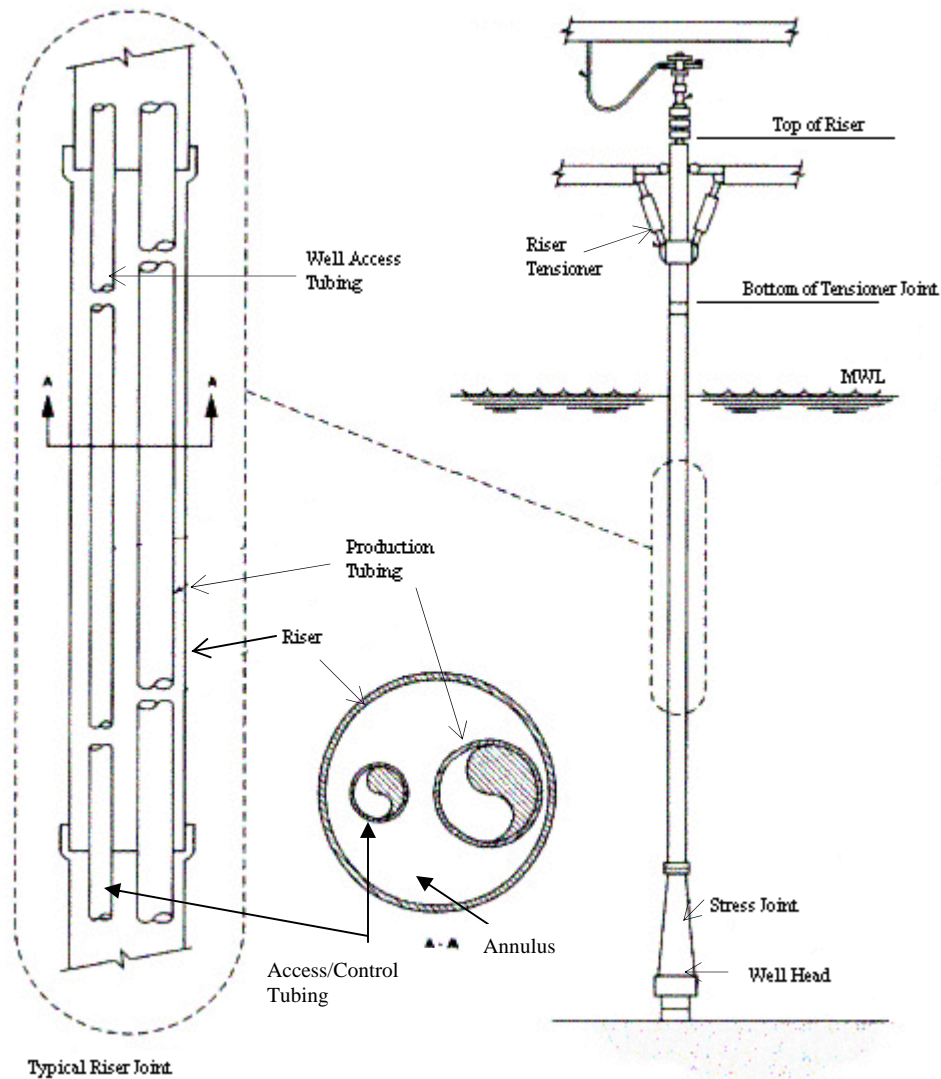


Figure 2-1: Schematic Illustration of Top-Tensioned Production Riser, API 2RD (1998)

- c. *Tensioner Joint*: The uppermost pipe segment is called the tensioner joint. This joint's function is to withstand the high axial loads in the riser at the top due to its

weight. Some intermediate joints may contain buoyancy or have buoyancy components attached to reduce the weight of the riser string in the water column.

- d. *Annulus*: The space inside in the riser, not occupied by the production tubing, is the annulus.
- e. *Weld Connections*: Two joints are connected to each other through a weld and the connection is called the weld connection.

2.3 Operation Phases of Production Riser

A production riser is subjected to different phases of operation during its life time, which are as follows:

- i. *Installation Phase*: During the installation phase, the riser joints are welded together and the riser is attached to the well-head and platform.
- ii. *Production Phase*: During the production phase, the riser is used to produce oil. It carries the inner production tubing and well-control access tubing. The annulus may contain liquid or gas, which insulates and protects the production tubing.
- iii. *Drilling Phase*: During operations are conducted periodically throughout the life of the riser to maintain and extend the well. During this mode, the production and access/control tubing are removed and replaced with drill pipe. The annulus is filled with drilling mud to provide a hydrostatic balance to the reservoir pressure.
- iv. *Shut-in Phase*: Production shut in is done to stop the production flow, which occurs periodically in anticipation of a hurricane or extreme sea conditions or due to operational disruptions.

2.4 Design Considerations for a Production Riser

There are two primary design considerations for a production riser:

- i) *Structural Integrity*: The production riser is the interface between a static structure on the ocean floor and the dynamic floating structure at the ocean's

surface and is thus subjected to a variety of static and dynamic loads. It is also subjected to pressure differentials between the inside and the outside.

- ii) *Containment*: The riser needs to contain the production fluids during a tubing leak if it were to occur during production and the drilling fluids during drilling in order to protect the environment.

Riser stress analysis is performed to determine if the pipeline stresses are acceptable during all its operational phases. The analysis performed to verify that stresses experienced are acceptable include: yield, burst, collapse, and propagating pressure collapse.

2.4.1 Yielding

The three principal stresses are calculated at all critical locations in the production risers. For standard joints, these principal stresses are in the axial, hoop and radial directions. The following principal stress combinations are compared to yield stress, Y , according to API RP 2RD (1998).

Primary Principal Stress: If a primary normal or shear stress exceeds the yield strength, either failure or gross structural yielding will occur. The two types of primary principal stress are

- a. *Primary Membrane Stress*: This is the average stress across the thickness of a solid section, excluding the effects of discontinuities and stress concentrations. For example, the general primary membrane stress in a pipe loaded in pure tension is the tension divided by the cross-sectional area.

For a thick walled pipe, the three principal membrane stress components are σ_{rr} , $\sigma_{\theta\theta}$, σ_{zz} , where r , θ , and z refer to radial, hoop and axial stresses.

$$\sigma_{rr} = -\frac{P_o D_o + P_i D_i}{D_o + D_i} \quad \text{Eq 2-1}$$

$$\sigma_{\theta\theta} = (P_i - P_o) \frac{D_o}{2t} - P_i \quad \text{Eq 2-2}$$

$$\sigma_{zz} = \frac{T}{A} \pm \frac{M}{2I} (D_o - t) \quad \text{Eq 2-3}$$

where:

P_i, P_o : Internal Pressure and External Pressure

D_o, D_i : Outside and Inside Diameter

t : Thickness of the Riser Pipe

A : Cross-section Area = $\pi/4(D_o^2 - D_i^2)$

T : True Wall Tension in Pipe at Section being Analyzed

M : Global Bending Moment in Pipe

I : Moment of Inertia = $\pi/64(D_o^4 - D_i^4)$

All these stress components at the section of the riser are combined using the von-Misses yield criterion, API 2RD RP (1998), to find the net primary stress, σ_p , due to the loads.

$$\sigma_p = \frac{1}{\sqrt{2}} \sqrt{(\sigma_{rr} - \sigma_{zz})^2 + (\sigma_{rr} - \sigma_{\theta\theta})^2 + (\sigma_{zz} - \sigma_{\theta\theta})^2} \quad \text{Eq 2-4}$$

A failure may result if the above von Misses stress exceeds the yield strength, Y , times the design case factor, C_f . API 2RD RP (1998) requires the C_f to be between .66 and 1, depending on the loading condition. Yong Bai (2001) suggests it to be .72.

- b. *Primary Bending Membrane Stress*: This stress is the portion of primary stress proportional to the distance from the centroid of a cross section, excluding the effects of discontinuities and stress concentrations. As suggested in API RP 2RD (1998) this stress is displacement controlled and thus is considered as secondary stresses.

Bending stresses that exceed yield strength do not in general cause gross structural yielding and failure.

Secondary Stress: This stress is any normal or shear stress that develops as a result of material restraint. This type of stress is self limiting which means that local yielding can relieve the conditions that cause the stress, and an event where this stress exceeds the yield strength will not cause failure.

2.4.2 Burst Pressure

The riser pipe should be designed to withstand the maximum differential pressure between internal and external pressures that may occur during installation, production and drilling. The maximum differential pressure for burst occurs during drilling, when the drilling mud is used to kill the pressure of the well-bore. In addition, an unanticipated entry of formation fluids into the well-bore during drilling, due to a loss of control of well (called a kick), may lead to the maximum differential pressure for burst. During production, a leak in production tubing may also lead to burst conditions.

API RP 1111 (1999) presents a formulation representing the burst capacity of pipelines as shown in Eq 2-5. A burst or parting of the riser occurs when the maximum internal differential pressure exceeds the burst capacity times the burst design factor, f_d . API RP 1111 (1999) requires this factor to be .75 for risers.

$$p_b = .45(Y + U) \log\left(\frac{D_o}{D_i}\right) \quad \text{Eq 2-5}$$

where,

U : Ultimate Tensile Strength

Y : Yield Strength

2.4.3 Collapse Pressure

Collapse of the riser pipe could occur when the external pressure is higher than the internal pressure. This condition occurs mainly during installation conditions when there is no fluid inside and thus no internal pressure. For deepwater risers, this condition is more crucial, as there is a high hydrostatic external pressure

The collapse of the riser is governed by its collapse strength, which explains the maximum external differential pressure, the riser can hold without failure. API RP 2RD (1998) suggests a formulation for the collapse pressure strength as shown in Eq 2-6. The effect tension was also accounted by it, unlike the formulation presented in API RP 1111 (1999). A riser collapses, when the maximum external differential pressure exceeds the collapse strength times the design factor, D_f . Both API RP 2RD (1998) and API RP 1111 (1999) suggests this design factor to be 0.7.

$$P_c = \frac{P_y P_e}{\sqrt{P_y^2 + P_e^2}} \quad \text{Eq 2-6}$$

where,

$$P_y : \text{Yield Pressure at Collapse} = \frac{2Y_r t}{D_o}$$

$$P_e : \text{Elastic Collapse Pressure} = 2E \frac{\left(\frac{t}{D_o}\right)^3}{(1-\nu^2)}$$

$$Y_r : \text{Reduced Yield strength due to axial stress} = \left[\sqrt{1 - .75(S_a/Y)^2} - .5(S_a/Y) \right] Y$$

S_a : Axial Stress

ν : Poisson's Ratio (0.3 for steel)

E : Modulus of Elasticity

2.4.4 Propagating Collapse Pressure

Dents induced by impact by foreign objects, local buckles induced by excessive bending during installation or under operational off-design conditions and wall thickness reduction due to wear and corrosion can locally reduce the collapse pressure strength of a riser pipe and induce local collapse. This local collapse can initiate a buckle which propagates at high speed and has the potential of becoming a global collapse. The lowest pressure at which such a buckle propagates is the propagation pressure (P_p), a characteristic pressure of the pipe. The propagation pressure is typically only one-fourth to one-eighth of the collapse pressure (P_c). Periodic placement of buckle arrestors along the line can ensure that collapse only affects the length of pipe between the two arrestors on either side of the initiation site. The arrestor spacing is usually driven by practical considerations.

In order to avoid this collapse, the external differential pressure should be less than the propagation pressure (P_p) times the design factor, D_p . API RP 2RD (1998) suggests a formulation of the propagation pressure as shown in Eq 2-7, with the design factor as 0.72. It also suggests that the collapse criterion (Section 2.4.3) is met if pipe design is sufficient to meet the propagation pressure criterion.

$$P_p = 24Y \left[\frac{t}{D_o} \right]^{2.4} \quad \text{Eq 2-7}$$

2.4.5 Fatigue

The integrity of the riser pipe is only as good as the welds between joints. In these welds, cracks induced by the welding process may grow under cyclic loading and lead to a failure of the pipe when the crack extends through the weld (called a through wall crack). The growth of a crack depends on the number of cycles of different stress amplitudes applied to the weld over its lifetime. Generally a large number of cycles of working stresses govern failure versus a small number of cycles. Since the fatigue behavior is

dependent on a number of parameters including initial crack geometry, stress history and the material characteristics, it is difficult to develop general fatigue design guidelines and thus this factor is not included in the conventional design.

2.5 Summary

This chapter gives background information on production risers. Production risers are made up of three types of joints standard joints, stress joint and tensioner joint. It is subjected to four types of operational phases in its lifetime: installation phase, production phase, drilling phase and shut-in phase. Primary design considerations of a production riser are to maintain structural integrity and containment of fluids. A production riser can fail through yielding, bursting, collapsing and fatigue.

Chapter 3: Design of the Study Riser

The study riser selected for analysis in this research is a top tensioned riser on a Tension Leg Platform (TLP) in 6000 feet of water. This riser is typical of existing systems and technologies that are currently being used in Gulf of Mexico because these systems and technologies have been approved and therefore represent acceptable risks. Thus this riser faces all the environment loads prevalent in Gulf of Mexico. The design for the study riser was developed for this research by Stress Engineering. The design load cases used by Stress Engineering are discussed and component dimensions presented.

3.1 Design Approach

The following criteria were used to develop the conceptual description for the study riser.

- 1) The study riser is a top tensioned riser in Tension Leg Platform (TLP).
- 2) The study riser has to stand a water column of 6000 feet in Gulf of Mexico.
- 3) Design properties for the Riser pipe steel is shown in Table 3-1

Table 3-1: Design Properties for Riser Pipe Steel

T_o	Top Tension (lbs)	860,000
σ_y	Yield Strength (psi)	70,000
U	Ultimate Tensile Strength (psi)	80,000
E	Modulus of Elasticity (psi)	30,000,000
ν	Poisson's ratio	0.3

- 4) The key issues in strength design are loads, resistance and acceptance criteria.

Acceptance design criteria are typically formulated as explained in Section 2.4. The resistance consists of characteristic resistance and design factors. The characteristic resistance is defined for yielding, bursting, collapsing, propagating pressure collapsing as yield strength, burst strength, collapse strength and propagating pressure respectively, which are also explained in Section 2.4.

The loads are classified to 3 categories as functional, environmental and accidental loads. Some load cases, called design load cases, are defined which are a combination of the different categories and which govern the design of the riser. These load cases are dependent on the kind of region and presented by Stress Engineering for Gulf of Mexico as shown in Section 3.2.

3.2 Design Load Cases

Various design cases were developed by Stress Engineering based on standard practices for riser design. These load cases are presented in Table 3-2 and their rationale in Table 3-3. Each load case is a combination of the following load categories.

- i) *Riser condition*: It tells the operating condition of the riser
- ii) *Contents*: The density of the fluid in the annulus and production tubing in pounds per gallon (ppg)
- iii) *Internal Pressure*: The internal pressure of the annulus and production tubing in psi
- iv) *Design Environment*: The type of extreme environment condition
- v) *Damage Condition*: Represents riser damage condition of the riser
- vi) *Tensioner factor*: This is the ratio of the top tension to the weight of the riser

Table 3-2: Design Load Cases

Case	Riser Condition	Contents (ppg)		Int. Press. (psi)		Design Environment	Damage Condition	Tension Factor
		Annulus	Tubing	Annulus	Tubing			
WPT-1	Riser Pressure Test	8.60	NA	10,000	NA	1 Yr. Winter Storm	Intact	1.30
PNS-1	Normal Shut-in	0.04	5.50	0	8,500	1 Yr. Winter Storm	Intact	1.30
PHN-1	Shut-in w/ Hurricane	0.04	5.50	100	8,500	100 Yr. Hurricane	Intact	1.30
PCN-1	Maximum Producing	0.04	5.50	100	8,500	100 Yr. Loop Current	Intact	1.60
PCL-1	Shut-in w/ Leak	5.50	5.50	8,500	8,500	100 Yr. Loop Current	Intact	1.60
PCK-T1	Well Killed-Tubing	15.50	15.50	0	0	100 Yr. Loop Current	Intact	1.60
PNK-T1D	Well Killed-Tubing	15.50	15.50	0	0	1 Yr. Winter Storm	Lost 1 Ten. Cyl.	1.08

Table 3-3: Design Load Cases Rationale

Case	Rationale
WPT-1	Maximum Internal Pressure, govern Burst failure
PNS-1	Maximum pressure with a normal operating stress criterion
PHN-1	Maximum storm condition with extreme stress criterion
PCN-1	Maximum Producing
PCL-1	Maximum pressure condition with survival stress criterion
PCK-T1	Heaviest riser with an extreme storm condition
PNK-T1D	Heaviest riser with lowest tension

3.3 Study Riser Design

Based on the above design approach and load cases, a global analysis of the study riser was performed by Stress Engineering to estimate the stresses during each load cases. The different riser joints and their positions along the riser are described in Table 3-4 and shown on Figure 3-1. Four top tension cylinders were used to maintain a top tension of 860 kips.

Table 3-4: Design of Steel Production Riser

Region	O.D. (in.)	I.D. (in.)	Region Extremities		Joint Length (ft.)	Air Wts		Submerged Wts		Ext. Fluid Density (ppg)	Intl. Fluid Density (ppg)
			Bottom (ft.)	Top (ft.)		Joint (lbs)	Unit (lbs/ft)	Joint (lbs)	Unit (lbs/ft)		
Foundation Casing	36	32	-20	10	30	21808	726.93	18960	632	8.56	0.04
Stress Jt. Btm. Straight Reg.	15.722	9.722	10	12	2	1310	655.16	1139	569.6	8.56	0.04
Stress Jt. Taper Reg.	15.722	9.722	12	42	30	8655	288.49	7524	250.8	8.56	0.04
Stress Jt. Straight Reg.	11.75	9.722	42	54	12	1780	148.34	1547	129	8.56	0.04
Bare Std. Jt.	11.75	9.722	54	4004	62	7692	124.07	6687	107.9	8.56	0.04
Std. Jt. With Fairings	11.75	9.722	4004	5988	62	8214	132.48	6838	110.3	8.56	0.04
Std. Jt. Below MWL	11.75	9.722	5988	6000	62	7692	124.07	6687	107.9	8.56	0.04
Bare Std. Jt.	11.75	9.722	6000	6050	62	7692	124.07	7692	124.1	0	0.04
Tensioner Joint - Reg. 1	11.75	9.722	6050	6055	5	849	169.83	849	169.8	0	0.04
Tensioner Joint - Reg. 2	15	9.722	6055	6065	10	3487	348.72	3487	348.7	0	0.04
Tensioner Joint - Reg. 3	15.25	9.722	6065	6088	23	8485	368.93	8485	368.9	0	0.04
Production Tubing	5.5	4.67	10	6088	40	902	22.56	902	22.55	0.04	5.5

The stress joint at the bottom is tapered and has a greater thickness than the standard joints due to high bending stresses at the bottom. At bottom of the riser, the axial stresses

are less due to the top tension making the bottom more vulnerable to high bending stresses. At the top, there are high axial stresses due to tension and the motion of the platform. To handle the high axial stresses, the tensioner joint also has a larger wall thickness. The study section consists of only standard joints and shown in Figure 3-1.

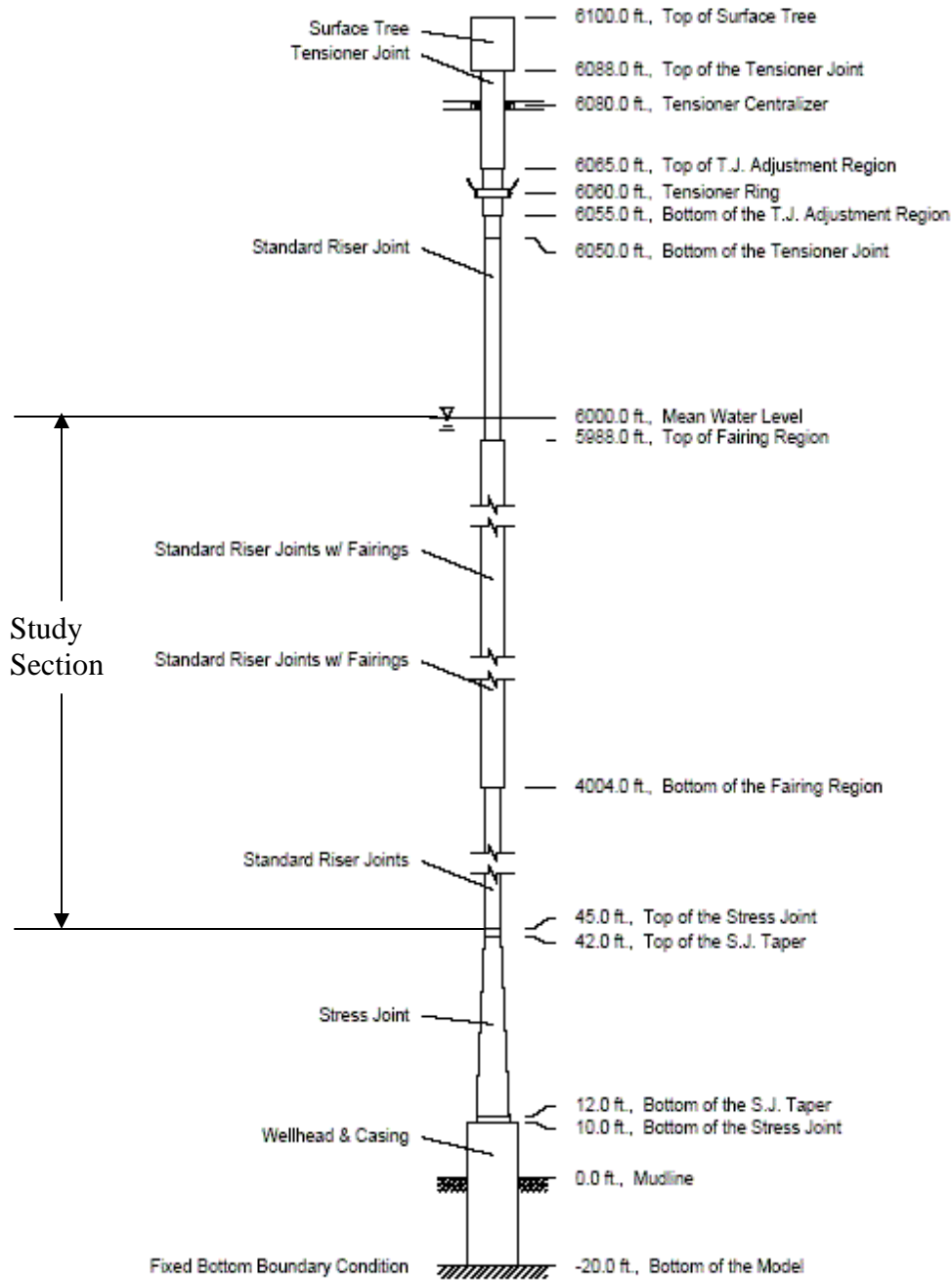


Figure 3-1: Riser Design

Chapter 4: Failure Analysis of the Study Riser

The objective of this chapter is to present an analysis of the potential failure modes for the study riser. The approach for this analysis is to first develop a fault tree representing all the failure modes and understand the likelihood of the various events leading to the top event in the fault tree.

4.1 Methodology

Failure modes for the study riser were identified through a series of five meetings (between January 2004 and August 2004). Each meeting, comprising of a group of experts, went for approximately eight hours and was held at Stress Engineering Services, Houston. A table listing all the meetings with the date, participants and the focus of discussion is shown in Table 4-1.

Table 4-1: List of Meetings

No	Date	Participants	Focus of Discussion
Meeting #1	21 Jan'04	Chuck Miller, Early Denison, E.G. Ward, Ozden Ochoa, Robert Gilbert	Develop System Description
Meeting #2	7 Feb'04	Chuck Miller, Early Denison, E.G. Ward, Ozden Ochoa, Robert Gilbert,	Steel Riser Failure Mode Identification
Meeting #3	March'04	Chuck Miller, Early Denison, E.G. Ward, Ozden Ochoa, Robert Gilbert,	Design of Study Riser
Meeting #4	19 May'04	Chuck Miller, Early Denison, E.G. Ward, Ozden Ochoa, Robert Gilbert	Likelihood of Failure modes
Meeting #5	24 Aug'04	Chuck Miller, Early Denison, E.G. Ward, Ozden Ochoa, Robert Gilbert, Julie B. McNeil	Review the findings and prepare for final outcomes for steel riser

Preliminary information was distributed among the participants at the beginning of the meetings to understand the basic objective of the project and the conceptual design of the study riser. The meetings were then focused on understanding the preliminary information and identifying the possible failure scenarios. Meeting #1 was focused mainly on establishing the scope of the project and time boundaries and describing the physical and operational features of the system. Meeting #2 was focused on defining the risks failure and identification of the possible failure scenarios of the steel riser. Meeting #3 was focused on global analysis of the study riser and establishing design basis for it. An objective of Meeting #3 and Meeting #4 was to elicit thoughts on the likelihood of the possible failure scenarios and identify the critical scenario. Preliminary analyses were done to elicit quantitative information from the technical experts during these meetings and to maximize the value of the information obtained from the experts.

4.2 Fault Tree

The objective of a fault tree is to identify and model the various system conditions that can result in the occurrence of a given undesired event, know as the “top event” or the failure. Before identifying the conditions leading to a failure, it is first required to define the “top event” or the failure.

In Section 2.4, it was mentioned that a production riser has two main design considerations, to maintain structural integrity and to contain the fluids inside. A riser will compromise on both of them, if and only if there is a through wall crack in the riser. Thus a riser through-wall crack was defined as the failure and assumed as the “top event” for the fault tree. Many scenarios were identified which would lead to failure of the risers during the meetings. The scenarios are listed as follows:

- i) During drilling, the production tubing is removed and the annulus is filled with drilling mud to provide a hydrostatic balance to the reservoir pressure. Due to the loss of control of the well (called pressure kick), unanticipated

entry of the formation fluids can lead to high internal differential pressure. This may lead to bursting of the pipe.

- ii) A surface control sub-sea safety valve (SCSSV), in the production tubing, controls the flow of the fluid/gas from the reservoir to the platform. It is located above the wellhead as shown in Figure 4-1. If, for some reason, there is a leak in the production tubing below the SCSSV, then there is no way of disconnecting the high pressure of the reservoir, which will subject the riser to contain the high pressure and thus may lead to burst. But if the leak is above the SCSSV, then the valve can disconnect the reservoir and thus avoiding a failure situation.

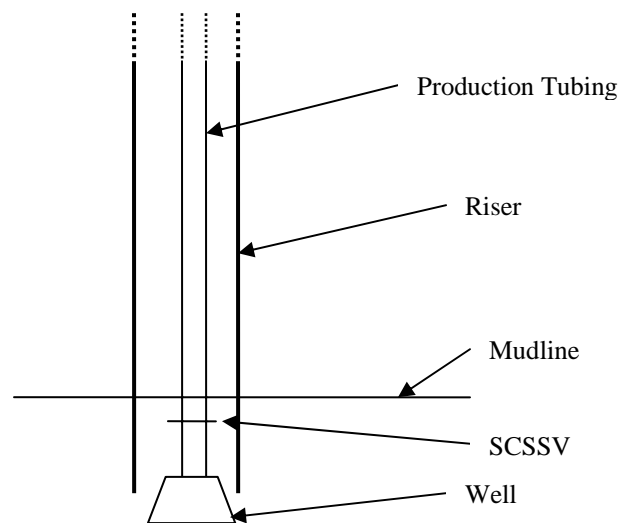


Figure 4-1: Schematic Representation of a Riser with SCSSV

- iii) In deepwater, the risers are required to stand against the high hydrostatic pressure. A hydrostatic overbalance may lead to collapse of the riser, due to high external pressure.
- iv) Impacts due to dropped objects like supply boats, or riser interference may also lead to damage on riser which can lead to riser yielding.
- v) Vortex Induced Vibrations (VIVs) occur due to loop currents, which develop vortices around the riser and results in its vibrations. These vibrations result in

load cycles and thus can lead to fatigue failure. There is a particular phenomenon called lock-in, during which the frequency of the vibrations match the natural frequency of the risers. At this point, the vibrations get very intense and lead to high fatigue damage.

- vi) The ocean waves put loads on the surface platform and vibrations are produced on the platform. These platform vibrations result in riser vibrations and stress amplitude load cycles. Due to the stress amplitude load cycles, fatigue damage can lead to riser failure. The kind of sea-state determines the amount of fatigue damage done.

All the above probable failure scenarios are represented through a fault tree as shown in Figure 4-2.

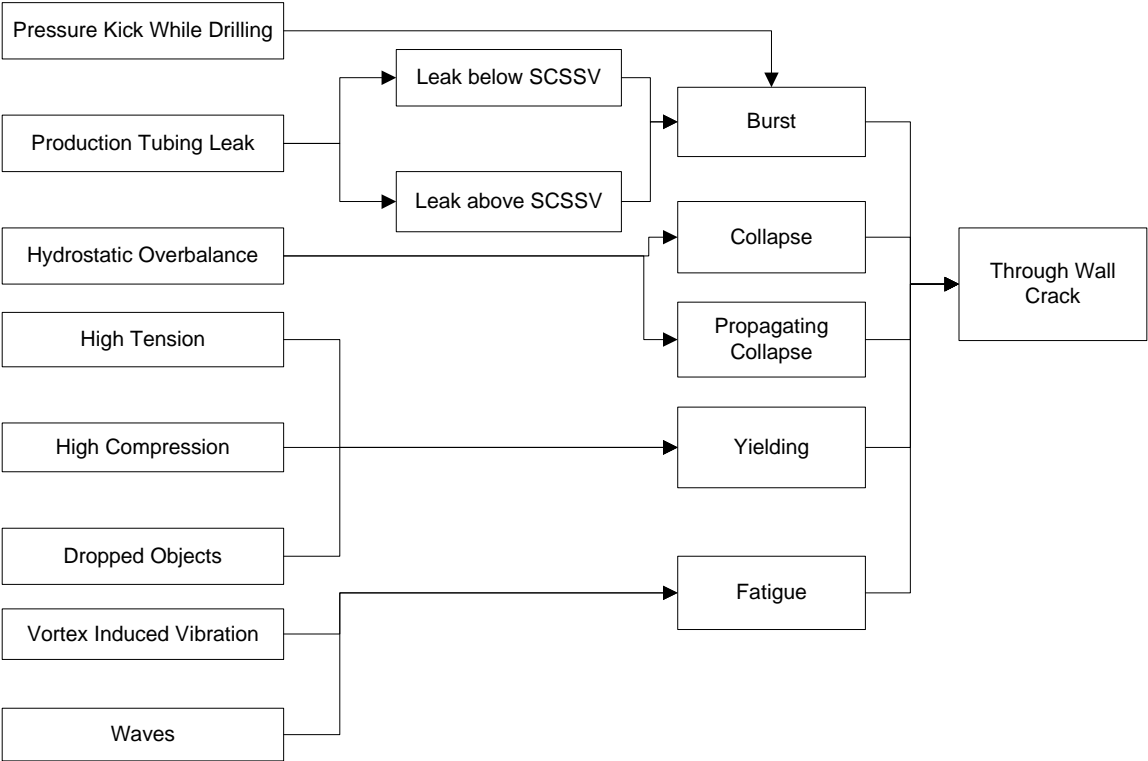


Figure 4-2: Fault Tree Leading to a Through Wall Crack.

4.3 Analysis of Fault Tree

The events leading to the riser failure were evaluated to understand their likelihood of occurrence. These events were analyzed based on the failure mechanisms as follows:

4.3.1 Collapse

The collapse of the riser is due to high external hydrostatic pressure compared to internal pressure. An extreme condition would be the case similar to PNS-1, when there is no internal pressure in the annulus, especially at the bottom of the riser. The hydrostatic pressure outside of the riser increases with the water depth and thus would be highest at the bottom of the riser. Wall thickness of the study riser between the elevations of 54 feet and 6000 feet is 1.014 inches. The wall thickness is constant for the change in the elevation, external pressure reduces with the increase in elevation and the internal pressure is zero for the design load case PNS-1, which would make it an extreme condition for the collapse of the riser. Since the first bare standard joint starts at 54 feet, which is also the point where the composite riser joint is recommended to replace the steel, it is a critical point to understand the collapse behavior. The maximum external hydrostatic pressure that can be experienced by the riser, represented by this load case, is calculated as shown below for 54 feet elevation above mud-line.

$$\rho_w = 8.5 \text{ ppg}$$

$$\begin{aligned} \text{Hydrostatic pressure} &= (6000 - 54) * \rho_w * 7.48/144 \text{ psi} && \text{Eq 4-1} \\ &= 2625.32 \text{ psi} \end{aligned}$$

Internal pressure is assumed to be zero for the extreme condition and thus around 2625 psi external pressure needs to be contained by the riser. As outlined in Section 2.4.3, the collapse strength of the riser at the 54 feet elevation above mud-line is calculated as shown in Table 4-2. The collapse pressure strength calculations are based on the riser material characteristics, as represented in Table 3-1.

Table 4-2: Calculation of Collapse Strength of the riser

Top Tension, lbs	T_e	864000
Production Tubing Weight (W_1), lbs	$W_1=(6088-10)*22.56$	137120
Tensioner Joint1, lbs	W_2	849
Tensioner Joint2, lbs	W_3	3487
Tensioner Joint3, lbs	W_4	8485
bare std joint (6000"-6050"), lbs	W_5	6203
bare std joint (5988"-6000"), lbs	W_6	1294
Std joint with fairings(4004-5988), lbs	W_7	218796
Bare Std Joint (54"-4004"), lbs	W_8	426047
True Wall Tension, lbs	$T=T_e-(W_1+W_2+W_3+W_4+W_5+W_6+W_7+W_8)$	61719
Thickness, in	T	1
Internal Diameter , in	D_i	9.722
Outside Diameter, in	D_o	11.75
Area, in ²	$A=\pi*(D_o^2-D_i^2)/4$	34.20033
Axial Stress, psi	$\sigma_{zz}=T/A$	1804.641
Yield Strength, psi	σ_y	70000
Reduced Yield Strength, psi	$Y_r=\sigma_y*(\text{SQRT}(1-0.75*(\sigma_{zz}/\sigma_y)^2)-0.5*\sigma_{zz}/\sigma_y)$	69080.23
Yield Pressure Collapse, psi	$P_y=2*Y_r*t/D_o$	11922.95
Elastic Collapse Pressure, psi	$P_e=2*E*((t/D_o)^3)/(1-\nu^2)$	42375.04
Collapse Strength, psi	$P_c=P_y.P_e/\text{SQRT}(P_y^2+P_e^2)$	11477.29

It is found that collapse strength at 54 feet elevation above mud-line is 11535 psi, which is approximately 4.3 times of the pressure required during an extreme condition and at the most critical point of the riser. The design safety factor is approximately 1.43 as suggested in Section 2.4.3, which is way below than what is found here. Thus the riser is self sufficient to stand by the maximum expected external hydrostatic pressure. The safety margin is too high to consider the uncertainties in the material properties. This makes collapse failure to be a highly unlikely event to take place during the life of the riser and thus is not considered for the evaluation of risks.

4.3.2 Bursting

During the consideration of the design load cases, WPT-1 represented the case of the maximum internal pressure, which might lead to bursting of pipe. It was argued that

bursting is a very unlikely event to take place because of the high burst strength of the study riser. Since the consequences of bursting are high, safety margin for failure of the study riser needs to be evaluated during an extreme condition.

An extreme condition that might lead to failure will be during the production tubing leak, which will make the outer casing of the riser vulnerable to the high internal pressure. WPT-1 case represents the condition of the high internal pressure that can result because of the leak. First the internal pressure at the different elevations of the riser was found as shown in Table 4-3.

Table 4-3: Internal Pressure Calculations for Case WPT-1

Elevation above mud line, ft	X
Shut In Pressure, psi	$P_{st}=1000$
Internal Fluid Density, ppg	$\rho_i=8.6$
Density of water, ppg	$\rho_w=8.5$
Internal Pressure (P_i), psi	$=P_{st}-X \cdot \rho_i \cdot 7.48/144$
External Pressure (P_o), psi	$=P_{at}+(6000-X) \cdot \rho_w \cdot 7.48/144$
Net Internal Pressure, psi	$=P_i-P_o$

Burst strengths of a pipe was found using API RP 1111 (1999), and as discussed in section 2.4.2. It is seen from the burst strength equation, that it doesn't depend on the true wall tension or the axial stresses. It was mentioned in API Bulletin 5C3 (2004) that Reduced Yield strength, Y_r , which takes into affect of the axial stresses, should be used in the calculations as the axial stresses do reduce the strength of the material.

Burst strength was found, P_b , considering the affect of axial stresses. Table 4-4 show the calculations of P_b for elevations between 4004 feet and 5988 feet, while Table 4-5 shows the changes in calculation needed to be done for elevations between 54 feet and 4004 feet.

Table 4-4: Burst Strength Calculations for (4004feet<X<5988feet)

Elevation above mud line, ft	X (4004<X<5988)
Top Tension, lbs	$T_e=864,000$
Production Tubing Weight, lbs	$W_1=(6088-10)*22.56=137120$
Tensioner Joint1, lbs	$W_2=849$
Tensioner Joint2, lbs	$W_3=3487$
Tensioner Joint3, lbs	$W_4=8485$
Bare Std Joint (6000'-6050'), lbs	$W_5=6203$
Bare Std Joint (5988'-6000'), lbs	$W_6=1294$
Std Joint with fairings(4004'-5988'), lbs/ft	$w_7=110.28$
True Wall Tension, lbs	$T=T_e-(W_1+W_2+W_3+W_4+W_5+W_6)-(5988-X)*w_7$
Internal Diameter, in	$D_i=9.722$
Outside Diameter, in	$D_o=11.75$
Area, in ²	$A=\pi*(D_o^2-D_i^2)/4=34.2$
Axial Stress, psi	$\sigma_{zz}=T/A$
Yield Strength, psi	$\sigma_y=70,000$
Reduced Yield Strength, psi	$Y_r=\sigma_y*(SQRT(1-0.75*(\sigma_{zz}/\sigma_y)^2)-0.5*\sigma_{zz}/\sigma_y)$
Ultimate Tensile Strength, psi	$U=80,000$
Burst Strength, psi	$P_b=0.45*(U+Y_r)*\ln(D_o/D_i)$

Table 4-5: Burst Strength Calculation Changes for (54feet<X<4004feet)

Elevation above mud line, ft	X (54'<X<4004')
Std Joint with fairings(4004'-5988'), lbs	$W_7=218795.5$
Bare Std Joint (54'-4004'), lbs/ft	$w_8=107.86$
True Wall Tension, lbs	$T=T_e-(W_1+W_2+W_3+W_4+W_5+W_6+W_7)-(4004-X)*w_8$

Figure 4-3 shows the net internal pressure during the extreme condition along the length of the riser with the burst strength, P_b . It is clearly seen that the capacities of containing the internal pressure is too high along the extreme condition, whose chances of occurrence is very rare. Even if there were uncertainties in the material, it was argued that the burst capacities won't be too low to consider bursting to be a critical failure mechanism. Thus bursting was left out of scope of evaluating the risks for the production riser.

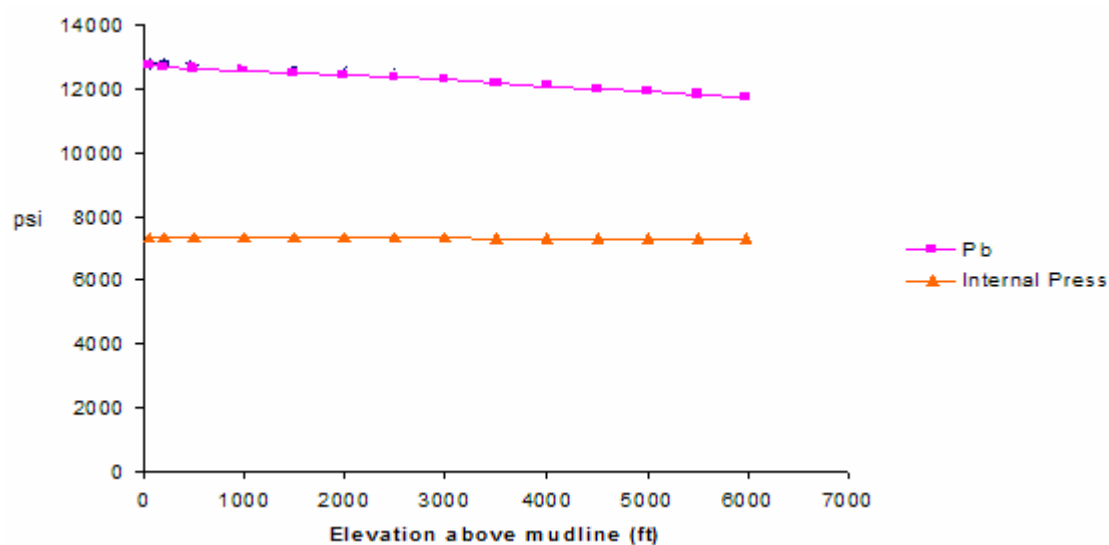


Figure 4-3: Net Inter Pressure and Burst Strengths

4.3.3 Yielding

Yielding occurs due to high tension, high compression or dropped objects. Due to high top tension, an event representing high compression is very unlikely. Von-misses stresses were found at the Tensioner and Stress joint for some extreme sea-states and compared with the allowable stresses. This analysis was done by Stress Engineering again and the results are presented in Table 4-6.

It is seen that the maximum stresses are within the allowable limits at the points of extreme loadings and during extreme environment conditions. This would mean that the

any other point of the riser would also be invulnerable to yielding due to its high capacity. If it is vulnerable, the chances of occurrence of failure due to yielding are very remote and the consequences are not comparable to that of bursting and collapse. Thus evaluation of risks due to yielding was also left out.

Table 4-6: Summary of Maximum Stress during extreme Sea- States

Load Case-1	Allowable Stress (ksi)	Stress Joint		Tensioner Joint	
		Max Stress (ksi)	% of Allowable	Max Stress (ksi)	% of Allowable
PNS-1: 1 year Winter Storm	53.3	32.0	60%	23.3	44%
PHN-1: 100 Yr Hurricane	64.0	58.0	91%	30.9	48%
PCN-1: 100 Year Loop Current	64.0	60.8	95%	32.4	51%

4.3.4 Propagating Collapse

Dents induced by dropped objects, riser interference, boat impacts can lead to local buckling, which can initiate a buckle that propagates at high speed. This buckle has the potential of leading to a global collapse unless the external differential pressure is less than the propagating pressure times the design factor. If the external differential pressure exceeds the propagating pressure, the riser could fail. This threshold pressure is dependent on the thickness, outer diameter and the yield strength. Since these parameters are constant for riser elevation between 54 feet and 6000 feet above mud-line, only one threshold exist for the whole riser, which is calculated as shown in Table 4-7.

Table 4-7: Calculations for Propagating Collapse

Outside Diameter, inch	$D_o=11.75$
Inside Diameter, inch	$D_i=9.722$
Thickness, inch	$t=1.014$
Yield Strength, psi	$Y=70000$
Propagating Pressure, psi	$P_r=4695.799$

The maximum external differential pressure found during the collapse analysis was 2600 psi. It is seen that the safety factor for the study riser is approximately 1.8 and the

required margin of safety is 1.4. Since the likelihood of an impact is very low and it still has a higher safety margin than what is required, this failure mechanism is considered to be unlikely.

4.3.5 Fatigue Failure

Fatigue is a failure mechanism which prevails even in the normal operating conditions, due to its dependence on the stress range cycles rather than the absolute values of stresses. There are multiple variables which affect the failure chances of a riser due to fatigue that are uncertain. Therefore, a probabilistic analysis of fatigue is the major focus of this study.

4.4 Summary

In this chapter, multiple failure scenarios were discussed with the perspective of the type of mechanism they go through. A fault tree, representing the failure paths was constructed. Through a preliminary analysis, it was found that burst, collapse, propagating collapse, yielding are not very likely scenarios. The safety factors for the study riser were found to be considerably greater than the conventional design factors for these failure mechanisms. Fatigue was identified as the most likely mechanism of failure and risk of fatigue is the focus in the remainder of this thesis.

Chapter 5: Probabilistic Fatigue Analysis of Study Riser

The objective of this chapter is to present a model to analyze the fatigue failure mode probability. First, a literature review is presented. Next, model for the fatigue analysis is adopted. The implementation of this model is verified by comparing results with the one in the literature. Finally, an analysis is conducted to evaluate the significance of the load path with this fatigue model.

5.1 Literature Review on Fatigue Crack Growth Models

When a piece of metal is subjected to a periodically varying load, microscopic inhomogeneities can develop into open cracks, leading to fatigue failure after a random time. There are two approaches to do the fatigue analysis, Klesnil and Lukas (1992), one using S-N (stress-cycles) approach and the other using fracture mechanics.

- i) *S-N curve approach*: For evaluation of the fatigue strength of materials, the S-N curve has been used from a long time. It is defined as the dependence of the stress amplitude on the number of cycles to fracture (Figure 5.1).

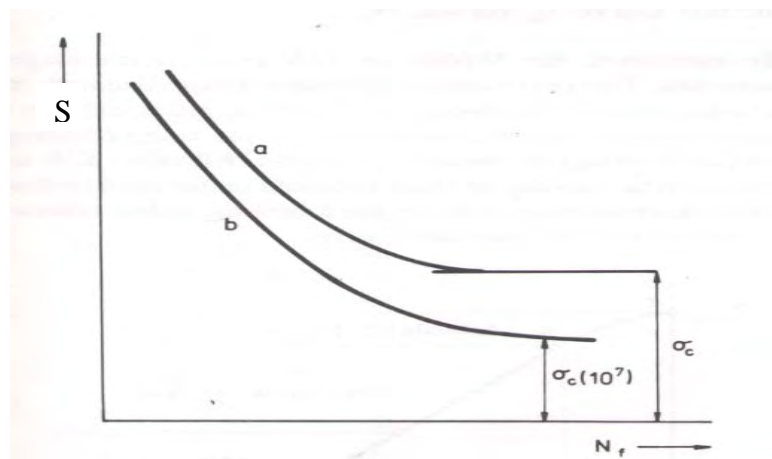


Figure 5-1: Schematic S-N curve, Klesnil and Lukas (1992)

This curve can be determined experimentally for any type of loading and body. However, only one type of S-N curve can be considered as a representative of the material characteristic and mean stress. If the material characteristics or the mean stress changes, this curve should change too. These S-N curves are based on previous empirical findings and statistical inference. It is seen that this approach doesn't mention anywhere about the type of fatigue damage done. Ertas, et al. (1992) mentions in his paper that S-N curve approach provides conservative results in determining fatigue damage of a pipe. It also mentions that researchers have constrained the use of S-N diagram as it usually has a lot of scatter.

- ii) *Fracture Mechanics approach:* Here fracture mechanics is used to track the fatigue damage due to load cycles, which is represented by the crack length. Parker (1981) presents the generic crack growth model, called Paris Law, with number of cycles using fracture mechanics. The Paris Law is represented as shown in Eq 5-1.

$$\frac{da}{dN} = C(\Delta K)^m = C(s\sqrt{\pi a} f(a))^m \quad \text{Eq 5-1}$$

where,

$f(a)$: Correction Factor depending on the geometry of the crack.

a : Crack Length

s : Stress Range in the j^{th} Cycle

m, C : Model Parameters

$(s_{max})_j$: Max Stress in j^{th} Fatigue Cycle

$(s_{min})_j$: Min Stress in j^{th} Fatigue Cycle

K : Stress Intensity Factor (S.I.F) = $s\sqrt{\pi a}$

$\Delta K = K_{max} - K_{min}$

a_N : Final Crack Length after N cycles

Schematic dependence of the crack growth on cyclic stress range is shown in Figure 5-2. Fatigue failure happens when the stress intensity factor, K , reaches fracture toughness, called K_c . The fracture toughness is the property of the material and at the threshold, the crack length increases infinitely, leading to the failure. Thus failure criterion with the fracture mechanics approach is $K > K_c$.

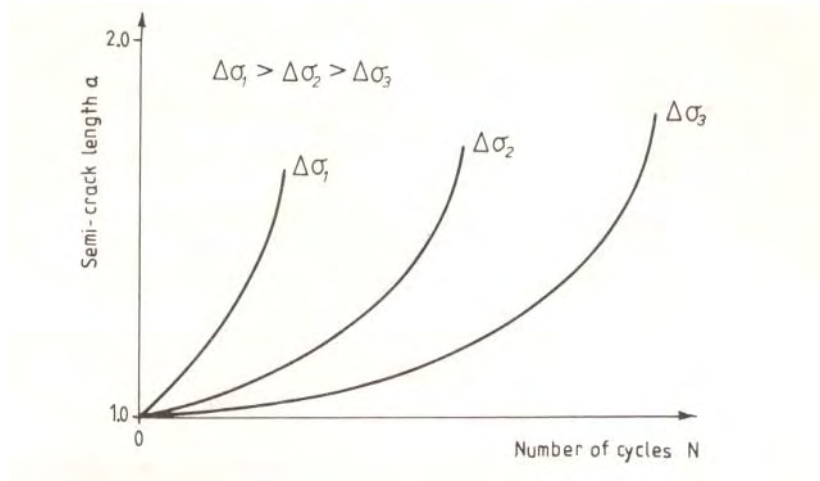


Figure 5-2: Crack length vs Number of Cycles for Different Stress Amplitudes, Parker (1991)

The above crack growth model can be used only for constant load cycles. Some changes have to be made in order to incorporate variable stresses.

Stress Engineering argued that fracture toughness for the study riser is too high to be taken into perspective. The crack will become a through wall crack before the stress intensity factor exceeds the fracture toughness.

Garbatov and Soares (2004) used Eq 5-1 to study the influence of steel strength on the fatigue reliability of welded structural components. Four different steel types were compared and they concluded that the fatigue behavior between the materials is almost the same during the crack initiation phase and very different during the crack propagation phase. This means that effect of material properties, namely C and m in Eq 5-1, have a significant impact on the fatigue life.

Zhao, et al. (2002) gave a very good description about the probabilistic models of uncertainties in fatigue analysis. However, the paper fails to present a fatigue model that would be able to use the probabilistic models in a convenient way. This paper is enlightening in providing a summary of available research on quantifying the uncertainties of the factors affecting fatigue.

Jiao, et al. (1990) present a probabilistic analysis of fatigue due to a Gaussian load processes. It uses the S-N approach and models the load in terms of the spectral density function of a Gaussian process, which is wide-banded. This paper gives a good description of the load processes typically encountered in offshore applications.

Huang, et al. (1989) present an approach for reliability analysis of fatigue crack growth under random loading to predict the distribution of crack lengths after a given number of cycles. This paper neglects the interaction between two cycles. Thus, the crack growth during any cycle depends only on the first crack length rather than on the crack length in the previous cycle. Newman, et al. [27], presents an approach for fatigue assessment under variable amplitude loads using small crack theory. They introduce to the concept of a crack closure, which is more relevant for small cracks under less intensive loadings, than the riser applications.

An approach for fatigue lifetime evaluation of welded joints is presented by Colombi and Dolinski (2001). They consider the retardation affect in crack growth due to overloading and under-loading, which is not evident from the Paris Law itself. They provided an excellent analysis for determining the fatigue life-cycles considering the loading stochastic process as Gaussian. Although the retardation effects are generally negligible, this paper provides an excellent description of the approach adopted for this study.

Wang, et al. (1996) present a reliability model which can be directly used for the current study. They present an approach that consider a random Rayleigh distribution for the

cyclic stress and therefore account for the variation in final crack length. No unreasonable assumptions were used, which could compromise the practicality of the model.

Parker (1981) suggests that the relative proximity of the stress intensity factor, K , to the fracture toughness, K_c , will affect the crack growth rate. This means the mean stress has an impact on the crack growth rate, which is not explained by Eq 5-1. He suggests including a correction factor, R , in the model. He also mentioned that the effect of varying the correction factor is limited in the case of steels, while it may be very sensitive to aluminium alloys.

5.2 Integration of Random Load Cycles Fatigue Model

The Paris law, Eq 5-1, gives the relationship of the crack growth with the constant load cycles. A modification is required in the model to integrate it with the random load cycles. An approach similar to that described by Wang et al. (1996) is used here to incorporate the uncertainties in the final crack length due to the random load cycles.

Equation 5.1 can be re-arranged and written as follows

$$\int_{a_i}^{a_N} \frac{dx}{(\sqrt{\pi x} f(x))^m} = \sum_{j=1}^N C(s_j)^m \quad \text{Eq 5-2}$$

where,

s_j : Stress Range in j^{th} Cycle

N : Total Number of Cycles

Thus when a crack of size, a_i is exposed to N cycles having s_j as the stress range in the j^{th} cycle, then a_N is the final crack size.

Define $Z(a_N)$ as

$$Z(a_N) = \int_{a_i}^{a_N} \frac{dx}{(\sqrt{\pi x} f(x))^m} \quad \text{Eq 5-3}$$

After integration in equation 5-3 with $f(a)=1$:

$$Z(a_N) = \frac{2.[a_N^{1-m/2} - a_i^{1-m/2}]}{\pi^{m/2}(2-m)} \quad \text{Eq 5-4}$$

It is also seen from equation 5-2 and equation 5-3 that $Z(a_N)$ is also equal to

$$Z(a_N) = \sum_{j=1}^N C(s_j)^m \quad \text{Eq 5-5}$$

When s_j are identically and independently distributed and N is constant, it is found from Appendix A that

$$E[Z(a_N)] = N C E[s^m] \quad \text{Eq 5-6}$$

$$V[Z(a_N)] = N C^2 V[s^m] \quad \text{Eq 5-7}$$

Expectation and variance of $Z(a_N)$ are utilized to find the expectation and variance of a_N . Due to non-linear relationship between Z and a_N , approximations are required to estimate the moments of a_N . Wang, et al. (1996) assumed Z to be normally distributed and transformed the distribution from Z to a_N , which doesn't belong to any standard distributions.

5.3 Verification of Model

Implementation of the fatigue model designed in section 5.2 requires numerical integration. To verify the implemented model, an example by Darcis, et al. [15], was used. This example is for fillet welds where cracks emanate from the weld toe. Using the material constants (C, m) provided by Darcis, et al. [15], the crack length vs life (cycles) relationship was studied for different constant stress amplitudes, for the linear relationship between da/dN and ΔK . In their analysis, $m=3$ and $C= 3 \times 10^{-13}$ (for da/dN in mm/cycle and s in MPa). The crack growth was started with an initial crack length of .5 mm. Figure 5-4 shows the path of crack growth for two different stress levels of 100 MPa and 150 MPa and it was seen that it exactly coincides with the plots of Figure 5-3,

which is the Figure 4 of [15]. Therefore, the model has apparently been implemented correctly.

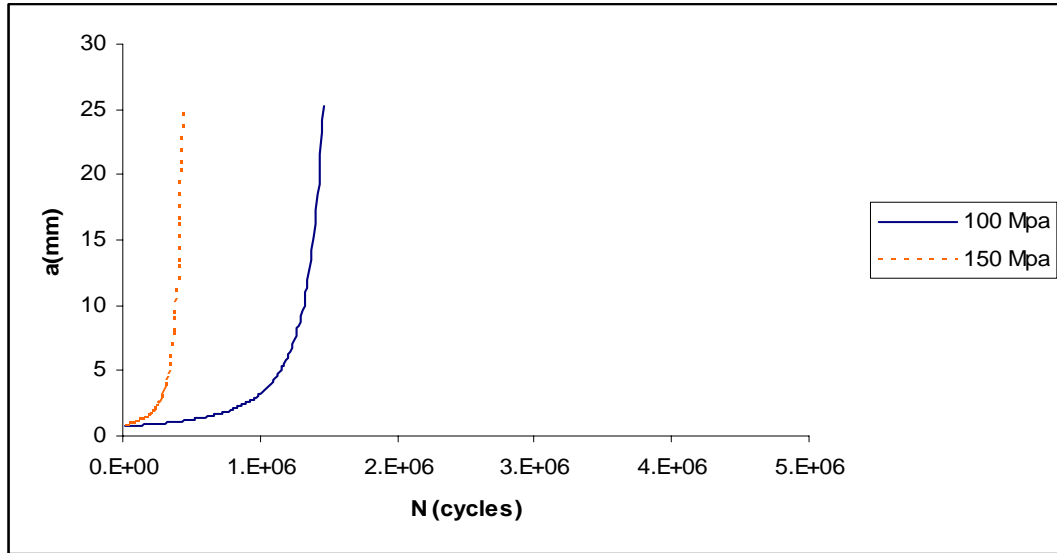


Figure 5-3: Crack growth at Stress Amplitude of 100 MPa and 150 MPa, as in Figure 4 of Ref [15](reproduced and scaled)

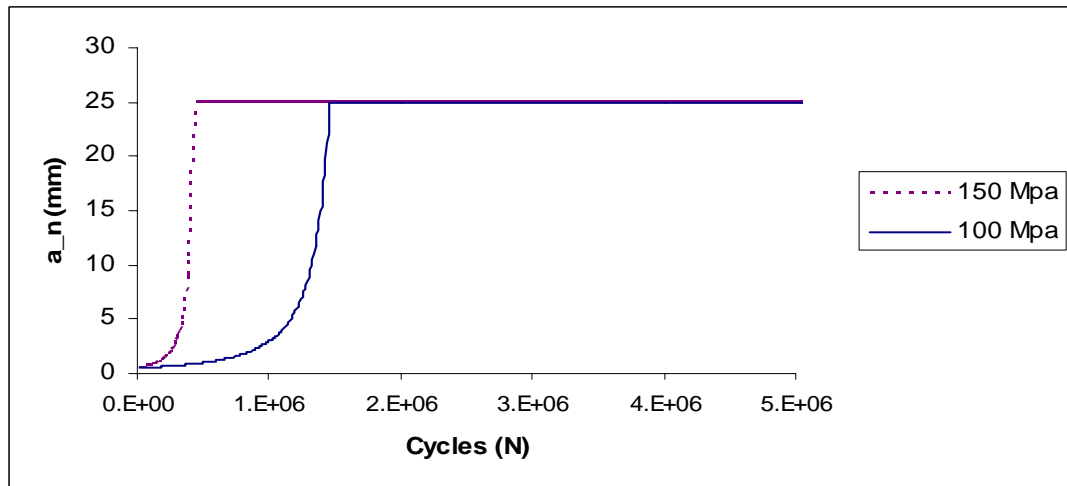


Figure 5-4: Crack Growth at Stress Amplitude of 100 MPa and 150 MPa

5.4 Evaluation of Final Crack Length with Stress Path

One concern that comes on looking the non-linear fatigue model, Eq 5-1, is that sequence of applied stress could affect the crack growth and hence the final crack length. In order

to explore it, two paths of the stress load cycles were studied. A reasonable stress histogram, applicable on the study riser, was supplied by Stress Engineering as shown in Figure 5-5. The first path considered is forward along the stress histogram with all the cycles of the least stress being imposed first and then all the cycles of the second least and so on. The other path considered is backward along the stress histogram with all the cycles of the maximum stress being imposed first, then all the cycles of the second maximum one and so on. The crack growth was studied for these two stress paths for different value of m as shown in Figure 5-6.

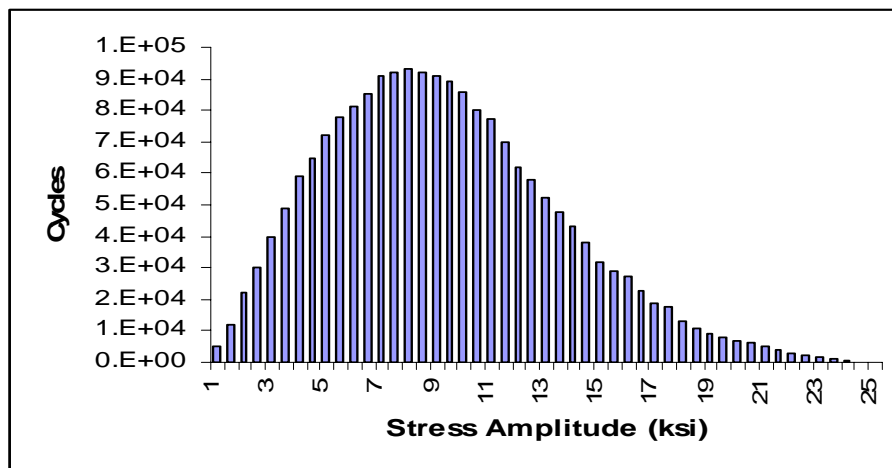


Figure 5-5: Stress Histogram

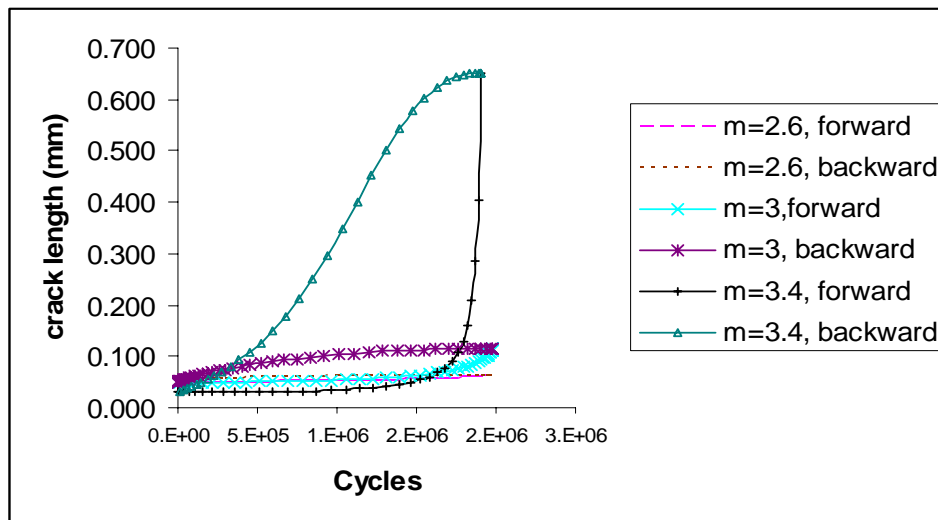


Figure 5-6: Fatigue Crack Growth for Different Stress Paths

It was found from Figure 5-6 that for each m , the final crack length is insensitive to the forward and backward load paths, although the crack growth path is different. Thus, although the crack takes different path for each different load path, the final crack length at the end of the loading is independent of it, if the stress histogram is given to be same. This conclusion is very important in the context of quantification of the uncertainties of the final crack length, which apparently can't be proven mathematically. This leads to the fact that the uncertainty in the load path history has no affect on the final crack length.

5.5 Flowchart for Probabilistic Fatigue Analysis

Crack growth depends on the number of cycles of different stress amplitude, initial crack-length and material properties (m and C). Any uncertainty in these factors will lead to uncertainty in the final crack length and thus will affect the failure probability, the probability that crack length exceeds the riser wall thickness. Uncertainty in these factors needs to be incorporated, in order to calculate the failure probability for fatigue. A brief summary about the approach required to quantify it for each of the factors is shown below:

- i) Stress amplitude load cycles, s_j and N_j : These load cycles are related to multiple sea-states prevalent in the life of the riser. The random nature of waves in a sea-state is a time-series phenomenon and is quantified using spectral analysis, which is explained in more detail in Chapter 6. Uncertainty in the occurrence of each sea-state also affects the overall uncertainty in the final crack length.
- ii) Initial crack length, a_i : This is a variable that depends on the quality of weld and the crack inspection technique used for quality control. The frequency of cracks also is an uncertain variable. This is discussed in Chapter 8.
- iii) Material properties, m and C : These factors are dependent on material properties of the weld. The uncertainties in these factors are addressed in Chapter 8.

Figure 5-7 presents the flow of the probabilistic analysis that is done to capture the uncertainties in the factors and to quantify the probability of fatigue failure.

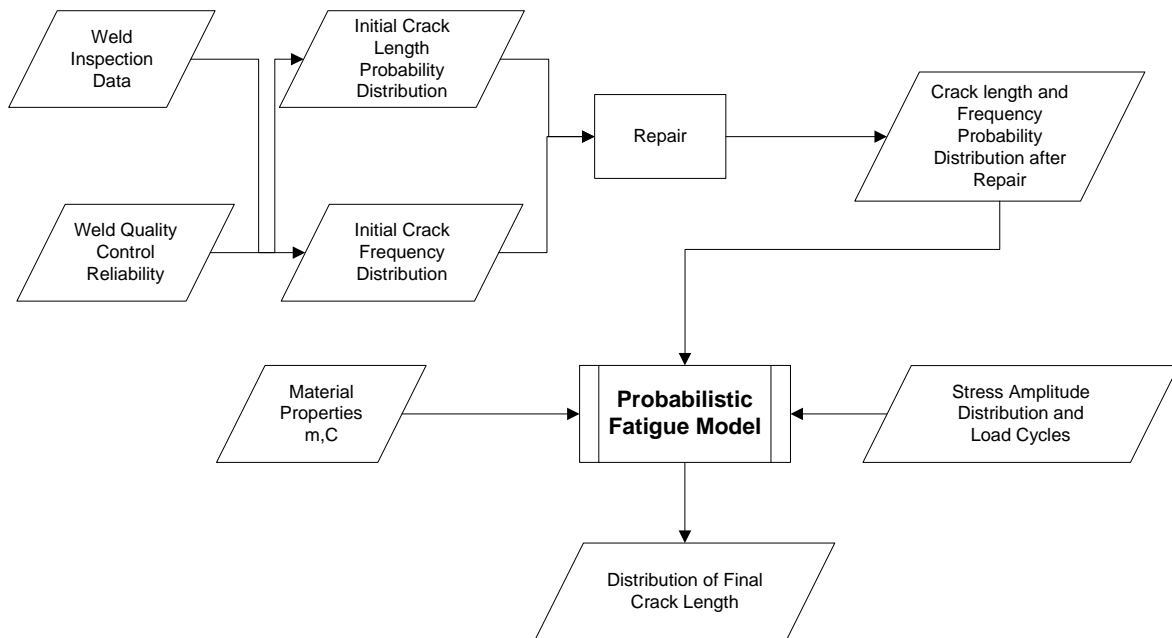


Figure 5-7: Flowchart of the Data Flow among the Key Components of Fatigue

5.6 Summary

This chapter presented the fatigue model to predict the distribution of the final crack length under random stress range cycles for the study riser. The deterministic model was verified with the data given in the published literature. It was concluded that the final crack length is independent of the stress path and only depends on the stress histogram. Thus the uncertainty in the path of the stress will not affect the uncertainty in the final crack length, which simplifies the analysis. It was concluded that final crack length is dependent on the stress amplitude, number of stress cycles, and material properties. A flowchart was presented, which explains the flow of the analysis required to be able to estimate the fatigue failure probability.

Chapter 6: Stress Amplitude Distribution for Study Riser

The objective of this chapter is to present the stress amplitude distribution for the study riser. First, a description of how the probability distribution of the stress amplitude load cycles obtained is presented. Next, the results for the steel riser, obtained by Stress Engineering are presented. These results are explained in the context of the requirements of fatigue analysis.

6.1 Introduction

Fatigue fracture damage is due to load cycles, which are due to waves, winds and currents for the study riser. Loads on risers for its life time are derived as a function of various sea-states. Each sea-state, which is typically assumed to last for 3hrs in the Gulf of Mexico, is characterized as follows:

- i)* Main wave direction, θ_{mj} ;
- ii)* Significant wave height, H_S , defined as the average of upper third of the wave heights;
- iii)* Mean zero up-crossing period, T_Z , defined as the time between successive up-crossing of the still water, averaged over the number of waves.

The current and wind speeds and directions are defined as a function of H_S and θ_{mj} respectively. The wave climate experienced by a vessel during its life time is described by models of two different time scales:

- i.* A short term model, which describes waves during a sea state as random and assumes it as a stationary process (wave spectrum model).
- ii.* A long term model, which defines the frequency distribution of sea states (Wave scatter diagram).

Spectral analysis, conducted in the frequency domain, is used to generate the distribution of wave heights, frequencies of currents and winds during a sea state. A finite element model of the floating structure is then used to determine loads during a sea state. It is conventionally assumed that stress processes are stationary with a narrow band, so that the stress amplitudes from each wave approximately have a Rayleigh distribution.

6.2 Wave Scatter Diagram

A wave scatter diagram specifies the probability density function of the joint occurrence of the three main parameters defining a sea state, $p(H_s, T_p, \theta_m)$. The wave scatter diagram for the Gulf of Mexico with 0° heading, used by Stress Engineering for the stress analysis of the study riser is shown in Figure 6-1.

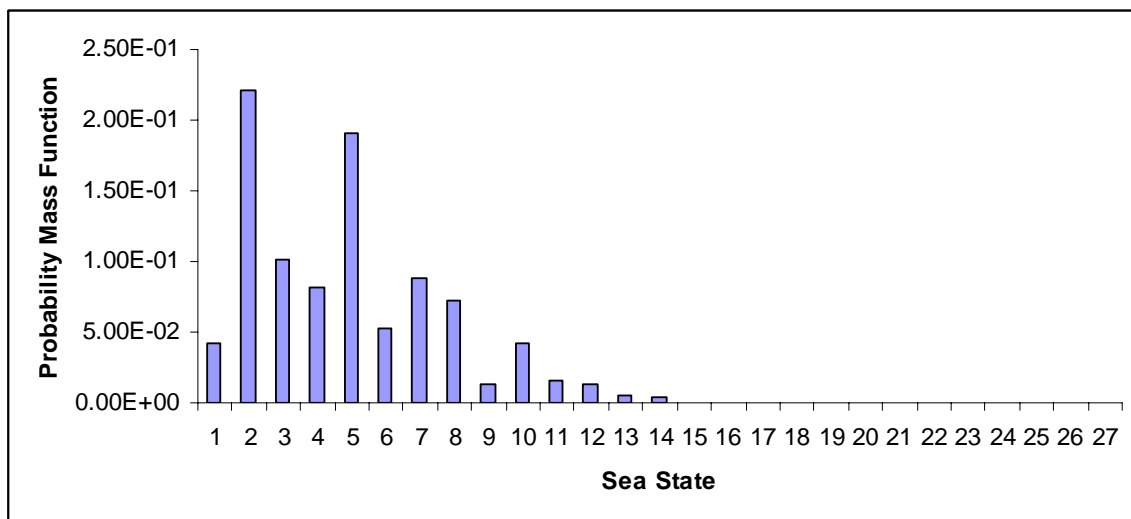


Figure 6-1: Frequency Distribution of the 27 Sea States

6.3 Wave Spectrum

The wave spectrum is an important environmental input to fatigue as it expresses the distribution of wave energy over the wave frequency range in a given sea state. For a specified sea state, the wave spectrum is estimated by modeling waves as a stationary, random process.

Michel (1967) explains a sea state as “A collection of a great number of simple, regular waves of different lengths, all of small height and all mixed together with no apparent relation to each other except that they are all there and are all traveling in the same direction”. The result is an irregular sea, with no set pattern to the wave height or period.

It can be seen from Figure 6-2 how an irregular wave can be obtained by combining only 4 component regular waves. A large number of component waves (around 200 waves) results in a very irregular resultant wave pattern. However, irregular waves can be characterized in simple terms of energy as the total energies of regular component waves that make up the sea.

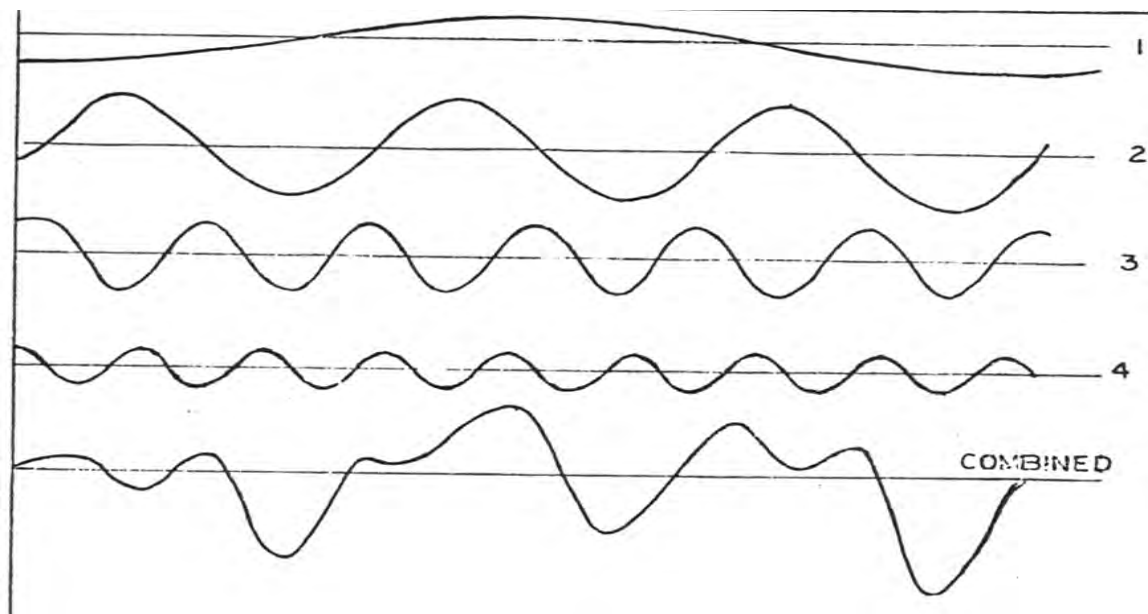


Figure 6-2: Wave Pattern from Combining Four Regular Waves, Michel (1967)

There is one question about the issue of randomness, as to how the resultant wave is random when everything is known about the component waves. It is true that everything is known about the component waves individually, but the relative position of the waves or the phase angle is unknown. Since the phase relationship of one regular wave to another is unknown, it is difficult to predict when a number of waves will group together to form a high sea-wave or when they will tend to cancel out in any systematic manner.

Characteristic relationship for deep water waves are summarized in Table 6-1. The energy of one component wave for each square foot of water surface is proportional to the square of the wave heights. Total energy of an irregular wave surface is the sum of the individual component energies, which is a constant multiplied by the sum of the squares of the heights of the component waves.

Table 6-1: Deep Water Characteristics of Regular Waves, [18]

Wave Period (T)	T
Wave Height (L)	H
Wave Length (L)	$L=gT^2/2\pi$
Wave Speed (L/T)	$c=L/T=gT/2\pi$
Cyclic Frequency (cycles/T)	$f=1/T$
Circular frequency (rad/T)	$\omega=2\pi/T$
Energy (per unit area of water surface),(FL/L ²)	$E=\rho gH^2/8$

Thus energy is used to characterize the sea-state and it is possible to show the contribution of energy for all the waves according to their frequencies. This distribution is called the energy spectrum, $E(\omega)$.

As an example, if there are 4 component waves as described in Figure 6-2, then the energy spectrum for each of the frequencies can be described by Figure 6-3. The ordinate of the curve is expressed as FT/L and abscissa as T^{-1} , so that the total area under the curve represents the total energy in the resultant wave. Thus energy spectrum is used to characterize the energy of the resultant wave according to frequencies of the regular, small waves as described by Figure 6-3.

Note that energy is a constant times the square of the height or the amplitude of the wave. The power spectral density or the wave spectrum, $S(\omega)$, gives the intensity in terms of the square of the amplitude for each frequency, ω , and is calculated as follows:

$$S(\omega) = \frac{E(\omega) * 8}{\rho g} L^2/T \quad \text{Eq 6-1}$$

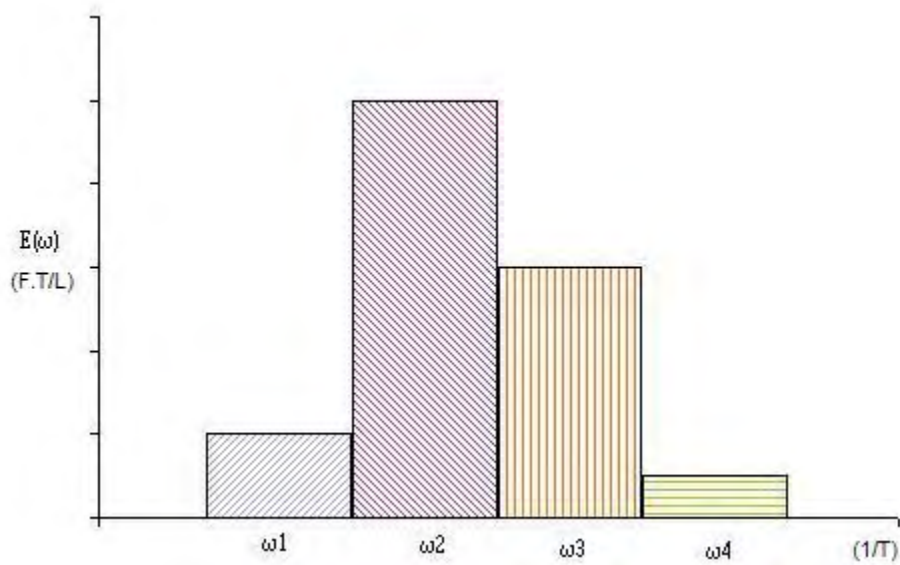


Figure 6-3: Energy Spectrum for the Resultant Wave Depicted in Figure 6-2, Michel (1967)

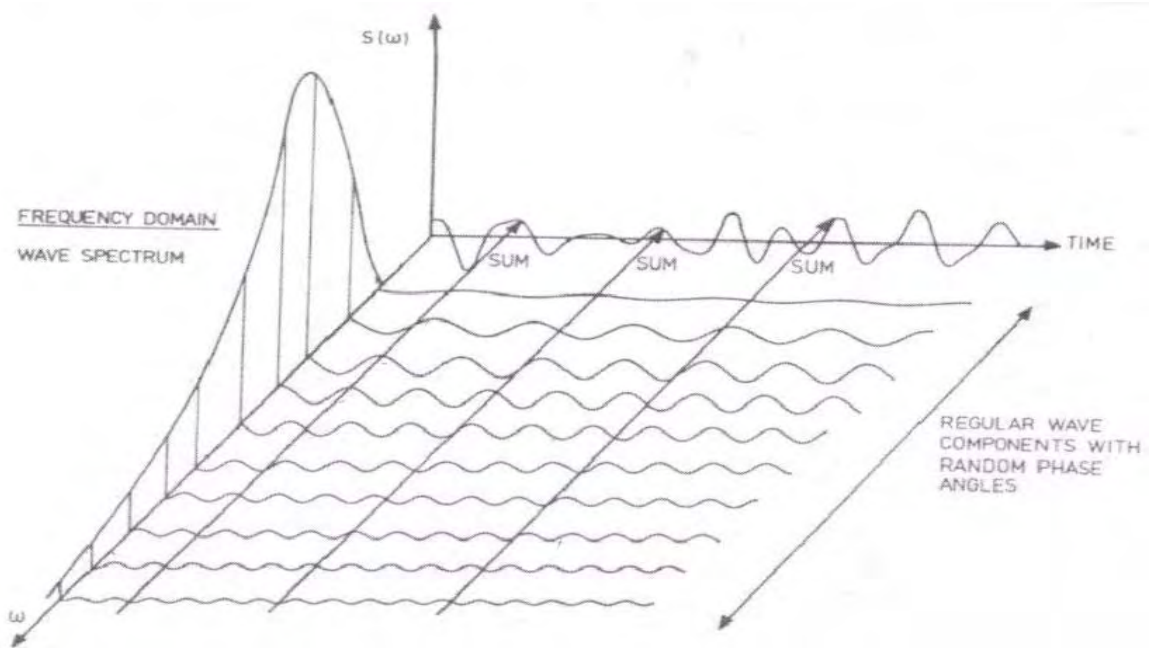


Figure 6-4: Figure Illustrating the Connection between a Frequency Domain and Time Domain Representation of Waves in a Short Term Sea-State, Stress Engineering

Thus total Energy for a sea-state is the area under the Energy Spectrum or $(\rho g/8)$ times the area under the power Spectral density, $S(\omega)$. Figure 6-4 shows the relationship of the time-domain and frequency domain wave characterization of a sea-state.

Many mathematical models for the relationship of spectral density, $S(\omega)$, with H_S and T_Z have been discussed in [18]. In general, [10], a Gamma Spectrum is employed to capture the energy for the frequency range for a given sea state.

$$S_{\eta}(\omega | h_s, t_p) = A \omega^{-\xi} \exp(-B \omega^{-\zeta}), \quad \omega > 0 \quad \text{Eq 6-2}$$

The parameter ξ represents the power of the high-frequency tail and the parameter ζ describes the steepness of the low-frequency part. The most common two parameter spectrum models are the Bretschneider, Scott, Pierson-Moskowitz, JONSWAP spectrums. For this analysis, Stress Engineering used the following JONSWAP spectrum, $S_{\eta}(\omega)$, Eq 6-3.

$$S_{\eta}(\omega) = \alpha H_s^2 \frac{\omega^{-5}}{\omega_o^{-4}} \exp\left[-1.25\left(\frac{\omega}{\omega_o}\right)^{-4}\right] \gamma^{\exp\left[-(\omega-\omega_o)^2/(2\tau^2\omega_o^2)\right]} \quad \text{Eq 6-3}$$

where,

$$\alpha = \frac{.0624}{.230 + .0336\gamma - .185(1.9 + \gamma)^{-1}}$$

$$\omega_o = 2\pi / T_Z$$

$$\tau = .07 \text{ for } \omega \leq \omega_o, \quad \tau = .09 \text{ for } \omega > \omega_o$$

γ : Peakedness Parameter of JONSWAP

τ : Shape Parameter of JONSWAP

6.4 Stress Response

When a linear system, [11], is subjected to harmonic excitation at a particular frequency (the input), the response of the system (the output) is also harmonic, with the same frequency and a phase shift between input and output. The transfer function is defined as

the ratio of the amplitude of the output to the amplitude of the input, which is also known as the Response Amplitude Operator or RAO. The complete operator between the input and the output, comprising both the RAO and the phase shift, is referred to as the frequency response function. Both the RAO and the phase shift are frequency dependent. The frequency response function is thus a complex valued function of frequency. The transfer function (or RAO) is the modulus of the frequency response function and hence a real function of frequency. Both the frequency response and the transfer functions are system properties and do not depend on the magnitude of the excitation. This distinction in terminology is, however, not always adhered to and the terms frequency response function and transfer function are often considered as synonyms.

The frequency response function is found as follows. First, waves for a range of wave frequencies and heights are selected and stresses in the risers are computed for each wave condition, which is called global performance analysis. Various steps including global performance analysis are:

Step 1. Select the sea-state from one of the bin shown in Figure 6-1 and develop the wave power spectral density $S_{\eta}(\omega)$

Step 2. The abscissa of the Spectral density, $S_{\eta}(\omega)$, is divided into N components such that almost all the range is considered. Thus ω_j will be the frequency of the j^{th} component wave where j will vary from 1 to N . Note the larger the value of N , better the approximation.

Step 3. Calculate the amplitude of the j^{th} component wave, A_j ,

$$A_j = \sqrt{2S(\omega_j)\Delta\omega} \quad \text{Eq 6-4}$$

Step 4. Simulate ' N ' regular waves of amplitude A_j and frequency ω_j with random phase angles. Note superimposing these N regular waves will result in the irregular wave depicting the characteristics of the considered fatigue bin or sea-state.

Step 5. Find the unit response of the vessel (vertical stress/foot of wave) is found, which is called be $RAO(\omega_j)$. Thus finding the RAO for each of the component wave will

result in getting the transfer function required to get the spectral density of the stress response, $S_X(\omega)$, for the considered sea-state as follows.

$$S_X(\omega | H_S, T_Z) = RAO(\omega)^2 S_\eta(\omega | H_S, T_Z) \quad \text{Eq 6-5}$$

The variance of the response is calculated using the following equation,

$$\sigma_X^2 = \int_0^\infty S_X(\omega) d\omega \quad \text{Eq 6-6}$$

These steps are repeated to find the standard deviation of the stress response, σ_i , at the fatigue critical points of the riser for each fatigue bin 'i'. The stress amplitude response is approximately described by Rayleigh distribution, Vanmarcke (1988), with variance σ_i^2 , for this Gaussian process.

6.5 Stress Amplitude versus Number of Cycles

The chance of occurrence for any sea-state or fatigue bin is described by the probability mass function shown in Figure 6-1. The waves for each respective bin are irregular with respect to time and thus would have a random response on the risers. For each i^{th} bin, these waves were simulated and the variance of the stress amplitude for the cycle, σ_i^2 , and the zero-crossing time period, t_i , was calculated and recorded by Stress Engineering. An example of the variation in the standard-deviation and zero-crossing time periods of the stress range cycles in the riser at 54 ft elevation above mud-line is shown in Figure 6-5 and Figure 6-6. The relevant data is provided in Appendix C.

The stress amplitude will follow Rayleigh distribution, as suggested by Vanmarcke (1988), for the Gaussian random process that is stationary.

Let $f_i(s) \sim \text{Rayleigh}(k_i) \sim \text{Weibull}(2, k_i\sqrt{2}, 0)$

$$f_i(s) = \frac{s}{k_i^2} \exp\left[-\frac{s^2}{2k_i^2}\right] \quad \text{i= 1 to 27} \quad \text{Eq 6-7}$$

where

$f_i(s)$ = probability density function (PDF) of the stress range per cycle for the i^{th} sea state at a given point of riser

s = stress range per cycle during the i^{th} sea-state

k_i = parameter for the Rayleigh distribution for i^{th} sea state

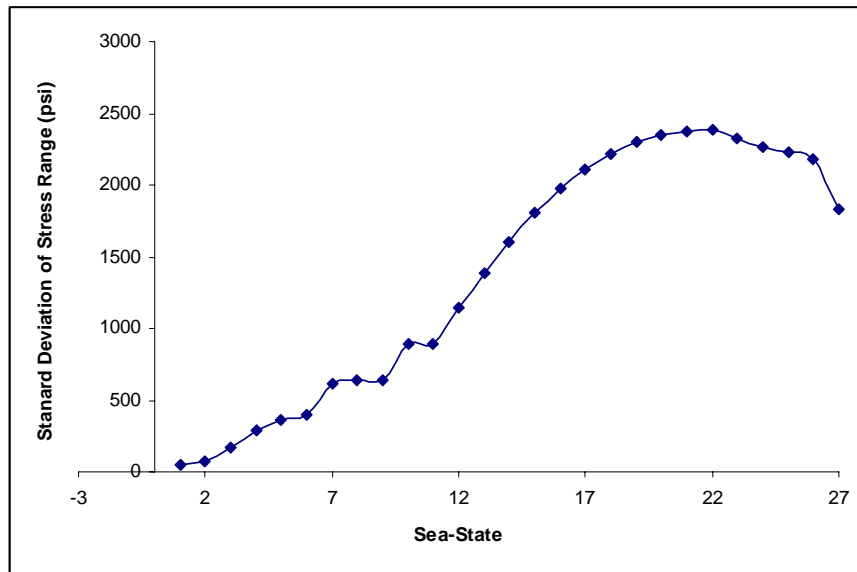


Figure 6-5: An Example of Stand Deviations of Stress Ranges for Sea-states at 54feet Elevation above Mud-line, Stress Engineering

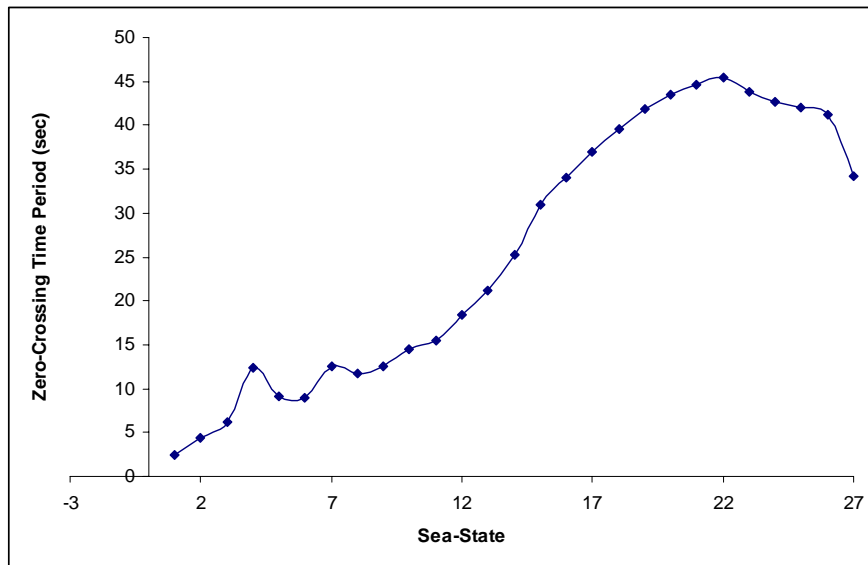


Figure 6-6: An Example of Zero-Crossing Time Period of Stress Load Cycles for Different Sea-States at 54feet Elevation above Mud-line

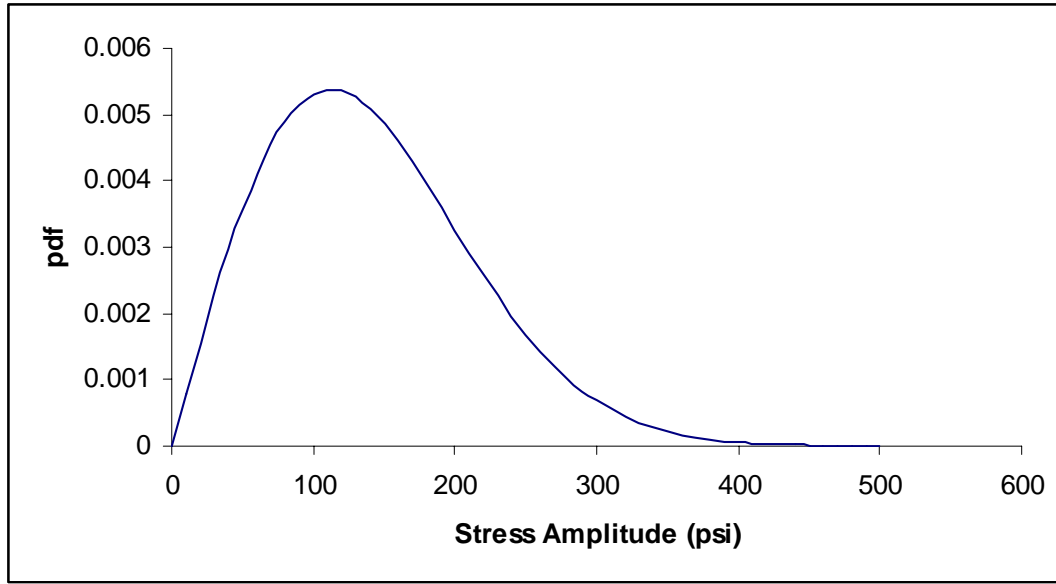


Figure 6-7: Example, Rayleigh Distribution Function for the Stress Amplitude at 54feet Elevation above Mud line under 2nd Sea State

For the above Rayleigh distribution, it is known from Appendix B that

$$\text{Variance}_i[s] = k_i^2 \left[2 - \frac{\pi}{2} \right] \quad \text{Eq 6-8}$$

$$\text{Mean}_i[s] = k_i \sqrt{\frac{\pi}{2}} \quad \text{Eq 6-9}$$

$$E_i[s^m] = (\sqrt{2}k_i)^m \cdot \Gamma\left(\frac{m}{2} + 1\right) \quad \text{Eq 6-10}$$

Using Eq 6-8, the parameter k_i can be found from the standard deviation of the stress range for the i^{th} sea state, σ_i , as shown in Eq 6-11

$$k_i = \sigma_i \sqrt{\frac{2}{4 - \pi}} \quad \text{Eq 6-11}$$

The fatigue analysis also requires total number of load cycles for i^{th} sea-state, N_i , which is calculated as follows:

$$N_i = \frac{L * 365 * 3600 * 24 * p_i}{T_i} \quad \text{Eq 6-12}$$

where,

N_i = Number of cycles for the i^{th} sea state; T_i = zero crossing time period (secs)

p_i = probability of the occurrence of the i^{th} sea state;

L = Life of the riser considered (yrs)

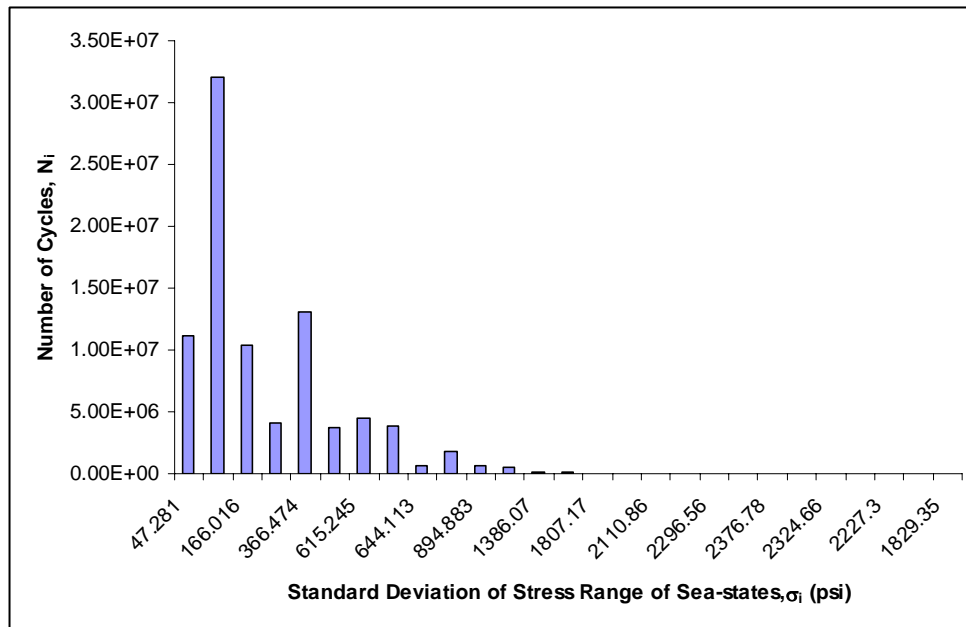


Figure 6-8: Expected Number of Stress Range Load Cycles vs its Standard Deviation

6.6 Summary

Approach used by Stress Engineering to find the stress cycles histogram was explained in this chapter. A wave scatter diagram was presented which include twenty seven sea states. A JONSWAP spectrum was adopted, which characterize a sea-state. Spectral analysis was performed by Stress Engineering to determine the stress amplitude levels under each sea state. The stress amplitude in the study riser was found to follow Rayleigh distribution and the parameter characterizing it was presented by Stress Engineering. The stress amplitude cycles histogram will be used further for the probabilistic fatigue failure analysis.

Chapter 7: Fatigue Failure Analysis with Random Load for Study Riser

The objective of this chapter is to study the variation of the final crack length with the stress range load cycle distribution. The sensitivities of the final crack length to the initial crack length, material properties m and C , and the location of the joint on the riser are addressed.

The uncertainty in the final crack length, a_N , depends on the variability in the loading history. Due to the non-linear relationship between the loading history and final crack length, it is difficult to directly quantify the uncertainty in the final crack length. To overcome this difficulty, uncertainty in final crack length was found through a two step approach.

- i) The mean and variance of random variable, Z , are established from the uncertainties in the load history.
- ii) The mean and variance of a_N are estimated from that of Z based on the relationship between a_N and Z (Eq 5-4).

7.1 Moments of Z

It is understood from Equation 5-5 that

$$Z(a_N) = \sum_{j=1}^N c(s_j)^m \quad \text{Eq 7-1}$$

The expectation and variance expressions, shown by Eq 5-6 and Eq 5-7 respectively, are valid when s_j are identically and independently distributed. However when there are many sea-states possible, s_j variables are no longer identically distributed. Therefore the distribution of the stress amplitudes of each sea state are first combined into a single resultant distribution describing the stress range load cycles.

It is known that stress amplitude will follow a Rayleigh(k_i) distribution with N_i/N chances in N cycles of load over the lifetime. The stress range s can be from any of the sea states. Thus

$$Event[S = s] = Event[S_1 = s \cup S_2 = s \cup S_3 = s \cup \dots \cup S_{27} = s] \quad \text{Eq 7-2}$$

where

S_i : Random Variable for stress range for i^{th} sea state

Since all the sea states are mutually exclusive, it follows

$$Pr ob[S = s] = \sum_{i=1}^{i=27} Pr ob[i^{th} \text{ sea state}] Pr ob[S_i = s] \quad \text{Eq 7-3}$$

Thus a combined PDF for the stress range per cycle, which will give its probability density for the entire life of the riser, is computed as follows:

$$f(s) = \sum_{i=1}^{27} p_i f_i(s) \quad \text{Eq 7-4}$$

where

$f(s)$: Distribution of the stress range over the entire life of the riser

p_i : Chances of occurrence of a stress cycle from i^{th} sea state in N load cycles $=N_i/N$

$f_i(s)$: Distribution of the stress range for the i^{th} sea-state

N : Total number of cycles contributing for the i^{th} sea-state $= \sum_{i=1}^{27} N_i$

Thus Z can be written as

$$Z = C \sum_{j=1}^N s_j^m$$

where s_j are independent for each cycle and follow $f(s)$ distribution as shown above.

Let $E_i[s^m]$ and $V_i[s^m]$ be the expectation and variance of the stress amplitude for i^{th} sea state, which are found as shown in Appendix B.

The m^{th} moment of s_j is obtained as follows:

$$\begin{aligned}
E[s^m] &= \int s^m f(s) ds \\
&= \frac{\int s^m \left(\sum_{i=1}^{27} N_i f_i(s) \right) ds}{N} = \frac{\sum_{i=1}^{27} N_i \int s^m f_i(s) ds}{N} \\
&= \frac{\sum_{i=1}^{27} N_i E_i[s^m]}{N}
\end{aligned} \tag{Eq 7-5}$$

Since s_j are independent and identically distributed, the expectation and variance of Z are found as follows using Eq 5-6 and Eq 5-7

$$\begin{aligned}
E[Z] &= N C E[s^m] \\
&= C \sum_{i=1}^{27} N_i E_i[s^m]
\end{aligned} \tag{Eq 7-6}$$

Similarly,

$$\begin{aligned}
V[Z] &= N C^2 V[s^m] \\
&= N C^2 \left[E[s^{2m}] - E[s^m]^2 \right] \\
&= N C^2 \left[\frac{\sum_{i=1}^{27} N_i \cdot E_i[s^{2m}]}{N} - \left(\frac{E[Z]}{N C} \right)^2 \right] \\
&= C^2 \left[\sum_{i=1}^{27} N_i \cdot (V_i[s^m] + E_i[s^m]^2) \right] - \frac{E[Z]^2}{N}
\end{aligned} \tag{Eq 7-7}$$

7.2 Coefficient of Variation of Z

Using the expressions for mean and variance of Z , the coefficient of variation (c.o.v.) of Z for the entire length of the riser is shown in Figure 7-1 for different value of m . Since Z is proportional to C , its c.o.v. is independent of C and thus the effect of C on the c.o.v. need not be considered.

From Figure 7-1 it is seen that the maximum value of c.o.v. is .016, near the base. Further above, c.o.v has a maximum value of low .006.

There low c.o.v values of Z are the effect of averaging over the whole life of riser. The larger the life of riser, the more the averaging affect and less are the variations in Z . At a particular instant there might be high variations due to stresses and thus high c.o.v. But if the whole life is considered, the increase in variations is not comparable with the increase in mean, thus leading to relatively low c.o.v

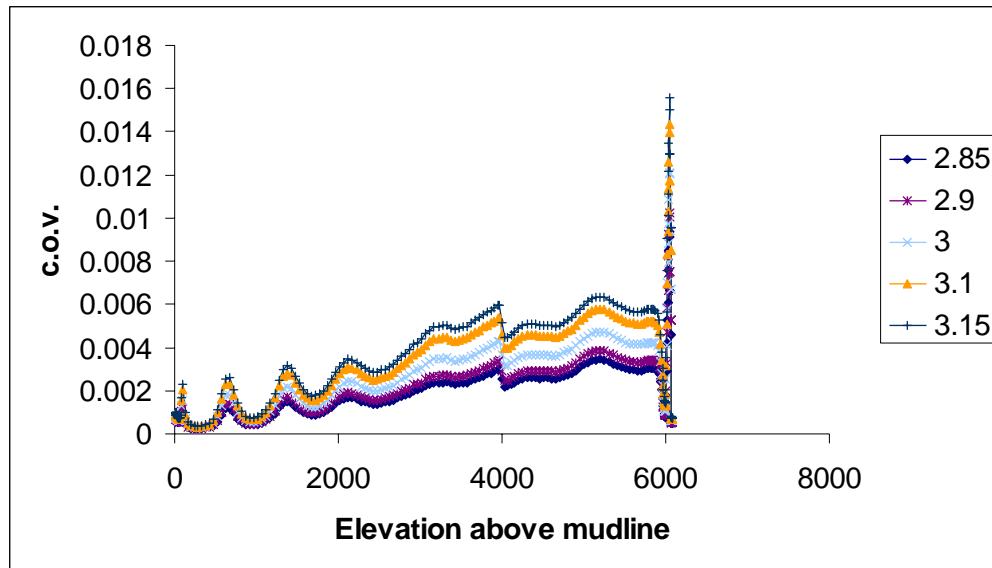


Figure 7-1: C.o.v. of Z at Different Points of Riser for Different m Values

7.3 Final Crack length: Uncertainty Analysis

Since the final crack length, a_N , is a function of Z , the mean and variance for a_N can be obtained from that for Z . However, since the relationship between a_N and Z (Eq 5-4) is non linear (Figure 7-2), an approximation is used to relate the moments for the two variables.

For $a_i=.5$, $m=3$ and $C=1E-13$, the variation of a_N with respect to Z is seen as shown in Figure 7-2. It is seen that a_N is an increasing function of Z . In this case, the relationship of a_N and Z is not far from linear. Knowing the fact that the variation in Z is low, the relationship is seen to be almost linear, when looked into small ranges of Z .

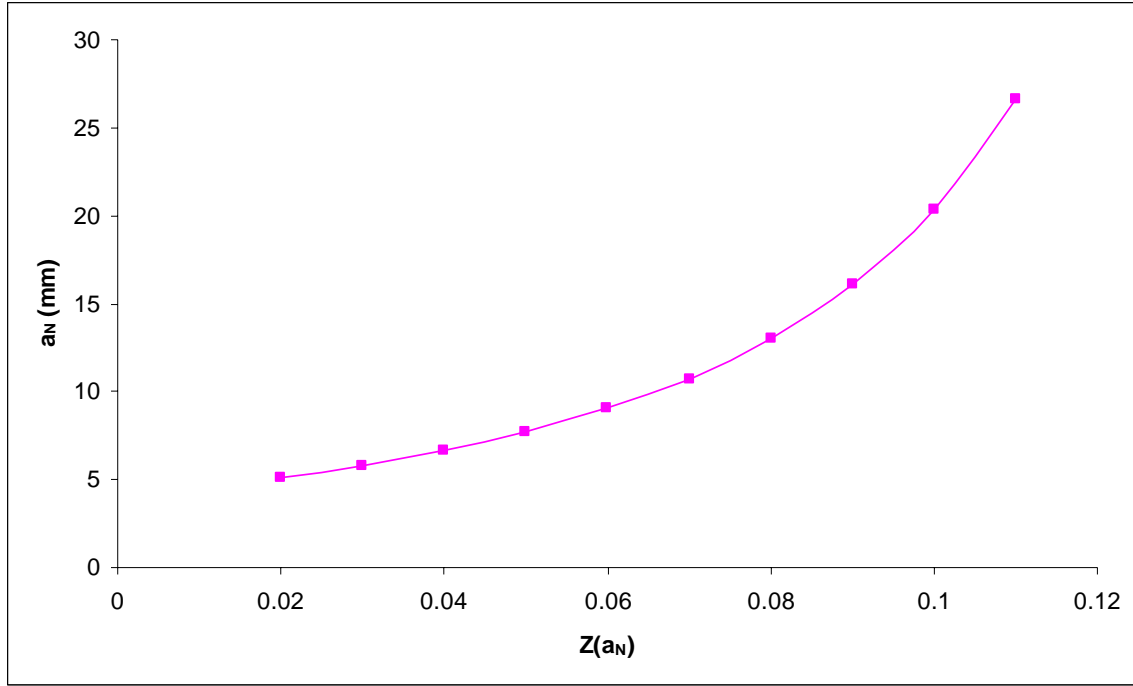


Figure 7-2: Variation of a_N with Z for $a_i=.5$, $m=3$ and $C=1e-13$ at 54feet of Elevation above Mud-line.

For a first order Taylor series approximation, Ang and Tang (1990), the mean and variance of a_N are given as follows

$$E[a_N] = g^{-1}(E[z]) \quad \text{Eq 7-8}$$

where $Z=g(a_N)$ (Eq 5-4)

$$Var[a_N] = \left(\frac{d g^{-1}(Z)}{dZ} \right)_{Z=E[Z]}^2 Var[Z] \quad \text{Eq 7-9}$$

After rearranging Eq 5-4, the derivative of a_N with respect to Z , is as shown below:

$$\frac{da_N}{dZ} = \left[Z\pi^{m/2} (1 - m/2) + a_i^{1-m/2} \right]^{2-m} \pi^{m/2} (1 - m/2) \quad \text{Eq 7-10}$$

For $m < 2$, the above derivative is always positive for positive values of Z . As Z is the sum of stress range values raise to the power m , Z is also positive. This concludes that a_N is an increasing function of Z for $m < 2$.

For $m > 2$, the derivative is positive for $E[Z].\pi^{m/2}(\frac{m}{2}-1) < a_i^{1-m/2}$, while negative otherwise. It is explained a little later, that the fatigue model doesn't work on $E[Z].\pi^{m/2}(\frac{m}{2}-1) > a_i^{1-m/2}$. This means that a_N is an increasing function of Z for $m > 2$ at all the reasonable values of Z . This concludes that a_N and Z has one to one relationship and inverse of $Z=g(a_N)$ exists.

As an example, at 54feet elevation above mud-line and assuming m and C to be 3 and $7e-13$, which are reasonable for the case-study, the

$$E[Z]=.020739$$

$$\text{Var}[Z]= 1.55E-10$$

Thus from Eq 7-8 and Eq 7-9, the expectation and variance of a_N are

$$E[a_N] \cong 5.112 \text{ mm}$$

$$\text{Var}[a_N] \cong 1.6E-07 \text{ mm}^2$$

$$\text{Std.Dev}[a_N] \cong .0004 \text{ mm}$$

Thus coefficient of variation of a_N is $7.8E-05$, which is negligibly small. This leads to the conclusion that the variation of a_N due to random load can be neglected and it can safely be estimated using the first order approximation in Eq 5-5 as follows:

For $m < 2$

$$a_N = \left[E[Z].\pi^{m/2} (1 - m/2) + a_i^{1-m/2} \right]^{2/2-m} \quad \text{Eq 7-11}$$

For $m > 2$

$$a_N = \left[a_i^{1-m/2} - E[Z].\pi^{m/2} (\frac{m}{2}-1) \right]^{2/2-m} \quad \text{Eq 7-12}$$

For $m > 2$, It is noted from Eq 7-13 that a_N increases as $E[Z]$ increases.

At $E[Z].\pi^{m/2}(\frac{m}{2}-1) = a_i^{1-m/2}$, a_N goes infinity, or the crack becomes a through wall crack, after which the fatigue law doesn't hold, as there is a point of discontinuity. Thus

during the analysis, it is important to understand the above relation and a check need to made to ensure that above equation is not used for $E[Z].\pi^{m/2}(\frac{m}{2}-1) > a_i^{1-m/2}$.

7.4 Sensitivity of Crack Growth to Weld Joints

The riser is considered to have failed when a crack in a weld becomes a through-wall crack. Thus it becomes imperative to understand the conditions which might lead to a through wall crack, i.e. when the crack length gets equal to the thickness of the riser outer casing. With the change in elevation of the point in consideration, the stress range cycles change and so does $E[s^m]$. The Paris Law factors m and C depend on the material strength and thus are assumed to be constant relative to the elevation. The circumstances and the type of welding used to join the riser joints will also be constant relative to the elevation distance. This leads to the fact that if the stresses were to remain the same at different points of riser and the initial crack length is same every where, the fatigue failure events could happen simultaneously and the probability of failure would increase as the number of welds (or length of riser) increases.

It is understood from the fatigue crack growth equation that the final crack length is an increasing function of $E[s^m]$. Thus the point of occurrence of maximum $E[s^m]$ will be the point of maximum crack length or the most likely location of failure.

Figure 7-4 shows the relation of the $E[s^m]$ with location in the riser above the mud line. First riser joint considered in this study is located above the stress joint at an elevation of 54 feet above mud line. It is also noted from the figure that $E[s^m]$ decreases with increasing elevation, making the point 'A', i.e. elevation of 54 feet, the most critical point. However, the riser failure can also occur at elevations higher than 54 feet. If there are big cracks prominent at the high elevations, even the less intensive load cycles can lead to failure. The likelihood of this situation is studied later, while the sensitivities of final crack length are studied at 54 feet, which is a critical point of failure.

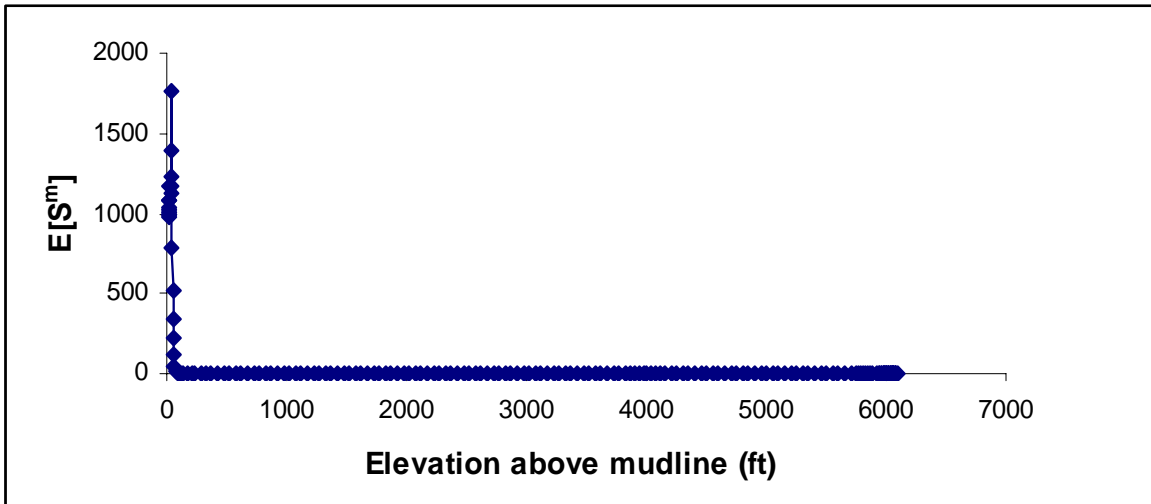


Figure 7-3: Change in $E[s^m]$ with the Location of Weld in Riser

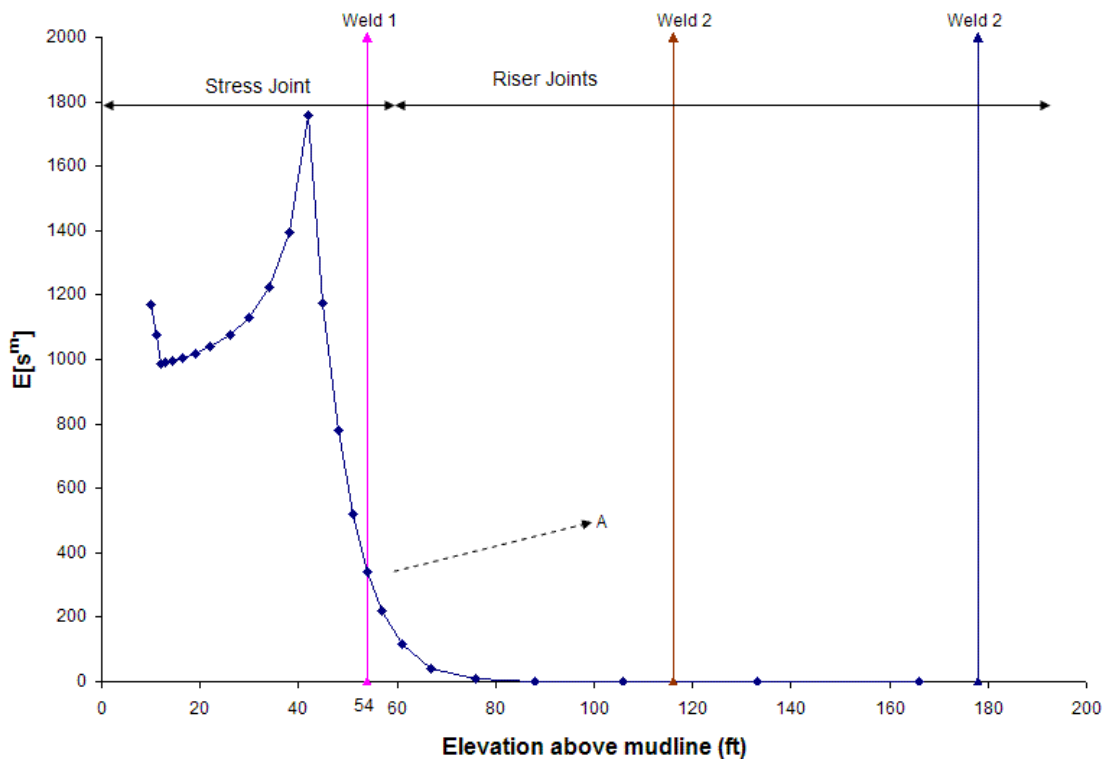


Figure 7-4: Change in $E[s^m]$ with the Elevation Point of Riser, Magnified for Range between 0 feet and 180 feet

7.5 Sensitivity of Crack Growth with Material Properties

The sensitivity of crack growth with material properties m , C , a_i , were studied at 54 feet, since it was decided to be a critical joint. The objective is to understand the behavior of the final crack length with respect to the material properties. Two of the factors were changed at a time in this analysis.

Figure 7-5 shows the variations in the final crack length with the change in m and C . It is found that the final crack length increases with an increase in m and C , or it is a non-decreasing function of m . This is also evident from Paris Law also as the rate of crack growth is a positive function of m and C . It is seen for some values of C , the curve is only a horizontal line and no variations are seen with the change in m . This result occurs because the wall thickness is assumed to be 30mm and the final crack length has become a through-wall crack. If there is a failure for some small value of m and knowing that the crack length is a non-decreasing function of it, then there will be a failure for a greater value of m too.

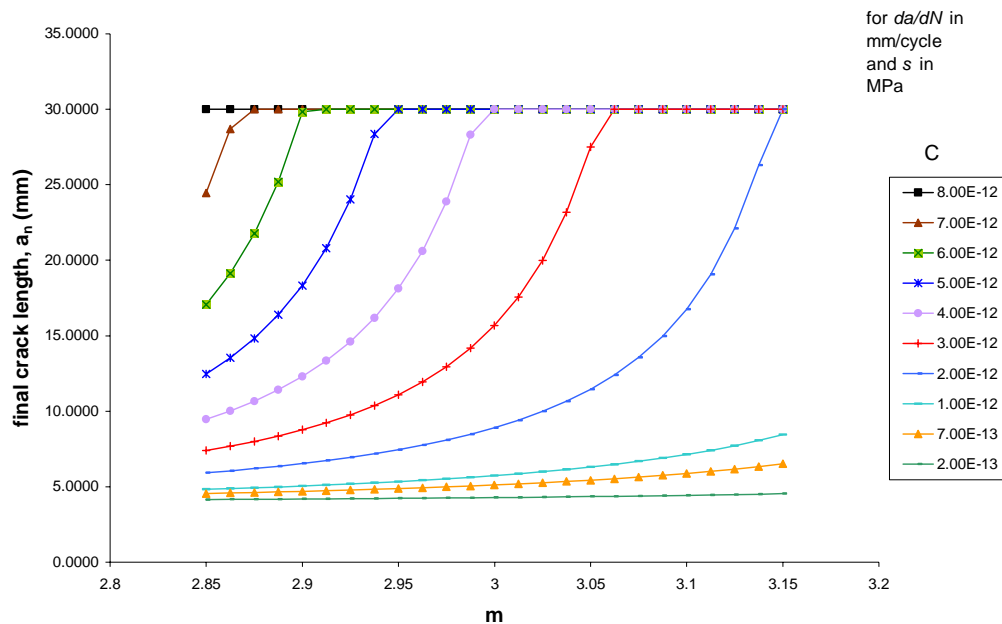


Figure 7-5: Sensitivity of the Final Crack Length with m for Different C at 54 feet of Elevation above Mud-line for $a_i=4\text{mm}$

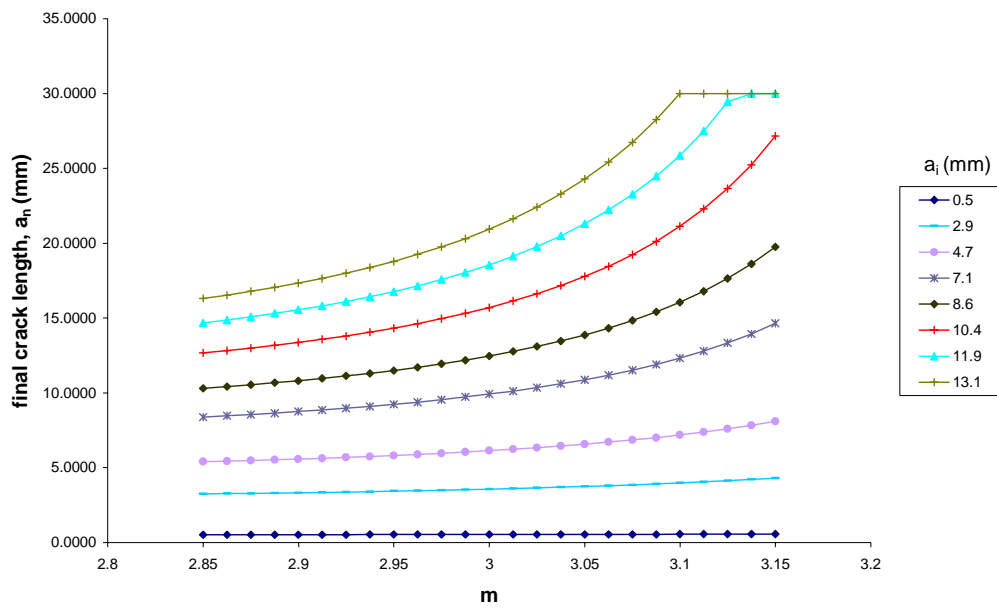


Figure 7-6: Sensitivity of the Final Crack Length with m for Different a_i at 54 feet of Elevation above Mud-line for $C=7E-13$

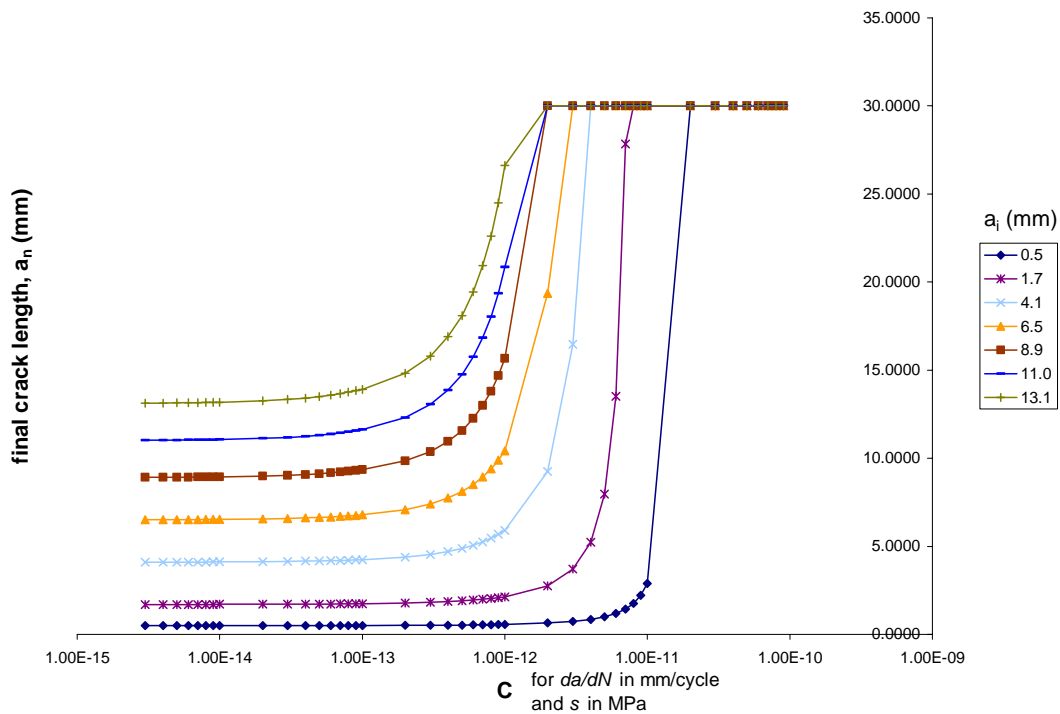


Figure 7-7: Sensitivity of the Final Crack Length with C for Different a_i at 54 feet of Elevation above Mud-line for $m=3$

Figure 7-6 shows variations in the final crack length with the change in m and a_i for a constant C . Final crack length increases with an increase in m or a_i ; it is a non-decreasing function of m . This is also evident from Paris Law also as the rate of crack growth is a positive function of m and a_i . From Figure 7-6 and Figure 7-7, it is concluded that the final crack length will also be a non-decreasing function a_i and C . High sensitivity of crack propagation to the material parameters, m and C , is also consistent with data in Garbatov and Soares (2004). They found the fatigue life to be very different on four different grades of steel.

7.6 Failure Envelope

Two dimensional analyses helps in understanding the sensitivity of crack growth with respect to two variables with the third variable constant. During the risk analysis, the fundamental problem is to know the failure scenarios in the life of the riser. In order to help evaluate the failure regions, failure envelopes were developed depicting the conditions of failure. The failure envelope curve, Figure 7-8, is an expected critical relationship between initial crack length, a_i , and Paris Law factor, C , for a constant m , which gives the boundary condition for the fatigue failure. Any point above the curve is a point of failure, while a point below the curve doesn't result in failure. The failure envelopes move down with an increase in m , resulting in the increase in the size of the failure region.

7.7 Sensitivity of Crack Growth with Life of Study Riser

Sensitivity of the crack growth of the study riser with its life was studied through Figure 7-9. With the increase in the life of the riser, there is an increase in the number of stress load cycles, resulting in more fatigue damage. But the damage will depend on the material properties and thus this sensitivity was checked at different values of C . The crack growth was too sensitive for $C > 1E-12$. at $m=3$ and initial crack length of 0.5mm.

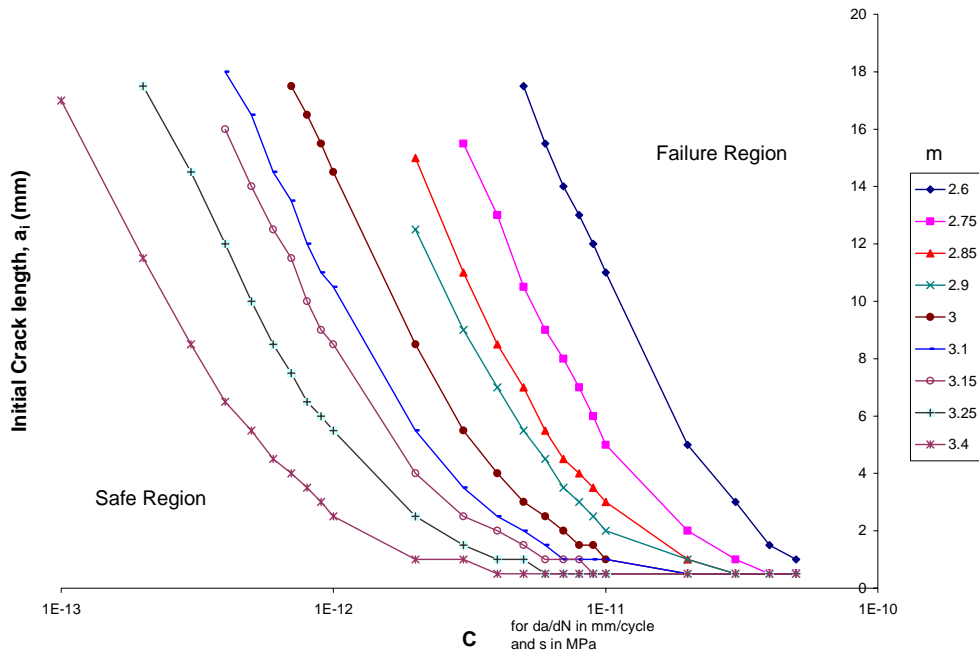


Figure 7-8: Failure Envelope with Respect to m , C , a_i at 54 feet of Elevation above Mud-line

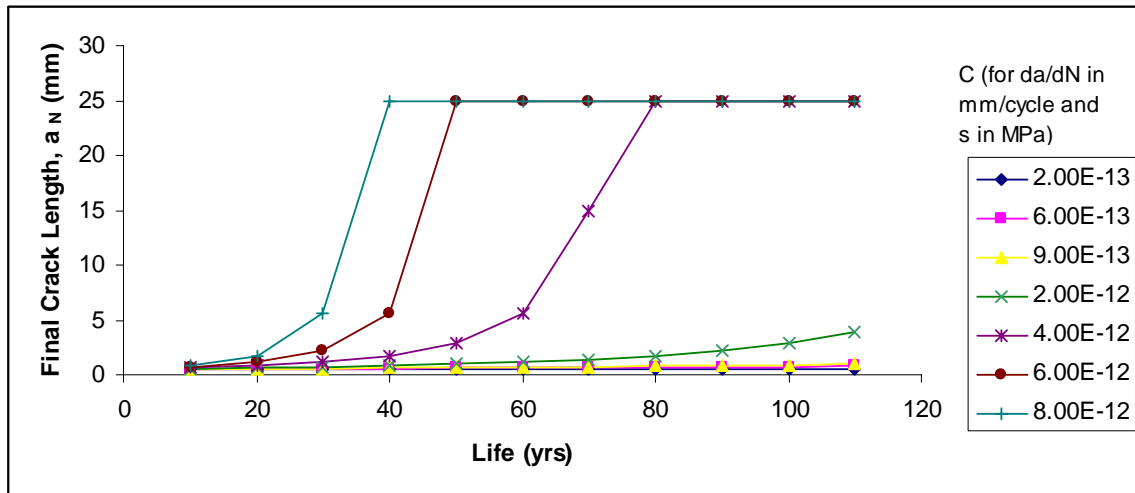


Figure 7-9: Sensitivity of Crack Growth with Life of Study Riser at $m=3$ and $a_i=.5$ mm

7.8 Summary

This chapter established the connection between the random stress range cycles with the final crack length. The information of the random stress load history is contained in the random variable Z , which is used to make inference about the final crack length.

The coefficient of variation of Z was negligibly small. Low variation in Z doesn't directly imply that the variation in final crack length is also small. Due to the non-linear relationship between Z and final crack length, the moments of the final crack were approximated from that of Z , using first order Taylor series approximation. Variance of a_N was too low to be considered and uncertainty in it was neglected.

It was further seen that final crack length is an increasing function of $E[Z]$ and $E[Z]$ is an increasing function of $E[S^m]$. Thus a critical point on the riser will be the point of maximum $E[S^m]$, which would have maximum final crack length. It was found that weld joint at 54 feet elevation above mud-line has the maximum $E[S^m]$ and thus is a critical point.

Sensitivity analyses of final crack length with respect to initial crack length and material properties were conducted and it was found that it is highly sensitive to C and m . Failure envelopes were developed which define the boundary of failure region with respect to the C , m and a_i . These failure envelopes will be used in the next section to find the probability of fatigue failure, considering uncertainty in C , m and a_i .

Sensitivity of the crack growth with the life of the study riser was assessed too. It was concluded that the crack growth is highly sensitive for $C > 1E-12$ at $m=3$ and initial crack length of 0.5 mm.

Chapter 8: Fatigue Failure Probability for Study Riser

The objective of this chapter is to quantify the uncertainties in initial crack length a_i , crack frequency, and material parameters, m and C . Limited information was provided by the experts regarding these parameters and the results will be based on past experiments and findings in published literature, referenced. The final fatigue failure probability is then evaluated with the help of the law of total probability.

8.1 Uncertainty in Initial Crack Length, a_i

Fatigue failures in metal structures are frequently caused by the unchecked propagation of flaws or cracks in metal and welds. Due to the microscopic nature of flaw sizes, there isn't any technique which is able to detect all flaw sizes. The operation characteristic of nondestructive testing (NDT) techniques is governed by a detectability curve, $P(x)$. $P(x)$ relates the probability of detecting a flaw of size 'x' for the respective NDT technique used for inspection. Thus uncertainty in the flaw size is dependent on the kind of inspection techniques used, the repair criteria and on the quality of welding.

Tang and Wilson (1973) presented a Bayesian model to find the distribution of the initial crack length after fabrication and repair. This model is powerful because it considers all the relevant factors and it doesn't require specific assumptions about inputs to the model.

Moan, et al. (2000) assume the crack length (before repair) follows an exponential distribution with the mean crack length as the unknown parameter. The probability of detection curve is approximated by a cumulative exponential function with the unknown parameter for crack depth. The parameters are then found through Bayesian updating using the evidence from inspection results.

Simola and Pulkkinen (1998) describe the use of statistical models for the evaluation of the reliability of non-destructive inspections. The flaw sizing models considered were based on logarithmic and logit transformations of the flaw sizes. A model containing unknown parameters was formed and the probability distribution was found using maximum likelihood estimation and Bayesian estimation of the unknown parameters.

In almost all the papers discussed, the common theme was the use of Bayesian estimation and the inspection results to find the probability density function of the initial crack size, which is described below.

Let

$f'_x(x)$ = original probability distribution function (p.d.f.) of flaw size after fabrication

$f''_x(x)$ = probability distribution function of flaw size for detected (observed) flaws.

Then using Bayes' theorem

$$f''_x(x) = \frac{P(x)f'_x(x)}{k} \quad \text{Eq 8-1}$$

$$f'_x(x) = \frac{k_1 f''_x(x)}{P(x)} \quad \text{Eq 8-2}$$

where ' k_1 ' is the probability of detection and the normalizing constant such that $f'_x(x)$ is a probability density function. Thus we can have the p.d.f. of the initial crack size after fabrication, which will be further truncated due to repair operations after inspections, as discussed later in the section.

Probability of detection data (POD) for the non-destructive testing techniques is generally described, [14], by the following expression.

$$P(x) = 1 - \frac{1}{1 + \left(\frac{x}{x_0}\right)^b} \quad \text{Eq 8-3}$$

where, x_o and b will depend on the type of inspection technique used. But x_o is not readily available, while it is easier to get to know the crack length, which has around 90% chances of detection. Thus the above equation is modified to the following.

$$P(x) = 1 - \frac{1}{1 + 9\left(\frac{x}{a_{90}}\right)^b} \quad \text{Eq 8-4}$$

Where,

a_{90} is the crack length having 90% chances of detection. This is called the 90th percentile detectability limit of the inspection technique.

The a_{90} and b values for Magnetic particle inspection above water and on a ground test surface are given in reference [14] as 22mm and 1.297 respectively with 95% confidence level. For the purpose of the study, 22mm seems to be a very high value for a_{90} . A very conservative value of 13mm is used for the analysis, which is based on the experience of the experts. With a_{90} to be 13mm and b to be 1.297, the POD curve is plotted as shown in Figure 8-1.

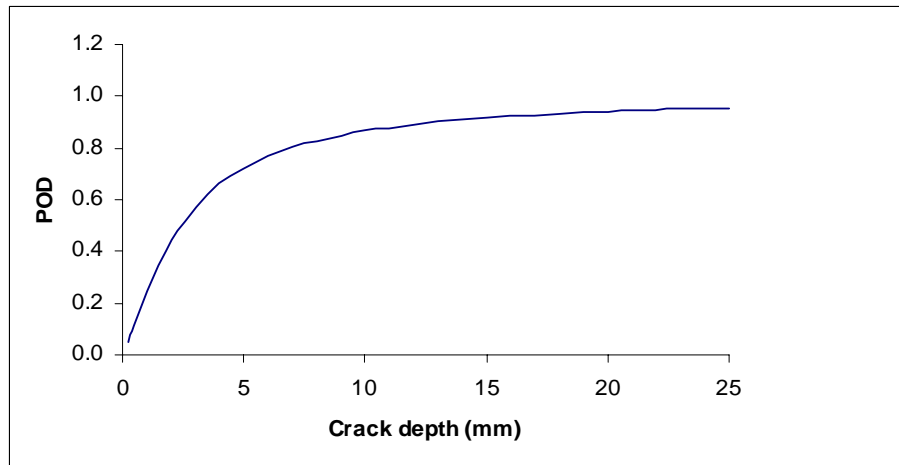


Figure 8-1: Probability of Detection Curve Based on ref [14]

It should be understood that any function should be as accurate as possible at the tail of the distribution. The goodness for fit is not critical for small defect sizes as such defects do not play an important role in determining the probability of failure. Also, the observed

distribution of small defects is likely to be more subjective to the measurement error (i.e. on NDT reliability) than that of large defects. An analysis was carried out to understand the nature of distribution of the flaws observed after magnetic particle inspection and ultrasonic inspection by Rogerson, et al. (1982). They concluded after several experiments that flaw size distribution observed after the NDT is best described by a Weibull distribution, which has the ability to capture the probability density for large defects.

Thus for the fatigue analysis, the observed defect distribution after NDT is

$$f_x''(x) = \text{Weibull}(\alpha, \beta, \gamma)$$

where α is the shape parameter, β is the scale parameter and γ is the location parameter.

Its pdf is as follows

$$f_x''(x) = \frac{\alpha}{\beta} \left[\frac{x-\gamma}{\beta} \right]^{\alpha-1} \exp \left[- \left(\frac{x-\gamma}{\beta} \right)^\alpha \right] \quad \text{Eq 8-5}$$

After the NDT, the detected cracks, which don't meet the acceptance criteria, are repaired by either re-welding or by cutting and replacing the defected portion. If all the cracks less than a_c are accepted, this means that all the detected cracks having length greater than a_c are repaired. Once the initial distribution of the cracks after fabrication, $f'(x)$, is found from Equation 8-2, the distribution of the cracks after fabrication and repair, $f'''(x)$, is found as follows.

$$\begin{aligned} f_x'''(x) &= f_x'(x) \cdot [1 - P(x)] \cdot k_3 & \text{if } x > a_c \\ &= f_x'(x) \cdot k_3 & \text{if } x \leq a_c \end{aligned} \quad \text{Eq 8-6}$$

where k_3 is the normalizing constant such that $f'''(x)$ is a pdf.

It is noted that the uncertainty in the flaw size after repair and fabrication is affected by the POD and the pdf would be a truncated distribution, as shown in Figure 8-2.

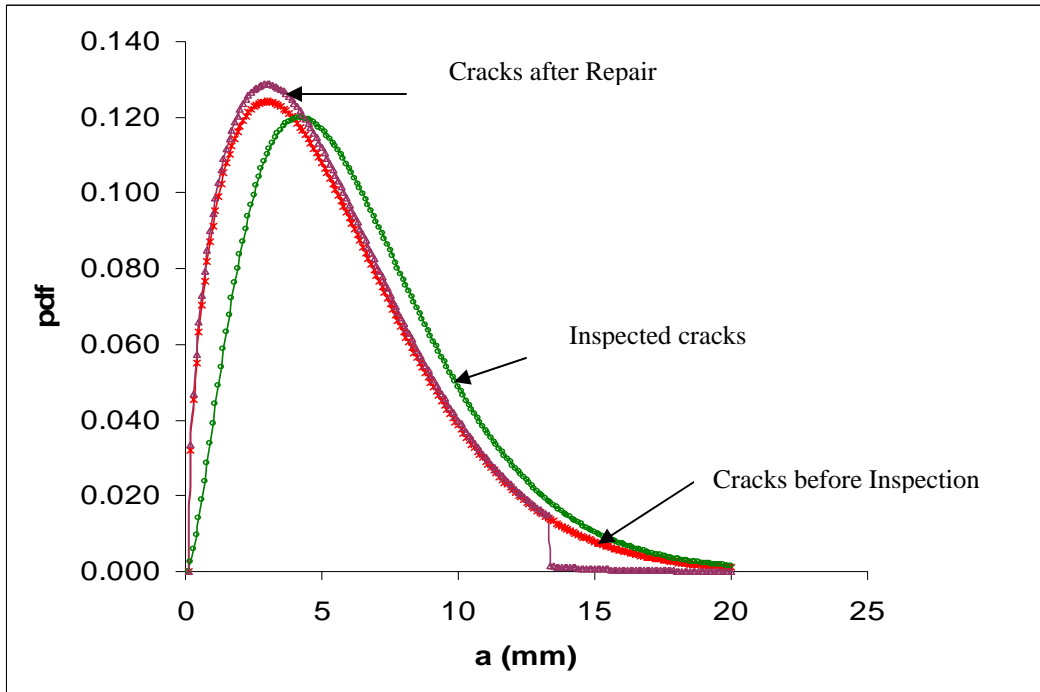


Figure 8-2: Probability Density Function of the Crack Length

8.2 Uncertainty in Initial Crack Density, v_i

The frequency of cracks also has a high impact on the failure probability as greater the number of cracks, the greater the chances of failure. Thus it is required to understand the probability distribution of the crack density before evaluating the final fatigue probability. Tang and Wilson (1973) argued that the inspection results can also help in establishing the distribution of the crack density. He assumed the number of cracks detected given some density function to be Poisson and used the prior distribution of the crack density as Gamma. Since the Gamma distribution is a conjugate pair for Poisson sampling, this serves as a very convenient distribution to quantify the uncertainties in the crack density.

Early Denison mentioned that approximately 5% of the welds are repaired after the non destructive testing. From the design of the study riser, it is known that the riser outer diameter (D_o) is approximately 1 feet.

Let x welded joints have only one crack.

v : number of cracks / unit length (feet)

$E[v]$: mean value of the number of cracks/length (feet)

D_o : Riser outer diameter= 1 feet

L : Length of weld = $\pi D_o = 3.14$ feet

Expected number of cracks in 1 weld = $3.14 E[v]$

Expected number of cracks in x welds = $3.14 x E[v] = 1$

Percentage number of welds having a crack = $100/x = 314 \cdot E[v]$

Prob (repair given one crack) = Prob (crack size greater 13 mm after inspection) = .0549

Percentage number of welds repaired = $314 \cdot E[v] \cdot 0.0549 = 5$

Thus $E[v]$ is approximately .29 cracks/feet. The results presented by Tang and Wilson (1973) about the gamma parameters were modified to attain a reasonable value of the mean of the crack frequency. A reasonable gamma distribution which represents the above results is.

$$v = \text{Gamma}(0.1, 3.114) \quad \text{Eq 8-7}$$

The above distribution function is continuous and thus needs to be numerically discretized for the simple calculations.

$$P(g \text{ cracks}) = \int_{\frac{g}{L}}^{\frac{g+1}{L}} f_v(v) \cdot dv \quad \text{Eq 8-8}$$

Table 8-1: Numerically Solved to Find the Chances of g Cracks in a Weld

g cracks	Prob	g cracks	Prob
0	0.44242	5	1.38E-05
1	0.47858	6	5.48E-07
2	0.07311	7	2.00E-08
3	0.00557	8	6.81E-10
4	0.00030	9	2.28E-11

8.3 Uncertainty in m and C

These parameters are dependent on material and the properties of weld. Since there is uncertainty in material properties, there is uncertainty in m and C . It is seen from the sensitivity graphs that m and C are very important factors affecting the crack growth and thus riser failure. Thus it is imperative to understand the variations in these parameters and model it to be able to estimate the riser failure probability. Zhao, et al. (2002) mentioned that there are two main methods to model the crack growth variability through the use of random variables, C and m .

- i) C and m are negatively correlated variables
- ii) m is deterministic and C is a variable dependent on m

The second method is adopted here because of the convenience and the availability of sufficient literature on this method to quantify the uncertainties. Zhao, et al. (2002) also mentioned that $\ln C$ is approximately Normal distributed for some deterministic value of m , but the mean and variance changes with m .

If m is also normally distributed, then $(\ln C, m)$ can be modeled as bivariate normal distributions as shown in Ang and Tang (1990), pg 291.

$$\ln C / m \sim Normal(E[\ln C / m], Std[\ln C / m]) \quad \text{Eq 8-9}$$

Where,

$$E[\ln C / m] = E[\ln C] + \rho \frac{Std[\ln C]}{Std[m]} (m - E[m]) \quad \text{Eq 8-10}$$

$$Std[\ln C / m] = Std[\ln C] \sqrt{1 - \rho^2} \quad \text{Eq 8-11}$$

Table 8-2 lists some of the adopted values of the expectation of m and C . The scenario referred by Zhao, et al. (2002) regarding the welds subjected to water is closest to this study and the expectation and variance of m and C are adopted corresponding to this

scenario. He used lognormal distribution to model C and normal to model m. The same approach is adopted to model these parameters. Thus

$$E[C] = 1.28 \text{ E-13 (for da/dN in mm/cycle and s in MPa)}$$

$$\text{Std.dev}[C] = 7.59 \text{ E-14}$$

$$E[m] = 3.1$$

Table 8-2: Probabilistic Models of C and m

Reference	E[m]	E[C] (for da/dN in mm/cycle and s in MPa)	Std[C]	Scenario
Garbatov and Soares (2004)	3.5	8.85E-15		Steel with Yield strength 38ksi
Garbatov and Soares (2004)	3	3.80E-13		Steel with Yield strength 45ksi
Garbatov and Soares (2004)	2.4	1.75E-11		Steel with Yield strength 64ksi
Garbatov and Soares (2004)	2.6	5.27E-12		Steel with Yield strength 58ksi
Zhao et al (2002)	3.1	1.28E-13	7.59E-14	Welds in Air
Zhao et al (2002)	3	1.92E-13	4.67E-14	Welds in Air
Zhao et al (2002)	2.8	9.97E-13	2.32E-13	Welds in Air
Zhao et al (2002)	3.5	4.58E-14	4.12E-14	Weld Subjected to Sea Water
Zhao et al (2002)	3.1	1.28E-13	7.59E-14	Weld Subjected to Sea Water
Darci et al	3	1.85E-13	5.75E-14	Fillet welded joints

8.4 Critical Failure Point

It was mentioned before that the fatigue failure at higher elevations than 54 feet can also lead to riser failure, where there are less intensive load cycles. In order for the fatigue failure at elevations above 54 feet to be the cause of riser failure, there should be no failure at 54 feet. The likelihood of occurrence of this situation is understood from fatigue analysis at the next joint above 54 feet, which is at 116 feet.

Figure 8-3 and Figure 8-4 show the fatigue failure envelopes at an elevation of 116 feet and 54 feet. It is concluded from Figure 8-3 and Figure 8-4 that

- Welded joint at 54 feet and 116 feet is in safe region for $C < 1\text{E-13}$ for all reasonable values of a_i and m .
- There is a possibility of failure for a welded joint at 54 feet, while welded joint at 116 feet lies in the safe region for $1\text{E-13} < C < 1\text{E-10}$.

- There is a possibility of failure for a welded joint at 116 feet, while welded joint at 54 feet lies in the failure region for $1E-13 < C < 1E-10$.
- Both the welded joints at 54 feet and 116 feet lies in the failure region for $C > 1E-10$.

These facts are summarized in Table 8-3.

Table 8-3: Failure or Safe Regions for Welded Joints at 54feet and 106feet Elevation

Range of C	54 feet elevation	106 feet elevation
$C < 1e-13$	Safe Region	Safe Region
$1e-13 < C < 1e-10$	Safe and Failure Region	Safe Region
$1e-10 < C < 1e-8$	Failure Region	Safe and Failure Region
$C > 1e-8$	Failure Region	Failure Region

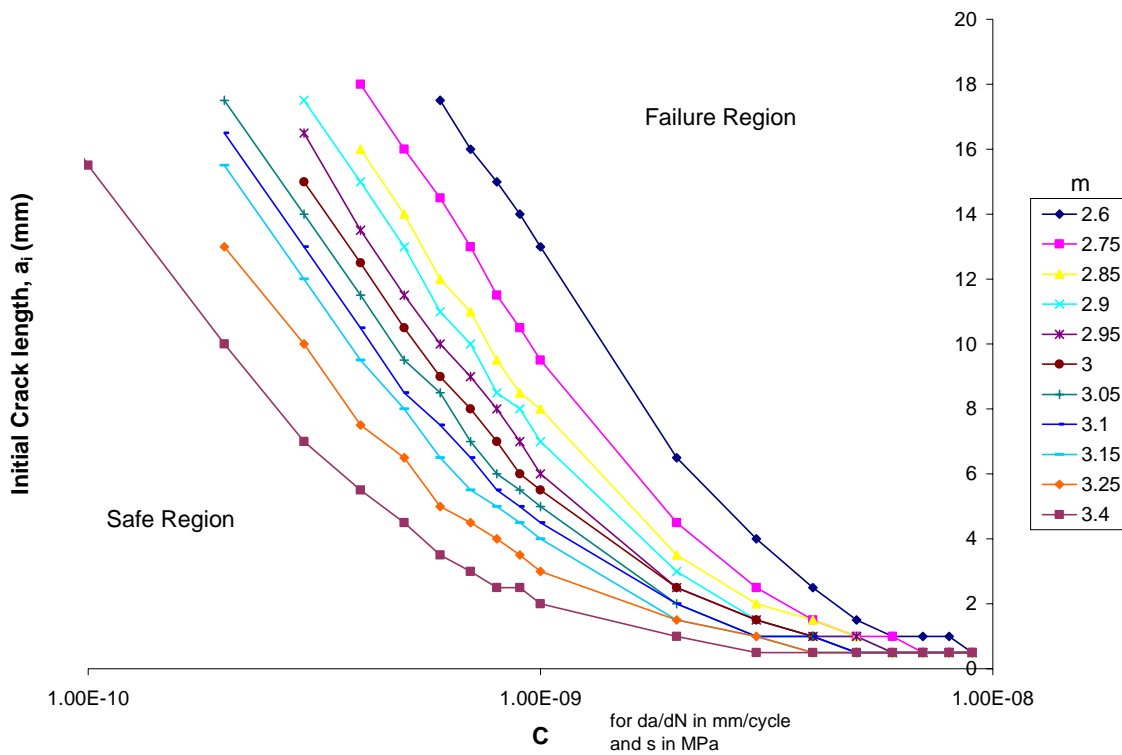


Figure 8-3: Failure Envelope w.r to m , C , a_i at 106 feet Elevation above Mud-line

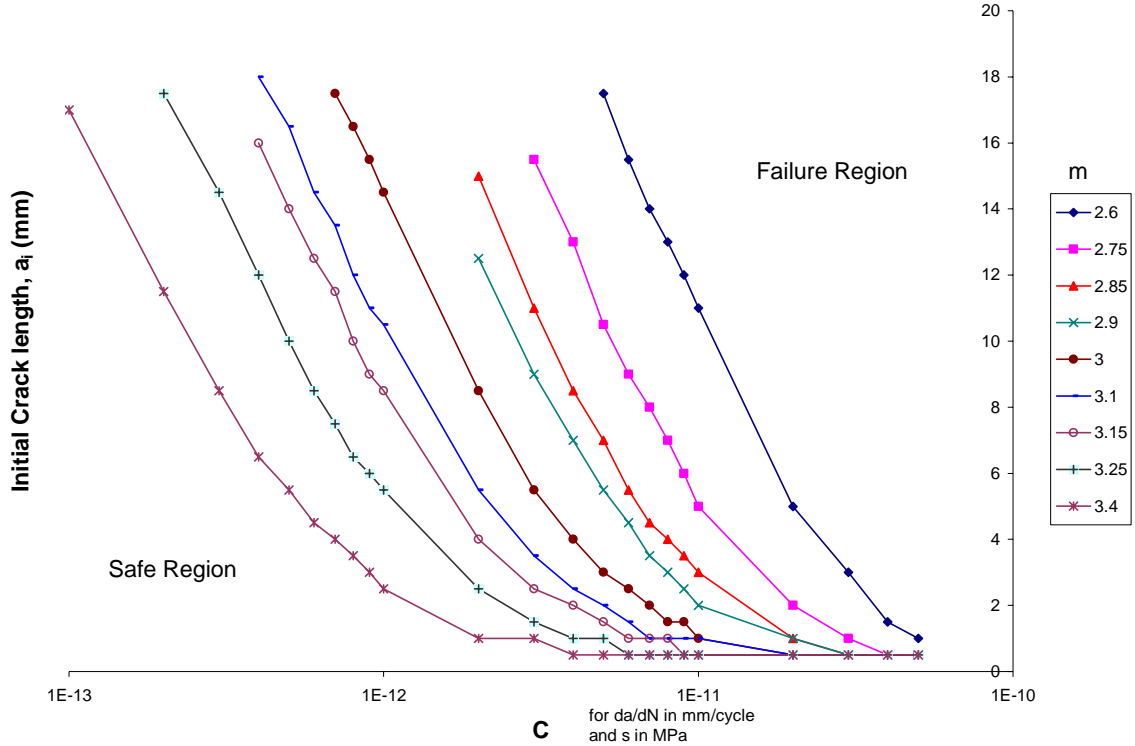


Figure 8-4: Failure Envelope w.r to m , C , a_i at 54 feet Elevation above Mud-line

It is seen from Figure 7-4 that $E[s^m]$ is a non-increasing function of elevation above mud-line. Thus it is highly unlikely that the riser will fail due to any other joint above the welding joint at 54 feet of elevation. To support the argument, the probabilities of failure are calculated with reasonable probabilistic models of m and C .

8.5 Fatigue Failure Probability

8.5.1 Fatigue Failure probability with constant m and C

Fatigue failure probability is found for known values of m and C and using the uncertainty in initial crack length a_i and number of cracks. For constant m and C , a value of a_i is found from the failure envelope curve depicting the boundary condition for fatigue failure. For the considered values of m and C , fatigue failure occurs for every

value of crack length greater than a_i . Thus if there is only one crack in the welded joint, then using the law of total probability, probability of failure is as follows:

$$P_{1,m,C} = P(\text{failure} | \text{one crack}, m, C) = \int_{a_i}^{25} f_x'''(x).dx \quad \text{Eq 8-12}$$

$$P_{n,m,C} = P(\text{failure} | n \text{ cracks}, m, C) = 1 - (1 - P_{1,m,C})^n \quad \text{Eq 8-13}$$

$$P_{f,m,C} = P(\text{failure} | m, C) = \sum_{\forall g} P_{g,m,C} \cdot P(g \text{ cracks}) \quad \text{Eq 8-14}$$

8.5.2 Final Fatigue Failure Probability

Final fatigue failure probability is found by summing up the product of failure probability found with known m and C , probability of m and probability of C given m . Law of total probability is again used here as shown in Eq 8-15.

$$P_F = \sum_{\forall m} \sum_{\forall C} P_{f,m,C} \cdot P(m) \cdot P(C/m) \quad \text{Eq 8-15}$$

For the reasonable probabilistic models adopted for each factors, the probability of failure due to fatigue is 0.00138. The results for the failure probabilities at 54 feet above elevation are shown in Appendix D. It is seen that as m increases, the chances of having a smaller C also increases, which is explained by the negative correlation assumed between them.

8.6 Sensitivity of Final Fatigue Failure Probability with $E[C]$ and $E[m]$

Sensitivity of final fatigue failure probability with $E[C]$ and $E[m]$ is studies at welded joints located at 54 feet and 116 feet.

At 54 feet above elevation (Figure 8-5), the probability of failure is very sensitive to both $E[C]$ and $E[m]$ in the range $1e-12 < E[C] < 5E-11$. The failure probability becomes steady after some value of $E[C]$. This occurs because the welded joint is in the failure region as represented by the failure envelopes. The failure probability doesn't increase

beyond 0.51 in the failure region due to the chances of no crack in the weld. If the material properties are such that the $E[C] < 5E-14$, the probability of failure is essentially zero, even if the initial crack size is high. Non-destructive inspection and repair of the cracks reduces the chances of the crack above a critical size drastically, reducing the likelihood of failure.

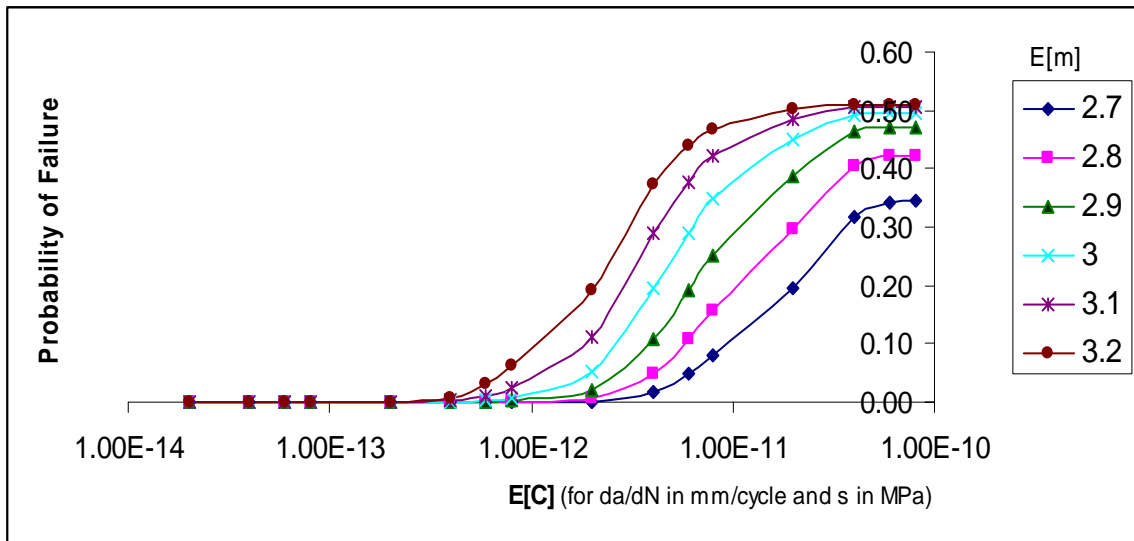


Figure 8-5: Sensitivity of Probability of Failure with $E[C]$ and $E[m]$ at 54 feet Elevation above Mud-line

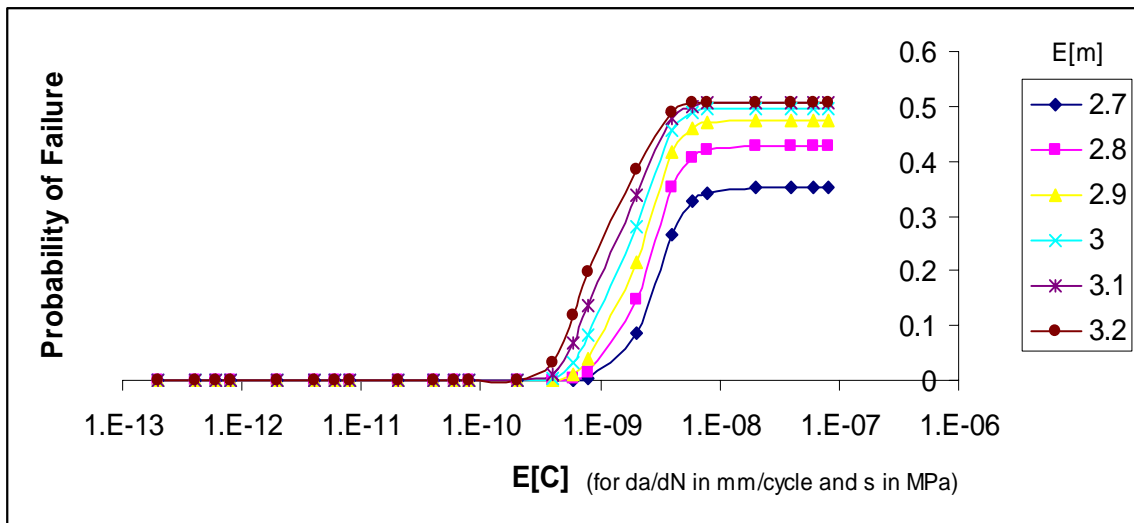


Figure 8-6: Sensitivity of Probability of Failure with $E[C]$ and $E[m]$ at 116 feet Elevation above Mud-line

From Figure 8-5 and Figure 8-6, the arguments presented in Section 8.4 about the critical failure point are supported. Thus, for reasonable expected values of C and m , which are $5E-13$ and 3 respectively, the failure probability is governed by the welded joint at 54 feet elevation above mud-line.

8.7 Summary

In this chapter, the uncertainties of the initial crack length, total number of cracks, and Paris law factors, m and C , were quantified. During the identification of the critical point in the riser, it was concluded that 54 feet elevation above mud-line is the critical point. The law of total probability was used to find the final fatigue failure probability by combining the probabilities of each of the random factors in the failure region, shown by the failure envelopes. A failure probability of 1 in 1000 in a 20 yr riser was estimated for reasonable inputs for the material parameters and the weld quality. This value is consistent with the existing technological standard in the oil and gas offshore industry.

Sensitivity of the final fatigue probability was seen to be very high with respect to $E[C]$. This sensitivity measure can be used to select material properties of the riser during the design phase to make sure that failure probability is low.

Chapter 9: Conclusions

A probabilistic assessment methodology to quantify the uncertainties in the failure mechanisms of a steel production riser in deepwater applications has been developed. First the background on the steel production riser was presented, detailing its functions, main components, operational phases and design considerations. Next, the study riser, developed by Stress Engineering, was described with the design basis. Failure scenarios were shown through a fault tree followed with the analyses to determine the likelihood of their occurrences. Fatigue was found to be main failure mechanism affecting the risks of the production riser. Probabilistic fatigue analysis was carried out, which included development of the probabilistic model and quantifying the uncertainties affecting it. Finally fatigue failure probability was found and its sensitivity calculated with the material parameters.

9.1 Conclusions

The following conclusions were drawn through the analyses:

- i) Fatigue failure mechanism is the most important factor contributing to the risks, while bursting, collapsing, yielding are not much likely.
- ii) Path of the stress cycles has no effect on the final crack length and thus only the stress load cycles histogram is required for the probabilistic fatigue analyses.
- iii) Factors affecting fatigue failure are the stress cycles histogram, weld quality, and the material properties.
- iv) Coefficient of variation of final crack length due to random load cycles was found to be negligible. This result was mainly due to averaging affect of large number of cycles during the life of the riser.

- v) First order Taylor approximation used to estimate the final crack length due to the random load cycles over the life of the study riser
- vi) Final crack length increases with the increase in C , m and a_i .
- vii) Final crack length is highly sensitive to the material parameters, C and m and thus accurately designing the riser considering these parameters can drastically reduce the risks associated with fatigue.
- viii) Final crack length is highly sensitive to the life of the riser for $C > 1E-12$ (for da/dN in mm/cycle and s in MPa)
- ix) The riser fatigue failure probability is governed by the fatigue of the welded joint located at 54 feet elevation above mud line of the study riser.
- x) Final fatigue failure probability of the study riser is .00138 with reasonable probabilistic models considered for the material and weld quality parameters.
- xi) The failure probability is highly sensitive to the material parameters C .

9.2 Future Work

Following are the items that could be considered for future work on this topic:

- i) The fatigue failure considered crack growth in only one dimension. Crack growth in one dimension is a conservative approach and more accurate results can be found using the theory of crack growth in two dimensions.
- ii) More information about the uncertainties in the initial crack, and the material parameters needs to be collected to make the probability distributions to be more reasonable.
- iii) Although the likelihood of failure due to bursting and collapsing were argued to be less, the consequences of these failure scenarios are extreme and thus risks found might be more. Uncertainty analysis can be extended to these failure scenarios too.
- iv) Failure analysis due to riser interference was left out in this thesis. Although the failure is not very likely in normal operating conditions, it might have good chances

during installation condition. This condition might be an issue for the comparative risk analyses of the steel and composite risers.

- v) The consequences for having a fatigue failure were not discussed. Event trees could be identified for this particular kind of failure to understand the possible escalation factors after the failure and then mitigation strategies can be developed to reduce the risks due to them.
- vi) Failure mechanisms of a composite riser need to be identified to be able to compare the risks of the steel with composite production riser.

Appendix A: Expectation and Variance of 'Z'

$$Z(a_N) = \sum_{j=1}^N C(s_j)^m \quad \text{Eq A-1}$$

$$\rightarrow Z(a_N) = C \sum_{j=1}^N (s_j)^m \quad \text{Eq A-2}$$

$$\text{Let } X = \sum_{j=1}^N (s_j)^m \quad \text{Eq A-3}$$

Since s_j are independent and identically distributed,

$$\rightarrow E[X] = N E[s^m] \quad \text{Eq A-4}$$

$$\rightarrow V[X] = N \text{Var}[s^m] \quad \text{Eq A-5}$$

From Eq A-2,

$$\rightarrow Z = CX \quad \text{Eq A-6}$$

Since X is a random variable and C is assumed to be constant,

$$\rightarrow E[Z] = CE[X] \quad \text{Eq A-7}$$

$$\rightarrow \text{Var}[Z] = C^2 \text{Var}[X] \quad \text{Eq A-8}$$

Now using Eq A-4, and Eq A-5,

$$\rightarrow E[Z] = NC E[s^m] \quad \text{Eq A-9}$$

$$\rightarrow V[Z] = NC^2 \text{Var}[s^m] \quad \text{Eq A-10}$$

Appendix B: Moments of a Rayleigh distribution

When $S \sim \text{Rayleigh}(a)$

$$\text{i.e. } f(s) = \frac{s}{a^2} \exp\left[-\frac{s^2}{2a^2}\right]$$

$$E[s^m] = \int_0^{\infty} s^m \frac{s}{a^2} \exp\left[-\frac{s^2}{2a^2}\right] ds$$

let

$$u = \frac{s^2}{2a^2}$$
$$a^2 du = s ds$$

Thus

$$E[s^m] = \int_0^{\infty} (\sqrt{2a})^m \cdot u^{m/2+1-1} \exp[-u] ds$$

$$E[s^m] = (\sqrt{2a})^m \cdot \int_0^{\infty} u^{m/2+1-1} \exp[-u] ds$$

$$E[s^m] = (\sqrt{2a})^m \cdot \Gamma(m/2 + 1)$$

$$\text{Mean} = E[s]$$

$$\text{Variance} = E[s^2] - E[s]^2$$

Thus

$$\text{Variance}[s] = a^2 \left[2 - \frac{\pi}{2}\right]$$

$$\text{Mean}[s] = a \sqrt{\frac{\pi}{2}}$$

Appendix C: Dynamic Stresses along the Length of the Riser for 27 Sea States

Elevation (ft. above Mudline)	Fatigue Bin 1		Fatigue Bin = 2		Fatigue Bin = 3		Fatigue Bin = 4		Fatigue Bin = 5		Fatigue Bin = 6		Fatigue Bin = 7		Fatigue Bin = 8	
	Stress	Zero Cross.	Stress Std. Dev.	Zero Cross.	Stress	Zero Cross.	Stress	Zero Cross.								
	Std. Dev. (psi)	Period (sec.)	Dev. (psi)	Period (sec.)	Dev. (psi)	Period (sec.)	Dev. (psi)	Period (sec.)	Dev. (psi)	Period (sec.)	Dev. (psi)	Period (sec.)	Std. Dev. (psi)	Period (sec.)	Std. Dev. (psi)	Period (sec.)
10.00	112.806	1.911	126.751	3.714	262.199	6.059	440.869	9.253	564.369	8.693	613.419	8.634	936.867	11.776	981.779	11.273
11.00	109.383	1.914	123.130	3.718	254.832	6.059	428.512	9.270	548.547	8.695	596.221	8.635	910.591	11.779	954.241	11.274
12.00	106.007	1.918	119.556	3.723	247.562	6.060	416.318	9.287	532.933	8.697	579.250	8.637	884.665	11.782	927.070	11.276
13.00	105.896	1.922	119.672	3.728	247.931	6.061	416.971	9.305	533.767	8.700	580.157	8.638	886.035	11.785	928.505	11.277
14.50	105.711	1.928	119.848	3.735	248.505	6.062	417.991	9.334	535.067	8.703	581.571	8.639	888.177	11.790	930.748	11.279
16.50	105.416	1.937	120.074	3.746	249.280	6.064	419.382	9.376	536.838	8.708	583.495	8.642	891.104	11.797	933.811	11.283
19.00	104.976	1.951	120.366	3.762	250.315	6.066	421.262	9.436	539.223	8.716	586.086	8.646	895.067	11.808	937.955	11.289
22.00	104.360	1.969	120.766	3.783	251.743	6.069	423.882	9.519	542.534	8.727	589.681	8.652	900.607	11.824	943.743	11.297
26.00	103.432	2.000	121.488	3.818	254.216	6.074	428.444	9.656	548.281	8.744	595.919	8.662	910.288	11.850	953.852	11.312
30.00	102.521	2.040	122.687	3.860	257.944	6.081	435.298	9.828	556.902	8.767	605.273	8.674	924.872	11.886	969.079	11.332
34.00	101.912	2.091	124.863	3.913	264.072	6.088	446.460	10.046	570.943	8.796	620.507	8.691	948.651	11.932	993.909	11.360
38.00	102.201	2.158	128.999	3.977	274.835	6.098	465.851	10.324	595.367	8.834	647.008	8.713	989.969	11.993	1037.069	11.398
42.00	104.699	2.242	137.199	4.054	294.989	6.109	501.805	10.673	640.730	8.882	696.237	8.741	1066.553	12.073	1117.102	11.448
45.00	87.173	2.316	118.232	4.121	256.353	6.119	437.725	10.997	558.289	8.929	606.577	8.770	930.584	12.155	974.486	11.502
48.00	71.817	2.391	101.516	4.195	222.338	6.131	381.528	11.385	485.884	8.987	527.819	8.807	811.364	12.258	849.409	11.571
51.00	58.523	2.435	86.799	4.270	192.389	6.144	332.265	11.833	422.300	9.059	458.640	8.853	706.847	12.387	739.731	11.659
54.00	47.281	2.373	73.861	4.333	166.016	6.158	289.109	12.314	366.474	9.147	397.886	8.911	615.245	12.546	643.578	11.770
57.00	38.194	2.124	62.508	4.355	142.772	6.173	251.320	12.761	317.444	9.254	344.511	8.983	534.952	12.742	559.267	11.911
61.00	30.428	1.609	49.567	4.239	115.977	6.191	208.175	13.035	261.202	9.432	283.249	9.110	443.070	13.076	462.740	12.158
67.00	28.877	1.205	34.408	3.516	83.271	6.196	156.485	11.710	193.137	9.785	209.017	9.394	332.270	13.763	346.233	12.717
76.00	38.641	1.202	21.086	2.006	47.209	5.949	102.059	6.999	119.398	10.381	128.284	10.199	212.755	15.135	220.295	14.329
88.00	52.938	1.338	20.707	1.559	17.179	3.581	61.874	3.313	59.568	8.436	61.644	12.380	114.770	13.288	116.412	19.229
106.00	65.563	1.532	30.925	1.943	19.746	3.171	48.163	2.138	36.649	3.822	34.255	5.685	58.592	4.988	56.554	7.684
133.00	68.748	1.823	40.661	2.502	39.796	4.482	57.082	2.455	60.174	4.462	62.015	5.615	74.404	4.504	76.803	5.679

Elevation (ft. above Mudline)	Fatigue Bin = 1		Fatigue Bin = 2		Fatigue Bin = 3		Fatigue Bin = 4		Fatigue Bin = 5		Fatigue Bin = 6		Fatigue Bin = 7		Fatigue Bin = 8	
	Stress	Zero	Stress	Zero	Stress	Zero	Stress	Zero	Stress	Zero	Stress	Zero	Stress	Zero	Stress	Zero
	Std. Dev. (psi)	Cross. Period (sec.)	Std. Dev. (psi)	Cross. Period (sec.)	Std. Dev. (psi)	Period (sec.)	Std. Dev. (psi)	Period (sec.)								
166.00	62.405	1.839	45.390	2.884	52.750	5.144	63.794	2.860	79.687	5.150	84.455	5.948	97.773	5.151	103.731	5.959
202.00	54.740	1.656	46.239	2.899	61.113	5.492	64.568	2.892	92.315	5.494	99.311	6.145	113.290	5.487	121.948	6.149
240.00	52.066	1.607	44.062	3.133	66.476	5.587	61.318	3.089	100.413	5.581	109.352	6.230	123.259	5.576	134.280	6.234
281.00	52.957	1.480	41.093	2.907	69.021	5.684	56.980	2.869	104.286	5.688	115.092	6.258	128.073	5.691	141.361	6.263
325.00	48.862	1.530	37.508	2.702	68.408	5.791	52.354	2.681	103.453	5.788	115.816	6.302	127.154	5.789	142.322	6.304
372.00	48.444	1.526	33.837	2.779	64.494	5.755	48.295	2.737	97.662	5.734	110.962	6.357	120.170	5.731	136.459	6.356
422.00	52.806	1.628	32.344	2.413	57.233	5.676	46.665	2.427	86.788	5.674	100.426	6.368	106.928	5.676	123.623	6.369
472.00	54.570	1.659	30.620	2.493	47.630	5.550	44.535	2.495	72.370	5.535	85.612	6.360	89.314	5.530	105.528	6.364
522.00	50.002	1.585	30.434	2.425	36.916	5.150	43.191	2.410	56.217	5.130	68.103	6.359	70.785	5.413	84.519	6.732
572.00	43.786	1.534	30.494	2.355	26.740	4.474	42.097	2.480	40.745	4.518	50.098	6.189	54.356	5.083	64.732	6.808
622.00	46.365	1.547	29.129	2.452	20.074	3.790	41.716	2.458	31.852	4.014	35.798	5.842	45.400	4.643	50.193	6.644
672.00	48.706	1.551	28.369	2.483	21.462	3.979	41.892	2.540	34.365	4.125	32.968	5.486	47.983	4.646	47.077	6.342
722.00	44.492	1.572	28.876	2.430	28.137	4.524	42.869	2.541	43.934	4.646	40.948	5.594	58.445	5.022	55.605	6.152
772.00	42.682	1.529	29.512	2.634	35.542	4.949	43.656	2.659	54.775	5.017	52.808	5.774	70.841	5.278	68.952	6.116
822.00	45.021	1.596	30.608	2.652	41.748	5.283	44.175	2.698	63.970	5.316	63.996	5.945	81.623	5.509	81.947	6.181
872.00	46.380	1.560	31.244	2.862	46.081	5.473	43.890	2.775	70.414	5.515	72.733	6.080	89.284	5.682	92.272	6.262
922.00	40.756	1.515	31.469	2.685	48.278	5.574	42.921	2.741	73.725	5.618	78.352	6.171	93.279	5.763	98.985	6.324
972.00	38.496	1.626	29.599	2.666	48.326	5.658	41.075	2.667	73.871	5.694	80.672	6.250	93.512	5.829	101.787	6.391
1022.00	45.393	1.486	26.696	2.684	46.448	5.663	38.714	2.596	71.157	5.693	79.834	6.331	90.308	5.841	100.809	6.471
1072.00	39.749	1.536	24.756	2.275	42.970	5.624	36.442	2.386	66.042	5.649	76.229	6.396	84.230	5.815	96.504	6.546
1122.00	34.579	1.545	22.693	2.495	38.338	5.586	33.936	2.494	59.161	5.617	70.409	6.446	76.042	5.817	89.540	6.618
1172.00	41.446	1.520	22.984	2.206	33.158	5.412	33.470	2.329	51.407	5.479	63.069	6.499	66.815	5.748	80.765	6.708
1222.00	42.473	1.571	22.980	2.215	28.081	5.121	32.981	2.346	43.781	5.240	55.077	6.529	57.789	5.590	71.236	6.799
1272.00	36.483	1.556	22.070	2.393	23.895	4.876	32.173	2.450	37.487	5.002	47.479	6.473	50.381	5.411	62.207	6.830
1322.00	35.310	1.527	22.335	2.332	21.596	4.642	32.493	2.379	33.929	4.714	41.450	6.320	46.088	5.151	55.038	6.775
1372.00	37.846	1.429	23.193	2.667	22.266	4.590	33.113	2.502	34.029	4.555	38.091	6.131	45.569	5.009	50.941	6.644
1422.00	35.161	1.614	24.905	2.501	24.612	4.735	34.118	2.478	37.518	4.761	39.121	5.836	48.124	5.102	50.404	6.457
1472.00	37.236	1.492	24.958	2.541	27.548	4.928	34.188	2.533	42.000	4.936	42.358	5.804	52.422	4.959	53.529	5.870

Elevation (ft. above Mudline)	Fatigue Bin = 9		Fatigue Bin = 10		Fatigue Bin = 11		Fatigue Bin = 12		Fatigue Bin = 13		Fatigue Bin = 14		Fatigue Bin = 15		Fatigue Bin = 16	
	Stress	Zero Cross.														
	Std. Dev. (psi)	Period (sec.)														
10.00	980.537	12.076	1365.292	13.842	1363.542	14.840	1766.168	17.778	2165.829	20.691	2570.213	25.047	2984.420	31.687	3382.696	35.921
11.00	953.048	12.078	1326.852	13.842	1325.164	14.840	1716.073	17.776	2103.801	20.684	2495.583	25.031	2896.289	31.653	3280.919	35.871
12.00	925.924	12.079	1288.931	13.843	1287.305	14.841	1666.669	17.773	2042.650	20.677	2422.045	25.014	2809.498	31.620	3180.751	35.820
13.00	927.372	12.080	1290.769	13.844	1289.154	14.841	1668.656	17.770	2044.466	20.669	2423.144	24.996	2809.261	31.583	3178.558	35.765
14.50	929.635	12.082	1293.647	13.845	1292.051	14.841	1671.784	17.766	2047.346	20.657	2424.935	24.969	2809.011	31.527	3175.309	35.680
16.50	932.728	12.086	1297.583	13.847	1296.016	14.843	1676.059	17.761	2051.266	20.642	2427.338	24.932	2808.580	31.451	3170.715	35.565
19.00	936.913	12.091	1302.937	13.850	1301.408	14.845	1681.924	17.755	2056.728	20.623	2430.869	24.886	2808.448	31.354	3165.177	35.416
22.00	942.759	12.098	1310.491	13.857	1309.015	14.851	1690.366	17.751	2064.871	20.603	2436.765	24.832	2809.887	31.234	3159.919	35.230
26.00	952.957	12.112	1323.884	13.871	1322.492	14.863	1705.806	17.751	2080.603	20.581	2449.960	24.762	2817.335	31.070	3158.327	34.972
30.00	968.293	12.132	1344.398	13.892	1343.105	14.881	1730.300	17.758	2107.064	20.567	2475.228	24.697	2837.834	30.905	3170.281	34.702
34.00	993.257	12.158	1378.277	13.924	1377.104	14.910	1771.872	17.777	2153.951	20.565	2523.818	24.642	2884.059	30.741	3209.655	34.425
38.00	1036.587	12.194	1437.664	13.969	1436.635	14.952	1846.112	17.812	2240.096	20.580	2617.579	24.603	2980.641	30.587	3303.414	34.149
42.00	1116.848	12.242	1548.323	14.031	1547.474	15.011	1986.062	17.868	2405.390	20.620	2802.742	24.591	3179.644	30.456	3508.488	33.891
45.00	974.458	12.294	1351.018	14.104	1350.465	15.081	1732.278	17.949	2095.704	20.700	2437.574	24.652	2758.559	30.453	3034.711	33.813
48.00	849.586	12.361	1178.275	14.201	1177.987	15.175	1510.606	18.062	1825.884	20.822	2120.507	24.764	2394.417	30.516	2626.823	33.813
51.00	740.095	12.447	1027.059	14.325	1027.006	15.296	1317.005	18.212	1590.809	20.991	1845.196	24.940	2079.473	30.658	2275.569	33.908
54.00	644.113	12.556	894.723	14.484	894.883	15.451	1147.970	18.410	1386.069	21.221	1606.219	25.191	1807.173	30.897	1973.196	34.116
57.00	559.961	12.694	778.897	14.686	779.249	15.650	1000.376	18.668	1207.742	21.526	1398.784	25.538	1571.757	31.254	1712.934	34.465
61.00	463.630	12.937	646.582	15.046	647.164	16.004	832.248	19.132	1005.201	22.085	1164.127	26.193	1306.701	31.966	1421.427	35.205
67.00	347.384	13.491	487.393	15.863	488.271	16.812	630.790	20.204	763.523	23.393	885.748	27.761	994.405	33.732	1080.558	37.130
76.00	221.743	15.122	316.107	18.225	317.310	19.192	415.271	23.376	506.568	27.299	592.373	32.493	668.778	39.045	729.352	43.071
88.00	117.865	21.516	175.023	25.326	176.292	28.243	238.488	35.224	297.342	41.611	356.408	49.335	411.110	55.233	456.705	60.484
106.00	55.289	9.960	84.204	9.938	83.473	12.987	117.643	16.648	152.610	20.158	193.904	26.479	237.332	33.569	278.679	38.058
133.00	71.375	6.286	89.359	5.808	83.961	6.495	103.769	7.968	129.753	9.489	166.784	12.854	214.017	18.635	267.630	23.078

Elevation (ft. above Mudline)	Fatigue Bin = 9		Fatigue Bin = 10		Fatigue Bin = 11		Fatigue Bin = 12		Fatigue Bin = 13		Fatigue Bin = 14		Fatigue Bin = 15		Fatigue Bin = 16	
	Stress	Zero Cross.														
	Std. Dev. (psi)	Period (sec.)														
166.00	96.348	6.384	122.488	6.542	114.854	7.105	138.646	7.993	165.888	9.160	199.295	11.743	239.311	16.785	288.081	20.670
202.00	113.266	6.484	142.338	6.668	133.011	7.080	156.906	7.790	183.324	8.729	213.196	10.827	248.048	15.155	294.218	18.565
240.00	124.910	6.556	155.241	6.684	144.976	7.054	168.627	7.652	194.243	8.454	221.591	10.273	252.918	14.133	297.669	17.228
281.00	132.021	6.598	162.611	6.667	152.198	7.037	175.701	7.571	200.845	8.294	226.783	9.968	256.076	13.563	300.050	16.463
325.00	133.904	6.632	163.553	6.695	153.949	7.044	177.388	7.555	202.405	8.249	228.196	9.871	257.192	13.368	300.976	16.176
372.00	129.898	6.689	157.300	6.768	149.472	7.112	172.888	7.643	198.111	8.362	225.126	10.014	255.785	13.552	300.010	16.366
422.00	119.819	6.782	143.795	6.840	138.593	7.265	162.061	7.872	187.857	8.685	217.457	10.488	251.732	14.205	297.018	17.124
472.00	105.197	6.898	125.111	6.972	123.100	7.501	146.824	8.262	173.575	9.256	206.710	11.371	245.847	15.420	292.590	18.530
522.00	87.855	7.051	103.814	7.269	105.203	7.881	129.568	8.914	157.668	10.211	194.804	12.799	239.196	17.307	287.518	20.671
572.00	70.101	7.295	83.561	7.678	87.741	8.540	113.224	10.033	142.912	11.801	183.788	14.945	232.882	19.845	282.623	23.467
622.00	55.276	8.064	69.353	7.957	74.403	9.375	101.118	11.484	132.123	13.838	175.480	17.564	227.818	22.489	278.583	26.315
672.00	49.774	7.792	66.148	7.737	68.939	9.308	95.997	11.712	127.311	14.383	171.046	18.817	224.552	23.869	275.814	27.916
722.00	53.637	7.085	73.810	7.142	72.235	8.303	98.263	10.335	128.652	12.716	170.643	17.242	223.197	23.028	274.422	27.349
772.00	63.052	6.717	86.806	6.760	81.135	7.572	105.613	9.086	134.451	10.966	173.420	14.835	223.468	20.874	274.238	25.289
822.00	73.584	6.589	100.090	6.639	91.618	7.208	114.863	8.353	142.232	9.838	177.950	13.052	224.811	18.725	274.897	22.988
872.00	82.665	6.557	110.949	6.624	100.956	7.041	123.470	7.962	149.780	9.189	182.770	11.952	226.575	17.120	275.950	21.121
922.00	89.077	6.578	118.138	6.635	107.684	6.989	129.854	7.785	155.551	8.861	186.720	11.330	228.165	16.098	276.964	19.847
972.00	92.356	6.636	121.192	6.680	111.173	7.014	133.241	7.752	158.696	8.755	189.055	11.048	229.150	15.561	277.605	19.124
1022.00	92.503	6.717	120.181	6.763	111.351	7.090	133.452	7.820	158.952	8.811	189.449	11.041	229.302	15.413	277.682	18.868
1072.00	89.821	6.812	115.574	6.860	108.513	7.205	130.734	7.969	156.497	8.999	187.944	11.279	228.595	15.591	277.148	19.007
1122.00	84.826	6.931	108.106	6.975	103.219	7.367	125.632	8.210	151.831	9.330	184.875	11.753	227.161	16.061	276.083	19.485
1172.00	78.215	7.086	98.722	7.141	96.234	7.597	118.922	8.570	145.686	9.838	180.776	12.469	225.247	16.800	274.658	20.262
1222.00	70.851	7.274	88.600	7.352	88.506	7.898	111.550	9.062	138.951	10.546	176.279	13.438	223.158	17.768	273.088	21.277
1272.00	63.726	7.465	79.092	7.546	81.094	8.240	104.538	9.654	132.556	11.417	172.019	14.638	221.201	18.858	271.599	22.418
1322.00	57.874	7.610	71.573	7.670	75.044	8.553	98.831	10.244	127.324	12.318	168.540	15.902	219.635	19.877	270.383	23.491
1372.00	54.180	7.648	67.161	7.665	71.186	8.726	95.117	10.643	123.825	12.989	166.209	16.865	218.626	20.584	269.575	24.256
1422.00	53.064	7.542	66.262	7.472	69.877	8.661	93.667	10.662	122.276	13.140	165.162	17.160	218.235	20.813	269.230	24.535
1472.00	54.246	7.344	68.276	7.203	70.851	8.402	94.260	10.321	122.510	12.744	165.298	16.778	218.419	20.575	269.328	24.319

Elevation (ft. above Mudline)	Fatigue Bin = 17		Fatigue Bin = 18		Fatigue Bin = 19		Fatigue Bin = 20		Fatigue Bin = 21		Fatigue Bin = 22		Fatigue Bin = 23		Fatigue Bin = 24	
	Stress	Zero Cross.														
	Std. Dev. (psi)	Period (sec.)														
10.00	3773.495	39.941	4150.792	43.892	4511.180	46.890	4850.548	49.941	5164.284	51.205	5423.218	52.911	5529.271	50.351	5614.053	49.910
11.00	3657.654	39.875	4020.688	43.808	4366.696	46.805	4691.775	49.844	4991.710	51.128	5238.763	52.831	5337.674	50.303	5416.539	49.860
12.00	3543.724	39.809	3892.820	43.723	4224.801	46.718	4535.964	49.744	4822.481	51.048	5057.999	52.747	5150.041	50.252	5223.223	49.807
13.00	3538.934	39.738	3884.842	43.632	4213.023	46.625	4519.867	49.636	4801.812	50.962	5033.087	52.657	5121.134	50.196	5190.932	49.748
14.50	3531.703	39.628	3872.722	43.492	4195.081	46.480	4495.309	49.469	4770.261	50.826	4995.052	52.514	5077.002	50.105	5141.640	49.653
16.50	3521.595	39.477	3855.853	43.298	4170.178	46.278	4461.290	49.235	4726.628	50.632	4942.522	52.309	5016.131	49.969	5073.726	49.511
19.00	3508.883	39.281	3834.344	43.043	4138.227	46.010	4417.503	48.922	4670.389	50.366	4874.782	52.025	4937.633	49.775	4986.164	49.306
22.00	3494.684	39.033	3809.144	42.720	4099.965	45.663	4364.433	48.513	4601.779	50.010	4791.849	51.642	4841.298	49.499	4878.575	49.014
26.00	3480.804	38.682	3779.999	42.256	4052.621	45.155	4296.403	47.908	4512.088	49.463	4682.231	51.045	4712.932	49.045	4734.532	48.529
30.00	3480.581	38.307	3764.259	41.753	4018.132	44.590	4240.412	47.225	4433.582	48.819	4583.016	50.334	4593.863	48.469	4598.952	47.912
34.00	3508.908	37.912	3777.657	41.213	4012.902	43.966	4213.375	46.459	4383.602	48.068	4511.856	49.491	4501.542	47.747	4489.138	47.134
38.00	3594.742	37.504	3850.781	40.644	4068.812	43.290	4248.132	45.616	4395.750	47.205	4502.886	48.512	4469.606	46.863	4438.336	46.174
42.00	3799.124	37.105	4047.999	40.070	4252.781	42.586	4413.406	44.723	4540.085	46.255	4626.984	47.420	4567.558	45.828	4514.910	45.047
45.00	3274.879	36.936	3476.213	39.788	3637.220	42.206	3758.288	44.210	3849.932	45.678	3909.007	46.737	3843.484	45.150	3786.545	44.296
48.00	2825.711	36.857	2988.768	39.605	3115.231	41.929	3205.816	43.807	3270.995	45.203	3309.472	46.157	3241.846	44.554	3183.821	43.627
51.00	2440.718	36.885	2573.002	39.544	2672.278	41.780	2739.505	43.544	2784.837	44.863	2808.197	45.719	2741.175	44.083	2684.171	43.084
54.00	2110.862	37.043	2218.524	39.630	2296.563	41.789	2346.107	43.452	2376.781	44.697	2389.251	45.463	2324.662	43.783	2270.059	42.717
57.00	1828.302	37.360	1916.384	39.897	1977.989	41.992	2014.362	43.574	2034.438	44.749	2039.269	45.440	1978.303	43.706	1926.951	42.578
61.00	1513.606	38.095	1581.858	40.605	1627.441	42.643	1651.679	44.152	1662.424	45.253	1660.838	45.872	1605.761	44.057	1559.437	42.856
67.00	1148.664	40.111	1197.270	42.696	1228.100	44.714	1242.473	46.221	1246.451	47.249	1240.789	47.848	1195.474	45.888	1157.142	44.617
76.00	777.656	46.415	811.802	49.480	833.975	51.497	845.219	53.323	849.093	54.112	844.926	54.986	814.603	52.517	801.463	22.604
88.00	496.184	62.468	526.761	66.170	551.264	64.890	569.763	66.999	583.799	63.777	644.792	26.588	712.309	25.776	759.858	26.746
106.00	320.702	39.625	358.951	43.018	426.616	28.235	501.924	31.579	580.297	31.362	640.040	33.402	688.341	31.147	720.327	31.817
133.00	328.081	26.626	387.093	30.759	450.574	32.256	510.361	35.713	570.636	35.158	614.964	37.071	647.624	34.196	668.063	34.675

Elevation (ft. above Mudline)	Fatigue Bin = 17		Fatigue Bin = 18		Fatigue Bin = 19		Fatigue Bin = 20		Fatigue Bin = 21		Fatigue Bin = 22		Fatigue Bin = 23		Fatigue Bin = 24	
	Stress	Zero Cross.														
	Std. Dev. (psi)	Period (sec.)														
166.00	342.277	24.349	394.612	28.425	450.456	30.747	502.984	34.411	555.793	34.616	594.206	36.658	621.524	34.120	638.249	34.633
202.00	345.790	22.059	395.715	25.905	449.221	28.581	499.659	32.286	550.616	33.084	587.653	35.241	614.033	33.144	630.111	33.741
240.00	348.089	20.531	397.139	24.167	450.018	26.954	499.946	30.615	550.633	31.754	587.467	33.966	613.922	32.197	629.981	32.857
281.00	349.938	19.622	398.653	23.099	451.428	25.898	501.281	29.483	552.092	30.795	588.983	33.016	615.711	31.457	631.856	32.149
325.00	350.819	19.257	399.560	22.637	452.527	25.403	502.530	28.912	553.635	30.267	590.690	32.465	617.759	30.996	634.035	31.692
372.00	350.320	19.432	399.448	22.778	452.896	25.478	503.261	28.919	554.813	30.201	592.130	32.352	619.596	30.855	636.053	31.527
422.00	348.301	20.228	398.172	23.591	452.384	26.168	503.323	29.537	555.471	30.616	593.150	32.695	621.064	31.046	637.754	31.670
472.00	345.168	21.688	395.997	25.091	451.142	27.442	502.781	30.713	555.607	31.446	593.703	33.427	622.076	31.517	639.029	32.072
522.00	341.496	23.829	393.342	27.256	449.472	29.209	501.848	32.332	555.373	32.568	593.907	34.428	622.728	32.169	639.953	32.644
572.00	337.888	26.474	390.657	29.874	447.705	31.230	500.765	34.165	554.953	33.791	593.907	35.525	623.142	32.878	640.631	33.274
622.00	334.849	29.005	388.328	32.362	446.131	33.040	499.757	35.816	554.518	34.850	593.842	36.491	623.444	33.492	641.170	33.832
672.00	332.694	30.398	386.609	33.826	444.955	34.071	498.983	36.822	554.199	35.477	593.825	37.096	623.734	33.872	641.662	34.195
722.00	331.522	30.027	385.597	33.694	444.265	34.006	498.527	36.902	554.069	35.522	593.922	37.201	624.077	33.934	642.167	34.287
772.00	331.233	28.346	385.243	32.266	444.039	33.019	498.391	36.147	554.141	35.030	594.154	36.824	624.496	33.683	642.712	34.100
822.00	331.586	26.279	385.387	30.318	444.174	31.575	498.511	34.910	554.376	34.196	594.498	36.111	624.978	33.201	643.291	33.696
872.00	332.267	24.451	385.811	28.467	444.517	30.103	498.784	33.565	554.700	33.244	594.900	35.254	625.481	32.607	643.872	33.173
922.00	332.966	23.100	386.288	27.010	444.902	28.857	499.093	32.365	555.028	32.352	595.296	34.420	625.948	32.010	644.410	32.629
972.00	333.427	22.256	386.622	26.033	445.180	27.952	499.330	31.443	555.275	31.629	595.619	33.717	626.323	31.490	644.857	32.142
1022.00	333.490	21.874	386.684	25.527	445.247	27.414	499.414	30.847	555.378	31.127	595.817	33.204	626.557	31.096	645.172	31.759
1072.00	333.102	21.892	386.416	25.445	445.050	27.228	499.299	30.579	555.299	30.860	595.857	32.903	626.620	30.850	645.327	31.507
1122.00	332.302	22.246	385.838	25.724	444.592	27.349	498.982	30.609	555.031	30.817	595.730	32.808	626.504	30.755	645.314	31.389
1172.00	331.205	22.874	385.024	26.294	443.921	27.719	498.494	30.887	554.595	30.968	595.453	32.895	626.220	30.797	645.140	31.398
1222.00	329.963	23.704	384.085	27.067	443.119	28.263	497.892	31.343	554.036	31.266	595.058	33.126	625.799	30.953	644.833	31.513
1272.00	328.742	24.631	383.144	27.935	442.279	28.892	497.248	31.890	553.412	31.651	594.594	33.448	625.283	31.189	644.428	31.705
1322.00	327.686	25.509	382.316	28.763	441.494	29.508	496.633	32.435	552.782	32.057	594.111	33.802	624.723	31.464	643.971	31.940
1372.00	326.906	26.169	381.689	29.403	440.837	30.014	496.108	32.890	552.203	32.423	593.660	34.129	624.167	31.738	643.506	32.181
1422.00	326.457	26.478	381.314	29.731	440.358	30.332	495.718	33.186	551.717	32.699	593.278	34.383	623.658	31.976	643.073	32.396
1472.00	326.337	26.407	381.200	29.705	440.076	30.422	495.482	33.285	551.348	32.857	592.992	34.534	623.225	32.154	642.704	32.560

Elevation (ft. above Mudline)	Fatigue Bin = 25		Fatigue Bin = 26		Fatigue Bin = 27	
	Stress	Zero Cross.	Stress	Zero Cross.	Stress	Zero Cross.
	Std. Dev. (psi)	Period (sec.)	Std. Dev. (psi)	Period (sec.)	Std. Dev. (psi)	Period (sec.)
10.00	5705.671	48.049	5780.864	47.879	6347.503	49.701
11.00	5502.039	48.034	5571.994	47.864	6100.739	49.599
12.00	5302.848	48.016	5367.778	47.845	5859.967	49.491
13.00	5267.179	47.995	5329.131	47.823	5799.801	49.374
14.50	5212.750	47.957	5270.174	47.783	5707.903	49.184
16.50	5137.845	47.893	5189.111	47.716	5581.605	48.901
19.00	5041.333	47.789	5084.717	47.607	5418.528	48.495
22.00	4922.710	47.622	4956.379	47.430	5216.509	47.915
26.00	4763.465	47.308	4783.755	47.095	4939.661	46.948
30.00	4612.136	46.859	4618.553	46.613	4662.490	45.702
34.00	4486.004	46.236	4478.019	45.942	4400.484	44.108
38.00	4418.140	45.404	4395.030	45.044	4182.945	42.114
42.00	4476.164	44.362	4436.462	43.915	4068.778	39.742
45.00	3743.177	43.631	3700.185	43.115	3305.796	38.097
48.00	3138.919	42.957	3095.269	42.374	2697.780	36.584
51.00	2639.718	42.391	2597.069	41.744	2213.618	35.280
54.00	2227.304	41.988	2186.678	41.282	1829.347	34.269
57.00	1886.624	41.805	1848.592	41.048	1525.486	33.633
61.00	1522.889	42.021	1488.690	41.209	1218.666	33.534
67.00	1126.570	43.681	1098.191	42.835	1203.009	22.757
76.00	879.895	22.392	930.224	23.098	1256.002	28.279
88.00	824.023	25.748	864.926	26.400	1221.780	33.604
106.00	763.720	29.790	790.705	30.246	1105.161	38.120
133.00	697.472	32.243	715.159	32.582	977.890	40.451

Elevation (ft. above Mudline)	Fatigue Bin = 25		Fatigue Bin = 26		Fatigue Bin = 27	
	Stress	Zero Cross.	Stress	Zero Cross.	Stress	Zero Cross.
	Std. Dev. (psi)	Period (sec.)	Std. Dev. (psi)	Period (sec.)	Std. Dev. (psi)	Period (sec.)
166.00	663.242	32.423	678.149	32.783	918.844	40.610
202.00	654.351	31.844	668.808	32.261	932.062	36.696
240.00	654.251	31.211	670.577	28.024	934.300	36.153
281.00	656.307	30.678	670.766	31.175	933.353	35.698
325.00	658.733	30.308	673.249	30.818	931.684	35.374
372.00	661.061	30.139	675.671	30.642	929.735	35.222
422.00	663.138	30.184	677.883	30.662	927.549	35.267
472.00	664.818	30.408	679.726	30.848	925.265	35.497
522.00	666.154	30.746	681.243	31.142	922.918	35.873
572.00	667.227	31.120	682.500	31.472	920.555	36.346
622.00	668.122	31.447	683.570	31.767	922.068	39.109
672.00	668.914	31.654	684.519	31.961	923.521	39.259
722.00	669.655	31.697	685.397	32.012	924.847	39.293
772.00	670.372	31.569	686.228	31.912	926.068	39.202
822.00	671.063	31.302	687.016	31.685	927.193	39.002
872.00	671.708	30.954	687.746	31.377	928.219	38.729
922.00	672.274	30.585	688.390	31.042	929.136	38.427
972.00	672.722	30.247	688.918	30.728	929.930	38.140
1022.00	673.021	29.978	689.304	30.471	930.588	37.901
1072.00	673.151	29.797	689.528	30.291	931.105	37.735
1122.00	673.106	29.712	689.586	30.196	931.480	37.651
1172.00	672.896	29.717	689.486	30.185	931.720	37.648
1222.00	672.544	29.802	689.249	30.246	931.842	37.719
1272.00	672.085	29.947	688.906	30.365	931.867	37.849
1322.00	671.560	30.130	688.493	30.521	931.819	38.019
1372.00	671.013	30.328	688.050	30.693	931.724	38.209
1422.00	670.482	30.516	687.613	30.860	931.608	38.401
1472.00	670.000	30.678	687.214	31.006	931.492	38.577

Appendix D: Results

$E[m]$	3	$E[C]$	5.00E-13
$Std[m]$	0.2	$Std[C]$	1.65E-13
$\rho_{m,C}$	-0.6	<i>c.o.v.</i>	3.30E-01

Number of cracks (n)	1	2	3	4	5	6	7	8	9
Prob (n cracks)	0.478583	0.073108	0.005571	0.000305	1.4E-05	5.5E-07	2E-08	6.8E-10	2.3E-11

m	C	a_i	Probability (Failure/n cracks,m,C), $P_{n,m,C}$									P(failure/m,C), $P_{f,m,c}$	$P(m)$	$P(C/m)$	P(failure), P_F
			1	2	3	4	5	6	7	8	9				
2.6	5E-12	17.5	0.000	0.000	0.000	0.000	0.000	0.000	0.000	0.000	0.000	0.000	0.083	9.88E-15	0
2.6	6E-12	15.5	0.000	0.000	0.000	0.000	0.000	0.000	0.000	0.000	0.000	0.000	0.083	0	0
2.6	7E-12	14	0.000	0.000	0.000	0.000	0.000	0.000	0.000	0.000	0.000	0.000	0.083	0	0
2.6	8E-12	13	0.000	0.000	0.000	0.000	0.000	0.000	0.000	0.000	0.000	0.000	0.083	0	0
2.6	9E-12	12	0.000	0.000	0.000	0.000	0.000	0.000	0.000	0.000	0.000	0.000	0.083	0	0
2.6	1E-11	11	0.000	0.000	0.000	0.000	0.000	0.000	0.000	0.000	0.000	0.000	0.083	0	0
2.6	2E-11	5	0.379	0.614	0.760	0.851	0.907	0.942	0.964	0.978	0.986	0.231	0.083	0	0
2.6	3E-11	3	0.625	0.859	0.947	0.980	0.993	0.997	0.999	1.000	1.000	0.367	0.083	0	0
2.6	4E-11	1.5	0.809	0.964	0.993	0.999	1.000	1.000	1.000	1.000	1.000	0.464	0.083	0	0
2.6	5E-11	1	0.860	0.981	0.997	1.000	1.000	1.000	1.000	1.000	1.000	0.489	0.083	0	0
2.75	3E-12	15.5	0.000	0.000	0.000	0.000	0.000	0.000	0.000	0.000	0.000	0.000	0.121	2.35E-10	0
2.75	4E-12	13	0.000	0.000	0.000	0.000	0.000	0.000	0.000	0.000	0.000	0.000	0.121	1.01E-13	0
2.75	5E-12	10.5	0.000	0.000	0.000	0.000	0.000	0.000	0.000	0.000	0.000	0.000	0.121	0	0
2.75	6E-12	9	0.050	0.098	0.144	0.187	0.228	0.266	0.303	0.338	0.372	0.032	0.121	0	0
2.75	7E-12	8	0.110	0.207	0.294	0.371	0.440	0.502	0.556	0.605	0.648	0.069	0.121	0	0

2.75	8E-12	7	0.184	0.333	0.456	0.556	0.637	0.704	0.758	0.803	0.839	0.115	0.121	0	0
2.75	9E-12	6	0.273	0.472	0.616	0.721	0.797	0.853	0.893	0.922	0.944	0.169	0.121	0	0
2.75	1E-11	5	0.379	0.614	0.760	0.851	0.907	0.942	0.964	0.978	0.986	0.231	0.121	0	0
2.75	2E-11	2	0.751	0.938	0.985	0.996	0.999	1.000	1.000	1.000	1.000	0.434	0.121	0	0
2.75	3E-11	1	0.860	0.981	0.997	1.000	1.000	1.000	1.000	1.000	1.000	0.489	0.121	0	0
2.75	4E-11	0.5	0.900	0.990	0.999	1.000	1.000	1.000	1.000	1.000	1.000	0.509	0.121	0	0
2.75	5E-11	0.5	0.900	0.990	0.999	1.000	1.000	1.000	1.000	1.000	1.000	0.509	0.121	0	0
2.85	2E-12	15	0.000	0.000	0.000	0.000	0.000	0.000	0.000	0.000	0.000	0.000	0.082	2.48E-07	0
2.85	3E-12	11	0.000	0.000	0.000	0.000	0.000	0.000	0.000	0.000	0.000	0.000	0.082	2E-11	0
2.85	4E-12	8.5	0.078	0.150	0.217	0.278	0.335	0.387	0.435	0.479	0.520	0.050	0.082	5.77E-15	2.35E-17
2.85	5E-12	7	0.184	0.333	0.456	0.556	0.637	0.704	0.758	0.803	0.839	0.115	0.082	0	0
2.85	6E-12	5.5	0.324	0.543	0.691	0.791	0.859	0.905	0.936	0.956	0.971	0.199	0.082	0	0
2.85	7E-12	4.5	0.437	0.683	0.821	0.899	0.943	0.968	0.982	0.990	0.994	0.264	0.082	0	0
2.85	8E-12	4	0.498	0.748	0.873	0.936	0.968	0.984	0.992	0.996	0.998	0.298	0.082	0	0
2.85	9E-12	3.5	0.561	0.807	0.915	0.963	0.984	0.993	0.997	0.999	0.999	0.333	0.082	0	0
2.85	1E-11	3	0.625	0.859	0.947	0.980	0.993	0.997	0.999	1.000	1.000	0.367	0.082	0	0
2.85	2E-11	1	0.860	0.981	0.997	1.000	1.000	1.000	1.000	1.000	1.000	0.489	0.082	0	0
2.85	3E-11	0.5	0.900	0.990	0.999	1.000	1.000	1.000	1.000	1.000	1.000	0.509	0.082	0	0
2.85	4E-11	0.5	0.900	0.990	0.999	1.000	1.000	1.000	1.000	1.000	1.000	0.509	0.082	0	0
2.85	5E-11	0.5	0.900	0.990	0.999	1.000	1.000	1.000	1.000	1.000	1.000	0.509	0.082	0	0
2.9	2E-12	12.5	0.000	0.000	0.000	0.000	0.000	0.000	0.000	0.000	0.000	0.000	0.093	9.17E-08	0
2.9	3E-12	9	0.050	0.098	0.144	0.187	0.228	0.266	0.303	0.338	0.372	0.032	0.093	5.56E-12	1.66E-14
2.9	4E-12	7	0.184	0.333	0.456	0.556	0.637	0.704	0.758	0.803	0.839	0.115	0.093	0	0
2.9	5E-12	5.5	0.324	0.543	0.691	0.791	0.859	0.905	0.936	0.956	0.971	0.199	0.093	0	0
2.9	6E-12	4.5	0.437	0.683	0.821	0.899	0.943	0.968	0.982	0.990	0.994	0.264	0.093	0	0
2.9	7E-12	3.5	0.561	0.807	0.915	0.963	0.984	0.993	0.997	0.999	0.999	0.333	0.093	0	0
2.9	8E-12	3	0.625	0.859	0.947	0.980	0.993	0.997	0.999	1.000	1.000	0.367	0.093	0	0
2.9	9E-12	2.5	0.689	0.903	0.970	0.991	0.997	0.999	1.000	1.000	1.000	0.401	0.093	0	0
2.9	1E-11	2	0.751	0.938	0.985	0.996	0.999	1.000	1.000	1.000	1.000	0.434	0.093	0	0
2.9	2E-11	1	0.860	0.981	0.997	1.000	1.000	1.000	1.000	1.000	1.000	0.489	0.093	0	0
2.9	3E-11	0.5	0.900	0.990	0.999	1.000	1.000	1.000	1.000	1.000	1.000	0.509	0.093	0	0
2.9	4E-11	0.5	0.900	0.990	0.999	1.000	1.000	1.000	1.000	1.000	1.000	0.509	0.093	0	0

2.9	5E-11	0.5	0.900	0.990	0.999	1.000	1.000	1.000	1.000	1.000	1.000	0.509	0.093	0	0
2.95	9E-13	17.5	0.000	0.000	0.000	0.000	0.000	0.000	0.000	0.000	0.000	0.000	0.099	0.00738	0
2.95	1E-12	16.5	0.000	0.000	0.000	0.000	0.000	0.000	0.000	0.000	0.000	0.000	0.099	0.003381	0
2.95	2E-12	10.5	0.000	0.000	0.000	0.000	0.000	0.000	0.000	0.000	0.000	0.000	0.099	3.28E-08	0
2.95	3E-12	7	0.184	0.333	0.456	0.556	0.637	0.704	0.758	0.803	0.839	0.115	0.099	1.49E-12	1.69E-14
2.95	4E-12	5.5	0.324	0.543	0.691	0.791	0.859	0.905	0.936	0.956	0.971	0.199	0.099	0	0
2.95	5E-12	4	0.498	0.748	0.873	0.936	0.968	0.984	0.992	0.996	0.998	0.298	0.099	0	0
2.95	6E-12	3	0.625	0.859	0.947	0.980	0.993	0.997	0.999	1.000	1.000	0.367	0.099	0	0
2.95	7E-12	2.5	0.689	0.903	0.970	0.991	0.997	0.999	1.000	1.000	1.000	0.401	0.099	0	0
2.95	8E-12	2	0.751	0.938	0.985	0.996	0.999	1.000	1.000	1.000	1.000	0.434	0.099	0	0
2.95	9E-12	2	0.751	0.938	0.985	0.996	0.999	1.000	1.000	1.000	1.000	0.434	0.099	0	0
2.95	1E-11	1.5	0.809	0.964	0.993	0.999	1.000	1.000	1.000	1.000	1.000	0.464	0.099	0	0
2.95	2E-11	0.5	0.900	0.990	0.999	1.000	1.000	1.000	1.000	1.000	1.000	0.509	0.099	0	0
2.95	3E-11	0.5	0.900	0.990	0.999	1.000	1.000	1.000	1.000	1.000	1.000	0.509	0.099	0	0
2.95	4E-11	0.5	0.900	0.990	0.999	1.000	1.000	1.000	1.000	1.000	1.000	0.509	0.099	0	0
2.95	5E-11	0.5	0.900	0.990	0.999	1.000	1.000	1.000	1.000	1.000	1.000	0.509	0.099	0	0
3	7E-13	17.5	0.000	0.000	0.000	0.000	0.000	0.000	0.000	0.000	0.000	0.000	0.099	0.044368	0
3	8E-13	16.5	0.000	0.000	0.000	0.000	0.000	0.000	0.000	0.000	0.000	0.000	0.099	0.01481	0
3	9E-13	15.5	0.000	0.000	0.000	0.000	0.000	0.000	0.000	0.000	0.000	0.000	0.099	0.004565	0
3	1E-12	14.5	0.000	0.000	0.000	0.000	0.000	0.000	0.000	0.000	0.000	0.000	0.099	0.001891	0
3	2E-12	8.5	0.078	0.150	0.217	0.278	0.335	0.387	0.435	0.479	0.520	0.050	0.099	1.13E-08	5.56E-11
3	3E-12	5.5	0.324	0.543	0.691	0.791	0.859	0.905	0.936	0.956	0.971	0.199	0.099	3.85E-13	7.57E-15
3	4E-12	4	0.498	0.748	0.873	0.936	0.968	0.984	0.992	0.996	0.998	0.298	0.099	0	0
3	5E-12	3	0.625	0.859	0.947	0.980	0.993	0.997	0.999	1.000	1.000	0.367	0.099	0	0
3	6E-12	2.5	0.689	0.903	0.970	0.991	0.997	0.999	1.000	1.000	1.000	0.401	0.099	0	0
3	7E-12	2	0.751	0.938	0.985	0.996	0.999	1.000	1.000	1.000	1.000	0.434	0.099	0	0
3	8E-12	1.5	0.809	0.964	0.993	0.999	1.000	1.000	1.000	1.000	1.000	0.464	0.099	0	0
3	9E-12	1.5	0.809	0.964	0.993	0.999	1.000	1.000	1.000	1.000	1.000	0.464	0.099	0	0
3	1E-11	1	0.860	0.981	0.997	1.000	1.000	1.000	1.000	1.000	1.000	0.489	0.099	0	0
3	2E-11	0.5	0.900	0.990	0.999	1.000	1.000	1.000	1.000	1.000	1.000	0.509	0.099	0	0
3	3E-11	0.5	0.900	0.990	0.999	1.000	1.000	1.000	1.000	1.000	1.000	0.509	0.099	0	0
3	4E-11	0.5	0.900	0.990	0.999	1.000	1.000	1.000	1.000	1.000	1.000	0.509	0.099	0	0

3	5E-11	0.5	0.900	0.990	0.999	1.000	1.000	1.000	1.000	1.000	1.000	0.509	0.099	0	0
3.05	6E-13	17	0.000	0.000	0.000	0.000	0.000	0.000	0.000	0.000	0.000	0.000	0.093	0.091372	0
3.05	7E-13	15.5	0.000	0.000	0.000	0.000	0.000	0.000	0.000	0.000	0.000	0.000	0.093	0.031531	0
3.05	8E-13	14.5	0.000	0.000	0.000	0.000	0.000	0.000	0.000	0.000	0.000	0.000	0.093	0.009602	0
3.05	9E-13	13.5	0.000	0.000	0.000	0.000	0.000	0.000	0.000	0.000	0.000	0.000	0.093	0.002727	0
3.05	1E-12	12.5	0.000	0.000	0.000	0.000	0.000	0.000	0.000	0.000	0.000	0.000	0.093	0.001024	0
3.05	2E-12	7	0.184	0.333	0.456	0.556	0.637	0.704	0.758	0.803	0.839	0.115	0.093	3.79E-09	4.04E-11
3.05	3E-12	4.5	0.437	0.683	0.821	0.899	0.943	0.968	0.982	0.990	0.994	0.264	0.093	9.65E-14	2.36E-15
3.05	4E-12	3	0.625	0.859	0.947	0.980	0.993	0.997	0.999	1.000	1.000	0.367	0.093	0	0
3.05	5E-12	2.5	0.689	0.903	0.970	0.991	0.997	0.999	1.000	1.000	1.000	0.401	0.093	0	0
3.05	6E-12	2	0.751	0.938	0.985	0.996	0.999	1.000	1.000	1.000	1.000	0.434	0.093	0	0
3.05	7E-12	1.5	0.809	0.964	0.993	0.999	1.000	1.000	1.000	1.000	1.000	0.464	0.093	0	0
3.05	8E-12	1.5	0.809	0.964	0.993	0.999	1.000	1.000	1.000	1.000	1.000	0.464	0.093	0	0
3.05	9E-12	1	0.860	0.981	0.997	1.000	1.000	1.000	1.000	1.000	1.000	0.489	0.093	0	0
3.05	1E-11	1	0.860	0.981	0.997	1.000	1.000	1.000	1.000	1.000	1.000	0.489	0.093	0	0
3.05	2E-11	0.5	0.900	0.990	0.999	1.000	1.000	1.000	1.000	1.000	1.000	0.509	0.093	0	0
3.05	3E-11	0.5	0.900	0.990	0.999	1.000	1.000	1.000	1.000	1.000	1.000	0.509	0.093	0	0
3.05	4E-11	0.5	0.900	0.990	0.999	1.000	1.000	1.000	1.000	1.000	1.000	0.509	0.093	0	0
3.05	5E-11	0.5	0.900	0.990	0.999	1.000	1.000	1.000	1.000	1.000	1.000	0.509	0.093	0	0
3.1	4E-13	18	0.000	0.000	0.000	0.000	0.000	0.000	0.000	0.000	0.000	0.000	0.082	0.332384	0
3.1	5E-13	16.5	0.000	0.000	0.000	0.000	0.000	0.000	0.000	0.000	0.000	0.000	0.082	0.182894	0
3.1	6E-13	14.5	0.000	0.000	0.000	0.000	0.000	0.000	0.000	0.000	0.000	0.000	0.082	0.069658	0
3.1	7E-13	13.5	0.000	0.000	0.000	0.000	0.000	0.000	0.000	0.000	0.000	0.000	0.082	0.02165	0
3.1	8E-13	12	0.000	0.000	0.000	0.000	0.000	0.000	0.000	0.000	0.000	0.000	0.082	0.006014	0
3.1	9E-13	11	0.000	0.000	0.000	0.000	0.000	0.000	0.000	0.000	0.000	0.000	0.082	0.001574	0
3.1	1E-12	10.5	0.000	0.000	0.000	0.000	0.000	0.000	0.000	0.000	0.000	0.000	0.082	0.000536	0
3.1	2E-12	5.5	0.324	0.543	0.691	0.791	0.859	0.905	0.936	0.956	0.971	0.199	0.082	1.22E-09	1.99E-11
3.1	3E-12	3.5	0.561	0.807	0.915	0.963	0.984	0.993	0.997	0.999	0.999	0.333	0.082	2.33E-14	6.35E-16
3.1	4E-12	2.5	0.689	0.903	0.970	0.991	0.997	0.999	1.000	1.000	1.000	0.401	0.082	0	0
3.1	5E-12	2	0.751	0.938	0.985	0.996	0.999	1.000	1.000	1.000	1.000	0.434	0.082	0	0
3.1	6E-12	1.5	0.809	0.964	0.993	0.999	1.000	1.000	1.000	1.000	1.000	0.464	0.082	0	0
3.1	7E-12	1	0.860	0.981	0.997	1.000	1.000	1.000	1.000	1.000	1.000	0.489	0.082	0	0

3.1	8E-12	1	0.860	0.981	0.997	1.000	1.000	1.000	1.000	1.000	1.000	0.489	0.082	0	0
3.1	9E-12	1	0.860	0.981	0.997	1.000	1.000	1.000	1.000	1.000	1.000	0.489	0.082	0	0
3.1	1E-11	1	0.860	0.981	0.997	1.000	1.000	1.000	1.000	1.000	1.000	0.489	0.082	0	0
3.1	2E-11	0.5	0.900	0.990	0.999	1.000	1.000	1.000	1.000	1.000	1.000	0.509	0.082	0	0
3.1	3E-11	0.5	0.900	0.990	0.999	1.000	1.000	1.000	1.000	1.000	1.000	0.509	0.082	0	0
3.1	4E-11	0.5	0.900	0.990	0.999	1.000	1.000	1.000	1.000	1.000	1.000	0.509	0.082	0	0
3.1	5E-11	0.5	0.900	0.990	0.999	1.000	1.000	1.000	1.000	1.000	1.000	0.509	0.082	0	0
3.15	4E-13	16	0.000	0.000	0.000	0.000	0.000	0.000	0.000	0.000	0.000	0.000	0.121	0.318863	0
3.15	5E-13	14	0.000	0.000	0.000	0.000	0.000	0.000	0.000	0.000	0.000	0.000	0.121	0.152128	0
3.15	6E-13	12.5	0.000	0.000	0.000	0.000	0.000	0.000	0.000	0.000	0.000	0.000	0.121	0.05132	0
3.15	7E-13	11.5	0.000	0.000	0.000	0.000	0.000	0.000	0.000	0.000	0.000	0.000	0.121	0.014363	0
3.15	8E-13	10	0.004	0.008	0.012	0.016	0.020	0.024	0.028	0.032	0.035	0.003	0.121	0.003639	1.13E-06
3.15	9E-13	9	0.050	0.098	0.144	0.187	0.228	0.266	0.303	0.338	0.372	0.032	0.121	0.000877	3.41E-06
3.15	1E-12	8.5	0.078	0.150	0.217	0.278	0.335	0.387	0.435	0.479	0.520	0.050	0.121	0.000272	1.64E-06
3.15	2E-12	4	0.498	0.748	0.873	0.936	0.968	0.984	0.992	0.996	0.998	0.298	0.121	3.81E-10	1.37E-11
3.15	3E-12	2.5	0.689	0.903	0.970	0.991	0.997	0.999	1.000	1.000	1.000	0.401	0.121	5.44E-15	2.64E-16
3.15	4E-12	2	0.751	0.938	0.985	0.996	0.999	1.000	1.000	1.000	1.000	0.434	0.121	0	0
3.15	5E-12	1.5	0.809	0.964	0.993	0.999	1.000	1.000	1.000	1.000	1.000	0.464	0.121	0	0
3.15	6E-12	1	0.860	0.981	0.997	1.000	1.000	1.000	1.000	1.000	1.000	0.489	0.121	0	0
3.15	7E-12	1	0.860	0.981	0.997	1.000	1.000	1.000	1.000	1.000	1.000	0.489	0.121	0	0
3.15	8E-12	1	0.860	0.981	0.997	1.000	1.000	1.000	1.000	1.000	1.000	0.489	0.121	0	0
3.15	9E-12	0.5	0.900	0.990	0.999	1.000	1.000	1.000	1.000	1.000	1.000	0.509	0.121	0	0
3.15	1E-11	0.5	0.900	0.990	0.999	1.000	1.000	1.000	1.000	1.000	1.000	0.509	0.121	0	0
3.15	2E-11	0.5	0.900	0.990	0.999	1.000	1.000	1.000	1.000	1.000	1.000	0.509	0.121	0	0
3.15	3E-11	0.5	0.900	0.990	0.999	1.000	1.000	1.000	1.000	1.000	1.000	0.509	0.121	0	0
3.15	4E-11	0.5	0.900	0.990	0.999	1.000	1.000	1.000	1.000	1.000	1.000	0.509	0.121	0	0
3.15	5E-11	0.5	0.900	0.990	0.999	1.000	1.000	1.000	1.000	1.000	1.000	0.509	0.121	0	0
3.25	2E-13	17.5	0.000	0.000	0.000	0.000	0.000	0.000	0.000	0.000	0.000	0.000	0.083	0.190656	0
3.25	3E-13	14.5	0.000	0.000	0.000	0.000	0.000	0.000	0.000	0.000	0.000	0.000	0.083	0.408428	0
3.25	4E-13	12	0.000	0.000	0.000	0.000	0.000	0.000	0.000	0.000	0.000	0.000	0.083	0.265773	0
3.25	5E-13	10	0.004	0.008	0.012	0.016	0.020	0.024	0.028	0.032	0.035	0.003	0.083	0.095115	2.03E-05
3.25	6E-13	8.5	0.078	0.150	0.217	0.278	0.335	0.387	0.435	0.479	0.520	0.050	0.083	0.025142	0.000104

3.25	7E-13	7.5	0.145	0.268	0.374	0.465	0.542	0.608	0.665	0.714	0.755	0.091	0.083	0.005701	4.3E-05
3.25	8E-13	6.5	0.226	0.402	0.537	0.642	0.723	0.786	0.834	0.872	0.901	0.141	0.083	0.001201	1.4E-05
3.25	9E-13	6	0.273	0.472	0.616	0.721	0.797	0.853	0.893	0.922	0.944	0.169	0.083	0.000246	3.44E-06
3.25	1E-12	5.5	0.324	0.543	0.691	0.791	0.859	0.905	0.936	0.956	0.971	0.199	0.083	6.32E-05	1.04E-06
3.25	2E-12	2.5	0.689	0.903	0.970	0.991	0.997	0.999	1.000	1.000	1.000	0.401	0.083	3.34E-11	1.11E-12
3.25	3E-12	1.5	0.809	0.964	0.993	0.999	1.000	1.000	1.000	1.000	1.000	0.464	0.083	0	0
3.25	4E-12	1	0.860	0.981	0.997	1.000	1.000	1.000	1.000	1.000	1.000	0.489	0.083	0	0
3.25	5E-12	1	0.860	0.981	0.997	1.000	1.000	1.000	1.000	1.000	1.000	0.489	0.083	0	0
3.25	6E-12	0.5	0.900	0.990	0.999	1.000	1.000	1.000	1.000	1.000	1.000	0.509	0.083	0	0
3.25	7E-12	0.5	0.900	0.990	0.999	1.000	1.000	1.000	1.000	1.000	1.000	0.509	0.083	0	0
3.25	8E-12	0.5	0.900	0.990	0.999	1.000	1.000	1.000	1.000	1.000	1.000	0.509	0.083	0	0
3.25	9E-12	0.5	0.900	0.990	0.999	1.000	1.000	1.000	1.000	1.000	1.000	0.509	0.083	0	0
3.25	1E-11	0.5	0.900	0.990	0.999	1.000	1.000	1.000	1.000	1.000	1.000	0.509	0.083	0	0
3.25	2E-11	0.5	0.900	0.990	0.999	1.000	1.000	1.000	1.000	1.000	1.000	0.509	0.083	0	0
3.25	3E-11	0.5	0.900	0.990	0.999	1.000	1.000	1.000	1.000	1.000	1.000	0.509	0.083	0	0
3.25	4E-11	0.5	0.900	0.990	0.999	1.000	1.000	1.000	1.000	1.000	1.000	0.509	0.083	0	0
3.25	5E-11	0.5	0.900	0.990	0.999	1.000	1.000	1.000	1.000	1.000	1.000	0.509	0.083	0	0
3.4	1E-13	17	0.000	0.000	0.000	0.000	0.000	0.000	0.000	0.000	0.000	0.000	0.023	0.031333	0
3.4	2E-13	11.5	0.000	0.000	0.000	0.000	0.000	0.000	0.000	0.000	0.000	0.000	0.023	0.356448	0
3.4	3E-13	8.5	0.078	0.150	0.217	0.278	0.335	0.387	0.435	0.479	0.520	0.050	0.023	0.409901	0.000464
3.4	4E-13	6.5	0.226	0.402	0.537	0.642	0.723	0.786	0.834	0.872	0.901	0.141	0.023	0.157838	0.000506
3.4	5E-13	5.5	0.324	0.543	0.691	0.791	0.859	0.905	0.936	0.956	0.971	0.199	0.023	0.036496	0.000165
3.4	6E-13	4.5	0.437	0.683	0.821	0.899	0.943	0.968	0.982	0.990	0.994	0.264	0.023	0.006671	4E-05
3.4	7E-13	4	0.498	0.748	0.873	0.936	0.968	0.984	0.992	0.996	0.998	0.298	0.023	0.001101	7.46E-06
3.4	8E-13	3.5	0.561	0.807	0.915	0.963	0.984	0.993	0.997	0.999	0.999	0.333	0.023	0.000176	1.33E-06
3.4	9E-13	3	0.625	0.859	0.947	0.980	0.993	0.997	0.999	1.000	1.000	0.367	0.023	2.81E-05	2.35E-07
3.4	1E-12	2.5	0.689	0.903	0.970	0.991	0.997	0.999	1.000	1.000	1.000	0.401	0.023	5.52E-06	5.04E-08
3.4	2E-12	1	0.860	0.981	0.997	1.000	1.000	1.000	1.000	1.000	1.000	0.489	0.023	6.72E-13	7.48E-15
3.4	3E-12	1	0.860	0.981	0.997	1.000	1.000	1.000	1.000	1.000	1.000	0.489	0.023	0	0
3.4	4E-12	0.5	0.900	0.990	0.999	1.000	1.000	1.000	1.000	1.000	1.000	0.509	0.023	0	0
3.4	5E-12	0.5	0.900	0.990	0.999	1.000	1.000	1.000	1.000	1.000	1.000	0.509	0.023	0	0
3.4	6E-12	0.5	0.900	0.990	0.999	1.000	1.000	1.000	1.000	1.000	1.000	0.509	0.023	0	0

3.4	7E-12	0.5	0.900	0.990	0.999	1.000	1.000	1.000	1.000	1.000	1.000	1.000	0.509	0.023	0	0
3.4	8E-12	0.5	0.900	0.990	0.999	1.000	1.000	1.000	1.000	1.000	1.000	1.000	0.509	0.023	0	0
3.4	9E-12	0.5	0.900	0.990	0.999	1.000	1.000	1.000	1.000	1.000	1.000	1.000	0.509	0.023	0	0
3.4	1E-11	0.5	0.900	0.990	0.999	1.000	1.000	1.000	1.000	1.000	1.000	1.000	0.509	0.023	0	0
3.4	2E-11	0.5	0.900	0.990	0.999	1.000	1.000	1.000	1.000	1.000	1.000	1.000	0.509	0.023	0	0
3.4	3E-11	0.5	0.900	0.990	0.999	1.000	1.000	1.000	1.000	1.000	1.000	1.000	0.509	0.023	0	0
3.4	4E-11	0.5	0.900	0.990	0.999	1.000	1.000	1.000	1.000	1.000	1.000	1.000	0.509	0.023	0	0
3.4	5E-11	0.5	0.900	0.990	0.999	1.000	1.000	1.000	1.000	1.000	1.000	1.000	0.509	0.023	0	0

Total = **.00138**

References

1. "Different Riser Materials Compete for Acceptance", *Drilling Contractor*, May/June 2003, pp 30-31.
2. American Petroleum Institution, 1998, "Design, Construction, Operation and Maintenance of Offshore Hydrocarbon Pipelines (Limit State design)", *American Petroleum Institution Recommended Practice (API RP) 1111*, Third Edition, July 1999
3. American Petroleum Institution, 1998, "Design of Risers for Floating Production Systems and Tension Leg Platforms", *American Petroleum Institution Recommended Practice (API RP) 2RD*, First Edition, June 1998.
4. American Petroleum Institution, 1994, "Bulletin on Formulas and Calculations for Casing, Tubing, Drill Pipe, and Line Pipe properties", *American Petroleum Institution Bulletin*, API Bulletin 5C3, Sixth Edition, October 1994
5. American Petroleum Institution, 2004, "Specification on Line Pipe", *American Petroleum Institution*, API Specification 5L, Forty Third Edition, March 2004
6. Mechanics of Wave Forces on Offshore Structures
7. Faltinsen, "Sea Loads on Ships and Offshore Structures"
8. Winterstein, Steven R., Satyendra Kumar, 1995, "Reliability of Floating Structures: Extreme Response and Load Factor Design", *Proceedings of Offshore Technology Conference*, OTC 7758, pp 569-578
9. Hansen, Peter Friis, 1994, "Reliability Analysis of a Mid-ship Section", Thesis, Department of Naval architecture and Offshore Engineering, Technical University of Denmark.
10. ISO/CD 19902, 2001, " Petroleum and Natural Gas Industries – Fixed Steel Offshore Structures", Clause 16,
11. http://www.galbraithconsulting.co.uk/iso/19902/Clause_16_CD.PDF
12. Baldwin, D.D., N.L. NewHouse, Lincoln Composites, 1997, "Composite Production Riser Design", *Proceedings of Offshore Technology Conference*, OTC 8431
13. <http://www.engin.brown.edu/courses/EN175/>
14. "Guideline for offshore structure reliability Analysis", DNV report No 95-2018, Chapter 7, pg 184.
15. Cramer, E.H., R. Loseth and E. Bitner, 1993, " Fatigue in side shell longitudinal due to

- external wave pressure”, OMAE proceedings, Safety and Reliability, Vol. II, pp 267-272
16. Wang, K.S., S.T. Chang and Y.C. Shen, 1996, “Dynamic Reliability models for fatigue crack growth problem”, *Engineering Fracture Mechanics*, Vol. 54, No 4, pp 543-556
 17. Darcis, Philippe, Diego Santarosa, Naman Recho and Tom Lassen, “A Fracture Mechanics Approach for the Crack growth in welded joints with reference to the BS 7910”
 18. Michel, Walter H., 1967, “Sea Spectra Simplified”, *For Presentation meeting of Gulf Section, The society of Naval Architects and Marine Engineers*, April 1967
 19. ABS, Commentary of fatigue Assessment of offshore Structures, pg 55
 20. Ertas, A., G. Mustafa, O. Cuvalci, 1992, “Comparison of Fracture Mechanics and S-N approaches in Designing Drill Pipe”, *Journal of offshore Mechanics and Arctic Engineering*, Vol 114, pp 205-211.
 21. Leira, Bernt J., Tore Holmas, Kjell Herfjord, 2002, “Probabilistic Modeling and Analysis of Riser Collision”, *Transactions of ASME*, Vol. 124, Aug 2002, pp 132-138.
 22. Garbatov, Y., C. Guedes Soares, 2004, “Influence of Steel strength on the fatigue reliability of welded structural components”, *International Journal of Fatigue*, October 2003, Vol. 26, pp 753-762
 23. Zhao W., A. Stacey, P. Prakash, 2002, “ Probabilistic Models in Uncertainties in fatigue and fracture reliability analysis”, *21st International Conference on Offshore Mechanics and Arctic Engineering (OMAE), Proceedings of OMAE '02*, pp 557-574
 24. British Standard Institution, 2000, “Guidance on Methods for Assessing the Acceptability of flaws in fusion welded structures”, *British Standards Institution*, BS7910
 25. Jiao, G., T. Moan, “ Probabilistic Analysis of Fatigue due to Gaussian load process”, *Probabilistic Engineering Mechanics*, 1990, Vol. 5, No2, pp 76-83
 26. Huang, X. and J.W. Hancock, 1989, “A Reliability Analysis of Fatigue crack growth under random loading”, *Fatigue Fracture Engineering Material. Structure*, 1989, Vol. 12, No. 3, pp 247-258
 27. Newman, J.C., E. P. Phillips, R.A. Everett, “ Fatigue Analysis Under Constant and Variable amplitude loading using small crack theory”, *NASA Langley Research Center*
 28. Rogerson, John H and W. Khean Wong, 1982, “Weld Defect Distributions in Offshore Structures and their influence on Structural Reliability”, *Proceedings of Offshore Technology Conference*, OTC 4237.
 29. Colombi, P., K. Dolinski, 2001, “ Fatigue lifetime of welded joints under random loading: rainflow cycle vs cycle sequence method”, *Probabilistic Engineering Mechanics*, 2001, Vol. 16, pp 61-71

30. Tang, Wilson H., "Probabilistic Updating of Flaw Information", *Journal of testing and Evaluation, JTEVA*, Nov 1973, Vol. 1, No. 6, pp 459-467
31. Moan, Torgeir, Ole T. Vardal, Nils-C. Hellevig, Knut Skjoldli, 2000, "Initial Crack Depth and POD Values Inferred from in Service Observations of Cracks in North Sea-Jackets", *Journal of Offshore Mechanics and Arctic Engineering*, Aug 2000, Vol. 122, pp 157-162.
32. Simola, Kaisa, Urho Pulkkinen, 1998, "Models for Non-destructive Inspection Data", *Reliability Engineering and System Safety*, 1998, Vol. 60, pp 1-12
33. Tang, Wilson H., Alfredo H-S. Ang, 1990, "Probability Concepts in Engineering Planning and Design", *Decision Risk and Reliability*, Vol. II, Wiley John and Sons, ISBN: 0471032018
34. Bai, Yong, 2001, "Pipelines and Risers", *Elsevier Ocean Engineering Book Series*, Vol. 3, First Edition, 2001.
35. Klesnil, Mirko, Petr Lukas, 1992, "Fatigue of Metallic Materials", *Elsevier Science and Publishing Company*, Material Science Monographs, 71, Second Revised Edition, 1992.
36. Parker, A. P., 1981, "The Mechanics of Fracture and Fatigue: An Introduction", *E. and F. N. Spon*, First Edition, 1981.
37. Vanmarcke, Erik, 1988, "Random Fields: Analysis and Synthesis", *The MIT Press*, Third Printing, 1988, pp 160-161

Vita

Anubhav Jain, son of Mr. Sharad Jain and Mrs. Abha Jain, was born in Meerut, India on 14th Sep, 1980. After completing high school at St. Mary's Academy, Meerut, India, in 1998, he attended the Indian Institute of Technology (IIT), Delhi, India where he obtained his Bachelor of Technology degree in Production and Industrial Engineering in May 2002. He entered the graduate school of The University of Texas at Austin in the Fall of 2002 to begin work on graduate study in Operations Research and Industrial Engineering.

Permanent Address: Kishan Flour Mills,
Railway Road,
Meerut, Uttar Pradesh,
INDIA-250002

This report was typed by Anubhav Jain.